ANNUAL REPORTS ON NMR SPECTROSCOPY

Volume 11B

ANNUAL REPORTS ON

NMR SPECTROSCOPY

This Page Intentionally Left Blank

ANNUAL REPORTS ON

NMR SPECTROSCOPY

Edited by

G. A. WEBB

Department of Chemistry, University of Surrey, Guildford, Surrey, England

VOLUME 11B

Nitrogen NMR Spectroscopy

M. WITANOWSKI, L. STEFANIAK and G. A. WEBB

1981

ACADEMIC PRESS

A Subsidiary of Harcourt Brace Jovanovich, Publishers

London • New York • Toronto • Sydney • San Francisco

ACADEMIC PRESS INC. (LONDON) LTD.
24–28 Oval Road,
London, NW1 7DX

U.S. Edition Published by

ACADEMIC PRESS INC.
111 Fifth Avenue
New York, New York 10003

British Library Cataloguing in Publication Data

Annual reports on NMR spectroscopy. – Vol. 11B
1. Nuclear magnetic resonance spectroscopy
541.2'8 QD96.N8 68–17678

ISBN 0–12–505349–5

Printed in Great Britain by J. W. Arrowsmith Ltd.
Bristol BS3 2NT

LIST OF CONTRIBUTORS

L. STEFANIAK, *Institute of Organic Chemistry, Polish Academy of Sciences, Warsaw, Poland.*

G. A. WEBB, *Department of Chemistry, University of Surrey, Guildford, Surrey GU2 5XH, England.*

M. WITANOWSKI, *Institute of Organic Chemistry, Polish Academy of Sciences, Warsaw, Poland.*

This Page Intentionally Left Blank

PREFACE

Largely on account of a continued expansion in the applications of nitrogen NMR, Volume 11 of Annual Reports is divided into two parts. An indication of the range of areas of molecular science which are critically dependent upon NMR investigations is provided by the diverse choice of topics covered in Volume 11A. The review on amino acids, peptides and proteins by Dr H. W. E. Rattle provides a current account of an area previously covered in Volume 6B of this series. Biologically important areas of research are also taken into account in the chapter by Professor S. Forsén and Dr B. Lindman on ^{25}Mg and ^{43}Ca NMR. The remaining three reports in Volume 11A deal with material which, although previously dealt with *inter alia*, is specifically covered for the first time in this series, the topics in question being ^{13}C–^{13}C couplings by Dr's P. E. Hansen and V. Wray and the ^{13}C NMR of Group VIII organometallic compounds by Dr P. S. Pregosin.

Volume 11B is devoted to a comprehensive and up-to-date account of nitrogen NMR by Professor M. Witanowski and his coworkers. This review serves to expand upon those provided previously, in Volumes 2, 5A and 7, on this important topic.

It gives me great pleasure to express my gratitude to all of the contributors to Volume 11 for their diligence and willing cooperation which has provided the basis for this volume.

University of Surrey,
Guildford, Surrey,
England

G. A. WEBB
May 1981

This Page Intentionally Left Blank

CONTENTS

Nitrogen NMR Spectroscopy

M. WITANOWSKI, L. STEFANIAK AND G. A. WEBB

CONTENTS OF VOLUME 11A

Nitrogen NMR Spectroscopy

M. WITANOWSKI AND L. STEFANIAK

Institute of Organic Chemistry, Polish Academy of Sciences, Warsaw, Poland

and

G. A. WEBB

Department of Chemistry, University of Surrey, Guildford, Surrey, England

I. INTRODUCTION

Our main aim in preparing this report is to present a comprehensive survey of the nitrogen NMR literature that has appeared since our last review.[1] Thus the present coverage extends from 1977 to late 1980. In discussing

the numerous developments that have occurred during this period liberal reference is made to our previous accounts of nitrogen NMR.[1-3]

Progress has been recorded in both experimental and theoretical aspects of nitrogen NMR during the review period. The widespread utilization of ^{15}N NMR as a practical structure elucidation technique has been referred to in a monograph[4] and in two reviews.[5,6] Concomitantly the more abundant ^{14}N nucleus has continued to be employed in a large range of chemical shift and quadrupolar relaxation studies.

The complementarity of the magnetic and electric properties of the two stable isotopes is in part responsible for the extensiveness of the applications of nitrogen NMR. A further important factor is the importance of nitrogen in many areas of chemistry, while the final necessary ingredient is the fact that, at about 900 ppm, the range of nitrogen chemical shifts is the largest to be found amongst the first- and second-row nuclei.

The rather large range of nitrogen chemical shifts reflects the importance of the lone-pair electrons to the nitrogen nuclear shielding. When the lone pair is actively engaged in bonding, the shielding usually increases by a substantial amount. The broad range of bonding situations available to nitrogen is thus graphically demonstrated by its range of chemical shifts. Consequently subtle changes in molecular structure are more likely to produce significant screening differences in nitrogen NMR spectra than in those of other commonly studied nuclei such as ^{1}H, ^{13}C, ^{19}F, or ^{31}P.

II. THEORY OF NITROGEN NMR PARAMETERS

Some theoretical aspects of NMR parameters have recently been presented in a treatise relating to NMR and the periodic table.[7] Thus only a brief account of the theoretical background to nuclear screening and spin–spin interactions is presented here.

A. Calculations of nitrogen shieldings

Nuclear shielding in the presence of a magnetic field is described by a second-order tensor. Quantum mechanical expressions for its components were first provided by Ramsey.[8] However, this approach has shortcomings which have been documented elsewhere.[9] Perhaps the most troublesome of these is the production of gauge-dependent shielding data when limited basis sets are used in the calculation. Such basis sets are usually necessary, even for diatomic molecules, in order to perform the calculations within a reasonable amount of computer time.

Coupled Hartree–Fock calculations of the nitrogen shielding tensor of ammonia have been reported.[10] The wavefunctions employed are expanded over basis sets of Gaussian functions. Four such wavefunctions, of increasing

accuracy, are employed. By choosing the origin at the centre of mass it is found that the diamagnetic part of the shielding tensor is almost independent of the choice of basis set, whereas the averaged paramagnetic component varies from −228·36 to −89·96 ppm as the basis set improves in accuracy. These values have to be compared with an experimental determination of −89·7 ppm for the averaged paramagnetic contribution to the nitrogen shielding of ammonia.[11]

In all four cases the results of the calculations are found to be gauge-dependent. The extent of this dependence decreases as the accuracy of the basis set increases. Thus a demonstration is provided of the sensitivity of *ab initio* calculations of nuclear shielding to the choice of basis set.

The equations-of-motion method, which appears to have a greater generality than the coupled Hartree–Fock theory, has been applied to the N_2 molecule.[12] This approach provides a value of −110·6 ppm for the mean nitrogen shielding, which is in good agreement with the experimental value of -101 ± 20 ppm.[13]

In nitrogen NMR spectroscopy the main interest lies in relative shielding constants, i.e. chemical shifts, for molecules somewhat larger than N_2 and NH_3. Consequently a model giving gauge-dependent results with limited basis sets leads to problems when larger molecules are under consideration.

The gauge-dependence of the calculated nuclear shielding can be removed by the use of a molecular orbital theory incorporating gauge-dependent atomic orbitals.[14] Although some criticisms of this method have been raised, it does give good nuclear screening results even when small basis sets are employed.[16]

Most semiempirical calculations of nitrogen shielding data are based upon the gauge-dependent atomic orbital formulation. Within this framework[14] the nuclear shielding, σ, is expressed as a sum

$$\sigma = \sigma^{d}_{loc} + \sigma^{d}_{non\text{-}loc} + \sigma^{d}_{inter} + \sigma^{p}_{loc} + \sigma^{p}_{non\text{-}loc} + \sigma^{p}_{inter} \quad (1)$$

The local diamagnetic and paramagnetic terms, σ^{d}_{loc} and σ^{p}_{loc} respectively, arise from electronic currents localized on the atom containing the nucleus of interest. The corresponding non-local contributions are due to currents on neighbouring atoms, while the interatomic terms are related to non-localized currents. These latter terms usually produce a shielding contribution of a few ppm at most, which is negligible when compared with the nitrogen chemical shift range of about 900 ppm.

As noted elsewhere,[7,9] by considering only the nitrogen 2s and 2p atomic orbitals the expressions for the rotationally averaged local terms in equation (1), for nucleus A, become

$$\sigma^{d}_{Aloc} = \frac{\mu_0 e^2}{12\pi m} \sum_{\nu} P_{\nu\nu} \langle \nu | r^{-1}_{\nu A} | \nu \rangle \quad (2)$$

and

$$\sigma^{p}_{Aloc} = -\frac{\mu_0 \hbar^2 e^2}{6\pi m^2}\langle r^{-3}\rangle_{2p} \sum_{j}^{occ}\sum_{k}^{unocc} (E_k - E_j)^{-1}$$
$$\times (C_{j,z_A}C_{k,y_A} - C_{j,y_A}C_{k,z_A}) \sum_{B} (C_{j,z_B}C_{k,y_B} - C_{j,y_B}C_{k,z_B})$$
$$+ (C_{j,z_A}C_{k,x_A} - C_{j,x_A}C_{k,z_A}) \sum_{B} (C_{j,z_B}C_{k,x_B} - C_{j,x_B}C_{k,z_B})$$
$$+ (C_{j,x_A}C_{k,y_A} - C_{j,y_A}C_{k,x_A}) \sum_{B} (C_{j,x_B}C_{k,y_B} - C_{j,y_B}C_{k,x_B}) \quad (3)$$

where $r_{\nu A}$ represents the separation of the electrons in orbital ν from nucleus A, $P_{\nu\nu}$ is the charge density relating to orbital ν, C_{j,x_A} is the LCAO coefficient of the $2p_x$ orbital on atom A in the molecular orbital j etc. whose energy is represented by E_j, and $\langle r^{-3}\rangle_{2p}$ is the mean inverse cube radius for the 2p orbitals on atom A.

Expressions analogous to equations (2) and (3) are available for the corresponding non-local terms. In general $\sigma^{d}_{non\text{-}loc}$ is negligible but $\sigma^{p}_{non\text{-}loc}$ can be appreciable, particularly in cases of multiple bonding[17,18] as demonstrated in Table 1. Consequently both the local and non-local contributions to the paramagnetic component of the nitrogen shielding tensor should be taken into account.

As noted previously,[1,7,9] σ^{d}_{loc} is approximately constant for nitrogen nuclei in a variety of molecular environments. Further work[19] has substantiated this claim by comparison with X-ray PE data.

By suitable evaluation,[1,7,9] equation (2) may be expressed as

$$\sigma^{d}_{loc} = 202{\cdot}353 + 4{\cdot}437[3{\cdot}25 - 0{\cdot}35(q-5)]q \quad (4)$$

where q is the total charge density on the nitrogen atom concerned. By means of equation (4) the largest change in σ^{d}_{loc} is found to be about 15 ppm.[19] This occurs between NOF_3 and OCN^- and corresponds to about 4·5% of the value of σ^{d}_{loc} for nitrogen. The nitrogen chemical shift difference between these two species is about 170 ppm.

It seems very probable that NOF_3 and OCN^- represent the limits of charge density for nitrogen molecular environments, and thus, from equation (4), the limits on the range of values for σ^{d}_{loc}. A report[20] based upon a similar series of calculations exaggerates the changes in σ^{d}_{loc} for a number of nitrogen-containing species. This discrepancy probably arises from excluding the effects of nuclear shielding on the nitrogen 2p electrons, such that the following equation rather than equation (4) is used to evaluate σ^{d}_{loc}:

$$\sigma^{d}_{loc} = 202{\cdot}353 + 14{\cdot}42q \quad (5)$$

As a consequence of this, changes in σ^{d}_{loc} are overestimated.

Hence, in general, it appears that changes in σ^{d}_{loc} are not of major significance in discussing nitrogen chemical shift differences. Usually changes due to solvent effects outweigh those arising from σ^{d}_{loc}.[1]

INDO parameterized calculations of nitrogen shielding have been reported which include two-centre integrals of the type $\langle\phi_{\nu B}|O_A|\phi_{\mu B}\rangle$,[21] where ϕ_μ and ϕ_ν are atomic orbitals centred on atom B, and O_A is an operator relating to atom A. The resulting diamagnetic contributions to the nitrogen shielding tensors in NH_3, HCN, N_2O, and CH_3CN are comparable to those obtained from gauge-dependent *ab initio* calculations. It is suggested[21] that this approach may supersede the empirical atom–dipole model[1,7,9] as a means of estimating the molecular, Ramsey-type, diamagnetic shielding terms. It cannot be stressed too frequently that such terms are not to be compared with the gauge-independent ones represented in equations (1) and (2).

In the period under review the significance of the contributions from the excited electronic states to the paramagnetic term has been investigated by comparing the results of calculations using various semiempirical parameter sets. The INDO scheme usually provides a serious overestimate of the energy separation between the ground and various excited states.[21] Thus parameters that have been specifically chosen to describe electronic transitions, such as the CNDO/S and INDO/S sets, are preferable for calculations of the paramagnetic contribution to the nuclear shielding.[17,18] Since the diamagnetic term relies only on calculated charge densities, there seems to be little to choose between the various semiempirical sets when considering this term.

Clearly the MINDO/3 set is inadequate for a reliable estimate of second-order properties such as nuclear shielding and spin–spin coupling constants.[22–24] In calculations of nitrogen shielding a significant improvement in the comparison with experimental data is obtained when the coefficients in equation (3) evaluated from MINDO/3 calculations are combined with excitation energies obtained from INDO/S parameterized calculations.[22] This is illustrated by calculations on nitromethane, which is recommended as the reference standard for nitrogen NMR. The value of the nitrogen shielding obtained from a MINDO/3 calculation is −325·33 ppm whereas the inclusion in equation (3) of energies obtained from an INDO/S calculation yields a value of −208·05 ppm.[22] When equation (3) is evaluated entirely by the INDO/S procedure the corresponding result is −112·46 ppm,[18] which is in reasonable agreement with about −130 ppm obtained from a comparison of the spin–rotation data for ammonia and the chemical shift data for ammonia and nitromethane.[18]

It should be remembered that the model usually chosen for nuclear shielding calculations is based upon an isolated molecule in a vacuum. For

a more realistic comparison with experimental NMR data some account of the medium employed should be taken. From the theoretical standpoint this is not a simple problem. So far, the few calculations that have been made for nitrogen nuclear shielding in the presence of solvation effects are based upon the solvaton model.[25] Within this model both Pople's procedure, as demonstrated by equations (2) and (3), and the finite perturbation approach have been employed. In general, significant nitrogen chemical shift differences are predicted as the dielectric constant of the medium varies. Taking nitromethane as an example, the nitrogen screening is predicted by using Pople's approach to decrease by about 29 ppm as the dielectric constant increases from 1 to 80. For pyridine an increase of about 16 ppm is predicted in hydrogen-bonding solvents. This arises from a decrease in the paramagnetic contribution due to the effective removal of nitrogen lone-pairs upon hydrogen-bond formation, and is in reasonable agreement with the measured[26] increase in nitrogen shielding of about 25 ppm (Section V.J).

Recently some high precision ^{14}N shielding measurements for nitroalkanes in various solvents have been reported.[120] In all cases the nitrogen shielding increases as the dielectric constant of the medium decreases. This trend is both qualitatively and quantitatively reproduced by INDO/S parameterized calculations based upon the solvaton and Pople models. Consequently, the nitrogen shielding changes appear to monitor satisfactorily the electronic redistributions which occur in the nitroalkanes as the solvent is changed.[121] The shielding variations, predicted by the finite perturbation procedure for nitromethane, are found to be too small for a reliable comparison with the experimental data.

The question of establishing an absolute shielding scale for nitrogen[1] has been raised again.[27] From the theoretical point of view, estimations of nitrogen shielding results appear in general to be satisfactorily accounted for by employing equations (2) and (3) together with INDO/S parameters.[18] Expressing these as chemical shifts can lead to poorer agreement with experiment owing to the introduction of medium effects. Hence theoreticians would welcome the introduction of an absolute shielding scale. However, it seems that such a suggestion is premature from the experimental aspect.[27] Thus the nitrogen shielding data are reported here in ppm on the nitromethane scale[1] (Section III).

The majority of applications of Pople's shielding model incorporate the average excitation energy (AEE) approximation in the paramagnetic term. In this procedure equation (3) becomes

$$\sigma^{p}_{Aloc} = -\frac{\mu_0 \hbar^2 e^2}{8\pi m^2} \frac{1}{\Delta E} \langle r^{-3} \rangle_{2p} \sum_{B} Q_{AB} \tag{6}$$

where the summation over B includes atom A, and

$$Q_{AB} = \tfrac{4}{3}\delta_{AB}(P_{x_Ax_B} + P_{y_Ay_B} + P_{z_Az_B}) - \tfrac{2}{3}(P_{x_Ax_B}P_{y_Ay_B} + P_{x_Ax_B}P_{z_Az_B} + P_{y_Ay_B}P_{z_Az_B}) + \tfrac{2}{3}(P_{x_Ay_B}P_{x_By_A} + P_{x_Az_B}P_{x_Bz_A} + P_{y_Az_B}P_{y_Bz_A}) \quad (7)$$

where δ_{AB} is the Kronecker delta, the P's are the elements of the charge-density bond order matrix, and ΔE is the AEE.

In general this method is reasonably successful in accounting for gross chemical shift trends in series of closely related molecules. However, any attempt to choose a suitable value for ΔE gives rise to difficulties since it is not directly related to any of the individually observed electronic transitions in the molecules concerned.

That great care must be exercised in invoking the AEE approximation is demonstrated by the results shown in Table 2. The average energies expressed in the final column of Table 2 are obtained by weighting the energies of the transitions contributing to the paramagnetic term by the magnitude of their contributions. The large variation in these data indicates that the AEE approach is not a very realistic method for estimating the shielding of the diverse nitrogen environments represented in Table 2.

From equations (6) and (7) it follows that if ΔE, $\langle r^{-3}\rangle_{2p}$, and the nitrogen bond orders remain reasonably constant, or produce cancelling changes for a given series of molecules, then the corresponding nitrogen chemical shifts are expected to follow charge density differences. A linear relationship between nitrogen chemical shift and charge density has been reported for various nitrogen-containing molecules,[28] some diazo compounds,[29] triazenes,[30] substituted pyrimidines,[31] flavins,[32] azoles,[33] borazines,[34] methyl-substituted anilines,[35] some 1,2,4-triazines[36] and their N-oxides.[307] The nitrogen charge densities are obtained by any one of a number of semiempirical molecular orbital procedures.

An example of a successful application of the AEE method to the interpretation of nitrogen shielding data is shown in Fig. 1 for some N-oxide groups of polyazine mono-N-oxides.[307]

By using INDO/S estimates of the charge density and bond order matrix elements in equations (6) and (7) it is possible to evaluate the product $\sigma_N^p \Delta E$ for the N-oxides and to plot this against observed nitrogen shielding with respect to nitromethane. The open circles in Fig. 1 correspond to measured N-oxide screenings and the solid circle represents the unknown compound quinazoline-1-oxide for which additivity rules[313] have been used to estimate its nitrogen shielding.

The correlation coefficient of 0·996 for the least-squares fit of the results given in Fig. 1 indicates the satisfactory nature of the AEE results. The corresponding value of ΔE is estimated to be $5{\cdot}3 \pm 0{\cdot}1$ eV. Although not comparable to any experimental electronic transition, this value of ΔE is

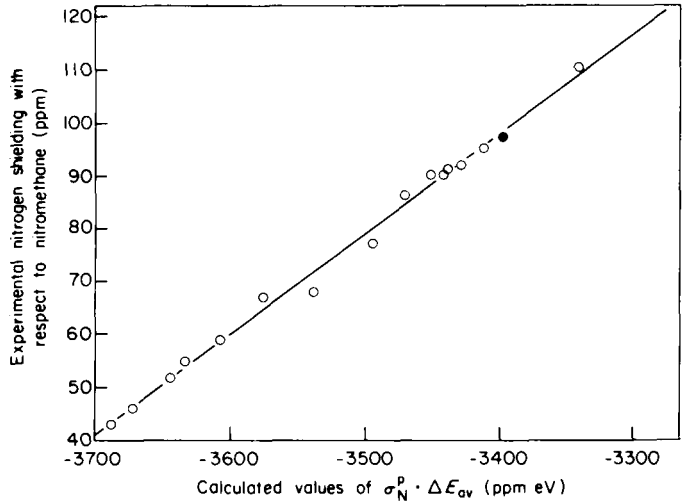

FIG. 1. Comparison of observed nitrogen shielding for some *N*-oxide groups of polyazine mono-*N*-oxides with estimates obtained from the AEE procedure using INDO/S parameterized calculations.[81]

higher than that reported for the parent azines.[1] This is quite reasonable since the azine nitrogen lone-pair electrons will be involved in the formation of the *N*-oxide bond, and thus low-energy n $\rightarrow \pi^*$ transitions will no longer be available to contribute to the paramagnetic component of the nitrogen shielding tensor.

Hence for a closely related series of molecules the AEE approximation can have practical consequences in that it can be easily used, for example to assign the *N*-oxide resonance in polyazine mono-*N*-oxides. Within these confines further applications are expected.

In the case of some picolines and lutidines,[37] the nitrogen chemical shifts are found not to correlate with INDO charge densities owing to significant changes in the $\langle r^{-3} \rangle_{2p}$ term in equation (6). However, the range of nitrogen shieldings observed for the molecules considered is too small for the conclusions reached to be of great significance. For some azo compounds[38] and some 2-coordinate nitrogen compounds[39] a crude linear relationship appears between the nitrogen shielding and the reciprocal energy of the lowest energy electronic transition. Such a relationship is probably largely fortuitous since, as shown in Table 2, the lowest energy electronic transition is not necessarily the largest contributor to the nitrogen shielding constant. Even when it makes the greatest contribution this is usually outweighed by the sum of the contributions from the other transitions concerned.

Attempts have been reported to interpret nitrogen chemical shifts in terms of rotation barriers for N–C bonds in amides, thioamides, and related

compounds,[40] some enamines,[41] some alkyl- and aryl-substituted ureas,[42] and a series of *para*-substituted *N,N*-dimethylbenzamides.[43] A similar approach has been adopted for the N–Si bond in silylamines[44] and the N–N bond in nitrosamines, hydrazones, triazenes, and related protonated species.[45] In general, satisfactory correlations are observed between the nitrogen chemical shifts and the activation energies for rotation around the bond in question (Section V.I).

Any proposal to extend this interpretation such that nitrogen chemical shifts are considered as a means of predicting activation energies for bond rotation should be treated with caution. Excluding those molecules where the rotation barrier depends upon steric effects, it is clear from equations (6) and (7) that changes in bond order, charge density, and the terms ΔE and $\langle r^{-3}\rangle_{2p}$ can be instrumental in producing nitrogen shielding differences. To imply that nitrogen chemical shifts depend linearly on bond order and charge density changes, and thus activation energies for rotation about those bonds,[40] necessitates that ΔE and $\langle r^{-3}\rangle_{2p}$ either remain constant over the series of molecules considered or vary in a compensatory manner.

In so far as transitions involving the nitrogen lone pair of electrons contribute to σ^{p}_{loc}, increased delocalization of these electrons will tend to lead to a larger value of ΔE and thus to an overall increase in nitrogen screening. If the delocalization results in a higher N–X bond order, $\langle r^{-3}\rangle_{2p}$ is expected to increase,[1-3] thus producing a decrease in the nitrogen shielding constant. Consequently, if these opposing contributions to the nitrogen shielding nullify each other, it is not unreasonable to interpret the chemical shift differences in terms of local changes in charge densities and bond orders. However, it is not easy to predict when such circumstances may obtain.

Recently some dynamic ^{13}C and ^{1}H NMR results, for the temperature range 0–150 °C, have been applied to the estimation of barriers to N–C internal rotation in tetramethylurea, tetramethylthiourea, *N*-methylaniline, and *p*-nitro-*N*-methylaniline.[46] For the first two of these molecules the barrier is estimated to be $6{\cdot}3 \pm 0{\cdot}1$ kcal mol^{-1}, compared with predictions of 11·6 and 3·2 kcal mol^{-1} respectively from ^{15}N chemical shifts.[40] The poor agreement between the calculated barrier heights, from these two sets of experimental data, is attributed to cross-conjugation between the nitrogen atoms and the carbonyl or thiocarbonyl groups.[46]

In the case of *N*-methylaniline the question of cross-conjugation between two equivalent nitrogen atoms, as encountered in the ureas, does not arise. Consequently the barrier heights predicted by the dynamic NMR and ^{15}N chemical shift procedures are in reasonable agreement. The values reported for *N*-methylaniline are $6{\cdot}1 \pm 0{\cdot}1$ and 5·3 kcal mol^{-1} from the dynamic NMR and ^{15}N chemical shift measurements respectively; the corresponding data for *p*-nitro-*N*-methylaniline are about 10–11 and 8·7 kcal mol^{-1}.[46,47]

An alternative explanation has been suggested[78,79] for the apparently poor results for the ureas obtained from the ^{15}N chemical shift approach. This is based upon the presence of steric hindrance in the substituted ureas. In the rotational transition state the steric effects may produce a barrier which is not a function of electronic distribution in the ground state. Consequently the ^{15}N chemical shift will not relate to the barrier height in such a case since the ^{15}N nuclear shielding is closely dependent upon the ground state electronic structure.

The variable agreement of the estimate of N–C barrier from these two experimental techniques, depending upon the degree of cross-conjugation or steric hindrance, provides a further reason for exercising caution in using the (indirect) ^{15}N chemical shift procedure.

An attempt has been made, based upon a dipole–dipole model of nucleus–electron interactions, to estimate the effects of ring currents on the nitrogen shielding of some heterocycles and corresponding cations.[28] The largest calculated effect occurs for the nitrogen of indolizine, for which the value of about 6 ppm is obtained. For the other species considered the ring current induced shift is estimated to be in the range 1–3 ppm which is negligible in comparison with the effects of solvation and experimental error usually found in ^{15}N NMR data.

Interest in the nuclear shielding of gaseous molecules appears to be increasing.[48] In NMR experiments the dependence of nuclear shielding upon the state of molecular rotation and vibration may be reflected in the temperature variation of the shielding and in the observation of isotope shifts.

The temperature dependence of the shielding arises from a variation in the populations of the various molecular rotational and vibrational levels and from intermolecular interactions. For a nucleus in a gaseous molecule the shielding may be expressed[48] as a function of the density (ρ) at a given temperature (T) by means of the equation

$$\sigma(T) = \sigma_0(T) + \sigma_1(T)\rho + \sigma_2(T)\rho^2 + \cdots \tag{8}$$

where $\sigma_0(T)$ is the shielding constant of an isolated molecule and $\sigma_1(T)$ and $\sigma_2(T)$ describe intermolecular effects. Usually $\sigma_2(T)$ is negligibly small; $\sigma_0(T)$ and $\sigma_1(T)$ may be determined by measuring σ as a function of temperature and pressure.

The first determination of $\sigma_0(T)$ and $\sigma_1(T)$ for ^{15}N has been reported for N_2O.[49] The magnitude of σ_1 for the terminal nitrogen atom is about four times that for the central nitrogen. This is consistent with the terminal nitrogen being the more exposed of the two, as is demonstrated by its higher shielding sensitivity in the presence of perturbing molecules.

In addition, the terminal nitrogen shielding has the greater temperature dependence. This is most probably due to the rate of change of σ_1 with

respect to the nitrogen–nitrogen separation being about twice as great for the terminal as for the central nitrogen atom.

It seems likely that further shielding studies on nitrogen nuclei in gaseous molecules will soon be performed.[50] Such investigations should provide a basis for understanding the importance of isotope effects, hydrogen-bonding, and various neighbouring interactions as contributors to nitrogen nuclear shielding.

B. Calculations of nitrogen spin–spin couplings

The calculation and interpretation of indirect nuclear spin–spin interactions are usually based on Ramsey's model.[53] Within this framework the spin–spin coupling constant, J(A–B), between nuclei A and B is expressed as a summation

$$J(\text{A–B}) = J(\text{A–B})_{\text{C}} + J(\text{A–B})_{\text{O}} + J(\text{A–B})_{\text{D}} \tag{9}$$

of contributions arising from the contact, orbital, and dipolar interactions respectively. The semiempirical molecular orbital expressions for these terms, which involve contributions from various excited electronic states, are given elsewhere.[7]

The contact interaction depends upon the product of the s electron densities at the coupled nuclei, $S_{\text{A}}^2(0)S_{\text{B}}^2(0)$, whereas both the orbital and dipolar terms are proportional to the product of the one-centre integrals, $\langle r^{-3}\rangle_{\text{A}}\langle r^{-3}\rangle_{\text{B}}$, relating to the valence p electrons on nuclei A and B.

Consequently equation (9) may be rewritten as

$$J(\text{A–B}) = aJ'(\text{A–B})_{\text{C}} + b[J'(\text{A–B})_{\text{O}} + J'(\text{A–B})_{\text{D}}] \tag{10}$$

where

$$a = S_{\text{A}}^2(0)S_{\text{B}}^2(0) \tag{11}$$

$$b = \langle r^{-3}\rangle_{\text{A}}\langle r^{-3}\rangle_{\text{B}} \tag{12}$$

Thus $J'(\text{A–B})_{\text{C}}$, $J'(\text{A–B})_{\text{O}}$, and $J'(\text{A–B})_{\text{D}}$ refer to the contact, orbital, and dipolar contributions respectively, omitting the integral products given by equations (11) and (12).

From equations (10)–(12) it is apparent that only a contact contribution is expected for couplings involving protons, whereas all three terms in equation (10) may contribute to coupling between other nuclei.

The coupling expressions appropriate to the terms in equation (10) are usually evaluated by the sum-over-states (SOS) perturbation,[54] finite perturbation (FP),[55] or self-consistent perturbation (SCP)[56] techniques. The computational aspects of these procedures have been reviewed by Kowalewski.[57] The INDO parameterization scheme at present appears to provide the most successful semiempirical approach to these calculations.

INDO parameters have been employed in calculations involving nitrogen within the SOS, FP, and SCP schemes. These usually involve taking a and b, from equations (11) and (12), as empirical parameters which are adjusted to give the best agreement between theory and experiment by means of a least-squares fitting procedure.

Both FP[58] and SOS[59] calculations of $^nJ(^{15}N-^{13}C)$ for a variety of molecules show that the major coupling contribution usually arises from the contact interaction. The lone-pair electrons may play a very important role in determining the magnitude of the contact term. An illustration of this is provided by a comparison of $^1J(^{15}N-^{13}C)$ for pyridine and the pyridinium ion. For the former the contact contribution is calculated to be $-0{\cdot}7$ Hz whereas it is $-13{\cdot}7$ Hz for the latter.[58]

This large difference arises from a low energy transition from the highest filled non-bonding orbital in pyridine which provides a large positive contribution to the contact term. This contribution largely cancels other negative contributions from different electronic transitions. The absence of the nitrogen lone pair in the pyridinium ion removes this possibility and results in a large and negative contact contribution to the $^{15}N-^{13}C$ coupling. Consequently, for "pyridine" type nitrogen atoms the major contribution to $^1J(^{15}N-^{13}C)$ usually arises from the orbital term in equation (9), whereas the contact term dominates most couplings involving "pyrrole" type nitrogens.[59]

Equations (10) and (11) indicate that, when the contact term is dominant, the spin–spin coupling will depend upon the amount of s-character in the single bond joining the nuclei. Thus the empirical relationship

$$^1J(^{15}N-^{13}C) = KS_NS_C \tag{13}$$

is expected to be valid in this case. FP calculations show that the constant K in equation (13) takes a value of -94.[60] However, some deviations from the linearity implied by equation (13) are observed for singly bound $^1J(^{15}N-^{13}C)$ values even when the contact term dominates the coupling. These are attributed to the effects of lone-pair electrons in orbitals with s-character on the coupled nuclei.[60] The presence of lone pairs in orbitals with p-character does not interfere with the linear relationship given by equation (13).

A similar effect has been revealed by FP[61] and SOS[62] calculations of some $^{15}N-^{15}N$ couplings. In this case the presence of a lone pair with s-character produces a large and negative contribution to the contact term due to the negative value of the ^{15}N magnetogyric ratio. An example of this effect is shown by $(Z)\beta$-acetylphenylhydrazine in Table 3. An analysis of the various transitions contributing to the contact term of $^1J(^{15}N-^{15}N)$ reveals negative contributions from $n(s) \rightarrow \sigma^*$ transitions whereas those

from $\sigma \rightarrow \sigma^*$ transitions can be of either sign. In $(Z)\beta$-acetylphenylhydrazine the nitrogen lone pair resides in a p atomic orbital thus precluding the possibility of a contribution from n(s) $\rightarrow \sigma^*$ transitions. Consequently the contact term is small and its positive sign is dictated by the resultant of various $\sigma \rightarrow \sigma^*$ transitions.

A further illustration of the importance of p lone pairs is afforded by the various nitramines given in Table 3. For the planar molecules the lone pairs are in p orbitals and the contact terms are small and negative, whereas for molecules 7 and 8 a tetrahedral nitrogen atom is present resulting in a more negative contact term and a larger value for $^1J(^{15}N–^{15}N)$.[62] Calculations of $^1J(^{15}N=^{15}N)$ and $^1J(^{15}N\equiv^{15}N)$ also predict negative values with larger contributions arising from the non-contact terms.[62] The importance of the effect of geometry on the value of $^1J(^{15}N–^{15}N)$ is shown in Fig. 2.

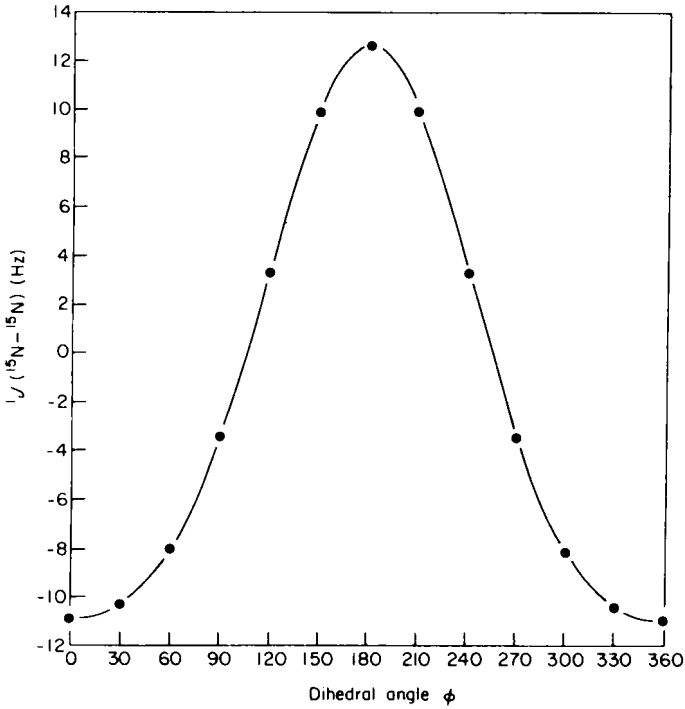

FIG. 2. Variation of $^1J(^{15}N–^{15}N)$ of hydrazine as a function of dihedral angle between nitrogen lone pairs.

Both the sign and magnitude of $^1J(^{15}N–^{15}N)$ for hydrazine are shown to depend critically on the dihedral angle between the nitrogen lone pairs.[61]

Calculations of $^1J(^{15}N–^{13}C)$ for some anilines and related molecules reveal that the coupling is dominated by the contact interaction.[58,59,63,64]

An FP calculation of $^{1}J(^{15}N-^{13}C)$ for diazomethane has used the CNDO/S parameter scheme.[65] This reveals that the coupling constant is negative in sign and dominated by the contact mechanism. A similar conclusion is drawn from INDO-based SCP calculations of $^{1}J(^{15}N-^{13}C)$ for 1-methylguanidine[66] and methyl diazoacetate.[67] Calculations involving the contact term only have been reported for $^{15}N-^{13}C$ couplings in azaadamantane and its hydrochloride[68] and for some aromatic oximes.[69] Not surprisingly, the absence of the non-contact terms makes for a poor correlation with experiment in the latter case. In general, longer range $^{15}N-^{13}C$ couplings are dominated by the contact interaction.[70]

When multiple bonding occurs the non-contact terms increase in magnitude and can dominate the spin–spin interaction.[58,71] The increased importance of the orbital and dipolar terms is reflected in the relevant values of the one-centre integral products given by a and b in equations (11) and (12). SCP calculations on 36 values of $^{1}J(^{15}N-^{13}C)$ produce 14·48 and 2·45 au^{-6} for a and b, whereas the corresponding data are reported to be 10·44 and 17·66 au^{-6} respectively for 19 $^{1}J(^{15}N\equiv^{13}C)$ couplings.[71] The small decrease in a and the large increase in b for the triple-bond couplings, compared with those for the single-bond case, appear to be reasonable. The decrease in a most probably reflects the decrease in s electron density at the nuclei due to an increase in σ overlap. The concomitant increase in b follows the smaller separation of the coupled nuclei in the triple-bonded arrangement. All the $^{1}J(^{15}N\equiv^{13}C)$ couplings considered are predicted to have a negative sign.

SOS and SCP calculations of some $^{n}J(^{19}F-^{15}N)$ values have also been reported.[72] All the $^{1}J(^{19}F-^{15}N)$ couplings are predicted to be positive, whereas the ^{2}J, ^{3}J, and ^{4}J couplings can be of either sign. Most of the couplings are dominated by the contact interaction but the non-contact terms can be important in some cases. The presence of lone pairs with s-character entails a large positive contact contribution to all the $^{1}J(^{19}F-^{15}N)$ values considered.[72]

A CNDO/2 parameterized series of FP calculations has been reported for some $^{1}J(^{31}P-^{15}N)$ couplings.[73] The calculations involve only the contact term and show satisfactory agreement with the available experimental data. A linear dependence of the calculated coupling constant on the bond order between the coupled nuclei is reported.[73]

III. CALIBRATION OF SPECTRA

The confusion that has previously existed in the calibration of nitrogen NMR spectra[1,2,4] seems to persist still, but there are some signs[80,81] that neat nitromethane ($MeNO_2$) will be considered as the primary external standard for referencing both for ^{14}N and ^{15}N NMR spectra. However, a

suggestion[81] that nitrogen chemical shifts should be referred experimentally to external neat nitromethane and then recalculated to a hypothetical ammonia reference signal at 380·2 ppm to higher fields (lower frequencies) from $MeNO_2$ seems to be untenable since it introduces some additional confusion, namely that concerned with bulk magnetic susceptibility effects. This point is discussed further in the present section.

There are several sources of error and inconsistency as far as the measurement of nitrogen chemical shifts is concerned. First of all, there are experimental errors in the measurement of the relative positions of the nitrogen resonance signals, including that of the standard employed. These can be reduced by modern experimental techniques to below 0·1 ppm for both ^{15}N and ^{14}N NMR. For the latter isotope, this requires a careful lineshape fitting, since the quadrupolar relaxation of ^{14}N nuclei causes the corresponding signal half-height width to range from a few Hz to several kHz. However, the signals of the non-quadrupolar ^{15}N nuclei can attain widths of 10–20 Hz, even if dynamic broadening effects are excluded; if one relies entirely on computerized algorithms which look simply for maximum readings within certain ranges of digitized spectra, an error of 0·5–1 ppm can easily result for noisy spectra, even at high magnetic fields and correspondingly high resonance frequencies.

Even the most accurate estimates of the relative positions of nitrogen resonance signals can be wasted if unreliable standards are used.[80] Since no internal standard (that dissolved in the sample examined) is immune to medium effects on its resonance position,[80,81] external standards are recommended. However, some popular standards, such as NH_4^+, NO_3^-, HNO_3, and Me_4N^+, are known to display considerable shifts of their nitrogen resonances with changes in the corresponding counterions, salt concentration, etc. (Table 6). If the exact composition of a standard is not reported, the uncertainty of the nitrogen shift can reach as much as 30 ppm. One should also remember that some apparent discrepancies can result from temperature differences between samples. If no temperature control is provided, particularly when the pulsed Fourier-transform technique for ^{15}N with proton decoupling is employed, the sample temperature can vary from one experiment to another and give rise to apparent shifts.

Another source of confusion is the problem of the sign conventions used with nitrogen shifts. The plus sign is used to denote either an increasing or decreasing shielding referred to an arbitrary standard. The latter system comes from the common practice in ^1H and ^{13}C NMR spectroscopy as well as from some general recommendations. We feel, however, that the best way to avoid confusion is to use precisely defined physical quantities or constants. In the case of the so-called chemical shift, one is interested ultimately in changes in the nuclear shielding involved, and it seems reasonable to express results in terms of the latter; this corresponds to assigning

the plus sign to the direction of increasing magnetic shielding of a nucleus.* In order to be completely clear at this point, we shall abandon the term "chemical shift" from now on and express all experimental and theoretical results in terms of *nitrogen shielding* in ppm referred to that in *neat liquid nitromethane* as an *external standard.*

One should also consider the common use of so-called *paramagnetic relaxation reagents* in ^{15}N NMR spectroscopy as a source of perturbation in measurements of nitrogen shielding. The reagents can introduce apparent changes in the shielding through changes in the bulk magnetic susceptibility of solutions, when external standards are employed. Large disturbances of this kind are observed[83] in ^{15}N measurements for nitrobenzenes in the presence of the chromium tris(acetylacetonate), $Cr(acac)_3$, reagent. One can theoretically eliminate such systematic errors by measuring the susceptibility and introducing due corrections, but the reagents can still induce intrinsic changes in the shielding, due to interactions with the molecules investigated. There have been some attempts[84] to resolve such effects for pyridine derivatives and $Cr(acac)_3$, but the technique employed (cylindrical samples, external and internal standards) only reveals that bulk susceptibility effects are significant. Only very recently have such intrinsic shifts induced by relaxation reagents been measured with reasonable accuracy (Table 7) for a variety of molecules, using a high-precision ^{14}N technique and concentric spherical containers for sample and standard in order to eliminate bulk susceptibility effects.[85] The data in Table 7 indicate that $Cr(acac)_3$, the most widely used reagent, does not induce appreciable intrinsic changes in the nitrogen shielding at concentrations that are effective for reducing the relaxation times of nitrogen nuclei. Only in the case of pyridine-type nitrogen atoms can such induced shifts exceed experimental errors from other sources. However, one should be more cautious with chelates of gadolinium, e.g. $Gd(dpm)_3$ which induces appreciable shifts (Table 7) at concentrations approaching 1 : 1000 molar ratio.

Even if we assume that our measurements of nitrogen shielding are accurate from the point of view of the errors considered, there is still a source of apparent discrepancy between results obtained by different techniques which may amount to a few ppm. This comes from the use of external standards and the fact that standards and samples examined generally have different *bulk magnetic susceptibilities* (Table 5). This problem can be evaded by employing concentric spherical sample and standard containers. This can be easily done in ^{14}N NMR spectroscopy, where sample spinning is not necessary; it is much more difficult in ^{15}N NMR, where sample spinning, in order to average field inhomogeneities, is critical from

* Although this is opposite to the frequency scale for chemical shifts it is consistent with the data in references 1 and 2 to which this review refers frequently.

the point of view of the signal/noise ratio. In the latter case it is common practice to use cylindrical sample tubes. The true difference in the shielding between a sample and an external reference is given by the equation

$$(\sigma_{\text{sample}} - \sigma_{\text{ref.}})_{\text{true}} = (\sigma_{\text{sample}} - \sigma_{\text{ref.}})_{\text{observed}} - (\tfrac{4}{3}\pi - \alpha)(\chi_{\text{ref.}} - \chi_{\text{sample}}) \qquad (14)$$

where χ is the corresponding volume magnetic susceptibility (Table 5) and the constant α depends on sample geometry (Table 4). Thus, systematic errors arise when external standards and samples are placed in cylindrical tubes, but even larger discrepancies are predicted between values obtained from measurements on electromagnet systems (external field perpendicular to sample tube) and those on superconducting magnets (external field parallel to sample tube). The deviation from a true shielding in the latter case is twice as large in absolute magnitude and opposite in sign with respect to that in the former case. Thus, even accurate results obtained in electromagnet and superconducting magnet systems can show appreciable differences, up to about 3·5 ppm, as calculated from the values of volume susceptibilities in Table 5 and equation (14). Larger discrepancies can occur when paramagnetic substances are examined; this includes the presence of relaxation reagents. One should be wary also of the fact that the values of α (Table 4) used in equation (14) for cylindrical samples actually refer to infinitely long cylinders. In modern spectrometers, sample tubes of large diameter are commonly used in order to improve sensitivity, particularly in the case of nitrogen nuclei. Such sample tubes and the samples involved can hardly be considered as infinite cylinders, and this can lead to further uncertainties about the bulk susceptibility effects.

If one wants to convert experimental nitrogen shieldings reported in the literature to a common scale, e.g. that based on neat nitromethane as external standard, it is necessary not only to have accurate values of nitrogen shieldings of various standards referred to the primary standard, but also experimental details which can affect the influence of bulk susceptibilities. The apparently simple process of the conversion from a given reference substance (ref. II) to the primary standard (ref. I) is complicated by the fact that either the experimental shift or the conversion constant or both can contain bulk susceptibility effects. All such combinations, and their results, are given in Table 4. In such conversions, we adopt the system of using experimental values, such as they were measured, and refer the reader to Table 4 for the conversion scheme used. Thus, conversion scheme II means that an apparent shielding referred to an arbitrary standard has been added algebraically to the true shielding of the standard referred to neat nitromethane, and that the resulting shielding referred to neat nitromethane contains the effect of the difference between the bulk susceptibilities of the arbitrary standard and the sample for a given spectrometer geometry (field parallel or perpendicular to sample tube). Conversion scheme IV, which is also commonly used, means that two apparent values

have been added algebraically, and that the result contains the effect of the susceptibility difference between neat nitromethane and the sample involved.

From this point of view, the suggestion[4,81] of referring experimental nitrogen shieldings to neat nitromethane and recalculating them to the ammonia standard at 380·2 ppm introduces more confusion than expected. This arises because the latter value was measured in concentric tubes with long axes perpendicular to the external magnetic field, not to speak of the fact that the shielding in NH_3 is quite sensitive to temperature, traces of water, etc. Thus, the use of any fictitious "standard" is not recommended.

The nitrogen shieldings of various standards referred to that of neat nitromethane are given in Table 6. The values in parentheses have been calculated from the data in Tables 4 and 5, and from equation (14). Only the experimental values are used as conversion constants for nitrogen shielding data reported in the literature. The calculated apparent shieldings are given in order to show how bulk susceptibility effects can affect observations under different experimental conditions.

Let us consider an example which should show the apparent discrepancies that may result from bulk susceptibility effects. For neat liquid pyridine at 30 °C, a shielding of $+62{\cdot}03 \pm 0{\cdot}11$ ppm referred to neat nitromethane in concentric spherical sample and standard containers (no bulk susceptibility effects) is reported from precise ^{14}N measurements.[80,85] From ^{15}N measurements[26] in concentric cylindrical tubes with the external field parallel to the tubes, shieldings of $+57{\cdot}3 \pm 0{\cdot}2$ ppm (uncorrected for bulk susceptibility) and 57·7 ppm (corrected) referred to 1 M aqueous DNO_3 are obtained; in addition there is a shielding of +6·2 ppm (uncorrected) for the latter standard referred to neat nitromethane. A simple conversion of these data to the neat nitromethane scale gives +63·5 and +63·9 ppm, respectively. However, the former result corresponds to scheme IV (Table 4), and contains a contribution from the bulk susceptibility difference between nitromethane and pyridine; the other value corresponds to scheme III, and contains a contribution from the bulk susceptibility difference between nitromethane and aqueous DNO_3. If due corrections are calculated from the data in Table 5, a value of $+62{\cdot}5 \pm 0{\cdot}3$ is obtained, practically within the limits of experimental error and isotope effects from the ^{14}N shielding. Almost perfect agreement is obtained if the "true" shielding of 1 M HNO_3 from Table 6 (+4·4 ppm) is used together with the corrected value of +57·7 ppm for pyridine referred to 1 M DNO_3.

IV. EXPERIMENTAL TECHNIQUES

As far as nitrogen NMR studies of liquids, solutions, and gaseous substances are concerned, the spectra of ^{15}N nuclei are obtained almost

exclusively by the pulsed Fourier-transform (PFT) technique, and occasionally by double-resonance methods. The spectra of ^{14}N nuclei are measured by either the continuous-wave method or the PFT technique; double-resonance methods have rather limited application here, since the quadrupolar relaxation of ^{14}N provides an effective mechanism for internal decoupling of ^{14}N from other nuclear spins.

Since it is often important to consider bulk susceptibility effects on nitrogen shielding (see Section III) when external standards are employed, one should have a simple check as to whether the external magnetic field was parallel or perpendicular to the long axis of the sample tube system used in a given experimental report. All spectrometer systems that are equipped with electromagnets have probes where the long sample tube axis is perpendicular to the external field. So far, only iron-core electromagnets have been in common use, which sets an upper limit of ~2·3 T for the field; the corresponding maximum values of resonance frequencies are 7·22 MHz for ^{14}N and 10·15 MHz for ^{15}N. All systems of superconducting magnets, where the long sample axis is always parallel to the direction of the field, generate fields of at least 4·2 T, which corresponds to minimum values of resonance frequencies of 13·0 MHz for ^{14}N and 18·2 MHz for ^{15}N. Thus, it is enough to know the resonance frequency or the field intensity employed in order to determine the relation between the field and the sample axis involved.

A. Pulsed Fourier-transform (PFT) technique

This is the most widely used method in ^{15}N NMR; it has already been discussed thoroughly elsewhere,[1,2,4,88] so only a few important points are raised here. In spite of the very low NMR sensitivity of ^{15}N nuclei, especially at their low (0·36%) natural abundance, the PFT technique has recently extended the scope of applications of ^{15}N NMR spectroscopy to cover large and complicated molecules in reasonably dilute solutions. Numerous examples of this can be found in Sections V and VI. However, the problem of sensitivity is still critical, and measurements of ^{15}N natural abundance spectra are far from being routine in execution.

Usually, in order to improve the signal/noise ratio, proton decoupling is employed in ^{15}N NMR. Since the magnetogyric ratio for ^{15}N is negative, a negative nuclear Overhauser effect (NOE) may operate, which can give an enhancement factor between 1 and −3·93 for short molecular rotation correlation times (extreme narrowing limit). Thus, for the values of the enhancement factor between 1 and −1, a net loss in signal intensity results, and even complete signal nulling can occur.[1] The decisive role in determining the magnitude of the NOE rests with the contribution of the dipole–dipole mechanism to the total relaxation rate of ^{15}N. For longer correlation

times, the limit of the NOE factor moves from −3·93 to +0·88, and the nulling contribution of the dipole–dipole interaction changes accordingly.

There is another source of serious trouble with ^{15}N spectra, that concerning the quite long (up to 100 s) relaxation times for ^{15}N nuclei in atoms that are not directly bonded to hydrogen atoms. Such slow relaxations can require excessively long delays between pulses and prohibitively long accumulation times for a signal to appear in the spectrum.

An unfavourable NOE can be eliminated, at least partly, by the so-called gated decoupling technique (ref. 88, p. 292) where the decoupler is on during the acquisition period (T_a) and is off during the delay period (T_d) between the end of acquisition and the next pulse, as expressed by the equation

$$\frac{\text{NOE}_{\text{gated}}}{\text{NOE}_{\text{continuous}}} = \frac{E_d(1-E_a)}{1-E_dE_a} \tag{15}$$

where $E_a = \exp(-T_a/T_1)$, $E_d = \exp(-T_d/T_1)$, and T_1 is the relaxation time for ^{15}N. However, the effectiveness of this method depends on the ^{15}N relaxation rate.

An inverse gated decoupling technique[88] can be used when the NOE is favourable, and should be retained if non-decoupled ^{15}N spectra are required. The decoupler is then on during the delay period T_d and is off during the acquisition time T_a. The retained NOE is expressed[88] by the equation

$$\frac{\text{NOE}_{\text{inv.gated}}}{\text{NOE}_{\text{continuous}}} = \frac{1-E_d}{1-E_dE_a} \tag{16}$$

Long relaxation times for ^{15}N nuclei can be substantially reduced by the addition of *paramagnetic relaxation reagents* to the experimental samples. Such reagents should be effective in reducing T_1 values, but simultaneously they should not produce significant signal broadening or induce significant changes in nitrogen shielding. One can divide relaxation reagents[89] into non-specific and specific (spin labels), from the point of view of whether they interact specifically with certain molecular sites. For general use, non-specific reagents are recommended, and the most popular one is $Cr(acac)_3$.[1,4,85,89] It has been argued[89] that, since Cr(III) is coordinatively saturated in $Cr(acac)_3$, the reagent should act via the outer-sphere relaxation mechanism; thus it should display only weak specificity towards acidic protons owing to possible hydrogen-bonding to its carbonyl groups. However, the recently measured[85] induced changes in nitrogen shieldings by $Cr(acac)_3$ reveal a weak specificity towards basic nitrogen sites, such as that in pyridine (Section III and Table 7). Needless to say, the reagent can

apparently influence nitrogen shieldings through bulk susceptibility effects (Section III). A specific (spin-label) relaxation reagent has been suggested recently;[89] it is Gd(III)tris(dipivaloylmethanate), $Gd(dpm)_3$, which is shown to be effective as a spin label specific to basic sites. This appears[89] to be due to the expansion of the coordination sphere of the lanthanide ion in such octahedral complexes. One should remember, however, that such gadolinium chelates are potent shift reagents[85] and can induce appreciable changes in nitrogen shieldings when their concentration approaches a 1 : 1000 molar ratio with respect to the molecules investigated (Section III). Such reagents should obviously give rise to considerable bulk susceptibility effects. The reagents considered can be applied in non-aqueous solutions, but recently $Gd(2:2:1)^{3+}$ cryptate has been suggested as a shiftless relaxation reagent for aqueous solutions.[90] An addition of $1{\cdot}6\times10^{-3}$ M of the cryptate to aqueous formamide results in a threefold decrease in the ^{15}N T_1 value, without any observed change in nitrogen shielding. However, since no measurements of the bulk susceptibility changes upon addition of the reagent were made, the lack of variation in the nitrogen shielding may result from the cancellation of opposing effects; thus further studies would be advisable.

Methods for NMR signal enhancement, based on the PFT technique with spin-polarization transfer in solid samples, have been known for some time (ref. 88, p. 342). Recently, significant ^{15}N enhancements in liquid samples were reported[91,93,95] using the *J cross-polarization* (*JCP*) technique which transfers spin polarization from e.g. protons to ^{15}N via the scalar couplings between the nuclear spins involved, e.g. $J(^{15}N-^{1}H)$. Theoretically, one can expect an enhancement of $\gamma(^{1}H)/\gamma(^{15}N) = 9{\cdot}9$ divided by the NOE enhancement factor inherent in the experiment. Such gains in ^{15}N signal intensity are actually observed[91] for NH_4Cl in acidified H_2O, methylammonium chloride in HCl/H_2O, neat liquid formamide, neat liquid pyridine, and aqueous ε-caprolactam. This method looks very attractive from the point of view of sensitivity in ^{15}N NMR, but it puts stringent requirements on spectrometer systems. Further gains in sensitivity can be expected within this method, since one may take advantage of the shorter relaxation times of protons and thus much faster pulse repetition rates.[91] One should notice, however, that in JCP experiments the cross-polarization time (τ) must be adjusted to a spin–spin coupling constant (J), since the polarization transfer involved depends on terms involving $\sin^2(A\tau J)$ where A is a constant. Thus, individual values of the cross-polarization time must be adjusted to individual ^{15}N signals. When coupling constants are of interest in a JCP spectrum, some complications arise because of phase shifts in multiplet components in such a spectrum. This can be dealt with using a modified, phase-corrected JCP technique[92] which has been tested on the ^{15}N spectrum of aqueous NH_4Cl.

As far as ^{14}N NMR spectra are concerned, the PFT technique has some evident disadvantages. The quadrupolar relaxation times of ^{14}N nuclei can cover three or four orders of magnitude, even in a single molecule; so do the corresponding signal widths. One can optimize the PFT technique only for a limited range of relaxation times (ref. 1, p. 147, and references therein); this can result in a complete loss or broadening of signals that have widths outside this range. Moreover, the free induction decay (FID) is fast for rapidly relaxing ^{14}N nuclei; since some of the FID has to be truncated in order to prevent pulse breakthrough, signal quenching occurs which increases with an increase in signal width. One can employ refocussing techniques (ref. 87, p. 129) in order to recover such broad signals, but the refocussing can be done only for a narrow range of relaxation rates (and signal widths). Consequently, one can only shift the minimum quenching range to some arbitrary signal width. Another aspect is that traces of pulse breakthrough can significantly influence the base-line of the spectrum measured, and make difficult (if not impossible) any reasonable lineshape fitting in order to obtain accurate results for nitrogen shieldings. Thus, the PFT technique is applicable mostly to collections of ^{14}N signals of comparable width or to cases where only one resonance is observed. However, in common practice one has to deal with a sharp ^{14}N signal of the reference used (e.g. nitromethane) and other signals of quite different widths from the sample examined.

B. Continuous-wave method

This method is currently used in ^{14}N but not in ^{15}N NMR. The most attractive variation thereof seems to be the differential saturation technique[1,80,85] which involves audiofrequency modulation of the external magnetic field in order to generate sidebands in addition to the central band spectrum. By adjusting the modulation index, one can introduce large differences between the effective radiofrequency-oscillating field (B_1) which gives rise to the central band and that responsible for the appearance of the sidebands. Thus, different saturation levels are observed within a single spectrum, which enables one to optimize sharp ^{14}N signals in the sidebands and broad signals in the central band. Lineshape fitting of theoretical spectral curves to such experimental spectra can give a precision of better than 0·1 ppm even for broad signals or complicated, overlapping spectra. In a recent modification of this method[85] a full theoretical expression for the lineshape was applied in the lineshape fitting procedure. This allows one to include in the set of variables fitted (in addition to nitrogen shieldings) signal widths, intensities, and base-line parameters, also a number of experimental parameters such as radiofrequency and audiofrequency phase angles, radiofrequency field intensity, and the modulation index. The

general lineshape function used for the least-squares fitting procedure is

$$F(\nu) = A + B\nu + \sum_n I^{(i)}(\nu) \tag{17}$$

where A and B are the parameters of the background line, n is the number of non-equivalent nuclei involved, and the I terms are given by

$$\begin{aligned} I^{(i)}(\nu) = {} & J_0 J_1 \gamma B_1 M_0^{(i)} \\ & \times \Bigg[\frac{b^{(i)}[\cos(\rho-\alpha)-\cos(\rho+\alpha)]+[\sin(\rho-\alpha)+\sin(\rho+\alpha)](\nu-\nu_i)}{(b^{(i)})^2+(\nu-\nu_i)^2+\gamma^2 B_1^2 J_0^2} \\ & - \frac{b^{(i)}\cos(\rho-\alpha)+(\nu-\nu_i-\nu_{mod})\sin(\rho-\alpha)}{(b^{(i)})^2+(\nu-\nu_i-\nu_{mod})^2+\gamma^2 B_1^2 J_1^2} \\ & + \frac{b^{(i)}\cos(\rho+\alpha)-(\nu-\nu_i+\nu_{mod})\sin(\rho+\alpha)}{(b^{(i)})^2+(\nu-\nu_i+\nu_{mod})^2+\gamma^2 B_1^2 J_1^2} \\ & - \frac{J_2}{J_0}\frac{b^{(i)}\cos(\rho+\alpha)-(\nu-\nu_i-\nu_{mod})\sin(\rho+\alpha)}{(b^{(i)})^2+(\nu-\nu_i-\nu_{mod})^2+\gamma^2 B_1^2 J_1^2} \\ & + \frac{J_2}{J_0}\frac{b^{(i)}\cos(\rho-\alpha)+(\nu-\nu_i+\nu_{mod})\sin(\rho-\alpha)}{(b^{(i)})^2+(\nu-\nu_i+\nu_{mod})^2+\gamma^2 B_1^2 J_1^2} \Bigg] \end{aligned} \tag{18}$$

where ν is the measured frequency, ν_i is the resonance frequency of nucleus i, ν_{mod} is the modulation frequency, ρ and α are the corresponding phase angles for the modulation and radiofrequency respectively, $b^{(i)} = 1/(2\pi T_2^{(i)})$ for nucleus i, $\gamma = \gamma/2\pi$, and the J's are the Bessel functions (of the first kind) of the modulation index $\beta = B_{mod}/\nu_{mod}$.

Such a procedure yields not only nitrogen shieldings but also quadrupolar relaxation times for individual nuclei, as well as the relative numbers of nuclei corresponding to individual signals.

Usually spectrum accumulation needs to be carried out in order to improve the signal/noise ratio; thus the sweep rates used require careful consideration. Since the relaxation times involved are rather short (for the sharp signal of nitromethane, T_1 is of the order of 0·03 s), high sweep rates can be employed. Equations (17) and (18) refer to steady-state spectra, but experimentally sweep rates of about 200 Hz s^{-1} are used without any significant deviation of the observed spectra from the lineshape described by equations (17) and (18).

In principle one could consider the application of so-called *correlation spectroscopy* to ^{14}N NMR spectra. This method employs very fast sweep rates which result in the appearance of transient effects in a spectrum, and a deconvolution of such spectra into those corresponding to the steady-state

condition (ref. 88, p. 78). However, this can be simply done only in the case of a linear response of the nuclei; this therefore excludes spectral conditions where the resonance signals can be saturated. Thus, the differential saturation technique cannot be employed within this procedure.

C. Double-resonance methods

These are used most simply and effectively for measurements of ^{15}N shieldings from the proton spectra of ^{15}N-labelled compounds. A necessary prerequisite for the application of such methods is a measurable coupling between ^{1}H and ^{15}N. Advantage is thus taken of the much higher sensitivity of proton NMR measurements as compared with those of ^{15}N NMR.

Recently, however, double-resonance methods based on the observation of very weak ^{15}N satellites in the proton spectra of compounds containing ^{15}N at its natural abundance concentration have been reported.[95,96] Generally, the methods employ the PFT technique for proton spectra with a suppression of the proton signals which arise from molecules containing ^{14}N, and a series of decoupling experiments on the ^{15}N satellites. The entire procedure can be incorporated into a proper pulse sequence[95] within a two-dimensional system which, after transformation, can yield a ^{15}N spectrum.

However, such methods do not have general utility. The two-dimensional method, apart from the possibility of generating artifacts, can be quite time-consuming, which may reduce the theoretically expected gain in sensitivity to a negligible level.

Double-resonance methods which involve the decoupling of ^{14}N nuclei are much less accurate, because of the internal decoupling mechanism via the quadrupolar relaxation of ^{14}N.[1,2] It has been shown, however, that the decoupling of ^{14}N can be used in ^{13}C NMR spectra in order to reveal weak ^{15}N satellites and the ^{13}C–^{15}N couplings involved.[97] In some specific cases, where the ^{14}N relaxation is slow (e.g. for simple isocyanides), double-resonance methods can be employed for determining the nitrogen shieldings and signs of coupling constants, as has been demonstrated for ^{14}N-decoupling in ^{13}C spectra.[98]

One should remember that in any consideration of a gain in sensitivity, that may be obtained by double-resonance methods, it is necessary to make allowance for the NOE which can operate in ^{15}N spectra. Usually double-resonance techniques are employed for nitrogen atoms with directly bonded hydrogen atoms, because of the large $^{1}J(^{15}N–^{1}H)$ involved. In such cases the NOE tends to yield a maximum enhancement factor of about 4. Since there is no NOE enhancement in the double-resonance technique, even the theoretical gain for ^{15}N-decoupled proton spectra can be closer to 2 rather than to $\gamma(^{1}H)/\gamma(^{15}N) = 9{\cdot}9$.

D. Measurement of relaxation times

Methods of measuring relaxation times have already been considered in detail elsewhere, for ^{14}N [1,2] as well as for ^{15}N.[4] The important point to note is that there are routine procedures available for measuring ^{15}N relaxation times in most modern spectrometer systems. As far as the relaxation times for ^{14}N nuclei are concerned, the differential saturation technique (Section IV.B) which is used for the accurate measurement of ^{14}N shieldings also gives, routinely, the relaxation rates. These can be used, according to a recent report,[99] as an aid in the nitrogen shielding assignment to individual nuclei in molecules that contain more than one nitrogen atom.

E. Quantitative nitrogen NMR

The problem of determining the relative numbers of nuclei from the corresponding NMR signals is of the utmost importance in applications of NMR spectroscopy. For the differential saturation method and the associated lineshape fitting in ^{14}N NMR, the problem is trivial, apart from errors that may arise from the signal/noise ratio. The procedure automatically yields the relative numbers of ^{14}N nuclei involved, in spite of the fact that the signals observed are usually saturated to various degrees. The situation is certainly non-trivial in PFT ^{15}N NMR spectroscopy. In proton-decoupled spectra, the NOE can, in principle, introduce infinite errors because of the possibility of a complete cancellation of some signals. Long relaxation times for some ^{15}N nuclei can give similar results, since saturation effects in the PFT technique can be complicated (ref. 88, p. 115); the outcome is that, for a fixed acquisition time of the free induction decay, they decrease the peak height of a signal without any effect on the signal width.

The question of quantitative measurements by ^{15}N NMR spectroscopic methods has been considered recently.[100] It is shown that such measurements are critically dependent upon the use of both the gated decoupling technique (in order to suppress the NOE) and effective relaxation reagents which should be non-specific for all molecular sites. However, even such measures do not guarantee quantitative results; the only remedy left is to increase the pulse intervals. It is also noted that even traces of paramagnetic impurities present in the samples examined can make impossible any quantitative analysis, since they may act preferentially on certain molecular structures.

F. Nitrogen NMR in nematic phases

Nitrogen NMR spectra of solutes in liquid crystals may provide information about molecular geometries, nitrogen shieldings and their anisotropies.

For ^{14}N nuclei, they can also yield the quadrupole coupling constants.[72] Since, in the latter case, the quadrupolar interactions are usually predominant and result in large splittings or signal broadening, it is advisable to use weakly orienting media[72] such as poly-γ-benzyl-L-glutamate (PBLG). If the anisotropy of the molecular motion and the temperature dependence of the relaxation times of ^{14}N are examined, it is necessary to use liquid crystals that form the nematic phase within a large range of temperatures.[101] For investigations of the ^{15}N natural abundance spectra of solutes in a nematic phase, it is possible to employ the double-resonance technique (Section IV.C) which suppresses the proton spectra of molecules containing ^{14}N and leaves the weak ^{15}N satellites.[102] The method is especially useful for the determination of direct ^{15}N–^{1}H couplings. Since the splittings observed in the ^{15}N spectra of oriented solutes considerably reduce the sensitivity of such measurements, ^{15}N labelling of molecules may be used profitably.[103]

A judicious use of liquid crystal solvents, those that produce linewidths of the order of 1–2 Hz, has led to the observation of ^{15}N satellites in a normal PFT proton spectrum of acetonitrile.[112]

The isotropic phases of *p*-azoxyanisole (a nematic liquid crystal) and diethyl azoxybenzoate (a smectic-A liquid crystal) have been investigated from the point of view of short-range order fluctuations by means of the lineshapes of the corresponding ^{14}N resonance signals.[113]

G. Solid-state nitrogen NMR

The resonance signals of ^{14}N in solid samples can be obtained by either direct or indirect (double-resonance) methods.[104] A direct method of observation of the ^{14}N resonance in a single-crystal of ammonium hydrogen oxalate,[104] using the PFT technique and proton decoupling, is reported to yield signals with about 300 Hz half-height widths. It is expected that this method will provide access to a variety of phenomena in solids, since the magnetogyric ratio of ^{14}N is low and nitrogen atoms can be considered to be magnetically dilute; therefore the homonuclear dipolar broadenings should be negligible. The linewidths observed, when compared with typical values of ^{14}N quadrupole coupling constants of 10^5–10^6 Hz, should provide good resolution.[104,107]

A separation of the quadrupolar splittings from ^{14}N–proton dipolar splittings is shown[105] to be easily performed using a two-dimensional PFT technique on single-crystals of L-histidine hydrochloride monohydrate for which complicated spectra are observed.

The PFT technique can also be applied to ^{14}N NMR studies of polycrystalline, powdered samples.[106] Recently, an exact theoretical treatment of the ^{14}N spectra of polycrystalline samples was presented.[108] The conventional

continuous-wave method was used, however, for obtaining the ^{15}N spectra of solid, polycrystalline $^{15}N_2$.[109]

The double-quantum cross-polarization technique in the PFT method can be employed profitably for both ^{14}N and ^{15}N NMR spectra of solids, resulting in a considerable gain in sensitivity for ^{15}N[111] and ^{14}N,[110] with a substantial signal narrowing for the latter isotope.[110] A combination of magic-angle spinning and the cross-polarization technique has been used[112] for the detection of the amide and amino moieties in ^{15}N-labelled soybean seeds, pods, and leaves; a resolution of about 10 ppm is achieved in such ^{15}N spectra.

H. Chemically induced dynamic nuclear polarization (CIDNP)

CIDNP effects on signal enhancement (as far as the absolute magnitude is concerned) have been employed in a determination of the mechanism of free-radical generation in the thermal decomposition of azo compounds[114] as shown in Table 9. One should note that the rules for predicting CIDNP effects should make allowance for the negative magnetogyric ratio of ^{15}N if ^{15}N NMR spectra are considered.

V. GENERAL CONSIDERATIONS OF NITROGEN SHIELDING

A. Isotope effects on nitrogen shielding

Thus far, the available data[1] have indicated that there should not be any significant difference between ^{15}N and ^{14}N shieldings. However, more recent data[74] based on a simple and convincing experiment with singly and doubly ^{15}N-labelled -N=N- moieties show that the shieldings for ^{15}N in the $-^{15}N=^{14}N-$ and $-^{15}N=^{15}N-$ isotopomers can differ by 0·1–0·3 ppm (Table 8). The measurement of such differences for mixtures of the isotopically isomeric species is straightforward, since the $-^{15}N=^{15}N-$ moiety in an unsymmetrical molecule gives rise to a spin–spin splitting pattern in the ^{15}N spectrum, owing to ^{15}N–^{15}N coupling across one bond. One may expect that the differences result from the slightly different vibrational levels of the molecules involved (due to a difference of 1 mass unit); therefore effects of the same order of magnitude can be expected in terms of ^{14}N and ^{15}N shielding differences, e.g. by changing from a ^{12}C–^{15}N to a ^{12}C–^{14}N bonding system. Nevertheless, the primary isotope effect between ^{14}N and ^{15}N shieldings seems to be small enough to be considered as insignificant in all but the most precise measurements of nitrogen shielding (Section III).

B. Absolute scale of nitrogen shielding

The question of the estimation of absolute, rather than relative, nitrogen shielding constants has already been discussed.[1] Some attempts have been

made (ref. 1, p. 143, and references therein) to calculate the absolute shieldings for simple molecules like N_2 and NH_3 using the available values of spin–rotational coupling constants. The latter are used in the calculation of the paramagnetic term of the shielding constant, while the diamagnetic term is calculated by other methods (ref. 27 and references therein). However, more recent data[27] on nitrogen shieldings and spin–rotational couplings for NH_3, N_2, HCN, and ClCN, as well as calculations of absolute shieldings,[27] indicate considerable discrepancies between the experimental and calculated relative shieldings of nitrogen nuclei. This can either mean that the calculation of the diamagnetic term is erroneous or that the reported values of the spin–rotational coupling constants contain errors larger than expected.[27] Anyway, it seems that so far there has not been any sound basis for establishing an absolute scale of nitrogen shieldings, in spite of claims to the contrary.[116]

C. Shift reagents in nitrogen NMR

It has already been shown (ref. 1, p. 214; ref. 2, p. 254) that lanthanide chelates can be used for inducing changes in nitrogen shieldings, the changes being characteristic of the various types of bonding available to nitrogen atoms. The most effective nitrogen shift reagents seem to be dysprosium chelates. Recently there have been two attempts at using lanthanide chelates for spectral assignments[115] or increasing the spectral resolution of ^{15}N signals.[244] In the former case, nitrogen shielding assignments to the *N*-oxide moiety and the pyridine-type nitrogen atoms in diazine *N*-oxides (Table 10) are compared with nitrogen shifts induced by $Yb(fod)_3$, where fod is $(CF_3CF_2CF_2COCHCOBu^t)^-$, in order to check whether such induced shifts can be helpful in distinguishing between the two types of nitrogen atom. However, since the reagent is probably bound preferentially to the oxygen atoms of the *N*-oxide moieties, the differentiation is not always clear. The other case (Table 11) is concerned with the use of $Eu(dpm)_3$, where dpm is $(Bu^tCOCHCOBu^t)^-$, and $Dy(fod)_3$ for increasing the relative shielding differences in the ^{15}N spectra of some model polypeptides.[244] The results show that dysprosium chelates are the most effective nitrogen shift reagents, that a ratio of 50 : 1 N/Dy cannot be exceeded because of signal broadening effects, and that shifts up to a maximum of 8 ppm can be induced under conditions of no significant broadening of the ^{15}N resonances. Since the useful range of effects is rather small when these reagents are used, simple solvent effects can be employed in order to increase the spectral resolution for ^{15}N signals of amino-acid residues. Moreover, the shift reagents cannot be employed in acidic solutions or in polar solvents; this further limits their utility in nitrogen NMR studies of peptides and polyamides.[244]

D. Nitrogen shielding assignments

Since nitrogen NMR spectra do not usually reveal spin–spin coupling patterns (because of the fast relaxation rates of ^{14}N nuclei, and because of the commonly used proton-decoupling in ^{15}N spectra), the question of the assignment of nitrogen shieldings is often non-trivial. Even in cases where it is possible to obtain a proton-coupled spectrum in the presence of natural abundance ^{15}N or when the sensitivity problem for the latter is overcome by ^{15}N isotope enrichment, the spin–spin splittings observed can generally be used only for the identification of NH, NH_2, and NH_3 moieties, owing to the large ^{15}N–^{1}H couplings across one bond. Other couplings are less informative, since their magnitudes do not depend clearly on the number of intervening bonds. Some general methods, those that are based on correlations of nitrogen shielding with structure, theoretical calculations, empirical additivity of shielding effects, or specific labelling with isotopes (^{15}N, ^{13}C; the latter can be used for the observation of ^{15}N–^{13}C couplings in ^{15}N spectra) can be employed in numerous cases. Nitrogen shift reagents (Section V.C) can also provide some information about nitrogen shielding assignments.

Recently, ^{14}N signal widths (and the corresponding relaxation times) have been suggested as an aid in the assignment[99] of nitrogen resonance signals within molecules that contain more than one type of nitrogen atom. The method is useful for molecular systems where the structure is rather rigid, without too much freedom for internal rotation. Such systems, which include heteroaromatic rings containing more than one nitrogen atom, pose some difficulties from the point of view of the nitrogen shielding assignments. The method is based on a rough assumption that, within a given rigid molecular structure, differences in rotational correlation times between individual nitrogen atoms do not contribute significantly to the relative relaxation rates of the corresponding ^{14}N nuclei (and the relative ^{14}N signal widths involved). It is also assumed that the order of increasing signal width follows that of the electric field gradients or, more precisely, that of the values of the product given in Table 12. The latter can be estimated from routine semiempirical molecular-orbital calculations, such as INDO (Table 12).

E. General characteristics of the nitrogen shielding range for diamagnetic species

The characteristic spectral ranges for nitrogen shielding in a variety of diamagnetic molecules and ions are presented in Table 13. Generally, the observed pattern is somewhat similar to that for ^{13}C shieldings (for example, ref. 117). The most screened nitrogen nuclei occur in alkylamino type moieties which can be considered as nitrogenous analogues of alkane chains.

At the other extreme the most deshielded nuclei occur in nitroso groups which can be considered as nitrogenous analogues of carbonyl groups. In between, there are nitrogen shieldings for C=N and N=N moieties. The overall correlation reaches even further, since for example both the nitrito group (R–O–N=O) in nitrogen NMR and the carbonyl group (R–O–C(=O)R) in ^{13}C NMR exhibit a considerable shielding increase relative to the nitroso group and the ketone carbonyl group respectively. A strong shielding increase is observed for the nitrogen atoms in aziridines (Table 23) and for the carbon atoms in cyclopropane. Since, however, nitrogen-containing compounds present a larger wealth of structures than those containing C, O, and H only, the analogy is a very rough one and includes only a selection of structures. It should also be noted that the range of nitrogen shieldings (~900 ppm) for diamagnetic molecules is about three times as large as that for carbon shieldings.

F. Alkyl group effects on nitrogen shielding

If an alkyl group is attached to a nitrogen atom which in turn can be a part of almost any molecular or ionic structure, the influence of the alkyl function on the nitrogen shielding can be expressed approximately in terms of the so-called α-, β-, γ-, and, eventually, δ-effects, each of which results from replacing a hydrogen atom with an alkyl group R at the corresponding carbon atom: $N^{\alpha}-C^{\beta}-C^{\gamma}-C^{\delta}$. The α-effect is variable and hardly predictable. The reasons for this are obvious, since replacing an NH structure with an *N*-alkyl moiety must affect hydrogen bonding influences and, possibly, the geometry of the bonds at the nitrogen atom concerned. The β-effect results in a considerable deshielding of the nitrogen nucleus, roughly by 10 ppm per C-β atom. The γ-effect is much smaller and in the direction of shielding; δ-effects can usually be ignored. Thus, the β-effect is primarily responsible for a span of about 30 ppm in nitrogen shieldings for any alkyl-substituted nitrogen moiety, if measurements are made for the same solvent and only one alkyl group is attached directly to the nitrogen atom. If two or more alkyl groups can be bound to the nitrogen atom, the range increases accordingly, as is the case for amines and amides and for ammonium ions. The β-effect is usually quenched with an increase in the number of C-β atoms at the same C-α atom; for example, the differences in nitrogen shielding in the sequence N-Me, N-Et, N-Pr^{i}, N-Bu^{t} tend to decrease. Recently, measurements for *N*-sulphinylamines (Table 131) have shown that the β-effect is reversed for Pr^{i}–N=S=O and Bu^{t}–N=S=O, since the latter compound is characterized by a more shielded nitrogen nucleus than that in the isopropyl derivative. Since there are strong arguments in favour of the "bent" or *syn* structure [1] for the *N*-sulphinylamine moiety,[118] it seems obvious that steric effects are responsible for

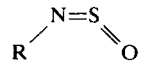

[1]

the observed quenching and reversal of the β-effect. Thus, the β-effect cannot be a result of steric effects. So far, no theoretical explanation of the β-effect has been given. The effect seems to be quite general, not only for nitrogen nuclei. It operates similarly for ^{13}C shieldings[117] and probably for other nuclei too. Since it usually dominates changes in the shielding of alkyl-substituted moieties, a host of linear correlations between the shieldings of alkyl-substituted nitrogen atoms and the ^{13}C shieldings of alkyl-substituted carbon atoms is obtained almost automatically.[119,170–172] There are usually attempts (for example Tables 18 and 50) to construct additivity schemes for alkyl-group effects on nitrogen shielding, by fitting a system of additivity parameters to a set of experimental data. However, there are some points that should be clearly understood as far as such additivity schemes are concerned. If they are simple enough, they provide a means of rough prediction of nitrogen shielding within a group of structurally related molecules. If they are more elaborate, and based on a large set of experimental data measured under uniform conditions, then much better agreement between the calculated and experimental values is usually obtained. However, the predictive value may become, ironically, close to zero. If the experimental set of molecules examined is large, any molecule from outside this set is almost certain to reveal additional effects, for example, an excessive steric hindrance or large departure from the mean geometry or rotamer population. This must result in serious deviations from the calculated values of shielding within the additivity scheme involved. On the other hand, no one would try to reproduce by this scheme any values that are experimentally available. The significance of such fittings of additivity schemes with sets of nitrogen shieldings lies mostly in revealing certain trends and dominating effects. When the internal rotation in molecules is limited, as is the case with alicyclic amines,[119] any attempt at constructing additivity schemes for nitrogen shielding has to include parameters that reflect geometrical factors, e.g. axial or equatorial positions of substituents etc. This must result in a significant complication of the scheme involved, and one should remember that the increasing number of parameters used can quickly bring the situation to a point where the result is equivalent to the absolutely true, and equally trivial, statement that every molecule has its own characteristic shielding.

G. Shielding of nitrogen atoms in conjugated ring systems

If an *N*-methyl moiety is replaced by an *N*-phenyl group, the effect on the nitrogen shielding is variable, but usually deshielding takes place. If

substituents are present in the phenyl ring, their effect on the shielding usually reflects, at least to some degree, their electron-donating or electron-attracting properties, especially when they occupy the *ortho* and *para* positions relative to the nitrogen atom. In most situations, electron-donating substituents induce some shielding of the nitrogen nuclei, while a deshielding is observed as the effect of electron-attracting substituents. This is observed for aniline derivatives (Table 37), phenylimines (Table 128), amides (Table 57), sulphonamides (Table 69), phenylhydrazones (Table 45), and, to some extent, for arylammonium ions (Table 40). Similar effects are reported for nitrogen atoms embedded in a conjugated ring system, such as that of pyridine and related azines (Tables 120 and 121); here the most effective are substituents in positions 2 and 4 relative to the nitrogen atom. However, there are some exceptions where the opposite trend of induced changes is observed, namely in *N*-sulphinylamines (Table 131) and aryl diazonium cations (Table 135), where electron-attracting substituents give rise to increased shielding.

If six-membered conjugated heterocycles are considered, there are rather clear and almost additive effects for the interactions between nitrogen atoms in the relative positions shown in structures [2]–[4] (Table 122). More complicated effects are observed in azoles and related structures (Table 112).

[2]
strong deshielding

[3]
moderate shielding

[4]
moderate deshielding

H. Protonation shifts in nitrogen shielding and related effects

Structural changes which may be described conventionally as those due to the protonation of a lone electron pair on the nitrogen atom considered can give rise to very characteristic changes in the shielding, which are valuable in the estimation of protonation sites. Generally, the four protonation shifts [5]–[8] are observed, from which it is obvious that two effects are in competition. The protonation of a nitrogen atom within a system of

[5] 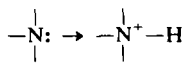

(alkyl amine)

slight deshielding (Table 34)

[6] 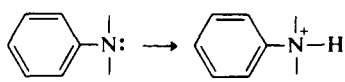

(aryl amine)

variable, usually slight, shielding (Table 40)

[7] 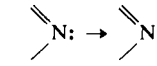 strong shielding (at least 100 ppm)

(including conjugated heterocycles)

[8] $\equiv N: \rightarrow \equiv N^+-H$ strong shielding

saturated bonds results in weak deshielding. In contrast, strong shielding is characteristic of nitrogen atoms in unsaturated systems upon protonation, as is found for the azine ring systems (Tables 122 and 123) and azoles (Table 112), azobenzene (Table 136), imines (Table 128), and nitriles (ref. 2, p. 204).

Analogous changes in shielding occur for *N*-oxides as compared with the parent structures. A deshielding is observed for alkylamine *N*-oxides as compared with the parent amines (ref. 2, p. 184), while shielding effects are found upon the *N*-oxidation of a nitrogen atom within an unsaturated system of bonds. The latter effect is evident if we compare the shieldings for azines (Tables 122 and 124) and their *N*-oxides, for oximes (Table 129) and nitrones (Table 130), for azo and azoxy compounds (Table 136), for nitroso (Table 140) and nitro groups (Table 133), and for nitriles (Table 108) and fulminates (Table 108).

I. Correlations between barriers to internal rotation and nitrogen shieldings

Recently, attempts have been made to find correlations between nitrogen shielding and the barrier to internal rotation in molecules where the possible delocalization of the lone-pair electrons from a nitrogen atom can hinder internal rotation around one of the adjacent bonds.[46,47] Such correlations (Tables 14 and 16) are used for predicting the barriers in molecules for which direct measurements have been either difficult or impossible to perform. However, one should note that the correlations are local, in the sense that they comprise only groups of structurally related molecules. If one wants to predict a barrier to internal rotation from the correlations, the assignment of a given structure to any of the groups can be quite arbitrary. Moreover, such correlations are bound to fail if simple steric hindrance is involved in the determination of the height of the barrier considered. This point has been raised recently,[40] and serious discrepancies are found between the measured barriers for tetramethylurea and tetramethylthiourea (Table 14) and those calculated from the nitrogen shielding. Additionally, rather poor correlations of this type are found for a number of urea derivatives.[42]

There is still another factor to be considered for such correlations. The data in Table 14 refer only to the rotation of the Me_2N moiety; if any other combination of alkyl groups is involved, significant effects on the

nitrogen shielding are expected (Section V.F) which do not have any evident relationship with the delocalization of the lone electron pair and the barriers to internal rotation. Thus, separate correlations are needed for every possible type of dialkyl substitution of the nitrogen atom considered.

J. Solvent effects on nitrogen shielding

The importance of solvent effects on the nitrogen shielding in almost any type of molecular structure has been appreciated only recently, since the modern techniques used in nitrogen NMR have provided a great deal of reasonably accurate data for fairly dilute solutions.

Even if one excludes from consideration protonation effects which may take place in acidic solvents, the range of solvent effects on nitrogen shieldings in a molecule can be comparable to that of substituent effects or other structural modifications. It is therefore important to consider solvent effects in all attempts at finding correlations between shielding and molecular structure, or in applications of such correlations to structural problems in the chemistry of nitrogen-containing compounds.

The nitrogen shielding in some types of molecule reveals a range of a few ppm for solvent effects, even if both aprotic and protic solvents are included. These are amines (Table 24), carbodiimides (Table 55), and diazo compounds (Table 138). Amides and related structures, oximes, and nitroalkanes (Tables 61, 129, and 133, respectively) show a range of 10–15 ppm for solvent effects on the shielding. In nitriles (Table 108) and azole ring systems (Table 112), the range may approach 20 ppm. In pyridine-type ring systems and imines (Tables 122 and 128, respectively), the largest changes are observed, up to 30 ppm. These values are on the cautious side since not always has a sufficient variety of solvents been examined at sufficiently low concentrations of the solutes.

For nitriles (Table 108), imines (Table 128), azoles (Table 112), and pyridine-like systems (Tables 122 and 123), there is a clear indication that hydrogen-bonding of protic solvents via the lone pair electrons on the nitrogen atom gives rise to a considerable shielding of the nucleus involved. Since the effects of hydrogen bonding are in the same direction as the protonation shifts (Section V.H), these must always be considered when estimates of protonation equilibria are made from nitrogen shieldings. An attempt has been made[120] to separate theoretically the effects of hydrogen bonding on the shielding in pyridine from other effects, by means of a linear regression analysis of the shieldings in terms of the Kamlet–Taft parameters which include the polarity of the solvent and its hydrogen-bond donating properties. It is shown that hydrogen-bonding effects account for about 80% of the observed range of nitrogen shielding in pyridine shown in Table 120.

Recently, it has been demonstrated for the nitrogen shielding in nitroalkanes (Table 133 and Section VI.W) that the effect of the polarity of the solvent used can be significant.[121] The entire range, of about 9 ppm, of solvent effects on the nitrogen shielding of nitromethane and other simple nitroalkanes is reproduced quantitatively by theoretical calculations within the solvaton approximation[25,121] which explicitly includes the dielectric constant of the solvent used. The solvaton model[122] represents the oriented solvent distribution around each atom in the solute molecule. It is assumed that, at infinite dilution of the solute, a number of charges (solvatons) are induced in the solvent, that associated with each atom of the solute molecule is a "solvaton" whose charge is equal in magnitude but opposite in sign to that of the atom with which it is associated, that there are no interactions between solvatons, and that the strength of the molecule–solvaton interaction depends upon the polarity of the solvent as expressed by its dielectric constant. Within this framework INDO/S calculations are carried out[122] to yield the nitrogen shielding according to the SOS procedure given by equations (2) and (3).

The latter results seem to be important from the point of view of monitoring changes in electron distribution, effected by changing the polarity of the medium, by nitrogen shieldings. Needless to say, any serious investigation of solvent effects on shieldings must be based on measurements that eliminate bulk susceptibility effects (Section III).

VI. NITROGEN SHIELDING IN VARIOUS CLASSES OF MOLECULE

A. Alkylamines and alkylammonium ions

The nitrogen nuclei in alkylamines are the most shielded among those occurring in diamagnetic molecules (Table 13). Recently, a considerable amount of data has been reported for this group of compounds (Tables 17–24). The shieldings in alkylamines with non-cyclic structures can be expressed in terms of the additivity of the effects of the β- and γ-carbon atoms (also Section V.F), as shown in Table 18 for solutions in cyclohexane and in MeOH. There is a considerable effect (*ca.* −20 ppm) on introducing the first β-carbon atom in primary (RNH_2) and secondary (R_2NH) amines; the second and third β-effects (those due to introducing further β-carbon atoms at the same C) are quenched consecutively by a few ppm each, which corresponds to the "branching" increments in Table 18. In tertiary amines (R_3N) the first β-effect is much smaller and the quenching is even more pronounced. Obviously, steric effects are involved and they tend to counteract the deshielding effect of β-carbon atoms. The introduction of γ-carbon atoms (the γ-effect) results in a slight shielding of the nitrogen

nuclei, but the mean values given in Table 18 cover small and variable effects which are of the order of magnitude of solvent effects on the shielding in alkylamines (Table 24), so any attempt at a detailed interpretation thereof can be premature.

Linear correlations between the nitrogen shieldings in alkylamines and the ^{13}C shifts of the corresponding carbon atoms in analogous alkane structures have been reported[119] separately for primary, secondary, and tertiary amines. Such correlations, as well as the additivity schemes considered above, show a deterioration upon passing from primary to secondary and then to tertiary amines. This is expected (see comments in Section V.F) since steric hindrance and deviations from an average geometry should be significant in considerably branched structures of secondary and especially tertiary alkylamines.

Solvent effects on the nitrogen shielding in alkylamines (Table 24) are only a few ppm and rather irregular. It seems that hydrogen-bonding generally results in a deshielding of the nitrogen nuclei in alkylamines, but various other effects of the same order of absolute magnitude must be in operation. This is in accord with the early investigations of solvent effects on the shielding in ammonia and trimethylamine (ref. 2, p. 247, and references therein).

The protonation of non-cyclic alkylamines to yield the corresponding alkylammonium ions (Table 34) seems to result in a deshielding of the nitrogen nuclei. The effect is not very large, up to −15 ppm when solutions in MeOH are involved. However, steric effects are also important, such that for diisopropylamine a positive (shielding) protonation shift is observed (Table 34). The nitrogen shieldings in alkylammonium ions can be fitted into an additivity scheme (Table 18) which is analogous to those found for alkylamines. One should note, however, that recent investigations have revealed a significant dependence of the shielding in alkylammonium ions on solvent, concentration, and counterion (Table 36). It is evident that the effects of ion aggregation can considerably influence the shielding, not to speak of the position of the protonation equilibrium involved. Thus, caution is advisable in the interpretation of protonation shifts.

For cyclic alkylamines, the situation is more complicated because of hindered internal rotation and possible ring strain effects. For non-strained ring systems, the nitrogen shielding does not depend appreciably on the ring size (Tables 19 and 21). The effect of the alkyl group in *N*-alkyl derivatives (Table 19) seems to be analogous to that in non-cyclic alkylamines. Linear correlations are found between the nitrogen shielding in piperidine and decahydroquinoline derivatives and the ^{13}C shifts of the corresponding cycloalkane carbon atoms.[127] However, some large deviations are observed which appear to arise in some molecules on account of the arrangement of the substituent group R in the NR moiety (or the

lone pair electron orbital) relative to the C–C bonds in the ring. The general structures [9] and [10] can be considered. If R = H, there is little difference in the nitrogen shielding between structures [9] and [10],[127,130] as shown in Table 20 [particularly data corresponding to note (d)]. If R = alkyl or another hydrocarbon chain, the structure with the lone pair antiperiplanar to the nearest C–C bond seems to give a strong shielding effect. This is most evident for quinuclidine (Table 20) where the nitrogen nucleus shows a shielding increase of ~40 ppm when compared with triethylamine (Et_3N) (Table 17). The effect of methyl substituents in the ring on the nitrogen shielding of piperidine and *N*-methylpiperidine (Table 22) is most pronounced when the methyl groups are in the 2- or 6-positions. This is predictable since the observed deshielding represents the well known β-effect; one should note, however, that the configuration of the substituents also has a significant effect.

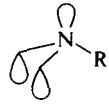

[9]

nitrogen lone-pair orbital is antiperiplanar to bonding C–C orbitals

[10]

nitrogen lone-pair orbital is antiperiplanar to bonding C–H orbitals

The protonation shifts of nitrogen shieldings for cyclic saturated amines are even more complicated than those for non-cyclic alkylamines. Generally, a slight deshielding is observed (Table 35), but numerous exceptions are found. Linear correlations with the corresponding ^{13}C shifts of cycloalkanes have been reported[133] and the additivity of effects of methyl substituents in various positions of the ring postulated.[133] Nonetheless recent results[82] on the influence of solvents, concentrations, and counterions (Table 36) on the shielding of cyclic ammonium ions suggest that caution is necessary in the interpretation of protonation shifts for any type of ammonium ion.

If we consider now the nitrogen shielding of cyclic amines where a considerable ring strain is expected, that is the three-membered ring system of aziridine and the four-membered ring system of azetidine (Tables 21 and 23), it is evident that the nitrogen nuclei involved are more shielded than those in the corresponding open-chain structures or any other cyclic structure. Generally, the effects of alkyl groups R in the NR moieties are analogous to those observed for other amines, with the exception of *N*-t-butylazetidine where the last β-effect results in shielding rather than deshielding. However, the concentrations used (as high as 4–5 M in $CDCl_3$) do not allow one to exclude intermolecular effects as a possible source of

the latter apparent shielding. There is a rough correlation between the nitrogen shielding in substituted aziridines and the ^{13}C shifts of the corresponding carbon atoms in cyclopropanes.[131] Additionally, the same general features, e.g. the β- and γ-effects, are observed. Attempts have been made to rationalize the nitrogen shielding of 2-phenyl-substituted aziridines (Table 23) in terms of conjugation between the phenyl ring and the aziridine ring,[131] but the arguments are based on an assumed perfect additivity of the effects of substituents and then on deviations therefrom. It seems, however, that without a study of solvent and concentration effects on the nitrogen shielding in aziridine systems, such arguments are not convincing. One should also be cautious in the use of chloroform as solvent for amines, since most amines react with it during the time required to obtain natural-abundance ^{15}N NMR spectra.[82]

Recently, an attempt has been made to determine the prevailing rotamers in diastereomeric 2,3-diamino- and 2-hydroxy-3-amino-butanes[134] on the basis of carbon and nitrogen shieldings and relaxation times. The nitrogen shielding data (recalculated to the nitromethane scale according to Table 6 from the original reference, saturated aqueous NH_4NO_3, by the conversion scheme II in Table 4) are:

$MeCHOHCHNH_2Me$	*erythro* *threo*	+348·1 ppm +346·8 ppm	(neat liquid)
$MeCHOHCH(NH_3^+)Me$	*erythro* *threo*	+337·0 ppm +336·3 ppm	(in H_2O)
$MeCH(NH_2)CH(NH_2)Me$	*meso* racemic	+346·9 ppm +346·1 ppm	(neat liquid)
$MeCH(NH_3^+)CH(NH_3^+)Me$	*meso* racemic	+336·7 ppm +336·2 ppm	(in H_2O)

which do not show any significant differences between the diastereomeric molecules involved. This is used as an argument against the *gauche* orientation between the OH and NH_2 groups (or two NH_2 groups) in the *threo* (or racemic) isomer.

B. Enamines and enaminoketones

The conjugation of the lone pair electrons of an amino group with an unsaturated system of bonds, as in enamines $R_2N–C(R)=CR_2$, results in a deshielding of the nitrogen nuclei involved (Tables 13, 26, and 27) when compared with analogous alkylamines. The effect is even more pronounced in enaminoketones $R_2N–C(R)=C(R)–C(=O)R$, which can be considered as amide vinylogues. The deshielding effect is largely reduced when there is some steric hindrance to a coplanar conformation of the amino moiety NR_2 and the double-bond system (Table 26).

A reasonably linear correlation is found[41] between the differences in nitrogen shielding for enamine–alkylamine pairs and the free enthalpy of activation of restricted rotation around the N–C(=C) bonds in enamines and enaminoketones. In a similar approach[40] the shieldings in enamines and enaminoketones are shown to fall into a linear correlation, together with those for amides, with the Arrhenius activation energies for internal rotation (Table 14). However, there are some limitations as far as such correlations are concerned (Section V.I).

C. Amino groups bound to elements other than carbon

If the carbon atom in the C–NR_2 moiety is replaced by that of another element, the effect on the nitrogen shielding can vary from nothing to a considerable reduction (Tables 25, 28–31). If silicon or phosphorus atoms are involved, there is little change from the shieldings in the analogous alkylamines, but the pattern of the shieldings is somewhat irregular from the point of view of correlation with structure. Large deshieldings are observed when Br, Cl, and especially F atoms are directly bonded to the amino group or when they are bound to the phosphorus atom in aminophosphines.

The silatrane structures (Table 29), where the nitrogen atom should be involved in dative bonding with the silicon atom, are characterized by a rather narrow range of nitrogen shielding values. However, the small variations in the shielding upon changing the R substituent on the silicon atom (Table 29) are explained[139] in terms of the Taft constants of the substituents:

$$\sigma_N(\text{ref. to } MeNO_2) = 356{\cdot}8 - 3{\cdot}54(\text{Taft constant})_R \qquad (19)$$

with a standard deviation of ±0·56 ppm and the correlation coefficient $r = 0{\cdot}989$, for dilute solutions in $CDCl_3$ [Table 29; data corresponding to note (a)]. For more concentrated solutions in acetone [Table 29; data corresponding to note (b)], a similar correlation is obtained:[124]

$$\sigma_N(\text{ref. to } MeNO_2) = 357{\cdot}35 - 3{\cdot}33(\text{Taft constant})_R \qquad (20)$$

with a standard deviation of ±1·28 ppm and $r = 0{\cdot}973$. These correlations can be considered as proof of the existence of the transannular bond between N and Si in silatranes, since otherwise the R substituent would be too far from the nitrogen to exert any significant inductive effect on it. For substituted silatranes with R = Me, $CH{=}CH_2$, Ph, and CH_2Cl, correlations are obtained[124] between the nitrogen shielding and calculated dipole moments of the N → Si bond. The moments are calculated from the differences between the measured moment for a given silatrane and the

sum of the moments for $RSi(OEt)_3$ and NEt_3. The resulting correlation is found to be:

$$\sigma_N(\text{ref. to } MeNO_2) = 368{\cdot}4 - 3{\cdot}62\mu(N \rightarrow Si) \quad (21)$$

with a standard deviation of ±0·94 ppm and $r = 0{\cdot}994$. Another approach[124] involves the differences between the experimental dipole moments for silatranes and those from standard values of bond moments (C–O 0·8 D; Si–O 1·54; C–N 0·5; Si–C 1·2; C–H 0·3) and from X-ray geometries. This gives

$$\sigma_N(\text{ref. to } MeNO_2) = 361{\cdot}1 - 2{\cdot}51\mu(N \rightarrow Si) \quad (22)$$

with a standard deviation of ±1·0 ppm and $r = 0{\cdot}940$.

The stannatrane structure [Table 29, note (c)] gives rise to two ^{15}N resonances, each flanked by satellites due to ^{119}Sn–^{15}N and ^{117}Sn–^{15}N couplings. The non-equivalence of the shieldings is explained in terms of a trimeric structure with two equivalent and one non-equivalent nitrogen atoms,[140] since the intensities involved are approximately 2 : 1; the more shielded nitrogen nuclei (Table 29) should be those in the terminal stannatrane moieties.

The nitrogen nuclei in silylamines (R_3Si–NR_2) (Table 28) seem to be more shielded than those in the analogous alkylamines (R_3C–NR_2)[137] but the conclusion that the $SiMe_3$ group exerts a positive inductive effect since it produces more shielding in comparison with the t-butyl group[137] seems to be based on a misunderstanding of the β-effects concerned. The β-effect (Section V.F) which results in a deshielding of the nitrogen nucleus in a R_3C–N moiety when the R's are changed from H atoms to C atoms is known[1,2] to act usually in the opposite direction to that produced by introducing electronegative substituents R. Thus, the increasingly positive inductive effect in such moieties seems to result in a deshielding rather than shielding of the nitrogen nuclei. In silylamines, additional complicating factors can affect the nitrogen shielding, since there is the possibility of so-called (p–d)π back-bonding between N and Si.[44,137] Such effects can depend critically on a large number of structural details of a molecule, which can explain the lack of regularity in the nitrogen shielding in silylamines. On the other hand, the alkyl groups, which are bonded directly to the nitrogen atom in Me_3Si–NR_2, reveal typical effects on the shielding which are described in Section V.F.

The small amount of data available for stannylamines (R_3SnNR_2) indicates that the nitrogen nuclei are generally more shielded than in the corresponding silylamines (Table 25).

The phosphoramidate structures R_2N–$P(O)(OMe)_2$ derived from cyclic saturated amines (Tables 21 and 30) show a slight deshielding of the nitrogen nuclei when compared with the latter; otherwise the shieldings

parallel those in saturated amines. Similar effects are observed for the nitrogen atoms in the dialkylamino groups in 1,2,3-diazaphospholanes [Table 30; data corresponding to note (h)].

The nitrogen shielding in aminophosphines (Table 30) tends to decrease with an increase in the number of Cl atoms on the P atom, and with an increasing number of phosphinyl groups on the nitrogen atom, but the overall pattern is complicated. This is probably due to (p–p)π interactions between P and N,[141] as well as to intermolecular effects (the data refer to neat liquids or concentrated solutions).

In aminoboranes R_2B–NR_2, the shielding seems to be reduced, in comparison with alkylamines, owing to the delocalization of the nitrogen lone pair towards the boron (ref. 1, p. 163, and references therein). Such effects should be more pronounced in cases where the delocalization can be extended over a larger conjugated system. This is actually shown[148] to be the case for aminoboranes which contain alkyne groups attached to the boron atom (Table 31).

D. Amino-sugars and related structures

The amino groups of amino-sugars are usually examined as the corresponding ammonium groups (in hydrochlorides) or amido groups (in *N*-acetyl derivatives). The distinction between these two moieties is straightforward from the point of view of nitrogen shielding (Table 32) since the amido groups show a considerable deshielding of their nitrogen nuclei when compared to ammonium ions (Table 13). Some attempts have been made to explain the rather small differences in shielding between the α- and β-anomers of amino-sugars[149] in terms of steric effects, mostly those of the *gauche* orientation of vicinal amino and hydroxy groups, but it seems that other effects are also important. In most cases (Table 32), the α/β anomer ratio determined from proton NMR is reproduced reasonably well by the relative peak heights in ^{15}N NMR.

If the 2-NH_2 group in an aminopyranose (Table 32) is in the equatorial position, there are two *gauche* relations thereof with respect to the two vicinal OH groups (those in positions 1 and 3) in both of the anomers, and the corresponding nitrogen shielding difference is small.[149,153] If the 2-NH_2 group is axial, as in the mannopyranose derivative (Table 32), there are two *gauche* relations in the α-anomer and only one in the β-anomer. The resulting difference in nitrogen shielding is then much larger, about 10 ppm, the β-anomer amino group being more shielded. Thus, it seems that such *gauche*-type interactions can largely offset differences in shielding between axial and equatorial amino groups in pyranose derivatives,[153] as observed for the α-anomers of glucopyranose and mannopyranose derivatives (Table 32). Generally, however, equatorial amino groups (or their derivatives)

show some deshielding in comparison with the axial groups. Additionally, the α-anomers are characterized by less shielding than the β-anomers.[150]

The shieldings of the amino/ammonium groups in components of the nebramycin complex of aminoglycoside antibiotics (Table 33) have been assigned on the basis of structural comparisons and the titration curves of both ^{15}N and ^{13}C shieldings.[151,152] The latter curves yield pK_a values for individual amino groups (Table 33). Usually, titration curves of nitrogen shieldings offer a formidable means of insight into properties of amino groups in complicated molecular systems, and they are superior in this respect to ^{13}C shift investigations. The case of nebramycin is a good example of this.

E. Arylamines, arylammonium ions, and related structures

Amino groups bound to conjugated ring systems show a deshielding of the nitrogen nuclei when compared with alkylamines (Tables 13, 37–40). The shieldings in arylamines are similar to those found in enamines (Section VI.B). It is quite evident that the deshielding results from the delocalization of the lone pair from the nitrogen atom through the conjugated system, since correlations are found between the nitrogen shieldings in substituted anilines and aminopyridines (Table 16; Section V.I) and the barriers to internal rotation of the amino groups.[47]

A consideration of substituent effects on the shielding in arylamines can be made most simply for aniline and its derivatives (Table 37). Since the range of solvent effects on the shielding in anilines can amount to about 10 ppm (Table 37), and the range of substituent effects is about 30 ppm, any comparison of substituent effects is reasonable only when solutions in the same solvents are considered. It is suggested[155] that the magnitude of substituent effects on the nitrogen shielding in anilines is characteristic of the delocalization of the lone pair electrons of the nitrogen atom. If the lone pair is not delocalized, as in the case of pyridine-type nitrogen atoms, only small effects should be observed. This is quite erroneous, since the comparison is made with the shielding changes in quinoline derivatives containing substituents in the ring that does not contain the nitrogen atom. If pyridine derivatives are considered (Table 120), the range of substituent effects turns out to be about twice as large as that for aniline derivatives.

Generally, electron-donating substituents in positions *ortho* and *para* to the amino group increase the shielding of the amino function whereas electron-attracting substituents in the same positions produce the opposite effect (Table 37). Halogen substituents should be considered separately, since they can act in a way that is a combination of electron attraction

(commonly termed the inductive effect) and electron release (due to the so-called back-bonding effect, which may be depicted as the delocalization of lone-pair electrons through the conjugated system). Their effects for acetone solutions of anilines,[155] according to Table 37, can be compared as follows, where the values are of the shielding effect in ppm relative to the amino nitrogen resonance of aniline:

F	*ortho*	+11·8	*para*	+3·4
Cl		+0·6		+0·5
Br		−4·2		(−1·0, in DMSO)
I		−11·9		−0·7

It seems evident that the back-bonding effect, which should decrease from F to I, plays an important role in determining the nitrogen shielding. The back-bonding effect of a halogen in positions *ortho* or *para* should generate a negative net charge at the carbon atom adjacent to the amino group. Thus it should reduce the delocalization of the lone pair of the latter. This conclusion is corroborated by the shielding effects of F and Cl on the nitrogen nucleus in pyridine (Table 120). However, substituents in the position *ortho* to the amino group can give additional effects owing to steric hindrance, direct interaction of electron charges, etc. The large deshielding produced by the 2-I substituent is probably of such an origin.

Steric effects of alkyl substituents in positions *ortho* to the NMe_2 group in *N,N*-dimethylaniline derivatives seem to result in a strong shielding of the nitrogen nuclei[164] owing to the inhibition of conjugation of the nitrogen lone electron pair (Table 38). However, the experimental techniques used cast doubt on the significance of the reported values (footnote in Table 38); therefore, the reported[164] correlations with carbon shieldings and ionization potentials should be accepted with reservation.

The influence of substituents in position 8 ("*peri*") in 1-naphthylamines (Table 39) seems to arise mainly from steric effects.[83]

The shielding for amino groups attached to pyridine-like heterocycles (Table 39) seems also to display conjugation effects. It is evident that amino groups in position 3 relative to the nitrogen atom in the ring reveal a shielding of about 20–30 ppm with respect to amino groups in positions 2 or 4; in the latter cases, the delocalization of the lone electron pair from the amino group should generate excess charge densities on the ring nitrogen atoms involved. Thus, nitrogen shieldings can simply distinguish between 3-NH_2 groups in pyridines and 5-NH_2 groups in pyrimidine derivatives respectively, and other amino groups in such systems. Since the amino groups in positions 2, 4, or 6 in the pyridine ring (and related azine ring systems) can be involved in tautomeric equilibria, [11] and [12], with

amidine-type systems, and since the amino groups in such systems show much greater shieldings (*ca.* +300 to +340 ppm; Table 39) than those for the =NH or =NR groups in the tautomeric amidines (*ca.* +180 ppm; Table 64), nitrogen NMR can be conveniently used for estimating the equilibrium constants involved.

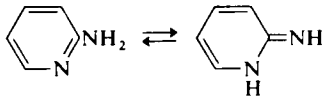

[11]

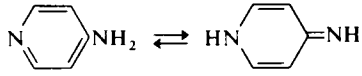

[12]

The protonation shifts of nitrogen shielding upon passing from an arylamine to the corresponding arylammonium ion are more complicated than in the case of alkylamines. Since protonation destroys the conjugation of the electron system of the amino group with the ring, the protonation shifts are likely to depend on the degree of delocalization of the lone pair electrons in the parent amine, as is shown by comparison of the data in Tables 37, 38, and 40. Thus, the largest shielding increases upon protonation are observed for 2-NO_2 and 4-NO_2 substituted anilines, and the smallest effects are found for electron-releasing substituents. One should note, however, that it is difficult to compare sensibly the shieldings in arylamines and their corresponding arylammonium ions if the changes are small, since both are influenced by solvents; the latter show also a dependence on the counterion involved (Tables 36 and 40). If steric hindrance inhibits conjugation in the parent amine (Table 38), protonation can produce a considerable deshielding of the nitrogen nucleus.

It is interesting to compare substituent effects on the nitrogen shielding in anilinium ions (Table 40) with those in aniline derivatives (Table 37). Halogen substituents exert comparable effects in both cases, but the nitro groups in positions 2 or 4 produce a strong deshielding in anilines, while the effect on the nitrogen resonance position in anilinium ions is small and can even result in a slight shielding (2-NO_2 substitution). The nitrogen shieldings in methyl-substituted anilinium ions show a fair correlation with the ^{13}C shieldings of the corresponding methyl groups in the analogous substituted toluenes,[35] but this is not the case with the parent anilines. Obviously, the delocalization effects in the latter do not allow one to compare the NH_2 groups with methyl groups.

Attempts have been made[55] to correlate INDO electron densities with the nitrogen shielding in methyl-substituted anilines and anilinium ions. It seems that the changes in the shielding exerted by methyl substituents (Tables 37 and 40) are too small, in comparison with solvent effects, to be rationalized in terms of theoretical calculations.

F. Amine *N*-oxides

In addition to the small amount of data (ref. 2, p. 186) on the nitrogen shieldings in amine *N*-oxides, we report some unpublished results from our own laboratories (nitrogen shielding in ppm referred to $MeNO_2$):

$Me_3N \rightarrow O$	satd. in acetone (ref. 2)	$+273 \pm 5$
$Et_3N \rightarrow O$	1 : 10 v/v in acetone	$+265 \pm 1$ (^{14}N)
$Me_2(Ph)N \rightarrow O$	1 : 10 v/v in acetone	$+266 \pm 1$ (^{14}N)
$Et_2(Ph)N \rightarrow O$	1 : 10 v/v in acetone	$+249 \pm 1$ (^{14}N)
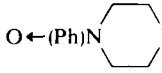	in CD_3OD	+264·1 (^{15}N)

These show that amine *N*-oxides reveal a considerable deshielding of their nitrogen nuclei with respect to the parent amines (Sections VI.A and VI.E) and analogous ammonium ions. The shieldings exhibit the usual β-effect for the ethyl substituents (Section V.F) as compared to the methyl-substituted moieties. The deshielding effect of *N*-oxidation is opposite to those observed for nitrogen atoms involved in unsaturated bonding systems (Section V.H; Tables 124, 130, and 136).

G. Hydrazines, hydroxylamines, hydrazides, hydrazones, and related structures

The nitrogen shieldings of hydrazines R_2N–NR_2 are smaller than those of amines (Tables 13, 41, and 43), but there is some overlap between their ranges of occurrence. Upon substituting one of the nitrogen atoms in H_2N–NH_2 with methyl groups, there appears to be a deshielding of the other nitrogen nucleus (Table 41) which is reminiscent of the β-effect exerted by hydrocarbon moieties (Section V.F). However, the deshielding can result from interactions between molecules, since replacing an NH moiety with an NMe group must significantly affect both solvation and hydrogen bonding influences. Consideration of the nitrogen shielding in Table 43 for tetraalkylhydrazines indicates that in most cases the effect of alkyl groups on the shielding of the nitrogen atom directly attached is comparable to that described in Section V.F.

For hydrazines, there is an additional factor which can complicate the shielding. In sterically unhindered hydrazines, the preferred conformation is such as to render the nitrogen lone-pair orbitals perpendicular to each other;[170] steric interactions or cyclic systems can force deviations therefrom, and these can result in significant interactions between the lone electron pairs. These seem to produce appreciable deshielding of the nitrogen nuclei involved, as can be seen from the data in Table 43. If the nitrogen shieldings for hydrazines are compared with the ^{13}C shifts in hydrocarbons derived

formally from them by replacing N with CH, a linear correlation is obtained[170] for strain-free hydrazines, but marked deviations are observed for all the cyclic hydrazines presented in Table 43. There may also be other factors that complicate the nitrogen shielding in hydrazines, such as flattening of the pyramidal conformation of the bonds at the nitrogen atoms due to the aggregation of bulky alkyl groups.

In bicyclic hydrazines (Table 42), a *trans-trans* double inversion of bond conformation at the nitrogen atoms can be observed in their ^{15}N, ^{13}C, and ^{1}H NMR spectra.[167] The values of the free enthalpies of activation for the inversion obtained by these three spectroscopic techniques show reasonable consistency.

A study[166] of NH proton transfer reactions in phenylhydrazine by means of proton-coupled ^{15}N spectra indicates that the rate of exchange at the NH_2 group in $PhNHNH_2$ is higher by about two orders of magnitude than that for the NH moiety, in all the solvents examined [Table 41; data corresponding to note (c)]. In trifluoroacetic acid, $PhNHNH_2$ seems to be protonated largely at the NH_2 moiety, as indicated by the deshielding for the latter relative to the NH_2 signal position found in other solvents (Table 41). In order to account for the fast proton exchange at NH_2, the dimers [13] are suggested where a simultaneous exchange of protons between the NH_2 groups can occur.[166]

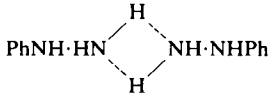

[13]

In hydrazide-type structures $RC(=X)NHNH_2$, where X = O or S, the nitrogen shielding for the C(=X)NH moiety is reduced, when compared with that for hydrazines, and falls within the range characteristic of amides and thioamides (Tables 13 and 41).

The data on the nitrogen shielding in hydroxylamine-type structures R_2N–OR are too few (Table 41) to allow one to draw any definite conclusions but it seems that their range should be similar to that for hydrazines.

Proton exchange reactions have been studied[169] for the three types of nitrogenous moiety that occur in hydrazine-carbothioamide structures [14] and [15], by means of the proton-coupled ^{15}N spectra of basic, neutral,

$H_2NC(=S)NHNH_2$ [14] $MeNHC(=S)NHNH_2$ [15]

and acidic solutions in DMSO. The hydrazino NH_2 group shows the fastest exchange of protons in acidic solutions, followed by the hydrazino NH

moiety; the slowest exchange occurs at the amido NH_2 group. In basic solutions, the exchange at the NH_2 group of the hydrazino moiety is the slowest and that for the hydrazino NH group is the fastest.

The Fischer indole reaction leading to indomethacin (Fig. 3) has been followed by natural-abundance ^{15}N NMR spectra.[168] The ^{15}N resonances characteristic of the starting hydrazide and those of the hydrazido-hydrazone intermediate decay with time, whilst two other signals emerge which are assigned to the amido-immonium intermediate in Fig. 3. This assignment is corroborated by a separate experiment where cyclohexanone is used in the first stage of synthesis; under such conditions, a relatively stable analogous intermediate [16] is formed whose shieldings are similar to those observed in Fig. 3. The reaction is carried out in CD_3COOH/HCl, and therefore protonated species are involved. The shieldings below 200 ppm from nitromethane are in accord with those observed for immonium ions (Table 128).

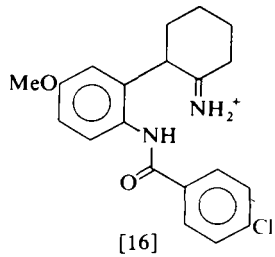

+193·3 ppm (=NH_2^+)
+243·8 ppm (NH)

[16]

The hydrazone-type structure $R_2C{=}N{-}NR_2$ is characterized by quite different shieldings for the =N– and NR_2 moieties (Table 45). The latter are close to those in hydrazines, but the former are smaller by ~250 ppm and fall into the range characteristic of doubly bonded C=N moieties, such as those in imines (Tables 13 and 128). Actually, the =N– shieldings in hydrazones, together with those in imines and related structures, are shown[171] to correlate linearly with the analogous ^{13}C shifts in the corresponding ethylene derivatives. The NR_2 shieldings in hydrazones are smaller by ~50 ppm than those in hydrazines, probably because of some delocalization of the lone pair electrons from the NR_2 moiety through the C=N–NR_2 system. The NMe_2 shieldings in dimethylhydrazones (Table 45) are shown to correlate with the barrier to internal rotation of the NMe_2 group about the N–N bond according to the equation

$$\Delta G^{\ddagger}_{298}(\pm 1{\cdot}7\ \text{kJ mol}^{-1}) = 172{\cdot}0 - 0{\cdot}5(\text{nitrogen shielding of } NMe_2 \text{ relative to } MeNO_2) \quad (23)$$

Equation (23) has been derived for a number of $Me_2N{-}N{=}X$ structures

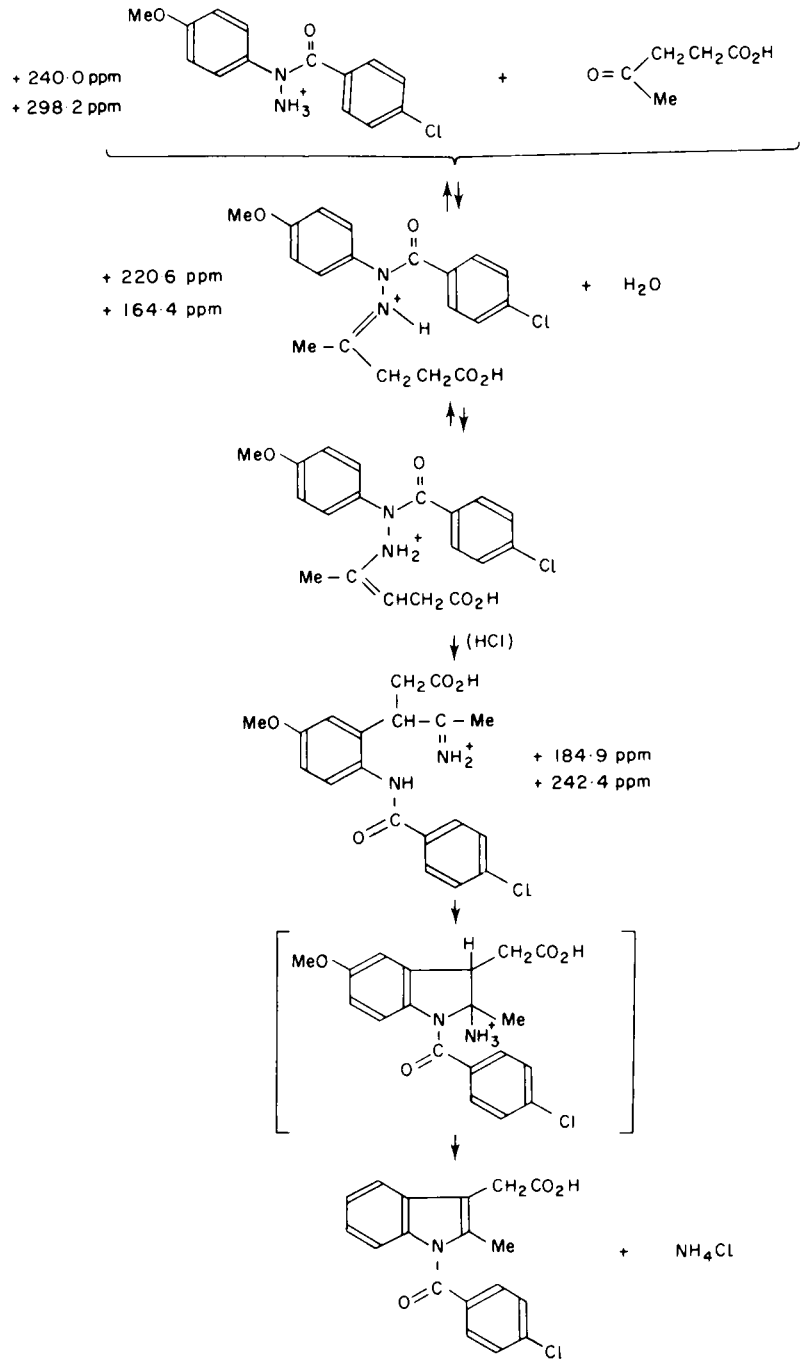

FIG. 3. Fischer indole reaction in the synthesis of indomethacin.

including hydrazones;[45] it is modified here in order to conform to the nitromethane scale of shieldings. An analogous correlation is found for the N–N bond lengths r for Me_2N–N=X structures:

$$r(\pm 0{\cdot}004\ \text{Å}) = 1{\cdot}224 + 0{\cdot}00064(\text{nitrogen shielding of } NMe_2 \text{ relative to } MeNO_2) \quad (24)$$

Thus, the delocalization of the lone pair electrons in hydrazones appears to be reflected rather clearly in the nitrogen shielding. This is corroborated further by the effects on the shieldings in pX·C_6H_4·CH=N–NHPh (Table 45) produced by changing substituent X. Both the =N– and NHPh shieldings show linear correlations with the Hammett constant of the substituent examined.[172]

A number of hydrazido-type complexes (Table 44) show shieldings that are similar to those for hydrazones. This suggests planar structures for the hydrazido ligands, analogous to those of hydrazones.[165]

Dihydrazone structures $R_2C{=}N{-}N{=}CR_2$ are characterized by nitrogen shieldings that are typical of C=N moieties (Tables 13 and 45).

H. Borazines and related ring systems

The borazine structure (Table 46) can be considered formally as that of an aminoborane (Section VI.C). However, the six-membered ring structure with six 2p electrons available for delocalization can reveal aromatic character. This is in accord with the considerable deshielding of the nitrogen nuclei in borazines when compared with alkylamines (Table 13) and simple aminoboranes (ref. 1, p. 159). Alkyl groups attached to the nitrogen atoms in borazines exert typical effects (Section V.F) on the nitrogen shielding. The substituents on the boron atoms appear to affect the nitrogen shielding in a way similar to that observed for conjugated systems such as arylamines (Table 37) and pyridines (Table 120).

I. Ureas, guanidines, and related structures

In structures such as $R_2N{-}C(=X){-}NR_2$, where X = O for ureas and X = NR for guanidines, the lone pair electrons of the NR_2 moieties can be delocalized and render some double-bond character to the C–NR_2 bonds. According to the considerations presented in the preceding subsections on various types of amino groups, the NR_2 moieties in the structures concerned should reveal a deshielding of their nitrogen nuclei when compared with those in alkylamino groups.

The shielding of the NR_2 groups in guanidines (Table 47) is comparable to those observed in enamines (Table 26). In some cases non-equivalence

of the groups is reported which results from the *syn* and *anti* positions relative to the C=NR system of bonds. The imino-type moiety C=N–R shows a deshielding of about 150 ppm relative to the NR_2 moieties (Table 47) but the nitrogen nuclei in the C=N–R fragments of guanidine structures are still shielded, by about 150 ppm, in comparison with those in imines (Tables 13 and 128).

Protonation of the C=NR nitrogen atom in a guanidine, to yield the corresponding guanidinium ion, removes the major structural difference between the C=NR and NR_2 moieties and the difference in shieldings apart from that which results from substituent effects (Table 47). The nitrogen nuclei in guanidinium ions are generally deshielded by a few ppm when compared with those of the amino-type groups of the parent guanidines, but there is a considerable shielding relative to the imino moieties involved.[176] Such protonation shifts of nitrogen shieldings have been used as an argument in favour of the tautomer [17] of aryl-guanidines.[176] The effect of *para* substituents on the phenyl ring of phenyl-guanidines [Table 47; data corresponding to note (f)] on the nitrogen shielding of the corresponding guanidinium ions is comparable to that observed in arylammonium ions (Table 40).

$$(\text{Aryl})\text{–N=C(NH}_2)_2$$

[17]

Proton-coupled ^{15}N spectra can give valuable information about nitrogen shielding assignments for guanidine structures, and about tautomeric forms thereof, provided that the proton exchange is slow and clear multiplet patterns are obtained. Such spectra, taken at the natural abundance level of ^{15}N, provide convincing arguments in favour of the structures shown in Table 47 for sulphaguanidine [note (b)] and amiloride [note (d)]. The same technique has been employed for nitrogen shielding assignments of the guanidinium moieties in streptomycin and dihydrostreptomycin (Table 48). It should be noted that the latter case shows how guanidinium moieties can be distinguished from ammonium moieties by means of their shielding; another example of this is provided by the ^{15}N spectrum of viomycin (Table 83).

The nitrogen shieldings in the guanidino moiety of L-arginine have been investigated within a broad range of pH values[66,174,187] and the results are given in Table 73. The δ-NH shielding is almost independent of pH, but the averaged signal for the remaining part of the guanidino moiety shows an increased shielding of the nitrogen nuclei upon protonation, in accord with the considerations presented above.

The structure of the guanidino moiety in the methyl ester of nitroarginine hydrochloride has been determined[188] on the basis of shieldings and ^{15}N signal multiplets in the proton-coupled ^{15}N NMR spectrum (Table 74).

It is interesting to note that the proton-coupled ^{15}N spectrum of L-arginine[187] shows that the rate of exchange of the protons in the δ-NH group is twice as fast as that for the terminal nitrogen atoms in the guanidino moiety.

In ureas $R_2NC(=O)NR_2$, the more electronegative oxygen atom (as compared with the =NR group in guanidines) should promote the delocalization of the lone pair electron from the NR_2 moieties. This should result in a deshielding of the nitrogen nuclei relative to those in guanidine NR_2 groups. The data in Table 49 show that this is actually the case. However, the shielding in ureas is generally greater than in the related amide-type structures (Tables 13 and 57). They are shown (see Section V.I) to depart significantly from the general correlations between shielding of amide-type structures and the barrier to internal rotation of the NR_2 moieties. The effects of alkyl groups on the nitrogen shielding in ureas can be expressed in terms of additive increments (Table 50); they are essentially the typical effects of alkyl groups described in Section V.F. However, the only significant parameters in Table 50 appear to be those corresponding to the β- and γ-effects, according to the considerations given in Section V.F. The shielding effect on the nitrogen nuclei of methyl groups introduced at the α-positions (Tables 49 and 50) is explained in terms of a decrease in the lone pair delocalization upon substitution,[42] but one should be cautious in making comparisons of the shielding in NH and NMe moieties since solvation and other intermolecular effects can play a significant role.

The proton-coupled ^{15}N spectra of urea, *N*-methylurea, *N,N'*-dimethylurea, *N*-methyl-*N'*-benzylurea, and *N*-methyl-*N'*-phenylurea provide information[180] about proton exchange rates in such molecules. For $MeNHC(=O)NH_2$ in basic aqueous solutions, the rate of exchange at NH_2 is about 3 times faster than at NH, and about 7·5 times faster in acidic solutions. In basic aqueous solutions the exchange in urea is 10 times faster than in $(MeNH)_2C=O$, but it is twice as slow in acidic solutions. For $MeNHC(=O)NHCH_2Ph$, the rates are approximately equal for the two NH moieties in basic DMSO solutions. If HCl is added, the rate of the MeNH moiety shows a four-fold increase. In MeNHC(=O)NHPh in DMSO the rate of MeNH is 50 times higher than of PhNH in basic solutions, but it is about 1000 times slower in acidic solutions.

An interesting application of nitrogen shieldings to sequence analysis of linear polyureas[184] is presented in Table 51 which reveals that there are small but clear changes in the nitrogen shielding with an increase in the number of CH_2 groups in the hydrocarbon bridges. Such small changes are hardly useful for structural analysis of monomeric species, but in polymers dissolved in CF_3COOH intermolecular effects on the shielding are small enough to render differences of the order of 1 ppm significant

for identification purposes. Moreover, the nitrogen shielding, in such circumstances, is sensitive to the neighbouring residues while the ^{13}C carbonyl shieldings are not.[184] It is therefore possible to use the nitrogen shieldings in random copolymers of urea units (Table 51) and diamine units for the identification of sequences thereof in the polymers.

The shielding effect on the nitrogen nuclei of steric crowding is observed for a number of urea derivatives containing cyclopropane rings [Table 49; note (h)].

Carbamate structures $R_2NC(=O)OR$ are characterized by nitrogen shieldings comparable to those found in ureas (Tables 13, 52, and 53). An analogous shielding effect of steric crowding is found (compare Tables 49 and 51) for some *N*-cyclopropyl derivatives of carbamates. Such shielding effects can be useful in the assignment of conformations.

Since arylamines, enamines, ureas, and carbamates are characterized by similar shielding ranges for their nitrogen nuclei (Table 13), it is sometimes difficult to assign nitrogen resonance signals if such structures occur together in complicated molecules. Proton-undecoupled ^{15}N spectra can, in favourable cases, provide some necessary additional information as shown for physostygmine (Table 54).

Ureas [18] are potentially tautomeric with isourea structures [19]. It has already been shown (ref. 1, p. 174) that the shielding of the NR_2 moiety is similar in both structures, but the shielding for the $=NR$ moiety in isourea systems is smaller by about 100 ppm.

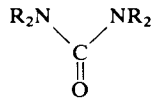

[18]

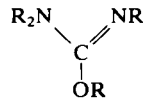

[19]

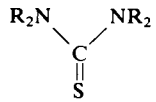

[20]

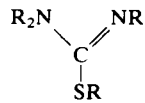

[21]

The nitrogen nuclei in thioureas $R_2NC(=S)NR_2$ are considerably less shielded than those in ureas (Table 68). In other aspects, the shieldings in thioureas resemble those found in ureas in that they are greater than those found in thioamides and amides, respectively. Moreover, the shielding of the NR_2 moiety is almost the same in thioureas [20] and isothioureas [21], while a deshielding by about 180 ppm is observed for the $=NR$ moiety in isothioureas (ref. 1, p. 174). The only example reported of the nitrogen shielding in an isothiouronium cation, $[(Me_2N)_2C]^+SMe$ (Table 68), seems to indicate that the NR_2 groups in such cations should be characterized by only a moderate deshielding of their nitrogen nuclei relative to those in

thioureas. This is similar to the rather small difference in nitrogen shielding observed between guanidine NR_2 groups and guanidinium ions (Table 47).

J. Carbodiimides and derived cations

In carbodiimides RN=C=NR, the nitrogen shieldings observed (Tables 13 and 55) are much greater than those for other structures containing C=N–R moieties, except isocyanates R–N=C=O and isothiocyanates R–N=C=S. In this respect they resemble the rather high shielding of the terminal carbon atoms of allenes $R_2C{=}C{=}CR_2$. Consequently, the nitrogen shielding is not unusual, as suggested in the literature,[189] but rather typical for X=C=Y linear structures. Carbodiimides are isomeric with cyanamides R_2N–C≡N, and the nitrogen shielding data for neat dimethylcyanamide [22][80] show that spectral distinction between the two types of structure is straightforward. The linear N–C≡N structure in cyanamides is also characterized by a rather high nitrogen shielding of the NR_2 moiety (when compared with any other NR_2 group connected to a system of unsaturated bonds) and the CN group (when compared with any other cyano group, Table 108, except in cyanates RO–CN, Table 106). The effect of alkyl groups R in RN=C=NR on the nitrogen shielding seems to follow the usual pattern (described in Section V.F).

Me_2N–C≡N [22] +371·8 ppm (NMe_2); +184·8 ppm (CN)

Alkylation of carbodiimides leads only occasionally to the corresponding carbodiimidium ions $R_2N^+{=}C{=}NR$; usually cyclic dimers are obtained which are clearly distinguished by means of nitrogen NMR spectra (Table 56).

K. Amides, thioamides, sulphonamides, and related structures

The nitrogen nuclei of amides $RC(=O)NR_2$ are more deshielded than those of arylamines, enamines, and ureas (Tables 13, 57–67) when compared with alkylamines. The deshielding most probably originates from the delocalization of the lone pair electrons from the NR_2 groups since it correlates with the height of the barrier to internal rotation of the groups in amide systems (Section V.I). The nitrogen shielding in amides can be significantly solvent-dependent (Table 61). The shieldings for a variety of amides and solvents from Table 61 have been subjected to a factor analysis.[196] The latter provides an indication that at least two factors are responsible for the solvent shifts of the nitrogen shieldings in amides; one is general, probably that concerned with a perturbation of the electronic

states in amides, and the other is specific, probably that concerned with the hydrogen-bonding properties of the NH moieties, where applicable. The importance of the first factor seems to be supported by the fact that the rotation of its eigenvector into a system of physically significant axes is reasonably successful only where the latter involve the solvatochromic shifts observed in the electronic absorption spectra given in Table 61. It should be noted, however, that the shieldings reported in Table 61 have not been corrected for bulk susceptibility effects; these can contribute about 0·7 ppm to the relative changes in the shielding obtained by the technique used. A detailed study on the shielding of *N*-methylacetamide (Table 58) in aqueous solutions shows that little change occurs in the shielding in basic solutions, but there are some significant shifts in acidic solutions. The latter do not necessarily result from the protonation of the oxygen atom in the amide, since even at low pH values the effect is cancelled by the addition of a solute that can compete with hydrogen-bonding of the carbonyl group of the amide.

The effect on the nitrogen shielding of the alkyl groups R in MeC(=O)NHR amides (Table 57) follows the regular pattern described in Section V.F. If R is a *para*-substituted phenyl group, the *para* substituent effects correlate roughly with the Hammett substituent constants,[190] but their magnitudes are much smaller than those found in the case of *p*-substituted anilines (Table 37). This difference is explained as being due to the result of competition between the delocalization of the lone pair through the carbonyl group and the phenyl ring,[190] but it is possible that one should also consider steric effects which can force the phenyl ring out of the plane of the amide system and thus reduce the conjugation of the π-electron systems involved. The nitrogen shielding of MeC(=O)NHR amides, where R = alkyl (Table 57), correlates reasonably well with the π-electron densities at the nitrogen atoms[207] calculated by the CNDO/2 method, but since the data refer to highly concentrated solutions in $CDCl_3$ the agreement may be fortuitous.

Recently, the *E* and *Z* isomers of unsymmetrically *N*-disubstituted amides have been shown[195] to give separate ^{15}N signals (Table 59). The nitrogen shielding difference between the isomers of a given amide is rather small, but dilution studies on aqueous solutions of *N*-methylformamide and *N*-t-butylformamide indicate[195] that the differences are not significantly disturbed upon dilution. This seems to exclude association effects as the source of the variation. If one assumes that the difference in the nitrogen shieldings comes from the difference in the delocalization of the lone pair electrons, one would expect that the nitrogen nuclei in the more abundant isomer would be less shielded. This is only in accord with the data for the first two amides in Table 59; obviously other effects, such as steric hindrance, have to be taken into account.

The protonation of an amide structure results in a considerable deshielding of the nitrogen nucleus, as shown in Table 57 [data corresponding to notes (i) and (j)]. This is in agreement with *O*-protonation which is thought to prevail for amides (ref. 192, and references therein), if we compare the nitrogen shieldings in $HC(=O)NMe_2$ and $Me_2N^+=CH-OMe$ (Table 57).

Amides are potentially tautomeric with isoamide structures. There is an appreciable difference between their nitrogen shieldings, as is shown (Table 57) for [23] and [24] in acetone solutions. The relatively low shielding of the nitrogen in $F_3CC(=O)N(SiMe_3)_2$ (Table 57) is assigned[193] to the existence of the tautomeric equilibrium [25]

$MeC(=O)NMe_2$ +282 ppm [23] $\qquad$ $MeC(OMe)=NMe$ +155 ppm [24]

$$F_3CC(=O)N(SiMe_3)_2 \rightleftarrows F_3CC(OSiMe_3)=NSiMe_3 \quad [25]$$

which should be shifted largely towards the isoamide structure.

Cyclic amides (lactams) usually represent the *cis* type of amide structure (the *cis* arrangement of NH and C=O) which is enforced by ring geometry. Their nitrogen shieldings do not depend significantly on ring size (Table 62). Only in the case of the nine-membered ring of 2-azacyclononanone (Table 62) can both the *cis* and *trans* isomers exist, and they show only a small difference in their nitrogen shieldings, analogous to those shown in Table 59 for the *E* and *Z* isomers of non-cyclic amides. In protonating media, such as CF_3COOH, the nitrogen shielding in lactams is decreased (Table 62), and a systematic study of the shielding[198] reveals that it decreases with an increase in ring size, but the effect is within about 10 ppm (from a five-membered to a nine-membered ring) and can be hidden by solvent effects.

The proton-coupled ^{15}N spectra of lactams have been employed in the determination of base-catalysed NH proton exchange rates.[191] For aqueous solutions, as well as those in DMSO, it is found that the rates decrease significantly with an increase in ring size, and the lowest rate is observed for *trans*-2-azacyclononanone. In a similar investigation[199] it was shown that 2-azacycloheptanone exchanges protons 1500 times more slowly than 2-azacycloheptathione.

A large number of nitrogen shieldings have been measured for the amido groups in penicillin derivatives and cephalosporins (Table 63). The exocyclic CONH moieties show shieldings typical of amides, but the four-membered lactam rings are characterized by a considerable deshielding of the nitrogen nuclei involved.

There are numerous structures for conjugated lactams which are tautomeric with the corresponding hydroxy derivatives of azine and azole

type heteroaromatic ring systems (Table 64). The nitrogen shielding in such lactams is smaller than those for any other amides, but is larger by about 100 ppm than those in the corresponding hydroxy-azine or hydroxy-azole tautomers (Tables 113, 120, and 121). Therefore, nitrogen shieldings can be used for estimating the positions of such tautomeric equilibria. For 2-OH and 4-OH substituted pyridines, and similar systems, the nitrogen shielding clearly indicates that the lactam ("pyridone") tautomers mainly prevail in the equilibria (Tables 113 and 120). Numerous examples of nitrogen shieldings in conjugated lactam forms are available from studies[202] on tetrahydropterin derivatives and folic acid (Table 64). Changes in the shieldings that occur upon conversion between the reduced and oxidized forms of riboflavin tetrabutyrate (Table 65) clearly reflect[203] the removal of hydrogen atoms from the enamino and lactam NH moieties involved. The differentiation between lactam, arylamine, and pyrrole type moieties by means of nitrogen shieldings is shown[204] by the example of chetomin, a toxic metabolite of *Chaetomium cochliodes* (Table 66).

Nitrogen shielding studies[132] on polyamide polymers dissolved in CF_3COOH appear to open an interesting perspective for applications of nitrogen NMR to the identification of various elements of copolymers (Table 67). The shielding reveals small, but reproducible, changes which depend on the diamine and the dicarboxylic acid units in the polymer chain. Such shieldings, characteristic of homopolymers, can be helpful in the identification of diamine units. However, as far as the diacid units are concerned, usually ^{13}C shieldings may be used for the differentiation between aliphatic and aromatic structures. An example of nitrogen shielding assignments in a copolymer chain, that of Trogamid T shown in Table 67, is based on the assumed shielding effect of γ-methyl groups (Section V.F).

In thioamide structures, the nitrogen nuclei are less shielded than in amides (Table 68). Conjugated thiolactams (Table 64), which are tautomeric with the corresponding SH-substituted heteroaromatic systems, show nitrogen shieldings larger by about 100 ppm than those in the latter systems (Table 120). They can also be employed in determinations of the tautomeric equilibria involved.[159,201] The nitrogen shielding indicates that 2-SH and 4-SH substituted pyridines largely exist in solution as the thiolactam tautomers (Tables 64 and 120). Thioamide nitrogen shieldings correlate with the height of the barrier to internal rotation of their NR_2 moieties, but they give a separate relationship from that found for amides (Section V.I and Table 14). In addition, tetramethylurea is found to depart significantly from the correlation.[40] Thus, the deshielding of the nitrogen nuclei in thioamides relative to those in amides bears no simple relationship to the relative magnitude of the barriers in the two types of structure.

In sulphonamides RSO_2NR_2, the nitrogen shieldings are slightly greater than those in amides (Table 69). This fact facilitates the spectral differenti-

ation between amide and sulphonamide type linkages in peptides (Table 102). The nitrogen shieldings in sulphonamides seem to be only slightly affected by protonating media such as CF_3COOH or aqueous HCl (Table 69), but they decrease in alkaline solutions, probably because of anion formation,[205] e.g.

$$MeSO_2NH_2 \underset{+H^+}{\overset{-H^+}{\rightleftharpoons}} MeSO_2NH^- \qquad [26]$$

The effect on the nitrogen shielding of *para* substituents in sulphonamides with *para*-substituted *N*-phenyl groups (Table 69) is similar to that observed in analogous amines and amides. The magnitude of such effects seems to decrease according to:

arylamines > *N*-phenylsulphonamides > *N*-phenylamides

L. Amino acids, peptides, polypeptides, and related structures

From the point of view of nitrogen NMR, amino acids are generally characterized by shieldings typical of amino and ammonium groups (Table 70). Some amino acids contain other nitrogenous moieties, such as guanidino groups, amido groups, and imidazole rings. The observed shielding depends appreciably on the equilibria between cations, anions, zwitterions, and neutral species. The increasing acidity of the solvent used usually results in a shielding of the amino/ammonium nitrogen in α-amino acids, but ω-amino acids show little effect,[210] as given in Table 70 [data corresponding to note (b)]. This means that the shielding in the former case mainly reflects the conversion [27]

$$R(NH_3^+)COO^- \xrightarrow{+H^+} R(NH_3^+)COOH \qquad [27]$$

but the effect is quenched when the NH_3^+ group is not on the same carbon atom as the $COO^-/COOH$ group. However, the shielding of the NH_3^+/NH_2 group in amino acids shows typical effects due to the hydrocarbon structure attached (Table 71), such as the β- and γ-effects (Section V.F). The difference in the shielding of the NH_3^+/NH_2 group of individual amino acids is often small and usually the corresponding titration curves of the shieldings are more informative. The latter can be used for determining pK_a values for individual nitrogenous moieties in amino acids. Such curves have been determined for histidine where additional complications arise owing to the tautomerism of its imidazole moiety (Table 72). The nitrogen shielding[208,212] indicates that the τ-H tautomer prevails under conditions where the imidazole ring contains only one NH group. However,

it is found[213] that the π-H tautomer dominates in histidine residues which are incorporated in α-lytic protease [see the corresponding nitrogen shieldings in Table 72, note (c)]. This apparently anomalous shift of the tautomeric equilibrium is explained[153,213] in terms of hydrogen-bonding effects between the π-NH of the histidyl residue and the COO^- group of the aspartic acid residue and eventually between the τ-N of the histidyl group and the OH group of serine. The three amino acid residues represent the catalytic triad of the protease.

There have been data galore reported on the nitrogen shieldings of arginine within a broad range of pH values (Table 73). The shieldings clearly indicate that the α-NH_3^+ and the terminal guanidino $C^+(NH_2)_2$ moieties undergo deprotonation at high pH values, while the δ-NH group remains unaffected. The shieldings of arginine turn out to be rather insensitive[174] to the presence of various anions (Table 73) which have been postulated to complex with the arginine residues in enzymes. For the nitroarginine derivative shown in Table 74, the nitrogen shieldings and ^{15}N signal splittings demonstrate that the nitroguanidine moiety exists in the R–NH–$C(NH_2)$=NNO_2 form.[188]

Amino acids labelled with ^{15}N can be used for tracing biosynthetic routes, since nitrogen NMR provides a simple means of insight into the fate of the ^{15}N label. This has been demonstrated by the incorporation of ^{15}N-labelled L-valine into the penicillin G structure (this is given in Table 63).[249]

Amino acid residues in peptides and other *N*-acyl derivatives of amino acids are characterized by a considerable deshielding of the nitrogen nuclei involved in the peptide linkages, when compared with the amino/ammonium shieldings representative of free amino acids. This is clearly predictable since the peptide linkage is actually an amido type structure R–C(=O)NH–R. The peptide shieldings are therefore analogous to those found in amides (Table 13). Simple *N*-acetyl derivatives of amino acids can be used as model compounds for the nitrogen shielding of peptides (Table 75). Such shielding data are actually employed[211] in the complete assignment of the nitrogen shieldings in the peptide hormone oxytocin (Table 82). For α-*N*-acetylhistidine, the nitrogen shieldings [Table 75; note (c)] indicate that the τ-H tautomer prevails, as in the case of histidine (Table 72).

Since CF_3COOH is a convenient solvent for large polypeptide structures, where it has been employed in numerous studies of peptide nitrogen shieldings (Tables 75–78, 80, 81, 95–99, and 102), caution is advisable when comparing the peptide shieldings for different peptide solutions. Trifluoroacetic acid can considerably affect the shieldings observed in comparison with those corresponding to other solvents (Table 75). The *N*-carboxyanhydrides of α-amino acids (Table 76), useful monomers for the preparation of polypeptides, show much smaller solvent effects on their

nitrogen shieldings than other amides. The values of the nitrogen shieldings are comparable to those found in carbamate structures (Tables 52 and 53).

Cyclic dipeptides of the 2,5-diketopiperazine type (Table 77) show substituent effects on the nitrogen shielding which are comparable to those found in amino acids (Table 71), but slightly different from those found in polypeptide polymers (Table 98), if solutions in CF_3COOH are compared. There is only a small difference in the nitrogen shielding between diastereomeric cyclodipeptides (Table 77). Such small differences can usually be resolved only in ^{15}N spectra taken at high magnetic fields in superconducting magnets.[175]

Since various protecting groups are commonly used in the syntheses of peptides, it is interesting to assess their influence on the nitrogen shielding in "protected" amino acids (Table 78). The effects are likely to be most pronounced in the case of the protected amino group of an amino acid residue, but they do not exceed 1·7 ppm for the next peptide nitrogen atom in the sequence of amino acid residues. Protecting groups that are bound to the terminal oxygen atom in a peptide seem to exert little influence on the nitrogen shielding (Tables 78 and 79).

A great deal of data on the nitrogen shielding of oligopeptides have been reported recently (Tables 80 and 81). The differentiation between terminal NH_3^+/NH_2 groups and peptide bridges is straightforward from the point of view of shielding which is much larger, by about 100 ppm, for the former groups. The protonation shift $NH_2 \rightarrow NH_3^+$ is towards deshielding but the opposite effect is observed for the peptide nitrogen atoms in C-terminal residues upon protonation of the carboxylate group, $COO^- \rightarrow COOH$. Since pH effects on the nitrogen shielding in aqueous solutions of oligopeptides can vary from one nitrogen atom to another, it is difficult to use such shieldings for the sequence analysis of amino acid residues. A reasonable method seems to be that employing CF_3COOH as the solvent,[217] since the shieldings are more reproducible under such conditions for amino acid residues linked to the same neighbouring residues in a peptide chain [Table 80; data corresponding to note (c)]. For example, the terminal Gly unit in R-Gly-Gly-OH shows a characteristic shielding of about 271 ppm. In some cases, where the differences between the nitrogen shieldings in amino acid residues are large (this happens mainly when the amino acid structures differ in the number of β-effects on the nitrogen shieldings; Table 71), the assignment of the observed shielding to individual residues may be simple, as in the case of cyclo(Gly-Pro-Gly-D-Ala-Pro) peptide [Table 80; note (e)]. The Pro and Ala shieldings are clearly distinguished from the Gly shieldings, but further assignments are less straightforward and can require ^{15}N labelling. The splitting of the resonances of the Gly units in an aqueous solution of the cyclopentapeptide (Table 80) is assigned to *cis-trans* isomerism of one of the peptide linkages, probably that of the first Gly unit.[218]

A detailed study of N- and C-protected oligopeptides composed of either norvaline or valine residues [Table 80; note (g)] shows that the nitrogen shielding of peptides is influenced by a number of factors, including solvent effects, temperature, and chain length.

The nitrogen shielding for the ^{15}N-labelled Pro residue in H-Ala-Pro-OH [Table 80; note (h)] reflects the presence of *trans* and *cis* isomers. The titration curves of the shieldings give the same pK_a value of 8·7 for the amino groups in both isomers, but two values (3·23 and 2·75) for the carboxylate group. It is suggested that the lower value corresponds to the *cis* isomer. This is the basis of the assignment given in Table 80.

The nitrogen shieldings in peptide chains are more sensitive to diastereomerism than ^{13}C or ^{1}H shieldings.[222] The data in Table 81 show that, under uniform experimental conditions, the differences are of the order of 1 ppm and these can be easily resolved at high magnetic fields. This question has been investigated further for a peptide polymer where diastereomeric Ala-Ala units are separated by achiral units (Table 81; -Aca-Ala-Ala- polymer). The L-L and L-D diastereomers are clearly resolved in the ^{15}N spectra,[223] and it is shown that considerable racemization takes place in the condensation polymerization process which starts from a single enantiomeric species of $SCN(CH_2)_5CO$-Ala-Ala-OH (Table 81).

A large number of peptide systems occurring in biologically important molecules have been investigated by ^{15}N NMR spectroscopy (Tables 92–94). The assignment of the nitrogen shielding in oxytocin and prolyl-leucyl-glycinamide has been made by a combination of ^{15}N labelling and comparison with the shieldings of *N*-acetyl amino acids (Table 82). The same procedure was applied to viomycin (Table 83), a cyclic peptide antibiotic, using the information involved in the one-bond N–H spin–spin splittings of the ^{15}N resonances and arguments based on the β- and γ-effects of alkyl groups, described in Section V.F. The assignment for N-9 is based on the slowest exchange of protons which is monitored by the ^{1}H-coupled ^{15}N spectra within a broad range of pH values.[224] The nitrogen shieldings of alumichrome (Table 84) are assigned on the basis of proton-decoupling and proton chemical shift assignments[225] for the peptide moieties. The shieldings for the hydroxamate nitrogens are measured directly,[226] and the partial non-equivalence thereof is explained in terms of a distortion of the octahedral configuration of the ligands. In the case of [Met^5]enkephalin, one of the endogenous peptides in mammalian brain,[227] the nitrogen shieldings (Table 85) are assigned rather simply by comparison with those in related model compounds. The titration curve for the nitrogen shielding in the terminal Met moiety yields a value of $pK_a = 2{\cdot}8$ for the terminal COOH group. The ^{15}N spectrum of bleomycin (Table 86) provides an additional argument in favour of the revised structure thereof,[228] showing eleven nitrogen atoms, two of them in primary amide structures. The

assignments rely upon signal multiplicities and general information on the characteristic shielding ranges for nitrogen nuclei, such as those given in Table 13. The tentative structure of the peptide antibiotic siomycin-A is supported by a comparison of its ^{15}N spectrum with that of thiostrepton (Table 87) whose structure is known. A complete assignment of nitrogen shieldings is reported for another naturally occurring antibiotic, gramicidin-S, which has a cyclic decapeptide structure (Table 88). The assignment is made on the basis of the nitrogen shielding of related peptides, solvent and deuterium exchange effects.[219] A trace of D_2O in the sample results in a considerable decrease in the signal intensities corresponding to the D-Phe and L-Orn moieties where the NH groups are exposed to solvent interactions. Shielding changes observed between solutions in DMSO and in CF_3CH_2OH also appear to reflect differences between solvent-exposed and internally hydrogen-bonded C=O groups. It is argued[219] that CF_3CH_2OH should form hydrogen bonds preferentially with the exposed carbonyl groups, those adjacent to the NH moieties of L-Pro, L-Leu, and L-Val residues. This is alleged to deshield the nitrogen nuclei in the NH groups, and actually such deshieldings are observed (Table 88), while for D-Phe the effect is much weaker and the NH moiety in L-Orn shows an increased shielding. The deshielding effect is attributed to an increased delocalization of the lone pair electrons from the NH moieties upon hydrogen-bonding of the adjacent carbonyl groups. This is in accord with the relationship between nitrogen shieldings and delocalization effects described in Section VI.K for amide type structures. It seems, therefore, that investigations of nitrogen shieldings in peptide structures can provide an insight into the conformations of both the NH and the CO groups in complicated molecules. In a similar study[230] on a model tetrapeptide with the amino acid sequence corresponding to that in tropoelastin (Table 89), deuterium exchange and solvent effects on ^{15}N NMR signals are used to delineate solvent-exposed and solvent-shielded nitrogen atoms. It is shown that the Gly^3 NH moiety should be exposed to solvent interactions and deuterium exchange. In MeOH solutions of the peptide, as compared with those in $CDCl_3$, significant deshieldings are found (Table 89) not only for the Gly^3 NH but also for the valine NH group. This is explained as the result of destroying some of the internal hydrogen bonds by the solvent. However, one can find an alternative explanation, missed by the authors. In the postulated, internally hydrogen-bonded structure,[230] the most exposed carbonyl group is that adjacent to the NH moiety in the Val residue. Using arguments such as those employed in the consideration of gramicidin-S above, one actually expects nitrogen deshielding for the latter residue in MeOH as solvent.

Recently, ^{15}N NMR has been shown to provide a deep insight into the structure of peptide type polymers and other polymers that contain amino

acid residues in bacterial cell walls (Tables 90–93). Studies have been undertaken[231–237] of the ^{15}N NMR spectra of intact cells, isolated cell walls, and cell wall digests. It is found that, upon broad-band proton decoupling, the ^{15}N spectra of such samples show essentially only the components of cell walls, since the NOE involved tends to null the resonances from the insides of the cells while those corresponding to the cell wall components are enhanced. The structures of the polymers contained in the cell walls of some Gram-positive bacteria are shown in Table 90 and Fig. 4. The ^{15}N

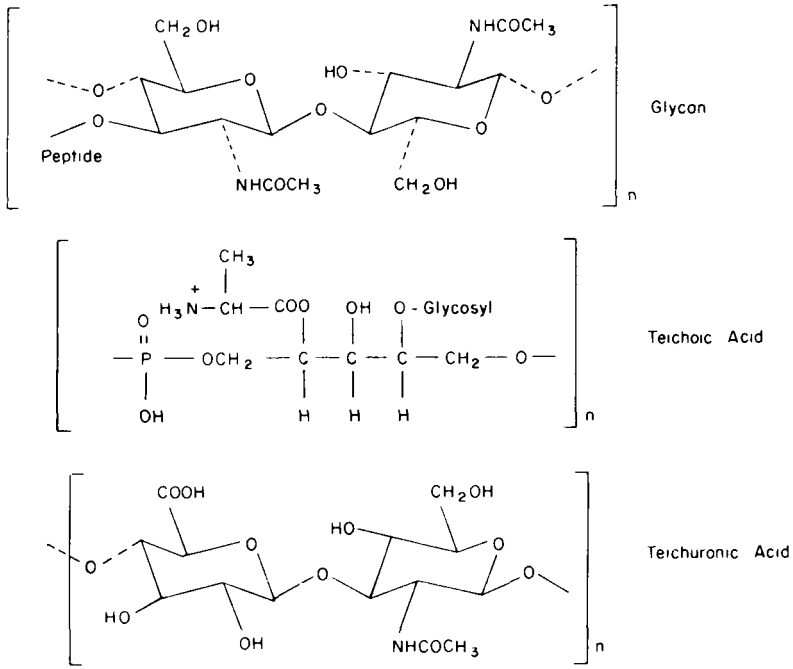

FIG. 4. Polymers in the cell walls of some Gram-positive bacteria.

spectra obtained from ^{15}N-labelled bacteria reveal well resolved signals of reasonable intensity owing to the relatively large mass of the cell wall components in the Gram-positive bacteria and the relatively small number of different types of nitrogenous moieties in the walls.[231] The latter include 5–10 types of peptide linkage, two types of free amino group, and 2–3 types of acetamido group bound to hexose rings (Table 90 and Fig. 4). Cell wall lysozyme digest turns out to be most suitable for the assignments of nitrogen shielding to the peptidoglycan structures, since the cleavage of the glycan strands upon digestion does not alter the primary structure of the peptide chains but it does increase the mobility of the latter. This results in sharper ^{15}N NMR signals and a favourable NOE. The nitrogen shieldings

of such digests are given in Table 91, together with their assignments. The latter are made from specific isotope labelling experiments, changes in the shieldings with pH, the data available for oligopeptides (Table 80), and, for *N*-acetyl derivatives of amino sugars (Table 32), cell wall fraction studies and comparisons between the digests.[231] When the assigned spectra of the digests are compared with those of intact cells,[231] it is found that the resonances of the peptidoglycan stems (Table 90) are missing, and the elimination of the NOE by gated decoupling shows that the apparent absence of the signals is not due to an unfavourable NOE. No resonances are observed, either, that can be assigned to the glycan strands. All this provides a strong argument in favour of the high rigidity of the glycan strands and the peptide stems in the peptidoglycans, and the high mobility of the crossbar and bridge regions. An exception to this is the mobile peptide system in the peptidoglycan of *Micrococcus lysodeikticus*, where the peptide chains are more sparsely distributed over the glycan strands. This is borne out by the ^{15}N spectra, since the same resonances are observed in both the digest and the intact cells.[231]

An interesting application of ^{15}N NMR to the elucidation of the role of antibiotics in the inhibition of bacterial growth has been reported.[233] Their action is associated with the inhibition of the biosynthesis of bacterial cell walls. The ^{15}N spectra of the cell wall lysozyme digests of *Bacillus licheniformis* (Table 92) show that there is no significant difference in the nitrogen shielding and the corresponding relative signal intensity between normal cells and those treated with lethal doses of vancomycin. This proves that there are no changes in the primary structure of cell wall peptidoglycan due to the action of vancomycin. However, analogous spectra of the whole cells show a decrease in the intensity of the ^{15}N resonances of teichuronic and teichoic acids upon vancomycin treatment, and comparison with the spectra of the lysozyme digests, as well as additional experiments on intact cells whose autolysins have been inactivated, indicate that the mobility of the acid polymers is affected by vancomycin. The reduction in mobility is probably associated with a rearrangement of teichuronic acid polymer chains and with a complexation of teichoic acid by vancomycin.[233]

A comparison of the ^{15}N spectra of *Escherichia coli* intact cells and their cell envelopes (Table 93) shows additional resonance signals in the latter. These can be assigned to the peptidoglycans, since the shieldings correspond to those found in the peptidoglycans of some Gram-positive bacteria (Tables 90 and 91; also Fig. 4). Thus, there should be much more mobility in the peptidoglycan structure of the prepared cell envelopes when compared with intact cells.[236]

The ^{15}N NMR signals of glycine units (marked with ^{15}N) in haemoglobin mixtures of Friend leukemic cells[260] show improved resolution upon exchanging the labile amide hydrogen atoms with deuterium.

The fate of the ^{15}N label in D-[α-^{15}N]lysine has been investigated by means of the ^{15}N spectra[380] of the fungus *Neurospora crassa*. The label is shown to migrate via L-pipecolinic acid into the α-position of L-lysine.

The elemental formula of the antibiotic nosiheptide has been determined using a combination of ^{15}N shielding and signal multiplicity with elemental analysis as well as ^{13}C and ^{1}H NMR spectra (Table 94). The ^{15}N spectrum provides key information about the number of nitrogen atoms and the number of hydrogen atoms directly attached to the nitrogen atoms. Since the ^{13}C spectra indicate 51 carbon atoms, 12 oxygen atoms attached to carbon atoms, and 32 hydrogen atoms attached to carbon atoms, as well as 3 hydrogen atoms in C–OH groups, and the proton spectrum shows 42 or 43 H atoms, the elemental formula is thus deduced.[238]

Nitrogen shielding can be employed for the characterization of synthetic peptide polymers. The results of extensive investigations of such systems are presented in Tables 95–102. Since there are solubility problems with such polymers, usually protonating solvents such as CF_3COOH are used. The nitrogen shielding of homopolymers of the Nylon-($N+1$) type, where N is the number of CH_2 groups between the peptide linkages, decreases with an increase in N. However, the deshielding effect declines exponentially, provided that solutions in the same solvent are compared (Table 95). This is explained as being due to the effect of increasing basicity of the peptide linkages with an increase in length of the intervening hydrocarbon chains, which makes the peptide moieties more susceptible to protonation. This explanation is corroborated by the fact that, for a given polyamide (Table 95), there is an evident deshielding effect in strongly protonating media which increases in the order $HCOOH < CF_3COOH < FSO_3H$. Trifluoroacetic acid seems to be preferred for spectral distinction between homopolyamide structures, since it produces only partial protonation of the peptide moieties and this results in maximum differentiation between the nitrogen shieldings. Strongly or weakly protonating media usually give much smaller changes in the shielding if one excludes the $(Gly)_n$ polymer. The nitrogen shielding of the homopolymers in CF_3COOH parallels those of the corresponding lactams (Table 62) in the same solvent. Thus, the nitrogen shieldings are not sensitive to *cis-trans* isomerism of the amide linkage.[198] Since the relaxation times of ^{15}N in peptide polymers can be long, paramagnetic additives may be used in order to enhance the relaxation rates, but there are limiting concentrations thereof beyond which the ^{15}N peak heights decline owing to signal broadening. Such limiting concentrations have been determined for some homopolypeptides (Table 96).

Nitrogen shift reagents (Table 11) were tested[244] as a means of introducing relative changes in the shielding of peptides in cases where the differences between individual amino acid residues are small. However, it turns

out that solvent effects can be more useful for the differentiation (Section V.C). The assignment of the nitrogen shielding of polypeptides with different amino acid residues within a polymer chain can be difficult if small differences in the shielding are involved. In some cases, selective ^{15}N labelling must be used,[239] but if the assignments are made for model polypeptides some simple rules can be established to aid the interpretation of the nitrogen NMR spectra of peptide polymers. For sequence polymers composed of (-X-Gly-Gly-) units, such rules are found (Table 97) where the corresponding homopolymers serve as reference substances for the nitrogen shielding. The data from Table 97 indicate that the strongest effect is exerted on the shielding of the peptide nitrogen in a given amino acid residue by the moieties that are adjacent to the N-terminal of the residue (the "primary" effect). It is difficult to explain the numerical values of such effects, but one should realize that the shielding of polypeptides dissolved in CF_3COOH is influenced not only by formal structural differences between the amino acid residues involved but also by protonation effects. Nevertheless, the simple rules can be used to distinguish between isomeric sequences of amino acid residues in sequence polymers on the basis of nitrogen shielding. Examples can be found in Table 95. The applicability of the rules is also clearly shown in Table 99 for sequence polymers composed of glycine and β-alanine units.[243] The identification of the individual types of peptide bridge is quite straightforward by means of nitrogen shielding. The characteristic values obtained from the sequence polymers can be applied to the identification of the peptide linkages in random polymers (Table 99). One should note that in the latter case some signal splitting is observed (Table 90) for the β-Ala-β-Ala linkages. This is ascribed to the effects of the next nearest pair of amino acid residues.

Since any rules that employ neighbouring residue effects on the nitrogen shielding of a given amino acid residue must assume some standard shielding for the latter, and since the logical choice for peptide polymers is homopolymers as the standards, it is interesting to compare the shielding in various polymers with that in polyglycine (Table 98). It is evident from the data given in Table 98 that there is some similarity in the shielding differences between individual amino acid residues within free amino acids, cyclodipeptides, and homopolypeptides, but the numerical values for the latter are significantly different from those for the other two groups.[175] Thus, only the data for homopolymers can be used as reference shieldings for heteropolymers.

The rather large difference in the shielding between various types of peptide linkage in polypeptides has important consequences from the point of view of the sequence analysis of peptide polymers.[250] A binary copolypeptide obtained from monomers A and B contains $-(A)_n-$ and $-(B)_m-$ units. If a spectroscopic technique such as proton NMR allows one

to distinguish only A and B, then the A/B ratio can be determined, but this does not provide any information about the average lengths (n and m) of the homopolymer blocks A_n and B_m. The ^{15}N spectra can usually

A–A B–B A–B B–A

[28]

distinguish between the four possible types of bonds [28] in such polypeptides, and the determination of the average values of n and m is made simple by using the equations

$$n = (I_{AA}/I_{BA}) + 1 \tag{25}$$

$$m = (I_{BB}/I_{AB}) + 1 \tag{26}$$

provided that the corresponding signal intensity (I) accurately reflects the relative numbers of nitrogen atoms involved. The latter problem can be solved by checking or correcting the relative ^{15}N signal intensities by means of the corresponding proton spectra, since the relevant intensities should obey the equation

$$\frac{I_A(^1H)}{I_B(^1H)} = \frac{I_{AA}(^{15}N) + I_{BA}(^{15}N)}{I_{BB}(^{15}N) + I_{AB}(^{15}N)} \tag{27}$$

Moreover, a single copolymerization experiment can then yield the reactivity ratios $r_A = k_{AA}/k_{AB}$ and $r_B = k_{BB}/k_{BA}$, where the k's are the rate constants for the four growing steps, since

$$r_A = (I_{AA}/I_{AB})(B'/A') \tag{28}$$

$$r_B = (I_{BB}/I_{BA})(A'/B') \tag{29}$$

where A' and B' are the starting concentrations of the monomers. In cases when it is possible to determine only one of the average block lengths, n or m [equations (25) and (26)], from nitrogen NMR, the A/B ratio obtained from the proton spectra can be used for the calculation of the other value, since $n/m = A/B$. Such cases occur[250] when one of the AA and BB signals in the nitrogen spectrum is beyond detection owing to either a low concentration of the BB bonds or the broadening of the corresponding signal. The copolymerization parameters have been determined by the method described[250] for a number of copolymerizations of glycine *N*-carboxyanhydride with γ-methylglutamate, *S*-benzylcysteine, leucine, and valine.

A similar problem arises when the copolymerization involves D and L enantiomers of the same amino acid derivative. The nitrogen shielding is often sufficiently sensitive to the diastereomerism which results from a combination of units (Table 80). If two such units are combined, two pairs of enantiomers [29] are obtained which should show some difference in

L–L D–D

L–D D–L

[29]

nitrogen shielding. It is reported[251] that the stereospecificity of the formation of the Bu^{t}OCO-D,L-Val-D,L-Val-OMe diastereomers from the corresponding D,L-valine derivatives can be simply observed in the ^{15}N spectra taken at high magnetic fields. In polypeptides the situation becomes more complicated since various successions of D and L units can occur, but it is usually sufficient to consider only the "tetrads" [30] and their enantiomeric

L–L–L–L D–L–L–D L–L–D–L D–L–D–D

D–L–L–L L–L–L–D D–L–D–L L–L–D–D

[30]

counterparts (D–D–D–D etc.). Thus, if only such short-distance effects on the nitrogen shielding are considered, there should be up to 8 different shieldings in a D,L-homopolypeptide. It is shown[252] that for poly-D,L-lysine the ^{15}N resonance is only broadened with respect to that in poly-L-lysine, but for poly-D,L-alanine at least four components are detected in the ^{15}N signal, with some further fine structure, and the range of the splitting is about 1·4 ppm. For poly(D,L-Phe) and poly(D,L-Ile) in CF_3COOH,[252] the range of splittings increases to 2·9 and 5·5 ppm, respectively, but the number of components in the signals is too large to be explained in terms of the tetrads. This effect can arise from conformational differences which should be most pronounced for bulky side-chains. Actually, the range of the splitting follows an increase in bulkiness of the side chain, Ala < Lys < Phe < Ile.

However, the influence of chiral centres on the nitrogen shielding in a peptide linkage along the carboxyl direction of the peptide chain can be different from that along the amino direction,[253] and the sets of "triads" [31] should be considered. The data for diastereomeric oligopeptides (Table 80) suggest that set A should be favoured, but one cannot exclude severe differences in solvent effects on the nitrogen shielding, since the results for oligopeptides refer to solutions in aprotic solvents while polypeptides are usually examined in solutions in CF_3COOH.[253] The identification of the shielding characteristic of the isotactic triads is relatively simple since the shielding is reproduced in the corresponding L-homopolymers and in random copolypeptides containing L-homopolymer blocks, provided that the polymers concerned do not differ in their secondary structures (e.g. helical or non-helical). This is proven for poly-D,L-valine, poly-L-valine, and copolymers of L-valine with glycine or leucine.[253] It is much more difficult to assign shieldings to the other triads, but fortunately the

identification of the ^{15}N signals representing the isotactic triads is sufficient for investigations of the stereospecificity of peptide polymerization.

Set A (stronger effect from the carboxyl end of the amino acid residue concerned)		Set B (stronger effect from the amino end of the amino acid residue concerned)
L–(CO–NH)–L···L	"isotactic"	L···L–(CO–NH)–L
L–(CO–NH)–L···D L–(CO–NH)–D···D	"heterotactic"	D···L–(CO–NH)–L L···L–(CO–NH)–D
L–(CO–NH)–D···L	"syndiotactic"	D···L–(CO–NH)–D

[31]

Another source of splitting of the ^{15}N resonances in polypeptides is the *cis-trans* isomerism of the amide moieties (Table 100). The effects of such isomerism are hardly detectable in the spectra of homopolymers with NH amide groups but they are clearly discernible in sarcosine polymers where N-Me moieties are present. The splittings observed are comparable to the difference in nitrogen shieldings of the *E* and *Z* isomers of amides (Table 59).

Nitrogen shielding can also differentiate between isomeric polymers where the isomerism results from the existence of more than one possibility of peptide bond formation by an amino acid unit. This point is illustrated by the example of polylysine [32] and isopolylysine [33]. The nitrogen shielding in (L-Lys)$_n$ and iso(L-Lys)$_n$, shown in Table 95 [note (e)], indicates that significant differences between the isomeric systems are found for the amino groups at low pH values. The peptide nitrogen shieldings are nearly identical in the two isomers.

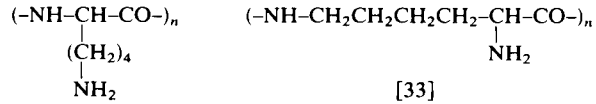

[32] [33]

Coil-to-helix transitions of the secondary structure of polypeptides can also be observed in ^{15}N NMR spectra. For (Lys)$_n$ polymer, the signals corresponding to the peptide nitrogens [Table 95; note (e)] show a small but clearly marked increase in the nitrogen shielding and simultaneously a significant broadening at pH 10·3. This is assigned to the helix formation upon increasing pH. A more detailed study of such transitions has been carried out for poly-L-ornithine (Table 101), where the spectra of the polymer are compared with those of *N*-methylacetamide[194] presented in Table 58. The comparison is made in order to distinguish the effect of a coil-to-helix transition from solvent effects. There is also a small shift of

the ^{15}N resonance of the peptide nitrogen atoms in polyornithine accompanied by signal broadening at a pH of about 10, while no such changes are found in the spectrum of *N*-Me-acetamide. This is again ascribed to helix formation upon increasing pH. There is a weak point in this argument since the comparison is only made with an amide, while the ornithine and lysine polymers contain both amido groups and amino/ammonium groups. The inflection in the titration curve of nitrogen shielding for the peptide moieties in the latter can simply reflect the deprotonation of the NH_3^+ group, and the transmission of the effect of deprotonation need not involve the coil-to-helix transformation of the structure.

Polyamides that contain sulphonamide linkages (Table 102) reveal characteristic nitrogen shieldings for the latter, comparable to those found in sulphonamides (Table 69). The nitrogen nuclei in the sulphonamide linkages are significantly shielded in comparison with those in peptide bonds. In alkaline solutions, the shielding decreases markedly, probably owing to the deprotonation of the $-SO_2NH-$ moieties. Isomeric sequence polymers that include sulphonamide linkages in addition to normal peptide bonds show appreciable differences in the nitrogen shielding (Table 102).

The ^{15}N spectrum of ^{15}N-labelled poly-L-lysine in aqueous solutions indicates that the side-chain amino groups bind Cu(II) ions since the ^{15}N signal corresponding to the amino groups [Table 95; note (i)] disappears from the spectra taken at pH values higher than 7 in the presence of $CuCl_2$.[242]

M. Azides

The azido group [34] is characterized by three distinct shieldings (Tables

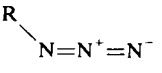

[34]

13 and 103). The most shielded is the nitrogen nucleus in the R–N moiety which resembles the highly shielded nuclei in carbodiimides (Table 55) and isocyanates (Table 106). The least shielded is usually the central nitrogen nucleus, but an interchange of its shielding with that of the terminal nucleus takes place when R is an electron-attracting group (Table 103). This is demonstrated for triply ^{15}N-labelled azido groups [Table 103; data corresponding to notes (a) and (b)] which give simple spin–spin splittings owing to the ^{15}N–^{15}N couplings across one bond in their ^{15}N spectra.[247,248] The assignment for *p*-toluenesulphonyl azide [Table 103; note (e)] is based on selective ^{15}N labelling[162] and the shieldings reported differ appreciably from those from the older data (ref. 2, p. 199). The shielding of the azido group bound to a phosphorus atom does not differ significantly from those for C-bound azido groups [Table 103; note (f)].

The shielding of the terminal nuclei in azido groups bound to C, P, or Ge increases linearly with the frequency of the symmetric stretching vibration of the group (observed at $\sim 1260\ cm^{-1}$)[256] but this is limited to alkyl derivatives. Other derivatives depart significantly from this correlation. The ^{15}N NMR spectra of azido groups bound to $SnMe_3$, $AlMe_2$, $GaMe_2$, and $AsMe_2$ show that the azido groups undergo exchange [Table 103; notes (g) and (h)]. For Me_3SnN_3 there are only two different nitrogen shieldings for the azide ion. For other metal derivatives the signals of the R–N and terminal atoms are distinct at low temperatures but they show coalescence at room temperature;[255,256] this also indicates that the azido group is exchanging on the NMR time scale.

The linear azide ion is characterized by two nitrogen shieldings owing to its symmetry [Table 103; notes (f) and (i)], and the assignments are based on the signal intensities.

It is shown by ^{15}N NMR that severe scrambling of the ^{15}N label takes place when *p*-toluenesulphonyl azide labelled with ^{15}N reacts with a nucleophile (Table 104). This provides a warning about the use of this versatile reagent in the syntheses of ^{15}N-labelled compounds.[257] The reactions [35]–[39] are postulated in order to explain the scrambling (Ts = *p*-toluenesulphonyl group).

[35] $$TsNN^{15}N + TsNH^- \rightleftarrows \begin{cases} TsNH^- + N^{15}NNTs \\ TsNHTs + (NN^{15}N)^- \end{cases}$$

[36] $$TsNN^{15}N + (NN^{15}N)^- \rightleftarrows \begin{cases} Ts^{15}NNN + (NN^{15}N)^- \\ Ts^- + 3N_2 \text{ containing } {}^{15}N \end{cases}$$

[37] $$Ts^- + TsNN^{15}N \rightleftarrows (TsNN^{15}NTs)^-$$

[38] $$TsNN^{15}N + TsNH^- \rightleftarrows TsN^- - N = {}^{15}N - NHTs \rightleftarrows TsNH - N = {}^{15}N - N^- Ts \rightleftarrows TsNH^- + N^{15}NNTs$$

[39] $$Ts^{15}NNN + TsNH^- \rightleftarrows Ts^{15}N^- - N = N - NHTs \rightleftarrows Ts^{15}NH - N = N - N^- Ts \rightleftarrows Ts^{15}NH^- + NNNTs$$

The results of the reaction of *p*-toluenesulphonyl azide with the azide ion (bottom of Table 104) can be explained[257] by a formal migration of the Ts group from TsN_3 to N_3^-. However, in order to account for the evolution of dinitrogen an unusual reaction [40] is invoked which is similar to reaction [36] considered above.

[40] $$TsN_3 + N_3^- \rightarrow Ts^- + 3N_2$$

N. Triaza- and diaza-pentadienium cations

The conjugated cations with two terminal NR_2 groups presented in Table 105 are characterized by nitrogen shieldings roughly comparable to those found in immonium cations (Table 128). Obviously, the structures given in Table 105 are conventional resonance structures since the positive charge should be distributed over the entire system involved, and for the 1,5-diaza- and 1,3,5-triaza-pentadienium cations the NR_2 groups should be equivalent. The equivalence is also shown in the shielding for symmetrically substituted NR_2 moieties.

The N-2 atoms in the 1,2,5-triazapentadienium salts reveal a considerable deshielding of their nuclei (Table 105), which is considered exceptional.[258] However, there is nothing unusual about the low shielding of the N-2 nucleus since it is well known (Table 13) that the N=N moieties are characterized by such shieldings provided that there are lone pair electrons on the atoms that are not involved in delocalized π-electron systems. The N-2 atoms obviously belong to this class.

O. Cyanates, isocyanates, thiocyanates, and isothiocyanates

The isomeric structures of cyanates [41] and isocyanates [42] are clearly distinguishable from each other by their nitrogen shieldings (Tables 13 and 106), and the same distinction is possible between thiocyanates [43] and isothiocyanates [44]. The relatively large shielding of the nitrogen nuclei

[41]	R–O–CN	*ca.* +200 ppm	nitrogen shielding ranges
[42]	R–N=C=O	+325 to +365 ppm	
[43]	R–S–CN	*ca.* +100 ppm	
[44]	R–N=C=S	+265 to +290 ppm	

in isocyanates and isothiocyanates is comparable to those observed in azides (Section VI.M; Table 103) and carbodiimides (Section VI.J; Table 55). Thus high shielding is characteristic of the R–N=X=Y structure with a linear N=X=Y moiety. In the bent NSO structure of *N*-sulphinylamines R–N=S=O (Table 131; Section VI.V), there is a significant deshielding in comparison with that of the linear structure considered.

The effect of alkyl and aryl groups on the nitrogen shielding in the compounds considered follows the general pattern described in Sections V.F and V.G.

The distinction between the nitrogen shielding in the cyanato and isocyanato structures, as well as that between the thiocyanato and isothiocyanato isomers, provides a simple means of determining the type of binding employed by the ambidentate ligands NCO and NCS in metal

complexes. A good example of the application of nitrogen shielding to such determinations is presented in Table 107.

The nitrogen shielding of Li(NCS) in various aprotic solvents is compared[261] with that of the $(NCS)^-$ anion in H_2O in order to examine association effects, and it is reported that in all cases Li(NCS) exhibits a higher shielding than the $(NCS)^-$ anion. This is erroneous, since the recalculated data in Table 106 [note (i)], compared with the precise shielding data for $(NCS)^-$, show that Li(NCS) in dimethylformamide reveals a significant deshielding of the nitrogen nucleus when compared with $(NCS)^-$ in H_2O. Nevertheless, there is a greater nitrogen shielding in Li(NCS) than in K(NCS) if the latter is dissolved in dimethylformamide. The solvents used (Table 106) represent a decreasing ionizing ability in the order: dimethylformamide > tetrahydrofuran > dimethyl carbonate > diethyl ether. The dilution curves[261] of the nitrogen shielding of Li(NCS) in these solvents are explained in terms of the equilibria [45] and [46], where the dimer structure [47] is assumed. For the S-bonded species, chain polymers [48] are suggested.

[45] free ions ⇄ ion pairs (in dimethylformamide)
ion pairs ⇄ dimers (in diethyl carbonate and ether)

[46] ion pairs ⇄ dimers ⇄ S-bonded species (in tetrahydrofuran)

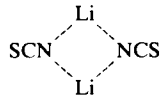

[47]

Li···NCS···Li

[48]

P. Cyano and isocyano groups, and related ions and *N*-oxides

The cyano group in covalent cyanides [49] (nitriles) is characterized by a narrow range of nitrogen shieldings (Table 108) which is quite distinct from that for the isomeric isocyanides [50] (isonitriles) and that for nitrile *N*-oxides (fulminates) [51].

[49]	R–CN	+110 to +140 ppm	nitrogen shielding ranges
[50]	R–NC	+180 to +220 ppm	
[51]	R–CNO	+160 to +180 ppm	

The protonation of a nitrile to yield the corresponding nitrilium ion $R–CNH^+$ increases the nitrogen shielding by about 100 ppm (Table 108). This is in accord with the considerations in Section V.H on the protonation shifts of shieldings for nitrogen atoms that are involved in multiple bond systems. The same applies to the increased shielding of nitrile *N*-oxides when compared with nitriles.

The effect of the group R in R–CN is rather small from the point of view of the nitrogen shielding, because of the intervening carbon atom of the cyano group, but solvent effects on the shielding can be considerable (Table 108; data for acetonitrile) since the lone electron pair on the nitrogen atom of the linear R–CN system is exposed to interactions with solvents.

Isocyanides R–NC exhibit the normal effects of alkyl groups R on nitrogen shielding (Section V.F) since the groups are bonded directly to the nitrogen atom concerned.

The nitrogen shielding in fulminates RCNO and the fulminate anion CNO^- is clearly different from those in the isomeric structures of cyanates R–OCN, isocyanates R–NCO, and the $(NCO)^-$ ion (Section VI.O).

It is evident, from the data in Table 108 for acetonitrile (MeCN), that both hydrogen-bonding and protonation effects act in the direction of increasing shielding. Thus, an involvement of the lone pair electrons of the nitrogen atom in any type of bonding seems to shield the nitrogen nucleus in the cyano group. This is amply supported by studies[266] on acetonitrile solutions of some inorganic salts, including $AgNO_3$ (Table 109). The latter induces a significant shielding in the CN group of acetonitrile, and it is known that within the range of concentrations used there are four MeCN molecules in the solvation sphere of Ag^+.

The nitrogen shielding of t-butyl isocyanide ligands in some palladium complexes (Table 110) does not differ appreciably from that for the free ligand (Table 108) but increases slightly with an increase in the electronegativity of the halogen atoms bound to Pd. The large deshieldings observed for the CN ligands in the paramagnetic systems of haemins and haemoproteins (Table 111) are quite sensitive to the structural environments involved,[267–269] including solvent effects. Since the ^{15}N NMR spectra of solutions also contain a signal for the free CN^- ion, the latter must be exchanging between the haem structure and the environment. The large deshieldings obey the Curie law, and their origin is undoubtedly that of direct binding to the paramagnetic centres such that some positive spin-density is induced on the nitrogen atom of CN (contact shifts). The effects of *cis* ligands, the peripheral substituent groups, on the shielding of the nitrogen nuclei in the axially bound CN ligands seem to be small, at least much smaller than solvent effects. On the other hand, there is a considerable influence on the shielding upon changing the *trans* ligand, e.g. one of the two CN ligands in dicyano-haemins (Table 110).

Q. Azole ring systems and related ions

Azole ring systems comprise five-membered rings of a considerably aromatic character (six delocalized π-electrons) with at least one nitrogen atom. They correspond to the general structures [52]–[55] where X = CH

or N. There are essentially two types of nitrogen atom in such ring systems. The nitrogen atom in the NR moiety in azoles, diazoles, etc. is bound

[52]
azoles,
diazoles,
triazoles,
tetrazoles,
pentazoles

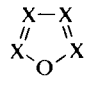

[53]
oxazoles,
oxadiazoles

[54]
thiazoles,
thiadiazoles

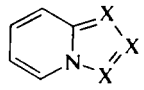

[55]
indolizines
(azoloazines)

directly to three other atoms in a plane, and it formally supplies two 2p electrons to the conjugated system. This is called the *pyrrole type* of nitrogen atom, since it occurs in all pyrrole derivatives. The *indolizine type* of

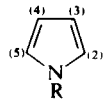

[56]
N-substituted pyrrole

nitrogen atom in structure [55] can be considered as a structural variation of the pyrrole type. The other kinds of nitrogen atom include those in positions X in the formulae given. This is called the *pyridine type* of nitrogen atom since its structural analogues are found in pyridine and other azine ring systems. The pyridine type of nitrogen atom is bound directly to only two other atoms; it supplies only one 2p electron to the conjugated π-electron system involved. Its lone pair electron orbital lies in the plane of the conjugated system and does not participate in the delocalized π-electron system.

There is usually a large difference between the shielding of a pyrrole type of nitrogen atom and that for any of the pyridine type nitrogen atoms that can occur in a given azole system (Table 112), the pyrrole type being more shielded. However, some overlap does occur in their characteristic shielding ranges (Table 13).

pyrrole type	+100 to +280 ppm	nitrogen shielding ranges
indolizine type	+120 to +200 ppm	
pyridine type (in azoles, oxazoles, thiazoles, etc.)	−60 to +145 ppm	

The indolizine type nitrogen atoms are usually less shielded, by about 40 ppm, than those in analogous *N*-methyl azoles (ref. 1, pp. 192–193, and references therein) and show a linear relationship with the latter, at least for simple unsubstituted structures.

The pyrrole type nitrogen atoms are structurally related to other nitrogen atoms whose lone pair electrons are delocalized over π-electron systems, e.g. arylamines, enamines, amides, and similar structures. Since the conjugated systems of azoles are characterized by a considerable delocalization of the lone pairs, and since the nitrogen shielding in such systems decreases with an increase in electron delocalization, it is not unusual for pyrrole type shieldings to be smaller than those for the other nitrogen types considered (Table 13), including amides. However, they are still larger than those of pyridine type nitrogen atoms and other moieties which contain formal C=N double bonds, with no participation of the nitrogen lone pairs in the delocalized π-electron systems (pyridine derivatives and other azines, imines, C=N groups in hydrazones, oximes), as is shown by the data in Table 13.

The shielding of pyrrole type nitrogen atoms is appreciably affected by solvents only when they are in NH moieties, but is largely unaffected in *N*-substituted derivatives (Table 112). This is opposite to the shielding trend for pyridine type atoms in azoles, which show large variations upon changing solvent (for example, the data for *N*-Me-pyrazole and *N*-Me-imidazole in Table 112). The latter are similar to those found for pyridine (Table 120) and other azine ring systems. The reason for this is rather obvious, since the pyridine type nitrogen atoms have their lone pair electrons exposed to interactions with solvents and other solutes. The latter point is clearly reflected in the behaviour of pyrrole and pyridine type nitrogen shieldings in the presence of shift reagents (e.g. lanthanide chelates), as is shown in ref. 2, p. 254, and references therein. The shielding of pyridine type nitrogen atoms shows large induced shifts by such reagents, while those of the pyrrole type do not change significantly.

Since the pyrrole type nitrogen shielding is fairly independent of the solvent used, approximate additivity rules have been established for them which express the influence of the various pyridine type nitrogen atoms that can occur in different positions of the azole ring system and the related indolizine system.[33] If we start with the shieldings of *N*-methylpyrrole [57] and indolizine [58] respectively, as references, the increments shown should be used.

	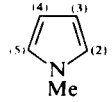 [57]	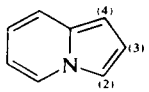 [58]
Reference shielding	+232 ppm	+191 ppm
N-2 or N-5 (each)	−54	−46
N-3 or N-4 (each)	−11	−9 (N-4) 0 (N-3)
N-2 and N-3 or N-4 and N-5 together (additionally for each pair)	−23	−20
N-3 and N-4 together (additionally)	+13	+8
N-2 and N-4 or N-2 and N-5 or N-5 and N-3 (additionally for each pair)	+7	+10

It should be noted that the numbering system for indolizine is chosen such as to conform to that of pyrrole.

One should be more cautious in setting up any additivity scheme for the shielding of the pyridine type nitrogen atoms in azoles, owing to the considerable range of solvent effects encountered. However, the following approximate additivity scheme is found[33] for the N-2 and N-3 atoms in azoles and related systems:

	Reference shielding		Increments for N–N interactions			
	N-2	N-3	2,3	2,4	2,5	3,4
N-methyl-azoles	+84 ppm	+123 ppm	−82	+4	−31	−41
oxazoles	+1 ppm	+126 ppm	?	+16	−34	−44
thiazoles	+83 ppm	+53 ppm	−114	+20	−48	−43
indolizines	+78 ppm	+137 ppm	−98	+18	—	−72 (N-4) −15 (N-3)

which show analogous changes in the shielding in all of the four groups of molecules considered.

The shieldings of both the pyrrole type (where applicable) and the pyridine type nitrogen atoms in azole systems (Table 112) usually provide

a clear differentiation between the various isomeric structures found in such systems. Only a few of the numerous examples in Table 112 are quoted here ([59]–[63]) in order to show the potential application of

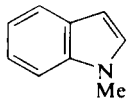

[59]

N-methylindole, +250 ppm

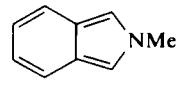

[60]

N-methylisoindole, +218 ppm

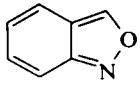

[61]

anthranil, +8 ppm

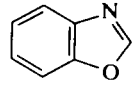

[62]

benzoxazole, +142 ppm

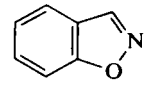

[63]

benzisoxazole, +27 ppm

nitrogen shielding to structural determination. The nitrogen shieldings are not only quite different for the different relative positions of the heteroatoms, but they distinguish between "benzenoid" structures (e.g. indole, benzisoxazole, benzoxazole) and "quinoid" structures (isoindole, anthranil).[201] A comparison of the spectral differentiation between isomeric thiadiazoles[33] [64]–[66] by ^{1}H, ^{13}C, and nitrogen NMR is also instructive. It is clear from the data given in Table 112 that the nitrogen shieldings of azole systems should be helpful in the determination of the tautomeric equilibria which can occur for azoles with NH groups, since the shielding of the corresponding isomeric *N*-methyl derivatives reveals significant differences between the isomeric species. Tautomerism in azoles often leads to dynamically averaged shieldings in their nitrogen NMR spectra.

	^{1}H shielding ref. to TMS	^{13}C shielding ref. to TMS	N shielding ref. to $MeNO_2$
 [64]	−8·95 ppm (coincident)	−148·6 (C-4) −137·9 (C-5)	−59 (N-3) −33 (N-2)
 [65]	−8·93	−151·6	+35
 [66]	−7·55	−152·7	+10

The effect of substituents on the nitrogen shielding in azoles cannot be explained in terms of any simple electronic theory. The data for substituted pyrroles (Table 113; see also ref. 1, pp. 179–185) indicate that electron-attracting groups in positions 3 or 4 tend to deshield the pyrrole type nitrogen nuclei, but it is difficult to explain the variation in magnitude of such effects. Substituents in positions 2 or 5 give rather unpredictable effects on the shielding. *N*-Phenyl and *N*-vinyl derivatives of pyrrole [Table 112; notes (b) and (d)] show a deshielding when compared to the *N*-methyl derivatives, probably due to the extension of the delocalized π-electron system. This is supported by the fact that *N*-vinylpyrroles, substituted at position 2, show an increase in shielding with respect to the parent compound[271] which can be explained in terms of non-planar structures for some of the possible rotamers in such derivatives which arise from steric interactions between the vinyl group and the substituent at position 2. Boron-containing substituents in position 2 or on the nitrogen atom of pyrrole result in a deshielding of the nitrogen nucleus, probably due to the extended delocalization of the π-electron system over the electron-deficient boron atoms [Table 112; notes (c) and (d)].

The protonation of a pyridine type nitrogen atom of an azole, to yield the corresponding azolium ion, results in a large increase in shielding for the nitrogen nucleus involved. This is typical of nitrogen atoms in unsaturated systems where the lone pair does not participate in the delocalized π-electron system (Section V.H). The protonation shifts of nitrogen shieldings for pyridine type nitrogen atoms in pyrazole and imidazole derivatives (Table 112) are in the same direction as the hydrogen-bonding effects but they are much larger than the latter.[273,274] The protonation or *N*-alkylation of a pyridine type nitrogen atom formally creates another pyrrole type nitrogen atom in the azole system involved. The shielding of such atoms in azolium cations does not significantly deviate from the values found for the pyrrole type nitrogen atoms in the corresponding parent azoles (Table 112).

The deprotonation of imidazole, which yields the corresponding anion [67] [Table 112; note (i)], has been investigated at high pH values[275] and the nitrogen shielding for the anion deduced from the titration curve. The shielding in the symmetric anion is much smaller than that in the symmetric imidazolium cation [68] (Table 112) but it is still greater than that for the pyridine type nitrogen atom in *N*-methylimidazole [69]. The spectra of the three species considered show clearly that, in general, there is no simple

[67]
+156 ppm (in H_2O)

[68]
+211 ppm (in H_2O)

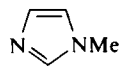

[69]
+218 ppm (NMe)
+135 ppm (N) (in H_2O)

relationship between nitrogen shielding and electron density in heteroaromatic systems, even if some local correlations are observed.

Two examples of the elucidation of the problem of tautomerism in azole systems are included in the data in Table 112. The nitrogen shielding of indazole shows[273] that the prevailing tautomer is such as indicated in the table [note (e)]. There is also an indication of tautomerism in *N*-phenyl-3-methyl-5-hydroxypyrazole[277] [Table 112; data corresponding to note (r)].

The complexation of imidazole by Zn(II) and Cd(II) is found to result in an average deshielding of the nitrogen nuclei (Table 114). Using previously determined values for the complexation constants, and nitrogen shielding data for various concentrations of the substrates, the shielding for individual complexes is calculated.[275,281] The dilution effects on the averaged nitrogen shielding in aqueous imidazole solutions[275,295] are small, and they indicate that there is no significant association of imidazole molecules in aqueous solution.

An example of spectral differentiation between pyrrole type nitrogen atoms and those in amino type groups is given in Table 115 which includes the shielding data for Rauwolfia alkaloids and related molecules.[128] The shielding for the indole moiety (N-12) is clearly different from that of the N-5 atoms. The former are not significantly affected by the structure of the saturated rings attached, but the latter seem to reflect the influence of *cis* and *trans* junctions between the saturated rings.

Azole ring systems constitute fundamental components of porphyrin ring systems (Table 116). Both pyrrole type and pyridine type nitrogen atoms can occur, and shielding can provide a simple means of spectral differentiation between them. The ^{15}N spectra of labelled compounds (selectively enriched with ^{13}C and ^{15}N) provide information about the unusual structure of the intermediate in the synthesis of uroporphyrinogen [Table 116; note (a)]. In studies on the ^{15}N spectra of octaethylporphyrin [Table 116; note (b)], it is found that the two central hydrogen atoms exchange positions among the four nitrogen atoms involved, but separate shieldings are observed for the NH and –N= moieties at low temperatures.[283,284] In the *N*-methyl derivative of octaethylporphyrin, the shieldings observed show that the NMe and NH moieties are in opposite positions with respect to each other, since a single shielding is found for the –N= moieties. The protonation of pyridine type nitrogen atoms in porphyrin systems results in an increased shielding which can be even larger than those observed for the pyrrole type nitrogen atoms in neutral molecules (Table 116). The exchange of hydrogen atoms between the NH and =N– moieties in porphyrin systems can be readily observed for ^{15}N-labelled compounds, since reduced, averaged NH splittings are found in the spectra of exchanging systems[283] rather than the normal one-bond NH couplings for non-exchanging NH moieties, provided that there is no significant exchange of

hydrogen atoms with the solvent. This is shown to be the case for the central hydrogen atoms in octaethylporphyrin and in the monocation of its *N,N'*-dimethyl derivative where the *N*-methyl groups occupy adjacent positions.

The same method has been used[290] for the observation of the tautomeric exchange of the central hydrogen atoms in protoporphyrin systems [Table 116; note (h)]. The exchange of the central hydrogen atoms is also indicated by the spectra of *meso*-tetraphenylporphyrin [Table 116; notes (d) and (e)].

The effect of metal atoms, in complexes of porphyrins, on the nitrogen shielding depends critically on whether the complexes are diamagnetic or paramagnetic. In the former case usually some increase in the shielding (referred to the average shielding of the parent system) is found (Table 116). Some subtle effects can be observed, as in the case of a Zn complex of *meso*-tetraphenylporphyrin [Table 116; note (g)]. The latter can be complexed with substituted pyridines, and the nitrogen shielding in such aggregates shows small changes which produce a reasonable correlation with the Hammett substituent constants.[289] A similar study of Cd(II) complexes[288] with *meso*-tetraphenylporphyrin and substituted pyridines indicates that the shielding of the porphyrin nitrogen nuclei is even less affected by substituents on the pyridine ring and the changes lie roughly parallel to those observed for the analogous Zn(II) complexes. The nitrogen shielding in complexes of Mg, Ni, Zn, and Cd with octaethylporphyrin follows the order of decreasing wavelength of the absorption maxima in their electronic spectra.[283–285] For Fe(II) low-spin complexes of octaethylporphyrin [Table 116; notes (b) and (c)], the nature of the bond between the axial ligand and Fe(II) seems to affect the nitrogen shielding of the porphyrin ring system.[285] If CO or isocyanide ligands are involved, the bond is of the π type, while pyridine and its derivatives are mostly σ-bonded; the former complexes are characterized by larger shieldings of the nitrogen nuclei in the porphyrin system.

Low-spin Fe(III) complexes of *meso*-tetraphenylporphyrin[296,297] show nitrogen shieldings that are larger by 2000–3000 ppm than those in the diamagnetic complex with Zn(II), which has a value of +179 ppm from neat nitromethane (Table 116). This is typical for paramagnetic species; the shieldings are found to increase linearly with the inverse of temperature.

The formation of an *N*-oxide from an azole system results in an increased shielding when compared with that for the parent pyridine type nitrogen atom, in agreement with the general rules considered in Section V.H. Examples of this can be found from the shieldings of furoxan systems [70] (Table 117) which are the *N*-oxides of furazans (1,2,5-oxadiazoles) [71]. Furoxan systems are known to undergo valence tautomerization,[278] and the barrier to the process [72], which probably occurs through the dinitroso

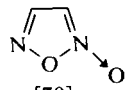

[70]

[71]

Nitrogen shielding *ca.* +20 ppm (N→O) −20 to −35 ppm
ca. 0 ppm (N) (Table 112)

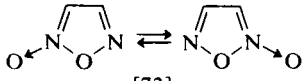

[72]

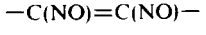

[73]

structure [73], is much higher for alkyl-substituted furoxans than for benzofuroxan structures. Thus, separate nitrogen signals are observed for the former at room temperature; in contrast an averaged signal is observed for benzofuroxan (Table 117) which splits at sufficiently low temperatures. There is a controversy about the assignment of the nitrogen shielding for furoxans.[278,279] It has been argued that, since the higher shielding is more influenced by hydrogen-bonding solvents (Table 117), it should be assigned to the pyridine type nitrogen atom,[278] by analogy with solvent effects on the shieldings in furazans and in other pyridine type nitrogen atoms. The weak point in this argument is that the oxygen atom in the N→O group is expected to be more exposed to interactions with solvents than the pyridine type nitrogen atom in a furoxan system. Thus the difference in the solvent effects may result from interactions with the *N*-oxide moiety. In contrast to this, the ^{14}N data[291] shown in Table 117 [note (c)] indicate that the resonances corresponding to the more shielded nuclei have much smaller widths, which is typical of *N*-oxide or nitro moieties. In addition, the higher shielding of the furoxan ring corresponds almost exactly to the shielding of the nitro groups of the nitrofuroxans examined. The *N*-oxide moiety in the furoxan ring is structurally similar to the nitro group; therefore the higher shieldings in Table 117 are assigned to the *N*-oxide groups.

The combination of ^{14}N and ^{15}N data [Table 117; notes (c) and (d)] indicates that the structures shown for the nitro derivatives of furoxans, as well as those for the benzo-bis- and -tris-furoxans, do not undergo valence tautomerism at rates that are fast on the nitrogen NMR time scale.[291] The valence tautomerism could in principle involve an oxygen shift within one furoxan ring, as considered above, but it could also include adjacent structures of furoxan rings and nitro groups, which is illustrated by [74]. The important point in this application of ^{14}N NMR spectroscopy is that the identification of the NO_2 resonance is made in a straightforward manner on the basis of the signal widths. In addition, unresolved ^{15}N resonances at about +20 ppm are indicated by ^{14}N NMR, since both the resolution and the determination of the relative numbers of nitrogen nuclei are simply

achieved by ^{14}N lineshape fitting and the differential saturation technique[291] described in Section IV.B.

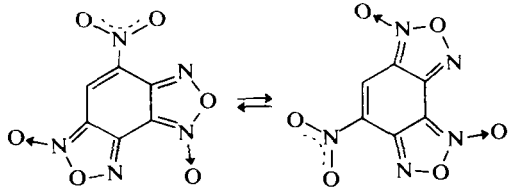

[74]

The nitrogen shielding of the oxide of the benzo derivative of 1,2,5-thiadiazole (Table 117) clearly shows the *N*-oxide rather than the *S*-oxide structure of the compound.[279]

In phosphadiazoles (Table 118), the hydrogen atom can exchange its position among three heteroatom centres including P.[292] The nitrogen shielding seems to exclude the latter possibility; comparison with the data for *N*-substituted derivatives favours tautomer A shown in Table 118.

Sydnones and related structures [75] are formally the betaine isomers of the corresponding 5-substituted 1,2,3-oxadiazoles [76] (Table 119). The

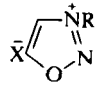

[75]

sydnone X = O
sydnonimine X = NH
acetylsydnonimine X = NC(=O)Me

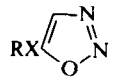

[76]

hypothetical 1,2,3-oxadiazole

assignment of the shieldings in Table 119 is facile because of the characteristically small linewidths in ^{14}N NMR and typical alkyl-group effects (Section V.F) on the shielding for the N^+–R moieties. The assignment may be verified by selective ^{15}N labelling,[264] as indicated in note (a) in Table 119. The nitrogen shielding shows that protonation of the sydnone-like structure occurs at the exocyclic X moiety, since there is little change in the shielding upon protonation; also the structure of the cation derived from sydnonimine shows a typical splitting for the NH_2 moiety labelled with ^{15}N, observed in the proton and ^{15}N spectra. It has already been pointed out that free sydnonimines are largely rearranged to isomeric cyanomethyl-alkyl-*N*-nitrosoamines (ref. 1, pp. 187–191, and references therein). However, the rearrangement is reversible, since upon acidification the corresponding sydnonimine cation is obtained; nitrogen shielding data provide unambiguous proof of the rearrangement (see Table 119). The present data on the ^{15}N-labelled compounds even show a distinction between the *E* and *Z* isomers of the nitrosoamine derivative involved.

The assignment of individual isomers is based on ^{15}N signal intensities and proton spectra.[264] It is interesting to note that the shieldings of the

NH_2 and NHC(=O)Me functions in the cations are typical of unsaturated amines and amides respectively (Table 13). This provides further evidence of the structure of the cations.

R. Azine ring systems and related *N*-oxides and ions

The nitrogen shielding in six-membered heteroaromatic ring systems (azines, diazines, etc.), which contain at least one nitrogen atom, covers a broad range (Tables 13, 120–122), i.e. −80 to +175 ppm from neat nitromethane. Since the nitrogen atoms involved obviously belong to the pyridine type, described at the beginning of the preceding section, the shielding of azines is comparable to those found for pyridine type nitrogen atoms in azoles (Section VI.Q), and for structurally related C=N moieties in imines (Table 13). Characteristic of the shielding are large solvent effects, particularly if hydrogen-bonding is involved. This is demonstrated by pyridine (Table 120) where hydrogen-bonding effects can induce shieldings of up to +30 ppm with respect to those observed in aprotic solvents. The protonation of the lone pair electrons to yield the corresponding azinium cation (Table 123) increases the shielding by about 100 ppm. The formation of an *N*-oxide structure yields a much smaller, but significant, increase in the shielding (Table 124). All this is typical of nitrogen nuclei in unsaturated systems where the lone pair electrons of the atom concerned do not participate in the delocalized π-electron system; it is considered in Sections V.H and V.J.

A considerable part of the observed range of nitrogen shielding in azine ring systems comes from interactions between nitrogen atoms located within the same ring (Table 122). The effects of such interactions on the shielding are simple and largely additive. Since the influence of solvents is large, a reasonable comparison can be made only for aprotic solvents, such as acetone or DMSO. If the data for simple (monocyclic) azines are compared (Table 122) one can reproduce the shielding within ±5 ppm using the additivity scheme [77] for nitrogen–nitrogen interaction effects with the increments shown. The ±5 ppm margin is quite small when compared with

			
reference shielding (from least-squares fit)	(1,2-interaction)	(1,3-interaction) [77]	(1,4-interaction)
+60·7 ppm	−85·4 ppm	+29·1 ppm	−12·4 ppm

the 140 ppm range of shielding. The presence of such simple effects provides an unambiguous assignment of the nitrogen shieldings in 1,2,4-triazine [78] [Table 122; note (e)] which themselves show the significance of such

nitrogen–nitrogen interactions within azine rings. These effects provide a formidable means of distinguishing between azine structures by nitrogen NMR.

[78] 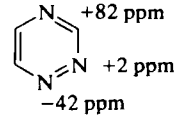

If both simple azines and their benzo derivatives are considered, the set of increments does not change appreciably:

reference shielding +64·1 ppm;

1,2-interaction −88·6 ppm; 1,3- +27·6 ppm; 1,4- −12·9 ppm

but the experimental values are reproduced to within ±13 ppm on the average, with phthalazine (Table 122) showing the largest discrepancy. The poorer fit is exemplified by significant differences in the shielding between the simplest systems (pyridine, quinoline, and isoquinoline) but the same general pattern of effects remains unchanged. The additivity scheme can be used for an unambiguous assignment of the shieldings of benzo-1,2,4-triazine [Table 122; note (e)].

The striking additivity of large effects in the nitrogen shielding of azines, which is indicated by empirical increments, is explained in terms of molecular orbital calculations by the INDO method employing the AEE approximation (Section II.A) in estimations of the relative shieldings in simple azine systems.[309] The calculations also provide[36] an independent proof for the assignment of the nitrogen shieldings in 1,2,4-triazine systems [Table 122; note (e)].

The question of shielding assignments for unsymmetrical benzodiazines (cinnoline, quinazoline; Table 122) is still open, but the fact that under the same experimental conditions the nitrogen nuclei in isoquinoline are more shielded than those in quinoline suggests[179] the tentative assignments given in Table 122.

A large amount of data on substituent effects on the nitrogen shielding in pyridine (Table 120) and pyrimidine (Table 121) have been recently reported. Sensible comparisons can be made only for solutions in the same solvent since most of the substituent effects are within the range of solvent effects. Substituents in position 3 of the pyridine ring do not significantly influence the shielding, and those for 2-substituted pyridines are hardly predictable. This is probably due to direct interactions between the substituent and the lone pair electrons on the nitrogen atom. Substituents in position 4 exert effects that can be compared to those found for *para*-substituted anilines (Table 37), but the latter are much weaker than those found in pyridine derivatives (Table 120). For example, the introduction

of an alkyl group into position 4 in pyridine increases the nitrogen shielding by about 8 ppm [Table 120; notes (c) and (h)], while in aniline the analogous *para*-substitution leads to a shift by +2 ppm (Table 37). For polar aprotic solvents such as acetone or DMSO the following approximate effects of substituents in position 4 on the shielding of pyridine can be deduced from the data in Table 120:

4-NH_2 (or NMe_2)	+41 ppm	4-Ph	+5 ppm	4-$CONH_2$	−8 ppm
4-OMe	+26	4-Cl (or Br)	+5	4-COMe	−10
4-F	+11	4-($CH{=}CH_2$)	+2	4-CHO	−15
4-(alkyl)	+7				

The largest effects (+40 to +50 ppm) are observed for 2-amino and 4-amino substituents as well as for the 2-F substituent (Table 120). Since the amino group in position 3 does not appreciably influence the shielding of the pyridine nitrogen atom, it is fairly easy to distinguish between various isomeric aminopyridines on the basis of the shielding of the pyridine nitrogen atoms. Fluorine substituents induce significant changes in the shielding, and their effects are approximately additive[301] for fluorinated pyridine derivatives; the following are the increments to the reference shielding (+62 ppm) in neat pyridine:

2-F or 6-F +43 ppm (each); 3-F or 5-F −10 ppm (each); 4-F +11 ppm

The values given above are slightly different from those originally reported[301] since the precise value of the shielding for neat pyridine (Table 120) is taken as reference. For pentafluoropyridine, the additivity scheme predicts a shielding of +150 ppm (referred to neat nitromethane) which compares favourably with the experimental value of about +148 ppm (Table 120). The increments are used for predictions of the shielding in unknown fluoropyridines.[301] The following list gives the positions of fluorine substituents in the pyridine ring followed by the predicted nitrogen shielding in ppm referred to neat nitromethane:

2,3	+95	2,6	+148	2,3,4	+106	2,4,5	+106	2,3,4,5	+96
2,4	+116	3,4	+63	2,3,5	+85	2,4,6	+159	2,3,4,6	+149
2,5	+95	3,5	+42	2,3,6	+138	3,4,5	+53	2,3,5,6	+128

It was recently shown[310] that, if a chiral substituent is present at position 2 of a pyridine ring, the enantiomers can be differentiated by the nitrogen shieldings when an optically active proton donor is added to the solution. The experiments have been carried out[310] with 8-benzyl-5,6,7,8-tetrahydroquinoline racemate [79], with the results shown. The shieldings are measured at 18·25 MHz (field parallel to sample tube), and originally referred to 1 M DNO_3, +6·2 ppm from neat nitromethane (Table 6). They are recalculated according to scheme IV in Table 4.

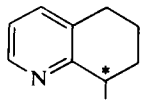

[79]

Optically active additive (mol %)	Solvent, and solute concentration (mol %)	Av. N shielding (ppm ref. to neat $MeNO_2$)	Difference between enantiomers (ppm)
R(−)-Mandelic acid			
(8·7)	tetrahydropyran (23·7)	+76·7	0·36
(8·0)	EtOH (13·5)	+98·9	0·27
(4·1)	CH_2Cl_2 (10·4)	+87·8	0·66
(6·7)	acetonitrile (16·0)	+87·9	0
S(+)-Lactic acid			
(23·0)	tetrahydropyran (23·0)	+88·6	0·16
R(+)-CF_3C(OMe) · (Ph)COOH			
(2·2)	CH_2Cl_2 (10·3)	+81·8	0·68
R(−)-CF_3CH(OH)Ph			
(17·2)	CH_2Cl_2 (17·0)	+78·6	0
β-Cyclodextrin hydrate			
(1·0)	DMSO (8·6)	+67·6	0·21

The effects of substituents on the shielding in pyrimidine derivatives [80] (Table 121) are complicated by the asymmetry introduced with substitution in positions 4 or 6. Substituents in position 5 do not induce appreciable changes, and this is analogous to the weak effect of substituents in position 3 of a pyridine ring [81]. Substituents in position 2 of a pyrimidine ring

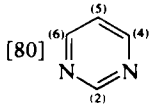

[80]

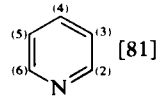

[81]

induce changes comparable to those of 2-substituted pyridines. Substituents in positions 4 or 6 in pyrimidines exert different effects on the shielding of N-1 and N-3 but they are comparable to those observed in 2- and 4-substituted pyridines respectively (Table 121). Table 121 does not include shielding values obtained from ^1H–{^{14}N} INDOR spectra[31] of 2-substituted pyrimidines, since they are rather inaccurate (±4 ppm) and do not differ significantly from those in the table. However, INDOR data provide some additional results; the following list of substituents gives the corresponding

increments to nitrogen shielding in pyrimidine (~5% solutions in acetone):

2-CN −19; 2-COOEt −13; 2-I −17; 2-SO_2Me +15; 2-F +47 ppm

There are two points of interest in the values given above. The large 2-F effect is comparable to that found in pyridines (Table 120), and the effect of 2-I is similar to that observed for aniline derivatives (Table 37).

Pyridine derivatives that contain substituents at positions 2 or 4 can be involved in tautomeric equilibria ([82] and [83]) provided that the substituents contain hydrogen atoms that dissociate easily. Since there are

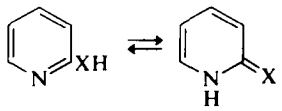

[82]

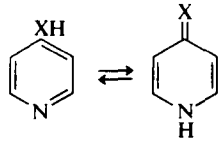

[83]

usually large differences in the shielding between the tautomeric pairs, often in excess of 100 ppm, the shielding provides a simple tool for the investigation of such equilibria (compare data in Tables 120 and 64). For hydroxypyridines (X = O), the shieldings show that the lactam ("pyridone") tautomers largely prevail in the equilibria; the same applies to the corresponding mercaptopyridines (X = S), as shown in a recent study.[159] The shieldings for the tautomeric derivatives, as well as those for the model compounds with NMe or XMe groups, are given in Tables 120 and 64. However, the data for fully fluorinated 4-OH and 4-OMe pyridines [Table 120; data corresponding to note (j)] suggest that the former exists as such rather than as the corresponding pyridone;[301] the same conclusion applies to the data on fully fluorinated 4-SH and 4-SMe pyridines. Thus, it seems that the equilibrium constants considered depend strongly on the character of the substituents in the ring systems.

In principle, one expects that the corresponding aminopyridines (X = NH or NR) can be involved in tautomeric equilibria with the amidine type tautomers, but the shieldings[301] for both ring nitrogen atoms and exocyclic amino/imino moieties (Tables 120 and 64) show that the aminopyridine forms largely prevail in the equilibria. In the case of aminopyrimidines (Table 121), the shieldings for 2-NH_2-pyrimidine, 2-NMe_2-pyrimidine, and the amidine type isomer show that the amino form dominates in the equilibrium.

There seems to be little influence on the shielding of nitrogen–nitrogen interactions when the nitrogen atoms are in different rings, as is shown for some naphthyridines (diazanaphthalenes).[311] The anisotropy of the nitrogen shielding in liquid pyridine has been estimated by a method based on relaxation time measurements made at various field strengths[312] but it relies

on an estimate of the absolute averaged shielding which is questionable (Section V.B).

Azinium ions, which are obtained by either the protonation or the *N*-alkylation of parent azines, are characterized by a significant nitrogen shielding when compared with the parent compounds (Table 123). However, the interpretation of such protonation shifts is complicated by the fact that the shielding of pyridine type nitrogen atoms is sensitive to hydrogen-bonding influences while that of the corresponding azinium ions is sensitive to the solvents and gegenions involved. *N*-Alkylazinium ions show much smaller influences on their shieldings due to solvents and anions (Table 123). The effects of substituents on the azinium nitrogen atoms seem to be similar to those found in parent azines. This is not unusual, since the protonation or *N*-alkylation does not fundamentally change the conjugated system of π-electrons. A different situation exists for arylammonium ions since the protonation of the amino group involved destroys the conjugation of the lone pair electrons with the ring system (Section VI.E).

Since the protonation shifts of pyridine type nitrogen atoms are large, they can be used to observe mono- and di-protonation processes in pyrimidine derivatives [Table 123; note (g)]. One can assume that 3-OH pyridine may be involved in a tautomeric equilibrium [84] with the zwitterion type ("betaine") isomer, but the nitrogen shielding of 3-OH- and 3-OMe-pyridines (Table 120; *ca.* +65 ppm) and *N*-Me-3-oxypyridyl betaine (Table 123; *ca.* +181 ppm) indicates that the 3-OH-pyridine structure largely prevails in the equilibrium.

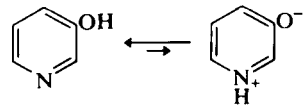

[84]

The *N*-oxides of azines (Table 124) are characterized by higher shieldings of their nitrogen nuclei, compared with the parent azines, but the change is smaller than that for the corresponding azinium ions (Section V.H). The protonation of an *N*-oxide to yield the corresponding *N*-hydroxyazinium ion (Table 124) results in a further increase in shielding. Azine *N*-oxides reveal significant solvent effects, comparable to those observed in azines. Hydrogen-bonding solvents tend to increase the shielding in both cases, in spite of the fact that in azines the hydrogen-bonding involves the nitrogen atoms while in azine *N*-oxides the oxygen atoms are most probably hydrogen-bonded to solvent molecules. This fact makes questionable the assignment of the nitrogen shielding of furoxan systems (Section VI.Q) based on solvent effects,[278] and provides some further support for the reverse assignment[279] based on nitrogen shielding and ^{14}N signal widths.

It has already been shown that the effect of ring substitution on the shielding of azine *N*-oxides is similar to those of the parent azines (ref. 1, pp. 196–198, and references therein). This is supported by the recent data presented in Table 124. The *N*-oxides of 2-hydroxy- and 4-hydroxy-pyridines can in principle exist in tautomeric equilibria [85], but this is one of the rare cases where the nitrogen shieldings do not differ significantly between the tautomers, as can be estimated from the data for the methylated derivatives given in Table 124. Thus no information about the equilibrium is obtained from nitrogen NMR measurements.[305] The lack of any significant difference in the shieldings in this case, when compared with that of the parent azines, is understandable in view of the fact that the tautomeric shift of the hydrogen atom between the two oxygen atoms does not essentially alter the bonding system of the nitrogen atom.

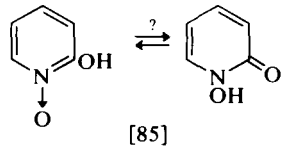

[85]

The question of the assignment of the nitrogen NMR spectra of *N*-oxides derived from di- and tri-azines is not easy to answer if one relies only on the shielding, since the difference between the latter for the NO and pyridine type nitrogen atoms is sometimes not sufficiently large when both types of nitrogen atom are present in the same ring (Table 124). However, the assignment is simple if ^{14}N NMR data are available, since the signal widths for the *N*-oxide moieties are known to be much smaller than for pyridine type nitrogen atoms (ref. 1, p. 196). This has recently been verified by the calculation of electric field gradients at the nitrogen nuclei of polyazine *N*-oxides,[306] using the method described in Section V.D and Table 12.[99] The results of the calculations[306] are quoted for structures [86]–[96]; the significance of the electric field gradient term is explained in Table 12. The calculations indicate that the field gradients at the nitrogen nuclei in the *N*-oxide moieties are so much smaller than those for the other nuclei considered that the sharpest ^{14}N signals are clearly predicted to represent the *N*-oxide function.

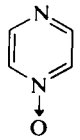

[86]

0·0063 (N → O)
0·1919 (N-4)

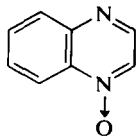

[87]

0·0070 (N → O)
0·1820 (N-4)

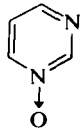

[88]

0·0015 (N → O)
0·2462 (N-3)

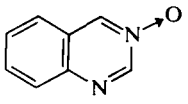

[89]

0·0013 (N → O)
0·2415 (N-1)

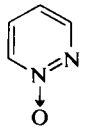

[90]

0·0034 (N → O)
0·2303 (N-2)

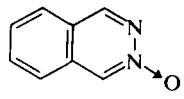

[91]

0·0051 (N → O)
0·2185 (N-3)

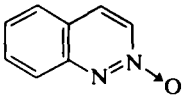

[92]

0·0044 (N → O)
0·2751 (N-1)

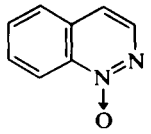

[93]

0·0047 (N → O)
0·2541 (N-2)

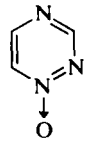

[94]

0·0065 (N → O)
0·2463 (N-2)
0·1879 (N-4)

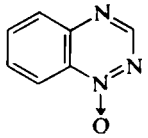

[95]

0·0091 (N → O)
0·2739 (N-2)
0·1765 (N-4)

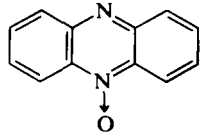

[96]

0·0099 (N → O)
0·1720 (N)

Once the question of the assignment of the shielding to *N*-oxide moieties in polyazine *N*-oxide has been settled they can be used for the localization of the *N*-oxide functions in such ring systems. For example, the oxidation of 1,2,4-triazine can lead to the isomeric *N*-oxides [97]–[99]. The values

N-oxide shielding data

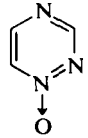

[97]

+37 ppm (predicted)
+43 ppm (found)

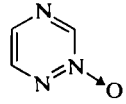

[98]

+60 ppm (predicted)

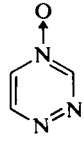

[99]

+73 ppm (predicted)

of the shielding for the *N*-oxide moieties can be predicted from the previously reported additivity rules.[313] Comparison with the experimental value for [97], the only product isolated,[307] shows that the oxygen atom is attached to N-1; the same has been demonstrated to be the case for

benzo-1,2,4-triazine mono-*N*-oxide [Table 124; data corresponding to note (i)]. The experimental values of the shielding of the *N*-oxide groups in azines give an excellent correlation with shieldings obtained from AEE calculations[307] (Section II.A). This correlation provides further support for the assignment of the 1,2,4-triazine *N*-oxide spectra and for the predicted shielding of the *N*-oxide moiety of the hitherto unknown isomer [100] of quinazoline mono-*N*-oxide.

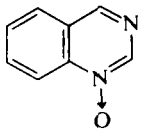

predicted N → O shielding[307,313]
+92 ppm (ref. to neat $MeNO_2$)

[100]

An interesting example of shielding assignments for azine, azinium, and azolium type nitrogen atoms is provided in Table 125 for thiamine and its protonated form vitamin B_1.[308] The data indicate that protonation occurs at N-1, provided that the assignment is correct. The ^{15}N triplet at +274 ppm shows that the NH_2 group is not protonated in vitamin B_1. The large increase in only one of the other shieldings indicates that only one of the pyrimidine nitrogen atoms in vitamin B_1 is protonated. The assignment of the shieldings to N-1, N-3, and the thiazolium nitrogen atom are then made on the basis of selective proton-decoupling and deuterium exchange effects.

S. Nucleosides, nucleotides, and related structures

Nucleosides and related systems (Table 126) contain pyridine type nitrogen atoms in azine and azole rings, pyrrole type nitrogen atoms, conjugated lactam moieties, and amino groups. We consider them separately because of the importance of this class of compound in biochemistry and biology, and because they contain essentially only two types of nitrogenous structure, those of purine and pyrimidine. As far as the shieldings are concerned for nucleoside systems, there is a simple distinction between the amino groups (*ca.* +300 ppm), the pyrrole type nitrogen atoms and lactam moieties (*ca.* +200 ppm), and pyridine type nitrogen atoms (*ca.* +150 ppm). Nitrogen shieldings are useful in the observation of protonation sites in nucleoside systems (because of the large increase in shielding upon protonation of a pyridine type nitrogen atom) and tautomerism (because of the large relative shielding difference of the nitrogen nuclei in lactam moieties when compared with pyridine type nitrogen atoms).

The detailed assignment of the shieldings for purine and pyrimidine type nucleosides [Table 126; data corresponding to notes (a) and (b)] is

made from observations of ^{15}N–H couplings, protonation shifts, NOE, and a comparison of the shielding differences between various molecules.[158,181] The only assignments that can be considered as tentative are those for N-1 and N-3 in adenine derivatives (Table 126), since arguments based on a comparison of the analogous shieldings in quinazoline[158] rely upon arbitrary assignments for the latter. The problem of the assignment of shieldings in quinazoline and other unsymmetrical benzodiazines seems to be still open (see Table 122 and Section VI.R), and the reverse assignment is suggested from a comparison of the shieldings in quinoline and isoquinoline. The higher shielding for N-3 in the adenosine system, as compared with N-1, is also claimed on the basis of a comparison with ^{15}N-1 labelled adenosine.[314,315] Curiously enough, the work quoted,[314,315] which is alleged to contain data for the ^{15}N-1 labelled compound, is not concerned with any aspect of nitrogen shielding. Thus, the only real argument in favour of the relative N-1 and N-3 assignments in the nitrogen NMR spectra of adenine derivatives comes from the fact that N-1 is supposed to undergo protonation,[314,315] but this amounts to an information transfer to, rather than from, the nitrogen spectra. Nitrogen shieldings can therefore constitute a simple tool for identification of protonation sites in nucleosides and nucleotides, provided that there is no ambiguity in their assignment. The latter often require specific ^{15}N-labelling of model compounds.

There remains the interesting question of how shieldings reflect association ("base pairing") between different nitrogenous bases of nucleosides and nucleotides. No significant effects are found[181] for the uridine–adenosine pair, which is explained[316] as being due to the use of an unsuitable solvent, DMSO. Investigation[316] of the ^{15}N-3 shielding in [3-^{15}N]-2′,3′,5′-tri-*O*-benzoyluridine in $CDCl_3$ reveals that addition of 5′-acetyl-2′,3′-isopropylideneadenosine decreases the shielding [Table 126; data corresponding to note (d)]. A similar study[318] has been undertaken on the nitrogen shielding in fully ^{15}N-labelled 2′,3′,5′-tri-*O*-acetyladenosine in $CDCl_3$ as a function of concentration and mole fraction of 1-cyclohexyluracil. Only the NH_2 resonance shows an increase in shielding upon dilution. The addition of the uracil derivative affects all the shieldings except that for N-9. The N-1, N-3, and N-7 shieldings increase by a few ppm, while a deshielding is observed for the NH_2 resonance. The largest change among the resonances of the ring nitrogen atoms occurs for N-1, provided that the assignments for N-1 and N-3 are correct.

T. Cyclophosphazenes

Cyclophosphazene ring systems (Table 127) are characterized by rather large nitrogen shieldings when compared with those in azines (Section

VI.R). This is attributed to the different π-electron system in the former which includes the phosphorus 3d orbitals, and to the non-planarity of cyclophosphazene rings.[143] The nitrogen shielding in cyclophosphazenes is comparable to that in the puckered ring of cyclothiazene S_4N_4, *ca.* +247 ppm (ref. 2, p. 339, and references therein).

The effects of phosphorus substituents on the shielding are appreciable (Table 127). Qualitatively they follow the trends observed in substituted pyridines (Table 120).

There are indications, however, that at least some of the cyclophosphazene structures given in Table 127 are planar,[324] which complicates the interpretation of the shielding in such systems.

U. Imines, nitrones, oximes, and related ions

The nitrogen shielding in the C=N moiety of imines (Table 128) is comparable to that of pyridine type nitrogen atoms in azines and azoles (Table 13; also Sections VI.Q and VI.R). The large increase in the shielding upon protonation of the nitrogen atom, to yield the corresponding immonium cation (Table 128), and the smaller but significant increase in shielding upon the formation of the *N*-oxide structure (nitrone; Table 130) are characteristic of this type of nitrogen atom (Section V.H) which also includes the pyridine type of nitrogen atom in heteroaromatic rings. Changes due to solvent effects, particularly the characteristic increase in shielding in hydrogen-bonding solvents (Table 128), are typical of this class of nitrogen atom (Section V.J).

The effects of alkyl groups R in C=N–R on the shielding conform to the general rules (Section V.F), including the significant deshielding arising from the presence of β-carbon atoms (the β-effect). For phenyl derivatives of imines, the effect of substituents in the phenyl ring of PhCH=NR is greater than in R_2C=NPh (Table 128). The effects correlate with the Hammett substituent constants,[172] and are comparable to those found in the shielding of arylamines (Sections V.G and VI.E). Linear correlations are also found[171,172] between the nitrogen shielding of imines and the ^{13}C shieldings for the corresponding carbon atoms in analogous alkenes. The effect of substituents is similar in the corresponding phenyl derivatives of immonium cations (Table 128), which is analogous to the situation of nitrogen shieldings in azines and the corresponding azinium ions (Section VI.R). The same applies to nitrones (imine *N*-oxides), at least for the limited set of data in Table 130.

The large difference in shielding between the amino and imino groups (Table 13) can be used in investigations of amino–imino tautomerism, as is shown for 1-phenylamino-7-phenylimino-1,3,5-cycloheptatriene [Table 128; note (h)].

The nitrogen shielding of the imino moiety (C=N) [101] is strongly dependent on π-electron delocalization effects, as indicated above for phenyl derivatives of imines. The most pronounced effect of this type can be found in amidine structures [102] [Table 128; note (a)] where the lone pair from the amino moiety can be delocalized over the imino moiety.

	$R_2C{=}N{-}R$	$R_2N{-}C(R){=}N{-}R$
	[101]	[102]
Nitrogen shielding ranges	+20 to +90 ppm	+140 to +180 ppm (=N-R)

The shieldings of some immonium ions are used to predict the barrier to rotation of the NR_2 group in $R_2C{=}NR_2^+$ (Table 14 and Section V.I). If the lone pair electrons of the C=N moieties are involved in bonding in a complex [Table 128; data corresponding to note (g)] there is an increase in the shielding, similar to that occurring in the case of *N*-protonation or *N*-oxidation. There is a large difference in the nitrogen shielding between the C=N and S=N moieties, as indicated by the data in Table 128 [note (i)].

	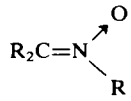	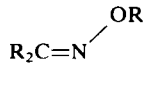
	[103]	[104]
Nitrogen shielding ranges	+70 to +110 ppm	−30 to +60 ppm

Imine *N*-oxides (nitrones) [103] and oximes [104] are isomeric but there is a clear distinction between their nitrogen shieldings. The shielding in oximes (Table 129) reveals a strong dependence on solvent effects, but a much smaller influence from the nature of the groups R. The *E,Z*-isomers of oximes with different groups R in a molecule, when compared in the same solvent, show rather small differences in their shielding, comparable to that for unsymmetrical amides (Table 59). There are rather large differences in the shielding between oximes and their ethers (Table 129), evidently because of strong hydrogen-bonding and association in oximes. Generally, for a given oxime, the smallest shielding is observed for solutions in hydrogen-bonding acceptors, like DMSO, and the largest nitrogen shielding is found for solutions in hydrogen-bonding donors, such as CF_3CH_2OH.[321] Since there is a difference of about 500 ppm between the shielding of

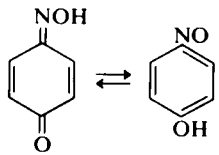

[105]

oximes (−30 to +60 ppm from $MeNO_2$) and of the nitroso group (*ca.* −500 ppm from $MeNO_2$; Table 140), nitrogen NMR data can be readily applied to the determination of tautomeric equilibria (ref. 1, pp. 201–202, and references therein) of the type [105].

V. *N*-Sulphinylamines, thionitrites, sulphodiimides, and related structures

The low shielding of the nitrogen nuclei in *N*-sulphinylamines RN=S=O (Table 131) is in contrast with the high shielding typical of RN=X=Y structures, such as isocyanates (RN=C=O; Table 13), isothiocyanates (RN=C=S), azides ($RN=N^+=N^-$), and carbodiimides (RN=C=NR). However, in the latter structures, the N=X=Y moieties are linear, while it is known that the N=S=O moiety is bent (refs 118 and 259, and references therein) and can theoretically exist in an equilibrium [106]. Thus, the large shieldings are characteristic only of linear N=X=Y moieties. The same applies to the small shielding of the nitrogen nuclei in the sulphodiimide structure of PhN=S=NPh (Table 131) when compared with carbodiimides (RN=C=NR; Table 13).

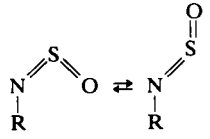

[106]

"*cis*" "*trans*"

The effect of alkyl groups R on the shielding in RN=S=O compounds is typical (Section V.F), with one notable exception.[118] There is a reversed β-effect on the shielding upon passing from R = Pr^i (or any secondary alkyl) to R = Bu^t. Since the "*cis*" structure brings the oxygen atom close to the methyl groups of R = Bu^t, this observation provides the basis of a strong argument in favour of the "*cis*" conformation of alkyl-*N*-sulphinylamines.[118] It indicates also that the β-effect of alkyl groups on nitrogen shieldings is quenched, or even reversed, by steric interactions (Section V.F). In principle, steric interactions can either result in a deformation of the more stable "*cis*" form, or simply shift the equilibrium towards the "*trans*" isomer. However, the rather abrupt change of the β-effect observed for the Bu^t derivative and the results of CNDO/S calculations[118] favour the deformation of the more stable "*cis*" isomer.

N-Sulphinylamines [107] are isomeric with thionitrites [108] but there is a vast difference in their nitrogen shieldings, the latter being characteristic of the nitroso structure (Table 140).

	R–N=S=O	R–S–N=O
	[107]	[108]
Nitrogen shielding ranges	+25 to +80 ppm	−300 to −400 ppm

W. Nitro groups, nitrates, and nitramines

Nitro groups have a characteristic range of shieldings extending from −30 to +70 ppm with respect to that of neat nitromethane (Tables 13, 132, 133), but some clear subdivisions of the range can be made. The nitrogen nuclei of the nitro groups of nitroalkanes are deshielded relative to that of $MeNO_2$, while conjugated nitro groups show a shielding increase together with those nitroalkanes that bear strongly electron-attracting groups on the carbon atoms directly bonded to the NO_2 groups (Table 133; also ref. 1, p. 203, and ref. 2, pp. 233–244). The largest shielding is observed for the *O*-nitro and *N*-nitro groups in nitrates and nitramines respectively (Tables 132 and 133).

Nitroalkanes that have hydrogen atoms on C-α [109] can be converted into the corresponding *aci*-nitro isomers [111] which can be considered as

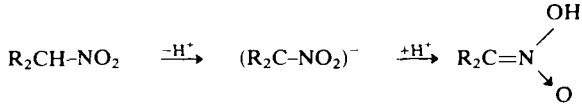

	[109]	[110]	[111]
Nitrogen shielding ranges	0 to −30 ppm	+20 to +60 ppm (ref. 2)	*ca.* +70 ppm (ref. 1)

oxime *N*-oxides. The latter usually rearrange slowly to the nitroalkane structure. An analogous distinction between the nitro [112] and *aci*-nitro *E,Z*-isomeric structures [113] and [114] by means of nitrogen shielding is possible for nitramines,[263] as shown in Table 132. The shielding of

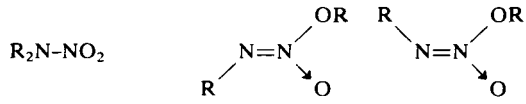

	[112]	[113]	[114]
Nitrogen shielding ranges	+20 to +40 ppm (NO_2) +100 to +220 ppm (NR_2)	+50 to +70 ppm (=NOOR) +90 to +110 ppm (RN=)	

MeN=N(O)OMe (Table 132) shows appreciable differences for the *E* and *Z* isomers involved. The nitramino structures also occur in nitrourethanes RO–C(=O)–N(R)–NO_2, and are characterized by shieldings comparable to those in nitramines.

In spite of the fact that the nitrogen atom in a nitro group occupies a central rather than a peripheral position, there are appreciable solvent effects on the shielding of the nitrogen nucleus (Table 133). However, hydrogen-bonding effects are insignificant, at least when compared with

those on the shielding of pyridine type nitrogen atoms (Sections VI.Q and VI.R), in imines (Section VI.U), their *N*-oxides, and related structures. It has been recently shown[121] that medium polarity (dielectric constant) is mainly responsible for the observed range of solvent effects on the shieldings in nitroalkanes. The changes induced by aprotic solvents have been reproduced theoretically using the solvaton model (Section V.J). This is an important point, since it shows that nitrogen shieldings can clearly reflect changes in the distribution of the electron charge in a molecule which are induced by changing the polarity of the medium. For example, the observed and calculated shieldings shown for nitromethane (since the calculations

$MeNO_2$ (0·30 M solutions)

Solvent	Dielectric constant at 30 °C	Nitrogen shielding (ppm) obs.	calc.
DMSO	45·8	−2·0	−0·6
dimethylformamide	37·5	−0·7	−0·5
none	35·9	0·000	−0·4
MeCN	36·6	+0·2	−0·4
acetone	20·4	+0·8	0·0
CH_2Cl_2	9·50	+3·2	+1·3
CH_2Br_2	6·78	+3·4	+2·3
$CHCl_3$	5·07	+3·8	+4·3
Et_2O	4·79	+3·9	+4·8
CCl_4	2·71	+7·1	+8·8

yield absolute shieldings, a conversion constant is introduced by a least-squares fitting procedure) have a range of about 10 ppm for medium polarity effects. The experimental shieldings come from high-precision ^{14}N measurements,[80,121] with the elimination of bulk susceptibility effects by the use of concentric spherical sample and standard containers. A similar agreement[121] between the observed and calculated effects of medium polarity on shielding is found for other nitroalkanes, namely those listed in Table 133 [note (b)].

The effect on the shielding of the structure of the alkane chain bonded to a nitro group is typical for alkyl group effects (Section V.F), provided that solutions in solvents of about the same dielectric constant are compared (Table 133). The effects make possible a simple distinction between primary, secondary, and tertiary nitroalkanes (RCH_2NO_2, R_2CHNO_2, and R_3CNO_2 respectively). Nitrogen shielding provides a simple means of distinguishing between nitroalkanes [115] and the isomeric alkyl nitrites [116].

	$R-NO_2$	R-O-N=O
	[115]	[116]
Nitrogen shielding ranges	0 to −30 ppm	*ca.* −190 ppm (Table 140)

The shielding of the nitro groups attached to an aryl function does not follow any simple rules when substituent effects are considered (Table 133 and ref. 2, p. 239). Electron-accepting groups appear to increase the shielding, but there seems to be little differentiation between *para*, *meta*, and *ortho* positions of substituents relative to the nitro group. The only deshielding effect relative to nitrobenzene (Table 133 and ref. 2) seems to be exerted by amino substituents.

Covalent nitrates $RONO_2$ are characterized by a relatively large shielding of their NO_2 moieties (Table 133) when compared with nitro groups. In contrast to this the nitrate ion NO_3^- has a shielding comparable to that of nitromethane. The shielding of nitric acid is extremely sensitive to its concentration in aqueous solutions. For dilute solutions, the shielding is essentially that for the NO_3^- ion, but for neat $HONO_2$ the shielding corresponds exactly to that of the covalent nitrate (Table 133). Thus, nitrogen shielding appears to reflect the equilibrium [117], but this is

$$H^+ + NO_3^- \rightleftarrows HO\text{–}NO_2 \qquad [117]$$

probably an oversimplification, since other nitrogenous ions can be involved (Table 141) such as the NO_2^+ ion. The large change in the shielding between dilute and concentrated solutions of HNO_3 is also reflected in the sensitivity of the NO_3^- shielding to the presence of acids [Table 133; note (a)]. The ^{14}N spectra of mixtures of anhydrous HNO_3 with acetic acid anhydride[327] show signals of HNO_3 and $MeC(=O)ONO_2$ which can be used for the observation of changes in the equilibrium [118]. The addition of concentrated H_2SO_4 results, after some time, in the appearance of a signal at 47 ppm which is evidently that of tetranitromethane $C(NO_2)_4$ (Table 133).

$$\underset{+42.5\text{ ppm}}{HNO_3} + (MeCO)_2O \rightleftarrows \underset{+68\text{ ppm}}{MeCOONO_2} + MeCOOH \qquad [118]$$

X. Diazo compounds and diazonium salts

The terminal nitrogen nuclei ($=N^-$) of diazo compounds $R_2C{=}N^+{=}N^-$ are substantially deshielded when compared with the central nuclei ($=N^+=$). The assignments in Table 134 are verified by selective ^{15}N-labelling and this has solved the controversy concerning their assignment (ref. 1, p. 210, and references therein). The large relative deshielding observed for the terminal nitrogen atoms in diazo moieties is also reproduced in diazonium cations (Table 135). This is opposite to the trend of the relative shieldings of the central and terminal atoms in azides (Section VI.M and Table 103), where the central atoms are usually less shielded. One should note that in one report[29] on the shielding of diazo compounds

there is a considerable error in the referencing of the shielding, as indicated in note (b) in Table 134.

When one compares the data in Table 134 with the shieldings of diazomethane [119] (ref. 1, p. 210, and references therein; assignments reversed in order to conform to the considerations mentioned above), a large deshielding, by about 50 ppm, is observed for the terminal atoms upon substituting the hydrogen atoms in diazomethane with phenyl groups. An analogous effect is observed when fused benzene rings are added to the structure of diazocyclopentadiene (Table 134).

$$CH_2{=}N^+{=}N^-$$

[119]

+95 ppm (=N^+=); −9 ppm (=N^-)

The shieldings of diazoketones $RC(=O)\text{–}C(R){=}N^+{=}N^-$ do not significantly differ from those of diazo compounds. The same applies to diazoesters $ROOC\text{–}C(R){=}N^+{=}N^-$, as is shown in Table 134. In the latter compounds, the rotation of the COOR moiety can give rise to *Z,E*-isomerism which has been observed in their nitrogen NMR spectra [Table 134; note (d)].

Nitrogen shieldings can simply distinguish between isomeric diazo moieties and diazirine rings [120] owing to the equivalence of the nitrogen atoms in the latter.

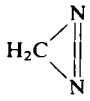

[120]

+47·5 ppm (Table 136)

The effects of substituents on the shieldings in *p*-substituted benzenediazonium cations (Table 135) can be simply accounted for[162] in terms of electron charge distribution, expressed by varying contributions from the resonance structures [121] to the actual structure. An increase in the

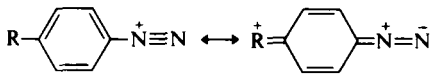

[A] [B]

[121]

electron-donating properties of R should cause the electron distribution to approach that of structure [B], which should thus result in changing the shielding to values characteristic of diazo moieties. This is actually observed in the data presented in Table 135 when compared with those in Table 134. In contrast to this the shieldings of the diazo moieties of cyano-substituted diazocyclopentadiene and diazo-diazacyclopentadiene (Table 134) are very similar to those of diazonium salts. This can be accounted

for[162] in terms of the dominant contribution of the electron charge distribution depicted by the structures [122] and [123], which resemble [A], to

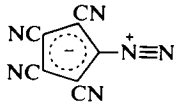

[122]

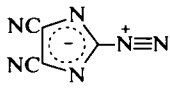

[123]

the actual structure of these compounds. One should be cautious, however, in employing such simple analogies. In particular, the effect on the shielding of diazo compounds produced by additional benzene rings, introduced either as phenyl substituents of diazomethane or as fused rings of diazocyclopentadiene, is just opposite to that expected for the structures given above (Table 134), i.e. deshielding is observed especially for the terminal nitrogen atoms. According to the simple theory considered, the benzene rings should assist in the delocalization of the excess electron charge over the hydrocarbon moiety, thus causing the electron structure of the NN moiety to resemble that of a diazonium ion. In order to rationalize this discrepancy, non-linear structures of the diazo moiety are invoked,[162] but this must be considered as pure speculation, at least in the absence of any clear supporting evidence from other sources.

In addition to the data in Table 134, nitrogen shieldings have been reported[340] for a number of organometallic derivatives of diazomethane (in deuterotoluene; 10·1 MHz; field perpendicular to sample tube; referred originally to neat aniline, +325·9 ppm from neat nitromethane; Table 37; conversion scheme II, Table 4; ^{15}N-enriched samples):

	Nitrogen shielding (ppm) ref. to neat $MeNO_2$			
$Me_3SiCH{=}N^+{=}N^-$	$=N^+=$	+102·0	$=N^-$	+38·6
$(Me_3Si)_2C{=}N^+{=}N^-$		+102·2		+38·9
$(Me_3Ge)_2C{=}N^+{=}N^-$		+110·9		?
$(Me_3Sn)_2C{=}N^+{=}N^-$		+117·9		+108·9
$(Me_3Pb)_2C{=}N^+{=}N^-$		+106·9		+104·0
$Me_2AsCH{=}N^+{=}N^-$		+100·9		+19·9
$(Me_2As)_2C{=}N^+{=}N^-$		+106·9		+52·9

The shieldings are greater than those for diazomethane (this section), but the largest changes occur for the terminal atoms. A comparison of the reactivity [124] of such organometallic derivatives of diazomethane with

$$R_2C{=}N^+{=}N^- + PR'_3 \rightarrow R_2C{=}N{-}N{=}PR'_3$$

[124]

phosphines[340] shows that the diazo derivatives, which are reactive, are characterized by differences between the shielding of the central and terminal nitrogen atoms of at least 50–60 ppm. This indicates that the

polarity of the diazo group rather than steric effects is probably responsible for the reactivity towards phosphines.

Y. Azo and azoxy compounds, azimines, triazenes, and related structures

The nitrogen nuclei of azo compounds RN=NR are usually strongly deshielded when compared with other nitrogenous compounds (Tables 13 and 136) except those containing nitroso type groups (Tables 138 and 140). There are two examples that depart significantly from the typical range of shieldings of azo moieties, namely the +47·5 ppm value for aziridine and the −618 ppm value for $Me_3SiN{=}NSiMe_3$ (Table 136). The latter compound reveals the greatest nitrogen deshielding that has so far been observed in diamagnetic compounds. If these two shieldings are included in the set of data for azo compounds, a roughly linear correlation of the shieldings is observed[38] with increase in wavenumber of the lowest-energy $n \rightarrow \pi^*$ transition in the corresponding UV spectra. However, the quality of the correlation critically depends on the inclusion of the two limiting values which deviate considerably from the other values; thus, only gross changes in the shieldings can be accounted for by this simple relationship.

The protonation of azo compounds [Table 136; note (a)] leads to a significant increase in the shielding, which is typical of nitrogen atoms in unsaturated systems with lone pairs that are not involved in the π-electron system (Section V.H). Azoxy compounds, which are *N*-oxides of azo compounds, also reveal a considerable shielding of their nitrogen atoms when compared with that of azo compounds (Table 136). This is in accord with the general rules given in Section V.H and with the observation of the nitrogen shielding in furoxans (Section VI.Q and Table 117). A similar increase in the shielding for the N=N moiety, when compared with that in azo compounds [125], is found in azimines [126] [Table 136; note (d)] which are structural analogues of azoxy compounds [127] in the sense that

Nitrogen shielding data for N=N groups

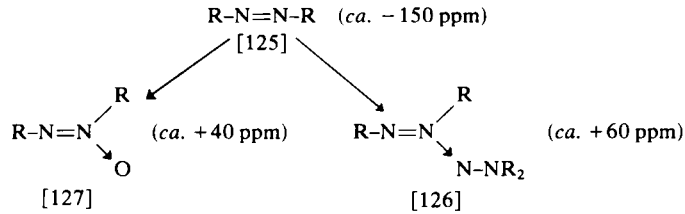

the azimine structure contains an N→N dative bond in place of the N→O bond in the azoxy structure. Since both of the atoms in the N=N moiety in azoxy compounds as well as in azimines show a considerable increase in shielding with respect to that of azo compounds, there arises the question

of the assignment of the shieldings. A study of azimines labelled with ^{15}N in their N=N moieties suggests,[329] on the basis of ^{15}N–^{1}H couplings and the quadrupolar relaxation effects of the ^{14}N nuclei in the remaining part of the nitrogenous chain, that the atoms in N=N bonded to the N–N moiety are characterized by a larger shielding (Table 136). This argument has subsequently been used in assigning the higher shieldings of azoxy moieties to the N→O groups.

Azoxy compounds that can exist as geometrical isomers show significant differences in shielding between the isomers (e.g. *cis*- and *trans*-azoxybenzene; Table 136).

In tetrazenes $R_2NN{=}NNR_2$ [128] the shielding of the azo moiety (N=N) is higher by about 100 ppm than that of azo compounds (Table 136), but the nuclei involved are still considerably deshielded when compared with nitrogen nuclei in other diamagnetic compounds (Table 13). The shielding of the amino moiety NR_2 is typical of enamino structures (Table 27).

R_2N–N=N–NR_2 [128]

−25 to −40 ppm (N=N)
+280 to +310 ppm (NR_2)

In triazenes one should separately consider two possible structures ([129] and [130]) for which the common name is used. The shielding values for

		$\overset{(1)}{R}\text{–}\overset{(2)}{N}{=}\overset{(3)}{N}\text{–}NR'_2$ [129]	$\overset{(1)}{R}\text{–}\overset{(2)}{N}{=}\overset{(3)}{N}\text{–}N{=}R'$ [130]
Nitrogen shielding ranges	N-1	+20 to +33 ppm	−24 to −43 ppm
	N-2	−65 to −75 ppm	−68 to −105 ppm
	N-3	+215 to +230 ppm	*ca.* +92 ppm

the amino-azo type [129] are taken from Table 136 and ref. 1, p. 209, and references therein, for compounds where R = *p*-substituted phenyl and R′ = Me; the assignments for N-1 and N-2 are tentative, based on the effects of *para*-substituents (OMe, Cl, NO_2) on the shielding.[76] The values for the imino-azo type [130] are based on a study[30] of ^{15}N selectively and

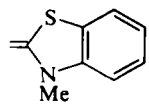

[131]

totally labelled compounds where R = *p*-substituted phenyl and R′ is given by [131]. The study also includes cations [133] derived from the triazene structure [132]. The shieldings are referred to neat nitromethane, but some complications are involved in their recalculation from the original data;[30] the ^{15}N spectra (9·12 MHz) were referred originally to saturated aqueous

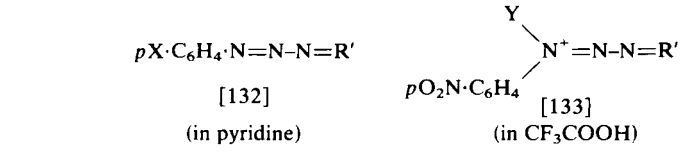

		X=H	X = OMe	Y = H	Y = Et
cis-isomers	N-1	−27·1 ppm	−23·8 ppm		
	N-2	−77·2	−70·8		
	N-3	+91.6	+92·2		
trans-isomers	N-1	−43·1	−43·4	+174·4 ppm	+159·1 ppm
	N-2	−105·0	−96·8	−68·4	−69·1
	N-3	+91·5	+92·7	+56·7	+62·2

KNO_2 (−228·9 ppm from neat nitromethane; Table 6), but the results were reported as deshieldings from saturated NH_4Cl in acidified H_2O whose shielding relative to KNO_2 was measured to be 590·7 ppm. This gives a shielding of +361·8 ppm for the latter relative to nitromethane; this value has been used in the recalculation, but it differs by about 10 ppm from the values for NH_4Cl given in Table 6. Thus, there is some uncertainty about the calibration procedure and the standards used in the original report. Nevertheless, the data clearly show that protonation of the imino-azo type of triazene structure occurs at N-1.

Azo compounds can be involved in tautomeric equilibria with hydrazone type isomers, such as presented in Table 137. Since there are large differences in the nitrogen shieldings between azo compounds and hydrazones (Tables 13, 45, 136, and 137), the shieldings observed for potentially tautomeric systems involving these structures should provide a facile measure of the tautomerization equilibrium constants. However, the situation is not so simple, since the shieldings in model compounds (Table 137) show large effects due to internal hydrogen-bonding.[331] Therefore it is not possible to approximate the shieldings in the actual tautomers by those in the corresponding analogues where the NH and OH groups are replaced by NMe and OMe respectively. A very interesting solution of the problem has been recently offered.[331] The method employs model compounds that are not simple derivatives of the tautomers concerned. They correspond closely, however, to the hydrogen-bonded structures of the tautomers (Table 137). Their nitrogen shieldings over a wide range of temperatures indicate that they do not tautomerize to any significant extent. The assumed models look quite arbitrary, but the example in Table 137 provides an internal check for the calculation of the tautomeric equilibrium since two nitrogen shieldings can be used independently for this purpose.

The observation of chemically induced dynamic nuclear polarization effects in the ^{15}N NMR spectra of some azo compounds undergoing thermal decomposition is presented in Table 9 and Section IV.H.

Z. Nitroso compounds, nitrosoamines, and nitrites

The nitrogen nuclei of nitroso groups (Tables 13, 138, and 140) are characterized by large deshieldings when compared with those of other diamagnetic systems. It is therefore quite simple to identify such groups by means of shielding data. There are also considerable differences in the shielding between *N*-nitroso [134], *O*-nitroso [135], and *C*-nitroso [136]

			Nitrogen shielding range
[134]	$R_2N-N=O$	nitrosoamines	+110 to +160 ppm (R_2N) −175 to −150 ppm (N=O)
[135]	R–O–N=O	covalent nitrites	*ca.* −190 ppm
[136]	R–N=O	nitrosoalkanes and aromatic nitroso compounds	−580 to −430 ppm

groups. The relatively small shielding of the NR_2 groups in nitrosoamines when compared with that of triazenes ($RN=NNR_2$; Section VI.Y), hydrazones ($R_2C=NNR_2$; Table 45), and amides ($RCONR_2$; Tables 14, 57, 59), can be explained, at least in part, by the considerable delocalization of the lone pair from the NR_2 moiety over the N–N=O system of a nitrosoamine. This is reflected in the rather high barrier to internal rotation (*ca.* 90–100 kJ mol^{-1}; ref. 45 and references therein) about the N–N bonds in nitrosoamines [137]. The same effect is probably responsible for the

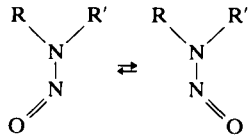

[137]

rather high shielding of the nitroso groups of nitrosoamines when compared with *C*-nitroso compounds (Tables 138 and 140). For some unsymmetrically substituted nitrosoamines, it is possible to observe a separate shielding for the *E* and *Z* isomers (Table 138), but the difference between them is often small. The effect of alkyl groups on the shielding in the NR_2 moieties of nitrosoamines follows the general rules described in Section V.F. Since the effects are not connected with the delocalization considered above, there is no correlation between the NR_2 shielding in nitrosoamines and the barrier to internal rotation within this class of compounds. However, the NMe_2 moieties in different classes of structures that contain $=N-NMe_2$ systems can be compared from the point of view of shielding and rotational barrier:[45]

Structure	Nitrogen shielding (ppm) for NMe_2	Free enthalpy of activation of NMe_2 rotation (kJ mol^{-1})	N–N bond length (Å)
Me_2N–N=O	*ca.* +150	96	1·344
Me_2N–NO_2	*ca.* +218	(62)?	1·382
Me_2N–N=NPh	*ca.* +225	57	(1·393)?
Me_2N–N=CHR	*ca.* +282	(31)?	1·43
Me_2N–NH_2	*ca.* +323	(12)?	1·45

The values in parentheses are predicted,[45] as far as the shieldings are concerned, from the least-squares linear correlation fit with the barrier height for a rather limited set of molecules, including Me_2N–NO and a few triazenes of the Me_2N–N=NPh type. The set seems, however, to be too small (only two types of structure are involved) to justify the extrapolation made. A somewhat better situation exists for predicting the N–N bond length in the triazenes from a consideration of the above data.

One should note some discrepancy between the shieldings in Me_2NNO and Et_2NNO (Table 138), as measured from ^{15}N [note (b)] and ^{14}N spectra [note (a)]. This comes, most probably, from bulk susceptibility effects on the ^{15}N measurements where $Cr(acac)_3$ is added[45] to the samples, according to considerations discussed in Section III; the ^{14}N data do not contain such effects, as indicated in note (a) in Table 138.

The protonation of nitrosoamines leads to cations (Tables 138 and 139) which are characterized by smaller differences in the shielding between their R_2N and =N–OH moieties than those between R_2N and N=O in the parent nitrosoamines. The observation of changes in the shielding of dimethylnitrosoamine upon addition of CF_3COOH and FSO_3H (Table 139) is used[45] for calculating the shielding of the cations and the equilibrium constant for protonation.

The nitrogen shielding in ethyl nitrite Et–ONO can be considered to be representative of alkyl nitrites, since only weak effects are expected upon exchanging the ethyl group for other alkyls. This can be inferred from the negligible difference between the alkyl nitrates $MeONO_2$ and $EtONO_2$ (Table 133). There is a large difference between the shielding of nitroalkanes R–NO_2 (Table 133) and that for the isomeric structure of an alkyl nitrite R–O–N=O (Table 140).

In nitrosoalkanes R–NO the shielding of the NO group occurs within the rather narrow range of −560 to −580 ppm (Table 140) provided that there are no substituents other than alkyl groups on the C-α atoms. In conjugated nitroso compounds, the small amount of data available indicates that substituents on the conjugated rings can severely affect the shielding,

as shown by the difference of about 100 ppm between the values for nitrosobenzene and *p*-methoxy-nitrosobenzene (Table 140).

Conjugated nitroso compounds that contain OH groups in positions *para* or *ortho* to NO can be involved in tautomeric equilibria with quinone-oxime structures (Section VI.U), and since there is a large difference in the shielding between the tautomeric species they can be used in an estimation of the relevant tautomerization equilibrium constants.

The nitrite ion NO_2^- shows some deshielding of its nitrogen nucleus when compared with that in ethyl nitrite (Table 140). This is analogous to the difference in the shielding between alkyl nitrates and the nitrate ion NO_3^- (Table 133).

The difference in the shielding between the isomeric nitro and *O*-nitroso (nitrito) structures is also present in the corresponding ionic species (Table 141), as has been shown[333] for the reactions [138] and [139].

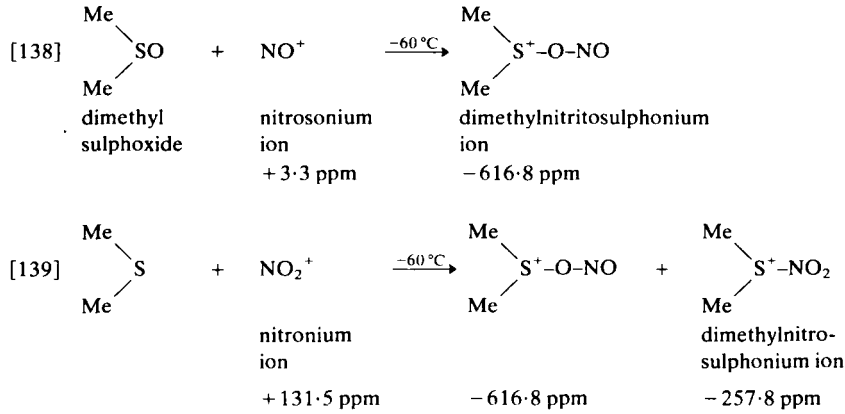

AA. Dinitrogen and its complexes

The shielding of N_2 molecules is interesting from the point of view of an absolute scale of nitrogen screening constants (Section V.B, also Section II.A). In addition, *ab initio* theoretical calculations can be carried out only for relatively simple molecules such as N_2. The anisotropy of the solid N_2 shielding tensor is reported[109] to be 603 ± 28 ppm. This agrees satisfactorily with earlier estimates[1] and with the value of 566·82 ppm given in Table 1 as a result of some INDO/S parameterized calculations.[18] Recent data on the shielding of N_2 (Table 142) can contain systematic errors of a few ppm due to the calibration procedures involved. Some of the data [notes (a), (b), and (d)] refer to solutions at low temperatures, for which the calibration was probably carried out by the sample replacement method, using aqueous $NaNO_3$ or HNO_3 as reference. For the measurement of gaseous N_2 [note

(c)], neat nitromethane containing some $Cr(acac)_3$ was employed as an external standard. This can result in significant bulk susceptibility effects, much larger than those calculated from equation (14) employing values of volume susceptibilities given in Table 5.

The ^{15}N spectra of some complexes of N_2 with molybdenum and tungsten (Table 142) clearly show the inequivalence of the nitrogen atoms in the N_2 ligands. The assignment of the shielding to metal-bound and terminal nitrogen atoms is tentative (N-α denotes metal-bound atoms), since it is based on the assumption of a larger absolute value for ^{15}N–^{31}P coupling across two bonds than across three bonds.[330] In a binuclear complex of zirconium with N_2 [Table 142; note (d)], the shieldings are compatible with the structure of the complex in the solid state as determined by X-ray methods.[332] Since $^{15}N_2$ molecules are studied, the assignments are based on the observation of ^{15}N–^{15}N couplings for the terminal N_2 ligands and a singlet signal for the central N_2 moiety. At temperatures above +12 °C, the resonances of the terminal ligands show dynamic broadening and they collapse at about +50 °C, indicating a dissociation–association process which probably occurs through free N_2 molecules [140]. An analysis of the dynamic ^{15}N NMR spectra of the complex in toluene solution yields[332] rate constants for the exchange and an activation energy of about 50 kJ mol^{-1}.

$$\text{M–N}\equiv\text{N} \rightleftarrows \underset{(+\text{M})}{\text{N}\equiv\text{N}} \rightleftarrows \text{N}\equiv\text{N–M} \qquad [140]$$

BB. Some miscellaneous complexes containing nitrogenous ligands and some free radicals

Nitrogen shielding provides a simple distinction between the "singly bent" and "doubly bent" structures of diazenido ligands,[334] as shown in Table 143. The protonation of a doubly bent ligand leads to a considerable increase in the shielding involved, following the rules described in Section V.H.

The data for a number of ammino (NH_3) and nitrosyl (NO) complexes of Co, Ru, and Os [Table 144; notes (a) and (b)] indicate that the two ligands can be simply distinguished by means of nitrogen shielding, but the accuracy of most of the results reported is too low for any correlation with the structure of the complexes to be made.

The shielding of the n-hexylamine ligands in complexes with Pt and Pd [Table 144; note (c)] of the general formula [141] shows significant changes upon changing the ligand R. There is a good linear correlation between the shielding of Pt complexes and that of the corresponding Pd complexes. The correlation may be useful for investigations of the structure of the

palladium complexes, since metal–ligand coupling constants are not observed in the spectra of the latter[337] while they are available for the Pt complexes. There seems also to be a significant difference between the shielding of the amine ligand for the isomeric complexes with R in the *trans* or *cis* position relative to the amine ligand. If we compare the data for the complexes considered with a value of +360 ppm which is characteristic of straight-chain primary amines (Table 17), the complexation induces changes in the shielding which can be of either sign, depending on the substituent R.

$$(R)XCl_2(\text{n-hexylamine}) \qquad X = Pt \text{ or } Pd$$

[141]

In rhodium(III) complexes with diaminoalkane ligands and aza-aromatic ligands [Table 144; note (d)], an increased shielding is observed relative to the free ligands[125] [Table 17, note (i); Table 122, note (h)].

The data for some cyclopentadienyl-nitrosyl complexes of Cr, Mo, and W, which have the general structure shown in Table 144 [data corresponding to note (e)], indicate that the shielding of NO increases with an increase in the atomic weight of the metal.[338]

In the Pb(II) complex of 1,4,8,11-tetraazacyclotetradecane [Table 144; note (f)], the NH ligands are known to occupy pairwise the non-equivalent positions around Pb(II); this is clearly reflected in the nitrogen shieldings.[339]

Investigations of imidazole in aqueous solutions containing zinc(II)[275] and cadmium(II)[419] ions have been reported. Hexacoordination is found in the zinc(II) solutions and tetracoordination in the case of cadmium(II) ions. Upon coordination with zinc(II) the imidazole nitrogen shielding increases by 10–20 ppm; the corresponding increase is 8–12 ppm in the case of cadmium(II).

The ^{14}N spectrum of the hexanitrocobaltate(III) ion shows that a time-dependent decomposition of the ion leads to the production of a cobalt(II) complex and nitrate ion in the solution.[420] It appears likely that this decomposition is responsible for the misassignment of the ^{14}N spectrum of this ion by earlier workers.[421] The value of $^{1}J(^{59}Co–^{14}N)$ is estimated to be 46 ± 4 Hz. In the light of these findings on hexanitrocobaltate(III) it would seem to be reasonable to re-examine the conclusions drawn from a previous ^{14}N study on the nitro complexes of platinum and palladium.[421]

The induced ^{14}N chemical shifts observed in aqueous thiocyanate solutions, in the presence of praseodymium(III), neodymium(III), europium(III), terbium(III), dysprosium(III), holmium(III), and ytterbium(III) ions, are reported to be due to contact interactions.[422] The dependence of the shifts upon thiocyanate ion concentration suggests the formation of inner-sphere complexes.[422] Solvent effects on the ^{15}N spectrum of 1-methylsilatrane have been investigated for a variety of solvents. A range of induced shifts of about 12 ppm is reported.[423]

Direct dipole–dipole coupling between ^{207}Pb and ^{14}N has been reported for a single-crystal of lead nitrate.[424] This coupling results in a linewidth dependence on orientation for the ^{207}Pb signal which may be used to assign the ^{207}Pb signals to the different sites in the cubic unit cell of lead nitrate.

A well resolved splitting of the ^{14}N signal of some non-stoicheiometric cubic manganese nitrides has been reported.[425] The splitting decreases with increasing temperature and is attributed to the presence of nitrogen vacancies in the lattice.

Studies on methyl isocyanide complexes of gold(I), palladium(II), platinum(II), and platinum(IV) show that the ^{14}N chemical shifts of the complexed ligands fall almost equally either side of that of the free isocyanide.[432] It appears that the shifts are more sensitive to the substitution of *cis*-halides than to those in the *trans* position.[432]

A ^{14}N NMR investigation of α,α-diphenyl-β-picrylhydrazyl (DPPH) has revealed a hyperfine splitting constant of $-0{\cdot}042 \pm 0{\cdot}005$ mT for the nitro group.[426] For such small ^{14}N splittings in free radicals the NMR method appears to have advantages over ELDOR, ENDOR, and triple-resonance techniques.

The nitrogen ENDOR lines of ^{15}N-labelled DPPH are readily detected.[427] When taken together with NMR, ESR, and triple-resonance results, the ENDOR data provide a consistent description of the electronic structure and dynamic processes of DPPH. ^{14}N ENDOR data are available for single-crystals of silver(II)- and copper(II)-tetraphenylporphyrin[428] and for single-crystals of X-irradiated hippuric acid,[429] oxovanadium(IV)-porphyrin in solid solution,[430] and Coppinger's radical both in isotropic solution and in liquid crystals.[431]

VII. CORRELATION OF NITROGEN SPIN–SPIN COUPLINGS WITH MOLECULAR STRUCTURE

Problems concerning the magnitudes, signs, and structural correlations of spin–spin couplings between ^{15}N and other nuclei have already been considered in detail.[1,2,4] Nitrogen coupling constants, until recently, have been mostly measured from the spectra of ^{15}N-coupled nuclei. With the advent of NMR spectrometers that employ high magnetic fields and large-bore sample containers, it has become feasible to measure ^{1}H-coupled ^{15}N spectra within reasonable accumulation times, even at the natural-abundance concentration of ^{15}N. The same applies to the spectra of ^{15}N nuclei which are coupled to other nuclei with a spin of 1/2, provided that the latter are either abundant in nature or introduced as labels.

Spin–spin couplings of ^{14}N with other nuclei are observed only occasionally, because of the rapid quadrupolar relaxation of ^{14}N nuclei in most

molecules. Where available, couplings involving ^{14}N can be converted to the corresponding ^{15}N coupling constant by using the equation

$$J(^{15}N\text{–}X) = -1{\cdot}4027J(^{14}N\text{–}X) \quad (30)$$

Thus, only ^{15}N coupling constants are considered here. Spin–spin couplings involving ^{15}N play an important role in the application of nitrogen NMR to the structure determination of nitrogen-containing molecules, since their values are often characteristic of the character and number of intervening bonds between the nuclei concerned. Multiplet patterns which result from the couplings, which can be observed in undecoupled ^{15}N spectra (occasionally also in ^{14}N spectra) often provide a means of unambiguously assigning the resonance signal and the corresponding shielding to individual nitrogenous moieties in molecules. It is convenient therefore to classify ^{15}N couplings $^{n}J(^{15}N\text{–}X)$ according to the coupled nuclei X and the number n of intervening bonds.

A. $^{1}J(^{15}N\text{–}^{1}H)$

The couplings across one bond between ^{15}N and ^{1}H are negative, and their absolute magnitudes are considerably larger than those of $^{15}N\text{–}^{1}H$ couplings across more bonds.[1,2,4] Recent values of one-bond NH couplings for a number of molecules and ions are presented in Table 145. The simplest application of one-bond NH couplings to nitrogen shielding assignments is concerned with the corresponding multiplet patterns in proton-coupled nitrogen NMR spectra which allow one to identify the resonance signals of NH_3^+, NH_2 (or NH_2^+), and NH (or NH^+) moieties, provided that intermolecular proton exchange is sufficiently slow. Numerous examples of such applications can be found in Section VI and the corresponding tables. If protons are exchanged within the same molecule, as is the case with some porphyrins (Table 116; references 283 and 284), the observed value of the coupling represents a weighted average which includes the couplings with a given proton at the other sites of residence. Since the absolute values of $^{15}N\text{–}^{1}H$ couplings across more than one bond are much smaller than that across one bond, the apparent $^{1}J(^{15}N\text{–}^{1}H)$ is reduced significantly in such systems. This reduction in magnitude is indicative of the intramolecular exchange of protons. A good example of this phenomenon is provided by the ^{15}N spectra of ^{15}N-labelled octaethylporphyrin [142] in $CDCl_3$.[283,284] At $-53\,°C$, the spectrum contains a singlet and a doublet split by 98 Hz; the latter value is typical of $^{1}J(^{15}N\text{–}^{1}H)$ in pyrrole type systems. At $+28\,°C$, only a quintet is observed, split by 24 Hz, which is almost a quarter of the spacing at low temperatures. This indicates that the NH protons are exchanged among the four nitrogen atoms, and the long-range N–H couplings are close to zero.

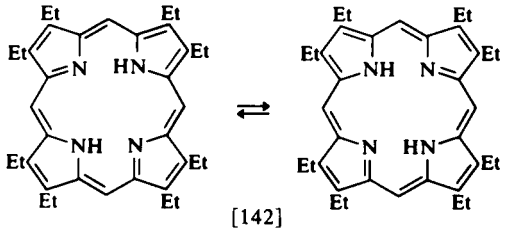

[142]

If major structural differences between molecules are considered, the corresponding $^1J(^{15}N-^1H)$ values often show a reasonable correlation with the amount of s-character of the N–H bonds involved, but notable exceptions are known.[2] Thus it is generally unsound to try and estimate the s-character of an N–H bond from the $^1J(^{15}N-^1H)$ data. However, such a correlation, which actually represents the dominating contribution of the contact term to the coupling in numerous cases (Section II.B), makes

Structure	Approximate character of N–H bond	Approximate value of $^1J(^{15}N-^1H)$ (Hz)
Alkylamine	sp^3–s	*ca.* −65
Arylamine	sp^2–s	−80 to −90
 (pyrrole type structures)	sp^2–s	*ca.* −95
Alkylammonium and arylammonium ions	sp^3–s	*ca.* −75
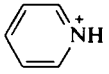 (pyridinium type ions)	sp^2–s	*ca.* −96
$R-C\equiv\overset{+}{N}-H$ (nitrilium ions)	sp–s	*ca.* −135
$R_2C=NH$ (ketimines)	sp^2–s	*ca.* −50 (anomalously low)
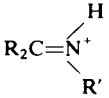 (immonium ions)	sp^2–s	*ca.* −91 (typical of sp^2–s bond)
R–C(=O)–NHR′ (amides)	sp^2–s	*ca.* −90

possible a simple distinction between a variety of structures on the basis of $^1J(^{15}N-^1H)$ values. The values quoted are based on those in Table 145 and in references 1, 2, and 4.

A rather high absolute value of $^1J(^{15}N-^1H)$, (−)86·7 Hz, is found[341] in the amino NH group which links two carbohydrate ring systems in bis(methyl-2-*O*-acetyl-4,6-*O*-benzylidene-3-deoxy-α-D-altropyranosid-3-yl)amine; this is accounted for in terms of steric repulsions which may have resulted in a flattening of the bonding arrangement in the amino moiety.

In a study of pyrrole and its substituted derivatives[280] no evident changes in the $^1J(^{15}N-^1H)$ values are observed upon a change in solvent, temperature, or concentration. This has been used as an argument against any appreciable tautomerization [143] of acetylpyrroles into the isomeric imino form.

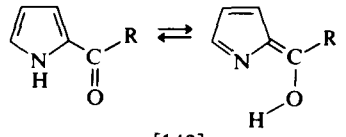

[143]

The data in Table 145 show that there is a small but regular difference between the $^1J(^{15}N-^1H)$ values for *trans*- [144] and *cis*-amide [145] structures, but this difference seems to largely vanish in polyamides dissolved in CF_3COOH.[198]

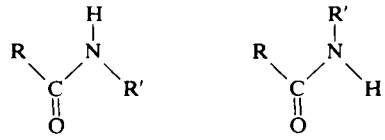

[144] [145]

$|^1J(^{15}N-^1H)| > |^1J(^{15}N-^1H)|$

The $^1J(^{15}N-^1H)$ couplings of α-amino-acid *N*-carboxyanhydrides (Table 145; ref. 185) are significantly stronger than those of amido type structures. This is interesting, since they contain *cis*-amide type moieties, which are usually characterized by weaker N–H couplings than the corresponding *trans*-forms.

Since absolute values of $^1J(^{15}N-^1H)$ are of the order of about 100 Hz, the collapse of multiplet patterns of NH moieties in ^{15}N NMR spectra can be used for monitoring proton exchange processes which occur at rates of the order of 100 s^{-1}. This has actually been done for ureas,[180] lactams,[191] arginine,[66] and histidine.[276]

B. $^2J(^{15}N-^1H)$

The two-bond $^{15}N-C-^1H$ couplings across a saturated (tetracoordinate) carbon atom are quite small in absolute magnitude, and the data in Table 146 indicate that they are generally positive in sign. It is known[2] that such couplings reveal a dependence of the orientation of the lone pair electrons on the nitrogen atom with respect to the C–H bond. The largest values are observed when the bond is *cis* to the lone pair.[2] This explains the differences in the $^2J(^{15}N-^1H)$ couplings observed in alumichrome (Table 146; ref. 356). Attention is drawn to the small values of $^2J(^{15}N-^1H)$ in silatranes (Table 146, ref. 124, and Table 29 for the geometry of their structures), where the lone electron pair is involved in a dative bond to Si, and the relevant dihedral angle is about 120°. If the intervening atom is N or O, the corresponding $^2J(^{15}N-N-^1H)$ and $^2J(^{15}N-O-^1H)$ couplings are also small (Table 146; refs 77 and 357), comparable in value to the $^2J(^{15}N-C-H)$ coupling across a saturated carbon atom.

The situation is quite different when the intervening carbon atom is tricoordinate as in [146] and [147]. The two-bond couplings across a carbonyl carbon atom [146] are quite large (Table 146; ref. 373) in absolute magnitude and can be distinguished easily from the coupling across a saturated carbon atom.

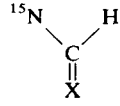

[146]

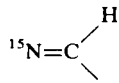

[147]

When the coupling occurs in an imino type moiety [147], which also includes those in the aza-aromatic systems of azines and azoles, the values of $^2J(^{15}N=C-^1H)$ depend critically on the structure of the bonds at the nitrogen atom involved, as is shown in Tables 146 and 147. If N is a pyridine type nitrogen atom or, generally, one with a lone pair of electrons (in imines, oximes, etc.), the coupling is large and negative. In addition its absolute value decreases significantly upon protonation of the lone pair. An even more dramatic change occurs when an *N*-oxide is formed, since the coupling can take a small positive value. Quite analogous observations have been made for conjugated cyclic lactams of the uracil type (Table 146; ref. 355). The coupling is large (in absolute magnitude) if N bears a lone pair, as is the case in the anion of 3-methyluracil, but it is reduced considerably in the parent molecule where a hydrogen (or deuterium) atom is attached to N. In azole systems, the two-bond N=C–H coupling is stronger for pyridine type nitrogen atoms than for pyrrole type nitrogen

atoms where the lone pair is involved in a delocalized π-electron system (Table 146; refs. 208, 209, 276, 277).

C. $^3J(^{15}N–^1H)$

In saturated systems, the coupling across three bonds ($^{15}N–C–C–^1H$) can be larger in absolute magnitude than that across two bonds.[2] However, the former depends on the dihedral angle between the N–C and C–H bonds, and should attain a maximum absolute value for 0° (*cis* arrangement) and 180° (*trans* arrangement), and a minimum at about 90°. Thus, in the *gauche* arrangement where the angle is about 60°, rather small absolute values of $^3J(^{15}N–^1H)$ are expected. All this is corroborated by the recent data presented in Table 148 (references 367–369). A number of equations have been suggested which relate the dihedral angle to $^3J(^{15}N–C–C–^1H)$. The data for ammonium ions (Table 148; ref. 369) have been fitted to a three-parameter function

$$^3J(^{15}N–C–C–^1H) = A + B\cos\phi + C\cos(2\phi) \qquad (31)$$

where ϕ is the dihedral angle, and the following values are obtained (the actual values refer to the coupling of ^{14}N, and are recalculated here to ^{15}N couplings):

$$A = 1{\cdot}98 \qquad B = -0{\cdot}79 \qquad C = 2{\cdot}12$$

which yield a standard deviation of about 0·3 Hz between the observed and calculated couplings.[369] Somewhat different equations are suggested for $^3J(^{15}N–C–C–^1H)$ couplings in amino acids,[367,368,804] those of the type

$$^3J(^{15}N–C–C–^1H) = A\cos^2\phi + B\cos\phi + C \qquad (32)$$

For ornithyl residues in alumichrome,[804] the values of the parameters are found to be

$$A = -4{\cdot}4 \qquad B = 1{\cdot}2 \qquad C = 0{\cdot}15$$

but the $^3J(^{15}N–^1H)$ couplings between different amino acid residues (those across a carbonyl carbon atom) are not fitted into such a scheme. This is in contrast with the suggested relationships (ref. 1, p. 224, and references therein) between the dihedral angles and $^3J(^{15}N–^1H)$ data in the systems [148]. However, one should remember that in establishing or evaluating

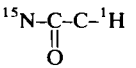

[148]

such correlations, the values of the angles are often taken from crystallographic data and the latter do not necessarily correspond to those in solution.

The three-bond ^{15}N–^{1}H couplings in unsaturated systems, including aza-aromatic structures, do not differ appreciably in absolute magnitude from those in saturated systems. This is clearly different from the situation with $^{2}J(^{15}N$–$^{1}H)$ values (Tables 146 and 147). Thus, in pyridine ring systems, and in azoles (Table 148), the absolute values of $^{3}J(^{15}N$–$^{1}H)$ are smaller than those of the corresponding $^{2}J(^{15}N$–$^{1}H)$ but this is reversed in the derived cations and *N*-oxides. It should be noted that there are opposite trends between the $^{3}J(^{15}N$–$^{1}H)$ and $^{2}J(^{15}N$–$^{1}H)$ data in the following set of aza-aromatic systems:

	$^{3}J(^{15}N$–$^{1}H)$ (Hz)	$^{2}J(^{15}N$–$^{1}H)$ (Hz)
Pyridine	−1·48	−10·8
Pyridinium ion	−3·98	−3·0
Pyridine *N*-oxide	−5·32	+0·5

In azole ring systems, the $^{3}J(^{15}N$–$^{1}H)$ results are often comparable to those across only two bonds (compare Tables 148 and 146). Thus, in aza-aromatic ring systems, the assignment and interpretation of $^{3}J(^{15}N$–$^{1}H)$ data are not straightforward.

The $^{3}J(^{15}N$–$^{1}H)$ coupling in the systems [149], which can be found in imines and oximes, shows some effect of the geometrical relation between

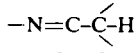

[149]

the lone pair on the nitrogen atom and the position of the CH moiety (Table 148; refs 357, 363, and 365). When the CH moiety is *cis* to the lone pair [150], the coupling is always stronger (in absolute magnitude) than that in the isomeric *trans* arrangement of the CH moiety and the lone pair [151]. These observations are useful for the identification of *Z* and

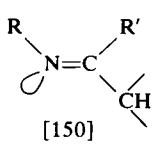

[150]

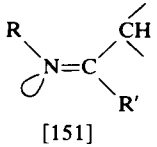

[151]

$^{3}J(^{15}N{=}C{-}C{-}^{1}H)$ *ca.* −4 Hz *ca.* −2 Hz

E isomers of oximes and imines by means of $^{3}J(^{15}N{=}C{-}C{-}^{1}H)$ couplings, in spite of the fact that the difference seems to be small, since the available data (Table 148) show that the individual values do not depart significantly (±0·5 Hz) from the approximate values given above. The effect of the lone

pair orientation relative to the CH moiety is even more pronounced in oxaziridine ring systems (Table 148; ref. 363). The difference almost vanishes when the lone pair is replaced by a bond to an oxygen atom, as is shown for isomeric nitrones [152] and [153] (Table 148; ref. 363) where

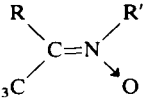

[152]

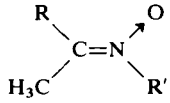

[153]

$^3J(^{15}N{=}C{-}C{-}^1H)$ −3·4 Hz −3·2 Hz

R = 4-nitrophenyl and R′ = t-butyl. The same lack of significant differences between the three-bond $^{15}N{=}N{-}C{-}^1H$ couplings is found (Table 148; ref. 263) in *aci*-nitro isomers of nitramines [154] and [155] where R = methyl and the nitrogen atoms involved in the coupling do not bear lone pair electrons.

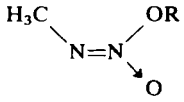

[154]

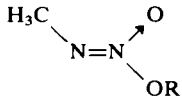

[155]

$^3J(N{=}N{-}C{-}H)$ (−?)5·3 Hz (−?)5·3 Hz

The data available in Table 148 suggest that the $^3J(^{15}N{-}^1H)$ couplings should be negative and some doubts may arise only for those with absolute values close to zero.

D. $^{15}N{-}^1H$ coupling across more than three bonds

Some long-range $^{15}N{-}^1H$ couplings have been observed recently in conjugated systems (Table 149). In pyridine, its cation, and its *N*-oxide, the couplings across four bonds are small and positive, and show an increase in this order; thus, the trend is in the same direction (an algebraic increase) as that observed in the corresponding $^2J(^{15}N{-}^1H)$ couplings (Section VII.B). However, in pyridazine (ref. 1, p. 226, and references therein), the $^4J(^{15}N{-}^1H)$ coupling is negative, −0·367 Hz.

The four-bond and five-bond $^{15}N{-}^1H$ couplings in nitrobenzene (Table 149) are small and negative. They are of the same sign and magnitude as those found in nitropyrroles (ref. 1, p. 226, and references therein).

E. $^1J(^{15}N{-}^{13}C)$

One-bond $^{15}N{-}^{13}C$ couplings have been reported to occur within the range from +4·9 Hz (an oxaziridine derivative) to −77·5 Hz (2,4,6-trimethylbenzonitrile *N*-oxide), but they are usually negative in sign and

absolute magnitudes do not normally exceed 35 Hz.[413] There have been attempts to correlate $^{1}J(^{15}N-^{13}C)$ data with the amount of s-character of the N–C bonds involved, but further studies tend to discourage such attempts.[1,2,413] Generally, the absolute magnitude of carbon–nitrogen couplings across one bond (Table 150) is larger than those for the coupling across more bonds (Table 151), and this may tempt investigators to use the couplings for the localization of direct N–C bonds in ^{13}C-labelled compounds. However, the procedure can be misleading, since some $^{1}J(^{15}N-^{13}C)$ coupling values can be close to zero, and smaller (in absolute magnitude) than the corresponding long-range couplings. Such exceptions are found when the nitrogen atoms involved bear lone pairs with considerable s-character.[413] These include pyridine type nitrogen atoms in azines and azoles, and imino type nitrogen atoms in imines and oximes. For pyridine (Table 150; ref. 359) the $^{1}J(^{15}N-^{13}C)$ coupling is $+0{\cdot}62$ while $^{2}J(^{15}N-^{13}C) = +2{\cdot}53$ and $^{3}J(^{15}N-^{13}C) = -3{\cdot}85$ Hz (Table 151). Similarly, the coupling between 3-N and 4-C in *N*-methylimidazole (Table 150; ref. 276) is only $+0{\cdot}9$ Hz. In *N*-phenylpyrazole (Tables 150 and 151; ref. 277), the coupling between 2-N and 3-C is $(\pm)1{\cdot}2$ Hz while that between 2-N and 4-C is larger in absolute magnitude. As far as imines are concerned, recent examples show (Table 150; ref. 389) that in [156] derivatives with substituents on the *C*-phenyl ring, the $^{1}J(^{15}N=^{13}C)$ couplings are larger in

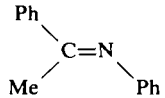

[156]

absolute magnitude than 5 Hz (contrary to reports in ref. 413), but the $^{1}J(^{15}N-^{13}C)$ coupling which involves the adjacent carbon atom of the *N*-phenyl ring is small, i.e. about 1 Hz. In oximes (Tables 150 and 151; refs 64, 69, and 390), the absolute values of the $^{1}J(^{15}N=^{13}C)$ couplings are about 4 Hz, but some of the corresponding $^{2}J(^{15}N=C-^{13}C)$ data are larger.

An attempt has been made to detect $^{13}C-^{15}N$ units by the corresponding $^{1}J(^{15}N-^{13}C)$ data in adenine obtained by simply heating formamide with hydrogen cyanide.[387] When doubly labelled $H^{13}C^{15}N$ is used, three such units are detected (Table 150; ref. 387) in the adenine obtained, but when doubly labelled formamide $H^{13}CO^{15}NH_2$ is employed, no detectable $^{1}J(^{15}N-^{13}C)$ couplings are observed in the product. This is used as an argument in favour of a thermal fission and re-formation of the C–N bonds in formamide molecules in the process examined. The latter conclusion has been strongly criticized[386] using arguments based upon the fact that $^{1}J(^{15}N-^{13}C)$ values can be quite small in some instances, and experimental

data for adenosine are reported which show that some of the $^{1}J(^{15}N-^{13}C)$ couplings are undetectable (no coupling of 2-C is detected with two adjacent N atoms, and only one of the couplings of 8-C has been measured, either with 7-N or 9-N). The same should apply to the reported lack of measurable $^{1}J(^{15}N-^{13}C)$ data in purine obtained from doubly labelled formamide.[417] However, experiments with doubly labelled [^{13}C,^{15}N]formamide diluted with non-labelled formamide and heated to +164 °C show that thermal fission and recombination of the C–N bonds takes place,[416] since in the ^{13}C spectra taken at different times there is a decrease in the intensity of the resonances that reveal $^{15}N-^{13}C$ coupling and an increase in the intensity of singlet peaks.

Nevertheless, one should be wary of the limitations inherent in the use of $^{1}J(^{15}N-^{13}C)$ data for the detection of C–N bonds, especially when arguments are based on the absence of measurable couplings. In spite of the limitations, there have been numerous applications of $^{1}J(^{15}N-^{13}C)$ couplings in the identification of various structural fragments in molecules. The observation of $^{1}J(^{15}N-^{13}C)$ couplings in the benzylation products of 8-methylthioimidazo[4,5-g]quinazoline (Table 150; ref. 351) has led to the determination of the site of benzylation. The structure of the intermediate in the formation of urogen (Tables 116 and 150; ref. 282) is verified by the observation of a $^{13}C-^{15}N$ fragment by means of $^{1}J(^{15}N-^{13}C)$. The biosynthetic pathway of nitrogen in the formation of streptonigrin (Table 150; ref. 388) from doubly labelled (2-^{13}C,1-^{15}N in the indole moiety) tryptophan is traced down owing to the observation of $^{1}J(^{15}N-^{13}C)$ in the product. The ^{13}C resonance signals of the antibiotic nybomycin have been assigned on the basis of the detected $^{1}J(^{15}N-^{13}C)$ coupling in biosynthetically ^{15}N-labelled nybomycin (Table 150; ref. 382). The $^{1}J(^{15}N-^{13}C)$ couplings in chetomin (Table 150; ref. 204) play an important role in the determination of its structure.

One-bond $^{15}N-^{13}C$ couplings in saturated systems (Table 150) have absolute magnitudes of a few Hz, and they are presumably negative in sign.[71,413] The only exception so far found is for oxaziridines (ref. 413 and references therein), but the recent data on aziridine derivatives (Table 150; ref. 378) provide the largest positive values of $^{1}J(^{15}N-^{13}C)$ ever observed, i.e. +5 to +8 Hz. These values lie slightly outside the range of $^{1}J(^{15}N-^{13}C)$ couplings reported[413] and quoted at the beginning of this section. They seem to indicate that there is relatively very little s-character in the C–N bonds of the three-membered rings of aziridine derivatives.[378]

There is a slight increase in the absolute value of $^{1}J(^{15}N-^{13}C)$ upon passing from a saturated amine to the corresponding ammonium ion (Table 150; refs 68 and 374). In alkylammonium ions[375] there are small but definite differences between the $^{1}J(^{15}N-^{13}C)$ couplings for the systems [157]–[160] when the N atom is bound to four carbon atoms. The increase

in the absolute value of $^1J(^{15}N-^{13}C)$ which occurs upon protonation of amino groups is also evident in amino acids (Table 150; refs 221 and 376).

		Absolute values of $^1J(^{15}N-^{13}C)$(Hz)
[157]	$^+N-CH_3$	4·9 to 6·0
[158]	$^+N-CH_2$	3·5 to 4·6
[159]	^+N-CH	1·7 to 2·5
[160]	^+N-C (quaternary)	*ca.* 1·0

One-bond $^{15}N-^{13}C$ couplings with carbonyl carbon atoms have much larger absolute magnitudes than those involving alkyl carbons and they can be readily distinguished from each other. The absolute values of the former range from 12 to 26 Hz, as shown by the data in Table 150, while the latter do not exceed 10 Hz.

In arylamines, the absolute values of $^1J(^{15}N-^{13}C)$ couplings with conjugated carbon atoms occur within a range of 10–18 Hz. Protonation of the nitrogen atoms in arylamines results in a decrease of the corresponding absolute values. This is opposite to the protonation effects observed in saturated amines (Table 150). The couplings in *N*-aryl moieties belonging to other structures, e.g. amides, pyrrole type nitrogen atoms in azoles, and conjugated nitro compounds, are comparable to those found in arylamines. However, if the nitrogen atoms involved bear lone pair electrons with considerable s-character, as is the case for imines [161], azo type structures [162], etc., the absolute values of $^1J(^{15}N-^{13}C)$ involving conjugated carbons are greatly reduced (to less than 4 Hz). Good examples of this effect are

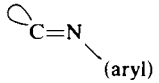

[161]

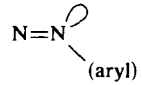

[162]

provided by the $^1J(^{15}N-^{13}C)$ data of azimines and azoxybenzenes (Table 150; ref. 329). The corresponding theoretical aspects of these observations are dealt with in Section II.B. One-bond $^{15}N-^{13}C$ couplings across conjugated or double C–N bonds depend critically upon whether the nitrogen atoms bear lone pairs with significant s-character. If such pairs are present, as in pyridine type nitrogen atoms in azine and azole ring systems, imines, and oximes, the couplings attain values from +1 to −7 Hz; the smallest absolute magnitudes are found for pyridine type nitrogen atoms, and the largest for the C=N moieties in imines (Table 150). Protonation of the lone pair or its replacement with an *N*-oxide bond results in quite large and negative couplings ranging from −10 to −22 Hz. Typical examples of such effects can be found in pyridine [163] and related structures [164] and [165],[359] as well as in imines [166] and their *N*-oxides (nitrones)

[163]	Pyridine	+0·62	$^1J(^{15}N-^{13}C)$ (Hz)
[164]	Pyridinium ion	−11·85	
[165]	Pyridine *N*-oxide	−15·23	

[166]	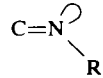	*ca.* (−)7	$^1J(^{15}N=^{13}C)$ (Hz)
[167]	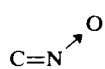	*ca.* −21	

[167].[363,389] Such effects are also observed in azole ring systems (Table 150) where pyridine type nitrogen atoms are characterized by small $^1J(^{15}N-^{13}C)$ values compared with pyrrole type nitrogen atoms, but the difference is largely removed upon protonation of the former.

Large absolute couplings are observed in the C=$^+$N moieties of diazo compounds (Table 150; refs 29 and 67) which are comparable to those found in nitrones.[363]

The largest absolute $^1J(^{15}N-^{13}C)$ value in Table 150 is that found for the N–C≡ moiety in PhN(Me)–C≡CMe,[343] but the coupling across triple bonds in nitriles [170] and isonitriles [169][392] is much weaker. The absolute

[168]	$R_2N-C(\equiv C-R)$	*ca.* (−)36 Hz
[169]	$R-N^+\equiv C^-$	*ca.* (−)10 Hz
[170]	$R-C\equiv N$	*ca.* (−)16 Hz

value of $^1J(^{15}N-^{13}C)$ in an isonitrile increases significantly upon complexation with myoglobin and synthetic Fe(II)-porphyrin complexes (Table 150; ref. 393). There is also some differentiation between the $^1J(^{15}N-^{13}C)$ value for the free cyanide ion and its square-planar and tetrahedral complexes with metals (Table 150; ref. 394). In hydrogen cyanide [171],[414] a deuterium isotope effect on the $^1J(^{15}N-^{13}C)$ interaction has been observed.

[171]	$HC\equiv{}^{15}N$	−18·5 ± 0·10	$^1J(^{15}N-^{13}C)$ (Hz)
[172]	$DC\equiv{}^{15}N$	−18·8 ± 0·10	

F. $^{15}N-^{13}C$ coupling across more than one bond

Two-bond $^{15}N-^{13}C$ *couplings* in saturated systems of amines and ammonium ions are usually smaller than those across one bond (Table 151), with minor exceptions. If the coupling is across a carbonyl carbon atom, the absolute value of $^2J(^{15}N-^{13}C)$ increases significantly, to about 4–12 Hz, and this makes it possible to distinguish between the molecular fragments [173] and [174] on the basis of two-bond couplings. The difference is removed, however, in strongly protonating media where the carbonyl oxygen is protonated; such protonation reduces the coupling

across the carbonyl carbon atom to values characteristic of couplings across a tetracoordinate carbon atom (Table 151; refs 374 and 362). The coupling is significantly reduced when the nitrogen atom involved bears a lone pair with significant s-character, as shown for the anion derived from 1-methyluracil (Table 151; ref. 355).

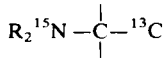

[173]

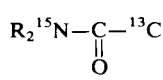

[174]

	[173]	[174]
Absolute $^2J(^{15}N-^{13}C)$ values	0–5 Hz	4–12 Hz

If the two-bond coupling occurs within an unsaturated or conjugated system, and the nitrogen atom bears a lone electron pair with significant s-character, its sign and magnitude appear to depend critically on whether the ^{13}C nucleus involved in the coupling is *cis* [176] or *trans* [175] to the

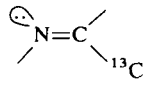

[175]

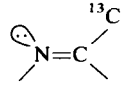

[176]

	[175]	[176]
$^2J(^{15}N-^{13}C)$	+1 to +3 Hz	−7 to −11 Hz

lone pair as can be estimated from the data in Table 151 for pyridine and related heterocycles, imines, and oximes. In pyridine type heterocycles (azines), the relevant ring carbon atoms are always *trans* to the lone pair, and the couplings are small and presumably positive in sign. When such ring systems bear methyl substituents that are *cis* to the lone pair of the nitrogen atom involved, the two-bond coupling with the methyl carbon is fairly large and presumably negative in sign (data in Table 151 corresponding to ref. 385). The effect seems to stem from a *cis* interaction between the lone pair and the carbon atom concerned, since the coupling in the *trans* arrangement is largely the same as in the case when the lone pair is protonated or replaced by an *N*-oxide bond. The latter is shown by the rather small difference in the $^2J(^{15}N-^{13}C)$ values between pyridine, its cation, and its *N*-oxide (Table 151; ref. 359). An analogous *cis-trans* effect on the $^2J(^{15}N-^{13}C)$ data is observed in azimines (Table 151; ref. 329), where the coupling occurs across a nitrogen atom, $^{15}N{=}N-^{13}C$.

The rules considered above predict small absolute $^2J(^{15}N-^{13}C)$ couplings of pyridine type nitrogen atoms in azoles, and large absolute couplings of such atoms with methyl substituents on the neighbouring carbon atoms. The data in Table 151 seem to support these predictions.[276,277]

In conjugated systems and imino type systems where the nitrogen atoms involved bear lone pairs with appreciable s-character, the $^2J(^{15}N-^{13}C)$

couplings can be larger in absolute magnitude than the corresponding $^1J(^{15}N–^{13}C)$ data (compare the results in Tables 150 and 151).

Three-bond $^{15}N–^{13}C$ couplings are, in general, negative in sign.[413] For saturated systems, equations analogous to equation (32) have been suggested (ref. 413, and references therein) which relate $^3J(^{15}N–^{13}C)$ values with the dihedral angles between the C–C and N–C bonds in N–C–C–C systems. Such equations predict maximum absolute values of $^3J(^{15}N–^{13}C)$ for dihedral angles of 0° and 180°, and minimum values for about 90°. Recent data on ammonium ions and amines (Table 151; refs 68 and 375) provide some support for such correlations of $^3J(^{15}N–^{13}C)$ data with the dihedral angles of 180°, 120°, and 60°, but severe discrepancies are observed for an angle of 0°, since the absolute value of $^3J(^{15}N–^{13}C)$ ranges from 6·7 Hz to about zero.[375]

Three-bond $^{15}N–^{13}C$ couplings are usually weak (their absolute magnitudes rarely exceed 5 Hz) but in some cases they are stronger than those across two bonds. This occurs mostly in saturated ammonium ions[375] but also in pyridine, the pyridinium ion, and pyridine *N*-oxide (Table 151; ref. 359). In pyridine itself, the $^3J(^{15}N–^{13}C)$ coupling is larger in absolute magnitude than any of the other pyridine $^{15}N–^{13}C$ couplings. In nitrobenzene (Table 151; ref. 364), the absolute value of $^3J(^{15}N–^{13}C)$ is slightly larger than that of $^2J(^{15}N–^{13}C)$. Significant $^3J(^{15}N–^{13}C)$ interactions are observed in $^{15}N{=}C–C{=}^{13}C$ systems, such as those of oximes (Table 151; refs 64, 69, and 390).

The couplings between ^{15}N and ^{13}C that occur *across more than three bonds* are generally weak, less than 1 Hz in absolute magnitude (Table 151). The only exception so far observed is for a derivative of 1,2,4-triazine (Table 151; ref. 385) where a coupling of 3·9 Hz is found between 1-N and a methyl group attached to a vinyl substituent (coupling across four bonds).

G. $^{15}N–^{15}N$ couplings

A considerable amount of data on $^{15}N–^{15}N$ couplings has been reported recently (Table 152). Most of them are concerned with $^1J(^{15}N–^{15}N)$ couplings. Some additional data are reported in Table 3 together with the results of some theoretical calculations. The latter show that $^1J(^{15}N–^{15}N)$ is predicted to be negative, with the possible exception of hydrazine type systems.

The largest $^{15}N–^{15}N$ coupling is observed in *N*-nitrosoamines, and the smallest in hydrazino moieties, nitramines, and molecular N_2. Generally, in N=N moieties, the absolute values of the coupling occur within a range of 10–20 Hz, with some exceptions. The latter include the $N^+{=}N^-$ moieties in diazo compounds $R_2C{=}N^+{=}N^-$ and in azides $RN{=}N^+{=}N^-$ (Table 152; refs 67, 248, and 256), where the coupling is less than 10 Hz. There

is a striking difference in the absolute value of $^{1}J(^{15}N-^{15}N)$ between nitramines [177] and their isomeric *aci* forms [178]. Two-bond $^{15}N-^{15}N$

	R_2N-NO_2	R-N=N(O)OR
	[177]	[178]
Absolute $^{1}J(^{15}N-^{15}N)$ values	*ca.* 6 Hz	*ca.* 13 Hz

couplings across a nitrogen atom are close to zero in azides,[247,248,256] but they can attain absolute values as high as about 11 Hz in some isomers of imino type triazenes (Table 152; ref. 30). In the latter, the small amount of data available indicates that the two-bond coupling can be critically influenced by the geometry of the system involved. Two-bond $^{15}N-^{15}N$ couplings across a carbon atom can also be significant, particularly when the intervening carbon atom is tricoordinate, i.e. belonging to a conjugated system or to a carbonyl group. Quite interesting are the two-bond $^{15}N-^{15}N$ couplings between different nitrogenous ligands in Pt complexes (Table 152; refs 395 and 396), since they occur across the central Pt atom; they indicate clearly the binding of individual nitrogen atoms to Pt. An example of $^{2}J(^{15}N-^{15}N)$ coupling across a phosphorus atom has also been reported (Table 152; ref. 142).

H. $^{31}P-^{15}N$ couplings

One-bond $^{15}N-^{31}P$ couplings (Table 153) cover a fairly broad range of both positive and negative values. Therefore, their interpretation is not straightforward when only absolute values are known.

In aminophosphines R_2N-PR_2, the couplings are large and positive,[73,141,142] and theoretical calculations[402] suggest that $^{1}J(^{31}P-^{15}N)$ should depend critically on the dihedral angle between the nitrogen and phosphorus lone pairs, provided that there is a pyramidal geometry of bonds at the nitrogen atom. No appreciable change is predicted[402] for a trigonal geometry of the nitrogen bonds involved. The importance of the lone electron pair on P in the coupling is supported by the drastic reduction in the magnitude of $^{1}J(^{31}P-^{15}N)$ in aminophosphonium ions $R_2N-P^{+}R_3$, as compared with aminophosphines (Table 153).

There also seems to be a significant algebraic decrease in $^{1}J(^{31}P-^{15}N)$ which can lead to large negative values thereof, upon passing from tricoordinate P atoms to tetracoordinate P atoms in the series [179]–[182]. The

[179]	R_2N-PR_2	algebraic decrease in $^{1}J(^{31}P-^{15}N)$
[180]	$R_2N-P(=Se)R_2$	
[181]	$R_2N-P(=S)R_2$	
[182]	$R_2N-P(=O)R_2$	

$^{1}J(^{31}P-^{15}N)$ couplings in cyclic systems are shown to reflect such structural

details as ring size[146] and conformation of substituents,[399] as shown by the data in Table 153. In cyclophosphazenes (Tables 127 and 153; references 254, 326, 400, and 401), the $^{1}J(^{31}P-^{15}N)$ coupling shows appreciable changes upon passing from six-membered to larger ring systems. The changes probably reflect the non-planarity of the larger rings.

A number of two-bond $^{31}P-^{15}N$ couplings have been observed across metal atoms in various complexes (Table 153; refs 330, 337, 346, and 396). There is a clear difference in the magnitude of the coupling in square-planar complexes between the *trans* [183] and *cis* [184] arrangements of the ligands involved in the $^{15}N-X-^{31}P$ coupling. The stronger

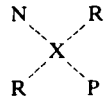

[183]

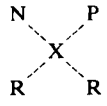

[184]

$^{31}P-^{15}N$ coupling between *trans* ligands seems to be attractive from the point of view of structural investigations, since it has been observed for a variety of metals and ligands.

I. $^{19}F-^{15}N$ couplings

One-bond $^{19}F-^{15}N$ couplings are large, i.e. 150–460 Hz (ref. 2, p. 290, and references therein), and positive in sign according to the calculations considered in Section II.B.

Recently, a number of nitrogen–fluorine couplings across two or more bonds have been reported (Table 154). Of these only $^{2}J(^{19}F-^{15}N)$ interactions have significantly large absolute values. The data include the couplings between ligands in complexes of Mo and W (Table 154; refs 346 and 404).

J. $^{195}Pt-^{15}N$ couplings

One-bond couplings between ^{195}Pt and ^{15}N have large absolute values, from 100 to 580 Hz (Table 155). The couplings are sensitive to the nature and arrangement of the ligands in square-planar complexes of Pt. In a systematic study of $^{1}J(^{195}Pt-^{15}N)$ values of platinum complexes that contain NH_3, Cl^-, and $(CH_3)_2SO$ ligands it is possible to identify isomeric complexes on the basis of the couplings (Table 155; ref. 405). The largest influence on the coupling is exerted by the ligand that is *trans* to the nitrogen atom involved.[337,405] There is a linear correlation between the $^{1}J(^{195}Pt-^{15}N)$ and $^{1}J(^{195}Pt-^{31}P)$ data for platinum complexes containing both nitrogenous and phosphine ligands.[337]

The coupling between ^{195}Pt and ^{15}N in complexes where the nitrogenous ligands contain more than one kind of nitrogen atom can be used for the

identification of the binding sites of platinum, as is shown for *N*-methylimidazole ligands (Table 155; ref. 395). It is interesting to note that quite appreciable couplings between ^{195}Pt and ^{15}N across three bonds are found, i.e. 25–33 Hz, but those across one bond are larger by an order of magnitude.[395]

The formation of the 2-ammonioethanido ligand CH_2^-–CH_2–N^+HMe_2 from CH_2=CH_2 upon the addition of dimethylamine to *trans*-$PtCl_2(CH_2{=}CH_2)(NHMe_2)$ in $CDCl_3$ has been monitored by the changes observed in ^{195}Pt–^{15}N couplings (Table 155; ref. 408). The three-bond ^{195}Pt–^{15}N coupling observed in the product is comparable to the three-bond couplings in the imidazole ligands considered above.

K. Some miscellaneous ^{15}N couplings

Some of these are collected in Table 156; they comprise mostly couplings across one bond between ^{15}N and a metal. Such couplings can be useful for the identification of nitrogen atoms that are bound directly to metal atoms. In the case of stannatranes, the coupling (Table 156; ref. 140) reflects the existence of the transannular bond between N and Sn shown in Table 29. The coupling between ^{103}Rh and ^{15}N in a complex[409] with an *N*-sulphinylamine (Table 156) is indicative of direct Rh–N bonding. The bonding modes of ambidentate ligands such as $(NCO)^-$ or $(NCS)^-$ can be readily established when the coupling between their nitrogen atom and the metal atom in a complex is observed (Table 156; ref. 410). The equivalence of the coupling between ^{199}Hg and the terminal nitrogen atoms in the phenyltriazene derivative shown in Table 156 (ref. 412) indicates that the structure must be symmetric or that the HgPh moiety must migrate between the terminal nitrogen atoms. There is a large difference in the couplings between ^{207}Pb and ^{15}N in the complex shown in Tables 144 and 156 (ref. 339) as far as the axial and equatorial positions of the nitrogen atoms are concerned. The larger coupling is attributed to the equatorial nitrogen nuclei.

It has been assumed that the large difference in values of these couplings is primarily due to contact interactions.[433] While this is probably true, the neglect of an orbital contribution in the absence of π bonding may not be justified. It is only within the AEE approximation that the orbital term disappears for coupling between non-hydrogen nuclei.[7] The use of this approximation can often lead to errors in the interpretation of coupling constants.[7]

Some diamagnetic iron(III) bis-amine complexes of *meso*-tetraphenylporphyrin are reported to have $^1J(^{57}Fe$–$^{15}N)$ values in the region of 7·5–8·0 Hz.[411] These couplings and the nitrogen chemical shifts are considered in relation to the influence of the axial ligand on the iron–porphyrin binding

profiles. A similar study has been performed on some comparable complexes of octaethylporphyrin.[285]

The value of $^{1}J(^{15}N-^{13}C)$ for some alkyl isocyanides, bound to the haem iron(II) atom in myoglobin and tetraphenyl- and octaethyl-porphyrin iron(II), is reported to be sensitive to the variation of the alkyl group.[393] The nitrogen nuclear screenings appear to be less sensitive in this respect.

^{15}N NMR studies have revealed $^{1}J(^{59}Co-^{15}N)$ values of $62{\cdot}5(\pm 1{\cdot}0)$ Hz and $63{\cdot}8(\pm 1{\cdot}0)$ Hz respectively for the hexaamminecobalt(III) and tris(ethylenediamine)cobalt(III) complex ions.[335] A single ^{15}N resonance has been observed for some mono- and di-nitroso complexes of some Group VIB elements containing also the cyclopentadienyl ligand.[338] Both ^{14}N and ^{15}N data are reported for the metal carbonyl cluster anion $[Rh_6N(CO)_{15}]^-$.[434] The ^{15}N signal is split into a septet and the value of $^{1}J(^{103}Rh-^{15}N)$ is 6·1 Hz. It is concluded that nitrogen is held interstitially in the anion.

L. Some notes on recent advances in the measurement of nitrogen couplings

Until recently, most of the data on nitrogen couplings were obtained from ^{15}N-enriched samples or from ^{14}N couplings when the relevant ^{14}N relaxation is sufficiently slow. The improvement in sensitivity obtained in modern NMR spectrometers has resulted in a breakthrough as far as the possibility of measuring natural-abundance ^{15}N spectra with retained spin–spin splittings is concerned, but the problem of sensitivity is still a major one. The same problem arises in the measurement of the couplings from very weak ^{15}N satellites in the spectra of nuclei coupled to nitrogen. Recent applications of the cross polarization technique to the observation of ^{15}N multiplet patterns[92,348,358,415] have shown that the transfer of polarization from ^{1}H to ^{15}N, and eventually a second transfer thereof back to ^{1}H,[415] can yield such an improvement in sensitivity from the point of view of multiplet patterns of ^{15}N resonances that the latter can be obtained with a single pulse.[348] There are also methods[95,96] for extracting weak ^{15}N satellites from the spectra of nuclei coupled to nitrogen by suppression of the signals that represent molecules containing ^{14}N.

The couplings that involve ^{14}N nuclei can also be measured indirectly, from the corresponding proton transverse relaxation time as a function of the 180° pulse separation in the Carr–Purcell sequence.[418]

VIII. RELAXATION PHENOMENA

The ^{14}N nuclear relaxation is usually dominated by the quadrupolar mechanism. This results in broad lines, both in the ^{14}N NMR spectrum

and in the spectra of nuclei spin–spin coupled to nitrogen. Since the ^{15}N nucleus has $I = \frac{1}{2}$ its relaxation is controlled by one or more of the less efficient relaxation processes.

A. ^{14}N relaxation

In low viscosity solutions, the extreme narrowing conditions

$$(2\pi\nu\tau_c)^2 \ll 1 \tag{33}$$

are usually obeyed, where ν is the resonance frequency of the nucleus of interest and τ_c the corresponding correlation time. When these conditions obtain, the effect of the quadrupole moment of a ^{14}N nucleus on its relaxation time T_Q is given by

$$\frac{1}{T_Q} = \frac{3}{8}\left(1 + \frac{\eta^2}{3}\right)\chi^2\tau_c \tag{34}$$

in which the nuclear quadrupole coupling constant χ (in frequency units) between the quadrupole moment eQ and the electric field gradient eq at the nucleus is given by

$$\chi = eqeQ/h \tag{35}$$

where η describes the deviation of the electric field gradient from axial symmetry. Since it is apparent from equation (35) that quadrupolar relaxation only occurs in the presence of a resultant electric field gradient at the nucleus, the variation of this gradient due to molecular motions may be studied by means of ^{14}N NMR.

In the case of the neat liquids pyrimidine and pyridazine, ^{14}N quadrupolar relaxation rates are combined with ^{13}C–^{1}H dipolar relaxation data to determine the rotational correlation times for motion about each principal axis.[435] Similar ^{14}N data are reported for pyrazine but its molecular motion has not been analysed.[435]

The three reorientational correlation times and the orientation of the ^{14}N quadrupole coupling tensor have been obtained for nitrobenzene.[436] However, disagreement has been noted[455] between the ^{14}N relaxation rate data and those obtained by electric field effect measurements on the ^{14}N NMR spectrum of nitrobenzene.[456] This appears to arise from the use of solid-state quadrupole coupling constant measurements for the interpretation of liquid-state NMR data. The discrepancy is removed if environmental effects on the value of χ are taken into account.[410]

By knowing the principal components of the rotational diffusion tensor, the unambiguous assignment of the ^{15}N nuclear screening tensor for nitrobenzene is obtained.[436]

^{14}N NMR relaxation rates have been measured for several singly charged ions including the ammonium ion and those of some pseudohalogens. The results indicate that the binding of these ions to a metal ion produces only relatively small changes in the field gradient at the site of the nitrogen nuclei.[437] Consequently metal macromolecule binding sites are unlikely to be easily studied by means of ^{14}N relaxation measurements.

^{14}N relaxation data have been reported for aqueous solutions of n-hexadecyltrimethylammonium bromide (CTAB) and the corresponding chloride (CTAC) as functions of concentration.[397] The measurements reveal that CTAC forms spherical micelles while CTAB produces larger aggregates at higher concentrations. Ammonium ions in a cationic mesophase comprising water, ammonium chloride, and decylammonium chloride have been investigated by ^{14}N NMR.[438] The value of χ for the ^{14}N nucleus of the ammonium ion is reported to be $3{\cdot}1 \pm 0{\cdot}3$ MHz along the bond axis. ^{14}N quadrupolar splittings have also been observed in a counterion binding study of the tetramethylammonium octanoate–heavy water and ammonium octanoate–heavy water systems.[439] Similar ^{14}N splittings have been reported for ND_4^+ and $N(CD_3)_4^+$ in three lyotropic lamellar systems, thus indicating orientation of the ions.[440]

The anisotropic motion of acetonitrile dissolved in a thermotropic liquid crystal (Merck's licrystal, phase V) has been investigated.[101] The ^{14}N relaxation data are obtained from the ^{13}C linewidth due to the incomplete averaging of the dipolar interactions in the nematic phase. It appears that equations which describe the isotropic phase are not suitable for application to a molecule dissolved in a nematic phase merely by adapting them to incorporate the partial orientation present in the nematic phase.

^{14}N linewidths and relaxation times are reported for succinonitrile in the liquid and solid I phases.[441] In the case of formamide, the ^{14}N relaxation data are found to be very sensitive to the presence of both cations and anions.[442] These results, and other spectroscopic information, provide direct evidence for specific ion–amide interactions and a tentative model for the interaction of electrolytes in liquid formamide.[442]

The ^{14}N and ^{1}H relaxation rates of liquid cyanoacetylene provide information on the translational and rotational molecular motions.[443]

Recently the first observation of a quadrupolar split ^{14}N spectrum for a model membrane system has been reported.[499] The system studied is an aqueous dispersion of dipalmitoylphosphatidylcholine (DPPC) between 3 and 65 °C. In both the liquid-crystal and gel phases the splittings are of the order of 10 kHz, suggesting a small order parameter for the choline headgroup. The studies are being extended to sphingomyelin and phosphatidylethanolamine.[499] It seems likely that ^{14}N NMR will act as a complementary probe to ^{31}P and ^{2}H, and thus it will provide a significant

contribution to the determination of headgroup conformation and dynamics in model and biological membranes.

High resolution ^{14}N NMR spectra have been obtained for single-crystals of ammonium hydrogen oxalate hemihydrate[104] and *N*-acetyl-*dl*-valine.[107] In the latter case the N–H bond length is found to be 0·106 nm. The results obtained indicate that ^{14}N NMR spectra are relatively easy to obtain for single-crystals and that structural determinations of moderately sized peptides are feasible provided that the assignment of the various nitrogen resonances can be accomplished. Exact theoretical results have been presented for ^{14}N nuclei in polycrystalline samples and applied to hexamethylenetetramine.[108]

N_2O dissolved in poly-γ-benzyl-L-glutamate(PBLG)–$CDCl_3$ and MBBA has been studied by ^{14}N quadrupole splittings and relaxation times.[444] In the case of the PBLG–$CDCl_3$ sample the ratio of the central and terminal nitrogen quadrupole coupling constants of N_2O agrees very well with microwave data but in MBBA a discrepancy is observed which could be due to molecular distortions.

^{14}N relaxation data for a quinuclidine in its plastic phase rule out the possibility of isotropic motion.[445] It is concluded that the molecules reorient by $\pm 90°$ jumps about the crystallographic C_4 axes with a residence time of $(22{\cdot}2 \pm 2) \times 10^{-12}$ s and by $\pm 120°$ jumps about the molecular C_3 axes with a residence time of $(5{\cdot}25 \pm 2{\cdot}8) \times 10^{-12}$ s at room temperature.

^{14}N relaxation times have been reported for a series of alkyl-substituted nucleic acid bases and mixtures thereof in DMSO-d_6.[446] With the exception of the guanine NH nitrogen no significant changes in the nitrogen electronic environment are found for any combination of bases.

From a comparison of equations (6) and (35) it appears that both $\sigma^{P}_{loc}\Delta E$ and χ depend upon the imbalance of electronic charge around nitrogen. Thus, not surprisingly, a rough correlation between nitrogen chemical shifts and values of χ is observed for some nitroso compounds.[447]

^{14}N relaxation data have been reported for pyrrole, both as a pure liquid and in 1,4-dioxan solution,[448] 3,5-lutidine,[448] 2-fluoropyridine,[448] nitromethane,[449] a series of nucleosides and nucleoside bases,[344] some indole derivatives,[344] some 1,3- and 1,4-diethylpyridinium bromides,[450] some palladium(II) complexes of t-butyl isocyanide,[265] some thiocyanate complexes of aluminium(III) and gallium(III), and sodium nitrite.[451] The value of χ for the ^{14}N nucleus of pyridine-*N*-oxide has also been evaluated.[303]

The utility of ^{14}N linewidths as an aid to the assignment of nitrogen chemical shifts in N-heterocycles has been further demonstrated.[99] INDO results, used in conjunction with the Townes–Daily model, provide a satisfactory account of the relative ^{14}N quadrupolar linewidths of various nitrogen environments in a given molecule.[99] The results obtained are used

to assign the nitrogen NMR spectra of some rigid N-heterocycles containing non-equivalent nitrogen environments.

Some MNDO and MINDO/3 calculations of the ^{14}N coupling constants of some fluorinated pyridines are reported to be in reasonable agreement with experiment.[452]

In the presence of a paramagnetic centre both the hyperfine and the quadrupole coupling tensors may be evaluated. ENDOR data on solutions of vitamin B_{12r} at liquid helium temperatures have been recorded.[453] Analysis of the results has yielded values for both the hyperfine and quadrupole coupling tensors of the ^{14}N nucleus present in the benzimidazole moiety.[453] Copper(II) complexes with imidazole have a value of 1·75 MHz for the ^{14}N hyperfine interaction.[454] The size of this interaction permits the observation of the zero-field quadrupolar frequencies of ^{14}N nuclei in the electron spin-echo envelope. ^{14}N hyperfine coupling constants have been reported for thiocyanate ions in the presence of some trivalent lanthanide ions.[422]

Some *ab initio* molecular orbital calculations of values of χ for the ^{14}N nuclei in some 5-membered ring oxygen and sulphur heterocycles are found to provide satisfactory agreement with both NQR and microwave measurements.[457] In those cases where a nitrogen atom is flanked by sulphur and nitrogen lone-pairs, the former is reported to be the more dominant in its effect upon the nitrogen electric field gradient.[457]

The ^{14}N nuclear quadrupole coupling has been investigated for some thermochromic and photochromic *N*-salicylideneanilines by means of a ^{1}H–^{14}N double resonance technique applied to solids.[458,459] The thermochromism appears to be accompanied by intramolecular proton transfer and an enol–keto transformation.[459]

Proton–nitrogen double resonance has been employed in order to determine the quadrupole coupling parameters for ^{14}N in the two chemically inequivalent sites in paraelectric ammonium sulphate over the temperature range 225–365 K.[460] At 296·1 K the values of χ and η for site I are 154·53 kHz and 0·684, whereas for site II the corresponding data are 115·71 kHz and 0·749. It is concluded that hydrogen-bonding to sulphate is an important feature in determining the ammonium ion charge distribution and thus the nitrogen field gradient tensor.

The photoexcited triplet state of phenazine has been studied by optically detected magnetic resonance (ODMR).[461] This has given rise to the determination of the ^{14}N quadrupole tensor for the lowest excited triplet state.

Although not strictly within the confines of the present review, some references to ^{14}N quadrupole coupling constants obtained by NQR and microwave spectroscopy are included for the sake of completeness.

Microwave data have been reported for isoxazole-4D,[462] *cis*-thionylimide,[463] and iminosulphur oxydifluoride.[463] ^{14}N NQR results are available for some methylbenzonitriles,[464] coordinated 1,2-dipiperidinoethane,[465] coordinated thiocyanate,[466] coordinated imidazole[467] and imidazolate,[468] carbonatotetraminecobalt(II) bromide,[469] sodium, potassium, and ammonium thiocyanates,[470] some salts of hexamethylenetetramine,[471,472] trimethylenetrinitramine,[473] the low temperature phase of 1,4-diazabicyclo[2,2,2]octane,[474] some explosives,[475] sulphuric diamide and methanesulphonamide,[476] tetracyanoquinodimethane,[477] various substituted nitrobenzenes,[478,479] several hydroxypyrimidines,[480] *p*-azoxyanisole and some related compounds,[481] some *p*-substituted benzene diazonium salts,[482] several barbiturates,[483] some molecular complexes of urea,[481] some binary systems of acetonitrile and various electron donors and acceptors,[485] some azines,[150] sodium nitrite,[486] antiferromagnetic copper(II) formate diurea dihydrate,[487] some hexanitrocopper(II) complexes,[488] K-TCNQ at various temperatures,[489] the magnetic phase transition at 6 K of dichloro(dimethylnitrosamine)copper(II),[490] some compounds with nitrogen–sulphur bonds,[491] *p*-chloroaniline with *p*-toluidine as an impurity,[492] and some liquid crystals in their solid state.[493] ^{14}N and ^{2}H NQR studies have revealed that cytosine hydrobromide exists in two different crystalline forms; the difference arises from their hydrogen-bonding schemes.[494]

Finally, mention is made of the presentation of the true second-order theory of the Zeeman effect of ^{14}N NQR with polycrystalline samples,[495] and of a pulsed fast FT NQR spectrometer for ^{14}N studies.[496]

B. ^{15}N relaxation

The relaxation of the ^{15}N nucleus is subject to varying contributions from the dipole–dipole, spin–rotation, chemical shielding anisotropy, and scalar coupling mechanisms. If the ^{15}N nucleus has an attached proton, the dipole–dipole interaction is usually the dominant one.[123]

The ^{15}N nuclei in *trans*-azobenzene, dissolved in $CDCl_3$, relax due to a mixture of the spin–rotation, dipole–dipole, and chemical shielding anisotropy interactions.[497] The relative proportions of these mechanisms are found to change considerably over the temperature range 5–80 °C. In contrast, the ^{15}N relaxation in n-butyl nitrite occurs almost entirely by the spin–(internal rotation) mechanism throughout the same temperature range.[497]

In the case of cyanide ion the ^{15}N relaxation is apparently controlled by a combination of the chemical shielding anisotropy and spin–rotation interactions.[498]

^{15}N relaxation rates and nuclear Overhauser enhancements (NOE) have been reported for some substituted anilines, aminobenzoic acids, and related compounds.[157] The dipole–dipole interaction dominates the ^{15}N relaxation process. In the cases of aniline and some substituted anilines the NH_2 or NH_3^+ groups appear to undergo rapid, but not free, internal rotation at rates comparable to those of overall reorientation for these molecules. Dipolar relaxation is reported to dominate the ^{15}N relaxation of the peptide hormone oxytocin.[211] Isotropic motion of the tocin ring is observed.

The ^{15}N T_1 values of a number of aldoximes and ketoximes appear in the region of 25–50 s.[322] Although dipolar relaxation is a significant contributor, other mechanisms account for 50–65% of the ^{15}N relaxation. It seems likely that the other processes concerned are chemical shielding anisotropy and interactions due to the presence of paramagnetic impurities.

The effects of the addition of paramagnetic relaxation reagents on ^{15}N relaxation have been studied.[84,89] The tris-acac complexes of chromium(III) and iron(III) appear to affect the ^{15}N chemical shifts of some methyl-substituted pyridines to an extent comparable to the substituent effects.[84] This is thought to be largely due to changes in bulk susceptibility upon addition of the relaxation reagent. Consequently the problem can be obviated by using an internal reference and an external lock.[84]

The acac and dpm complexes of chromium(III) appear to influence the ^{15}N relaxation of a series of amines, either by means of an outer sphere mechanism or by translational motion not involving any interaction.[89] In contrast the corresponding gadolinium(III) complexes are found to be specific for the basic sites of amines. The relaxation rate enhancement is reported to be closely dependent upon the availability of the nitrogen lone pair. This gives rise to the possibility of ^{15}N spin labelling due to the differences of basicity and steric effects. An example of such spin labelling is afforded by α-methyltryptamine [185]. In the absence of a relaxation reagent two, almost equally intense, ^{15}N signals are observed. The addition of $Gd(dpm)_3$ causes the more highly screened resonance to be nulled whereas the other remains unchanged. The greater basicity of the primary amine nitrogen suggests that its signal is the one influenced by the relaxation reagent. Stereoselective sensitivity to $Gd(dpm)_3$ is shown by both acetaldoxime and propanaldoxime.[322] The preference of the relaxation agent is about three times as great for the *syn* isomer as it is for the *anti* isomer.

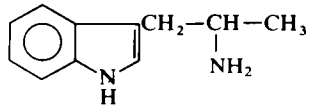

[185]

This Page Intentionally Left Blank

TABLES 1–156

Note: Shieldings are expressed throughout in ppm.

A complete list of tables is given on p. 489.

TABLE 1

The results of some INDO/S calculations of the paramagnetic contributions to some nitrogen shielding tensors, their average values and anisotropy, and some nitrogen chemical shifts compared with experimental data[18]

Molecule	Calculated (ppm)					Experimental (ppm)			Ref.
	σ^{p}_{loc}	$\sigma^{p}_{non\text{-}loc}$	σ^{av}	$\Delta\sigma$	δ	σ^{av}	$\Delta\sigma$	δ	
N_2	−377·88	−8·51	−61·76	566·82	−50·70	−69 −100 ± 20	603 ± 28 657 ± 20	−70·2 ± 1·5	1
CN^-	−338·52	−9·72	−18·41	507·78	−94·05			−102·48 ± 0·09	1
$[O{=}N{=}O]^+$	−309·62	−10·99	−6·21	464·38	−106·25			−129 ± 2	1
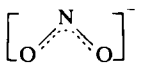	−621·77	7·16	−290·07	712·60	177·61			228·89 ± 0·25	1
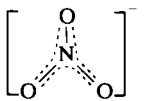	−416·29	2·83	−94·98	420·50	−17·48	−115 ± 20	210 ± 5	3·70 ± 0·12	1
$O{=}C{=}\bar{N}$	−294·48	−3·58	32·71	441·18	−145·17	155		−302·91 ± 0·14	1
$CH_3\text{-}\overset{+}{N}{\equiv}\bar{C}$	−228·64	−5·69	91·46	355·75	−203·92	130 ± 20 85	360 ± 73	−218 ± 0·5	51
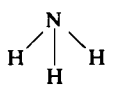	−214·84	0·0	112·12	63·03	−224·58	260 ± 20 264	39 ± 10	−381·93 ± 0·14	1
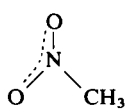	−440·64	9·07	−112·46	444·94	0·0			0·0	

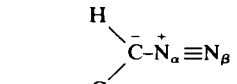	(N_α)	−322·37	4·35	3·20	101·0	−115·66	−113·70 −165·79 −24 ± 7*	67 29 52
	(N_β)	−456·87	−1·40	−132·60	166·0	20·14	0·6 −49·49 −115 ± 2*	67 29 52
Z-isomer								
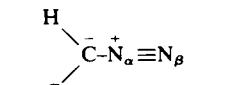	(N_α)	−318·09	4·21	7·47	91·50	−119·93	−113·70 −165·79 −24 ± 7*	67 29 52
	(N_β)	−452·01	−1·29	−127·51	153·0	15·05	8·0 −49·49 −115 ± 2*	67 29 52
E-isomer								
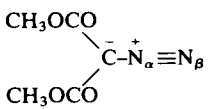	(N_α)	−293·36	1·99	29·52	164·06	−141·98	−177·49	29
	(N_β)	−398·62	−2·25	−75·70	71·34	−36·76	−58·19	29
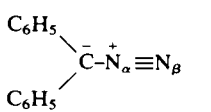	(N_α)	−357·43	6·74	−28·45	57·70	−84·01	−130·69 55 ± 2*	29 52
	(N_β)	−498·39	1·08	−170·98	284·61	58·52	5·41 −86 ± 2*	29 52
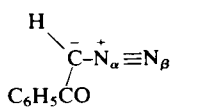	(N_α)	−312·21	3·66	12·70	105·0	−125·16	−165·19	29
	(N_β)	−447·09	−1·46	−122·84	164·0	10·38	−59·59	29

* Reversed assignments are suggested as a result of the calculations reported here.

TABLE 2

Some contributions to the paramagnetic component of the nitrogen shielding tensor (ppm) from various electronic transitions[18]

Molecule	$\sigma \rightarrow \sigma^*$	$n \rightarrow \sigma^*$	$\sigma \rightarrow \pi^*$	$n \rightarrow \pi^*$	$\pi \rightarrow \sigma^*$	Average weighted value of transition energies (eV)
N_2			−12·47	−281·68	−83·70	10·69
CN^-			−14·90	−242·57	−81·03	9·29
NO_2^+			−197·03		−112·57	17·89
NO_2^-	−54·11	6·54	−146·68	−351·00	−76·58	7·91
NO_3^-	−55·57	7·29	−195·28	−77·27	−98·27	14·08
OCN^-		−5·05	−6·77	−116·15	−167·50	9·76
CH_3NC			−114·07		−104·76	15·53
$\bar{C}H_2-\overset{\cdot}{\overset{+}{N}}\equiv N$	−59·69	−58·23	−50·65	−52·71	−162·54	11·91
$\bar{C}H_2-\overset{+}{N}\equiv \overset{\cdot}{N}$	−39·52	−98·59	28·16	−59·87	−408·76	6·52
$[N-\overset{\cdot}{N}-N]^-$			−40·68	−122·09	−98·28	18·13
$[\overset{\cdot}{N}-N-N]^-$			−5·19	−105·15	−123·95	12·02
NH_3	−79·46	−131·82				14·66
CH_3NO_2	−83·98	10·09	−164·78	−130·38	−45·53	12·64

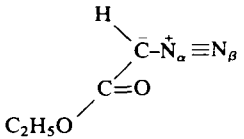	*Z*	(N_α)	−62·08	−43·30	−43·24	−39·26	−125·20	14·36
		(N_β)	−43·92	−71·78	3·20	−51·58	−278·59	8·32
	E	(N_α)	−69·52	−29·11	−50·81	−28·39	−121·67	14·53
		(N_β)	−59·55	−50·29	−5·81	−39·77	−279·35	8·40
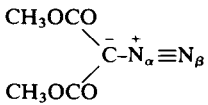		(N_α)	−84·63	−21·25	−64·16	−20·39	−96·91	15·76
		(N_β)	−88·57	−32·42	−27·82	−23·58	−220·33	9·63
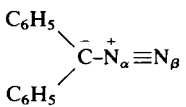		(N_α)	−81·34	−17·17	−52·29	−15·56	−169·99	12·71
		(N_β)	−67·41	−45·22	0·60	−28·40	−340·4	7·67
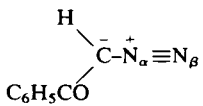		(N_α)	−109·08	−42·81	−42·28	−29·85	−68·57	14·82
		(N_β)	−70·20	−66·49	3·80	−38·93	−242·67	8·49

* Transitions contributing less than 5 ppm to σ^P have been omitted.

TABLE 3

The results of some INDO-SOS calculations of ^1J(N–N) compared with experiment (Hz)[62]

Species	Calculated				Experimental	Ref.
	contact	orbital	dipolar	total		
1. 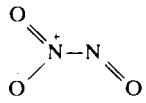	−23·01	1·17	6·35	−15·49	±11·7	74
2. 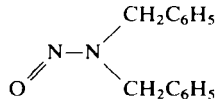	−18·25	0·87	0·69	−16·69	±19·0	75
3. 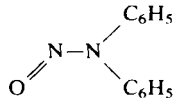	−18.39	4·26	−0·02	−22·68	±22·0	76
4. 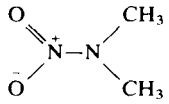	−3·00	−2·55	0·08	−5·47	±4·9	75, 76
5. 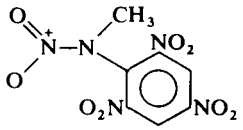	−2·27	−1·82	0·15	−3·94	±4·9	75
6. 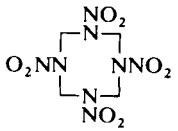	−3·53	−1·62	0·16	−4·99	±4·5	75
7. 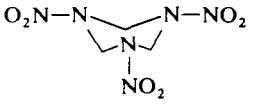	−7·12	0·43	0·49	−6·20	±8·9	75
8. 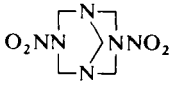	−5·72	−1·35	0·24	−6·83	±8·5	75

TABLE 3—*cont.*

Species	Calculated				Experimental	Ref.
	contact	orbital	dipolar	total		
9. 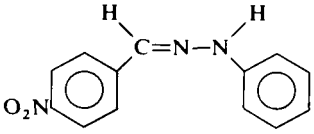	−10·61	−1·38	0·26	−11·72	±10·7	75
10. 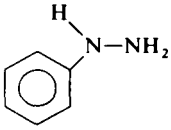	−4·36	0·65	0·67	−3·04	±6·7	75
11. 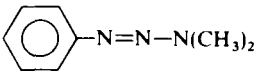	−13·69	−0·34	0·52	−13·52	±14·0	76
12. 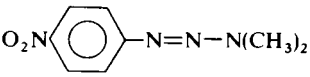	−12·91	−0·41	0·49	−12·83	±13·4	76
13. 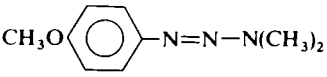	−13·12	−0·38	0·49	−13·02	±14·0	76
14. 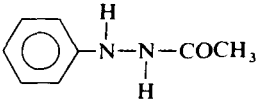 *Z*-isomer	2·31	0·90	0·64	3·85	±3·6	77

TABLE 4

Conversion schemes for shielding constants (σ) referred to different reference signals

No.	$(\sigma_{sample} - \sigma_{ref.II})$	$(\sigma_{ref.II} - \sigma_{ref.I})$	$(\sigma_{sample} - \sigma_{ref.II}) + (\sigma_{ref.II} - \sigma_{ref.I})$
I	true	true	$(\sigma_{sample} - \sigma_{ref.I})_{true}$ $(= \Delta\sigma_{ref.I})$
II	apparent	true	$\Delta\sigma_{ref.I} + (\frac{4}{3}\pi - \alpha)(\chi_{ref.II} - \chi_{sample})$
III	true	apparent	$\Delta\sigma_{ref.I} + (\frac{4}{3}\pi - \alpha)(\chi_{ref.I} - \chi_{ref.II})$
IV	apparent	apparent	$\Delta\sigma_{ref.I} + (\frac{4}{3}\pi - \alpha)(\chi_{ref.I} - \chi_{sample})$

ref. I = primary reference (external neat nitromethane is used in the present review)

ref. II = any secondary reference actually employed

true = true difference between shielding constants

apparent = apparent difference between shielding constants, as estimated from the positions of the resonance signals involved

$\alpha = 0$ for magnetic field (B_0) parallel to concentric cylindrical sample tubes

$\alpha = 2\pi$ for B_0 perpendicular to concentric cylindrical sample tubes

$\alpha = 4\pi/3$ for spherical sample containers

χ = volume magnetic susceptibility

TABLE 5

Volume bulk magnetic susceptibilities at 30 °C

Substance (neat liquid, if not stated otherwise)	Volume susceptibility $\times 10^6$	Ref.
$C(NO_2)_4$	−0·358	80
$MeNO_2$	−0·387	80
Acetone	−0·456	80
MeCN	−0·518	80
MeOH	−0·523	80
Et_2O	−0·522	80
MeCOOH	−0·549	80
n-Hexane	−0·558	80
$MeNH_2$ (liquid under pressure)	−0·564	80
EtOH	−0·569	80
n-Butylamine	−0·591	80
Dioxan	−0·591	80
Pyridine	−0·597	80
Diisopropylamine	−0·598	82
Benzene	−0·609	80
HNO_3 (70% w/w in H_2O)	−0·618	80
Dimethyl sulphoxide	−0·618	82
N-Methylpiperidine	−0·619	82
Cyclohexane	−0·623	80
cis-2,6-Dimethylpiperidine	−0·635	82
CCl_4	−0·684	80
CS_2	−0·693	80
HNO_3 (1 M in H_2O)	−0·715	82
H_2O	−0·716	80
CH_2Cl_2	−0·717	80
NH_4NO_3 (satd. in H_2O)	−0·722	80
H_2SO_4 (100%)	−0·723	80
$NaNO_3$ (satd. in H_2O)	−0·729	80
$CHCl_3$	−0·730	80
NH_4Cl (satd. in H_2O)	−0·769	80
CH_2Br_2	−0·932	80

TABLE 6

Nitrogen shieldings used as conversion factors for various reference substances[a]

Standard	Solution or state	Nitrogen shielding referred to neat nitromethane		
		true	apparent	
			external field perpendicular to sample tube	external field parallel to sample tube
$MeNO_2$	neat liquid	0·0000		
$NaNO_3$	satd. in H_2O	+3·7	(+3·0)[b]	(+5·1)[b]
	0·30 M in H_2O	+3·5	(+2·8)[b]	(+4·9)[b]
HNO_3 or DNO_3	1·0 M in H_2O	+4·4	(+3·7)[b]	+6·2[c] (+5·9)[b]
	7·0 M in H_2O	+12·6		
	10·0 M in H_2O	+18·2		
	15·7 M in H_2O (70% w/w)	+31·3		
NH_4NO_3	satd. in H_2O	+359·6 (NH_4) +4·0 (NO_3)	(+358·9)[b] (+3·3)[b]	(+361·0)[b] (+5·4)[b]
	4 M in 2 M HNO_3	+359·1 (NH_4) +5·6 (NO_3)	(+358·4)[b] (+4·9)[b]	(+360·5)[b] (+7·0)[b]
	5 M in 2 M HNO_3	+359·0 (NH_4) +4·6 (NO_3)	(+358·3)[b] (+3·9)[b]	(+360·4)[b] (+6·0)[b]
	5 M in 2 M HCl	+358·0 (NH_4) +5·2 (NO_3)		
	4·5 M in 3 M HCl	+357·1 (NH_4) +6·3 (NO_3)		
NH_4Cl	satd. in H_2O	+352·9	(+352·1)[b]	(+354·7)[b]
	satd. in 2 M HCl	+352·5		
	2·9 M in 1 M HCl		+355·3[d]	
	1 M in 10 M HCl	+349·9		
NH_3	neat liquid	+381·9	+380·2[d]	
$C(NO_2)_4$	neat liquid	+46·6		
$Me_4N^+Cl^-$	satd. in H_2O	+336·7		
	0·3 M in H_2O	+337·7	(+337·0)[b]	(+339·1)[b]
	2 M in H_2O			+339·0[c]
$Me_4N^+I^-$	0·3 M in H_2O	+337·3	(+336·6)[b]	(+338·7)[b]
$K^+(NCO)^-$	satd. in H_2O	+302·9		
	0·3 M in H_2O	+302·6		
$NaNO_2$	satd. in H_2O	−228·9		
	0·3 M in H_2O	−227·6		

(*a*) Data from ref. 80, if not stated otherwise.
(*b*) Calculated values; bulk susceptibilities from Table 5 are used.
(*c*) Data from ref. 82.
(*d*) Data from ref. 81 and ref. 4; the value for 2·9 M NH_4Cl in 1 M HCl seems to be unreliable, since the sample revealed a change of about 2 ppm in the shielding after 2 years of use.

TABLE 7

Changes in nitrogen shielding induced by some relaxation reagents

Compound	Nitrogen shielding referred to neat nitromethane (induced shielding in parentheses)		
	neat liquid	neat liquid + $Cr(acac)_3$ (1 : 100 molar ratio)	neat liquid + $Gd(dpm)_3$ (1 : 1000 molar ratio)
$MeNO_2$	0·0000	−0·07 ± 0·06	reagent insoluble
MeN=C=O	+365·42 ± 0·06	+365·30 ± 0·08 (−0·12 ± 0·10)	+365·24 ± 0·07 (−0·18 ± 0·12)
$HC(=O)NMe_2$	+277·01 ± 0·09	+277·13 ± 0·07 (+0·12 ± 0·11)	+278·07 ± 0·08 (+1·06 ± 0·12)
MeCN	+135·83 ± 0·06	+135·81 ± 0·07 (−0·02 ± 0·11)	+135·79 ± 0·16* (−0·04 ± 0·11)
Pyridine	+62·03 ± 0·11	+62·44 ± 0·06 (+0·41 ± 0·12)	+68·69 ± 0·12 (+6·61 ± 0·16)
NEt_3	+333·40 ± 0·14	reagent insoluble	+334·39 ± 0·12 (+0·99 ± 0·18)
MeN=C=S	+289·80 ± 0·07	+290·01 ± 0·07 (+0·21 ± 0·10)	+290·08 ± 0·02 (+0·28 ± 0·07)

Data from ref. 85; ^{14}N continuous-wave spectra; 4·33 MHz; high-precision differential saturation technique with full lineshape fitting; concentric spherical sample/standard containers in order to eliminate bulk susceptibility effects; 30 ± 1 °C.

* 1 : 10 000 molar ratio.

TABLE 8

Isotope effects on nitrogen shielding

Molecule	Solvent	Approximate shielding referred to external neat nitromethane		Difference in shielding between $^{14}N^{15}N$ and $^{15}N^{15}N$ isotopomers
$(ONNO_2)^{2-}$ $2Na^+$	D_2O	+43·5	(NO?)	+0·24
		+28	(NO_2?)	+0·13
$[ONN(O)SO_3]^{2-}$ $2K^+$	D_2O	−58	(ON?)	+0·21
		+47	(NSO_3?)	+0·10
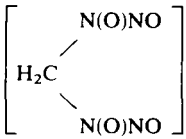 $2Na^+$	D_2O	+87·5	(NCH_2)	+0·14
		−37·5	(NO)	+0·21
$ON-NO_2$	CH_2Cl_2 (−100 °C)	−292		−0·37
		−63		−0·03
$[Et_2NN(O)NO]^-$ $Et_2NH_2^+$	$CDCl_3$ (−10 °C)	+138		?
		−33·5		+0·24

Data from ref. 74; 30% ^{15}N-enriched N–N moiety containing ~9% of $^{15}N^{15}N$ isotopomer; ^{15}N spectra; isotope effects estimated from unsymmetrical locations of $^{14}N^{15}N$ singlets inside the corresponding $^{15}N^{15}N$ doublets.

TABLE 9

Chemically induced dynamic nuclear polarization (CIDNP) effects on ^{15}N NMR spectra

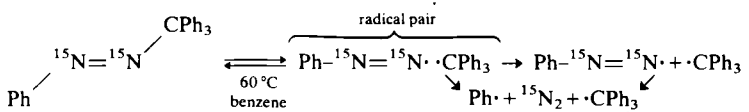

CIDNP	^{15}N–Ph	$^{15}NCPh_3$	$^{15}N_2$
Predicted	enhanced absorption; twice that of $NCPh_3$	enhanced absorption	emission
Found	enhanced absorption at −141; 2·6 times that of $NCPh_3$	enhanced absorption at −165	emission signal at +70·5

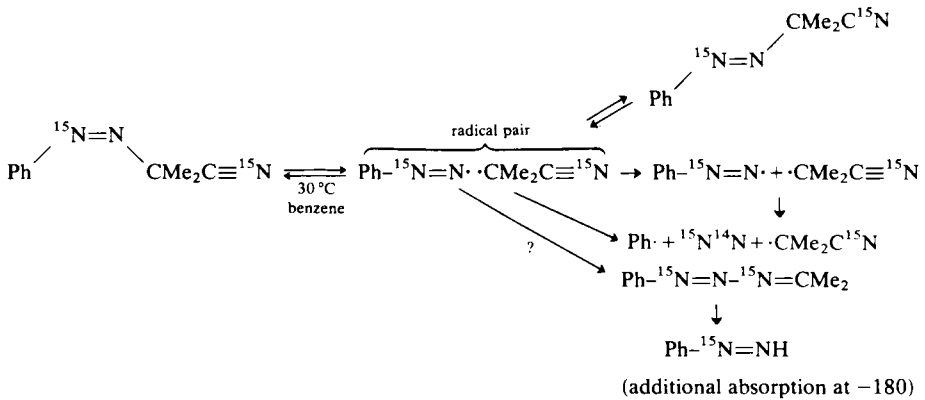

CIDNP	^{15}N–Ph	C≡^{15}N	^{15}N≡N
Predicted	enhanced absorption	emission	emission
Found	enhanced absorption at −150 (*cis*) and −128 (*trans*)	emission at +112 (*cis*) and +122 (*trans*)	emission signal at +70·5

Data from refs 114 and 86; ^{15}N NMR spectra of labelled compounds; 10·14 MHz; originally referred to external aqueous $NaNO_3$, +3·7 ppm from neat nitromethane (Table 6); recalculated to the latter standard.

TABLE 10

Nitrogen shieldings induced in model *N*-oxide structures by the Yb(fod)$_3$ shift reagent

Structure	Induced nitrogen shielding referred to parent compound without shift reagent	
	N→O	-N=
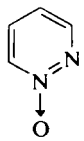	−119·3	−86·0
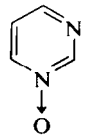	−31·6	+4·7
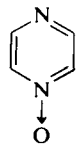	−85·6	−76·7
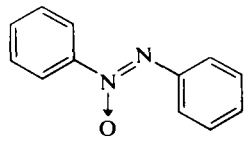	−44·5	−28·5

Data from ref. 115; solutions in $CHCl_3$; results extrapolated to 1 : 1 molar ratio of chelate to solute; ^{15}N spectra; 10·1 MHz; field perpendicular to sample tube; data uncorrected for bulk susceptibility effects.

TABLE 11

Effects of shift reagents on the nitrogen shieldings in polypeptides

Sample	Nitrogen shielding referred to neat $MeNO_2$*		
$PhCH_2OCO$-Gly-Leu-Leu-OMe			
0·5 M in CH_2Cl_2			
no reagent	+305·7	+261·8	+261·3
+Eu(dpm)$_3$ (1 : 60)	+306·8	+263·1	+267·4
+Dy(fod)$_3$ (1 : 60)	+310·6	+267·0	+264·5
+Dy(fod)$_3$ (1 : 20)	broad	broad	+273·9
0·5 M in HCOOH	+309·8	+259·5	+257·9
$PhCH_2OCO$-Ala-Leu-Leu-OMe			
0·5 M in CH_2Cl_2			
no reagent	+290·6	+260·8	+260·8
+Dy(fod)$_3$ (1 : 60)	+295·4	+265·3	+265·3
0·5 M in HCOOH	+288·1	+260·0	+257·5

Data from ref. 244; ^{15}N (natural abundance and ^{15}N-enriched compounds) spectra; 9·12 MHz; field perpendicular to sample tube; referred originally to NO_3^- in aqueous NH_4NO_3, +4·0 ppm from neat nitromethane (Table 6); conversion scheme II (Table 4); changes in shielding may contain a considerable share of bulk susceptibility effects.

* Assignments follow the sequence of amino acid residues in the corresponding formulae; Gly = glycine; Leu = leucine; Ala = alanine; dpm = $(Me_3CCOCHCOCMe_3)^-$; fod = $(CF_3CF_2CF_2COCHCOCMe_3)^-$.

TABLE 12

^{14}N signal linewidths as an aid to nitrogen shielding assignments[99]

Molecule	Nitrogen atom	Calculated value of electric field gradient term*	^{14}N signal half-height width (Hz)	Nitrogen shielding referred to neat $MeNO_2$
	N-2	0·2324	395	+20
	N-4	0·1302	117	+140
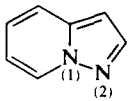	N-1	0·0715	89	+141
	N-2	0·2672	342	+75
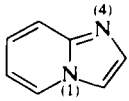	N-1	0·0577	54	+178
	N-4	0·1238	270	+132
$Me-N=N^+=N^-$	MeN	0·4439	126	+306·5
	=N=	0·0032	13	+131·7
	=N	0·0707	19	+168·9
Me_2N-CN	Me_2N	0·5261	280	+372
	CN	0·0234	125	+185

* This is expressed as $(eq_{max})^2(1+\eta^2/3)$, where eq_{max} is the maximum absolute component of electric field gradient at the nitrogen nucleus (in the principal axis system) and η is the asymmetry parameter; they are calculated by the INDO method; the term should be proportional to the quadrupolar relaxation rate for isotropic rotation and a constant correlation time.

TABLE 13

Characteristic nitrogen shielding ranges for various classes of molecule

Name	General formula	Nitrogen shielding referred to neat nitromethane	
		lower limit	upper limit
Ammonia	NH_3	+378	+400
Alkylamines	NR_3	+300	+390
Hydrazines	R_2N-NR_2	+255	+335
Hydroxylamines	R_2N-OR	+260	+330
Arylamines	(aryl)$-NR_2$	+290	+345
Silylamines	R_3Si-NR_2	+320	+380
Aminophosphines	R_2P-NR_2	+200	+370
Aminoboranes	R_2B-NR_2	+260	+370
Silatranes	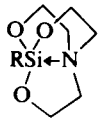	+345	+360
Chloramines	$RNCl_2$, R_2NCl	+180	+340
Ammonium ion	NH_4^+	+350	+360
Alkylammonium ions	NR_4^+	+310	+360
Arylammonium ions	(aryl)$-NR_3^+$	+320	+340
Enamines	$R_2C=CR-NR_2$	+300	+335
Isocyanates	$R-N=C=O$	+325	+365
Cyanamides	R_2N-CN	+320	+380 (R_2N)
		+180	+200 (CN)
Enaminoketones	$RC(=O)CR=CR-NR_2$	+270	+300
Ureas	$R_2N-C(=O)-NR_2$	+260	+320
Carbamates	$RO-C(=O)-NR_2$	+280	+315
Guanidines	$(R_2N)_2C=NR$	+295	+335 (R_2N)
		+175	+220 (=NR)
Guanidinium ions	$C^+(NR_2)_3$	+275	+310
Azides	$R-N=N^+=N^-$	+260	+320 (RN)
		+130	+150 ($=N^+=$)
		+140	+180 ($=N^-$)
Amides, lactams, peptides	$RC(=O)-NR_2$	+235	+285
Thioureas	$R_2N-C(=S)-NR_2$	+250	+300
Thioamides	$RC(=S)-NR_2$	+220	+250
Isothiocyanates	$R-N=C=S$	+265	+290
Hydrazones	$R_2C=N-NR_2$	+205	+285 (NR_2)
		+15	+60 (=N–)
Carbodiimides	$RN=C=NR$	+270	+300
Isocyanides (isonitriles)	$R-N^+\equiv C^-$	+180	+220
Cyanates	$R-O-CN$	+190	+210
Fulminates (nitrile *N*-oxides)	$R-C\equiv N\rightarrow O$	+160	+180
Cyanides (nitriles)	$R-CN$	+110	+140

TABLE 13—*cont.*

Name	General formula	Nitrogen shielding referred to neat nitromethane: lower limit	upper limit
Thiocyanates	R–S–CN	+85	+105
Imides	$(RC{=}O)_2NR$	+180	+200
Immonium ions	$R_2C{=}N^+R_2$	+160	+200
Nitrilium ions	$R{-}C{\equiv}N^+R$	+235	+250
Azoles (pyrrole type nitrogen atoms)		+100	+280
Azoles, oxazoles, thiazoles (pyridine type nitrogen atoms)	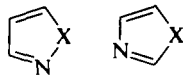 (X = NR, O, S)	−60	+145
Azolium ions	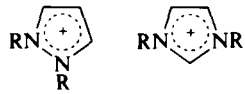	+170	+220
Sydnone type structures	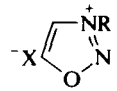	+80 +5	+115 (N^+R) +35 (–N=)
Furoxans	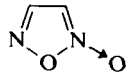	−5	+25
Azoloazines (indolizine type nitrogen atoms)	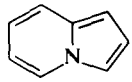	+120	+200
Azines (pyridine type nitrogen atoms)		−80	+175
Azinium ions		+160	+265
Azine *N*-oxides	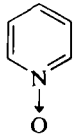	+40	+170
Imines	$R_2C{=}NR$	+20	+90
Oximes	$R_2C{=}N{-}OR$	−30	+60

TABLE 13—*cont.*

Name	General formula	Nitrogen shielding referred to neat nitromethane: lower limit	upper limit
Nitrones	$R_2C{=}N(\rightarrow O)R$	+70	+115
Diazonium ions	$R{-}N^+{\equiv}N$	+120	+160 (N^+)
		+15	+60 ($\equiv$N)
Diazo compounds	$R_2C{=}N^+{=}N^-$	+80	+155 (N^+)
		−70	+65 (=N^-)
Sulphinylamines	R–N=S=O	+25	+80
Nitrates	R–O–NO_2	+40	+70
Nitramines	$R_2N{-}NO_2$	+100	+225 (RN)
		+10	+45 (NO_2)
gem-Polynitroalkanes	$R_2C(NO_2)_2$, $RC(NO_2)_3$, $C(NO_2)_4$	0	+50
Aromatic nitro compounds	(aryl)–NO_2	+7	+40
Nitroalkanes	R–NO_2	−30	+2
Azoxy compounds	$R{-}N{=}N(\rightarrow O){-}R$	+20	+75 (N, NO)
Triazenes	$R{-}N{=}N{-}NR_2$	+20	+35 (RN)
		−75	−70 (=N–)
		+215	+230 (NR_2)
Nitrosoamines	$R_2N{-}N{=}O$	+110	+160 (R_2N)
		−175	−150 (NO)
Diazirine ring		*ca.* +50	
Nitrites	R–O–N=O	*ca.* −190	
Azo compounds	R–N=N–R (R = alkyl or aryl)	−170	−120
Azo bridges	X–N=N–X (X = heteroatom)	−620	−25
Thionitrites	R–S–N=O	−410	−330
Nitroso compounds	R–N=O	−580	−430
Some important inorganic molecules and ions			
Ammonium ion	NH_4^+	+350	+360
Ammonia	NH_3	+378	+400
Isocyanic acid	HNCO	*ca.* +355	
(Iso)cyanate ion	$(NCO)^-$	*ca.* +303	
Hydrazoic acid	$HN{=}N^+{=}N^-$	*ca.* +300 (HN)	
		ca. +130 (N^+)	
		ca. +165 (N^-)	
Azide ion	$(NNN)^-$	*ca.* +281 (terminal N)	
		ca. +132 (central N)	
Isothiocyanic acid	HNCS	*ca.* +265	
(Iso)thiocyanate ion	$(NCS)^-$	*ca.* +172	
Cyanide ion	CN^-	*ca.* +104	
Hydrogen cyanide	HCN	*ca.* +130	
Fulminate ion	$(CNO)^-$	*ca.* +175	

TABLE 13—*cont.*

Name	General formula	Nitrogen shielding referred to neat nitromethane	
		lower limit	upper limit
Nitrogen oxides	NNO	*ca.* +143 (central N)	
		ca. +227 (terminal N)	
	$ONNO_2$	*ca.* −300 (NO)	
		ca. −65 (NO_2)	
	N_2O_4	+11	+20
	N_2O_5	+48	+62
Nitric acid	$HONO_2$	+3	+40
Nitrate ion	NO_3^-	+3	+6
Nitrite ion	NO_2^-	*ca.* −228	
Nitronium ion	NO_2^+	*ca.* +130	
Nitrosyl ion	NO^+	*ca.* +3	

Data from this book and from refs 1 and 2 for diamagnetic substances.

TABLE 14

Correlations between nitrogen shieldings and barriers to internal rotation of the Me_2N moiety in amides, thioamides, and related structures[a]

Molecule (in neat liquid or chlorinated solvent)	Nitrogen shielding referred to neat nitromethane for the Me_2N moiety	Activation energy of rotation, E_a (kJ mol^{-1})
		experimental data
Me_2NCHO	+277·4	86·2
Me_2NCOMe	+283·9	77·5
Me_2NCOPh	+281·7	73·7
Me_2NCOCl	+286·3	72·9
$Me_2NCOCCl_3$	+289·5	67·8
$Me_2NCH{=}CHCHO$	+291·2	69·9
$Me_2NCH{=}CHCOMe$	+300·6	60·7
$Me_2NCH{=}NPh$	+301·8	61·5
$Me_2NCH{=}CHPh$	+326·2	37·7
Me_2NCHS	+227·8	92·1
Me_2NCSMe	+237·1	86·7
Me_2NCSCl	+236·0	79·5
$Me_2NCSSMe$	+246·6	67·0
$Me_2\dot{N}C^+(SMe)NMe_2$	+271·3	39·8
		values predicted from nitrogen shieldings
$Me_2N^+{=}CH_2(CF_3COO^-)$	+158·7	193·8
$Me_2N^+{=}CHCl\ (Cl^-)$	+218·0	140·2
$Me_2N^+{=}CHOMe\ (SO_3F^-)$	+238·1	121·8
$Me_2NCOMe{\cdot}AlCl_3$	+244·3	116·4
$(Me_2N)_2CO{\cdot}SbCl_5$	+308·5	58·2
$Me_2NCOOMe$	+315·7	51·5
$(Me_2N)_2CO$	+319·0	48·6 26·4 (found[b])
$Me_2NCH(CH_2)CHPh$	+347·9	22·2
$Me_2NCH{=}CHMe$	+353·0	17·6
$(Me_2N)_2CS$	+294·7	13·4 26·4 (found[b])

(*a*) Data from ref. 40 and references therein; originally referred or recalculated to aqueous $NaNO_3$ standard, +3·7 ppm from neat nitromethane (Table 6); the following correlations were suggested, separately for amides and thioamides:

amides and related structures

$$E_a(\pm 2{\cdot}8\ \text{kJ mol}^{-1}) = 338{\cdot}9 - 0{\cdot}9085(\text{nitrogen shielding of } Me_2N \text{ referred to } MeNO_2)$$

thioamides and related structures

$$E_a(\pm 3{\cdot}3\ \text{kJ mol}^{-1}) = 389{\cdot}9 - 1{\cdot}277(\text{nitrogen shielding of } Me_2N \text{ referred to } MeNO_2)$$

where the equations are modifications of the original ones which refer to kcal mol^{-1} units of E_a and deshieldings relative to that in aqueous $NaNO_3$.

(*b*) Data from ref. 46 where the predictions of barriers from nitrogen shielding data are criticized.

TABLE 15

Correlation between nitrogen shieldings and barriers to internal rotation in R_2N–N=X molecules

Molecule	Nitrogen shielding (ppm) referred to neat nitromethane for the R_2N moiety (solvent or state in parentheses)	$\Delta G^{\ddagger}_{298}$ for rotation around N–N bond (kJ mol^{-1})
Me_2N–N=O	+150·4 (neat liquid)	96·2 (in $PhNO_2$)
Me_2N–N=NPh	+229·9 (in $CDCl_3$)	57·3 (in $CDCl_3$)
Me_2N–N=N·C_6H_4·NO_2*p*	+219·2 (in $CDCl_3$)	65·6 (in $CDCl_3$)
Me_2N–N=N·C_6H_4·Cl*p*	+228·3 (in $CDCl_3$)	58·1 (in $CDCl_3$)
Me_2N–N=N·C_6H_4·CH_3*p*	+233·6 (in $CDCl_3$)	54·3 (in $CDCl_3$)
Me_2N–NO_2	+219·7	(62·2) (predicted)
Me_2N–N=CHR	+282·7	(31·0) (predicted)
Me_2N–NH_2	+320·3	(11·9) (predicted)
Et_2N–N=O	+126·0 (neat liquid)	97·0 (neat liquid)
$Pr^i{}_2N$–N=O	+110·9 (neat liquid)	98·2 (neat liquid)

Data from ref. 45 and references therein; originally referred or recalculated to aqueous $NaNO_3$ standard, +3·7 ppm from neat nitromethane (Table 6); correlation found for the Me_2N derivatives:

$\Delta G^{\ddagger}_{298}(Me_2NN{=}X)(\pm 1{\cdot}7\ \text{kJ mol}^{-1}) = 172{\cdot}0 - 0{\cdot}50(\text{nitrogen shielding referred to } MeNO_2)$

after introducing corrections due to conversion to neat nitromethane scale of nitrogen shieldings.

TABLE 16

Suggested correlations between barrier to internal rotation of the NR_2 moiety and nitrogen shielding

Type of structure	Correlation
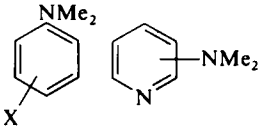	$\Delta G^{\ddagger} = 219{\cdot}6 - 0{\cdot}59$(nitrogen shielding of NMe_2 ref. to $MeNO_2$)
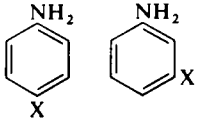	$\Delta G^{\ddagger} = 206{\cdot}9 - 0{\cdot}56$(nitrogen shielding of NH_2 ref. to $MeNO_2$)
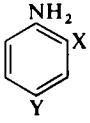	$\Delta G^{\ddagger} = 213{\cdot}2 - 0{\cdot}56$(nitrogen shielding of NH_2 ref. to $MeNO_2$)

Data from ref. 47 and references therein; original equations have been modified here in order to conform to nitrogen shieldings referred to neat nitromethane.

TABLE 17

Nitrogen shieldings in some alkyl amines

Compound	Solution	Nitrogen shielding referred to neat nitromethane	Notes
NH_3	neat liquid	+381·93 ± 0·14	(a)
		+380·2	(d)
	various solvents	see ref. 1, p. 151	
$MeNH_2$	neat liquid	+378·73 ± 0·15	(a)
	neat liquid, −20 °C	+382·2	(b)
	various solvents	see ref. 1, p. 151	
	2 M in MeOH	+377·3	(c)
$EtNH_2$	2 M in cyclohexane (0 °C)	+355·1	(c)
	2 M in MeOH (0 °C)	+355·4	(c)
Pr^nNH_2	2 M in cyclohexane	+360·7	(c)
	2 M in MeOH	+359·6	(c)
	various solvents	see Table 24	
Bu^nNH_2	2 M in cyclohexane	+360·4	(c)
	2 M in MeOH	+359·4	(c)
Bu^iNH_2	2 M in cyclohexane	+364·2	(c)
	2 M in MeOH	+362·7	(c)
$Me_2CHCH_2CH_2NH_2$	2 M in cyclohexane	+360·2	(c)
	2 M in MeOH	+359·3	(c)
$Me_3CCH_2NH_2$	2 M in cyclohexane	+368·7	(c)
	2 M in MeOH	+367·6	(c)
Pr^iNH_2	2 M in cyclohexane	+337·2	(c)
	2 M in MeOH	+338·1	(c)
Bu^sNH_2	2 M in cyclohexane	+342·4	(c)
	2 M in MeOH	+342·2	(c)
	neat liquid	+339·8	(d)
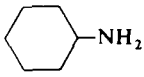	2 M in cyclohexane	+340·8	(c)
	2 M in MeOH	+340·4	(c)
	2 M in cyclohexane	+340·8	(c)
	2 M in MeOH	+340·4	(c)
	2 M in cyclohexane	+349·6	(c)
	2 M in MeOH	+349·7	(c)
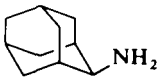	2 M in cyclohexane	+346·5	(c)
	2 M in MeOH	+346·5	(c)
Bu^tNH_2	2 M in cyclohexane	+322·4	(c)
	2 M in MeOH	+324·3	(c)
$(Et)Me_2CNH_2$	2 M in cyclohexane	+328·4	(c)
	2 M in MeOH	+328·6	(c)

TABLE 17—*cont.*

Compound	Solution	Nitrogen shielding referred to neat nitromethane	Notes
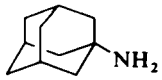	2 M in cyclohexane	+322·5	(c)
	2 M in MeOH	+323·7	(c)
Me_2NH	neat liquid, −20 °C	+374·3	(b)
	80% v/v in benzene	+372·2	(f)
	2 M in cyclohexane (0 °C)	+371·1	(c)
	2 M in MeOH (0 °C)	+369·5	(c)
(Me)(Et)NH	2 M in cyclohexane	+352·8	(c)
	2 M in MeOH	+352·0	(c)
Et_2NH	2 M in cyclohexane	+333·0	(c)
	2 M in MeOH	+333·7	(c)
$Pr^n{}_2NH$	2 M in cyclohexane	+342·2	(c)
	2 M in MeOH	+340·5	(c)
	various solvents	see Table 24	
$Bu^n{}_2NH$	2 M in cyclohexane	+341·7	(c)
	2 M in MeOH	+340·0	(c)
$Bu^i{}_2NH$	2 M in cyclohexane	+346·4	(c)
	2 M in MeOH	+345·2	(c)
$Pr^i{}_2NH$	2 M in cyclohexane	+305·1	(c)
	2 M in MeOH	+306·5	(c)
	various solvents	see Table 24	
Me_3N	neat liquid	+368·59 ± 0·10	(a)
	neat liquid, −20 °C	+372·7	(b)
	neat liquid, +4 °C	+372·2	(f)
	2 M in cyclohexane	+366·9	(c)
	2 M in MeOH	+363·1	(c)
	various solvents	see p. 151 of ref. 1	
$EtNMe_2$	2 M in cyclohexane	+355·2	(c)
	2 M in MeOH	+351·3	(c)
Pr^nNMe_2	neat liquid	+358·2	(b)(f)
	2 M in cyclohexane	+358·4	(c)
	2 M in MeOH	+352·8	(c)
Bu^nNMe_2	2 M in cyclohexane	+358·4	(c)
	2 M in MeOH	+352·8	(c)
Bu^iNMe_2	2 M in cyclohexane	+359·0	(c)
	2 M in MeOH	+354·8	(c)
$Me_2CHCH_2CH_2NMe_2$	2 M in cyclohexane	+358·4	(c)
	2 M in MeOH	+352·9	(c)
$MeNEt_2$	2 M in cyclohexane	+343·1	(c)
	2 M in MeOH	+340·5	(c)
Et_3N	neat liquid	+333·40 ± 0·14	(h)
		+331·9	(b)
	2 M in cyclohexane	+333·6	(c)
	2 M in MeOH	+332·0	(c)

TABLE 17—*cont.*

Compound	Solution	Nitrogen shielding referred to neat nitromethane	Notes
Pr^iNMe_2	2 M in cyclohexane	+353·0	(c)
	2 M in MeOH	+347·5	(c)
Bu^sNMe_2	2 M in cyclohexane	+358·9	(c)
	2 M in MeOH	+349·6	(c)
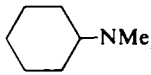	2 M in cyclohexane	+353·9	(c)
	2 M in MeOH	+347·7	(c)
	2 M in cyclohexane	+353·7	(c)
Bu^tNMe_2	2 M in cyclohexane	+348·8	(c)
	2 M in MeOH	+342·5	(c)
$(Et)Me_2CNMe_2$	2 M in cyclohexane	+354·6	(c)
	2 M in MeOH	+344·9	(c)
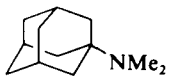	2 M in cyclohexane	+348·9	(c)
$MeNPr^n_2$	2 M in cyclohexane	+350·0	(c)
	2 M in MeOH	+343·8	(c)
$MeNBu^n_2$	2 M in cyclohexane	+349·7	(c)
	2 M in MeOH	+343·6	(c)
$MeNBu^i_2$	2 M in cyclohexane	+350·7	(c)
	2 M in MeOH	+349·4	(c)
$MeNPr^i_2$	2 M in cyclohexane	+336·5	(c)
	2 M in MeOH	+330·3	(c)
$Me_3CCH_2NMe_2$	2 M in cyclohexane	+364·9	(c)
$HOCH_2CH_2NH_2$	neat liquid	+362 ± 2	(e)
$HOCH_2CH_2CH_2NH_2$	neat liquid	+358 ± 2	(e)
$H_2NCH_2CH_2NH_2$	2 M in $CDCl_3$	+366·1	(i)
$MeCH(NH_2)CH_2NH_2$	2 M in $CDCl_3$	+369·0, +349·8	(i)
$H_2NCH_2CH_2CH_2NH_2$	2 M in $CDCl_3$	+354·1	(i)
$(HOCH_2CH_2)_3N$	0·3 M in $CDCl_3$	+354·0	(g)
	0·3 M in acetone	+355·4	(g)
	0·3 M in MeOH	+354·1	(g)
	0·3 M in H_2O	+348·3	(g)
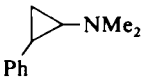	neat liquid	+347·9	(j)

(a) Data from ref. 80; ^{14}N continuous-wave spectra; 4·33 MHz; high-precision differential saturation technique with full lineshape fitting; 30 °C; concentric spherical sample/standard containers in order to eliminate bulk susceptibility effects; referred to neat nitromethane.

(b) Data from ref. 47; ^{15}N natural abundance spectra; 9·12 MHz; field perpendicular to sample tube; referred originally to aqueous $NaNO_3$, +3·7 ppm from neat nitromethane (Table 6); conversion scheme II (Table 4).

(c) Data from ref. 119; ^{15}N natural abundance spectra; 18·25 MHz; field parallel to sample tube; referred originally to 1 M DNO_3, +6·2 ppm from neat nitromethane (Table 6); conversion scheme IV (Table 4).

(d) Data from ref. 81; ^{15}N natural abundance spectra; 10·09 MHz; field perpendicular to sample tube; referred originally to neat nitromethane; uncorrected for bulk susceptibility effects.

(e) Data from ref. 123; ^{15}N natural abundance spectra; 27·4 MHz; low-precision measurements referred originally to Me_4N^+, +337 ppm from neat nitromethane (Table 6).

(f) Data from ref. 41; ^{15}N natural abundance spectra; 10·1 MHz; field perpendicular to sample tube; referred originally to NO_3^- in dilute aqueous NH_4NO_3, probably +3·7 ppm from neat nitromethane (Table 6); conversion scheme II (Table 4).

(g) Data from ref. 124; ^{15}N-labelled compound; ^{15}N spectrum; 9·12 MHz; field perpendicular to sample tube; referred originally to neat nitromethane; uncorrected for bulk susceptibility effects.

(h) Data from ref. 85; details as in note (a).

(i) Data from ref. 125; ^{15}N natural abundance spectra; 10·09 MHz; field perpendicular to sample tube; referred originally to what was reported as aqueous NH_4Cl (+352·9 ppm from neat nitromethane; Table 6), but the reported shift for pyridine suggests that aqueous NH_4NO_3 was used, +359·6 ppm from neat nitromethane (Table 6); conversion scheme II (Table 4).

(j) Data from ref. 40; ^{15}N natural abundance spectra; 6·08 MHz; field perpendicular to sample tube; referred originally to dilute HNO_3, probably +3·7 ppm from neat nitromethane (Table 6); conversion scheme II (Table 4).

TABLE 18

Additivity rules for alkyl effects on nitrogen shielding in amines and ammonium ions[119]

Parameter assignment*	Nitrogen shielding		
	amine (in cyclohexane)	amine (in MeOH)	hydrochloride (in MeOH)
Starting value for RNH_2 or RNH_3^+ (R=Me)	+378·8	+377·2	+361·8
Each C-β	−22·6	−21·3	−15·2
Each C-γ	+3·8	+3·4	+2·2
Each branching at C-α	+4·9	+5·0	+3·6
Additionally for each branching at C-α if there is C-γ at the same residue	+1·8	+0·6	−0·4
Starting value for R_2NH or $R_2NH_2^+$ (R=Me)	+361·3	+369·8	+356·6
Each C-β	−19·0	−18·3	−13·5
Each C-γ		same as for RNH_2 or RNH_3^+	
Branching effects		same as for RNH_2 or RNH_3^+	
Starting value for R_3N or R_3NH^+ (R=Me)	+366·7	+362·1	+349·2
Each C-β	−11·7	−10·5	−9·1
Each C-γ	+2·2	+1·8	+0·9
Each branching at C-α	+8·2	+5·7	+3·6
Additional branching effect		same as for RNH_2 or RNH_3^+	

* Starting values are recalculated in order to fit the neat nitromethane scale of nitrogen shieldings; the predicted value for any alkyl amine is obtained by summation of effects of all C-β and C-γ atoms and all branchings at C-α.

TABLE 19

Nitrogen shieldings in some simple cyclic amines

Substituent R	Nitrogen shielding referred to neat nitromethane (solvents and solutions specified in footnotes)				
			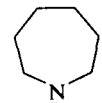	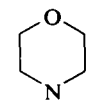	Et_2NR
H	+343·5 (a) +343·5 (d) +342·1 (e)	+343·2 (a) +342·5 (d) +343·2 (e) +342·1 (f)		+350·1 (a)	
Me	+339·5 (a)	+343·5 (a) +340·8 (c) +342·8 (d) +340·6 (e) +340·8 (f)		+347·7 (a)	
Et		+329·4 (d) +328·2 (e)			
Pr^n	+329·1 (a)	+333·4 (a)		+337·5 (a)	
Bu^i	+329·8 (a)	+334·1 (a)		+338·7 (a)	
Ph_2CHCH_2–	+330·3 (a)	+334·6 (a)		+338·9 (a)	
Cyclopentyl	+315·9 (a) +314·2 (b)	+320·9 (a) +320·5 (b)	+327·1 (b)	+324·5 (a) +324·7 (b)	+326·3 (b)
Cyclohexyl	+318·6 (a) +319·4 (b)	+327·1 (a) +327·0 (b)	+331·5 (b)	+330·2 (a) +330·1 (b)	+326·2 (b)
Cycloheptyl	+319·5 (b)			+328·7 (b)	
Cyclooctyl	+317·7 (b)				
2-Me-cyclohexyl	+319·1 (b)				
Pr^i		+326·5 (d) +342·2 (e)			

(a) Data from ref. 41; ^{15}N natural abundance spectra; 10·1 MHz; field perpendicular to sample tube; referred originally to NO_3^- in aqueous 0·5 M NH_4NO_3, probably +3·7 ppm from neat nitromethane (Table 6); conversion scheme II (Table 4); 80% v/v solutions in benzene-d_6.

(b) Data from ref. 126; ^{15}N natural abundance spectra; 18·25 MHz; field parallel to sample tube; referred originally to 1 M DNO_3, +6·2 ppm from neat nitromethane (Table 6); conversion scheme IV (Table 4); 20 mol % solutions in cyclohexane; $Cr(acac)_3$ added in order to shorten T_1 time.

(c) Data from ref. 81; ^{15}N natural abundance spectra; 10·09 MHz; field perpendicular to sample tube; referred originally to neat nitromethane; uncorrected for bulk susceptibility effects; neat liquids, $Cr(acac)_3$ added.

(d) Data from ref. 127; details as in note (b); 2 M solutions in cyclohexane.

(e) See footnote (d); 2 M solutions in MeOH.

(f) Data from ref. 128; ^{15}N natural abundance spectra; 10·09 MHz; field perpendicular to sample tube; referred originally to 2·9 M NH_4Cl in 1 M HCl, but reported relative to "anhydrous ammonia", +380·2 ppm from neat nitromethane (Table 6); conversion scheme II (Table 4); neat liquids.

TABLE 20

Some additional nitrogen shielding data for cyclic amines

Compound		Solution	Nitrogen shielding referred to neat nitromethane	Notes
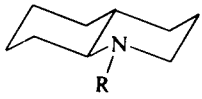	R=H	2 M in cyclohexane	+327·3	(a)
	R=Me	2 M in cyclohexane	+333·6	(a)
		2 M in MeOH	+330·9	(a)
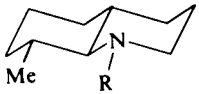	R=H	2 M in cyclohexane	+330·8	(a)
	R=Me	2 M in cyclohexane	+356·4	(a)
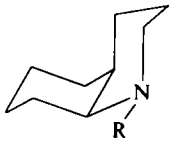	R=H	2 M in cyclohexane	+337·8	(a)
	R=Me	2 M in cyclohexane	+345·7	(a)
		2 M in MeOH	+341·6	(a)
Decahydroquinoline derivatives				
		neat liquid	+342·1	(b)
Piperidine				
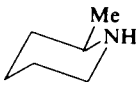		neat liquid	+324·9	(b)
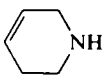		neat liquid	+352·2	(b)
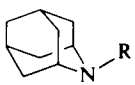	R=H	2 M in benzene	+322·0	(a)
		2 M in MeOH	+323·5	(a)
	R=Me	2 M in cyclohexane	+342·2	(a)
2-Azaadamantane				

TABLE 20—*cont.*

Compound	Solution	Nitrogen shielding referred to neat nitromethane	Notes
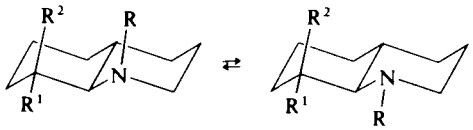 [A] ⇄ [B]	2–4 M in benzene		
R^1 R^2 predominant conformer			
R=H			
H Me B		+328·8	(d)
Me H B		+330·6	(d)
H Bu^t B		+324·5	(d)
Bu^t H A		+325·9	(d)
H H B		+325·9	(d)
R=Me			
H Me B		+334·4	(d)
Me H A		+354·2	(d)
H Bu^t B		+333·3	(d)
Bu^t H A		+352·0	(d)
H H B		+331·7	(d)
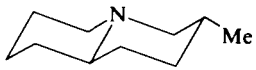	2 M in cyclohexane	+318·2	(a)
	2·1 M in $CDCl_3$	+317·9	(b)
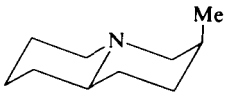	2 M in cyclohexane	+327·3	(a)
	0·3 M in $CDCl_3$	+327·0	(a)
Quinolizidine derivatives			
	in benzene	+372·7	(a)
	in H_2O	+361·2	(a)
Quinuclidine			
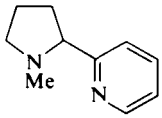	0·2 M in $CDCl_3$	+330·1 (NMe)	(c)

TABLE 20—*cont.*

Compound	Solution	Nitrogen shielding referred to neat nitromethane	Notes
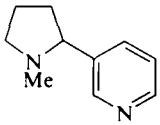 Nicotine	0·2 M in $CDCl_3$	+327·6 (NMe)	(c)
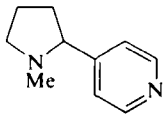	0·2 M in $CDCl_3$	+329·4 (NMe)	(c)
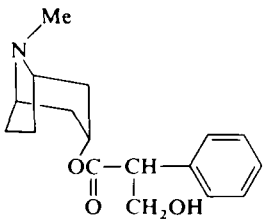 Atropine	in $CHCl_3$	+321·1	(a)
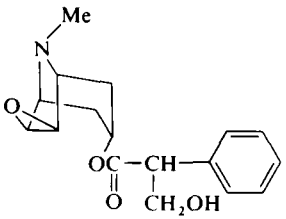 Scopolamine	in $CHCl_3$	+342·6	(a)

(a) Data from ref. 127; ^{15}N natural abundance spectra; 18·25 MHz; field parallel to sample tube; referred originally to 1 M DNO_3, +6·2 ppm from neat nitromethane (Table 6); conversion scheme IV (Table 4).

(b) Data from ref. 128; ^{15}N natural abundance spectra; 10·09 MHz; field perpendicular to sample tube; referred originally to 2·9 M NH_4Cl in 1 M HCl, but reported relative to "anhydrous ammonia", +380·2 ppm from neat nitromethane (Table 6); conversion scheme IV (Table 4).

(c) Data from ref. 129; ^{15}N natural abundance spectra; 10·1 MHz; field perpendicular to sample tube; referred originally to neat nitromethane; uncorrected for bulk susceptibility effects.

(d) Data from ref. 130; ^{15}N natural abundance spectra; 10·09 MHz; field perpendicular to sample tube; referred originally to neat nitromethane, but reported relative to NH_3, +380·2 ppm from neat nitromethane (Table 6); uncorrected for bulk susceptibility effects.

TABLE 21

Trends in nitrogen shieldings in cyclic amines

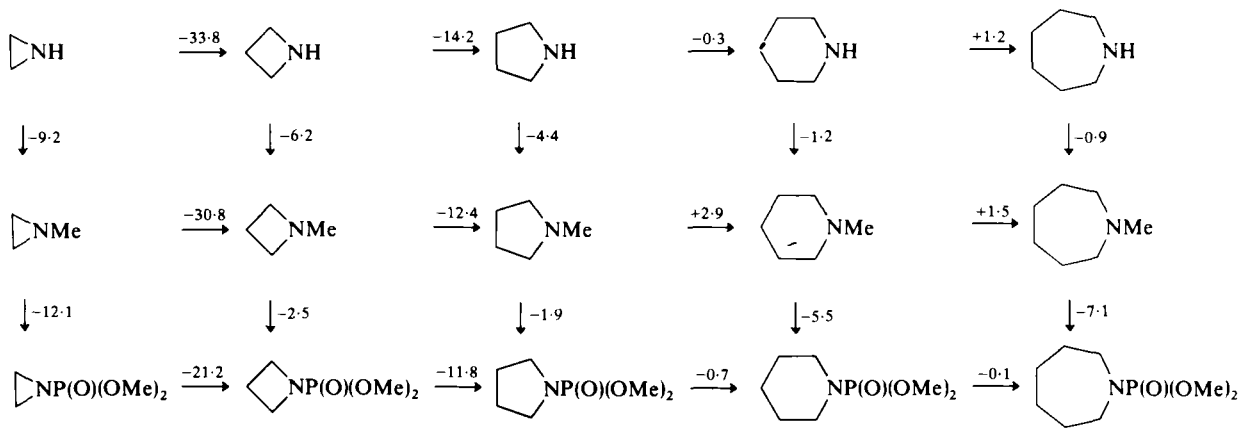

Data from ref. 131 for 4–8 M solutions in $CDCl_3$.

TABLE 22

Nitrogen shieldings in methyl-substituted piperidines

	Nitrogen shielding referred to neat nitromethane for structures and solutions specified			
	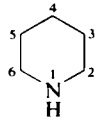		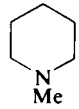	
Substituent	2 M in cyclohexane	2 M in MeOH	2 M in cyclohexane	2 M in MeOH
None	+342·5	+343·2	+342·5	+337·6
2-Me	+325·3	+326·8	+331·3	+329·3
3-Me	+343·2	+343·4	+343·8	+340·6
4-Me	+343·7	+344·2	+343·2	+340·8
cis-2,6-Me_2	+306·9	+309·7	+318·1	+317·2
trans-2,6-Me_2	+316·4	+317·7	+335·8	+331·7
cis-3,5-Me_2	+342·7	+342·6	+343·5	+340·5
trans-3,5-Me_2	+353·5	+353·6	+351·3	+347·9
cis-2,3-Me_2	+336·1			
trans-2,3-Me_2	+324·6		+331·1	
3,3-Me_2	+349·8	+350·4	+347·6	+344·9
4,4-Me_2	+343·9	+344·4	+342·9	
2,2,6,6-Me_4	+298·5	+298·8	+329·5	+324·7

Data from ref. 127; ^{15}N natural abundance spectra; 18·25 MHz; field parallel to sample tube; referred originally to 1 M DNO_3, +6·2 ppm from neat nitromethane (Table 6); conversion scheme IV (Table 4).

TABLE 23

Nitrogen shieldings in some aziridines and azetidines (4–5 M solutions in $CDCl_3$)

Substituents				Nitrogen shielding referred to neat nitromethane	
					
R					
H				+388·7	+388·7
Me				+379·5	+369·7
Et				+363·8	+372·3
Pr^n				+366·6	
Bu^n				+366·6	
Pr^i				+350·0	+372·9
Bu^t				+346·7	+376·8
R^1	R^2	R^3	R^4		
Me	Me	H	H	+351·6	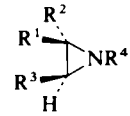
Me	H	H	Me	+364·3	
H	Me	Me	H	+349·5	
Me	H	Me	H	+355·2	
R^1	R^2	R^3			
H	H	H		+362·4	
Me	H	H		+347·1	
H	Me	H		+358·7	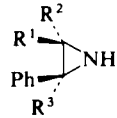
H	H	Me		+340·9	
Ph	H	H		+344·1	
H	Ph	H		+357·9	
H	H	Ph		+337·0	
Me	Me	H		+338·7	
R					
H				+354·9	
Me				+348·7	
Et				+335·2	
Pr^n				+337·8	
Pr^i				+323·9	
Bu^t				+328·2	

Data from ref. 131; ^{15}N natural abundance spectra; 10·09 MHz; field perpendicular to sample tube; referred originally to neat nitromethane (uncorrected for bulk susceptibility effects), but reported relative to "anhydrous ammonia", +380·2 ppm from neat nitromethane (Table 6).

TABLE 24

Solvent effects on nitrogen shielding in aliphatic amines and aniline[a]

Amine	Solvent and concentration (mol %)		Nitrogen shielding			
			ref. to neat $MeNO_2$		solvent shift ref. to solution in cyclohexane	protonation shift in MeOH[d]
			uncorrected[b]	corrected[c]		
Pr^nNH_2	cyclohexane	(19·4)	+360·7		0·0000	
	neat liquid	(100)	+359·6		−1·1	
	DMSO	(19·4)	+358·4		−2·3	
	Bu^tOH	(19·9)	+355·2		−5·5	
	MeOH	(8·3)	+359·6		−1·1	−11·7
	H_2O	(19·4)	+356·6		−4·1	
Et_2NH	cyclohexane	(19·4)	+333·0	+331·8	0·0000	
	neat liquid	(100)	+333·4	+332·6	+0·8	
	DMSO	(19·6)	+334·6	+333·9	+2·1	
	Bu^tOH	(19·0)	+332·3	+331·1	−0·7	
	MeOH	(19·4)	+333·7	+333·1	+1·3	−2·9
	H_2O	(19·4)	+332·5	+331·2	−0·6	
$Pr^n{}_2NH$	cyclohexane	(19·2)	+342·2		0·0000	
	neat liquid	(100)	+342·2		0·0	
	DMSO	(19·0)	+342·9		+0·7	
	Bu^tOH	(23·1)	+340·2		−2·0	
	MeOH	(23·1)	+340·5		−1·7	−8·4
$Pr^i{}_2NH$	cyclohexane	(19·4)	+305·1	+304·1	0·0000	
	neat liquid	(100)	+305·0	+303·7	−0·4	
	DMSO	(9·2)	+306·5	+305·7	+1·6	
	Bu^tOH	(21·4)	+304·6	+303·6	−0·5	
	MeOH	(8·3)	+306·5	+306·0	+1·9	+4·9

 Pyrrolidine	cyclohexane	(19·4)	+343·5	+342·4	0·0000	
	neat liquid	(100)	+343·7	+342·5	+0·1	
	DMSO	(19·4)	+342·9	+341·7	−0·7	
	$CHCl_3$	(19·4)	+342·2	+340·3	−2·1	
	Bu^tOH	(19·4)	+340·2	+338·9	−3·5	
	MeOH	(19·3)	+342·5	+341·4	−1·0	−10·4
	H_2O	(8·3)	+342·1	+341·3	−1·1	
		(19·4)	+340·8	+338·8	−3·6	
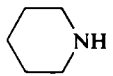 Piperidine	cyclohexane	(17·8)	+342·5	+341·4	0·0000	
	neat liquid	(100)	+342·8	+341·6	+0·2	
	DMSO	(19·4)	+343·3	+342·4	+1·0	
	$CHCl_3$	(19·4)	+342·2	+340·6	−0·8	
	Bu^tOH	(19·4)	+341·4	+340·2	−1·2	
	Pr^iOH	(19·4)	+342·1	+341·0	−0·4	
	EtOH	(19·4)	+342·8	+341·9	+0·5	
	MeOH	(19·9)	+343·2	+342·6	+1·2	−1·8
	H_2O	(19·4)	+341·9	+340·4	−1·0	
		(10·0)	+341·8	+340·4	−1·0	
 *cis*-2,6-Me_2-piperidine	cyclohexane	(19·4)	+306·8	+305·8	0·0000	
	Bu^tOH	(17·2)	+307·2	+306·2	+0·4	
	MeOH	(6·3)	+309·7	+309·0	+3·2	+7·4
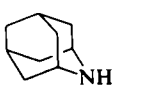 2-Azaadamantane	benzene	(8·2)	+322·0		0·0000	
	Bu^tOH	(8·6)	+319·8		−2·2	
	MeOH	(6·3)	+323·5		+1·5	+3·9

TABLE 24—*cont.*

Amine	Solvent and concentration (mol %)	Nitrogen shielding: ref. to neat $MeNO_2$ uncorrected[b]	Nitrogen shielding: ref. to neat $MeNO_2$ corrected[c]	Nitrogen shielding: solvent shift ref. to solution in cyclohexane	Nitrogen shielding: protonation shift in MeOH[d]
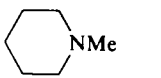	cyclohexane (19·4)	+342·8	+341·8	0·0000	
	neat liquid (100)	+342·7	+341·7	−0·1	
	DMSO (12·4)	+341·9	+340·8	−1·0	
	$CHCl_3$ (19·4)	+340·7	+338·8	−3·0	
	Bu^tOH (26·6)	+342·0	+340·9	−0·9	
	MeOH (19·4)	+340·6	+339·4	−2·4	−7·9
	H_2O (19·4)	+340·8	+339·1	−2·7	
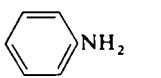	cyclohexane/benzene (4 : 1) (18·8)	+327·0	+325·9	0·0000	
	Bu^tOH (7·4)	+324·9	+323·5	−2·4	
	MeOH (8·3)	+328·5	+327·8	+1·9	+5·6

(*a*) Data from ref. 82; ^{15}N natural abundance spectra; 18·25 MHz; field parallel to sample tube; referred originally to 1 M DNO_3, +6·2 ppm (uncorrected) or +4·8 ppm (corrected) from neat nitromethane (Table 6).

(*b*) The values contain bulk susceptibility difference effects between nitromethane and sample (conversion scheme IV, Table 4).

(*c*) The values are taken from the original data and corrected for bulk susceptibility, using conversion scheme I (Table 4).

(*d*) The values represent nitrogen shielding in the corresponding hydrochloride in MeOH relative to the parent amine in the same solvent.

TABLE 25

Nitrogen shieldings in some miscellaneous alkylamino moieties

Compound (neat liquid)	Nitrogen shielding ref. to neat $MeNO_2$ (±3 ppm)	^{14}N resonance half-height width (Hz)
Bu^tNHMe	+334	275
$Bu^tN(BMe_2)_2$	+217	?
$Bu^tN(SnMe_3)_2$	+322	?
$N(SnMe_3)_3$	+385	?
$EtN(SnMe_3)_2$	+376	?
$[(Me_2N)_3Al]_2$	+372	850
Me_2NPMe_2	+373	204
$(Me_2N)_2S$	+332	342
Me_2NSCl	+306	235
Me_2NCl	+291	238
Bu^tNCl_2	+187	300
$MeNCl_2$	+221	260
Me_2N–SCN	+317 (Me_2N)	?

Data from ref. 137; ^{14}N continuous-wave spectra; 7·22 MHz; field perpendicular to sample tube; referred originally to saturated aqueous $NaNO_3$, +3·7 ppm from neat nitromethane (Table 6); conversion scheme II (Table 4).

TABLE 26

Nitrogen shieldings in some enamines, enaminoketones, and related structures

Unsaturated substituent R	Nitrogen shielding referred to neat nitromethane (solvents given in footnotes)						
	$RNMe_2$	$RNEt_2$			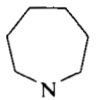		
	+335·1[a]	+310·7[b]	+310·4[a] +310·2[b]	+310·9[a] +310·0[b]	+312·7[b]	+315·3[a]	
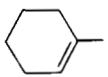	+333·8[a]	+310·2[b]	+306·7[a] +306·9[b]	+307·3[a] +307·3[b]	+311·9[b]	+312·1[a] +311·6[b]	+317·9[a]
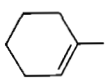 Me			+323·8[b]	+326·1[b]			
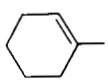 Me			+309·1[b]	+313·6[b]			
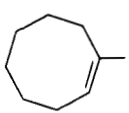			+307·4[b]				
MeCH=CH–	+353·0[c]						

trans-PhCH=CH–	+326·8 +326·2[c]	+301·1[a]	+303·6[a]	+309·8[a]
Me_2C=CH–	+351·2[a]	+322·2[a]	+325·6[a]	+330·1[a]
Ph_2C=CH–	+329·3[a]	+301·9[a]	+304·0[a]	+312·9[a]
trans-O_2NCH=CH–			+266·7[a] (amine)	
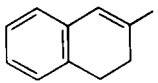	+326·9[a]			
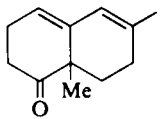		+301·2[a]		
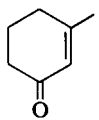	+299·0[a]	+274·6[a]	+280·4[a]	+291·7[a]
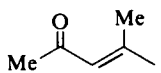	+297·9[a]	+272·9[a]	+276·3[a]	+284·6[a]
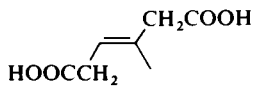	+274·6[a]			

(*a*) Data from ref. 41; ^{15}N natural abundance spectra; 10·1 MHz; field perpendicular to sample tube; referred originally to NO_3^- in 0·5 M NH_4NO_3, +3·7 ppm from neat nitromethane (Table 6); conversion scheme II (Table 4); $Cr(acac)_3$ added; 80% solutions in benzene-d_6.

(*b*) Data from ref. 126; ^{15}N natural abundance spectra; 18·25 MHz; field parallel to sample tube; referred originally to 1 M DNO_3, +6·2 ppm from neat nitromethane (Table 6); conversion scheme IV (Table 4); $Cr(acac)_3$ added; 20 mol % solutions in cyclohexane.

(*c*) Data from ref. 40; ^{15}N natural abundance spectra; 6·08 MHz; field perpendicular to sample tube; referred originally to aqueous $NaNO_3$, +3·7 ppm from neat nitromethane (Table 6); conversion scheme II (Table 4).

TABLE 27

Some additional data on nitrogen shielding in enamino type moieties

Compound	Solution	Nitrogen shielding referred to neat nitromethane	Notes
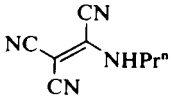	80% in benzene	+263·5	(a)
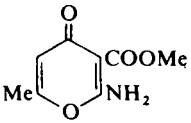	10% v/v in DMSO (70 °C)	+292	(b)
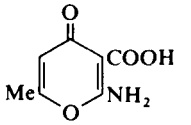	10% v/v in DMSO (70 °C)	+283	(b)
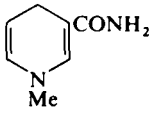	0·1 M in D_2O, pD = 7	+279·8 (NMe)	(c)
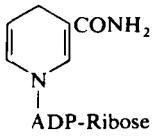	0·1 M in D_2O, pD = 7	+264·2 (N-ADP)	(c)
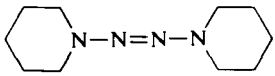	neat liquid	+312 ± 5	(d)
$MeNH-N{=}CMe_2$	neat liquid	+298 ± 3 (NH)	(d)
$Me_2N-N{=}N-NMe_2$	neat liquid	+279 ± 3 (NMe_2)	(d)
$Et_2N-N^+{\equiv}C^-$	neat liquid	+264 ± 3 (NEt_2)	(d)
$(Me_3Si)_2N-N{=}CH_2$	neat liquid	+241 ± 3 (NSi)	(d)
$(Me_3Si)_2N-N{=}CCl_2$	neat liquid	+216 ± 3 (NSi)	(d)
$(Me_3Si)_2N-N{=}CF_2$	neat liquid	+300 ± 3 (NSi)	(d)
$(Me_3Si)_2N-P{=}NSiMe_3$	neat liquid	+264 ± 3 (amine)	(d)

(a) Data from ref. 41; see footnote (a) in Table 26.

(b) Data from ref. 135; $^1H\{^{14}N\}$ INDOR spectra; 100/7·22 MHz; field perpendicular to sample tube; referred originally to $Me_4N^+Cl^-$, +336·7 ppm from neat nitromethane (Table 6); conversion scheme II (Table 4).

(c) Data from ref. 136; ^{15}N-labelled nitrogen atom in the ring system; ^{15}N spectra; 10·14 MHz; field perpendicular to sample tube; referred originally to 1 M ND_4Cl, +352·9 ppm from neat nitromethane (Table 6); conversion scheme II (Table 4).

(d) Data from ref. 137 and ref. 38; ^{14}N continuous-wave spectra; 7·22 MHz; field perpendicular to sample tube; referred originally to saturated aqueous $NaNO_3$, +3·7 ppm from neat nitromethane (Table 6); conversion scheme II (Table 4).

TABLE 28

Nitrogen shieldings in some silylamines and related structures

Compound	Solvent	Nitrogen shielding referred to neat nitromethane	^{14}N resonance half-height width (Hz)	Notes
$(H_3Si)_2NPF_2$	$CDCl_3/SiMe_4$	+330·2		(a)
$Me_3SiN(Me)Ph$	none	+326 ± 3	1200	(b)
$[(Me_3Si)_2N]_2Be$	none	+325 ± 1	192	(b)
$(Me_3Si)_2NPh$	none	+291 ± 3	1200	(b)
$(Me_3Si)_2NPMe_2$	none	+348 ± 1	135	(b)
$[(Me_3Si)_2N]_2S$	none	+345 ± 3	?	(b)
$(Me_3Si)_2NSSiMe_3$	none	+333 ± 3	?	(b)
$(Me_3Si)_2NSOSiMe_3$	none	+312 ± 3	1100	(b)
$(Me_3Si)_2NSBr$	none	+309 ± 3	?	(b)
$(Me_3Si)_2NCl$	none	+346 ± 1	180	(b)
$(Me_3Si)_2NBr$	none	+314 ± 3	355	(b)
$(Me_3Si)_2NI$	none	+416 ± 3	?	(b)
$(Me_3Si)_2N\text{-}NC$	none	+320 ± 3 (amine)	423	(b)
$(Me_3Si)_2N\text{-}N{=}C{=}S$	none	+266 ± 3 (amine)	?	(b)
$(Me_3Si)_2N\text{-}SCN$	none	+369 ± 3 (amine)	?	(b)
$(Me_3Si)_2NSi(Me)NCl_2$	none	+320 ± 5 (amine)	?	(b)
		+239 ± 5 (NCl_2)	?	(b)
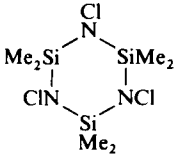	none	+298 ± 3	?	(b)
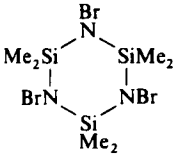	none	+269 ± 3	?	(b)
$(Me_3Si)_2NSnN(SiMe_3)_2$	benzene	+255 ± 3	317	(b)
	tetrahydrofuran	+248 ± 5	?	(b)
	none	+214 ± 15	?	(b)
$(Me_3Si)_2NPbN(SiMe_3)_2$	hexane	+174 ± 3	?	(b)
$(Me_3Si)_2NHgMe$	none	+291 ± 3	?	(b)
$(Me_3Si)_2NLi$	toluene	+326 ± 3	342	(b)
	tetrahydrofuran	+334 ± 3	280	(b)
	diglyme	+333 ± 3	271	(b)
$(Me_3Si)_2NNa$	toluene	+341 ± 3	348	(b)
	tetrahydrofuran	+337 ± 3	370	(b)
	diglyme	+340 ± 3	314	(b)
	diglyme/crown ether	+328 ± 3	?	(b)

TABLE 28—*cont.*

Compound	Solvent	Nitrogen shielding referred to neat nitromethane	^{14}N resonance half-height width (Hz)	Notes
$(Me_3Si)_2NK$	toluene	+315 ± 3	400	(b)
	tetrahydrofuran	+326 ± 3	433	(b)
	diglyme	+325 ± 3	387	(b)
$(Me_3Si)_2NBu^t$	none	+322 ± 3	?	(b)
$Me_3SiNHBu^t$	none	+325 ± 3	225	(b)
$(Me_3Si)_2NSiMe_2NH_2$	none	+360 ± 3 (NH)	?	(b)
		+341 ± 3 (NSi)	?	(b)
$Me_3SiNHSiMe_2NHSiMe_3$	none	+344 ± 1	100	(b)
Me_3SiNMe_2	$CDCl_3$	+381·0		(c)
$Me_2HSiNMe_2$	$CDCl_3$	+383·4		(c)
$Me_2(Ph)SiNMe_2$	$CDCl_3$	+384·0		(c)
$Ph_2(Me)SiNMe_2$	$CDCl_3$	+370·6		(c)
$Cl_2(Ph)SiNMe_2$	$CDCl_3$	+364·1		(c)
Cl_3SiNMe_2	$CDCl_3$	+357·1		(c)
Me_3SiNEt_2	$CDCl_3$	+354·0		(c)
$Me_2HSiNEt_2$	$CDCl_3$	+377·0		(c)
$Me_2(Bu^t)SiNEt_2$	$CDCl_3$	+353·6		(c)
$Me_2(Ph)SiNEt_2$	$CDCl_3$	+352·0		(c)
$Ph_2(Me)SiNEt_2$	$CDCl_3$	+345·0		(c)
$(Ph)(Me)(CH_2{=}CH)SiNEt_2$	$CDCl_3$	+340·0		(c)
$Ph_2(Cl)SiNEt_2$	$CDCl_3$	+341·1		(c)
$Cl_2(Ph)SiNEt_2$	$CDCl_3$	+334·0		(c)
Ph_3SiNEt_2	$CDCl_3$	+305·0		(c)
Cl_3SiNEt_2	$CDCl_3$	+327·6		(c)
$Ph_2(Cl)SiNPr^i_2$	$CDCl_3$	+318·6		(c)
$Cl_2(Ph)SiNPr^i_2$	$CDCl_3$	+313·5		(c)
$Cl_3SiNPr^i_2$	$CDCl_3$	+307·0		(c)

(a) Data from ref. 138; ^{15}N-labelled compound; $^1H\{^{15}N\}$ double-resonance spectra; 100/10·1 MHz; field perpendicular to sample tube; referred originally to aqueous NMe_4I, +337·3 ppm from neat nitromethane (Table 6); conversion scheme II (Table 4).

(b) Data from ref. 137; ^{14}N continuous-wave spectra; 7·22 MHz; field perpendicular to sample tube; referred originally to saturated aqueous $NaNO_3$, +3·7 ppm from neat nitromethane (Table 6); conversion scheme II (Table 4).

(c) Data from ref. 44; ^{15}N natural abundance spectra; 9·12 MHz; field perpendicular to sample tube; referred originally to aqueous $NaNO_3$, see note (b).

TABLE 29

Nitrogen shieldings in silatrane and stannatrane structures

Compound	Solution	Nitrogen shielding referred to neat nitromethane	Notes
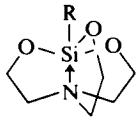			
Silatrane structure			
R=H	0·001 M in $CDCl_3$	+352·6	(a)
Me	0·001 M in $CDCl_3$	+357·8	(a)
	0·3 M in $CDCl_3$	+357·3	(b)
	0·3 M in acetone	+357·2	(b)
	0·3 M in CD_3OD	+356·5	(b)
CH_2=CH	0·001 M in $CDCl_3$	+355·2	(a)
	0·3 M in acetone	+356·0	(b)
Ph	0·001 M in $CDCl_3$	+354·7	(a)
	0·3 M in acetone	+355·5	(b)
$ClCH_2$	0·001 M in $CDCl_3$	+352·5	(a)
	0·3 M in $CDCl_3$	+352·5	(b)
	0·3 M in acetone	+353·0	(b)
MeO	0·3 M in acetone	+354·9	(b)
EtO	0·001 M in $CDCl_3$	+351·5	(a)
	0·3 M in acetone	+352·4	(b)
ICH_2	0·001 M in $CDCl_3$	+353·2	(a)
Cl_2CH	0·001 M in $CDCl_3$	+350·3	(a)
Cl	0·001 M in $CDCl_3$	+347·2	(a)
Br	0·001 M in $CDCl_3$	+346·5	(a)
$Et_3N^+CH_2$	0·001 M in $CDCl_3$	+350·2	(a)
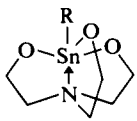			
Stannatrane structure			
R=Me	none	+358·2; +363·8	(c)

(a) Data from ref. 139; ^{15}N-labelled compounds; $^1H\{^{15}N\}$ double-resonance spectra; 90/9·12 MHz; field perpendicular to sample tube; referred to neat nitromethane; uncorrected for bulk susceptibility effects.

(b) Data from ref. 124; ^{15}N-labelled compounds; ^{15}N spectra; 9·2 MHz; field perpendicular to sample tube; referred to neat nitromethane; uncorrected for bulk susceptibility effects.

(c) Data from ref. 140; ^{15}N-labelled compound; ^{15}N spectrum; 9·12 MHz; field perpendicular to sample tube; referred originally to aqueous NO_3^-, probably +3·7 ppm from neat nitromethane (Table 6); conversion scheme II (Table 4).

TABLE 30

Nitrogen shieldings in amino groups bound to phosphorus atoms

Compound	Solvent	Nitrogen shielding referred to neat nitromethane	Notes
$P(NMe_2)_3$	none	+352 ± 2	(a)
		+340 ± 5	(d)
$MeP(NMe_2)_2$	CH_2Cl_2	+346 ± 2	(a)
Me_2PNMe_2	none	+373 ± 2	(a)
$(Me_2P)_2NMe_2$	none	+345 ± 3	(a)
$ClP(NMe_2)_2$	none	+334 ± 3	(a)
$BrP(NMe_2)_2$	none	+322 ± 3	(a)
$P(NEt_2)_3$	none	+329 ± 3	(a)
$ClP(NEt_2)_2$	none	+284 ± 3	(a)
F_2PNH_2	none	+315·9	(b)
F_2PNMe_2	none	+320 ± 2	(a)
Cl_2PNMe_2	none	+318 ± 2	(a)
Br_2PNMe_2	none	+311 ± 3	(a)
Cl_2PNEt_2	none	+264 ± 3	(a)
$Cl(Me)PNMe_2$	$CDCl_3$	+329 ± 3	(a)
$(F_2P)_2NH$	benzene-d_6	+251·0	(b)
$(Cl_2P)_2NMe$	none	+267 ± 3	(a)
$(F_2P)_3N$	benzene-d_6	+198·3	(b)
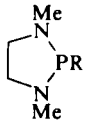			
R = Me	CH_2Cl_2	+344 ± 3	(a)
Cl	none	+322 ± 3	(a)
Br	CH_2Cl_2	+309 ± 3	(a)
OMe	CH_2Cl_2	+324 ± 3	(a)
SMe	CH_2Cl_2	+339 ± 3	(a)
NMe_2	benzene	+343·4 (NMe) +332·8 (NMe_2)	(h)
NEt_2	benzene	+345·7 (NMe) +302·7 (NEt_2)	(h)
NPr^i_2	CD_2Cl_2	+353·8 (NMe) +286·0 (NPr^i_2)	(h)
	none	+357·5 (NMe) +289·7 (NPr^i_2)	(c)
$N(Me)Pr^i$	benzene-d_6	+345·5 (NMe) +308·7 ($NMePr^i$)	(h)
NHPh	benzene	+284·2 (NHPh)	(b)
$O{=}P(NMe_2)_3$	none	+358 ± 5	(d)
$S{=}P(NMe_2)_3$	none	+348 ± 5	(d)

TABLE 30—*cont.*

Compound	Solvent	Nitrogen shielding referred to neat nitromethane	Notes
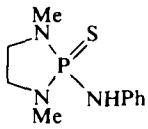	$CHCl_3$/benzene	+289·5 (NHPh)	(b)
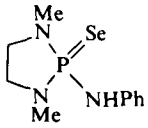	benzene	+284·2 (NHPh)	(b)
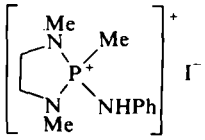	CH_2Cl_2	+370·7 (NHPh)	(b)
$Me_2NP(OMe)_2$	none	+322 ± 3	(a)
$Me_2NP(SMe)_2$	CH_2Cl_2	+326 ± 3	(a)
Me_2PNHPh	benzene	+309·1	(b)
$Me_2P(=O)NHPh$	DMSO	+293·6	(b)
$Me_2P(=S)NHPh$	dioxan	+301·0	(b)
$Me_2P(=Se)NHPh$	CH_2Cl_2	+304·6	(b)
$Me_2P(=Te)NHPh$	benzene/CH_2Cl_2	+308·0	(b)
$(Me_3P^+\text{-}NHPh)I^-$	CH_2Cl_2	+322·3	(b)
$[(MeS)Me_2P^+\text{-}NHPh]I^-$	$CHCl_3$	+315·9	(b)
$[Me_2P\text{-}N(BH_2)Ph]_n$	CH_2Cl_2	+285·3	(b)
Bu^t_2PNHPh	mesitylene	+321·6	(b)
$Bu^t_2P(=O)NHPh$	CH_2Cl_2/mesitylene	+316·7	(b)
$Bu^t_2P(=S)NHPh$	$CHCl_3$/mesitylene	+321·3	(b)
$Bu^t_2P(=Se)NHPh$	$CHCl_3$/mesitylene	+325·8	(b)
$[Bu^t_2P^+(Me)NHPh]I^-$	DMSO	+339·6	(b)
$[Bu^t_2P^+(SeMe)NHPh]I^-$	DMSO	+323·7	(b)
$Bu^t_2P\text{-}N(Ph)SnMe_3$	CH_2Cl_2/benzene	+340·3	(b)
$Me_2P\text{-}N(Ph)SnMe_3$	benzene	+332·8	(b)
$Me_2P(=S)\text{-}N(Ph)SnMe_3$	benzene	+307·8	(b)
$(Me_2N)_2P\text{-}NHPh$	benzene	+297·5 (NHPh)	(b)
$Me_2N\text{-}P(NHPh)_2$	benzene	+297·2 (NHPh)	(b)
$MeN{=}P(NMe_2)_3$	benzene-d_6	+354·4 (N=P)	(e)
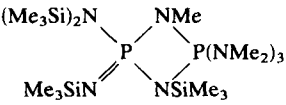	benzene-d_6	+309·7 (NMe)	(e)
$(H_3Si)_2NPF_2$	$CDCl_3$/$SiMe_4$	+330·2	(i)

TABLE 30—*cont.*

Compound	Solvent	Nitrogen shielding referred to neat nitromethane	Notes
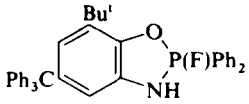	benzene	+313·0	(f)
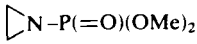	benzene-d_6	+367·4	(g)
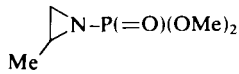	benzene-d_6	+352·2	(g)
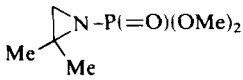	benzene-d_6	+340·9	(g)
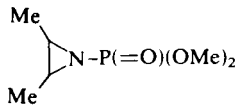	benzene-d_6	+338·4 (*cis*-Me_2) +338·1 (*trans*-Me_2)	(g) (g)
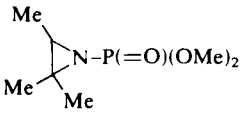	benzene-d_6	+327·2	(g)
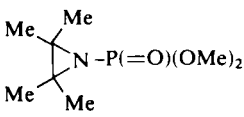	benzene-d_6	+320·5	(g)
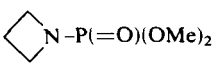	benzene-d_6	+346·2	(g)
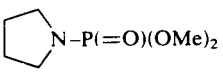	benzene-d_6	+334·4	(g)
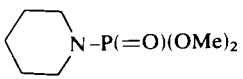	benzene-d_6	+333·7	(g)
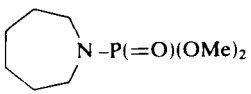	benzene-d_6	+333·6	(g)
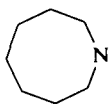	benzene-d_6	+337·0	(g)

TABLE 30—*cont.*

Compound	Solvent	Nitrogen shielding referred to neat nitromethane	Notes
	benzene-d_6	+335·4	(g)
Et_2N–P(=O)$(OMe)_2$	benzene-d_6	+335·4	(g)

(a) Data from ref. 141; ^{14}N continuous-wave spectra; 7·22 MHz; field perpendicular to sample tube; referred originally to saturated aqueous $NaNO_3$, +3·7 ppm from neat nitromethane (Table 6); conversion scheme II (Table 4).

(b) Data from ref. 142; ^{15}N-labelled compounds; $^1H\{^{15}N\}$ double-resonance spectra; 100/10·1 MHz; field perpendicular to sample tube; referred originally to aqueous $Me_4N^+I^-$, +337·3 ppm from neat nitromethane (Table 6); conversion scheme II (Table 4).

(c) Data quoted in ref. 141 [see note (a)] under ref. 4b there.

(d) Data from ref. 143; ^{14}N continuous-wave measurements (wide-line spectrometer); 3 MHz; referred originally to NH_4^+ in NH_4NO_3, +359·5 ppm from neat nitromethane (Table 6); low-precision results.

(e) Data from ref. 144; ^{15}N-labelled compounds; ^{15}N spectra; 9·12 MHz; field perpendicular to sample tube; referred originally to neat nitromethane; uncorrected for bulk susceptibility effects.

(f) Data from ref. 145; ^{15}N-labelled compound; ^{15}N spectrum; 9·12 MHz; field perpendicular to sample tube; referred originally to saturated aqueous $NaNO_3$, +3·7 ppm from neat nitromethane; see note (a).

(g) Data from ref. 146; ^{15}N natural abundance spectra; 10·138 MHz; field perpendicular to sample tube; referred originally to nitromethane (90% in C_6D_6); $Cr(acac)_3$ added.

(h) Data from ref. 147; ^{15}N natural abundance spectra; 18·25 MHz; field parallel to sample tube; referred originally to neat nitromethane; uncorrected for bulk susceptibility effects.

(i) Data from ref. 138; ^{15}N-labelled compound; $^1H\{^{15}N\}$ double-resonance spectrum; 100/10·1 MHz; details as in note (b).

TABLE 31

Nitrogen shieldings of amino groups in some alkynyl boranes

Compound (neat liquid)	Nitrogen shielding referred to neat nitromethane
$(Me_2N)_2BC{\equiv}CMe$	+327
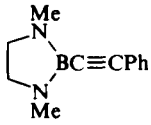	+314
$(Et_2N)_2BC{\equiv}CB(NEt_2)_2$	+249
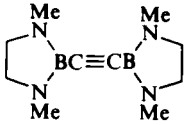	+309
$Et_2NB(C{\equiv}CH)_2$	+236
$Et_2NB(C{\equiv}CMe)_2$	+242

Data from ref. 148; ^{14}N continuous-wave spectra; 7·22 MHz; field perpendicular to sample tube; referred originally to saturated aqueous $NaNO_3$, +3·7 ppm from neat nitromethane (Table 6); conversion scheme II (Table 4).

TABLE 32

Nitrogen shieldings and relative signal intensities for some amino sugars and their derivatives

Compound (solutions specified in footnotes)	Nitrogen shielding referred to neat nitromethane		^{15}N peak height intensity ratio	^{1}H integral intensity ratio	Notes
	α-anomer	β-anomer	α/β	α/β	
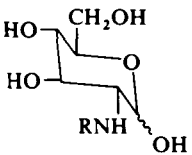					
2-Amino-2-deoxy-D-glucopyranose hydrochloride	+346·5	+348·1	61/39	63/37	(a)
(R=H+HCl)	+346·4	+348·8	63/37	63/37	(b)
2-Acetamido-2-deoxy-D-glucopyranose	+258·6	+259·3	69/31	68/32	(a)
(R=COMe)	+259·1	+259·9	64/36	68/32	(b)
2-Benzamido-2-deoxy-D-glucopyranose, in DMSO (R=COPh)	+267·0	+267·4	90/10	?	(a)
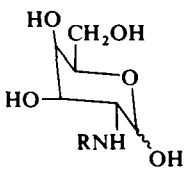					
2-Amino-2-deoxy-D-galactopyranose hydrochloride	+347·8	+349·2	55/45	42/53	(a)
(R=H+HCl)	+348·1	+350·2	63/37	58/42	(b)
2-Acetamido-2-deoxy-D-galactopyranose	+258·8	+259·6	56/44	65/35	(a)
(R=COMe)	+259·4	+260·2	63/37 (64/36, integral)	65/35	(b)

TABLE 32—*cont.*

Compound (solutions specified in footnotes)	Nitrogen shielding referred to neat nitromethane		^{15}N peak height intensity ratio	^{1}H integral intensity ratio	Notes
	α-anomer	β-anomer	α/β	α/β	
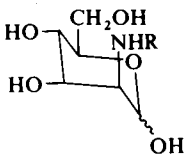					
2-Amino-2-deoxy-D-mannopyranose hydrochloride	+350·4	+357·8	40/60	43/57	(a)
(R=H+HCl)	+350·8	+358·3	43/57	43/57	(b)
2-Acetamido-2-deoxy-D-mannopyranose	+267·0	+267·4	60/40	57/43	(a)
(R=COMe)	+262·8	+269·6	63/37	57/43	(b)
6-Deoxy-1,2:3,5-di-*O*-isopropylidene-6-phthalimido-α-D-glucofuranose	+227·1				(c)
6-Deoxy-1,2:3,5-di-*O*-isopropylidene-6-phthalimido-α-D-glucopyranose	+226·6				(c)
Methyl 5-deoxy-1,2:3,4-di-*O*-isopropylidene-5-phthalimido-α-D-ribofuranoside	+226·5				(c)
2-Acetamido-1,3,4,6-tetra-*O*-acetyl-2-deoxy-α-D-glucopyranose	+270·4				(c)
6-Amino-6-deoxy-1,2:3,5-di-*O*-isopropylidene-α-D-glucofuranose	+368·1				(c)

6-Amino-6-deoxy-1,2:3,5-di-*O*-isopropylidene-α-D-galactopyranose	+367·5	(c)
2,3,4-Tri-*O*-acetyl-β-D-xylopyranosyl cyanide	+124·1 (cyano group)	(c)

(a) Data from ref. 149; ^{15}N natural abundance spectra; 18·25 MHz; field parallel to sample tube; referred originally to 1 M DNO_3, +6·2 ppm from neat nitromethane (Table 6); conversion scheme IV (Table 4); 25% aqueous solutions if not stated otherwise.

(b) Data from ref. 150; ^{15}N natural abundance spectra; 9·12 MHz; field perpendicular to sample tube; referred originally to NO_3^- in 4·5 M NH_4NO_3 in 3 M HCl, +6·3 ppm from neat nitromethane (Table 6); conversion scheme II (Table 4); 1·4 M solutions in H_2O/DMSO (9 : 1).

(c) See note (b), but solutions in $CDCl_3/C_6F_6$ (9 : 1).

TABLE 33

Nitrogen shieldings in aminoglycoside (Nebramycin) antibiotics from *Streptomyces tenebrarius* (0.5–1.0 M solutions in H_2O/D_2O, 9:1)

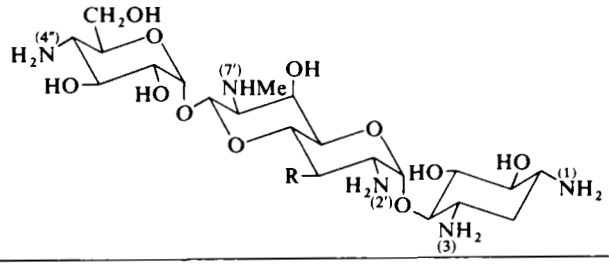

Substituent R (common name of compound)	pH	Nitrogen shieldings referred to neat nitromethane				
		N-1	N-3	N-2′	N-7′ (?)	N-4″ (?)
H ("factor-2", Apramycin)	3	+338·1	+339·6	+338·8	+343·9	+345·3
	4	+338·1	+339·5	+338·7	+343·9	+345·1
	5	+338·4	+339·6	+338·7	+344·3	+345·3
	6	+340·2	+339·9	+339·2	+346·7	+346·1
	7	+343·4	+340·7	+340·7	+351·4	+348·8
	8	+344·8	+342·9	+345·3	+354·1	+354·4
	9	+346·0	+346·0	+347·4	+355·3	+356·1
	10·3	+346·2	+347·1	+347·8	+355·3	+356·4
	11	+346·5	+347·4	+348·3	+355·3	+356·8
OH ("factor-7", Oxyapramycin)	4	+338·4	+339·8	+344·3	+343·9	+345·4
	9·5	+346·9	+347·3	+356·3	+355·3	+356·5

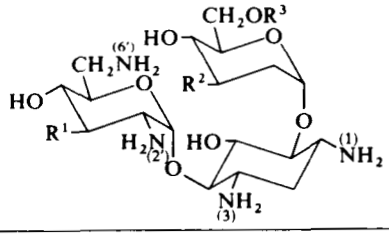

R^1	R^2	R^3	pH	N-1	N-3	N-2′	N-6′	R^2	R^3
OH	OH	H	4	+338·6	+340·7	+344·2	+351·4		
("factor-3")			10·4	+342·6	+347·6	+356·3	+363·8		
OH	NH_2	$CONH_2$	4	+338·6	+340·5	+344·0	+351·4	+345·4	+302·4
("factor-4")			10·5	+346·2	+347·7	+356·2	+363·8	+354·2	+303·3
OH	NH_2	H	4	+339·2	+340·4	+344·3	+351·4	+345·4	
("factor-5", Kanamycin-B)			9·5	+346·0	+347·4	+356·1	+363·2	+354·1	
			11	+346·2	+347·5	+356·2	+363·7	+354·1	

TABLE 33—*cont.*

R^1	R^2	R^3	pH	N-1	N-3	N-2′	N-6′	R^2	R^3
H	NH_2	$CONH_2$ ("factor-5′′′")	11	+346·1	+347·7	+347·8	?	?	+303·4
H	NH_2	H	3	+338·1	+340·1	+339·0	+350·8	+344·9	
("factor-6", Tobramycin)			4	+338·2	+340·1	+339·1	+350·8	+344·9	
			5	+338·7	+340·2	+339·1	+350·9	+345·0	
			6	+341·5	+340·9	+339·3	+351·2	+345·4	
			7	+343·6	+342·5	+341·2	+351·9	+347·8	
			8	+344·7	+345·3	+344·7	+354·3	+351·8	
			9	+345·4	+347·2	+347·2	+359·1	+353·5	
			10	+345·9	+347·3	+347·9	+362·1	+354·0	
			11	+346·0	+347·4	+348·0	+363·4	+354·1	
H	NH_2	H (N-6′-acetyl) ("factor N-6′-acetyl-6")	10	+346·7	+347·6	+348·2	+261·2	+354·2	

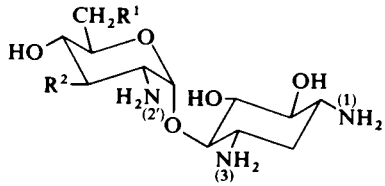

R^1	R^2	pH	N-1	N-3	N-2′	R^1
NH_2	H	10·7	+346·0	+347·4	+348·2	+363·0
("factor-8", Nebramine)						
OH	H	9·1	+346·1	+347·2	+347·9	
("factor-9", Lividamine)						

	pK_a values for nitrogen atoms in factors 2 and 6						
	N-1	N-3	N-2′	N-6′	N-7′	N-3″	N-4″
Factor-2	6·6	8·2	7·7		6·7		7·5
Factor-6	6·2	7·4	7·6	8·6		7·4	

Data from ref. 151 and ref. 152; ^{15}N natural abundance spectra; 10·09 MHz; field perpendicular to sample tube; referred originally to 2·9 M NH_4Cl in 1 M HCl, +355·3 from neat nitromethane (Table 6); conversion scheme IV (Table 4).

TABLE 34

Nitrogen shieldings in some alkylammonium ions

Compound	Solution	Nitrogen shielding: referred to neat nitromethane	Nitrogen shielding: referred to parent amine in MeOH (protonation shift)	Notes
NH_4^+		see Table 6		
$MeNH_3^+ Cl^-$	1 M in MeOH	+361·4	−15·9	(a)
$EtNH_3^+ Cl^-$	1 M in MeOH	+346·7	−8·7	(a)
$Pr^nNH_3^+ Cl^-$	1 M in MeOH	+349·0	−10·6	(a)
$Bu^nNH_3^+ Cl^-$	1 M in MeOH	+348·8	−10·6	(a)
$Bu^iNH_3^+ Cl^-$	1 M in MeOH	+351·1	−11·6	(a)
$Me_2CHCH_2CH_2NH_3^+ Cl^-$	1 M in MeOH	+348·7	−10·6	(a)
$Me_3CCH_2NH_3^+ Cl^-$	1 M in MeOH	+354·0	−13·6	(a)
$Pr^iNH_3^+ Cl^-$	1 M in MeOH	+334·0	−4·1	(a)
$Bu^sNH_3^+ Cl^-$	1 M in MeOH	+335·9	−6·3	(a)
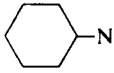	1 M in MeOH	+335·3	−5·1	(a)
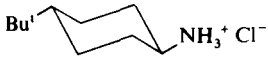	1 M in MeOH	+335·7	−5·3	(a)
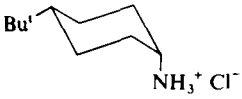	1 M in MeOH	+341·6	−8·1	(a)
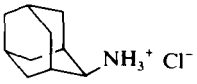	1 M in MeOH	+339·5	−7·0	(a)
$Bu^tNH_3^+ Cl^-$	1 M in MeOH	+323·7	−0·6	(a)
$(Et)Me_2CNH_3^+ Cl^-$	1 M in MeOH	+325·2	−3·4	(a)
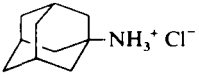	1 M in MeOH	+323·2	−0·4	(a)
$Me_2NH_2^+ Cl^-$	1 M in MeOH	+356·6	−12·9	(a)
$(Me)(Et)NH_2^+ Cl^-$	1 M in MeOH	+343·7	−8·3	(a)
$Et_2NH_2^+ Cl^-$	1 M in MeOH	+330·1	−3·6	(a)
$Pr^n{}_2NH_2^+ Cl^-$	1 M in MeOH	+333·8	−6·7	(a)
$Bu^n{}_2NH_2^+ Cl^-$	1 M in MeOH	+333·5	−6·5	(a)
$Bu^i{}_2NH_2^+ Cl^-$	1 M in MeOH	+337·8	−7·5	(a)
$Pr^i{}_2NH_2^+ Cl^-$	1 M in MeOH	+310·0	+3·5	(a)
$Me_3NH^+ Cl^-$	1 M in MeOH	+349·4	−13·4	(a)
$(Et)Me_2NH^+ Cl^-$	1 M in MeOH	+340·0	−11·3	(a)

TABLE 34—*cont.*

Compound	Solution	Nitrogen shielding: referred to neat nitromethane	Nitrogen shielding: referred to parent amine in MeOH (protonation shift)	Notes
$Pr^nMe_2NH^+\ Cl^-$	1 M in MeOH	+340·9	−11·9	(a)
$Bu^nMe_2NH^+\ Cl^-$	1 M in MeOH	+340·9	−11·9	(a)
$Bu^iMe_2NH^+\ Cl^-$	1 M in MeOH	+342·3	−12·5	(a)
$(Me_2CHCH_2CH_2)Me_2NH^+\ Cl^-$	1 M in MeOH	+340·8	−12·1	(a)
$(Me_3CCH_2)Me_2NH^+\ Cl^-$	1 M in MeOH	+343·5	?	(a)
$Pr^iMe_2NH^+\ Cl^-$	1 M in MeOH	+333·7	−13·8	(a)
$Bu^sMe_2NH^+\ Cl^-$	1 M in MeOH	+333·6	−16·0	(a)
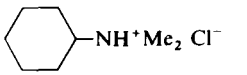	1 M in MeOH	+333·6	−14·1	(a)
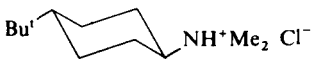	1 M in MeOH	+334·0	?	(a)
$Bu^tMe_2NH^+\ Cl^-$	1 M in MeOH	+326·5	−16·0	(a)
$(EtMe_2C)Me_2NH^+\ Cl^-$	1 M in MeOH	+326·7	−18·2	(a)
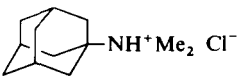	1 M in MeOH	+326·0	?	(a)
$Pr^n{}_2NH^+Me\ Cl^-$	1 M in MeOH	+333·2	−13·3	(a)
$Bu^n{}_2NH^+Me\ Cl^-$	1 M in MeOH	+332·4	−11·2	(a)
$Bu^i{}_2NH^+Me\ Cl^-$	1 M in MeOH	+335·1	−14·3	(a)
$Pr^i{}_2NH^+Me\ Cl^-$	1 M in MeOH	+317·0	−13·3	(a)
$Et_2NH^+Me\ Cl^-$	1 M in MeOH	+331·1	−9·4	(a)
$Et_3NH^+\ Cl^-$	1 M in MeOH	+322·8	−9·2	(a)
$Pr^n{}_3NH^+\ Cl^-$	0·3 M in H_2O	+334·0	−12·3	(d)
$H_3N^+CH_2CH_2NH_3^+\ (Cl^-)_2$	in HCl/H_2O	+344·3		(c)
$(CF_3COO^-)_2$	in CF_3COOH	+351·0		(b)
$H_3N^+(CH_2)_3NH_3^+\ (Cl^-)_2$	in HCl/H_2O	+342·6		(c)
$(CF_3COO^-)_2$	in CF_3COOH	+349·4		(b)
$H_3N^+(CH_2)_4NH_3^+(CF_3COO^-)_2$	in CF_3COOH	+348·9		(b)
$H_3N^+(CH_2)_6NH_3^+(CF_3COO^-)_2$	in CF_3COOH	+348·8		(b)
$H_3N^+(CH_2)_8NH_3^+(CF_3COO^-)_2$	in CF_3COOH	+348·8		(b)
$MeCH(NH_3^+)CH_2NH_3^+\ (Cl^-)_2$	in HCl/H_2O	+337·9, +351·9		(c)

(a) Data from ref. 119; ^{15}N natural abundance spectra; 18·25 MHz; field parallel to sample tube; referred originally to 1 M DNO_3, +6·2 ppm from neat nitromethane (Table 6); conversion scheme IV (Table 4).

Footnotes to Table 34 continued.

(b) Data from ref. 132; ^{15}N natural abundance spectra; 9·12 MHz; field perpendicular to sample tube; referred originally to NO_3^- in aqueous NH_4NO_3, +4·0 ppm from neat nitromethane (Table 6); conversion scheme II (Table 4).

(c) Data from ref. 125; ^{15}N natural abundance spectra; 10·09 MHz; field perpendicular to sample tube; referred originally to what was reported as aqueous NH_4Cl, but the reported shielding for pyridine in $CHCl_3$ suggests that NH_4NO_3 was used, +359·6 ppm from neat nitromethane (Table 6); conversion scheme II (Table 4).

(d) Data from ref. 124; ^{15}N-labelled compound; 9·12 MHz; field perpendicular to sample tube; referred originally to neat nitromethane; uncorrected for bulk susceptibility effects.

TABLE 35

Nitrogen shieldings in some cyclic ammonium ions

Compound	Nitrogen shielding in solvent specified (1 M solutions if not stated otherwise)			
	referred to neat nitromethane			referred to parent amine in MeOH (protonation shift)
	in $CHCl_3$	in $CHCl_3$/MeOH (82 : 18 mol ratio)	in MeOH	
		+337·5	+351·0	−2·2
2-Me	+324·1	+325·0	+328·3	+1·5
3-Me	+334·6	+336·0	+340·0	−3·3
4-Me	+335·8	+337·4	+341·3	−2·8
cis-2,6-Me_2		+313·5	+314·6	+4·9
trans-2,6-Me_2		+317·5	+319·2	+1·5
cis-3,5-Me_2	+333·6	+334·5	+338·3	−4·3
trans-3,5-Me_2	+339·3	+340·6	+344·9	−8·7
cis-2,3-Me_2	+326·9	+328·7	+331·8	?
trans-2,3-Me_2	+320·8	+324·6	+326·7	?
3,3-Me_2	+337·5	+338·7	+343·8	−6·6
4,4-Me_2	+336·2		+340·5	−3·9
2,2,6,6-Me_4		+301·8	+302·3	+3·5
		+325·9		+2·4
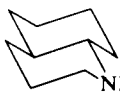		+325·8	+328·7	?
8(eq.)-Me			+332·3	?

TABLE 35—*cont.*

Compound		Nitrogen shielding in solvent specified (1 M solutions if not stated otherwise)			
		referred to neat nitromethane			referred to parent amine in MeOH (protonation shift)
		in $CHCl_3$	in $CHCl_3$/MeOH (82 : 18 mol ratio)	in MeOH	
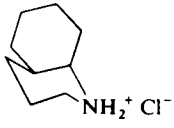			+331·2	+334·7	?
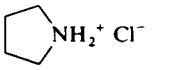		+328·4		+333·4	−9·1
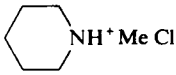		+334·1		+335·3	−5·3
2-Me	*trans*	+325·6		+325·9	−3·4
	cis	+330·9		+332·1	?
3-Me	*trans*	+338·1			?
	cis	+332·7		+334·0	−6·6
4-Me	*trans*	+334·0		+335·2	−5·6
	cis	+336·4			?
cis-2,6-Me_2	NMe(ax.)	+324·3		+324·1	?
	NMe(eq.)	+317·6		+316·6	−0·6
trans-2,6-Me_2		+320·7		+320·2	−9·5
cis-3,5-Me_2	NMe(ax.)	+336·6			?
	NMe(eq.)	+331·9		+333·2	−7·1
trans-3,5-Me_2		+335·9		+339·0	−8·9
cis-2,3-Me_2	*cis*/*cis*	+327·2		+328·1	?
	cis/*trans*	+330·5		+330·9	?
trans-2,3-Me_2	NMe(ax.)	+330·7		+330·7	?
	NMe(eq.)	+324·9		+325·6	?
3,3-Me_2		+335·2		+337·0	−7·2
4,4-Me_2		+334·0		+334·9	?
2,2,6,6-Me_4		+311·5		+309·1	−15·6
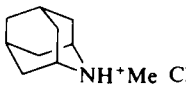		+326·2		+326·2	−11·3
					
	NMe(ax.)	+332·0		+333·4	?
	NMe(eq.)	+325·9		+326·6	−4·3
8(eq.)-Me		+334·0		+336·8	?

TABLE 35—*cont.*

Compound	Nitrogen shielding in solvent specified (1 M solutions if not stated otherwise)			
	referred to neat nitromethane			referred to parent amine in MeOH (protonation shift)
	in $CHCl_3$	in $CHCl_3$/MeOH (82 : 18 mol ratio)	in MeOH	
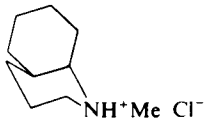				
NMe(inside)	+331·7		+334·0	−7·6
NMe(outside)	+327·5		+328·4	?
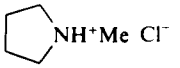	+323·8		+325·7	−10·7
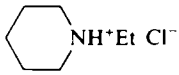	+326·2		+326·0	−2·2
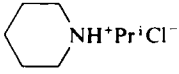	+320·6		+319·2	−5·0
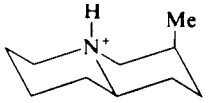	+325·0		+326·2	?
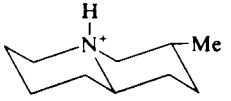	+319·0		+319·9	?
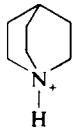			+348·5	−13·7

Data from ref. 133; ^{15}N natural abundance spectra; 18·25 MHz; field parallel to sample tube; referred originally to 1 M DNO_3, +6·2 ppm from neat nitromethane (Table 6); conversion scheme IV (Table 4).

TABLE 36

Solvent and gegenion effects on nitrogen shielding in ammonium ions and anilinium ion

Ammonium ion	Solvent	Concentration (mol %)	Gegenion	Nitrogen shielding referred to neat nitromethane: ammonium ion	Nitrogen shielding referred to neat nitromethane: parent amine in cyclohexane	protonation shift referred to parent amine in cyclohexane
$Bu^sNH_3^+$	$CHCl_3$	7·3	Cl^-	+324·1	+342·4	−18·3
		7·3	I^-	+319·5		−22·9
	CH_2Cl_2	5·1	I^-	+319·6		−22·8
	DMSO	5·6	I^-	+333·1		−9·3
	CF_3COOH	6·7	Cl^-	+333·2		−9·2
		7·4	CF_3COO^-	+336·0		−6·4
	MeOH	4·0	Cl^-	+335·9		−6·5
		3·8	I^-	+336·2		−6·2
		4·2	CF_3COO^-	+338·3		−4·1
 (2-Me-piperidinium)	$CHCl_3$	9·2	Cl^-	+324·1	+325·3	−1·2
		7·3	I^-	+321·3		−4·0
	MeOH	4·0	Cl^-	+328·3		+3·0
		3·8	I^-	+328·4		+3·1
 (*cis*-2,6-Me_2-piperidinium)	$CHCl_3$/MeOH (82:18)	7·9	Cl^-	+313·5	+306·9	+6·4
	MeOH	4·5	Cl^-	+314·6		+7·7

TABLE 36—*cont.*

Ammonium ion	Solvent	Concentration (mol %)	Gegenion	Nitrogen shielding referred to neat nitromethane: ammonium ion	Nitrogen shielding referred to neat nitromethane: parent amine in cyclohexane	Protonation shift referred to parent amine in cyclohexane
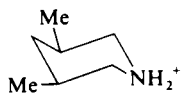 (*cis*-3,5-Me_2-piperidinium)	$CHCl_3$	10·8	Cl^-	+333·4	+342·7	−9·3
		7·7	Cl^-	+336·6		−6·1
		7·2	I^-	+329·6		−13·1
		7·7	CF_3COO^-	+340·7		−2·0
		7·7	BF_4^-	+341·3		−1·4
		8·0	$MeCOO^-$	+340·5		−2·2
	MeOH	8·5	Cl^-	+336·0		−6·3
		4·0	Cl^-	+338·3		−4·4
		3·8	I^-	+338·9		−3·8
		4·0	CF_3COO^-	+341·0		−1·7
		3·8	BF_4^-	+341·2		−1·5
		4·2	$MeCOO^-$	+340·5		−2·2
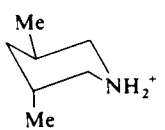 (*trans*-3,5-Me_2-piperidinium)	$CHCl_3$	10·8	Cl^-	+338·6	+353·5	−14·9
		7·7	Cl^-	+339·3		−14·2
		7·2	I^-	+334·9		−18·4
		7·7	CF_3COO^-	+347·1		−6·4
		7·7	BF_4^-	+348·5		−5·0
		8·0	$MeCOO^-$	+346·9		−6·6
	MeOH	8·5	Cl^-	+343·0		−10·5
		4·0	Cl^-	+344·9		−8·6
		3·8	I^-	+345·5		−8·0
		4·0	CF_3COO^-	+347·9		−5·4
		3·8	BF_4^-	+348·3		−5·2
		4·2	$MeCOO^-$	+347·2		−6·3

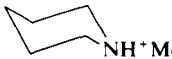	$CHCl_3$	7·7	Cl^-	+334·1	+342·8	−8·7
	DMSO	8·9	Cl^-	+334·8		−8·0
(*N*-Me-piperidinium)	MeOH	4·0	Cl^-	+335·3		−7·5
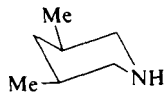	$CHCl_3$	13·1	Cl^-	+331·9	+343·4	−11·5
		9·0	Cl^-	+331·7		−11·7
		12·6	I^-	+329·8		−13·6
(*N,cis*-3,5-Me_3-piperidinium)		7·3	I^-	+330·0		−13·4
	MeOH	8·3	Cl^-	+332·6		−10·8
		4·6	Cl^-	+333·3		−10·1
		3·8	I^-	+333·5		−9·9
	H_2O	5·2	I^-	+333·9		−9·5
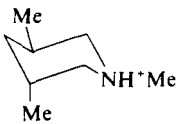	$CHCl_3$	13·1	Cl^-	+336·3	+351·3	−15·0
		9·0	Cl^-	+335·9		−15·4
		12·6	I^-	+334·5		−16·8
		7·3	I^-	+334·4		−16·9
(*N,trans*-3,5-Me_3-piperidinium)	MeOH	8·3	Cl^-	+338·0		−13·3
		4·6	Cl^-	+339·0		−12·3
		3·8	I^-	+339·2		−12·1
	H_2O	3·2	I^-	+339·7		−12·6
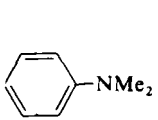	$CHCl_3$	0·9	Cl^-	+320·6	+326·5	−5·9
		8·0	I^-	+319·6		−6·9
	MeOH	4·2	Cl^-	+319·2		−7·3
		3·8	I^-	+319·2		−7·3
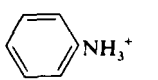	$CHCl_3$/MeOH (70:30)	5·2	Cl^-	+328·2	+327·0	+1·2
	MeOH	4·0	Cl^-	+332·6		+5·6

Data from ref. 82; ^{15}N natural abundance spectra; 18·25 MHz; field parallel to sample tube; referred originally to 1 M DNO_3, +6·2 ppm from neat nitromethane (Table 6); conversion scheme IV (Table 4).

TABLE 37

Nitrogen shieldings in aniline and its derivatives

Compound	Solution	Nitrogen shielding: referred to neat nitromethane	substituent effect referred to parent amine: in acetone	in DMSO	neat	Notes
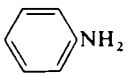	1 M in DMSO	+321·3		(0·000)		(a)
	25% in DMSO	+322·5		0·000		(b)
	1·0 M in acetone	+322·3	0·000			(c)
Aniline	neat+10% C_6D_6	+323·8				(d)
	neat liquid	+325·9			0·000	(b)
	2 M in cyclohexane	+327·0				(e)
	2 M in MeOH	+328·5				(e)
	see also Table 24					
Substituted anilines:						
2-F	1·0 M in acetone	+334·1	+11·8			(c)
2-OMe	1·0 M in acetone	+332·7	+10·4			(c)
4-NH_2	25% in DMSO	+329·5		+7·0		(b)
4-OH	25% in DMSO	+329·2		+6·7		(b)
4-OMe	neat liquid	+329·2			+3·4	(b)
	satd. in DMSO	+328·2		+5·8		(b)
4-F	1·0 M in acetone	+325·7	+3·4			(c)
4-Me	neat liquid	+328·7			+2·4	(b)
	satd. in DMSO	+325·0		+2·5		
2-Me	neat liquid	+328·0			+2·1	(b)
2-Cl	1·0 M in acetone	+322·9	+0·6			(c)
4-Cl	1·0 M in acetone	+322·8	+0·5			(c)
3-NH_2	neat liquid	+324·4			−1·5	(b)
	25% in DMSO	+322·8		+0·3		(b)
	6 mol % in DMSO	+322·1		(+0·8)		(f)

4-I	1·0 M in acetone	+321·6	−0·7			(c)
4-Br	satd. in DMSO	+321·5		−1·0		(b)
2-CF_3	1·0 M in acetone	+320·3	−2·0			(c)
2-CN	satd. in DMSO	+314·1 (NH_2)		−8·4		(b)
2-Br	1·0 M in acetone	+318·1	−4·2			(c)
4-SO_2NH_2	1 M in DMSO	+313·6 (aniline)		(−7·9)		(a)
4-$SO_2N{=}C(NH_2)_2$	8 g/18 ml DMSO	+315·5 (aniline)		−10·4		(g)
2-COPh	1·0 M in acetone	+311·4	−10·9			(c)
4-COMe	25% in DMSO	+311·2		−11·3		(b)
2,4,6-Br_3	1·0 M in acetone	+310·7	−11·6			(c)
2-I	1·0 M in acetone	+310·4	−11·9			(c)
2-COMe	neat liquid	+313·8			−12·1	(b)
4-CN	1 M in DMSO	+308·6 (aniline)		(−12·7)		(a)
4-NO_2	1·0 M in acetone	+307·4	−14·9			(c)
	25% in DMSO	+302·2		−20·3		(b)
	satd. in DMSO	+302·8				(b)
	3 M in DMSO	+302±2				(h)
	1 M in DMSO	+302·0		(−19·3)		(a)
2-Cl-4-NO_2	1·0 M in acetone	+307·1	−15·2			(c)
2-NO_2	1·0 M in acetone	+306·7	−15·6			(c)
2-NO_2-4-Cl	1·0 M in acetone	+305·4	−16·9			(c)
2,3-$(NO_2)_2$	satd. in DMSO	+289·8		−32·7		(b)
2-COOH	4 M in DMSO	+309·4		−16·3		(i)
2-COO^-Na^+	4 M in DMSO	+322·6		−3·3		(i)
3-COOH	4 M in DMSO	+316·0		−9·9		(i)
3-COO^-Na^+	4 M in DMSO	+323·5		−2·4		(i)
		+335(?)				(h)
4-COOH	4 M in DMSO	+306·2		−19·7		(i)
4-COO^-Na^+	4 M in D_2O	+315·5				(i)
	25% in DMSO	+337·2		0·000		(b)
	2 M in MeOH	+338·0				(e)
	2 M in cyclohexane	+339·7				(e)
N,N-Dimethylaniline	neat liquid	+339·8			0·000	(b)

TABLE 37—*cont.*

Compound	Solution	Nitrogen shielding: referred to neat nitromethane	substituent effect referred to parent amine: in acetone	in DMSO	neat	Notes
Substituted:						
4-OMe	25% in DMSO	+343·2		+6·0		(b)
4-Me	neat liquid	+342·1			+2·3	(b)
4-Br	neat liquid	+337·6			−2·2	(b)
4-COMe	neat liquid	+327·2			−12·6	(b)
4-COPh	neat liquid	+326·6			−13·2	(b)
4-CN	neat liquid	+325·4 (NMe_2)			−14·4	(b)
4-CHO	neat liquid	+323·1			−16·7	(b)
4-NO_2	10% in DMSO	+316·5 (NMe_2)		−20·7		(b)
4-NO	neat liquid	+309·5 (NMe_2)			−30·3	(b)

(a) Data from ref. 154; ^{15}N natural abundance spectra; 18·25 MHz; field parallel to sample tube; referred originally to 1 M DNO_3, +6·2 ppm from neat nitromethane (Table 6); conversion scheme IV (Table 4).

(b) Data from ref. 47; ^{15}N natural abundance spectra; 9·117 MHz; field perpendicular to sample tube; referred originally to saturated aqueous $NaNO_3$, +3·7 ppm from neat nitromethane (Table 6); conversion scheme II (Table 4).

(c) Data from ref. 155; ^{15}N-labelled amino group; $^1H\{^{15}N\}$ INDOR spectra; referred originally to ^1H acetone lock at 89 999 809·7 Hz and the corresponding TMS frequency of 89 999 622·1 Hz; for conversion, according to scheme II (Table 4) and for magnetic field perpendicular to sample tube, a value of 9·1230299 MHz was used for neat nitromethane resonance (calculated from data in ref. 80 and ref. 2, p. 172).

(d) Data from ref. 81; ^{15}N natural abundance spectra; 10·09 MHz; field perpendicular to sample tube; referred originally to neat nitromethane; uncorrected for bulk susceptibility effects.

(e) Data from ref. 119; details as in note (a).

(f) Data from ref. 83; details as in note (a).

(g) Data from ref. 156; details as in note (a); ^1H-coupled spectra.

(h) Data from ref. 123; ^{15}N natural abundance spectra; 27·4 MHz; field parallel to sample tube; referred originally to aqueous NH_4Cl, but reported relative to Me_4N^+, +337 ppm from neat nitromethane (Table 6), low-precision measurements (±2 ppm).

(i) Data from ref. 157; ^{15}N natural abundance spectra; 27·4 MHz; field parallel to sample tube; referred originally to saturated aqueous NH_4Cl, +352·9 ppm from neat nitromethane (Table 6); conversion scheme II (Table 4).

TABLE 38

Nitrogen shielding in methyl-substituted *N,N*-dimethylanilines and corresponding arylammonium ions

Compound	Nitrogen shielding referred to neat nitromethane	
	for parent amine (neat liquid)	for corresponding ammonium ion (2 M in C_6D_6+2 eq. of CF_3COOH)
	(+339·8; Table 37)	+329·2 (?)
2-Me	+350·5	+330·7
3-Me	+340·7	+329·2
4-Me	+342·4	+330·2
2,3-Me_2	+351·0	+331·0
2,6-Me_2	+367·3	+330·4
2,4,6-Me_3	+369·0	+331·2
2,4-Et_2	+371·3	+331·0
2,4-$Pr^i{}_2$	+374·0	+332·6

Data from ref. 164; ^{15}N natural abundance spectra; 10·1 MHz; originally referred to nitromethane in deuteriobenzene, but reported relative to 2·9 M NH_4Cl in 1 M HCl, +351·85 ppm from the nitromethane reference used; if this conversion constant is used in recalculation, severe discrepancies with the data in Table 37 are obtained, e.g. +332·2 instead of +339·8 for neat *N,N*-dimethylaniline, and therefore the latter value is used here as the reference shielding; the shieldings for the arylammonium ions are recalculated using the 351·85 ppm conversion constant, but since the content of deuteriobenzene in nitromethane was not reported, a systematic error up to about 4 ppm may be involved; since $Cr(acac)_3$ was added to the amines, this can produce additional uncertainty about the significance of the results.

TABLE 39

Nitrogen shieldings in aryl amines (other than simple aniline derivatives)

Compound	Solution	Nitrogen shielding: referred to neat nitromethane	Nitrogen shielding: referred to parent amine in: $CHCl_3$	Nitrogen shielding: referred to parent amine in: DMSO	Notes
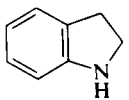	neat liquid	+312·9			(a)
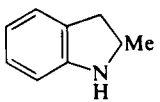	neat liquid+10% C_6D_6	+294·6			(b)
	neat liquid	+295·6			(a)
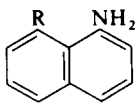					
R=H	6 mol % in $CHCl_3$	+329·2	0·00		(c)
	6 mol % in DMSO	+321·9		0·00	(c)
NO_2	6 mol % in $CHCl_3$	+324·5 (NH_2)	−4·7		(c)
	6 mol % in DMSO	+320·1 (NH_2)		−1·8	(c)
CN	6 mol % in DMSO	+319·5 (NH_2)		−2·4	(c)
NH_2	6 mol % in $CHCl_3$	+320·8	−8·4		(c)
	6 mol % in DMSO	+316·8		−5·1	(c)
Cl	6 mol % in $CHCl_3$	+320·4	−8·8		(c)
	6 mol % in DMSO	+314·8		−7·1	(c)
Br	6 mol % in $CHCl_3$	+319·5	−9·7		(c)
	6 mol % in DMSO	+314·5		−7·4	(c)
I	6 mol % in $CHCl_3$	+318·0	−11·2		(c)
	6 mol % in DMSO	+313·4		−8·5	(c)

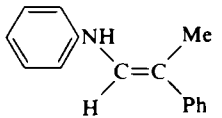	satd. in DMSO	+323·1	0·00		(d)
Substituent in phenyl ring:					
4-OMe	satd. in DMSO	+328·5	+5·4		(d)
4-Me	satd. in DMSO	+325·2	+2·1		(d)
4-Cl	satd. in DMSO	+322·5	−0·6		(d)
3-OMe	satd. in DMSO	+322·2	−0·9		(d)
3-Cl	satd. in DMSO	+321·3	−1·8		(d)
3-NO_2	satd. in DMSO	+317·6 (NH)	−5·5		(d)
4-NO_2	satd. in DMSO	+303·8 (NH)	−19·3		(d)
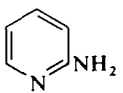	1 : 3 v/v in acetone	+311·8(NH_2)			(i)
		+310±3(NH_2)			(h)
	neat liquid	+310·6 (NH_2)			(e)
	satd. in DMSO	+308·3 (NH_2)		0·00	(e)
	0·5 M in DMSO	+307·3 (NH_2)			(f)
		+307·8 (NH_2)			(g)
Substituted:					
6-OH	25% in DMSO	+314·8 (NH_2)		+6·5	(e)
5-NO_2	25% in DMSO	+289·0 (NH_2)		−19·3	(e)
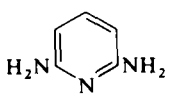	25% in DMSO	+309·6 (NH_2)			(e)
	0·5 M in DMSO	+309·1 (NH_2)			(f)
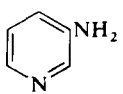	1 : 3 v/v in acetone	+328·3 (NH_2)			(i)
		+334±3 (NH_2)			(h)
	25% in DMSO	+329·5 (NH_2)		0·00	(e)
	0·5 M in DMSO	+325·3 (NH_2)			(f)
Substituted:					
6-OMe	25% in DMSO	+337·2 (NH_2)		+7·7	(e)

TABLE 39—*cont.*

Compound	Solution	Nitrogen shielding: referred to neat nitromethane	Nitrogen shielding: referred to parent amine	Notes
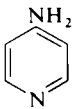	1 : 3 v/v in acetone	+317·2(NH_2)		(i)
		+323±3(NH_2)		(h)
	25% in DMSO	+312·2 (NH_2)		(e)
	0·5 M in DMSO	+312·0 (NH_2)		(f)
		+312·8 (NH_2)		(g)
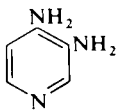	25% in DMSO	+338·3 (3-NH_2)		(e)
		+322·5 (4-NH_2)		(e)
	0·5 M in DMSO	+336·9 (3-NH_2)		(f)
		+322·0 (4-NH_2)		(f)
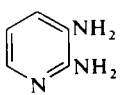	0·5 M in DMSO	+313·5 (2-NH_2)		(f)
		+330·4 (3-NH_2)		(f)
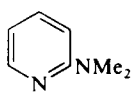	neat liquid+$Cr(acac)_3$	+324·1 (NMe_2)		(e)
	1 : 3 v/v in acetone	+323·0		(i)
		+319±3		(h)
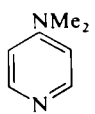	neat liquid+$Cr(acac)_3$	+328·6 (NMe_2)		(e)
	1 : 3 v/v in acetone	+328·6		(i)
		+329±3		(h)

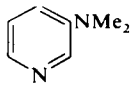	1 : 3 v/v in acetone	+340·0 +342±3	(i) (h)
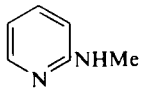	1 : 3 v/v in acetone	+308±3	(h)
	1 : 3 v/v in acetone	+318±3	(h)
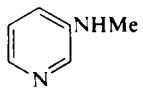	1 : 3 v/v in acetone	+336±3	(h)
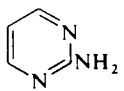	25% in DMSO 0·5 M in DMSO	+299·7 (NH_2) +297·9 (NH_2)	(e) (f)
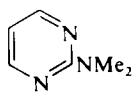	0·5 M in DMSO	+311·9 (NMe_2)	(f)
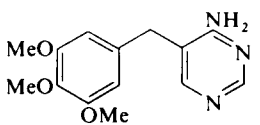	0·5 M in DMSO	+298·4 (NH_2)	(f)
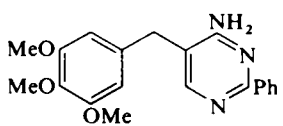	0·5 M in DMSO	+302·3 (NH_2)	(f)

TABLE 39—*cont.*

Compound	Solution	Nitrogen shielding: referred to neat nitromethane	Nitrogen shielding: referred to parent amine	Notes
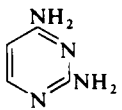	0·5 M in DMSO	+301·6 (2-NH_2) +299·6 (4-NH_2)		(f) (f)
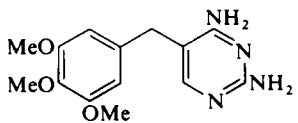	0·5 M in DMSO	+304·6 (2-NH_2) +302·3 (4-NH_2)		(f) (f)
	0·5 M in DMSO	+300·9 (2-NH_2?) +299·4 (4-NH_2?)		(f) (f)
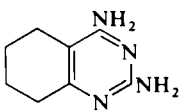	0·5 M in DMSO	+305·1 (2-NH_2) +302·6 (4-NH_2)		(f) (f)
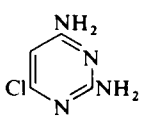	0·5 M in DMSO	+297·7 (2-NH_2) +296·6 (4-NH_2)		(f) (f)

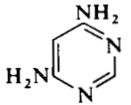	0·5 M in DMSO	+309·1 (NH_2)	(f)
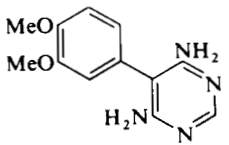	0·5 M in DMSO	+304·5 (NH_2)	(f)
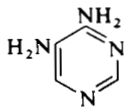	0·5 M in DMSO	+305·9 (4-NH_2) +338·0 (5-NH_2)	(f) (f)
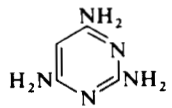	0·5 M in DMSO	+304·0 (2-NH_2) +306·0 (4-NH_2, 6-NH_2)	(f) (f)
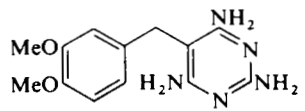	0·5 M in DMSO	+305·5 (2-NH_2) +306·4 (4-NH_2, 6-NH_2)	(f) (f)
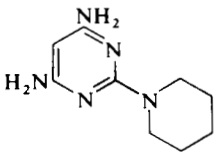	0·5 M in DMSO	+308·2 (piperidyl) +306·2 (4-NH_2, 6-NH_2)	(f) (f)
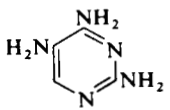	0·5 M in DMSO (dissolved as hydrochloride, 1 eq. 4 M NaOH added)	+311·2 (2-NH_2) +316·3 (4-NH_2) +357·3 (5-NH_2)	(f) (f) (f)

TABLE 39—*cont.*

Compound	Solution	Nitrogen shielding: referred to neat nitromethane	Nitrogen shielding: referred to parent amine	Notes
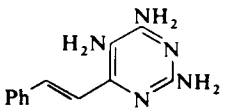	0·5 M in DMSO (dissolved as hydrochloride, 1 eq. 4 M NaOH added)	+303·4 (2-NH_2) +311·5 (4-NH_2) +341·9 (5-NH_2)		(f) (f) (f)
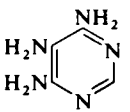	0·5 M in DMSO (dissolved as hydrochloride, 1 eq. 4 M NaOH added)	+309·6 (4-NH_2, 6-NH_2) +346·9 (5-NH_2)		(f) (f)
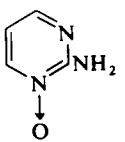	0·5 M in DMSO 0·5 M in H_2O	+304·8 (NH_2) +305·5 (NH_2)		(f) (f)
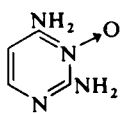	0·5 M in DMSO	+306·2 +307·4 (NH_2)		(f) (f)
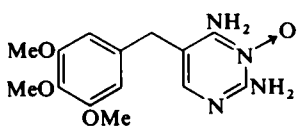	0·5 M in DMSO	+308·6 +309·5 (NH_2)		(f) (f)

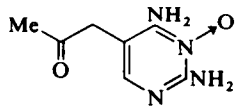	0·5 M in DMSO	+308·1 (NH$_2$) +311·1 (NH$_2$)	(f) (f)
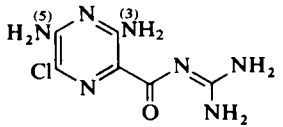	in DMSO	+298·6 (3-NH$_2$) +301·3 (5-NH$_2$)	(j) (j)
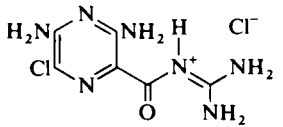	in DMSO	+297·7 (3-NH$_2$) +290·0 (5-NH$_2$)	(j) (j)
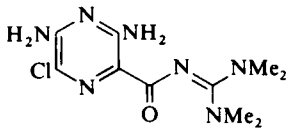	in DMSO	+300·5 (3-NH$_2$) +302·1 (5-NH$_2$)	(j) (j)
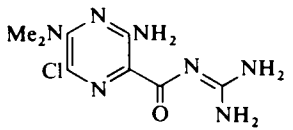	in DMSO	+298·4 (3-NH$_2$) +319·1 (5-NMe$_2$)	(j) (j)
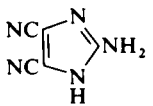	in DMSO/MeOH	+326·6 (NH$_2$)	(k)
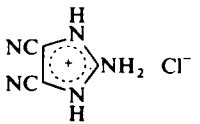	in DMSO/H$_2$O/HCl	+319·3 (NH$_2$)	(k)

TABLE 39—*cont.*

Compound	Solution	Nitrogen shielding		Notes
		referred to neat nitromethane	referred to parent amine	
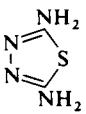	in DMSO	+324·0 (NH_2)		(l)
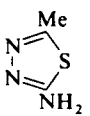	in DMSO	+318·8 (NH_2)		(l)
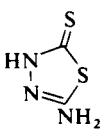	in DMSO	+314·9 (NH_2)		(l)

(a) Data from ref. 128; ^{15}N natural abundance spectra; 10·09 MHz; field perpendicular to sample tube; referred originally to 2·9 M NH_4Cl in 1 M HCl, but reported relative to "anhydrous ammonia", +380·2 ppm from neat nitromethane (Table 6); conversion scheme IV (Table 4).

(b) Data from ref. 81; ^{15}N natural abundance spectra; 10·09 MHz; field perpendicular to sample tube; referred originally to neat nitromethane; uncorrected for bulk susceptibility effects.

(c) Data from ref. 83; ^{15}N natural abundance spectra; 18·25 MHz; field parallel to sample tube; referred originally to 1 M DNO_3, +6·2 ppm from neat nitromethane (Table 6); conversion scheme IV (Table 4).

(d) Data from ref. 41; ^{15}N natural abundance spectra; 10·1 MHz; field perpendicular to sample tube; referred originally to NO_3^- in aqueous 0·5 M NH_4NO_3, +3·7 ppm from neat nitromethane (Table 6); conversion scheme II (Table 4).

(e) Data from ref. 47; ^{15}N natural abundance spectra; 9·117 MHz; field perpendicular to sample tube; referred originally to saturated aqueous $NaNO_3$, +3·7 ppm from neat nitromethane (Table 6); conversion scheme II (Table 4).

(f) Data from ref. 115; ^{15}N natural abundance spectra; 10·1 MHz; field perpendicular to sample tube; referred originally to NH_4NO_3 and originally recalculated to neat nitromethane scale; conversion scheme IV (Table 4).

(g) Data from ref. 158; ^{15}N natural abundance spectra; details as in note (c).

(h) Data from ref. 159; ^{14}N continuous-wave spectra with lineshape fitting; 4·33 MHz; field perpendicular to sample tube; referred originally to neat nitromethane.

(i) Data from ref. 160; ^{15}N natural abundance spectra; 18·25 MHz; field parallel to sample tube; referred originally to neat nitromethane; uncorrected for bulk susceptibility effects.

(j) Data from ref. 161; details as in note (c).

(k) Data from ref. 162; details as in note (c).

(l) Data from ref. 163; details as in note (c).

TABLE 40

Nitrogen shieldings in some arylammonium ions

Ion	Solution	Nitrogen shielding: referred to neat nitrogen methane	substituent effect referred to parent ion in: $HFSO_3$	C_6D_6	H_2O	protonation shift referred to parent amine	Notes
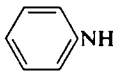	1·0 M in $HFSO_3$	+331·0	0·00				(a)
	2 M in CF_3COOH +10% C_6D_6	+329·2		0·00			(b)
	Cl^-, 2 M in H_2O	+330·1			0·00		(b)
	Cl^-, 2 M in MeOH	+332·6				+4·1	(c)
Substituent in phenyl ring:							
2-F	1·0 M in $HFSO_3$	+340·7	+9·7				(a)
2,6-Me_2	2 M in CF_3COOH	+334·8		+5·6			(b)
	Cl^-, 2 M in H_2O	+335·2			+5·1		(b)
2-NO_2-4-Cl	1·0 M in $HFSO_3$	+334·4	+3·4				(a)
2,4-Me_2	2 M in CF_3COOH	+332·4		+3·2			(b)
2-NO_2	1·0 M in $HFSO_3$	+333·6	+2·6				(a)
2,5-Me_2	2 M in CF_3COOH	+331·6		+2·4			(b)
2-Me	2 M in CF_3COOH	+331·5		+2·3			(b)
	Cl^-, 2 M in H_2O	+332·4			+2·3		(b)
2-Cl	1·0 M in $HFSO_3$	+333·1	+2·1				(a)
4-F	1·0 M in $HFSO_3$	+332·6	+1·6				(a)
4-Cl	1·0 M in $HFSO_3$	+332·2	+1·2				(a)
4-Me	2 M in CF_3COOH	+330·7		+1·5			(b)
	Cl^-, 2 M in H_2O	+331·0			+0·9		(b)
3,4-Me_2	2 M in CF_3COOH	+330·1		+0·9			(b)
4-Br	1·0 M in $HFSO_3$	+331·9	+0·9				(a)
3-Me	2 M in CF_3COOH	+330·0		+0·8			(b)
3-Br	1·0 M in $HFSO_3$	+331·6	+0·6				(a)
4-I	1·0 M in $HFSO_3$	+331·6	+0·6				(a)
4-NO_2-2-Cl	1·0 M in $HFSO_3$	+331·5	+0·5				(a)
3,5-Me_2	2 M in CF_3COOH	+329·6		+0·4			(b)
3-NO_2	1·0 M in $HFSO_3$	+330·9	−0·1				(a)
4-NO_2	1·0 M in $HFSO_3$	+329·9	−1·1				(a)
2-Br	1·0 M in $HFSO_3$	+328·2	−2·8				(a)
2,4,6-Br_3	1·0 M in $HFSO_3$	+325·3	−5·7				(a)
2-I	1·0 M in $HFSO_3$	+320·6	−10·4				(a)
2-COOH	4 M in DMSO +1 eq. CF_3COOH	+319·3					(d)
3-COOH	4 M in DMSO +1 eq. CF_3COOH	+325·1					(d)
4-COOH	4 M in DMSO +1 eq. CF_3COOH	+319·0					(d)

TABLE 40—*cont.*

Ion	Solution	Nitrogen shielding: referred to neat nitrogen methane	Nitrogen shielding: protonation shift referred to parent amine	Notes
 $NHMe_2^+$	2 M in MeOH, Cl^-	+330·8	−7·6	(c)

(a) Data from ref. 155; ^{15}N-labelled compounds; $^1H\{^{15}N\}$INDOR spectra; see note (c) in Table 37.

(b) Data from ref. 35; ^{15}N natural abundance spectra; 10·09 MHz; field perpendicular to sample tube; referred originally to 2·9 M NH_4Cl in 1 M HCl, +355·3 ppm from neat nitromethane (Table 6); conversion scheme IV (Table 4).

(c) Data from ref. 119; ^{15}N natural abundance spectrum; 18·25 MHz; field parallel to sample tube; referred originally to 1 M DNO_3, +6·2 ppm from neat nitromethane (Table 6); conversion scheme IV (Table 4).

(d) Data from ref. 157; ^{15}N natural abundance spectra; 27·4 MHz; field parallel to sample tube; referred originally to saturated aqueous NH_4Cl, +352·9 ppm from neat nitromethane (Table 6); conversion scheme II (Table 4).

TABLE 41

Nitrogen shieldings in some hydrazines, hydrazides, hydroxylamines, and related structures

Compound	Solution	Nitrogen shielding referred to neat nitromethane (assignments in order of nitrogen-containing moieties)	Notes
H_2NNH_2	neat liquid	+334·8	(a)
	in H_2O	+330·7	(a)
$H_2NNH_3^+HSO_4^-$	in H_2O	+335·6	(b)
$MeNHNH_2$	neat liquid	+328·0, +305·5	(a)
Me_2NNH_2	neat liquid	+322·7, +281·4	(a)
MeNHNHMe	neat liquid	+306·6	(a)
Me_2NNHMe	neat liquid	+307·7, +285·3	(a)
$PhNHNH_2$	neat liquid	+294·8, +320·0	(c)
	20% v/v in Et_3N	+294·8, +320·4	(c)
	20% v/v in DMSO	+294·5, +320·6	(c)
	20% v/v in $CHCl_3$	+295·2, +320·0	(c)
	20% v/v in EtOH (absolute)	+295·3, +320·3	(c)
	20% v/v in 80% EtOH	+296·5, +319·0	(c)
	20% v/v in CF_3CH_2OH	+297·7, +320·2	(c)
	20% v/v in CF_3COOH	+295·6, +315·4	(c)
PhNHNHPh	in dioxan	+287·6	(a)
Ph_2NNH_2	neat liquid	? , +293·2	(a)
$(Me_3Si)_2NN(SiMe_3)_2$	neat liquid	+296±3	(d)
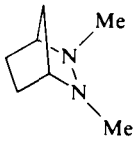	in $CDCl_3$(50 °C)	+269·6	(e)
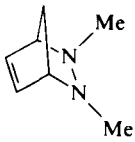	in $CDCl_3$(50 °C)	+277·7	(e)
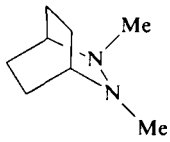	in $CDCl_3$(50 °C)	+285·6	(e)
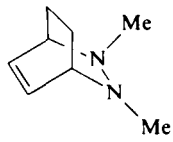	in $CDCl_3$(50 °C)	+282·6	(e)

TABLE 41—*cont.*

Compound	Solution	Nitrogen shielding referred to neat nitromethane (assignments in order of nitrogen-containing moieties)	Notes
	in CD_3COOH/HCl	+240·0 (N) +298·2 (NH_3^+)	(f) (f)
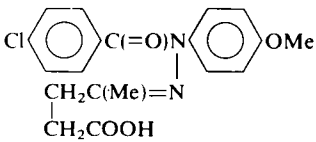	in CD_3COOH/HCl	+220·6 (N) +164·4 (C=N)	(f) (f)
$H_2NC(=S)NHNH_2$	in DMSO	+277·7, +255·6, +316·0	(g)
$MeNHC(=S)NHNH_2$	in DMSO	+273·9, +259·1, +319·2	(g)
H_2NOCH_2Ph	neat liquid	+254±3	(d)
$(Me_3Si)_2NOSiMe_3$	neat liquid	+334±3	(d)

(a) Data from ref. 1, p. 170, recalculated from R. L. Lichter and J. D. Roberts, *J. Amer. Chem. Soc.*, 1972, **94**, 4904; details as in note (c).

(b) Data from ref. 165; ^{15}N-labelled compound; ^{15}N spectrum; 18·24 MHz; field parallel to sample tube; referred originally to neat nitromethane; uncorrected for bulk susceptibility effects.

(c) Data from ref. 166; ^{15}N natural abundance spectra; 18·25 MHz; field parallel to sample tube; referred originally to 1 M DNO_3, +6·2 ppm from neat nitromethane (Table 6); conversion scheme IV (Table 4).

(d) Data from ref. 137; ^{14}N continuous-wave spectra; 7·22 MHz; field perpendicular to sample tube; referred originally to saturated aqueous $NaNO_3$, +3·7 ppm from neat nitromethane (Table 6); conversion scheme II (Table 4).

(e) Data from ref. 167, details as in note (c).

(f) Data from ref. 168; ^{15}N natural abundance spectra; 10·1 MHz; referred originally to *internal* NH_4Cl in acidic solution, assumed to correspond to a shielding of +352 ppm (Table 4).

(g) Data from ref. 169; details as in note (c); proton-decoupled and coupled ^{15}N natural abundance spectra.

TABLE 42

Comparison of $\Delta G^{\ddagger}$ values for *trans-trans* double inversion in cyclic hydrazines

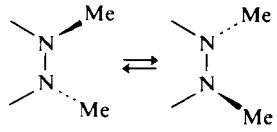

Compound	$\Delta G^{\ddagger}$ values from NMR spectra (kJ mol^{-1}) ^{15}N	^{1}H	^{13}C
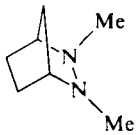	58·48 (at 209 K)	55·26	55·26
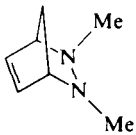	51·74 (at 281 K)	51·74	?
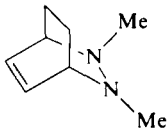	53·20 (at 252 K)	53·20	50·53

Data from ref. 167; originally reported in kcal mol^{-1}.

TABLE 43

Nitrogen shieldings in some tetraalkylhydrazines

Compound (1·5–3·0 M solutions in 1 : 1 acetone–nitromethane)	Nitrogen shielding referred to *internal* nitromethane standard
Me_2NNMe_2	+303·6
EtMeNNMeEt	+296·3
$Me_2NNMeEt$	+307·4 (NMe_2) +290·5 (NMeEt)
Me_2NNEt_2	+313·1 (NMe_2) +276·4 (NEt_2)
$Me_2NNMeBu^n$	+307·5 (NMe_2) +294·4 ($NMeBu^n$)
$Me_2NNMePr^n$	+307·6 (NMe_2) +294·5 ($NMePr^n$)
$Me_2NNMeBu^i$	+307·3 (NMe_2) +295·8 ($NMeBu^i$)
Et_2NNEt_2	+284·8
$Pr^n{}_2NNPr^n{}_2$	+290·0
$Pr^iMeNNMePr^i$	+291·6
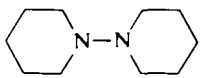	277·9
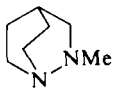	+303·7 +302·0
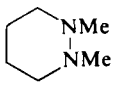	+284·4
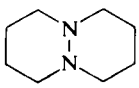	+259·2
	+285·1
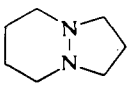	+258·2
	+285·1
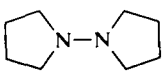	+272·4

TABLE 43—*cont.*

Compound (1·5–3·0 M solutions in 1 : 1 acetone–nitromethane)	Nitrogen shielding referred to *internal* nitromethane standard
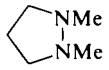	+271·3
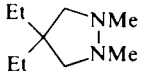	+270·1
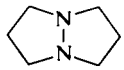	+256·9
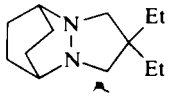	+277·8
H_2N-NH_2	+295·7

Data from ref. 170; ^{15}N natural abundance spectra; 10·1 MHz; referred originally to internal nitromethane, but reported relative to Me_2NNMe_2; 0·087 M $Cr(acac)_3$ content in the samples.

TABLE 44

Nitrogen shieldings in some hydrazido complexes

Complex (solution in CH_2Cl_2)	Nitrogen shielding referred to neat nitromethane	
	–N–	$-NH_2$
trans-$[MoF(NNH_2)(Ph_2PCH_2CH_2PPh_2)_2]BF_4$	+83·3	+243·9
trans-$[WF(NNH_2)(Ph_2PCH_2CH_2PPh_2)_2]BF_4$	+101·4	+255·1
$[Mo(NNH_2)(quinolin\text{-}8\text{-}olate)(PMe_2Ph)_3]Cl$	+64·3	+220·8
$[W(NNH_2)(quinolin\text{-}8\text{-}olate)(PMe_2Ph)_3]Cl$	+82·1	+241·6
$[MoCl(NNH_2)(pyridine)(PMe_2Ph)_3]Cl$	+72·8	+227·0
$[WCl(NNH_2)(pyridine)(PMe_2Ph)_3]Cl$	+90·6	+240·6

Data from ref. 165; ^{15}N-labelled compounds; ^{15}N spectra; 18·24 MHz; field parallel to sample tube; referred originally to neat nitromethane; uncorrected for bulk susceptibility effects.

TABLE 45

Nitrogen shieldings in some hydrazones

Compound (geometric isomer designation in parentheses)	Solution	Nitrogen shielding referred to neat nitromethane		Notes
		=N–	$-NR_2$	
(*E*)-MeCH=N-NMe_2	neat liquid	+26·6	+282·0	(a)
(*E*)-EtCH=N-NMe_2	neat liquid	+28·1	+283·0	(a)
(*E*)-Pr^nCH=N-NMe_2	neat liquid	+26·2	+282·6	(a)
(*E*)-Pr^iCH=N-NMe_2	neat liquid	+30·7	+284·0	(a)
(*E*)-Bu^iCH=N-NMe_2	neat liquid	+24·9	+281·7	(a)
(*E*)-PhCH=N-NMe_2	neat liquid	+27·4	+276·9	(a)(b)
(*E*)-$PhCH_2CH$=N-NMe_2	neat liquid	+26·8	+280·7	(a)(b)
Me_2C=N-NMe_2	neat liquid	+29·7	+289·7	(a)(b)
(*E*)-MeC(Et)=N-NMe_2	neat liquid	+25·2	+291·0	(a)(b)
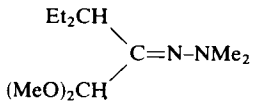	neat liquid	+17·9	+291·3	(a)
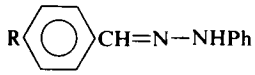				
R=OMe	20 mol % in DMSO	+60·0	+239·0	(c)
Me	20 mol % in DMSO	+56·4	+237·9	(c)
H	20 mol % in DMSO	+54·0	+237·0	(c)
Cl	20 mol % in DMSO	+52·8	+236·1	(c)
NO_2	20 mol % in DMSO	+43·4	+230·3	(c)
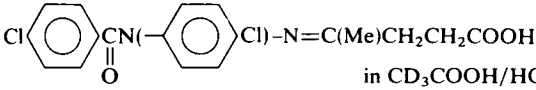	in CD_3COOH/HCl	+164·4	+220·6	(d)
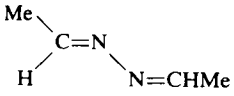	neat liquid	+17·2		(b)
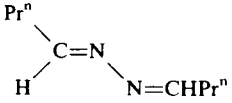	neat liquid	+14·5		(b)
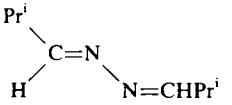	neat liquid	+21·4		(b)

TABLE 45—*cont.*

Compound (geometric isomer designation in parentheses)	Solution	Nitrogen shielding referred to neat nitromethane		Notes
		=N–	$-NR_2$	
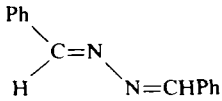	1 : 1 v/v in $CHCl_3$	+19·4		(b)
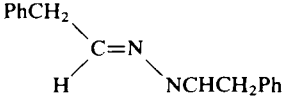	1 : 1 v/v in $CHCl_3$	+20·1		(b)
$CH_2{=}N{-}N(SiMe_3)_2$	neat liquid	+8±3	+241±3	(e)
$CCl_2{=}N{-}N(SiMe_3)_2$	neat liquid	+45±3	+216±3	(e)
$CF_2{=}N{-}N(SiMe_3)_2$	neat liquid	+182±3	+300±3	(e)

(a) Data from ref. 45; ^{15}N natural abundance spectra; 9·117 MHz; field perpendicular to sample tube; referred originally to aqueous $NaNO_3$, +3·7 ppm from neat nitromethane (Table 6); conversion scheme II (Table 4); samples contained 0·1 M $Cr(acac)_3$.

(b) Data from ref. 171; ^{15}N natural abundance spectra; details as in note (a).

(c) Data from ref. 172; ^{15}N natural abundance spectra; 18·25 MHz; field parallel to sample tube; referred originally to 1 M DNO_3, +6·2 ppm from neat nitromethane (Table 6); conversion scheme IV (Table 4).

(d) Data from ref. 168; ^{15}N natural abundance spectra; 10·1 MHz; field perpendicular to sample tube; referred originally to NH_4Cl internal standard in an acidic solution, *ca.* +352 ppm from neat nitromethane (Table 6).

(e) Data from ref. 137; ^{14}N continuous-wave spectra; 7·22 MHz; field perpendicular to sample tube; referred originally to saturated aqueous $NaNO_3$, +3·7 ppm from neat nitromethane (Table 6); conversion scheme II (Table 4).

TABLE 46

Nitrogen shieldings in borazines[34] and related structures[173]

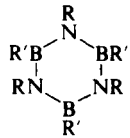

Borazine structure			Nitrogen shielding referred to neat nitromethane	^{14}N resonance half-height width (Hz)
R	R′	Solvent		
H	H	none	+282	?
Me	H	Et_2O	+275	116
Et	H	benzene	+257	155
$PhCH_2$	H	CH_2Cl_2	+239	?
H	Me	CH_2Cl_2	+294	105
Me	Me	CH_2Cl_2	+279	190
H	Et	benzene	+295	225
Me	Et	Et_2O	+279	773
H	Ph	CH_2Cl_2	+272	?
Me	C_6F_5	CH_2Cl_2	+249	?
H	F	benzene-d_6	+317	?
Me	F	CH_2Cl_2	+311	245
Et	F	benzene-d_6	+288	385
H	Cl	benzene-d_6	+284	197
Me	Cl	benzene-d_6	+278	266
Et	Cl	benzene-d_6	+260	305
$PhCH_2$	Cl	CH_2Cl_2	+249	?
Ph	Cl	CH_2Cl_2	+231	?
H	Br	benzene-d_6	+278	195
Me	Br	CH_2Cl_2	+258	267
Et	Br	CH_2Cl_2	+250	380
Et	NCO	CH_2Cl_2	+284 (NEt)	?
			+346 (NCO)	?
Me	NCS	CH_2Cl_2	+284 (NMe)	?
			+268 (NCS)	?
Et	NCS	CH_2Cl_2	+273 (unresolved)	?
Et	CN	CH_2Cl_2	+244 (NEt)	?
			+112 (CN)	?
H	OMe	CH_2Cl_2	+306	380
Me	SMe	CH_2Cl_2	+285	?
H	NMe_2	benzene-d_6	+316 (NH)	?
			+359 (NMe_2)	?

TABLE 46—*cont.*

	Solvent	Nitrogen shielding referred to neat nitromethane	^{14}N resonance half-height width (Hz)
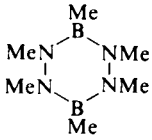	$CDCl_3$	+284	?
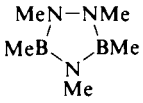	$CDCl_3$	+269	?

Data from refs 34 and 173; ^{14}N continuous-wave spectra; 7·22 MHz; field perpendicular to sample tube; referred originally to saturated aqueous $NaNO_3$, +3·7 ppm from neat nitromethane (Table 6); conversion scheme II (Table 4); accuracy not better than ±1 ppm for signals with half-height width of *ca.* 100 Hz, ±3 ppm for *ca.* 300 Hz, and at least ±5 ppm for broader signals.

TABLE 47

Nitrogen shieldings in guanidines and guanidinium ions

Compound	Solution	Nitrogen shielding referred to neat nitromethane	Notes
$PhN{=}C(NMe_2)_2$	in $CDCl_3$	+176·5 (N=C)	(e)
		+325·2, +324·8 (NMe_2)	(e)
	neat liquid	+175·4 (N=C)	(c)
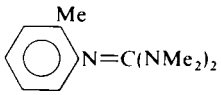	in $CDCl_3$	+174·7 (N=C)	(e)
		+325·3 (NMe_2)	(e)
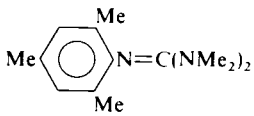	in $CDCl_3$	+175·1 (N=C)	(e)
		+327·9, +317·9 (NMe_2)	(e)
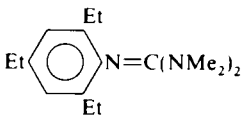	in $CDCl_3$	+174·9 (N=C)	(e)
		+327·7, +312·9 (NMe_2)	(e)

TABLE 47—*cont.*

Compound	Solution	Nitrogen shielding referred to neat nitromethane	Notes
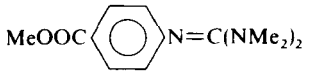	in $CDCl_3$	+179·1 (N=C) +322·3 (NMe_2)	(e) (e)
$PhCH_2N{=}C(NMe_2)_2$	in $CDCl_3$	+184·5 (N=C) +339·7, +321·9 (NMe_2)	(e) (e)
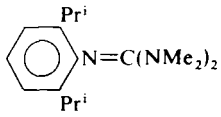	in $CDCl_3$	+178·5 (N=C) +327·3 (NMe_2)	(e) (e)
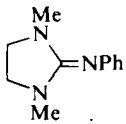	in $CDCl_3$	+205·7 (C=N) +312·0 (NMe)	(e) (e)
$HN{=}C(NMe_2)_2$	in $CDCl_3$	+211·1 (C=NH) +354·1 (NMe_2)	(e) (e)
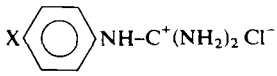			
X=OMe	16 mol % in DMSO	+303·3 (NH_2) +283·1 (NH)	(f) (f)
Me	14 mol % in DMSO	+302·7 (NH_2) +281·4 (NH)	(f) (f)
H	20 mol % in DMSO	+302·4 (NH_2) +280·4 (NH)	(f) (f)
Cl	20 mol % in DMSO	+301·5 (NH_2) +281·7 (NH)	(f) (f)
NO_2	6 mol % in DMSO	+297·7 (NH_2) +277·4 (NH) +11·7 (NO_2)	(f) (f) (f)
$C^+(NH_2)_3\ HCO_3^-$	2 M in H_2O +NaCl(1 : 1) +HPO_4(1 : 1) +HBF_4(1 : 1) +HCl(1 : 1)	+307·9 +307·2 +306·8 +308·9 +307·9	(a) (a) (a) (a) (a)
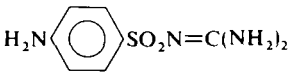	in DMSO	+315·5 (H_2N-aryl) +301·2 (=CNH_2) +218·5 (C=N)	(b) (b) (b)

TABLE 47—*cont.*

Compound	Solution	Nitrogen shielding referred to neat nitromethane	Notes
Arginine		see Table 73	
Viomycin		see Table 83	
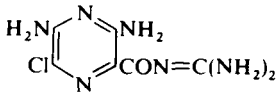	in DMSO	+296·6 (=CNH_2, triplet) +203·6 (N=C, singlet)	(d) (d)
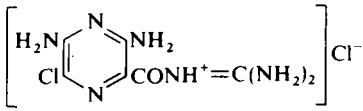 Amiloride	in DMSO	+293·6 (=CNH_2, triplet) +260·3 (NH^+, doublet)	(d) (d)
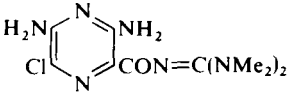	in DMSO	+309·6 (NMe_2) +176·8 (N=C)	(d) (d)
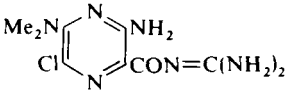	in DMSO	+296·9 (=CNH_2) +203·0 (N=C)	(d) (d)

(a) Data from ref. 174; ^{15}N natural abundance spectra; 18·25 MHz; field parallel to sample tube; referred originally to 1 M DNO_3, +6·2 ppm from neat nitromethane (Table 6); conversion scheme IV (Table 4).

(b) Data from ref. 156; details as in note (a); proton-undecoupled spectra.

(c) Data from ref. 175; ^{15}N natural abundance spectra; 9·12 MHz; field perpendicular to sample tube; referred originally to aqueous $NaNO_3$, +3·7 ppm from neat nitromethane (Table 6); conversion scheme II (Table 4); $Cr(acac)_3$ added.

(d) Data from ref. 161; undecoupled spectra; details as in note (a).

(e) Data from ref. 4, pp. 68–69, quoted as unpublished results by M. Franzen-Sieveking, D. Leibfritz, and R. L. Lichter; ^{15}N spectra; 10·1 MHz; field perpendicular to sample tube; referred originally to 2·9 M NH_4Cl in 1 M HCl, but reported relative to "anhydrous ammonia", +380·2 ppm from neat nitromethane (Table 6); conversion scheme IV (Table 4).

(f) Data from ref. 176; details as in note (a).

TABLE 48

Nitrogen shielding in streptomycin and dihydrostreptomycin

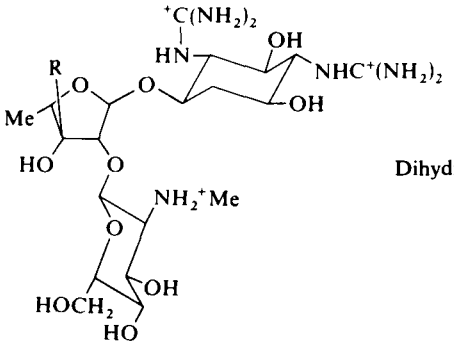

Streptomycin: R=–CHO $\overset{H_2O}{\rightleftharpoons}$ –$CH(OH)_2$

Dihydrostreptomycin: R=–CH_2OH

Type of nitrogen atom	Nitrogen shielding referred to neat nitromethane, and signal multiplicity due to NH coupling: Streptomycin sulphate ($3\times H_2SO_4$)	Dihydrostreptomycin sulphate ($3\times H_2SO_4$)
Guanidine NH	+292·3 (doublet)	+292·3 (doublet)
	+292·8 (doublet)	+293·0 (doublet)
Guanidinium $C^+(NH_2)_2$	+305·6 (triplet)	+305·6 (triplet)
	+306·3 (triplet)	+306·3 (triplet)
Ammonium $NH_2{}^+Me$	+344·8 (singlet)	+344·9 (singlet)

Data from ref. 177; ^{15}N natural abundance spectra of saturated aqueous solutions at pH 5; 36·48 MHz; field parallel to sample tube; referred originally to NO_3^- in aqueous NH_4NO_3, +4·0 ppm from neat nitromethane (Table 6); conversion scheme II (Table 4).

TABLE 49

Nitrogen shieldings in some ureas and related structures

Compound	Nitrogen shielding referred to neat nitromethane				
	4 M in dimethyl-formamide	2 M in dimethyl-formamide	4 M in DMSO	other solvents	Note
$(H_2N)_2C{=}O$	+305·2	+305·3	+302·6		(a)
				+302·2 (H_2O)	(b)
			+304·2		(c)
				+302·1 (H_2O)	(d)
				+305·0 (H_2O)	(e)
$MeNHC(=O)NH_2$	+311·2 (NH)	+311·5	+310·2		(a)
	+307·3 (NH_2)	+307·5	+304·7		(a)
				+307·5 (H_2O)	(e)
				+307·7 (H_2O)	(e)
$(MeNH)_2C{=}O$	+313·6	+313·6	+312·2		(a)
				+310·5 (H_2O)	(e)
$Me_2NC(=O)NH_2$	+314·7 (Me_2N)		+319·4		(a)
	+307·5 (NH_2)		+303·9		(a)
$Me_2NC(=O)NHMe$	+317·3 (Me_2N)		+316·7		(a)
	+312·6 (NH)		+311·5		(a)
$(Me_2N)_2C{=}O$	+316·7	+317·6	+316·7		(a)
				+319·0 (neat)	(f)
$EtNHC(=O)NH_2$	+293·0 (NH)	+293·5	+292·2		(a)
	+307·3 (NH_2)	+307·6	+307·6		(a)
$Pr^nNHC(=O)NH_2$	+296·5 (NH)	+296·6	+295·8		(a)
	+307·3 (NH_2)	+307·8	+305·1		(a)
$Pr^nNHC(=O)NHMe$				(Pr^nNH) +296·1 (H_2O)	(e)
				(NHMe) +310·7 (H_2O)	(e)
$Pr^iNHC(=O)NH_2$	+279·6 (NH)	+279·5	+278·5		(a)
	+308·4 (NH_2)	+307·2	+307·2		(a)
				+279·0 (H_2O)	(g)
				+305·5 (H_2O)	(g)

$Pr^iNHC(=O)NHMe$			(Pr^{i}NH) +281·6	+279·0 } (H$_2$O)	(e)
			(NHMe) +313·7	+310·6 }	(e)
$Bu^nNHC(=O)NH_2$	+296·4(NH)	+296·6	+295·6		(a)
	+307·3 (NH_2)	+307·6	+305·1		(a)
$Bu^iNHC(=O)NH_2$	+297·9 (NH)	+298·3			(a)
	+307·2 (NH_2)	+307·6			(a)
$Bu^tNHC(=O)NH_2$	+276·3 (NH)	+275·5	+275·0		(a)
	+306·1 (NH_2)	+306·4	+303·9		(a)
$Bu^tNHC(=O)NHMe$			+278·2 (Bu^{t}NH)		(e)
			+313·5 (NHMe)		(e)
$PhNHC(=O)NH_2$	+274·5 (NH)	+274·6	+273·4		(a)
	+302·7 (NH_2)	+303·2	+300·7		(a)
$PhNHC(=O)NHMe$			+276·2 (PhNH)		(e)
			+308·9 (NHMe)		(e)
$PhCH_2NHC(=O)NHMe$			+298·5 (CH_2NH)		(e)
			+313·5 (NHMe)		(e)
$(EtNH)_2C=O$	+295·3	+295·6	+294·5		(a)
$(Bu^nNH)_2C=O$	+297·8	+297·8	+294·5		(a)
$(PhNH)_2C=O$	+272·6	+272·6	+271·4		(a)
			+272·3		(b)
$H_2NC(=O)NHC(=O)NH_2$ (biuret)			+258·0 (NH)		(b)
			+297·0 (NH_2)		(b)

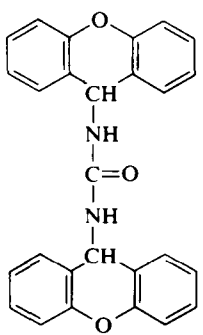

			+272·9 (30 °C)		(b)
			+273·6 (90 °C)		(b)

TABLE 49—*cont.*

Compound	Nitrogen shielding referred to neat nitromethane: 4 M in DMSO	other solvents	Note
	+272·6 (NH) +305·7 (NH_2)		(b) (b)
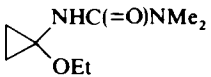		(NH) +285·3 (NMe_2) +315·8 } ($CDCl_3$)	(h) (h)
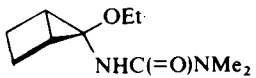		(NH) +296·8 (NMe_2) +316·0 } ($CDCl_3$)	(h) (h)
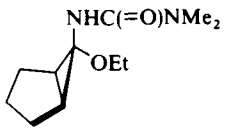		(NH) +292·7 (NMe_2) +315·6 } ($CDCl_3$)	(h) (h)
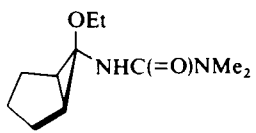		(NH) +282·1 ($CDCl_3$) (NMe_2) not observed	(h) (h)

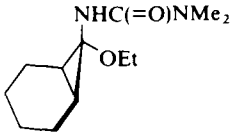

(NH) +292·7, (NMe$_2$) +315·5 } (CDCl$_3$) (h), (h)

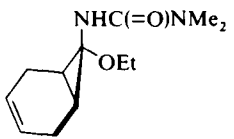

(NH) +295·5, (NMe$_2$) +315·3 } (CDCl$_3$) (h), (h)

(a) Data from ref. 42; ^{15}N natural abundance spectra; 10·09 MHz; field perpendicular to sample tube; referred originally to neat nitromethane but reported relative to "anhydrous ammonia", +380·2 ppm from neat nitromethane (Table 6); uncorrected for bulk susceptibility effects.

(b) Data from ref. 178; ^{15}N-labelled and non-labelled compounds; ^{15}N spectra; 9·12 MHz; field perpendicular to sample tube; referred originally to NO_3^- in saturated aqueous NH_4NO_3, +4·0 ppm from neat nitromethane (Table 6); conversion scheme II (Table 4).

(c) Data from ref. 66; ^{15}N-labelled compounds; ^{15}N spectra; 10·1 MHz; field perpendicular to sample tube; referred originally to Me_4N^+, +336·7 ppm from neat nitromethane (Table 6); conversion scheme II (Table 4).

(d) Data from ref. 179; continuous-wave ^{14}N spectra; 4·33 MHz; high-precision differential saturation technique with full lineshape fitting; concentric spherical sample/standard containers in order to eliminate bulk susceptibility effects; referred to neat nitromethane.

(e) Data from ref. 180; ^{15}N natural abundance spectra; 18·25 MHz; field parallel to sample tube; referred originally to 1 M DNO_3, +6·2 ppm from neat nitromethane (Table 6); conversion scheme IV (Table 4).

(f) Data from ref. 40; ^{15}N natural abundance spectra; 6·08 MHz; field perpendicular to sample tube; referred originally to dilute DNO_3, probably +3·7 ppm from neat nitromethane (Table 6); conversion scheme II (Table 4).

(g) Data from ref. 181; ^{15}N natural abundance spectra; 9·12 MHz; field perpendicular to sample tube; referred originally to NH_4^+ in 5 M NH_4NO_3 in 2 M HNO_3, +359·0 ppm from neat nitromethane (Table 6); conversion scheme II (Table 4).

(h) Data from refs 182 and 183; ^{15}N natural abundance spectra; 10·13 MHz; field perpendicular to sample tube; referred originally to 1 M 2-pyrrolidone, +265·5 ppm from neat nitromethane; conversion scheme II (Table 4).

TABLE 50

Nitrogen shielding increments for carbon atoms in ureas

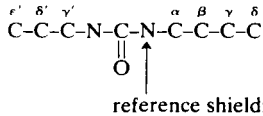

reference shielding = +307·62 ppm

Carbon atom position	Nitrogen shielding increment	Number of data involved
α	+4·64±0·40	13
β	−16·61±0·56	7
γ	+1·81±0·53	4
δ	+0·67±0·92	2
γ'	+0·99±0·37	12
δ'	−0·51±0·58	8
ε'	+0·36±0·87	4

Data from ref. 42; reference shift recalculated to neat nitromethane.

TABLE 51

Nitrogen shieldings in some linear polyureas

Polymer structure	Nitrogen shielding referred to neat nitromethane for solutions in CF_3COOH	
$-NH-(CH_2)_n-NH-CO-$		
$n=2$	+296·6	
3	+293·4	
4	+291·6	
6	+291·0	
8	+290·8	
12	+290·6	
$-NH-(CH_2)_6-NH-CO-NH-(CH_2)_n-NH-CO-$	$N(CH_2)_nN$	$N(CH_2)_6N$
$n=2$	+297·5	+289·5
3	+294·0	+290·0
4	+292·3	+290·7
6	+291·0	+291·0
8	+291·2	+290·6
12	+291·4	+290·5
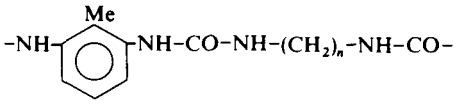	$N(CH_2)_nN$	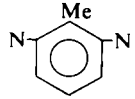
$n=2$	+294·1	+282·3
3	+290·8	+282·0
6	+287·2	+283·4

TABLE 51—*cont.*

Polymer structure	Nitrogen shielding referred to neat nitromethane for solutions in CF_3COOH	
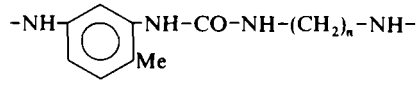	$N(CH_2)_nN$	
$n=2$	+286·9	+284·6, +281·8
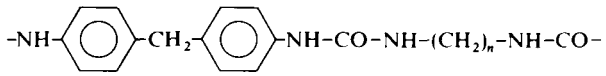		
	$N(CH_2)_nN$	N- $-CH_2-$ -N
$n=2$	+294·7	+279·1
3	+291·0	+280·1
4	+288·9	+280·6
6	+287·8	+281·0
12	+287·2	+281·2
$-NH-(CH_2)_6-NH-CO-NH-X-NH-CO-$	$N(CH_2)_6N$	NXN
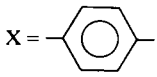	+286·7	+281·2
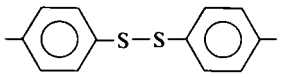	+287·4	+281·4
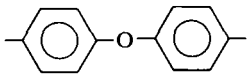	+287·6	+282·0
Random copolymer of urea unit* with		
1,3-diaminopropane unit	+294·1	
1,6-diaminohexane unit	+290·1	
1,3-diaminobenzene unit	+286·7	
	+280·6	
Random copolymer of urea unit† with		
1,3-diaminopropane unit	+294·1	
1,6-diaminohexane unit	+291·0	
1,3-diaminobenzene unit	+290·1	
	+286·7	
	+280·7	

Data from ref. 184; ^{15}N natural abundance spectra; 9·12 MHz; field perpendicular to sample tube; referred originally to NO_3^- in aqueous NH_4NO_3, +4·0 ppm from neat nitromethane (Table 6); conversion scheme II (Table 4); 1·5 g polymer in 7 ml CF_3COOH.

* Copolymer obtained from 1,3-diaminopropane, 1,3-diaminobenzene, and 1,6-hexamethylenediisocyanate.

† Copolymer obtained from 1,3-diaminopropane, 1,6-diaminohexane, 1,3-diaminobenzene, and 1,6-hexamethylenediisocyanate.

TABLE 52

Nitrogen shieldings in some carbamates

Compound	Solution	Nitrogen shielding referred to neat nitromethane	Notes
$MeOC(=O)NMe_2$	neat liquid	+315·7	(a)
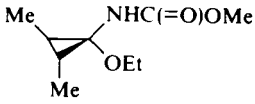	1 M in acetone	+287·7	(b)
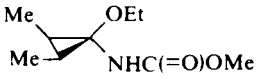	1 M in acetone	+280·7	(b)
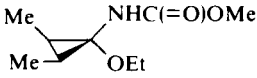	1 M in acetone	+293·5	(b)
Other carbamate structures		see Table 53	

(a) Data from ref. 40; ^{15}N natural abundance spectra; 6·08 MHz; field perpendicular to sample tube; referred originally to "dilute HNO_3", probably +3·7 ppm from neat nitromethane (Table 6); conversion scheme II (Table 4).

(b) Data from refs 182 and 183; ^{15}N nautral abundance spectra; 10·13 MHz; 1 M 2-pyrrolidone, +265·5 ppm from neat nitromethane; conversion scheme II (Table 4).

TABLE 53

Solvent effects on nitrogen shieldings in some carbamate structures

Compound	Nitrogen shielding referred to neat nitromethane for solutions in: CF_3COOH	HCOOH	H_2O	DMSO	pyridine
$EtOC(=O)NH_2$	+305·9	+305·9	+305·0	+305·3	+307·6
$PhCH_2OC(=O)NHCH_2COOH$		+303·7		+303·5	+304·2
 (2-oxazolidinone)	+299·3	+300·8	+302·8	+305·0	+305·6
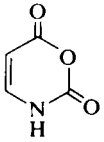 (1,3-oxazine-2,6-dione)	+259·3	+258·4		+255·3	

Data from ref. 185; ^{15}N enriched and non-enriched compounds; ^{15}N spectra; 9·12 MHz; field perpendicular to sample tube; referred originally to NO_3^- in aqueous NH_4NO_3, +4·0 ppm from neat nitromethane (Table 6); conversion scheme II (Table 4); 20% w/w solutions.

TABLE 54

Nitrogen shieldings in physostigmine

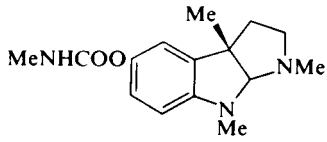

(saturated solution in $CDCl_3$)

Nitrogen shielding referred to neat nitromethane	Signal structure	Assignment
+308·1	doublet	MeNHC(=O)–
+308·8	singlet	Aryl–N(Me)–
+322·8	unresolved multiplet	–N(Me)–

Data from ref. 186; ^{15}N natural abundance spectra; gated decoupling (NOE and coupling retained) of protons; 10·09 MHz; field perpendicular to sample tube; referred originally to aqueous NH_4Cl, +352·9 ppm from neat nitromethane (Table 6); conversion scheme II (Table 4).

TABLE 55

Nitrogen shieldings in some carbodiimides

Compound $R^1N{=}C{=}NR^2$ R^1	R^2	Solution	Nitrogen shielding referred to neat nitromethane
Pr^i	Pr^i	20% v/v in cyclohexane	+277·9
		20% v/v in Et_3N	+277·4
		20% v/v in Me_2SO_4	+277·2
		20% v/v in MeI	+277·1
		neat liquid	+277·1
		20% v/v in $CHCl_3$	+276·6
		20% v/v in DMSO	+276·2
		20% v/v in CF_3CH_2OH	+274·0
		20% v/v in CF_3CH_2OH (80 °C)	+274·9 +252·1 (isourea derivative)
cyclohexyl	cyclohexyl	10% v/v in MeI	+281·2
		10% v/v in Me_2SO_4	+281·1
		10% v/v in $CHCl_3$	+280·7
Pr^i	Bu^t	20% v/v in cyclohexane	+275·8 ($Pr^iN{=}$) +267·6 ($Bu^tN{=}$)
Pr^i	Ph	20% v/v in DMSO	+283·7 (PhN=) +270·8 ($Pr^iN{=}$)
Et	$CH_2CH_2CH_2NMe_2$	neat liquid	+294·4 +297·2 +359·1 (NMe_2)

Data from ref. 189; ^{15}N natural abundance spectra; 18·25 MHz; field parallel to sample tube; referred originally to 1 M DNO_3, +6·2 ppm from neat nitromethane (Table 6); conversion scheme IV (Table 4).

TABLE 56

Nitrogen shieldings in cyclic dimeric cations derived from carbodiimides

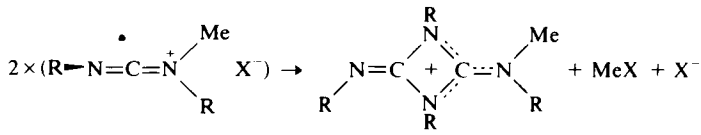

Nitrogen shielding referred to neat nitromethane

R	X	Solvent	RN=	RN⋮+	NMeR
cyclohexyl	I^-	MeI	+145·9	+241·5, +243·8	+264·4
	$MeSO_4^-$	Me_2SO_4	+145·1	+241·2, +243·0	+264·1
Pr^i	$MeSO_4^-$	Me_2SO_4	+142·0	+241·1, +242·8	+263·4

Data from ref. 189; ^{15}N natural abundance spectra; 18·25 MHz; field parallel to sample tube; referred originally to 1 M DNO_3, +6·2 ppm from neat nitromethane (Table 6); conversion scheme IV (Table 4).

TABLE 57

Nitrogen shieldings in some amides and related structures

Compound	Solution	Nitrogen shielding referred to neat nitromethane	Note
$HC(=O)NH_2$	neat liquid + 10% acetone	+267·8	(a)
	10 mol % in H_2O	+267·8	(b)
	various solvents	see Table 61	
$MeC(=O)NH_2$	4 mol % in $CDCl_3$	+276·8	(c)
HC(=O)NHMe	neat liquid	see Table 60	
	neat liquid + 10% C_6D_6	+269·8	(a)
MeC(=O)NHMe	neat liquid	see Table 60	
	neat liquid + 10% C_6D_6	+272·8	(a)
	1 : 3 v/v in acetone	+277·7	(d)
	1 : 1 v/v in acetone	+275·3	(e)
	1·5 M in DMSO	+276·2	(f)
	in H_2O, pH 6.5	+262·4	(f)
	pH 12·5	+262·2	(f)
	40 mol % in $CDCl_3$	+274·4	(c)
MeC(=O)NHEt	neat liquid	see Table 60	
	40 mol % in $CDCl_3$	+255·4	(c)
$MeC(=O)NHPr^i$	40 mol %in $CDCl_3$	+244·1	(c)
$MeC(=O)NHBu^t$	40 mol % in $CDCl_3$	+242·8	(c)
$MeC(=O)NHPr^n$	40 mol % in $CDCl_3$	+260·4	(c)
$MeC(=O)NHBu^i$	40 mol % in $CDCl_3$	+262·4	(c)
$MeC(=O)NHBu^n$	40 mol % in $CDCl_3$	+260·5	(c)
$MeC(=O)NH(CH_2)_4Me$	40 mol % in $CDCl_3$	+260·2	(c)
$MeC(=O)NHBu^s$	40 mol % in $CDCl_3$	+246·5	(c)
$MeC(=O)NHCMe_2Et$	40 mol % in $CDCl_3$	+245·5	(c)

TABLE 57—*cont.*

Compound	Solution	Nitrogen shielding referred to neat nitromethane	Note
$MeC(=O)NHCH_2CH_2Ph$	40 mol % in $CDCl_3$	+262·3	(c)
$MeC(=O)NH{\cdot}C_6H_4{\cdot}OMe$*p*	5 mol % in DMSO	+249·1	(c)
$MeC(=O)NH{\cdot}C_6H_4{\cdot}Me$*p*	5 mol % in DMSO	+247·8	(c)
$MeC(=O)NHPh$	5 mol % in DMSO	+247·0	(c)
$MeC(=O)NH{\cdot}C_6H_4{\cdot}Cl$*p*	5 mol % in DMSO	+248·2	(c)
$MeC(=O)NH{\cdot}C_6H_4{\cdot}NO_2$*p*	5 mol % in DMSO	+242·1 (NH)	(c)
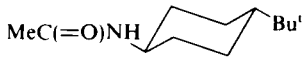	in $CDCl_3$	+246·7	(g)
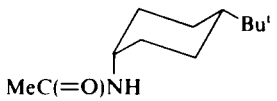	in $CDCl_3$	+255·0	(g)
$HC(=O)NMe_2$	neat liquid	+277·01 ± 0·09	(h)
		+277·4	(i)
	neat liquid + 10% C_6D_6	+276·4	(a)
	0·30 M in H_2O	+264·59 ± 0·10	(h)
	various solvents	see Table 61	
$MeC(=O)NMe_2$	neat liquid	+281·6	(e)
		+283·9	(i)
	1 : 1 v/v in acetone	+282·1	(e)
		+282·2	(d)
	2 M in Et_2O	+282·8	(e)
	1 M in Et_2O	+286·1	(e)
	0·5 M in Et_2O	+287·6	(e)
$MeC(OMe)=NMe$ (isoamide isomer)	1 : 1 v/v in acetone	+155·5	(e)
		+155·2	(d)
$MeC(=O)NMe_2{\cdot}HCl$	in $CDCl_3$	+210 ± 10	(j)
$(Me_2N^+=CH{-}OMe)\ FSO_3^-$	in $CHCl_2CHCl_2$	+238·1	(i)
$MeC(=O)NMe_2{\cdot}SbCl_5$	in $CHCl_2CHCl_2$	+308·5	(i)
$PhC(=O)NMe_2$	1 : 1 v/v in $CHCl_2CHCl_2$	+281·7	(i)
$ClC(=O)NMe_2$	neat liquid	+286·3	(i)
$Cl_3CC(=O)NMe_2$	neat liquid	+289·5	(i)
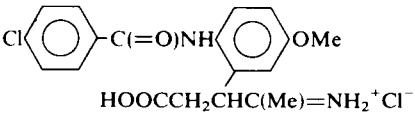	in CD_3COOD/HCl	+242·2 (amide)	(k)
		+184·7 (NH_2^+)	(k)
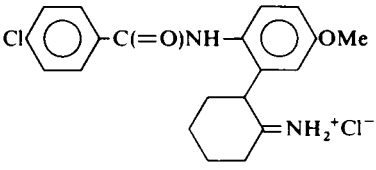	in CD_3COOD/HCl	+243·8 (amide)	(k)
		+193·3 (NH_2^+)	(k)

TABLE 57—*cont.*

Compound	Solution	Nitrogen shielding referred to neat nitromethane	Note
$MeC(=O)NHSiMe_3$	neat liquid	+258 ± 3	(l)
		+264 ± ?	(m)
$MeC(=O)N(Me)SiMe_3$	neat liquid	+286 ± ?	(m)
$HC(=O)N(SiMe_3)_2$	neat liquid	+259 ± ?	(m)
$F_3CC(=O)N(Me)SiMe_3$	neat liquid	+275 ± ?	(m)
$F_3CC(=O)N(SiMe_3)_2$	neat liquid	+177 (?)	(m)
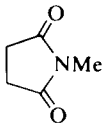	neat liquid	+199 ± 3	(l)
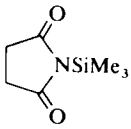	neat liquid	+181 ± 3	(l)

(a) Data from ref. 81: ^{15}N natural abundance spectra; 10·09 MHz; field perpendicular to sample tube; $Cr(acac)_3$ added in order to shorten T_1; referred to neat nitromethane; uncorrected for bulk susceptibility.

(b) Data from ref. 90; ^{15}N natural abundance spectra; 18·25 MHz; field parallel to sample tube; referred originally to 1 M DNO_3, +6·2 ppm from neat nitromethane (Table 6); conversion scheme IV (Table 4).

(c) Data from ref. 190; details as in note (b).

(d) Data from ref. 179; ^{15}N natural abundance spectra; 18·25 MHz; field parallel to sample tube; referred to neat nitromethane; uncorrected for bulk susceptibility.

(e) Data from ref. 179; continuous-wave ^{14}N spectra; 4·33 MHz; high-precision differential saturation technique with full lineshape fitting; 30 °C; concentric spherical sample/standard containers in order to eliminate bulk susceptibility effects; referred to neat nitromethane.

(f) Data from ref. 191; details as in note (b).

(g) Data from ref. 149; details as in note (b).

(h) Data from refs 80 and 85; details as in note (e).

(i) Data from ref. 40; ^{15}N natural abundance spectra; 6·08 MHz; field perpendicular to sample tube; $Cr(acac)_3$ added; referred originally to "dilute HNO_3", probably +3·7 ppm from neat nitromethane (Table 6); conversion scheme II (Table 4).

(j) Data from ref. 192; ^{14}N measurements; low precision; 4·33 MHz; originally reported as 70 ± 10 ppm deshielding relative to parent amide.

(k) Data from ref. 168; ^{15}N natural abundance spectra; 10·1 MHz; referred to internal NH_4Cl (dissolved in sample), probably +352·0 ppm from neat nitromethane (Table 6).

(l) Data from ref. 137; continuous-wave ^{14}N spectra; 7·22 MHz; low precision; referred originally to aqueous $NaNO_3$, +3·7 ppm from neat nitromethane (Table 6).

(m) Data from ref. 193; details as in note (l).

TABLE 58

Effects of additives on nitrogen shielding in *N*-methylacetamide (1·5 M in water)

pH	Additive	Nitrogen shielding referred to neat nitromethane
1	1 M HBr	+265·8
7	none	+267·4
14	1 M NaOH	+267·2
2	$Pr^nNH_2 \cdot HBr$ + 1 M HBr	+266·7
4	$Pr^nNH_2 \cdot HBr$ + 1 M HBr	+266·7
6	$Pr^nNH_2 \cdot HBr$	+266·7
7·5	$Pr^nNH_2 \cdot HBr$ + NaOH	+266·7
9·0	$Pr^nNH_2 \cdot HBr$ + NaOH	+266·7
10·0	$Pr^nNH_2 \cdot HBr$ + NaOH	+266·7
11·0	$Pr^nNH_2 \cdot HBr$ + NaOH	+266·7
12·0	$Pr^nNH_2 \cdot HBr$ + NaOH	+266·8
12·5	$Pr^nNH_2 \cdot HBr$ + NaOH	+266·8

Data from ref. 194; ^{15}N natural abundance spectra; 9·12 MHz; field perpendicular to sample tube; referred originally to NO_3^- in aqueous NH_4NO_3, +4·0 ppm from nest nitromethane (Table 6); conversion scheme II (Table 4).

TABLE 59

Nitrogen shieldings in *E,Z*-isomers of unsymmetrically substituted amides (neat liquids)

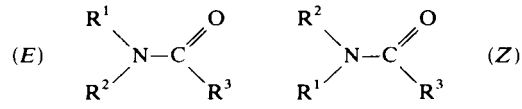

R^1	R^2	R^3	Nitrogen shielding relative to neat nitromethane isomer *E*	isomer *Z*
H	Me	H	+273·9 (10%)	+272·3 (90%)
H	Et	H	+256·2 (10%)	+255·2 (90%)
H	Bu^t	H	+233·3 (30%)	+235·6 (70%)
H	Ph	H	+241·2 (40%)	+243·8 (60%)
Me	Bu^n	H	(62%) 267·9	(38%)
Me	$PhCH_2$	H	(53%) 266·2	(47%)
Me	Bu^n	Me	+271·2 (45%)	+272·6 (55%)
Me	H	Me		+274·9 (100%)
Me	H	Et		+278·7 (100%)
Me	H	Pr^n		+276·9 (100%)
Me	H	Pr^i		+280·6 (100%)
Me	H	Ph (25% in $CDCl_3$)		+282·3 (100%)
Me	H	CH_2Cl		+276·1 (100%)
Me	H	CH_2OMe		+281·2 (100%)
Me	H	CH_2NMe_2 (amide)		+282·5 (100%)
Me	H	$PhCH_2$		+275·9 (100%)
Et	H	Me		+257·0 (100%)
$PhCH_2$	H	Me		+261·1 (100%)
Ph	H	Pr^i (30% in MeCN)		+252·9 (100%)
$MeOC(=O)CH_2$	H	Et	+273·7 (15%)	+275·0 (85%)
$MeOC(=O)C(Me)H$	H	Et (25% in $CDCl_3$)	(12%) +260·2	(88%)

Data from ref. 195; ^{15}N natural abundance spectra; 9·12 MHz; field perpendicular to sample tube; referred originally to aqueous $NaNO_3$, +3·7 ppm from neat nitromethane (Table 6); conversion scheme II (Table 4); isomer ratios quoted are obtained from proton spectra.

TABLE 60

Comparison of nitrogen shieldings in *cis* and *trans* isomers of *N*-alkyl-substituted formamides and acetamides

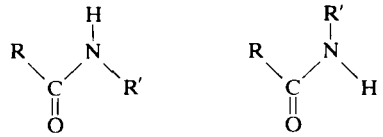

"*trans*" (*Z*) amide "*cis*" (*E*) amide

R	R′	State	Nitrogen shielding referred to neat nitromethane "*trans*"	"*cis*"	"*cis*" content
H	H	neat liquid	+268·6		
Me	H	1·5 M in $CHCl_3$	+275·2		
H	Me	neat liquid	+271·8	+273·8	8%
Me	Me	1·5 M in $CHCl_3$	+276·0		
H	Et	neat liquid	+253·9	+255·0	12%
H	Pr^n	neat liquid	+257·0	+258·4	14%
H	Bu^n	neat liquid	+257·1	+258·5	14%
H	$(CH_2)_4Me$	neat liquid	+257·0	+258·5	12%
H	Bu^i	neat liquid	+259·0	+260·6	12%
H	CH_2CMe_3	neat liquid	+261·2	+262·8	11%
Me	CH_2CMe_3	4·5 M in $CHCl_3$	+265·5		
H	CH_2Ph	10 M in DMSO	+257·8	+259·1	13%
Me	CH_2Ph	4·5 M in $CHCl_3$	+260·4		
H	CH_2CH_2Ph	neat liquid	+256·6	+260·0	14%
H	Pr^i	10 M in DMSO	+240·3	+241·9	14%
H	$CH(Me)CH_2Me$	neat liquid	+241·0	+244·9	16%
H	$CH(Me)CH_2CH_2Me$	10 M in DMSO	+241·1	+244·9	14%
Me	$CH(Me)CH_2CH_2Me$	4·5 M in $CHCl_3$	+245.8		
H	cyclopropyl	10 M in DMSO	+252·5	+255·4	18%
H	cyclopentyl	neat liquid	+243·8	+246·1	12%
H	cyclohexyl	neat liquid	+242·8	+243·5	14%
H	Bu^t	neat liquid	+237·0	+235·0	22%
H	$C(Me)_2CH_2Me$	neat liquid	+239·2	+236·8	22%
Me	$C(Me)_2CH_2Me$	4·5 M in $CHCl_3$	+245·6		

Data from ref. 373; ^{15}N natural abundance spectra; 18·25 MHz; field parallel to sample tube; referred originally to 1 M DNO_3, +6·2 ppm from neat nitromethane (Table 6); conversion scheme IV (Table 4).

TABLE 61

Solvent effects on nitrogen shielding in some simple amides

Amide	Nitrogen shielding referred to neat nitromethane, in									
	dioxan	$(EtOCH_2CH_2)_2O$	cyclo-hexanone	$P(NMe_2)_3$	DMSO	ethylene carbonate	$MeNO_2$	MeOH	ethylene glycol	H_2O
H_2NCHO	271·5	270·2	270·2	266·0	265·4	270·5	271·1	267·4	264·7	263·7
(*Z*)-MeNHCHO	271·5	271·9	271·2	270·4	268·9	270·1	270·4	267·4	264·9	263·0
(*E*)-Bu^{t}NHCHO	234·2	234·2	233·8	234·2	232·6	232·8	232·8	230·3	228·1	227·0
(*Z*)-Bu^{t}NHCHO	236·2	236·4	235·9	235·8	234·1	234·6	234·8	232·5	231·2	229·7
Me_2NCHO	278·4	279·4	278·4	278·1	275·8	275·4	276·5	272·9	270·2	267·8
$Me_2NC(=O)Me$	284·5	284·7	284·6	284·2	282·2	281·8	282·8	278·4	275·8	273·4
Bulk property of solvent										
Dielectric constant	2·2	5·7	18·3	29·6	48·9	89·6	38·6	32·6	37·7	78·5
Dipole moment (D)	0·4	?	2·9	5·5	3·9	4·9	3·1	1·6	2·0	1·8
E_T (kJ mol^{-1})*	150·7	157·0	170·8	171·2	188·3	?	193·8	232·3	235·6	264·1

Data from ref. 196; ^{15}N natural abundance spectra; 9·12 MHz; field perpendicular to sample tube; referred originally to aqueous $NaNO_3$, +3·7 ppm from neat nitromethane (Table 6); conversion scheme II (Table 4); shielding values contain bulk susceptibility effects (sample–aqueous $NaNO_3$).

* Solvatochromic shift measured from the UV absorption spectra of a pyridinium salt in a given solvent; K. Dimroth and C. Reichardt, *Liebigs Ann. Chem.*, 1969, **727**, 93.

TABLE 62

Nitrogen shieldings in some simple lactams

Compound	Solution	Nitrogen shielding referred to neat nitromethane	Notes
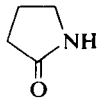	1·5 M in H_2O, pH 6·5	+260·4	(a)
	pH 12·5	+260·3	(a)
	1·5 M in DMSO	+265·5	(a)
	1·5 M in DMSO + NaOH	+264·1	(a)
2-Pyrrolidone	in CF_3COOH	+246·4	(b)
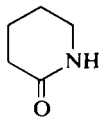	1·5 M in H_2O, pH 6·5	+260·7	(a)
	pH 12·5	+260·4	(a)
	in CF_3COOH	+243·6	(b)
2-Piperidone			
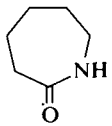	1·5 M in H_2O, pH 6·5	+257·8	(a)
	pH 12·5	+257·3	(a)
	1·5 M in DMSO	+263·0	(a)
		+262·4	(c)
	1·5 M in DMSO + NaOH	+262·1	(a)
ε-Caprolactam	in CF_3COOH	+239·7	(b)
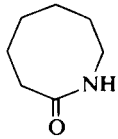	1·5 M in H_2O, pH 6·7	+257·8	(a)
	pH 12·5	+257·4	(a)
	pH 13·5	+255·7	(a)
	1·5 M in acetone	+264·5	(c)
	1·5 M in CF_3CH_2OH	+257·9	(c)
	1·5 M in HCOOH	+251·3	(c)
2-Perhydroazocinone	in CF_3COOH	+239·7	(b)
(2-Azacyclooctanone)	1·5 M in FSO_3H	+234·9	(c)
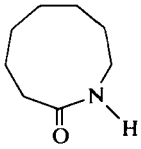	2·5 M in DMSO	+259·6	(a)(d)
	2·5 M in DMSO + $NaOH_{aq.}$	+257·9	(a)
	in CF_3COOH	+237·1	(b)
E-2-Azacyclononanone ("*cis*")			
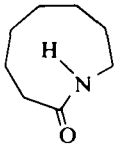	2·5 M in DMSO	+262·1	(a)(d)
	2·5 M in DMSO + $NaOH_{aq.}$	+260·6	(a)
Z-2-Azacyclononanone ("*trans*")			
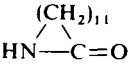	in CF_3COOH	+236·3	(b)
2-Azacyclotridecanone			

TABLE 62—*cont.*

Compound	Solution	Nitrogen shielding referred to neat nitromethane	Notes
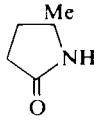	in CF_3COOH	+232·4	(b)
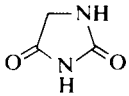 Hydantoin	2 M in DMSO	+296·4 (CH_2NHCO) +230·0 (CONHCO)	(e) (e)
	20% w/w in DMSO	+296·9 +230·5	(f) (f)
	20% w/w in H_2O	+293·8 +229·9	(f) (f)
	20% w/w in HCOOH	+294·6 +232·5	(f) (f)
	20% w/w in CF_3COOH	+294·3 +233·9	(f) (f)
 2-Imidazolidinone	20% w/w in pyridine	+302·4	(f)
	20% w/w in DMSO	+302·2	(f)
	20% w/w in H_2O	+299·7	(f)
	20% w/w in CF_3COOH	+298·9	(f)

(a) Data from ref. 191; ^{15}N natural abundance spectra; 18·25 MHz; field parallel to sample tube; referred originally to 1 M DNO_3, +6·2 ppm from neat nitromethane (Table 6); conversion scheme IV (Table 4).

(b) Data from ref. 198; ^{15}N natural abundance spectra; 9·12 MHz; field perpendicular to sample tube; referred originally to NO_3^- in aqueous NH_4NO_3, +4·0 ppm from neat nitromethane (Table 6); conversion scheme II (Table 4); 1·5 g substance in 7 ml CF_3COOH.

(c) Data from ref. 199; details as in note (a).

(d) Data from ref. 200; details as in note (a).

(e) Data from ref. 181; ^{15}N natural abundance spectra; 9·12 MHz; field perpendicular to sample tube; referred originally to NH_4^+ in 5 M NH_4NO_3 to 2 M HNO_3, +359·0 ppm from neat nitromethane (Table 6); conversion scheme II (Table 4).

(f) Data from ref. 185; natural abundance ^{15}N spectra; 9·12 MHz; field perpendicular to sample tube; referred originally to NO_3^- in aqueous NH_4NO_3, +4·0 ppm from neat nitromethane (Table 6); conversion scheme II (Table 4).

TABLE 63

Nitrogen shieldings of the amido groups in penicillins and cephalosporins

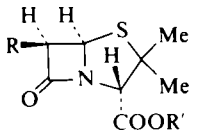

Penicillin structure

Molecule		Solvent	Nitrogen shielding referred to neat $MeNO_2$ N at ring junction	CONH and other moieties
Penicillin G	R = $PhCH_2CONH$, R′ = K	H_2O	+211·6	+264·6
		DMSO	+212·7	+268·7
its Me ester	R′ = Me	benzene	+221·0	+270·2
its procaine derivative	R′ = (H, $pH_2N{\cdot}C_6H_4{\cdot}COOCH_2CH_2NEt_2$)	DMSO	+218·2	+268·0 +310·1 (amino) +329·4 (amino)
Penicillin V	R = $PhOCH_2CONH$, R′ = Na	H_2O	+212·2	+269·8
its Me ester	R′ = Me	dioxan	+220·5	+274·8
Methicillin	R = 2,6-$(OMe)_2$-$C_6H_3{\cdot}CONH$, R′ = Na	H_2O	+210·8	+259·5
its Me ester	R′ = Me	benzene	+218·5	+271·9
Ampicillin	R = $PhCH(NH_2)CONH$, R′ = Na	H_2O	+210·8	+267·7 +345·7 (amino)
its Me ester	R′ = Me	benzene	+219·9	+277·1 +354·2 (amino)
Oxacillin	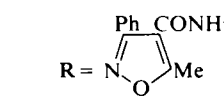 R′ = Na	H_2O	+211·2	+263·2 +93·0 (isoxazole)

TABLE 63—*cont.*

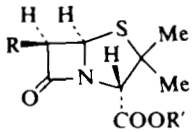

Penicillin structure

Molecule		Solvent	Nitrogen shielding referred to neat $MeNO_2$ N at ring junction	CONH and other moieties
its Me ester	R′ = Me	CH_2Cl_2/benzene	+219·9	+267·6 +80·4 (isoxazole)
Hetacillin	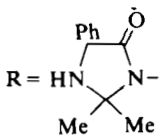			
	R′ = K	H_2O	+223·2	+269·3 (N) +306·7 (NH)
its Me ester	R′ = Me	CH_2Cl_2/benzene	+230·4	+276·9 (N) +319·5 (NH)
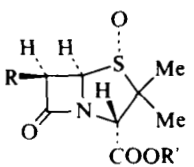				
Penicillin V α-sulphoxide				
	R = $PhOCH_2CONH$ R′ = Na	H_2O	+229·4	+272·9
its Me ester	R′ = Me	dioxan	+238·0	+276·4

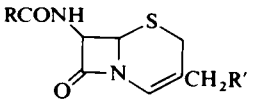

Cephalosporin structure

R = H R′ = OCOMe	H_2O	+226·0	+265·7
R = Me R′ = OCOMe	H_2O	+225·6	+267·8
R = $PhCH_2$ R′ = OCOMe	H_2O	+225·6	+268·6
R = $PhOCH_2$ R′ = OCOMe	H_2O	+226·0	+274·2
R = PhC(OH)H R′ = OCOMe	H_2O	+225·7	+273·9
R = 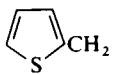 R′ = OCOMe	H_2O	+226·0	+269·8
R = 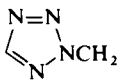 R′ = OCOMe	H_2O	+226·2	+271·8
R = 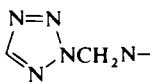 R′ = 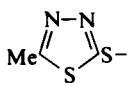	H_2O	+224·6	+271·6
R = $PhC(NH_2)H$ R′ = H	H_2O	+225·4	+271·6

Data from ref. 197; ^{15}N natural abundance spectra; 10·09 MHz; field perpendicular to sample tube; referred originally to 2·9 M NH_4Cl in 1 M HCl, +355·3 ppm from neat nitromethane (Table 6); conversion scheme IV (Table 4).

TABLE 64

Nitrogen shieldings in conjugated cyclic lactams, thiolactams, and amidines (tautomeric or isomeric forms of OH, SH, and NH_2 substituted azines and azoles)

Compound	Solution	Nitrogen shielding referred to neat $MeNO_2$	Notes
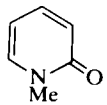	1 : 3 v/v in acetone	+216 ± 2	(a)
	neat liquid	+215 ± 3	(a)
	1 : 3 v/v in MeOH	+214 ± 1	(a)
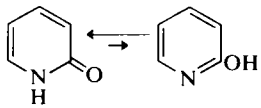	1 : 3 v/v in acetone	+209 ± 2	(a)
	1 : 3 v/v in MeOH	+212 ± 2	(a)
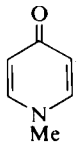	1 : 3 v/v in acetone	+248 ± 2	(a)
	1 : 3 v/v in MeOH	+240 ± 3	(a)
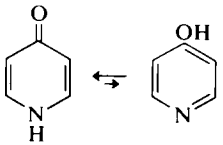	satd. in acetone	+222 ± 4	(a)
	1 : 3 v/v in MeOH	+227 ± 3	(a)
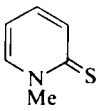	1 : 3 v/v in acetone	+189 ± 2	(b)
	1 : 3 v/v in MeOH	+188 ± 1	(b)
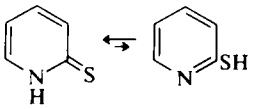	1 : 3 v/v in acetone	+187 ± 1	(b)
	1 : 3 v/v in MeOH	+186 ± 1	(b)
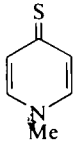	1 : 3 v/v in acetone + DMSO (4 : 1 v/v)	+225 ± 2	(b)
	1 : 3 v/v in MeOH	+222 ± 1	(b)
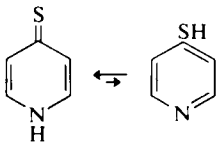	1 : 3 v/v in acetone	+225 ± 2	(b)
	1 : 3 v/v in MeOH	+218 ± 1	(b)
	1 : 3 v/v in acetone + DMSO (4 : 1 v/v)	+222 ± 1	(b)

TABLE 64—*cont.*

Compound	Solution	Nitrogen shielding referred to neat $MeNO_2$	Notes
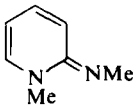	1 : 3 v/v in acetone	+195 ± 3 (=NMe) +237 ± 3 (NMe)	(b) (b)
	in acetone	+191·3 (=NMe) +239·3 (NMe)	(g) (g)
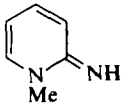	1 : 3 v/v in acetone	+192 ± 3 (=NH) +242 ± 3 (NMe)	(b) (b)
	in acetone	+194·2 (=NH) +242·6 (NMe)	(g) (g)
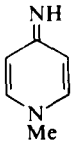	1 : 3 v/v in acetone	+168 ± 3 (=NH) +260 ± 3 (NMe)	(b) (b)
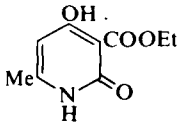	in DMSO	+217	(c)
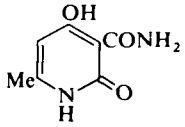	in DMSO	+223 (NH) +281 (NH_2)	(c) (c)
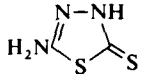	in DMSO	+166·7 (NH) +314·9 (NH_2)	(d) (d)
Riboflavin tetrabutyrate		see Table 65	
Tetrahydropterin derivatives			
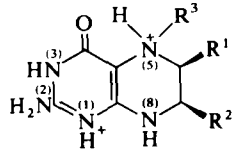	in CF_3COOH		
$R^1 = R^2 = Me$; $R^3 = H$		+269·4 (N-1) +246·3 (N-3) +333·2 (N-5) +287·4 (N-8) +296·5 (NH_2)	(e) (e) (e) (e) (e)

TABLE 64—*cont.*

Compound	Solution	Nitrogen shielding referred to neat $MeNO_2$	Notes
$R^1 = Me$; $R^2 = R^3 = H$	in CF_3COOH	+269·0 (N-1)	(e)
		+245·6 (N-3)	(e)
		+332·9 (N-5)	(e)
		+299·6 (N-8)	(e)
		+297·5 (NH_2)	(e)
$R^2 = Me$; $R^1 = R^3 = H$	in CF_3COOH	+268·1 (N-1)	(e)
		+247·1 (N-3)	(e)
		+346·3 (N-5)	(e)
		+286·1 (N-8)	(e)
		+297·3 (NH_2)	(e)
$R^1 = R^2 = R^3 = Me$	in CF_3COOH	+270·1 (N-1)	(e)
		+246·3 (N-3)	(e)
		+330·6 (N-5)	(e)
		+288·8 (N-8)	(e)
		+295·9 (NH_2)	(e)
$R^2 = R^3 = H$;	0·7 M in 6 M HCl	+267·7 (N-1)	(e)
$R^1 = -CH_2-NH_2^+$  $CONH-C_5H_7O_4$		+242·8 (N-3)	(e)
		+333·5 (N-5)	(e)
		+303·6 (N-8)	(e)
(tetrahydrofolic acid)		+295·5 (NH_2 at C^2)	(e)
		+319·7 (NH_2 in R^1)	(e)
		+261·4 (CONH)	(e)
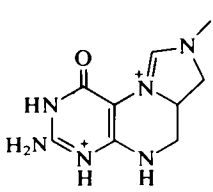	0·7 M in CF_3COOH	+268·3 (N-1)	(e)
		+245·5 (N-3)	(e)
		+251·3 (N-5)	(e)
		+300·7 (N-8)	(e)
		+298·1 (NH_2 at C^2)	(e)
		+245·5 (NCO)	(e)
		+262·1 (CONH)	(e)
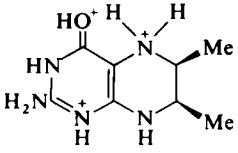	in FSO_3H	+263·2 (N-1)	(e)
		+257·9 (N-3)	(e)
		+337·2 (N-5)	(e)
		+265·2 (N-8)	(e)
		+288·1 (NH_2)	(e)
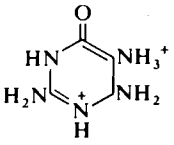	in $HCl_{aq.}$	+255·8 (N-1)	(e)
		+242·8 (N-3)	(e)
		+350·0 (N-5)	(e)
		+302·6 (N-8)	(e)
		+298·3 (NH_2 at C^2)	(e)
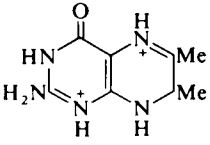	in $HCl_{aq.}$	+266·5 (N-1)	(e)
		+245·6 (N-3)	(e)
		+194·1 (N-5)	(e)
		+294·0 (N-8)	(e)
		+296·3 (NH_2)	(e)

TABLE 64—*cont.*

Compound	Solution	Nitrogen shielding referred to neat $MeNO_2$	Notes
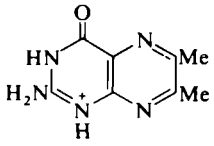	in CF_3COOH	+262·3 (N-1) +236·7 (N-3) +84·5 (N-5) +79·3 (N-8) +296·7 (NH_2)	(e) (e) (e) (e) (e)
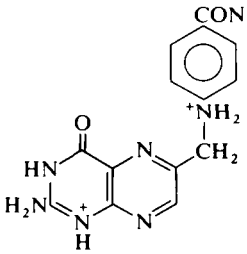 (folic acid)	in CF_3COOH	+264·1 (N-1) +238·0 (N-3) +78·5 (N-5) +58·3 (N-8) +294·8 (NH_2 at C^2) +332·5 (NH_2^+) +262·2 (CONH)	(e) (e) (e) (e) (e) (e) (e)
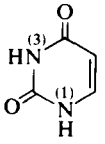 (uracil)	0·8 M in DMSO	+247·8 (N-1) +220·2 (N-3)	(f) (f)

(a) Data from ref. 1, pp. 172 and 190, and references therein; ^{14}N spectra.

(b) Data from ref. 159 and ref. 201; continuous-wave ^{14}N spectra; 4·33 MHz; referred to neat nitromethane; uncorrected for bulk susceptibility effects.

(c) Data from ref. 135; $^1H\{^{14}N\}$ INDOR spectra at 100/7·22 MHz; field perpendicular to sample tube; referred originally to $Me_4N^+Cl^-$, +337 ppm from neat nitromethane (Table 6); conversion scheme II (Table 4).

(d) Data from ref. 163; ^{15}N natural abundance spectra; 18·25 MHz; field parallel to sample tube; referred originally to 1 M DNO_3, +6·2 ppm from neat nitromethane (Table 6); conversion scheme IV (Table 4).

(e) Data from ref. 202; ^{15}N natural abundance spectra; 10·09 MHz; field perpendicular to sample tube; referred to neat nitromethane; uncorrected for bulk susceptibility effects.

(f) Data from ref. 181; ^{15}N natural abundance spectra; 18·25 MHz; field parallel to sample tube; referred originally to NH_4^+ in 5 M NH_4NO_3 in 2 M HNO_3, +359·0 ppm from neat nitromethane (Table 6); conversion scheme II (Table 4).

(g) Data from ref. 160; ^{15}N natural abundance spectra; 18·25 MHz; field parallel to sample tube; referred originally to neat nitromethane; uncorrected for bulk susceptibility effects.

TABLE 65

Nitrogen shielding in reduced and oxidized forms of riboflavin (vitamin B_2)-2′,3′,4′,5′-tetrabutyrate

R = ribose-2′,3′,4′,5′-tetrabutyrate

	Sample	Nitrogen shielding referred to neat nitromethane N-1	N-3	N-5
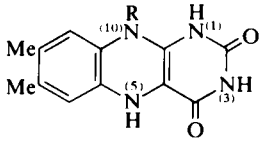	reduced form in $CDCl_3$	+261·5	+232·8	+322·7
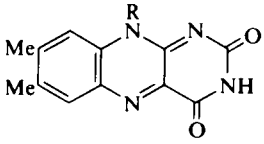	oxidized form in $CDCl_3$	+182·4	+223·0	+37·1

Data from ref. 203; ^{15}N-labelled riboflavin (N-1, N-3, and N-5); ^{15}N spectra; 10·09 MHz; field perpendicular to sample tube; referred originally to NO_3^- in NH_4NO_3 in DMSO, reported to be deshielded by 2·02 ppm from a solution in aqueous HCl; this results in an uncertainty about the actual shielding constant of the standard used (Table 6), but a value of +3·7 ppm from neat nitromethane is assumed here as a conversion factor according to scheme II (Table 4).

TABLE 66

Nitrogen shieldings in chetomin (toxic metabolite of *Chaetomium cochliodes*)

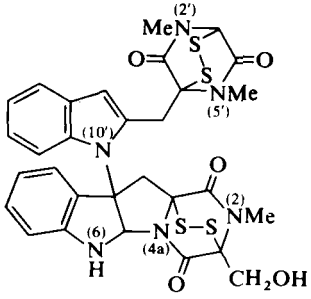

Nitrogen atom	Shielding referred to neat nitromethane	Type of moiety involved
N-2	+261·4	amide
N-4a	+229·5	amide
N-6	+301·5	arylamine
N-2′	+262·2	amide
N-5′	+257·2	amide
N-10′	+235·1	pyrrole

Data from ref. 204; biologically ^{15}N-enriched chetin; ^{15}N spectra; 10·14 MHz; field perpendicular to sample tube; referred originally to 4 M NH_4Cl in 2 M HCl, +352·5 ppm from neat nitromethane (Table 6); conversion scheme II (Table 4); assignments based on simultaneous ^{13}C-labelling and observation of ^{13}C–^{15}N one-bond couplings.

TABLE 67

Nitrogen shieldings in some polyamides dissolved in trifluoroacetic acid

Polymer	Nitrogen shielding referred to neat nitromethane
$[-NH-(CH_2)_m-NH-C(=O)-(CH_2)_k-C(=O)-]_n$	
$m = 2$ $k = 2$	+253·5
3 2	+249·0
4 2	+247·5
6 2	+246·3
8 2	+245·6
10 2	+245·5
2 3	+255·5
2 4	+253·2
2 6	+252·0
2 8	+251·5
2 12	+251·3
4 6	+241·6
6 3	+243·4
6 4	+240·3
6 6	+238·4
6 8	+238·6
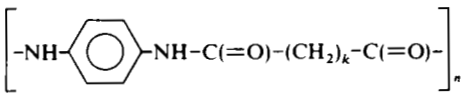	
$k = 2$	+240·5
3	+240·6
4	+240·7
6	+240·1
8	+240·9
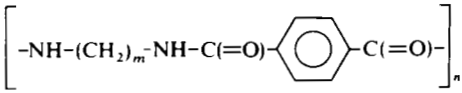	
$m = 2$	+261·1
3	+255·3
4	+251·4
6	+249·0
8	+246·5

TABLE 67—*cont.*

Polymer	Nitrogen shielding referred to neat nitromethane
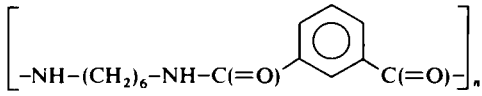	+248·7
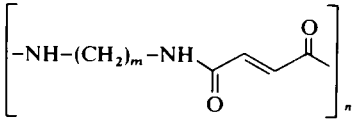	
m = 6	+243·5
10	+242·4
Mixed polymer "Trogamid T"	
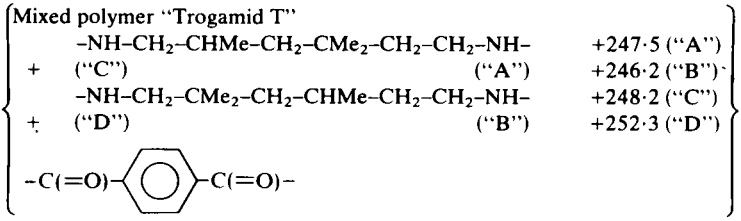	
-NH-CH_2-CHMe-CH_2-CMe_2-CH_2-CH_2-NH-	+247·5 ("A")
+ ("C") ("A")	+246·2 ("B")
-NH-CH_2-CMe_2-CH_2-CHMe-CH_2-CH_2-NH-	+248·2 ("C")
+ ("D") ("B")	+252·3 ("D")

Data from ref. 132; ^{15}N natural abundance spectra; 9·12 MHz; field perpendicular to sample tube; referred originally to NO_3^- in aqueous NH_4NO_3, +4·0 ppm from neat nitromethane (Table 6); conversion scheme II (Table 4).

TABLE 68

Nitrogen shieldings in some thioamides, thiourea derivatives, and related structures

Compound	Solution	Nitrogen shielding referred to neat nitromethane	Notes
$HC(=S)NMe_2$	in $CHCl_2CHCl_2$	+227·8	(a)
$MeC(=S)NMe_2$	in $CHCl_2CHCl_2$	+237·1	(a)
$ClC(=S)NMe_2$	in $CHCl_2CHCl_2$	+236·0	(a)
$MeSC(=S)NMe_2$	in $CHCl_2CHCl_2$	+246·6	(a)
$MeC(=S)NHMe$	neat	+228 ± 3	(b)
$(Me_2N)_2C=S$	in $CHCl_2CHCl_2$	+294·7	(a)
$Me_2N^+=C(SMe)-NMe_2$	in $CHCl_2CHCl_2$	+271·3	(a)
$H_2NC(=S)NHC(=S)NH_2$	1 M in DMSO	+250·7 (NH, doublet) +272·8 (NH_2, triplet)	(c) (c)
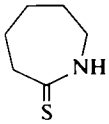	1·5 M in DMSO	+218·7	(d)

(a) Data from ref. 40; ^{15}N natural abundance spectra; 6·08 MHz; field perpendicular to sample tube; referred originally to "dilute HNO_3", probably +3·7 ppm from neat nitromethane (Table 6); conversion scheme II (Table 4).

(b) Data from ref. 137; continuous-wave ^{14}N spectra; 7·22 MHz; originally referred to aqueous $NaNO_3$, +3·7 ppm from neat nitromethane.

(c) Data from ref. 163; ^{15}N natural abundance spectra; 18·25 MHz; field parallel to sample tube; referred originally to 1 M DNO_3, +6·2 ppm from neat nitromethane (Table 6); conversion scheme IV (Table 4).

(d) Data from ref. 199; details as in note (c).

TABLE 69

Nitrogen shielding in some sulphonamides

Compound	Solution	Nitrogen shielding referred to neat nitromethane	Note
$MeSO_2NH_2$	3 M in H_2O		
	pH 1·0–1·1	+288·4	(a)
	pH 4·0–4·1	+288·4	(a)
	pH 6·4–6·5	+288·6	(a)
	pH 8·5–8·6	+288·5	(a)
	pH 10·0–10·1	+287·2 (broad)	(a)
	pH 11·1–11·2	+277·5	(a)
	pH 11·7–11·8	+277·6	(a)
	pH 12·3–12·4	+277·5	(a)
	3 M in 8 M $NaOH_{aq.}$	+275·8	(a)
	3 M in DMSO	+285·3	(a)
	3 M in acetone	+289·6	(a)
	3 M in MeOH	+291·1	(a)
	3 M in CF_3COOH	+293·0	(a)
$MeSO_2NHMe$	neat liquid	+299 ± 5	(b)
$MeSO_2NHSiMe_3$	neat liquid	+278 ± 3	(b)
$MeSO_2NHBu^t$	neat liquid	+281 ± 5	(b)
	3 M in DMSO	+285·7	(a)
	3 M in CF_3COOH	+293·3	(a)
$MeSO_2NHPh$	3 M in DMSO	+297·2	(a)
	3 M in CF_3COOH	+301·3	(a)
$p H_2N{\cdot}C_6H_4{\cdot}SO_2NH_2$	9 mol % in DMSO	+284·3, +285·9	(c)
$PhSO_2NH_2$	9 mol % in DMSO	+285·9	(c)
	in acetone	+289 ± 3	(d)
$p Me{\cdot}C_6H_4{\cdot}SO_2NH_2$	in acetone	+289 ± 3	(d)
$PhSO_2NHEt$	9 mol % in DMSO	+281·6	(c)
$PhSO_2NHCH_2Ph$	9 mol % in DMSO	+283·4	(c)
$PhSO_2NHCH(Me)(Pr^n)$	9 mol % in DMSO	+270·6	(c)
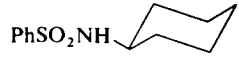	9 mol % in DMSO	+270·2	(c)
$PhSO_2NMe_2$	in Et_2O	+288 ± 3	(d)
$PhSO_2NEt_2$	9 mol % in DMSO	+280·2	(c)
$PhSO_2NPr^n{}_2$	9 mol % in DMSO	+282·9	(c)
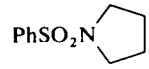	9 mol % in DMSO	+280·0	(c)
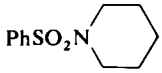	9 mol % in DMSO	+278·9	(c)
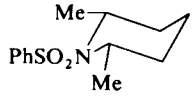	9 mol % in DMSO	+276·2	(c)

TABLE 69—*cont.*

Compound	Solution	Nitrogen shielding referred to neat nitromethane	Note
$PhSO_2N(CH_2Ph)_2$	9 mol % in DMSO	+279·3	(c)
$PhSO_2NH{\cdot}C_6H_4{\cdot}OMe$*p*	9 mol % in DMSO	+263·0	(c)
$PhSO_2NH{\cdot}C_6H_4{\cdot}F$*p*	9 mol % in DMSO	+261·4	(c)
$PhSO_2NH{\cdot}C_6H_4{\cdot}Me$*p*	9 mol % in DMSO	+261·2	(c)
$PhSO_2NH{\cdot}C_6H_4{\cdot}Br$*p*	9 mol % in DMSO	+259·7	(c)
$PhSO_2NHPh$	9 mol % in DMSO	+259·7	(c)
$PhSO_2NH{\cdot}C_6H_4{\cdot}CN$*p*	9 mol % in DMSO	+254·5 (NH)	(c)
$PhSO_2NH{\cdot}C_6H_4{\cdot}NO_2$*p*	9 mol % in DMSO	+253·3 (NH)	(c)
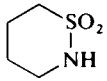	9 mol % in DMSO	+284·4	(c)
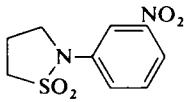	9 mol % in DMSO	+261·7 (NSO_2)	(c)
$PhSO_2NHC(=O)Me$	9 mol % in DMSO	+210·8	(c)
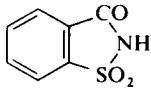	9 mol % in DMSO	+221·6	(c)

(a) Data from ref. 205; ^{15}N natural abundance spectra; 9·12 MHz; field perpendicular to sample tube; referred originally to NO_3^- in aqueous NH_4NO_3, +4·0 ppm from neat nitromethane (Table 6); conversion scheme II (Table 4).

(b) Data from ref. 137; continuous-wave ^{14}N spectra; 7·22 MHz; field perpendicular to sample tube; referred originally to aqueous $NaNO_3$, +3·7 ppm from neat nitromethane (Table 6); conversion scheme II (Table 4).

(c) Data from ref. 154; ^{15}N natural abundance spectra; 18·25 MHz; field parallel to sample tube; referred originally to 1 M DNO_3, +6·2 ppm from neat nitromethane (Table 6); conversion scheme IV (Table 4).

(d) Data from ref. 206; wide-line ^{14}N spectra; 3 MHz; referred originally to NH_4^+, in NH_4NO_3, +359·6 ppm from neat nitromethane; bulk susceptibility effects insignificant as compared with overall low precision.

TABLE 70

Structural formulae, abbreviations, and nitrogen shielding data for amino acids

Conventional formula, common name, and abbreviation	Solvent	Nitrogen shielding referred to neat nitromethane			Notes
		cation	amphion	anion	
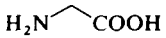 Glycine (Gly)	H_2O/HCl	+348·9	+347·3	356·6	(a)
	or NaOH	+351·2	+349·8		(b)
	H_2O/CF_3COOH	+352·7			(b)
	H_2O/H_2SO_4	+352·2			(b)
	HCOOH	+352·1			(b)
	CF_3COOH	+353·9			(b)
	97% H_2SO_4	+352·9			(b)
	FSO_3H	+354·0			(b)
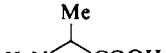 Alanine (Ala)	H_2O/HCl	+337·4	+337·1		(b)
	H_2O/CF_3COOH	+339·7			(b)
	H_2O/H_2SO_4	+339·4			(b)
	HCOOH	+339·5			(b)
	97% H_2SO_4	+339·8			(b)
	FSO_3H	+340·7			(b)
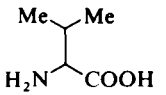 Valine (Val)	H_2O/HCl	+344·0	+344·1		(c)
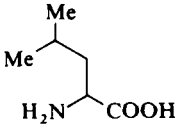 Leucine (Leu)	H_2O/HCl	+338·7			(c)
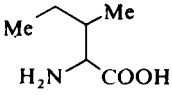 Isoleucine (Ile)	(L) H_2O/HCl	+343·1			(b)
	(L) HCOOH	+344·2			(b)
	(L) CF_3COOH	+345·1			(b)
	(L) 97% H_2SO_4	+344·0			(b)
	(D) H_2O/HCl	+345·7			(b)
	(D) HCOOH	+346·8			(b)
	(D) CF_3COOH	+348·1			(b)
	(D) 97% H_2SO_4	+347·5			(b)
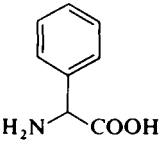 Phenylglycine (Phg)	CF_3COOH	+337·1			(d)

TABLE 70—*cont.*

Conventional formula, common name, and abbreviation	Solvent	Nitrogen shielding referred to neat nitromethane			Notes
		cation	amphion	anion	
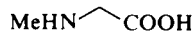 Sarcosine (Sar)	H_2O		+347·5		(b)
	HCOOH	+350·0			(b)
	CF_3COOH	+350·8			(b)
	97% H_2SO_4	+350·0			(b)
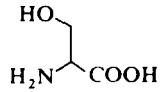 Serine (Ser)	H_2O/HCl	+344·0			(c)
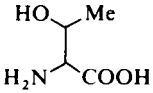 Threonine (Thr)	H_2O		+348		(c)
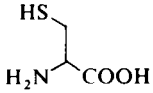 Cysteine [Cys(SH)]	H_2O/HCl	+338·1	+341		(c)
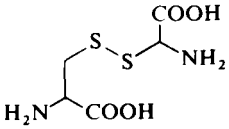 Cystine (Cys-Cys)	H_2O		+342		(c)
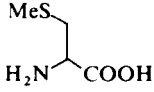 Methionine (Met)	H_2O		+341		(c)
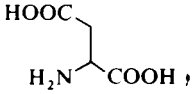 Aspartic acid (Asp)	H_2O/HCl	+340·3	+342		(c)

TABLE 70—*cont.*

Conventional formula, common name, and abbreviation	Solvent	Nitrogen shielding referred to neat nitromethane			Notes
		cation	amphion	anion	
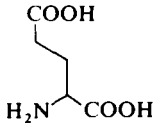 Glutamic acid (Glu)	H_2O/HCl	+338·9	+338		(c)
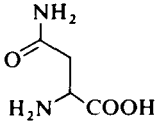 Asparagine (Asn)	H_2O		+339·7 (NH_3^+)		(c)
			+267·9 (amide)		(c)
	H_2O/HCl	+338·1 (NH_3^+)			(c)
		+268·1 (amide)			(c)
		+268·6 (amide)			(e)
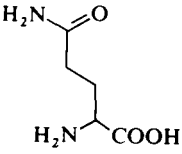 Glutamine (Gln)	H_2O		+340 (NH_3^+)		(c)
			+270 (amide)		(c)
			+266·4 (amide)		(a)
	H_2O/NaOH			+266·4	(a)
	H_2O/HCl	+340·0 (NH_3^+)			(b)
		+268·2 (amide)			(b)
	HCOOH	+340·7 (NH_3^+)			(b)
		+268·6 (amide)			(b)
	CF_3COOH	+341·7 (NH_3^+)			(b)
		+267·8 (amide)			(b)
	97% H_2SO_4	+341·1 (NH_3^+)			(b)
		+269·7 (amide)			(b)

TABLE 70—*cont.*

Conventional formula, common name, and abbreviation	Solvent	Nitrogen shielding referred to neat nitromethane			Notes
		cation	amphion	anion	
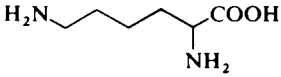	H_2O		+339·2 ($N\alpha$)		(b)
			+346·8 (N_ϵ)		(b)
Lysine (Lys)					
	HCOOH	+340·7 (N_α)			(b)
		+346·6 (N_ϵ)			(b)
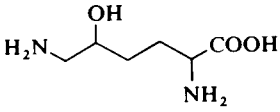	CF_3COOH	+340·2 (N_α)			(b)
		+346·8 (N_ϵ)			(b)
Hydroxylysine (Hyl)					
	H_2O		+342 (N_α)		(c)
			+354 (N_ϵ)		(c)
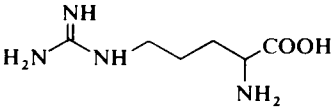		see Table 73			
Arginine (Arg)					
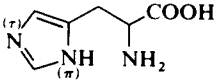		see Table 72			
Histidine (His)					
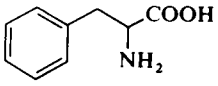	H_2O		+341·0		(c)
Phenylalanine (Phe)					
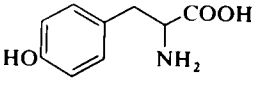	H_2O/HCl	+340·5			(c)
Tyrosine (Tyr)					

TABLE 70—*cont.*

Conventional formula, common name, and abbreviation	Solvent	Nitrogen shielding referred to neat nitromethane: cation	amphion	anion	Notes
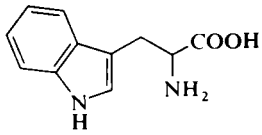 Tryptophan (Trp)			+349 (NH_3^+)		(c)
	H_2O		+299 (NH)		(c)
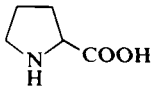 Proline (Pro)	H_2O		+324·7		(b)
			+323·0		(a)
	H_2O/HCl	+325·0			(a)
	HCOOH	+327·1			(b)
	CF_3COOH	+328·1			(b)
	97% H_2SO_4	+327·5			(b)
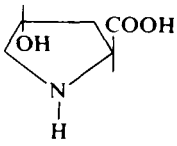 Hydroxyproline (Hyp)	H_2O		+329		(c)
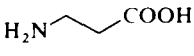 β-Alanine (β-Ala)	H_2O		+348·5		(b)
	H_2O/HCl	+347·8			(b)
	H_2O/H_2SO_4	+348·8			(b)
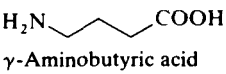 γ-Aminobutyric acid (γ-Abu)	H_2O		+347·3		(b)
	H_2O/HCl	+346·3			(b)
	H_2O/CF_3COOH	+347·8			(b)
	H_2O/H_2SO_4	+347·4			(b)
	HCOOH	+347·6			(b)
	CF_3COOH	+348·1			(b)
	97% H_2SO_4	+347·4			(b)
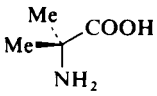 α-Aminoisobutyric acid (α-Aibu)					
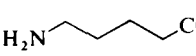 δ-Aminovaleric acid (δ-Ava)	H_2O		+347·8		(b)
	H_2O/H_2SO_4	+347·4			(b)
	97% H_2SO_4	+347·5			(b)

TABLE 70—*cont.*

Conventional formula, common name, and abbreviation	Solvent	Nitrogen shielding referred to neat nitromethane: cation	amphion	anion	Notes
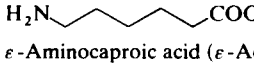 ε-Aminocaproic acid (ε-Aca)	H_2O		+347·7		(b)
	H_2O/H_2SO_4	+347·3			(b)
	HCOOH	+347·9			(b)
	CF_3COOH	+348·0			(b)
	97% H_2SO_4	+347·5			(b)
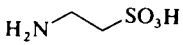 Taurine (Tau)	H_2O		+349		(c)
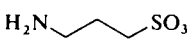 γ-Aminopropanesulphonic acid (γ-Aps)					
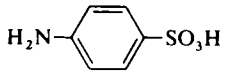 Sulphanilic acid (Sulf)					
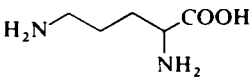 Ornithine (Orn)	H_2O		+345 (Nα)		(c)
			+349 (Nδ)		(c)
	H_2O/HCl	+338·9 (Nα)			(c)

(a) Data from ref. 208 and ref. 209; ^{15}N-enriched compounds; ^{15}N spectra; 9·12 MHz; field perpendicular to sample tube; referred originally to NH_4^+ in 4 M NH_4NO_3 in 2 M HNO_3, +359·1 ppm from neat nitromethane (Table 6); conversion scheme II (Table 4).

(b) Data from ref. 210; ^{15}N natural abundance spectra; 9·12 MHz; field perpendicular to sample tube; referred originally to NO_3^- in aqueous NH_4NO_3, +4·0 ppm from neat nitromethane (Table 6); conversion scheme II (Table 4).

(c) Data quoted in ref. 1, pp. 165–166, and references therein.

(d) Data from ref. 175; ^{15}N natural abundance spectra; details as in note (b).

(e) Data from ref. 211; ^{15}N natural abundance spectra; 9·12 MHz; field perpendicular to sample tube; referred originally to NH_4^+ in 5 M NH_4NO_3 in 2 M HNO_3, +359·0 ppm from neat nitromethane (Table 6); conversion scheme II (Table 4).

TABLE 71

Changes in nitrogen shielding in amino acids relative to that in glycine in the same solvent

Amino acid	Shielding change				Carbon atom effects
	H_2O	HCOOH	CF_3COOH	97% H_2SO_4	
Glycine	0	0	0	0	(arbitrary)
Alanine	+12·7	−12·6	−13·3	−13·1	$1\times\beta$
Isoleucine	L −8·1	−7·9	−8·8	−8·5	$1\times\beta+2\times\gamma$
	D −5·5	−5·3	−5·8	−5·4	
Sarcosine	−2·3	−2·1	−2·1	−2·9	$1\times\alpha$
Proline	−25·1	−25·0	−25·8	−25·4	$1\times\alpha+2\times\beta$
Glutamine (N_α)	−11·1	−11·4	−12·2	−11·8	$1\times\beta+1\times\gamma$
Lysine (N_α)	−10·6	−11·4	−13·7		$1\times\beta+1\times\gamma$
β-Alanine	−1·3			−3·8	
γ-Aminobutyric acid	−4·8	−4·5	−5·8	−5·6	
δ-Aminovaleric acid	−4·8			−5·4	
ε-Aminocaproic acid	−4·9	−4·2	−5·9	−5·4	

Data from ref. 210; ^{15}N natural abundance spectra; 9·12 MHz; carbon atom effects on nitrogen shielding refer to positions of carbon atoms according to the schematic formula $HOOC-C(NH_2)-C^{\alpha}-C^{\beta}-C^{\gamma}$.

TABLE 72

Nitrogen shielding in histidine and its derivatives

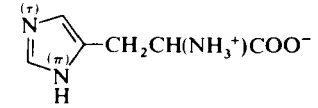

π-H tautomer

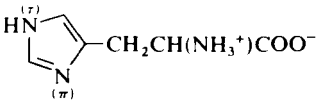

τ-H tautomer

Compound	Solution	Nitrogen shielding referred to neat nitromethane: cation	amphion	anion	Notes
Histidine	H_2O/(HCl or	+337·8 (NH_3^+)			(a)
	NaOH)	+205·0 ($N\tau$)			(a)
		+202·1 (N_π)			(a)
		+206·4 ($N\tau$)	+201·4 (N_τ)	+185·6 (N_τ)	(b)
		+204·0 (N_π)	+148·0 (N_π)	+162·0 (N_π)	(b)
Histidine in	H_2O/(HCl or	+210·4 (N_τ)	+144·2 (N_τ)		(c)
α-lytic protease	(NaOH)	+197·8 (N_π)	+205·6 (N_π)		(c)
τ-Methylhistidine	H_2O/HCl	+337·7 (NH_3^+)			(a)
		+202·9 (N_π)			(a)
π-Methylhistidine	H_2O/HCl	+337·5 (NH_3^+)			(a)
		+207·4 (N_τ)			(a)

(a) Data from ref. 212; ^{15}N natural abundance spectra; 10·14 MHz; field perpendicular to sample tube; referred originally to NO_3^- in aqueous NH_4NO_3, +4·0 ppm from neat nitromethane (Table 6); conversion scheme II (Table 4).

(b) Data from ref. 208 and ref. 209; ^{15}N-enriched compounds; ^{15}N spectra; 9·12 MHz; field perpendicular to sample tube; referred originally to NH_4^+ in 4 M NH_4NO_3 in 2 M HNO_3, +359·1 ppm from neat nitromethane (Table 6); conversion scheme II (Table 4).

(c) Data from ref. 213; ^{15}N-labelled (singly and doubly) imidazole ring of histidine; ^{15}N spectra; 18·25 MHz; field parallel to sample tube; referred originally to 1 M DNO_3, +6·2 ppm from neat nitromethane (Table 6); conversion scheme IV (Table 4).

TABLE 73

Nitrogen shielding in arginine at various pH values

$HOOC-CH(\overset{\alpha}{N}H_2)-CH_2-CH_2-CH_2-\overset{\delta}{N}H-C(=NH)NH_2$

Solution		Nitrogen shielding referred to neat nitromethane			Notes
		α-NH_2 or NH_3^+	δ-NH	terminal NH ⇄ NH_2 or $C^+(NH_2)_2$	
ca. 1 M in H_2O,	pH 14	+349·0	+298·0	+293·0	(a)
	pH 13·4	?	?	+300·9	(b)
	pH 12	+349·0	+296·0	+310·0	(a)
	pH 11·5	+348·9	+296·5	+310·6	(a)
		+348·7	+295·9	+309·9	(c)
	pH 10·4	?	?	+308·7	(b)
	pH 9·9	?	?	+307·5	(b)
	pH 7·8	+340·1	+296·4	+308·9	(c)
	pH 7	+341·0	+296·0	+310·0	(a)
	pH 6·0	+339·9	+296·4	+308·9	(c)
	pH 3·5	+340·0	+296·5	+308·9	(c)
	pH 1·5	+340·5	+296·6	+308·6	(c)
+NaCl,	pH 11·1	+348·9	+296·5	+310·6	(a)
$+HPO_4^{2-}$,	pH 10·6	+347·6	+295·8	+309·5	(a)
$+HBF_4$,	pH 8·9	+340·3	+297·4	+308·4	(a)
$+HPO_4^{2-}$ and $H_2PO_4^-$,	pH 7·3	+340·6	+296·7	+309·5	(a)
+HCl,	pH 6·0	+341·3	+297·0	+310·0	(a)
+ATP,	pH 4·4	+341·0	+297·2	+310·2	(a)
$+HBF_4$ and NaOH,	pH 6·3	?	+296·6	+310·2	(a)
$+HPO_4^{2-}$ and $H_2PO_4^-$ and NaOH,	pH 6·3	+340·7	+296·6	+309·3	(a)

(a) Data from ref. 174; ^{15}N natural abundance spectra; 18·25 MHz; field parallel to sample tube; referred originally to 1 M DNO_3, +6·2 ppm from neat nitromethane (Table 6); conversion scheme IV (Table 4).

(b) Data from ref. 66; ^{15}N selectively labelled arginine; ^{15}N spectra; 10·1 MHz; field perpendicular to sample tube; referred originally to Me_4N^+, +336·7 ppm from neat nitromethane (Table 6); conversion scheme II (Table 4).

(c) Data from ref. 187; details as in note (a).

TABLE 74

Structure evidence of nitroarginine methyl ester hydrochloride in aqueous solution

Structures considered	Nitrogen shieldings referred to neat nitromethane, and signal multiplicities	Assignments
$MeOC(=O)CH(NH_3^+)CH_2CH_2CH_2NHC(NH_2)=NNO_2$ [A]	+12·1 (singlet)	NO_2
	+142·2 (singlet)	C=N
$MeOC(=O)CH(NH_3^+)CH_2CH_2CH_2NHC(NHNO_2)=NH$ [B]	+284·7 (doublet)	NH
	+296·8 (triplet)	NH_2
$MeOC(=O)CH(NH_3^+)CH_2CH_2CH_2N=C(NH_2)NHNO_2$ [C]	+339·3 (multiplet)	NH_3^+
	Structure indicated: [A]	

Data from ref. 188; ^{15}N natural abundance spectra; proton-decoupled and undecoupled; 9·12 MHz; field perpendicular to sample tube; referred originally to 1 M $NaNO_3$, +3·7 ppm from neat nitromethane (Table 6); conversion scheme II (Table 4).

TABLE 75

Nitrogen shielding in some *N*-acetyl substituted amino acids

Compound (for abbreviations see Table 70)	Solution	Nitrogen shielding referred to neat nitromethane	Notes
MeCO-Gly-OH	2 M in DMSO	+269·6	(a)
	in CF_3COOH	+259·7	(b)
MeCO-Leu-OH	2 M in DMSO	+257·3	(a)
	in MeOH	+255·4	(b)
	in CF_3COOH	+245·8	(b)
MeCO-Ile-OH	2 M in DMSO	+260·0	(a)
MeCO-Asn-OH	2 M in DMSO	+269·8 ($CONH_2$)	(a)
		+257·4 (MeCONH)	(a)
MeCO-Gln-OH	2 M in DMSO	+270·4 ($CONH_2$)	(a)
		+256·9 (MeCONH)	(a)
MeCO-Cys(SH)-OH	2 M in DMSO	+260·0	(a)
MeCO-Tyr–OH	2 M in DMSO	+257·2	(a)
MeCO-His-OH	in H_2O	+203·6 (N_π, cation, zwitterion)	(c)
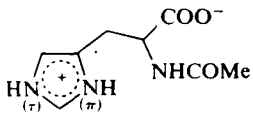	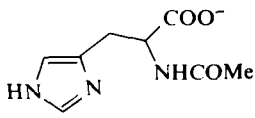	+158·3 (N_π, anion)	(c)
		+207·0 (N_τ, cation, zwitterion)	(c)
		+190·1 (N_τ, anion)	(c)

(a) Data from ref. 211; ^{15}N natural abundance spectra; 9·12 MHz; field perpendicular to sample tube; referred originally to NH_4^+ in 5 M NH_4NO_3 in 2 M HNO_3, +359·0 ppm from neat nitromethane (Table 6); conversion scheme II (Table 4).

(b) Data from ref. 215; ^{15}N natural abundance spectra; 9·12 MHz; field perpendicular to sample tube; for details see footnote * in Table 78.

(c) Data from ref. 209 and ref. 208; ^{15}N-labelled compounds (imidazole ring); ^{15}N spectra; 9·12 MHz; field perpendicular to sample tube; referred originally to NH_4^+ in 4 M NH_4NO_3 in 2 M HNO_3, +359·1 ppm from neat nitromethane (Table 6); conversion scheme II (Table 4).

TABLE 76

Nitrogen shieldings in some α-amino acid *N*-carboxyanhydrides (oxazolidine-2,5-diones)

Structure	Nitrogen shielding referred to neat nitromethane for solutions in: CF_3COOH	acetone	acetone/$CHCl_3$ (1:3 v/v)	Parent amino acid (abbreviations in Table 70)
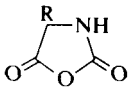				
R = H	+299·1			Gly-OH
Me	+285·9	+286·0	+286·7	Ala-OH
Pr^i	+291·8	+293·0		Val-OH
Bu^i	+287·4	+288·5	+289·2	Leu-OH
CH_2CH_2COOMe	+289·0			γ-OMe-Glu-OH
CH_2CH_2SMe	+289·2	+289·8		Met-OH
CH_2Ph	+288·9	+290·0		Phe-OH
Ph	+286·7	+287·4		Phg-OH

Data from ref. 185; ^{15}N 10% enriched compounds; ^{15}N spectra; 9·12 MHz; field perpendicular to sample tube; referred originally to NO_3^- in aqueous NH_4NO_3, +4·0 ppm from neat nitromethane (Table 6); conversion scheme II (Table 4); 6% w/w solutions.

TABLE 77

Nitrogen shieldings in some cyclic dipeptides (2,5-diketopiperazines) in CF_3COOH solutions

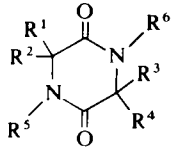

$R^2 = R^4 = R^5 = R^6 = H$ if not stated otherwise

Compound	Nitrogen shielding referred to neat nitromethane (assignments in order of amino acid residues)
cyclo(Gly-Gly), $R^1 = R^3 = H$	+267·4
cyclo(Ala-Ala), $R^1 = R^3 = Me$	+254·5
cyclo(L-Ala-D-Ala)	+254·9
cyclo(Leu-Leu), $R^1 = R^3 = CH_2CHMe_2$	+257·4
cyclo(L-Leu-D-Leu)	+257·8
cyclo(Val-Val), $R^1 = R^3 = Pr^i$	+260·3
cyclo(L-Val-D-Val)	+260·9
cyclo(Phe-Phe), $R^1 = R^3 = CH_2Ph$	+256·2
cyclo(L-Phe-D-Phe)	+256·5
cyclo(Tyr-Tyr), $R^1 = R^3 = CH_2 \cdot C_6H_4 \cdot OHp$	+256·7
cyclo(Sar-Sar), $R^1 = R^3 = H$; $R^5 = R^6 = Me$	+256·6
cyclo(Pro-Pro), $(R^1R^5) = (R^3R^6) = -CH_2CH_2CH_2-$	+238·9
cyclo(α-Aibu-α-Aibu), $R^1 = R^2 = R^3 = R^4 = Me$	+243·4
cyclo(Gly-Ala), $R^1 = H$; $R^3 = Me$	+269·9, +252·4
cyclo(Gly-Leu), $R^1 = H$; $R^3 = CH_2CHMe_2$	+269·5, +255·9
cyclo(Gly-Val), $R^1 = H$; $R^3 = Pr^i$	+267·5, +260·7
cyclo(Gly-Phe), $R^1 = H$; $R^3 = CH_2Ph$	+265·7, +257·1
cyclo(Gly-Phg), $R^1 = H$; $R^3 = Ph$	+269·0, +253·3
cyclo(Ala-Leu), $R^1 = Me$; $R^3 = CH_2CHMe_2$	+253·9, +257·6
cyclo(L-Ala-D-Leu)	+254·0, +258·4
cyclo(Ala-Val), $R^1 = Me$; $R^3 = Pr^i$	+251·7, +262·8
cyclo(L-Ala-D-Val)	+251·9, +263·3
cyclo(Ala-Phe), $R^1 = Me$; $R^3 = CH_2Ph$	+250·6, +257·6
cyclo(Ala-Sar), $R^1 = R^6 = Me$; $R^3 = H$	+253·9, +269·5

Data from ref. 175; ^{15}N natural abundance spectra; 9·12 MHz; field perpendicular to sample tube; referred originally to NO_3^- in aqueous NH_4NO_3, +4·0 ppm from neat nitromethane (Table 6); conversion scheme II (Table 4).

TABLE 78

Effects of protecting groups in Gly-Gly dipeptides on nitrogen shielding

Compound (in DMSO solution)	Nitrogen shielding referred to neat nitromethane	
	R-Gly	Gly-OR
R-Gly-Gly-OH		
R = pMe·C_6H_4·SO_2	+287·7*	+272·9*
$o$$O_2N$·$C_6H_4$·S	+362·4	+272·9
CF_3CO	+271·0	+273·9
MeCO	+269·0	+274·1
Bu^{t}CO	+277·9	+275·5
HCO	+263·4†	
S=C=N$(CH_2)_5$CO	+270·4	+274·5
$ClCH_2CO$	+271·2	+274·1
$PhCH_2OCO$-Ala-	+288·9 (Ala)	+274·9 (Gly-Gly)
Bu^{t}OCO	+301·2	+274·9
Ph_3C	?	+272·8
R-Gly-Gly-OEt		
R = $PhCH_2OCO$	+302·8	+276·0
$p$$O_2N$·$C_6H_4$·$CH_2OCO$	+302·4	+275·8
Cl_3CCH_2OCO	+301·6	+275·9
2,4-$(NO_2)_2$-C_6H_3	+290·5	+274·4
pMe·C_6H_4·SO_2	+287·8	+274·3
pMe·C_6H_4·SO_2-Gly-	+287·6, +275·5	+273·7
$PhCH_2OCO$-Ala-	+287·7 (Ala), +275·6,	+275·7
Bu^{t}OCO	+300·8	+276·4

R-Gly-Gly-OH	Shielding in R-Gly (in ppm) referred to R = HCO
R = HCO	0 (arbitrary)
MeCO	+5·6
S=C=N$(CH_2)_5$CO	+7·0
CF_3CO	+7·6
$PhCH_2OCONHCH_2CH_2CO$	+7·6
$ClCH_2CO$	+7·8
$MeCONHCH_2CO$	+10·7
$PhCH_2OCONHCH(Me)CO$	+11·5
Bu^{t}CO	+14·5
CCl_3CH_2OCO	+37·2
Bu^{t}OCO	+37·8
$p$$O_2N$·$C_6H_4$·$CH_2OCO$	+38·0
$PhCH_2OCO$	+38·5

Data from ref. 214; ^{15}N-labelled and non-labelled compounds; ^{15}N spectra; 20·27 MHz; field parallel to sample tube; 1 g peptide in 5 ml DMSO; referred originally to NO_3^- in aqueous NH_4NO_3, +4·0 ppm from neat nitromethane (Table 6); conversion scheme II (Table 4).

* Same as in above, but 9·12 MHz spectra and field perpendicular to sample tube.

† Quoted in ref. 214 (above), from G. E. Hawkes, E. W. Randall, and C. H. Bradley, *Nature*, 1975, **257**, 767.

TABLE 79

Solvent effects on nitrogen shielding in protected peptides

Peptide (for abbreviations see Table 70)	Solvent	Nitrogen shielding referred to neat nitromethane (assignments in order of amino acid residues)
$(Gly)_n$	HCOOH	+272·2
H-Gly-Gly-OH	HCOOH	+354·2, +272·4
H-Gly-Gly-OEt·HBr	CF_3COOH	+352·6, +272·4
MeCO-Gly-Gly-OH	H_2O	+266·4, +270·6*
	CF_3COOH	+260·1, +271·4*
	DMSO	+269·9, +275·0*
MeCO-Leu-Gly-OH	CF_3COOH	+246·3, +270·1*
	DMSO	+256·8, +274·4*
MeCO-Gly-Gly-Gly-OH	CF_3COOH	+261·3, +271·7, +271·7*
	DMSO	+269·3, +275·0, +275·0*
CF_3CO-Gly-Gly-OH	HCOOH	+274·2, +271·8
	DMSO	+272·1, +274·0
Bu^tOCO-Gly-Gly-OH	DMSO	+302·3, +274·0
	pyridine	+303·1, +276·1
*p*Me·C_6H_4·SO_2-Gly-Gly-OH	HCOOH	+290·1, +270·8
	DMSO	+288·8, +270·4
	pyridine	+288·1, +274·5
*p*Me·C_6H_4·SO_2-Gly-Gly-OEt	HCOOH	+290·0, +270·7
	DMSO	+290·9, +275·4
	pyridine	+288·2, +276·2
*p*Me·C_6H_4·SO_2-Gly-Gly-Gly-OEt	HCOOH	+289·8, +271·2, +271·8
	DMSO	+288·7, +274·8, +276·6
	pyridine	+288·3, +275·0, +277·6
CCl_3CH_2OCO-Gly-Gly-OEt	HCOOH	+302·3, +272·2
	DMSO	+302·7, +276·8
	pyridine	+303·6, +277·6
CF_3CO-Gly-Gly-OEt	HCOOH	+303·5, +272·1
	DMSO	+303·9, +276·2
	pyridine	+304·7, +277·6
CF_3CO-Gly-Gly-OBu^t	HCOOH	+303·5, +271·3
	DMSO	+303·8, +276·1
	pyridine	+304·7, +277·2
2,4-$(NO_2)_2$-C_6H_3·CH_2OCO-Gly-Gly-OEt	HCOOH	+303·8, +272·2
	DMSO	+303·6, +276·7
	pyridine	+304·4, +277·5
CF_3CO-β-Ala-Gly-Gly-OEt	HCOOH	+295·9, +267·2, +272·0
	DMSO	+297·5, +271·0, +276·5
H-Ala-Ala-OH	HCOOH	+340·6, +257·8
Bu^tOCO-Ala-Ala-OH	DMSO	+287·9, +262·2
	pyridine	+288·2, +262·0
CF_3CO-Ala-Ala-OH	HCOOH	+289·4, +258·2
	DMSO	+289·4, +261·7
	pyridine	+289·7, +261·7

TABLE 79—*cont.*

Peptide (for abbreviations see Table 70)	Solvent	Nitrogen shielding referred to neat nitromethane (assignments in order of amino acid residues)
CF_3CO-Ala-Ala-OEt	HCOOH	+289·5, +258·0
	DMSO	+289·5, +262·5
	pyridine	+290·0, +263·0
CF_3CO-Phe-Ala-Ala-OMe	HCOOH	+292·7, +255·5, +258·3
	DMSO	+292·7, +261·1, +261·1

Data from ref. 214 (except those corresponding to footnote*); ^{15}N natural abundance and labelled compounds; ^{15}N spectra; 9·12 MHz; field perpendicular to sample tube; referred originally to NO_3^- in aqueous NH_4NO_3, +4·0 ppm from neat nitromethane (Table 6); conversion scheme II (Table 4); 1 g peptide in 5 ml solvent.

* Data from ref. 215; ^{15}N natural abundance spectra; 9·12 MHz; field perpendicular to sample tube; referred originally to NH_4^+ in 5 M NH_4NO_3 in 2 M HNO_3, +359·1 ppm from neat nitromethane (Table 6); conversion scheme II (Table 4).

TABLE 80

Nitrogen shieldings in some oligopeptides

Peptide (for abbreviations see Table 70)	Solvent	Nitrogen shielding referred to neat nitromethane (assignments in order of amino acid residues)	Notes
H-Gly-Gly-OH	H_2O, pH 0·5	+352·3, +270·7	(a)
	pH 5·8	+352·8, +264·5	(a)
	isoelectric	+355·1, +266·6	(b)
H-Ala-Gly-OH	H_2O, isoelectric	+341·2, +266·6	(b)
H-Leu-Gly-OH	H_2O, isoelectric	+343·0, +263·3	(b)
H-Val-Gly-OH	H_2O, isoelectric	+346·4, +262·0	(b)
H-Gly-Ala-OH	H_2O, isoelectric	+354·6, +252·1	(b)
H-Gly-Leu-OH	H_2O, isoelectric	+355·1, +254·3	(b)
H-Ala-Ala-OH	H_2O, isoelectric	+341·6, +252·3	(b)
H-Phe-Gly-OH	H_2O, pH 4·9	+343·6, +263·5	(b)
H-Phe-Ala-OH	H_2O, pH 9	+353·1, +256·5	(b)
H-Phe-Leu-OH	H_2O, pH 12	+353·0, +252·8	(b)
H-Gly-Phe-OH	H_2O, pH 9	+355·3, +256·9	(b)
H-Gly-Tyr-OH	H_2O, pH 11	+355·2, +256·8	(b)
H-Gly-Gly-Gly-OH	H_2O, isoelectric	+355·1, +272·9, +266·9	(b)
	pH 0·5	+352·3, +270·1, +271·5	(a)
	pH 1·5	+355·0, +272·6, +273·4	(b)
	pH 11·9	+367·9, +273·0, +266·8	(b)
H-Ala-Gly-Gly-OH	H_2O, isoelectric	+340·9, +272·8, +266·8	(b)
H-Leu-Gly-Gly-OH	H_2O, isoelectric	+342·6, +269·9, +266·7	(b)
H-Val-Gly-Gly-OH	H_2O, isoelectric	+346·3, +268·5, +266·5	(b)
H-Gly-Gly-Ala-OH	H_2O, isoelectric	+355·1, +272·8, +250·7	(b)
H-Ala-Ala-Ala-OH	H_2O, isoelectric	+341·6, +258·0, +253·2	(b)
H-Gly-Ala-Gly-OH	H_2O, isoelectric	+355·8, +258·4, +267·9	(b)
H-Gly-Leu-Gly-OH	H_2O, isoelectric	+355·3, +260·0, +266·1	(b)
H-Phe-Gly-Gly-OH	CF_3COOH	+341·9, +267·7, +270·4	(c)
H-β-Ala-Gly-Gly-OH	CF_3COOH	+347·4, +266·5, +270·0	(c)
H-ε-Aca-Gly-Gly-OH	CF_3COOH	+347·8, +263·6, +271·8	(c)
H-Gly-Gly-Glu-OH	H_2O, pH 4·0	(?), +270·7, +256·1	(d)
	pH 1·9	(?), +269·7, +259·2	(d)
H-Gly-Gly-L-His-OH	H_2O, pH 3·5	(?), +270·5, +257·9	(d)
	pH 1·5	(?), +269·3, +261·3	(d)
H-Gly-Gly-L-Val-OH	H_2O, pH 5·2	(?), (?), +256·7	(d)
	pH 2·3	(?), +270·5, +260·6	(d)
H-Gly-Gly-L-Leu-OH	H_2O, pH 5·0	(?), (?), +252·3	(d)
	pH 2·7	(?), +270·7, +256·1	(d)
H-Gly-Gly-L-Ile-OH	H_2O, pH 5·4	(?), (?), +255·4	(d)
	pH 2·0	(?), +270·7, +259·3	(d)
H-Glu-Cys-Gly-OH | S | S | H-Glu-Cys-Gly-OH (glutathione, oxidized form)	H_2O, pH 0·4	+339·5, +256·8, +268·3	(a)
	pH 4·0	+337·9, +256·2, +264·8	(a)
	pH 7·3	+337·6, +256·2, +262·9	(a)
	pH 12·0	(?), +255·4, +262·4	(a)

TABLE 80—*cont.*

Peptide (for abbreviations see Table 70)	Solvent	Nitrogen shielding referred to neat nitromethane (assignments in order of amino acid residues)	Notes
H-Glu-Cys(SH)-Gly-OH	H_2O, pH 0·4	+340·0, +256·8, +268·3	(a)
(glutathione, reduced	pH 2·4	+339·5, +256·8, +267·7	(a)
form)	pH 7·5	(?), +256·0, +262·4	(a)
	pH 12·5	+347·0, +252·5, +262·4	(a)
H-β-Ala-His-OH	H_2O, pH 0·4	+347·0, +257·2, (+203·7, +206·8) imidazole ring	(a)
(Carnosin)	pH 4·5	+347·5, +253·7, (? , ?)	(a)
	pH 8·0	+348·3, +250·1, (? , ?)	(a)
	pH 10·8	(?), +249·1, (? , ?)	(a)
	pH 11·0	(?), +248·7, (? , ?)	(a)
cyclo(Gly-Pro-Gly-D-Ala-Pro)	MeOH	+274·6, +244·0, +262·9, +258·9, +244·0	(e)
	$CHCl_3$	(?), +244·0, +275·8, +261·1, +246·7	(e)
	$CHCl_3$/acetone	+276·9, +244·8, +275·7, +261·3, +244·8	(e)
	H_2O	{+273·2 / +270·8}, (?), {+271·8 / +271·3}, +255·5, (?)	(e)
Bu^{t}OCO-Gly-OH	DMSO	+296·0	(f)
Bu^{t}OCO-Val-Gly-OMe	DMSO	+288·6, +268·2	(f)
Bu^{t}OCO-Gly-Val-Gly-OMe	DMSO	+296·0, +261·9, +267·3	(f)
MeCO-Gly-Val-Gly-OMe	DMSO	+263·9, +260·9, +267·3	(f)
Bu^{t}OCO-L-Nva-OMe	CF_3CH_2OH (55 °C)	+292·0	(g)
Bu^{t}OCO-(L-Nva)$_2$-OMe	CF_3CH_2OH (25 °C)	+292·0, +262·7	(g)
	(63 °C)	+291·7, +263·7	(g)
	DMSO (52 °C)	+291·8, +266·1	(g)
Bu^{t}OCO-(L-Nva)$_3$OMe	CF_3CH_2OH (18 °C)	+292·2, +262·7, +261·7	(g)
	(36 °C)	+292·0, +262·9, +262·2	(g)
	(59 °C)	+291·9, +263·0, +262·2	(g)
	DMSO (24 °C)	+291·4, +265·1, +264·0	(g)
	(36 °C)	+291·7, +265·5, +264·6	(g)
	(60 °C)	+292·0, +266·1, +265·2	(g)
Bu^{t}OCO-(L-Nva)$_4$-OMe	CF_3CH_2OH (25 °C)	+291·9, +263·9, +262·5, +261·7	(g)
	(38 °C)	+291·9, +263·9, +263·9, +261·8	(g)
	(62 °C)	+291·8, +263·9, +263·9, +261·9	(g)
	DMSO (20 °C)	+291·5, +264·9, +264·6, +263·8	(g)
	(40 °C)	+291·7, +265·3, +265·1, +264·2	(g)
	(65 °C)	+292·0, +265·6, +265·6, +264·7	(g)
Bu^{t}OCO-L-Val-OH	CF_3CH_2OH (28 °C)	+296·2	(g)
Bu^{t}OCO-(L-Val)$_2$-OMe	CF_3CH_2OH (28 °C)	+294·9, +296·2	(g)
Bu^{t}OCO-(L-Val)$_3$-OMe	CF_3CH_2OH (28 °C)	+295·1, +262·3, +262·3	(g)

TABLE 80—*cont.*

Peptide (for abbreviations see Table 70)	Solvent	Nitrogen shielding referred to neat nitromethane (assignments in order of amino acid residues)	Notes
Bu^tOCO-(L-Val)$_4$-OMe	CF_3CH_2OH (28 °C)	+295·1, +261·7, +261·7, +259·8	(g)
	(56 °C)	+294·9, +262·7, +261·1, +260·4	(g)
MeCO-L-Val-OMe	CF_3CH_2OH(34 °C)	+261·5	(g)
Bu^tOCO-L-Val-NHMe	CF_3CH_2OH (35 °C)	+295·3, +274·9	(g)
H-Ala-Pro-OH			
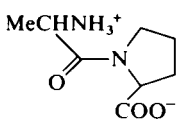 (*trans*)	H_2O	(?), +239·3 (cation)	(h)
		(?), +235·1 (amphion)	(h)
		(?), +234·8 (anion)	(h)
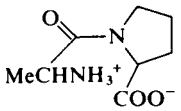 (*cis*)	H_2O	(?), +238·5 (cation)	(h)
		(?), +234·3 (amphion)	(h)
		(?), +234·2 (anion)	(h)

(a) Data from ref. 215; ^{15}N natural abundance spectra; 9·12 MHz; field perpendicular to sample tube; referred originally to NH_4^+ in 5 M NH_4NO_3 in 2 M HNO_3, +359·0 ppm from neat nitromethane (Table 6); conversion scheme II (Table 4); 0.8–1.2 M aqueous solutions.

(b) Data from ref. 216; ^{15}N natural abundance spectra; 18·25 MHz; field parallel to sample tube; referred originally to 1 M DNO_3, +6·2 ppm from neat nitromethane (Table 6); conversion scheme IV (Table 4).

(c) Data from ref. 217; ^{15}N-labelled and non-labelled compounds; ^{15}N spectra; 18·25 MHz; field parallel to sample tube; referred originally to NO_3^- in aqueous NH_4NO_3, +4·0 ppm from neat nitromethane (Table 6); conversion scheme II (Table 4).

(d) Data from ref. 96; ^{15}N natural abundance proton spectra; 90 MHz; AISEFT technique (extracting ^{15}N satellites and double resonance); field perpendicular to sample tube; referred to neat nitromethane; uncorrected for bulk susceptibility effects.

(e) Data from ref. 218; ^{15}N natural abundance and partly labelled Gly; details as in note (b).

(f) Data from ref. 219; ^{15}N-labelled compounds; ^{15}N spectra; 10·05 MHz; field perpendicular to sample tube; referred originally to 0·1 M NH_4Cl in 2 M HCl, +352·5 ppm from neat nitromethane (Table 6); conversion scheme II (Table 4).

(g) Data from ref. 220; details as in note (b); Nva = norvaline.

(h) Data from ref. 221; ^{15}N-enriched Pro; ^{15}N spectra; 9·12 MHz; field perpendicular to sample tube; referred originally to NH_4^+ in 4 M NH_4NO_3 in 2 M HNO_3, +359·1 ppm from neat nitromethane (Table 6); conversion scheme II (Table 4).

TABLE 81

Differentiation between diastereomeric peptide systems by means of nitrogen shielding

Peptide (R=Bu^{t}OCO)	Solution	Nitrogen shielding referred to neat nitromethane (assignments in order of amino acid residues)
R-L-Ala-L-Ala-OH	DMSO/acetone	+287·7, +262·0
	pyridine	+287·3, +262·0
	CF_3CH_2OH	+287·4, +259·6
	MeCOOH	+286·4, +257·2
	H_2O, pH 9	+284·7, +259·9
H-L-Ala-L-Ala-OH	CF_3COOH	+339·6, +256·3
R-L-Ala-D-Ala-OH	DMSO/acetone	+287·7, +262·4
	pyridine	+287·3, +262·4
	CF_3CH_2OH	+287·4, +259·6
	MeCOOH	+285·2, +260·3
	H_2O, pH 9	+284·7, +260·3
H-L-Ala-D-Ala-OH	CF_3COOH	+339·6, +256·3
R-L-Val-L-Val-OH	DMSO/acetone	+293·6, +265·2
R-L-Val-D-Val-OH	DMSO/acetone	+294·3, +265·9
R-L-Val-L-Val-L-Val-OH	DMSO/acetone	+293·0, +265·3, +263·7
R-L-Val-L-Val-D-Val-OH	DMSO/acetone	+292·7, +264·6, +264·6
R-L-Val-L-Val-L-Ala-OMe	DMSO/acetone	+292·7, +264·4, +257·5
R-L-Val-L-Val-D-Ala-OMe	DMSO/acetone	+293·1, +264·4, +257·9
R-L-Val-L-Val-L-Phe-OMe	DMSO/acetone	+293·0, +264·2, +261·0
R-L-Val-L-Val-D-Phe-OMe	DMSO/acetone	+293·2, +265·0, +261·4
R-L-Val-L-Val-Gly-OEt	DMSO/acetone	+293·0, +263·7, +262·9
R-L-Val-D-Val-Gly-OEt	DMSO/acetone	+294·0, +263·7, +263·2
R-L-Ala-L-Ala-D-Ala-OH	DMSO/acetone	+287·1, +262·4, +261·5
R-L-Ala-D-Ala-L-Ala-OH	DMSO/acetone	+286·9, +262·6, +261·5
R-L-Val-L-Val-D-Val-OMe	DMSO/acetone	+292·7, +264·6, +264·4
R-L-Val-D-Val-L-Val-OMe	DMSO/acetone	+293·8, +265·6, +264·5
$SCN(CH_2)_5CO$-D,L-Ala-D,L-Ala-OH	DMSO/acetone	+256·1, +262·1
(ε-Aca-D,L-Ala-D,L-Ala)$_n$		
L-L (D-D)	DMSO	+253·6, +259·1, +266·8
L-D (D-L)	DMSO	+254·5, +260·9, +266·5
L-L (D-D)	H_2O, pH 7	+250·5, +256·2, +260·5
L-D (D-L)	H_2O, pH 7	+250·5, +257·2, +260·0
L-L (D-D)	CF_3COOH	+246·0, +253·3, +255·3
L-D (D-L)	CF_3COOH	+246·0, +252·8, +255·3
L-L (D-D)	98% H_2SO_4	+232·9, +239·8, +245·1
L-D (D-L)	98% H_2SO_4	+232·9, +239·8, +244·6

Data from ref. 222 and ref. 223; ^{15}N partly labelled and non-labelled compounds; ^{15}N spectra; 36·48 MHz; field parallel to sample tube; referred originally to NO_3^- in aqueous NH_4NO_3, +4·0 ppm from neat nitromethane (Table 6); conversion scheme II (Table 4); *ca.* 1 g peptide in 4 ml solvent.

TABLE 82

Nitrogen shielding assignments in oxytocin

	Amino acid residue	Nitrogen shielding referred to neat nitromethane
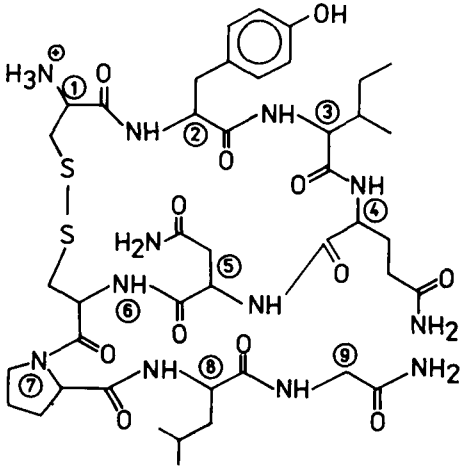	$Cys^1(NH_3^+)$	+342·0
	$Gly^9(NH_2)$	+273·2
	$Gly^9(NH)$	+269·7
	$Asn^5(NH_2)$	+267·9
	$Gln^4(NH_2)$	+268·2
	$Asn^5(NH)$	+263·7
	$Cys^6(NH)$	+260·3
	$Gln^4(NH)$	+260·3
	$Ile^3(NH)$	+260·3
	$Leu^8(NH)$	+257·8
	$Tyr^2(NH)$	+256·4
	$Pro^7(N)$	+242·9
Oxytocin		
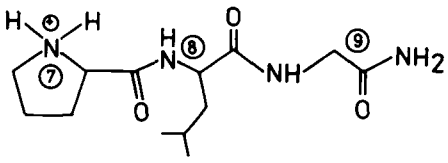	$Gly^9(NH_2)$	+273·1
	$Gly^9(NH)$	+268·6
	$Leu^8(NH)$	+257·7
	$Pro^7(NH_2^+)$	+327·3
Prolylleucylglycinamide		

Data from ref. 211; ^{15}N-labelled and non-labelled compounds; ^{15}N spectra; 18·25 MHz; field parallel to sample tube; referred originally to NH_4^+ in 5 M NH_4NO_3 in 2 M HNO_3, +359·0 ppm from neat nitromethane (Table 6); conversion scheme II (Table 4).

TABLE 83

Nitrogen shieldings in viomycin

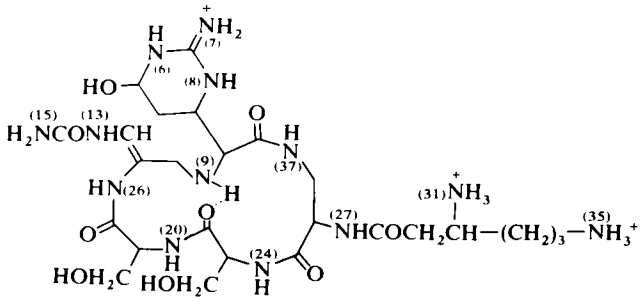

0·3 M solution in 90% H_2O/10% D_2O at pH 2·8

Nitrogen atom	Nitrogen shielding referred to neat nitromethane	Amino acid residues or other moieties
6	+281·1	guanidine moiety
7	+307·6	
8	+296·0	
9	+273·7	alanine type
13	+263·8	urea moiety
15	+296·3	
20	+262·8	serine
24	+256·9	serine
27	+257·0	α,β-diaminopropionic acid
31	+336·9	lysine-H^+
35	+346·7	lysine-H^+
37	+266·9	α,β-diaminopropionic acid

Data from ref. 224; ^{15}N natural abundance spectra; 27·36 and 36·48 MHz; field parallel to sample tube; referred originally to NH_4^+ in 5 M NH_4NO_3 in 2 M HNO_3, +359·0 ppm from neat nitromethane (Table 6); conversion scheme II (Table 4); somewhat different assignments are made elsewhere.

TABLE 84

Nitrogen shieldings in alumichrome

Al^{3+} cyclo(-Gly^1-Gly^2-Gly^3-Orn^1-Orn^2-Orn^3-)
Gly = glycine residue
Orn = δ-*N*-acetylhydroxyornithyl residue

Method	Solvent	Type of nitrogen atom	Nitrogen shielding referred to neat nitromethane					
			Gly^1	Gly^2	Gly^3	Orn^1	Orn^2	Orn^3
Double resonance*	DMSO (19 °C)	amide	(+) 266·9	265·5	275·7	265·5	261·3	264·0
	(70 °C)	amide	(+) 268·1	270·0	276·3	265·5	261·2	264·5
	CF_3CH_2OH (70 °C)	amide	(+) 268·2	273·5	274·1	262·0	257·7	260·4
Direct†	DMSO (45 °C)	amide	(+) 268·8	270·9	277·4	267·1	262·8	265·6
		hydroxamate				(+) 183·1	182·3	182·3

* Data from ref. 225; $^1H\{^{15}N\}$ double resonance spectra; 220/22·3 MHz; ^{15}N-labelled alumichrome; referred originally to tetramethylsilane proton signal at exactly 220 MHz; recalculated here to nitromethane using a frequency of 22 300 833·3 Hz for neat nitromethane at the same magnetic field (ref. 2, p. 172).

† Data from ref. 226; ^{15}N-labelled alumichrome; ^{15}N spectra; 10·13 MHz; field perpendicular to sample tube; referred originally to Orn^2 signal, reported to be at −39·3 ppm from that of urea (+302·1 ppm from neat nitromethane; Table 49).

TABLE 85

Nitrogen shielding in [Met^5]enkephalin and related peptides

Sample* (0·5 M aqueous solutions, pH 1·5)	Nitrogen shielding referred to neat nitromethane (assignments follow the sequence of amino acid residues)
H-Tyr-Gly-Gly-Phe-Met-OH (Enkephalin)	(+) 341·8, 268·0, 272·0, 260·8, 258·3
H-Phe-Met-OH	(+) 341·6, 257·0
H-Gly-Gly-Phe-Met-OH	(+) 335·9, 273·3, 260·5, 257·6
H-Gly-Gly-OH	(+) 352·4, 270·1
H-Tyr-Gly-Gly-OH	(+) 341·3, 267·6, 270·7
H-Tyr-Gly-OH	(+) 341·4, 267·6

Data from ref. 227; ^{15}N natural abundance spectra; 10·05 MHz; field perpendicular to sample tube; referred originally to NH_4^+ in aqueous NH_4NO_3 at pH 2, +359·0 ppm from neat nitromethane (Table 6); conversion scheme II (Table 4).

* Abbreviations used for amino acid residues: Gly = glycine; Tyr = tyrosine; Phe = phenylalanine; Met = methionine.

TABLE 86

Structure evidence of bleomycin by ^{15}N NMR

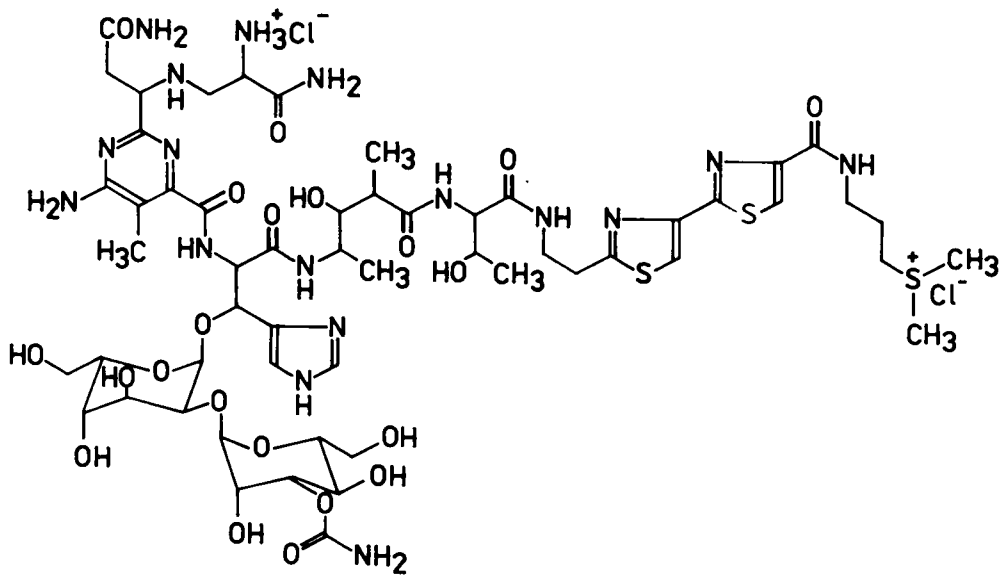

Nitrogen atom type	Nitrogen shielding relative to neat nitromethane and signal multiplicity due to N–H coupling
thiazole	+68·6 (singlet); +77·6 (singlet)
pyrimidine	+137·7 (singlet); +137·9 (singlet)
imidazole	+206·2 (broad, integral intensity suggests 2 atoms)
C-terminal amide bound to dithiazole	+263·6 (doublet)
$-C(=O)NH_2$ groups	+268·6 (triplet); +274·7 (triplet)
pyrimidine NH_2	+296·6 (triplet)
secondary amide (–CONH–)	+248·2 (doublet); +263·2 (doublet); +264·5 (doublet); +265·6 (doublet)
O-carbamoyl ($-O-CONH_2$)	+305·7 (triplet)
secondary amine (NH)	+343·5 (singlet, proton exchange)
ammonium group (NH_3^+)	+344·9 (singlet, proton exchange)

Data from ref. 228; ^{15}N natural abundance spectra for solution in methanol; undecoupled and those with inverse-gated decoupling of protons; 36·48 MHz; field parallel to sample tube; referred originally to NO_3^- in H_2O, probably $NaNO_3$, +3·7 ppm from neat nitromethane (Table 6); conversion scheme II (Table 4); key observations to structure determination: 17 nitrogen atoms including 2 primary amide moieties ($-CONH_2$).

TABLE 87

Tentative assignments of nitrogen shieldings in thiostrepton and siomycin A

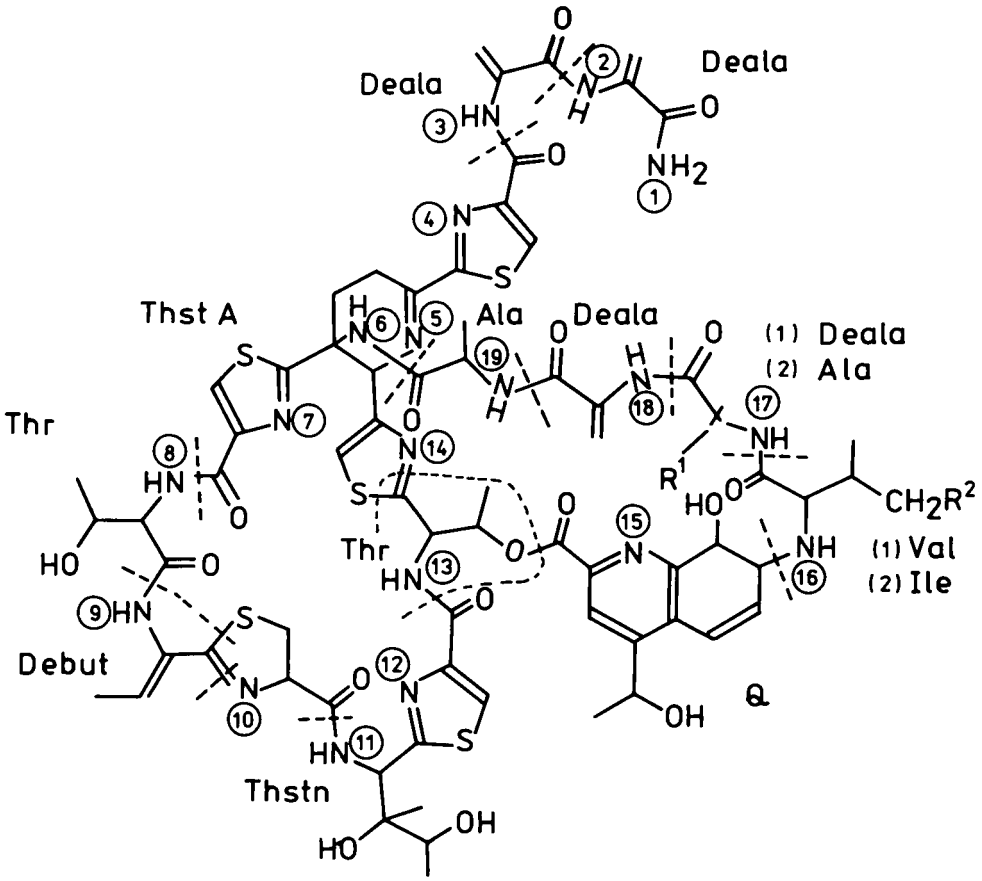

(1) X=C, R^1=CH_2, R^2=H
(2) X=CH, R^1=R^2=Me

Nitrogen atom number	Nitrogen shielding referred to neat nitromethane: Siomycin A (1)	Thiostrepton (2)
4, 5, 7, 10	(+)59·2, 67·6, 68·1, 70·6	(+)58·9, 67·5, 68·1, 70·1
12, 14, 15	(+)76·0, 89·3, 91·5	(+)76·2, 88·8, 91·4
17	+254·1	
6	+257·1	+257·2
2, 3	+257·8, 257·8	+257·9, +257·9
18		+258·8
17		+259·3
19	+260·8	+260·8
9	+263·2	+263·3
18	+263·5	

TABLE 87—*cont.*

Nitrogen atom number	Nitrogen shielding referred to neat nitromethane: Siomycin A (1)	Thiostrepton (2)
8, 13	+266·9, +268·5	+267·1, +268·7
11	+269·6	+269·4
1	+284·4	+284·9
16		+335·4
16	+340·5	

Data from ref. 229; solutions in $CDCl_3$/MeOH (8:2); ^{15}N natural abundance spectra; 36·48 MHz; field parallel to sample tube; referred originally to NO_3^- in aqueous NH_4NO_3, +4·0 ppm from neat nitromethane (Table 6); conversion scheme II (Table 4).

TABLE 88

Nitrogen shieldings in gramicidin-S

cyclo(-L-Val-L-Orn-L-Leu-D-Phe-L-Pro-)

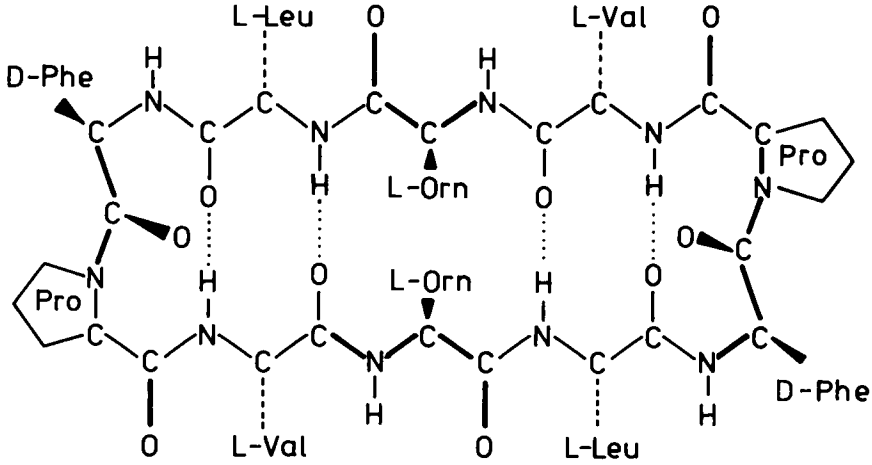

Amino acid residue	Nitrogen shielding referred to neat nitromethane: gramicidin-S in DMSO	gramicidin-S CF_3CH_2OH	gramicidin-S DMSO/MeOH (1:1)	*N*-Me-Phe derivative in DMSO/MeOH (1:1)
L-Val	+261·6	+254·6	+257·8	+256·1
L-Orn	+246·6	+248·2	+247·3	+247·8
L-Leu	+249·3	+244·4	+248·1	+248·9
D-Phe	+251·6	+248·3	+248·8	
(*N*-Me)D-Phe				+253·3
L-Pro	+240·5	+236·3	+238·6	+237·9

Data from ref. 219; ^{15}N natural abundance spectra at 52 °C; 10·05 MHz; field perpendicular to sample tube; originally referred to 0·1 M NH_4Cl in 2 M HCl, +352·5 ppm from neat nitromethane (Table 6); conversion scheme II (Table 4).

TABLE 89

Nitrogen shieldings in a model tetrapeptide for amino acid sequence in tropoelastin

Tetrapeptide structure: Bu^{t}OCO-Val-Pro-Gly-Gly-OMe

Solvent (0·015 M solutions)	Nitrogen shielding referred to neat nitromethane			
	Val	Pro	Gly	Gly-OMe
$CDCl_3$	+290·0	+237·7	+271·4	+266·8
$CDCl_3$/MeOH (9:1)	+289·2	+237·3	+269·8	+266·2
MeOH	+284·5	+235·5	+267·0	+264·3

Data from ref. 230; ^{15}N 20% enriched tetrapeptide; ^{15}N spectra; 10·093 MHz; field perpendicular to sample tube; referred originally to NH_4Cl in 2 M HCl, +352·5 ppm from neat nitromethane (Table 6); conversion scheme II (Table 4); since the shieldings are not corrected for bulk susceptibility effects, the observed solvent shifts ($CDCl_3$/MeOH) contain a contribution of about 0·5 ppm from the latter.

TABLE 90

Primary structures of cell wall peptidoglycans in some Gram-positive bacteria (according to ref. 231)

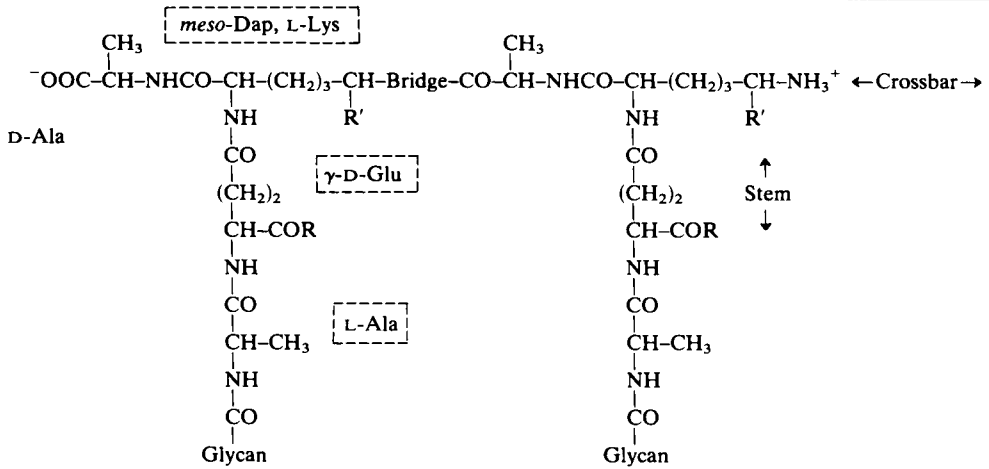

Bacteria	R	R′	Bridge	Accessory polymer
B. licheniformis	OH, NH_2	$COO^-, CONH_2$	direct	teichoic acid, teichuronic acid
B. subtilis	OH, NH_2	$COO^-, CONH_2$	direct	teichoic acid
S. faecalis	NH_2	H	$-NHCHCH_2CO-$ (CONH2)	polysaccharides
M. lysodeikticus	$NHCH_2COO^-$	H	$-(L\text{-}Ala\text{-}\gamma\text{-}D\text{-}Glu\text{-}L\text{-}Lys)_{1\text{-}6}-$ (Gly D-Ala)	traces of *N*-acetyl aminopolysaccharides
S. aureus	NH_2	H	$-(NHCH_2CO)_5-$	teichoic acid

TABLE 91

Nitrogen shieldings in cell-wall lysozyme digests of some Gram-positive bacteria

Bacteria	Nitrogen shielding referred to neat nitromethane	Assignments for structures in Table 90
Bacillus licheniformis lysozyme digest, pH 7	+247·2	C-terminal D-alanine
	+247·6, +250·3	alanine residues
	+250·9	D-alanine in crossbar
	+252·0	alanine residue
	+252·7, +253·6	D-glutamate and *meso*-diaminopimelic acid peptide groups adjacent to free carboxylic acid groups
	+254·4, +255·1	acetamido groups in glycan *N*-acetylmuramic acid residues and teichuronic acid *N*-acetylgalactosamine units
	+255·8, +258·2	D-glutamate and *meso*-diaminopimelic acid residues
	+268·9, +270·5	amidated carboxylate groups ($CONH_2$) of D-glutamate and *meso*-diaminopimelic acid residues
	+337·2	free amino groups of teichoic acid
	+339·5, +345·2	see *B. subtilis*
Bacillus subtilis lysozyme digest, pH 7	+247·7	C-terminal D-alanine
	+251·0	D-alanine in crossbar
	+251·9	L-alanine in stem
	+252·7	D-glutamate in stem
	+253·9	*meso*-diaminopimelic acid in crossbar
	+254·9, +255·9	α and β anomeric forms (*N*-acetyl groups) of glucosamine units of glycan
	+258·0	*meso*-diaminopimelic acid in stem
	+268·6, +270·4	$CONH_2$ groups in amidated glutamate and *meso*-diaminopimelic acid residues
	+337·3	free amino groups of teichoic acid
	+339·5	free amino groups of *meso*-diaminopimelic acid
	+345·2	lysine-N_ω free amino groups
Streptococcus faecalis lysozyme digest, pH 7·5	+251·7	alanine in stem and crossbar
	+255·3	*N*-acetyl groups in glycan
	+256·2	CONH in amidated glutamate residues
	+258·0	L-lysine-$N_{\alpha,\omega}$
	+261·2	D-isoasparagine peptide bond in bridge
	+270·3	$CONH_2$ in amidated glutamate residues
	+271·3	$CONH_2$ of D-isoasparagine in bridge
	+336·9	free amino groups of teichoic acid
	+344·9	L-lysine free amino groups

TABLE 91—*cont.*

Bacteria	Nitrogen shielding referred to neat nitromethane	Assignments for structures in Table 90
Micrococcus lysodeikticus lysozyme digest, pH 7	+248·6	C-terminal D-alanine
	+251·5	D-alanine in bridge
	+253·2	L-alanine peptide bond
	+255·1	D-glutamate substituted with glycyl groups
	+258·2	L-lysine-N_α peptide bond
	+258·7	?
	+261·4, +261·8	C-terminal glycine units in stem and bridge
Staphylococcus aureus autolysate, pH 7	+252·0	alanine in stem and crossbar
	+256·7	L-lysine amido group
	+268·9	glycine in pentaglycine bridge
	+337·2	?
	+345·5	free amino groups in L-lysine
	+350·8	N-terminal glycine residues in pentaglycine bridge

Data from refs. 231–235; ^{15}N-labelled (totally and selectively) bacteria; ^{15}N spectra; 9·12 MHz; field perpendicular to sample tube; referred originally to 4 M NH_4Cl in 2 M HCl, +352·5 ppm from neat nitromethane (Table 6), but reported relative to "HNO_3" at 352·5–350·9 = +1·6 ppm from neat nitromethane; conversion scheme II (Table 4).

TABLE 92

Relative intensities of ^{15}N resonance signals of cell wall lysozyme digests of *Bacillus licheniformis*

Resonance position (shielding relative to neat nitromethane)	Integral intensity (estimated from lineshape fitting and normalized to that of the resonance at +255·1 ppm)	
	normal cells	Vancomycin-treated cells
+247·2	0·23	0·26
+247·6	0·20	0·20
+250·3	0·11	0·12
+250·9	0·24	0·24
+252·0	0·25	0·25
+252·7	0·24	0·22
+253·6	0·22	0·22
+254·4	0·39	0·32
+255·1	1·00	1·00
+255·8	0·37	0·36
+258·2	0·21	0·19
+268·9	0·26	0·24
+270·5	0·23	0·22

Data from ref. 233; for details see footnote in Table 91.

TABLE 93

Nitrogen shieldings in *Escherichia coli* cell walls

Sample type	Nitrogen shielding referred to neat nitromethane	Assignments
Intact cells	+254·8, +258·3, +264·9	polypeptide amido groups
	+291·0	arginine-N_ε
	+304·2	arginine-$N_{\omega,\omega'}$
	+335·4	*meso*-diaminopimelic acid in peptidoglycan of cell envelope
	+342·8	lysine-N_ω
	+349·8	ammonium groups of phosphatidylethanolamine in cell envelopes
Cell envelopes	(additional signals)	
	+245·3, +250·3, +251·4, +252·9, +263·2	amido groups in peptidoglycan

Data from refs 236 and 237; ^{15}N-labelled bacteria; ^{15}N spectra; 9·12 MHz; field perpendicular to sample tube; referred originally to 2 M NH_4Cl in 2M HCl, +352·5 ppm from neat nitromethane (Table 6), but reported relative to "HNO_3", 352·5–352·7 = −0·2 ppm from neat nitromethane; conversion scheme II (Table 4).

TABLE 94

Structure determination of nosiheptide antibiotic by ^{15}N NMR

^{15}N resonance of nosiheptide in DMSO solution referred to neat nitromethane		Assignments and conclusions
+61·2, +63·7, +68·5, +72·7, +75·6, +81·4		assigned to five thiazole and one pyridine moieties; no thiazoline unit present
+258·6 (doublet)		assigned to indole unit
+259·6, +262·3, +265·8, +268·8, +270·1 (doublets)		assigned to five –C(=O)NH– groups
+279·5 (triplet)		assigned to single $-C(=O)NH_2$ group
total: 13 signals		13 nitrogen atoms, seven of them bound directly to H atoms, none bound directly to O atoms, eight H atoms bound to N atoms
Molecular formula deduced from elemental analysis for 13 N atoms	C: 49·6–52·4 H: 38·1–48·2 N: 13 O: 10·0–14·7 S: 5·8–6·2	Final formula deduced from experimental data $C_{51}H_{43}N_{13}O_{12}S_6$

Data from ref. 238; ^{15}N spectra; 18·25 MHz; field parallel to sample tube; referred originally to NO_3^- in aqueous NH_4NO_3, +4·0 ppm from neat nitromethane (Table 6); conversion scheme II (Table 4).

TABLE 95

Nitrogen shieldings in some polypeptides

Polypeptide (for abbreviations see Table 70)	Solvent	Nitrogen shielding referred to neat nitromethane (assignments follow the sequence of amino acid residues)	Notes
$(Gly)_n$, Nylon-2	CF_3COOH	+271·4	(a)
		+270·7	(b)
		+270·4	(c)
		+271·3	(d)
	HCOOH	+270·4	(e)
		+271·9	(f)
	FSO_3H	+257·2	(f)
	CF_3CH_2OH	+275·0	(f)
	DMSO	+276·4	(f)
$(\beta$-Ala$)_n$, Nylon-3	CF_3COOH	+251·9	(a)(f)
		+251·4	(c)
		+251·0	(d)
	HCOOH	+259·2	(f)
	FSO_3H	+238·4	(f)
$(\gamma$-Abu$)_n$, Nylon-4	CF_3COOH	+247·7	(a)
		+247·4	(c)
		+247·8	(d)
	HCOOH	+254·2	(f)
	FSO_3H	+236·7	(f)
	CF_3CH_2OH	+257·3	(f)
$(\delta$-Ava$)_n$, Nylon-5	CF_3COOH	+244·0	(a)(d)
		+243·8	(c)
	HCOOH	+253·3	(f)
	FSO_3H	+235·4	(f)
	CF_3CH_2OH	+257·4	(f)
$(\varepsilon$-Aca$)_n$, Nylon-6	CF_3COOH	+240·2	(a)(d)
		+240·1	(c)
	HCOOH	+252·3	(f)
	FSO_3H	+234·7	(f)
	CF_3CH_2OH	+257·4	(f)
Nylon-7	CF_3COOH	+238·7	(d)
Nylon-8	CF_3COOH	+237·7	(d)
	HCOOH	+251·1	(f)
	FSO_3H	+234·1	(f)
	CF_3CH_2OH	+256·4	(f)
Nylon-12	CF_3COOH	+237·2	(d)
Poly(3-aminobutyric acid)	CF_3COOH	+237·1	(d)

TABLE 95—*cont.*

Polypeptide (for abbreviations see Table 70)	Solvent	Nitrogen shielding referred to neat nitromethane (assignments follow the sequence of amino acid residues)	Notes
$(Ala)_n$	CF_3COOH	+256·3 (D:L=1:5)	(a)
		+255·7	(g)
$(Leu)_n$	CF_3COOH	+254·7 (D:L=1:5)	(a)
$(Val)_n$	CF_3COOH	+254·0 (D:L=1:5)	(a)
$(Phe)_n$	CF_3COOH	+254·8 (D:L=1:3)	(a)
$(Pro)_n$	CF_3COOH	+238·9	(a)
$(Sar)_n$	CF_3COOH	+270·3	(f)
	HCOOH	+272·1	(f)
$(Ala\text{-}Ala\text{-}Gly)_n$	CF_3COOH	+254·4, +256·2, +272·1	(a)
$(Ala\text{-}Gly\text{-}Gly)_n$	CF_3COOH	+255·5, +272·0, +271·6	(a)
	HCOOH	+257·0, +272·9, +272·3	(f)
	H_2O+25% HCOOH	+257·0, +272·9, +272·2	(f)
$(Leu\text{-}Gly\text{-}Gly)_n$	CF_3COOH	+257·2, +270·6, +271·1	(a)
		+255·82, +268·92, +269·97	(h)
$(Val\text{-}Gly\text{-}Gly)_n$	CF_3COOH	+259·5, +267·9, +271·1	(a)
$(Phe\text{-}Gly\text{-}Gly)_n$	CF_3COOH	+258·5, +268·5, +271·6	(a)
	HCOOH	+260·7, +270·5, +272·4	(f)
$(Pro\text{-}Gly\text{-}Gly)_n$	CF_3COOH	+241·9, +270·2, +271·1	(a)
$(\beta\text{-}Ala\text{-}Gly\text{-}Gly)_n$	CF_3COOH	+259·0, +265·6, +272·1	(a)
	HCOOH	+262·7, +267·4, +272·1	(f)
	FSO_3H	+240·0, +253·4, +256·1	(f)
$(\gamma\text{-}Abu\text{-}Gly\text{-}Gly)_n$	CF_3COOH	+256·6, +265·1, +271·0	(a)
$(\delta\text{-}Ava\text{-}Gly\text{-}Gly)_n$	CF_3COOH	+254·2, +264·6, +271·2	(a)
	HCOOH	+259·3, +267·8, +274·7	(f)
$(\varepsilon\text{-}Aca\text{-}Gly\text{-}Gly)_n$	CF_3COOH	+252·3, +264·3, +271·3	(a)
	HCOOH	+257·5, +267·8, +271·7	(f)
$(Phg)_n$	CF_3COOH	+254·8	(g)
$(Lys)_n$	H_2O, pH 7·4	+258 (amide), +349 (amine)	(i)
	pH 1	+256·3 (amide), +343·6 (amine)	(e)
	pH 10	+256·9 (amide), +348·4 (amine)	(e)
	HCOOH	+256·1 (amide)	(e)
	DMSO	+260·7 (amide)	(e)
$iso(Lys)_n$	H_2O, pH 1	+256·2 (amide), +340·5 (amine)	(e)
	pH 13	+256·6 (amide), +347·9 (amine)	(e)
	HCOOH	+255·9 (amide)	(e)

TABLE 95—*cont.*

Polypeptide (for abbreviations see Table 70)	Solvent	Nitrogen shielding referred to neat nitromethane (assignments follow the sequence of amino acid residues)	Notes
$(Ala\text{-}Gly)_n$	CF_3COOH	+255·2, +271·9	(a)
		+255·1, +271·3	(g)
$(Ala\text{-}Ala\text{-}Gly\text{-}Gly)_n$	CF_3COOH	+255·4, +255·8, +272·1, +271·9	(a)
		+254·36, +254·73, +270·28, +271·05	(h)
$(\gamma\text{-}Abu\text{-}\beta\text{-}Ala\text{-}Gly)_n$	CF_3COOH	+260·1, +246·5, +265·9	(a)
		+258·40, +246·28, +265·55	(j)
$(\beta\text{-}Ala\text{-}\gamma\text{-}Abu\text{-}Gly)_n$	CF_3COOH	+259·9, +247·2, +264·6	(a)
		+259·09, +247·01, +264·17	(j)
$(\gamma\text{-}Abu\text{-}Ala\text{-}Gly)_n$	CF_3COOH	+256·5, +246·5, +271·9	(a)
		+256·08, +246·31, +271·19	(j)
$(Ala\text{-}\gamma\text{-}Abu\text{-}Gly)_n$	CF_3COOH	+255·3, +257·5, +262·0	(a)
		+254·99, +256·98, +261·42	(j)
$(Val\text{-}Ala\text{-}Gly)_n$	CF_3COOH	+259·7, +251·9, +271·5	(a)
$(Ala\text{-}Val\text{-}Gly)_n$	CF_3COOH	+255·0, +257·7, +267·9	(a)
$(Phe\text{-}Gly)_n$	CF_3COOH	+259·0, +269·3	(g)
$(\beta\text{-}Ala\text{-}Gly)_n$	CF_3COOH	+258·9, +266·8	(k)
$(\beta\text{-}Ala\text{-}\beta\text{-}Ala\text{-}Gly)_n$	CF_3COOH	+259·6, +249·3, +266·5	(k)

(a) Data from ref. 239; ^{15}N-labelled and non-labelled peptides; ^{15}N spectra; 9·12 MHz; field perpendicular to sample tube; 1·4 g polymer in 2 ml CF_3COOH; referred originally to NO_3^- in aqueous NH_4NO_3, +4·0 ppm from neat nitromethane (Table 6); conversion scheme II (Table 4).

(b) Data from ref. 215; ^{15}N natural abundance spectra; 9·12 MHz; field perpendicular to sample tube; 0·8–1·2 M solutions in H_2O; referred originally to NH_4^+ in 5 M NH_4NO_3 in 2 M HNO_3, +359·0 ppm from neat nitromethane (Table 6); conversion scheme II (Table 4).

(c) Data from ref. 217; ^{15}N-labelled and non-labelled compounds; 18·25 MHz; field parallel to sample tube; details as in note (a).

(d) Data from ref. 198; ^{15}N natural abundance spectra; details as in note (a).

(e) Data from ref. 240; ^{15}N natural abundance spectra; details as in note (c).

(f) Data from ref. 241; details as in note (d).

(g) Data from ref. 175; details as in note (d).

(h) Data from ref. 239; ^{15}N natural abundance spectra; 36·48 MHz; field parallel to sample tube; 1 g polymer in 5 ml CF_3COOH; details as in note (a); accuracy of *ca.* ±0·07 ppm pertains to relative positions of signals in the same spectrum only (i.e. spectral resolution).

(i) Data from ref. 242; ^{15}N natural abundance spectra; 10·1 MHz; other details as in note (a).

(j) Data from ref. 239; details as in note (h), but 18·25 MHz spectra.

(k) Data from ref. 243; details as in note (h).

TABLE 96

Limiting concentrations of paramagnetic ions for slowly relaxing ^{15}N nuclei in polypeptides[244]

Peptide*	Ion	Solvent	Cation-to-solute (monomer) ratio†
$PhCH_2OCO$-Gly-OH	Mn^{2+}	acetone	10^{-4}
		DMSO	5×10^{-4}
		pyridine	10^{-4}
		HCOOH	10^{-4}
$(Sar)_n$	Mn^{2+}	H_2O	2×10^{-4}
$(Gly)_n$	Dy^{3+}	CF_3COOH	10^{-3}
	Cr^{3+}	CF_3COOH	5×10^{-3}
	Cu^{2+}	CF_3COOH	2×10^{-5}
	Mn^{2+}	CF_3COOH	2×10^{-6}
		FSO_3H	5×10^{-4}
$(\beta\text{-Ala})_n$	Mn^{2+}	HCOOH	2×10^{-5}
		CF_3COOH	10^{-5}
		FSO_3H	2×10^{-3}
	Cu^{2+}	CF_3COOH	10^{-4}

* Gly = glycine; Sar = sarcosine; β-Ala = β-alanine.
† That resulting in a 20% reduction of ^{15}N signal height.

TABLE 97

Neighbouring residue effects on nitrogen shielding in X-Gly-Gly polypeptides

X	Primary effect of X upon Gly	Primary + secondary + tertiary effect of Gly upon X	Secondary + tertiary effect of X upon Gly
Ala	+0·6	−0·8	+0·2
Leu	−0·8	+2·5	−0·3
Val	−3·5	+5·5	−0·3
Phe	−2·9	+3·8	+0·2
Pro	−1·2	+3·0	−0·3
β-Ala	−5·8	+7·1	+0·7
γ-Abu	−6·3	+8·9	+0·4
δ-Ava	−6·8	+10·2	−0·2
ε-Aca	−7·1	+12·1	+0·2
Calculated from difference in shieldings	$(X\text{-Gly-Gly})_n - (Gly)_n$	$(X\text{-Gly-Gly})_n - (X)_n$ for solutions in CF_3COOH	$(X\text{-Gly-Gly})_n - (Gly)_n$

Data from ref. 239; effects refer to the following scheme:

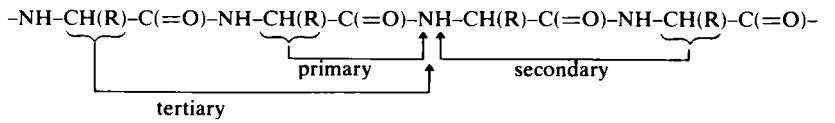

TABLE 98

Substituent effects on nitrogen shielding in amino acids, cyclodipeptides, and peptide homopolymers referred to that in the corresponding glycine moieties

	Nitrogen shielding referred to X = Gly		
X	H–X–OH in CF_3COOH	cyclo(X–X) in CF_3COOH	$(X)_n$ in CF_3COOH
Gly	0·0000	0·0000	0·0000 (arbitrary)
Ala	−13·3	−13·0	−15·0
Leu	−11·2	−10·1	−16·6
Val	−7·3	−7·3	−17·3
Phe	−9·4	−11·3	−16·5
Sar	−3·1	−1·9	−1·0
Pro	−25·8	−26·0	−32·4
Phg	−16·8		−16·5

Data from ref. 175; for abbreviations of amino acid residues see Table 70.

TABLE 99

Identification of amide linkages in glycine–β-alanine polymers by means of nitrogen shielding data

Peptide polymer	Nitrogen shielding, referred to neat nitromethane, for individual peptide linkages			
(solution in CF_3COOH)	β-Ala-β-Ala	Gly-β-Ala	β-Ala-Gly	Gly-Gly
$(Gly)_n$				+271·3
$(\beta\text{-Ala})_n$	+251·9			
$(\beta\text{-Ala-Gly})_n$		+258·9	+266·8	
$(\beta\text{-Ala-Gly-Gly})_n$		+259·0	+265·6	+272·1
$(\beta\text{-Ala-}\beta\text{-Ala-Gly})_n$	+249·3	+259·6	+266·5	
random $(Gly,\beta\text{-Ala})_n$	+250·8, +252·1	+259·6	+266·4	+271·8

↓

(Gly)-β-Ala-β-Ala-(β-Ala)
(β-Ala)-β-Ala-β-Ala(Gly)
(Gly)-β-Ala-β-Ala-(Gly)
(β-Ala)-β-Ala-β-Ala-(β-Ala)

Data from ref. 243; ^{15}N natural abundance spectra; 36·48 MHz; field parallel to sample tube; referred originally to NO_3^- in aqueous NH_4NO_3, +4·0 ppm from neat nitromethane (Table 6); conversion scheme II (Table 4); 1 g polymer in 5 ml solvent.

TABLE 100

Differentiation between *cis* and *trans* sarcosine bridges in polypeptides containing sarcosine residues

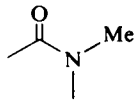

"*cis*"

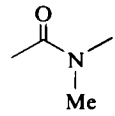

"*trans*"

Polypeptide	Solvent	Proton decoupling	Nitrogen shielding referred to neat nitromethane (values within parentheses represent amino acid moieties in order shown by formulae; plus signs are omitted)
$(Sar)_n$	H_2O	no	(270·45, 270·78, 270·89)
		yes	(271·12, 271·28, 271·41)
	DMSO	no	(276·27, 276·38, 276·55, 276·65)
		yes	(277·08, 277·16, 277·35, 277·43)
$(\beta$-Ala-Sar-Gly$)_n$	H_2O	no	(258·65; 263·70), (267·95; 268·90), *cis* + *trans* *cis* *trans* (266·47, 271·50; 267·50, 272·60) *cis* *trans*
		yes	(261·20; 261·41), (269·02; signal nulled), *trans* *cis* *trans* *cis* (269·02; 270·02) *cis* *trans*
$(\beta$-Ala-Sar-Ala$)_n$	H_2O	no	(259·60, 264·70), (267·90; 269·00), *cis*+*trans* *cis* *trans* (251·50, 256·60; 252·40, 257·51) *trans* *cis*
		yes	(262·23; 262·50), (269·00; signal nulled), *trans* *cis* *trans* *cis* (254·10; 255·06) *cis* *trans*

Data from ref. 245; ^{15}N natural abundance spectra; 18·25 MHz; field parallel to sample tube; referred originally to NO_3^- in aqueous NH_4NO_3, +4·0 ppm from neat nitromethane (Table 6); conversion scheme II (Table 4); 5 g polymer in 25 ml solvent; accuracy of *ca.* ±0·05 ppm refers only to relative positions of signals in the same spectrum.

TABLE 101

Nitrogen shieldings in poly-L-ornithine

Polypeptide	Solvent (0·8 M solutions)	pH	Nitrogen shielding referred to neat nitromethane NH	NH_2
$(Orn)_n$ $n = 45–50$ and 95–100	H_2O	0·5–0·6	+257·0	+346·4
		4·0–4·1	+257·0	+346·4
		6·0–6·1	+257·0	+346·4
		8·2–8·3	+257·0	+346·4
		9·0–9·1	+257·2	+346·8
		9·7–9·8	+257·4	+349·0
		10·5–10·6	+257·8	+352·0
		11·1–11·2	+257·9	+354·2
		12·0–12·1	+258·1	+354·9
		12·4–12·5	+258·1	+355·1
$(Orn)_n$ $n = 95–100$	H_2O/MeOH (7:3 v/v)	2·0–2·1	+257·9	+346·9
		5·0–5·1	+257·9	+346·9
		7·0–7·1	+257·9	+346·9
		8·0–8·1	+257·9	+346·9
		8·9–9·0	+257·9	+348·6
		9·9–10·0	+258·2	+351·6
		10·5–10·7	broad	+354·6
		11·4–11·5	broad	+355·7
		12·1–12·2	broad	+355·7

Data from ref. 194, ^{15}N natural abundance spectra; 9·12 MHz; field perpendicular to sample tube; referred originally to NO_3^- in aqueous NH_4NO_3, +4·0 ppm from neat nitromethane (Table 6); conversion scheme II (Table 4).

TABLE 102

Nitrogen shieldings in some polypeptides with sulphonamide linkages

Polypeptide (for abbreviations see Table 70)	Solvent	Nitrogen shielding referred to neat nitromethane (values for sulphonamide bridge are set in *italics*; assignments in order of residues)	Notes
$(\gamma\text{-Aps-}\beta\text{-Ala})_n$	CF_3COOH	+248·7, *+291·6*	(a)
$(\gamma\text{-Aps-}\varepsilon\text{-Aca})_n$	CF_3COOH	+245·6, *+292·3*	(b)
$(\text{Sulf-}\varepsilon\text{-Aca})_n$	CF_3COOH	+243·1, *+312·2*	(b)
$(\text{Tau-}\varepsilon\text{-Aca})_n$	CF_3COOH	+253·8, *+290·1*	(a)
		+254·3, *+291·1*	(b)
	HCOOH	+261·4, *+290·2*	(c)
	acetone/DMSO	+268·5, *+288·0*	(c)
$(\text{Tau-}\gamma\text{-Abu})_n$	CF_3COOH	+255·5, *+290·5*	(a)
$(\text{Tau-}\beta\text{-Ala})_n$	CF_3COOH	+256·6, *+290·9*	(a)
	H_2O, pH 13·6	+258·5, *+278·0*	(a)
$(\text{Tau-Gly})_n$	CF_3COOH	+264·3, *+294·9*	(a)
		+265·0, *+295·9*	(b)
$(\text{Tau-Gly-Gly})_n$	CF_3COOH	+265·2, *+295·7*, +271·2	(b)
$(\text{Tau-Gly-}\beta\text{-Ala})_n$	CF_3COOH	+259·2, *+295·9*, +257·1	(b)
$(\text{Tau-}\beta\text{-Ala-Gly})_n$	CF_3COOH	+264·7, *+292·0*, +265·4	(b)

(a) Data from ref. 246; ^{15}N natural abundance spectra; 9·12 MHz; field perpendicular to sample tube; referred originally to NO_3^- in aqueous NH_4NO_3, +4·0 ppm from neat nitromethane (Table 6); conversion scheme II (Table 4).

(b) Same as in note (a), but 18·25 MHz spectra, field parallel to sample tube.

(c) Data from ref. 241; details as in note (a).

TABLE 103

Nitrogen shieldings in some azides

Compound	Solution	Nitrogen shielding in the azido group referred to neat nitromethane RN	central N	terminal N	Notes
HN_3	in Et_2O	+324·5	+134·1	+178·6	(a)
ClN_3	in CD_2Cl_2	+273·1	+123·7	+114·1	(a)
MeN_3	30% in benzene	+321·7	+130·2	+171·5	(b)
PhN_3	25% in acetone	+288·5	+136·7	+147·4	(b)
EtN_3	neat liquid	+307·7	+132·0	+169·2	(c)
	0·30 M in CCl_4	+306·4	+132·1	+166·6	(c)
Bu^tN_3	neat liquid	+286 ± 2	+134 ± 2	+162 ± 2	(d)
$pO_2N{\cdot}C_6H_4{\cdot}N_3$	10% in DMSO	+282·0	+140·0	+144·1	(b)
$2,4,6\text{-}(NO_2)_3\text{-}C_6H_2{\cdot}N_3$	20% in DMSO	+289·3	+151·1	+142·7	(b)
$NC\text{–}N_3$	5% in MeCN	+315·3	+149·7	+147·5	(b)
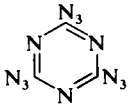	10% in CH_2Cl_2	+261·1	+145·6	+134·8	(b)
$p\text{Me}{\cdot}C_6H_4{\cdot}SO_2N_3$	in cyclohexane	+243·4	+148·1	+140·2	(e)
	in MeOH	?	+148·6	+139·4	(e)
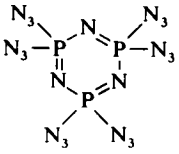	in toluene-d_8	+290·2	+151·4	+165·7	(f)
$Me_2P(O)N_3$	neat liquid	?	+146·7	+177	(f) (^{14}N)
	in $CDCl_3$	+294·8	+147·9	+175·5	(f)
$Me_2P(S)N_3$	in acetone-d_6	+289·9	+143·8	+170·3	(f)
$Me_2P(Se)N_3$	in benzene-d_6	+290·6	+142·8	+168·5	(f)
$Et_2P(O)N_3$	neat liquid	?	+146	+176	(f) (^{14}N)
	in benzene-d_6	+289·5	+145·4	+177·3	(f)
$Et_2P(S)N_3$	neat liquid	?	+137	+167	(f) (^{14}N)
	in benzene-d_6	+294·2	+143·4	+172·8	(f)
$(MeO)_2P(O)N_3$	in MeCN	+304·6	+148·7	+174·2	(f)
Me_3SnN_3	in pyridine				
	+71 °C	+272·9	+135·2	+272·9	(g)
	+35 °C	+272·2	+134·6	+272·2	(g)
	−38 °C	+272·0	+134·5	+272·0	(g)
	−48 °C	+272·2	+134·0	+272·2	(g)
$(Me_2AlN_3)_3$	in toluene				
	+35 °C	+316·1	+143·8	+180·5	(h)
	−59 °C	+316·0	+144·1	+181·0	(h)
	−109 °C	+315·3	+143·8	+180·9	(h)

TABLE 103—*cont.*

Compound	Solution	Nitrogen shielding in the azido group referred to neat nitromethane RN	central N	terminal N	Notes
$(Me_2GaN_3)_3$	in toluene				
	+35 °C	?	+139·5	?	(h)
	−40 °C	+314·7	+139·4	+189·6	(h)
	−90 °C	+315·1	+138·6	+190·5	(h)
Me_2AsN_3	neat liquid				
	+68 °C	?	+136·3	?	(h)
	+35 °C	?	+136·0	?	(h)
	−40 °C	+318·5	+135·9	+198·5	(h)
	−60 °C	+317·1	+135·9	+199·4	(h)
$Li^+N_3^-$	in H_2O	+280·4	+131·8	+280·4	(f)
$Na^+N_3^-$	0·30 M in H_2O	+280·6	+131·5	+280·6	(i)
	5·13 M in H_2O	+281·7	+132·2	+281·7	(i)
	in H_2O	+280·8	+131·4	+280·8	(f)

(a) Data from ref. 247; ^{15}N-labelled azido group; ^{15}N spectra; 10·4 MHz; field perpendicular to sample tube; referred originally to 1 M $NaNO_3$, +3·5 ppm from neat nitromethane (Table 6); conversion scheme II (Table 4).

(b) Data from ref. 248; see note (a).

(c) Data from ref. 179; ^{14}N continuous-wave spectra; 4·33 MHz; high-precision differential saturation technique with total lineshape fitting; concentric spherical sample/standard containers in order to eliminate bulk susceptibility effects; referred to neat nitromethane; standard deviation for the shielding is less than 0·1 ppm.

(d) Data quoted from ref. 1, p. 177, and references therein.

(e) Data from ref. 162; ^{15}N natural abundance spectra; 18·25 MHz; field parallel to sample tube; referred originally to 1 M DNO_3, +6·2 ppm from neat nitromethane (Table 6); conversion scheme IV (Table 4).

(f) Data from ref. 254; details as in note (a) if not stated otherwise, or ^{14}N continuous-wave spectra for neat liquids; 7·23 MHz; field perpendicular to sample tube; standard as in note (a).

(g) Data from ref. 255; see note (a).

(h) Data from ref. 256; see note (a).

(i) Data from ref. 80; details as in note (c).

TABLE 104

^{15}N spectral data for reaction of nitrogen scrambling in *p*-toluenesulphonyl azide

Starting reaction mixture (Ts = *p*Me·C_6H_4·SO_2–)	Nitrogen shieldings referred to neat nitromethane (signal multiplicities, and assignments for final stages of reaction)	
0·005 M $TsNH^-$ Na^+ 0·005 M $TsNH_2$ 0·0081 M $TsN{=}N^+{=}{}^{15}N^-$ in dry DMSO	+240·4 (singlet)	$Ts^{15}N{=}N^+{=}N^-$
	+148·2 (singlet)	$TsN{=}{}^{15}N^+{=}N^-$
	+138·3 (singlet)	$TsN{=}N^+{=}{}^{15}N^-$
	+277·7 (singlet)	$Na^+(^{15}NNN)^-$
	+132·0 (singlet)	$Na^+(N^{15}NN)^-$
	+285 (singlet first stage)	$Ts^{15}NH^- + Ts^{15}NH_2$ $Ts^{15}NH_2 + Ts^{15}NH^-$
	+285 (triplet, final stage)	$Ts^{15}NH_2$
	+217·8 (singlet, final stage)	$(Ts^{15}NTs)^-$
	+70·3	$^{15}N{\equiv}N$
	+30·3	$[TsN{=}N^{15}N^-Ts \leftrightarrow TsN^-N{=}{}^{15}NTs]$
$Ts^{15}N{=}N^+{=}N^-$ $TsN{=}{}^{15}N^+{=}N^-$ $TsN{=}N^+{=}{}^{15}N^-$ } 0·012 M 0·012 M $Na^+N_3^-$ (non-labelled) in DMSO	+240·4 (singlet)	$Ts^{15}NNN$
	+148·2 (singlet)	$TsN^{15}NN$
	+138·3 (singlet)	$TsNN^{15}N$
	+277·7 (singlet)	$Na^+(^{15}NNN)^-$
	+132·0 (singlet)	$Na^+(N^{15}NN)^-$
	+30·3 (singlet)	see above
	−154·1 (singlet)	$TsN{=}{}^{15}NN^-Ts$
	+70·3 (trace)	$^{15}N{\equiv}N$

Data from ref. 257; ^{15}N spectra; 18·25 MHz; field parallel to sample tube; referred originally to 1 M DNO_3, +6·2 ppm from neat nitromethane (Table 6); conversion scheme (Table 4).

TABLE 105

Nitrogen shieldings in triaza- and diaza-pentadienium salts (perchlorates, 0·6 M in DMSO)

Substituents				Nitrogen shielding referred to neat nitromethane for nitrogen atoms and structures specified			
R^1	R^2	R^3	R^4	N-1	N-2	N-3	N-5
				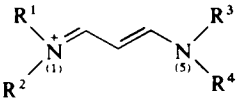			
Me	Me	Me	Me	+257·3			+257·3
Ph	H	Me	Me	+237·1			+247·0
Ph	H	Ph	H	+229·3			+229·3
				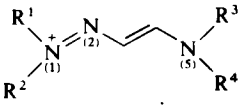			
Me	Me	Me	Me	+204·6	−28·8		+229·7
Ph	H	Me	Me	+173·1	−7·4		+215·9
Me	Me	Ph	H	+194·2	−33·3		+214·7
Ph	H	Ph	H	+184·4	−11·0		+200·0
				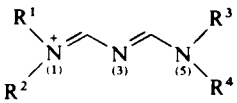			
Me	Me	Me	Me	+246·2		+164·9	+246·2

Data from ref. 258; ^{15}N natural abundance spectra; ^1H-undecoupled; 27·35 MHz; field parallel to sample tube; referred originally to NO_3^- in 5 M NH_4NO_3 in 2 M HNO_3, +4·64 ppm from neat nitromethane, but reported relative to NH_4^+; +356·25 ppm from the NO_3^- standard (assumed); thus, the conversion constant is 4·64 + 356·25 = 360·9 ppm, according to Table 6 and conversion scheme II (Table 4).

TABLE 106

Nitrogen shieldings in some cyanates, isocyanates, thiocyanates, and isothiocyanates

Compound	Solution	Nitrogen shielding referred to neat nitromethane	Notes
MeN=C=O	neat liquid	+365·42 ± 0·06	(a)
		+365·3	(b)
EtN=C=O	neat liquid	+348·6	(b)
$Bu^nN=C=O$	neat liquid	+352·1	(b)
$Pr^iN=C=O$	neat liquid	+335·5	(b)
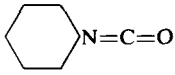	neat liquid	+338·3	(b)
$Bu^tN=C=O$	neat liquid	+326·0	(b)
PhN=C=O	neat liquid	+333·7	(b)
pCl·C_6H_4·N=C=O	3 M in DMSO	+334·2	(b)
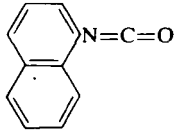	neat liquid	+338·0	(b)
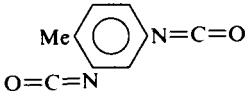	neat liquid	+335·5, +335·9	(b)
$P(NCO)_3$	in benzene	+329 ± 5	(c)
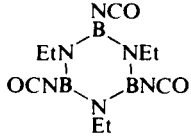	in CH_2Cl_2	+346 ± 3 (NCO)	(d)
EtOCN	in Et_2O	+222 ● 1	(g)
PhOCN	neat liquid	+211 ± 3	(e)
pMeO·C_6H_4·OCN	neat liquid	+215 ± 3	(e)
pCl·C_6H_4·OCN	neat liquid (75 °C)	+212 ± 3	(e)
pO_2N·C_6H_4·OCN	neat liquid (85 °C)	+189 ± 5 (OCN)	(e)
K^+ $(NCO)^-$	6·2 M in H_2O (satd.)	+302·91 ± 0·14	(f)
	0·30 M in H_2O	+302·60 ± 0·14	(f)
MeN=C=S	neat liquid (35 °C)	+289·80 ± 0·07	(a)
	3 M in DMSO	+289·9	(b)
EtN=C=S	neat liquid	+277·0	(b)
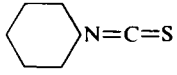	neat liquid	+268·2	(b)
PhN=C=S	neat liquid	+273·1	(b)

TABLE 106—*cont.*

Compound	Solution	Nitrogen shielding referred to neat nitromethane	Notes
$(Me_3Si)_2NN{=}C{=}S$	neat liquid	+266 ± 3 (NCS)	(h)
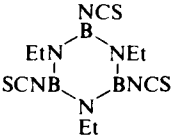	in CH_2Cl_2	+268 ± 3 (NCS)	(d)
EtSCN	neat liquid	+102 ± 2	(g)
Me_2NSCN	neat liquid	+86 ± 3 (SCN)	(h)
$(Me_3Si)_2NSCN$	neat liquid	+99 ± 3 (SCN)	(h)
K^+ $(NCS)^-$	9·51 M in H_2O (satd.)	+170·04 ± 0·11	(f)
	0·30 M in H_2O	+174·07 ± 0·17	(f)
	inf. dil. in dimethylformamide	+163·2	(i)
Li^+ $(NCS)^-$	inf. dil. in dimethylformamide	+164	(i)
	inf. dil. in dimethyl carbonate	+190	(i)
	inf. dil. in tetrahydrofuran	+196	(i)
	inf. dil. in Et_2O	+203	(i)

(a) Data from ref. 85; ^{14}N continuous-wave spectra; high-precision differential saturation technique with full lineshape fitting; 4·33 MHz; concentric spherical sample/standard containers in order to eliminate bulk susceptibility effects; referred to neat nitromethane.

(b) Data from ref. 259; ^{15}N natural abundance spectra; 18·25 MHz; field parallel to sample tube; referred originally to 1 M DNO_3, +6·2 ppm from neat nitromethane (Table 6); conversion scheme IV (Table 4).

(c) Data from ref. 143; ^{14}N continuous-wave measurements; wide-line spectrometer; 3 MHz; referred originally to NH_4^+ in saturated aqueous NH_4NO_3, +359·6 ppm from neat nitromethane; low-precision data.

(d) Data from ref. 34; ^{14}N continuous-wave spectra; 7·22 MHz; field perpendicular to sample tube; referred originally to saturated aqueous $NaNO_3$, +3·7 ppm from neat nitromethane (Table 6); conversion scheme II (Table 4).

(e) Data quoted from ref. 1, p. 175, and references therein.

(f) Data from ref. 80; see note (a).

(g) Data from ref. 2, p. 201, and references therein.

(h) Data from ref. 137; see note (d).

(i) Data from ref. 261; ^{15}N natural abundance spectra; 9·117 MHz; field perpendicular to sample tube; referred originally to aqueous $NaNO_3$, +3·7 ppm from neat nitromethane (Table 6); conversion scheme II (Table 4).

TABLE 107

Distinction between isothiocyanato and thiocyanato ligands from nitrogen shieldings

Complex (solution in CH_2Cl_2)	Nitrogen shielding referred to neat nitromethane	
S-bound ligands (thiocyanates)		
$(Bu_4N)_2[Pd(SCN)_4]$	+127·6	
$(Bu_4N)_2[Pt(SCN)_4]$	+128·8	
$(Bu_4N)_2[Hg(SCN)_4]$	+138·4	
N-bound ligands (isothiocyanates)		
$(Bu_4N)_2[Zn(NCS)_4]$	+221·8	
$(Bu_4N)_2[Cd(NCS)_4]$	+204·2	
trans-$[Pt(NCS)_2(PBu_3)_2]$	+309·7	(doublet)
trans-$[Pt(NCS)(SCN)(PBu_3)_2]$	+281·0	(NCS) (doublet)
	?	(SCN)

Data from ref. 262; ^{15}N enriched ligands; ^{15}N spectra; 9·12 MHz; field perpendicular to sample tube; referred originally to aqueous NH_4Cl, +352·9 ppm from neat nitromethane (Table 6); conversion scheme II (Table 4); assignments verified by ^{15}N–^{195}Pt couplings in nitrogen and platinum NMR spectra.

TABLE 108

Nitrogen shieldings in some nitriles, isonitriles, nitrile *N*-oxides (fulminates), and related structures

Compound	Solution	Nitrogen shielding referred to neat nitromethane	Notes
HCN	neat liquid (30 °C)	+129	(a)
ClCN	neat liquid (30 °C)	+144	(a)
MeCN	neat liquid	+135·83 ± 0·06	(b)
		+136·4 (+135·9)	(c)
	0·30 M in CCl_4	+127·44 ± 0·28	(d)
	0·30 M in $MeNO_2$	+137·77 ± 0·32	(d)
	0·30 M in acetone	+132·99 ± 0·13	(d)
	0·30 M in H_2O	+144·95 ± 0·26	(d)
	10% v/v in CF_3COOH	+152·8	(c)
$MeC{\equiv}NH^+$	10% v/v in 90% H_2SO_4	+252·2	(c)
EtCN	neat liquid	+136·68 ± 0·08	(e)
		+138·8	(f)
Pr^nCN	neat liquid	+133·17 ± 0·11	(e)
Pr^iCN	neat liquid	+135·60 ± 0·11	(e)
Bu^tCN	neat liquid	+135·92 ± 0·14	(e)
$K^+ (CN)^-$	8·5 M in H_2O (satd.)	+102·48 ± 0·09	(d)
	0·30 M in H_2O	+106·11 ± 0·12	(d)
$MeN(N{=}O)CH_2CN$	neat liquid	+133·2 (CN, isomer *Z*)	(g)
		+128·4 (CN, isomer *E*)	(g)
	2 M in MeOH	+131·1 (CN, isomer *Z*)	(h)
		+126·1 (CN, isomer *E*)	(h)
$Pr^iN(N{=}O)CH_2CN$	neat liquid	+133·2 (CN, isomer *Z*)	(g)
$MeN(N{=}O)CH(Me)CN$	neat liquid	+132·7 (CN, isomer *Z*)	(g)
		+126·5 (CN, isomer *E*)	(g)
trans-$PhN{=}NC(Me_2)CN$	in benzene	+122 (CN)	(i)
cis-$PhN{=}NC(Me_2)CN$	in benzene	+112 (CN)	(i)
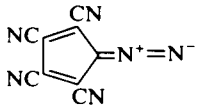	in DMSO	+103·9 +110·0 (CN)	(j)
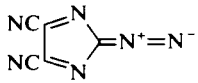	in DMSO	+114·2 (CN)	(j)
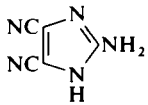	in DMSO/MeOH	+111·8 (CN)	(j)
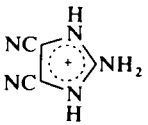	in $DMSO/H_2O/HCl$	+109·4 (CN)	(j)

TABLE 108—*cont.*

Compound	Solution	Nitrogen shielding referred to neat nitromethane	Notes
MeNC	neat liquid	+219·6	(k)
EtNC	neat liquid	+205·1	(k)
Pr^nNC	neat liquid	+206·0	(k)
Me_3CCH_2NC	neat liquid	+211·3	(k)
Pr^iNC	neat liquid	+193·4	(k)
Bu^tNC	neat liquid	+184·9	(k)
	in $CHCl_3$	+182·1	(l)
PhNC	neat liquid	+204	(k)
Et_2NNC	neat liquid	+199 (NC)	(m)
$(Me_3Si)_2NNC$	neat liquid	+215 ± 3	(m)
2,4,6-Me_3-C_6H_2·CNO	in CH_2Cl_2	+169	(k)
pO_2N·C_6H_4·CNO	in acetone	+179 (CNO)	(k)
	in benzene	+170 ± 3 (CNO)	(k)
Na^+ $(CNO)^-$	in H_2O	+180	(k)

(a) Data from ref. 27; ^{14}N continuous-wave spectra; 7·22 MHz; field perpendicular to sample tube; referred originally to saturated aqueous $NaNO_3$, +3·7 ppm from neat nitromethane (Table 6); conversion scheme II (Table 4).

(b) Data from ref. 85; ^{14}N continuous-wave spectra; high-precision differential saturation technique with full lineshape fitting; 4·33 MHz; concentric spherical sample/standard containers in order to eliminate bulk susceptibility effects; referred to neat nitromethane.

(c) Data from ref. 189; ^{15}N natural abundance spectra; 18·25 MHz; field parallel to sample tube; referred originally to 1 M DNO_3, +6·2 ppm from neat nitromethane (Table 6); conversion scheme IV (Table 4); if bulk susceptibility corrections are introduced for the value for MeCN (the corrected value is given in parentheses), an almost perfect agreement with the high-precision ^{14}N measurement [note (b)] is obtained.

(d) Data from ref. 80, details as in note (b).

(e) Data from ref. 179; details as in note (b).

(f) Data from ref. 263, ^{15}N natural abundance spectra; 9·12 MHz; field perpendicular to sample tube; referred originally as in note (a).

(g) Data from ref. 45; details as in note (f); $Cr(acac)_3$ added to the samples.

(h) Data from ref. 264; ^{15}N selectively labelled compounds; ^{15}N spectra; 18·25 MHz; field parallel to sample tube; referred originally to neat nitromethane (uncorrected for bulk susceptibility effects).

(i) Data from ref. 144; ^{15}N-labelled compounds; ^{15}N spectra; 10·1 MHz; field perpendicular to sample tube; referred originally to aqueous NO_3^-, +3·7 ppm from neat nitromethane (Table 6); conversion scheme II (Table 4).

(j) Data from ref. 162; details as in note (c).

(k) Data from ref. 2, p. 201, and references therein; +3·7 ppm was added to the values that were referred to external aqueous $NaNO_3$.

(l) Data from ref. 265; high-resolution ^{14}N continuous-wave spectra; 7·14 MHz; field perpendicular to sample tube; referred originally to NH_4^+ in aqueous NH_4NO_3, +359·6 ppm from neat nitromethane (Table 6); conversion scheme II (Table 4).

(m) Data from ref. 137; details as in note (a).

TABLE 109

Effects of solutes on nitrogen shielding in acetonitrile

Solute	Concentration (mol/kg solution)	Nitrogen shielding of CH_3CN as solvent: referred to neat nitromethane	Nitrogen shielding of CH_3CN as solvent: referred to neat CH_3CN
$AgNO_3$	0·98	+139·2	+3·4
	2·98	+145·1	+9·2
	5·07	+150·4	+14·5
	8·10	+156·6	+20·8
$Ba(ClO_4)_2$	1·00	+138·1	+2·2
	2·61	+140·8	+4·9
	3·25	+141·4	+5·6
$AlCl_3$	0·50	+136·1	+0·2
	1·18	+136·2	+0·3
	2·16	+136·4	+0·6

Data from ref. 266; natural abundance ^{15}N spectra; 9·115 MHz; field perpendicular to sample tube; referred originally to neat MeCN, +135·83 ppm from neat nitromethane (Table 6); conversion scheme IV (Table 4); the shifts are uncorrected for bulk susceptibility effects, and therefore the accuracy reported (±0·05 ppm) seems to be too optimistic.

TABLE 110

Nitrogen shieldings in t-butyl isocyanide complexes with palladium in $CDCl_3$ solutions

Structure	Nitrogen shielding for isocyanide groups referred to neat nitromethane		
	X = Cl	X = Br	X = I
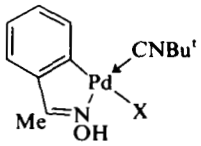	+186·1	+184·9	+181·6
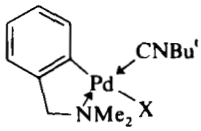	+189·2	+187·2	+183·4
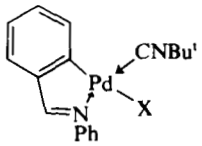	+188·0		

Data from ref. 265; high-resolution ^{14}N spectra; 7·14 MHz; field perpendicular to sample tube; referred originally to NH_4^+ in aqueous NH_4NO_3, +359·6 ppm from neat nitromethane (Table 6); conversion scheme II (Table 4); value for Bu^{t}NC in chloroform is +182·1 ppm from neat nitromethane.

TABLE 111

Nitrogen shieldings in the cyanide ion complexed with hemins and hemoproteins

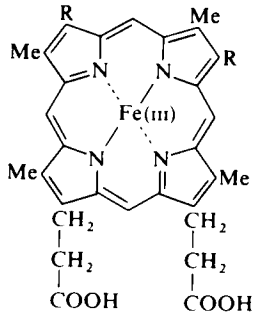

protohemin R = CH=CH$_2$
deuterohemin R = H
mesohemin R = Et
hematohemin R = CH(OH)Me

Py = pyridine

Compound	Solvent	Nitrogen shielding for CN, referred to neat nitromethane	Notes
Hemins			
protohemin(CN)$_2$	DMSO	−728	(a)(b)
	DMSO/D$_2$O(18 : 1)	−712	(a)
	DMSO/D$_2$O(18 : 2)	−695	(a)
	DMSO/D$_2$O(18 : 4)	−667	(a)
	pyridine	−692	(b)
	pyridine/D$_2$O(20 : 4)	−653	(a)
	pyridine/D$_2$O(20 : 5)	−648	(a)
	pyridine/D$_2$O(20 : 7)	−633	(a)
	MeOD	−502	(b)
		−496	(a)
	MeOD/D$_2$O(1 : 1)	−476	(b)
		−486	(a)
	H$_2$O, pH 9·4	−447	(b)
	H$_2$O, pH 9·2	−444	(b)
protohemin(Py)(CN)	pyridine/H$_2$O(5 : 1)	−996	(a)
	pyridine/H$_2$O(2 : 1)	−937	(a)
	pyridine/H$_2$O(3 : 2)	−927	(a)
	pyridine/D$_2$O(500 : 1 hemin)	−985	(b)
	pyridine/D$_2$O(230 : 1 hemin)	−1030	(b)
protohemin(3,5-Me$_2$-Py)(CN)	3,5-Me$_2$Py/D$_2$O (500 : 1 hemin)	−1066	(b)
protohemin(4-acetyl-Py)(CN)	4-acetyl-Py/D$_2$O (500 : 1 hemin)	−941	(b)
protohemin(*N*-Me-imidazole)(CN)	*N*-Me-imidazole/DMSO	−992	(b)
deuterohemin(CN)$_2$	DMSO	−734	(b)
	DMSO/D$_2$O(20 : 1)	−712	(b)
	MeOD	−505	(b)
deuterohemin(Py)(CN)	pyridine/D$_2$O(230 : 1 hemin)	−1036	(b)
mesohemin(CN)$_2$	DMSO	−716	(b)
	MeOD	−492	(b)
mesohemin(Py)(CN)	pyridine/D$_2$O(500 : 1 hemin)	−980	(b)

TABLE 111—*cont.*

Compound	Solvent	Nitrogen shielding for CN, referred to neat nitromethane	Notes
hematohemin$(CN)_2$	MeOD	−491	(b)
hematohemin(Py)(CN)	pyridine/D_2O(500 : 1 hemin)	−978	(b)
octaethylporphyrin$(CN)_2$	DMSO	−714	(b)
	MeOD	−470	(b)
Hemoproteins with CN ions bound to Fe(III) of heme			
horse myoglobin	H_2O, pH 6·9	−944	(c)
	pH 8·0	−935	(c)
	pH 9·0	−932	(c)
sperm whale myoglobin	H_2O, pH 8·8	−941	(c)
sperm whale mesomyoglobin	H_2O, pH 8·6	−906	(c)
human adult hemoglobin	H_2O, pH 7·3	−971 (α) −1043 (β)	(c) (c)
horse cytochrome c	H_2O, pH 6·6	−838	(c)
	pH 7·8	−843	(c)
	pH 9·0	−844	(c)
horse cytochrome c (carboxymethylated)	H_2O, pH 9·0	−848	(c)

(a) Data from ref. 267; ^{15}N-labelled KCN; ^{15}N spectra; 10·15 MHz; field perpendicular to sample tube; referred originally to *internal* NO_3^-, *ca.* +4 ppm from neat nitromethane (Table 6).
(b) Data from ref. 268; details as above.
(c) Data from ref. 269 and ref. 270; details as above.

TABLE 112

Nitrogen shieldings in some azoles

Compound	Solution	Nitrogen shielding referred to neat nitromethane	Notes
 (pyrrole)	neat liquid	+231·4 ± 0·4	(a)
	0·15 M in acetone	+229·6 ± 0·4	(a)
	0·15 M in DMSO	+222·3 ± 0·4	(a)
	0·10 M in CCl_4	+236·4 ± 0·4	(a)
	neat liquid	+231·4	(b)
	1·0 M in acetone	+231·6	(b)
			
X = $B(NMe_2)_2$	neat liquid	+230 (pyrrole)	(c)
$B(Me)NH_2$	neat liquid	+227 (pyrrole)	(c)
BEt_2	neat liquid	+214	(c)
$BCH_2CH_2CH_2CH_2$	neat liquid	+212	(c)
BCl_2	neat liquid	+210	(c)
	neat liquid	+202	(d)
	neat liquid	+206·5	(b)
	2·0 M in acetone	+205·6	(b)
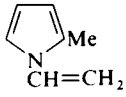	neat liquid	+208·5	(b)
	2·0 M in acetone	+207·5	(b)
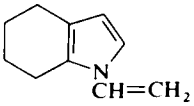	neat liquid	+216·9	(b)
	2·0 M in acetone	+212·9	(b)
			
X = $GeMe_2$	neat liquid	+221	(d)
$SnMe_2$	neat liquid	+222	(d)
$SiMe_3$	neat liquid	+221	(d)

TABLE 112—*cont.*

Compound	Solution	Nitrogen shielding referred to neat nitromethane	Notes
$PbMe_2$	neat liquid	+215	(d)
PMe_2	neat liquid	+227	(d)
BMe_2	satd. in Et_2O	+186 ± 10	(d)
 (pyrazole)	2 M in $CHCl_3$	+134·7 (N ⇄ NH)	(e)
	4 M in DMSO	+173·1 (NH)	(e)
		+79·8 (–N=)	(e)
	2 M in CF_3CH_2OH	+143·4 (N ⇄ NH)	(e)
	2 M in MeCOOH	+144·4 (N ⇄ NH)	(e)
	2 M in H_2O	+139·0 (N ⇄ NH)	(e)
	Cl^-, 2 M in MeCOOH	+184·9	(e)
	Cl^-, 2 M in MeOH	+182·0	(e)
	Cl^-, in H_2O pH 3·43	+145·5	(e)
	pH 1·10	+182·9	(e)
	pH 0·95	+183·9	(e)
	pH 0·45	+185·1	(e)
	pH 0·30	+185·3	(e)
	2 M in $CHCl_3$	+180·8 (NMe)	(e)
		+76·5 (N)	(e)
	2 M in CF_3CH_2OH	+182·2 (NMe)	(e)
		+94·4 (N)	(e)
	1 : 1 v/v in MeOH	+180 ± 2 (NMe)	(f)
		+80 ± 2 (N)	(f)
	2 M in MeCOOH	+181·4 (NMe)	(e)
		+93·6 (N)	(e)
	CF_3COO^-, 2 M in MeCOOH	+186·4 (NMe)	(e)
		+146·4 (NH)	(e)
	Cl^-, in H_2O, pH 5·96	+180·1 (NMe)	(e)
		+89·4 (NH)	(e)
	pH 2·10	+185·6 (NMe)	(e)
		+138·1 (NH)	(e)
	pH 1·71	+186·8 (NMe)	(e)
		+148·9 (NH)	(e)
	pH 1·04	+188·8 (NMe)	(e)
		+168·4 (NH)	(e)
	pH 0·06	+189·9 (NMe)	(e)
		+176·4 (NH)	(e)
	I^-, 2 M in MeOH	+184·2	(e)
	I^-, 2 M in H_2O	+185·7	(e)

TABLE 112—*cont.*

Compound	Solution	Nitrogen shielding referred to neat nitromethane		Notes
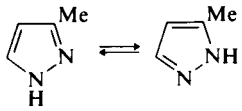	2 M in $CHCl_3$	+134·3	(NCMe)	(e)
		+139·8	(NCCCMe)	(e)
	2 M in CF_3CH_2OH	+145·7	(NCMe)	(e)
		+148·3	(NCCCMe)	(e)
	2 M in MeCOOH	+151·1	(NCMe)	(e)
		+155·9	(NCCCMe)	(e)
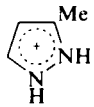	CF_3COO^-, 2 M in MeCOOH	+183·2	(NCMe)	(e)
		+185·7	(NCCCMe)	(e)
	Cl^-, 2 M in MeCOOH	+187·0	(NCMe)	(e)
		+189·7	(NCCCMe)	(e)
	Cl^-, 2 M in MeOH	+184·1	(NCMe)	(e)
		+187·4	(NCCCMe)	(e)
	Cl^-, in H_2O, pH 1·66	+186·1	(NCMe)	(e)
		+189·6	(NCCCMe)	(e)
	pH 0·6	+187·3	(NCMe)	(e)
		+190·8	(NCCCMe)	(e)
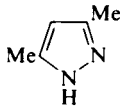	2 M in $CHCl_3$	+139·8	(N ⇄ NH)	(e)
	2 M in CF_3CH_2OH	+150·2	(N ⇄ NH)	(e)
	2 M in MeCOOH	+165·7	(N ⇄ NH)	(e)
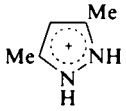	CF_3COO^-, 2 M in MeCOOH	+189·0		(e)
	Cl^-, 2 M in MeCOOH	+189·7		(e)
	Cl^-, 2 M in MeOH	+189·1		(e)
	Cl^-, in H_2O, pH 2·39	+190·7		(e)
	pH 1·66	+191·9		(e)
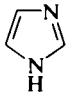 (imidazole)	2 M in $CHCl_3$	+172·6	(N ⇄ NH)	(g)
	2 M in H_2O	+177·2	(N ⇄ NH)	(g)(h)
	2 M in $CHCl_3$ + 1 eq. of CF_3CH_2OH	+178·6	(N ⇄ NH)	(g)
	2 M in CF_3CH_2OH	+182·4	(N ⇄ NH)	(g)
	2 M in $CHCl_3$ + 1 eq. of MeCOOH	+186·8	(N ⇄ NH)	(g)
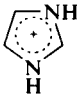	$MeCOO^-$, 2 M in MeCOOH	+206·0		(g)
	Cl^-, 1·2 M in MeOH	+206·5		(g)
	Cl^-, in H_2O	+208·2		(g)(h)
	Cl^-, 1 M in H_2O, pH 0·5	+207·0		(i)(j)
	1 M in H_2O, pH 10·4	+176·0		(i)
	pH 13	+175·0		(i)
	pH 14	+166·1		(i)
	deduced value	+156		(i)

TABLE 112—*cont.*

Compound	Solution	Nitrogen shielding referred to neat nitromethane		Notes
	27·4 mol % in cyclohexane	+221·9	(NMe)	(k)
		+117·2	(N)	(k)
	2 M in benzene	+221·9	(NMe)	(g)
		+117·6	(N)	(g)
	2 M in $CHCl_3$	+221·3	(NMe)	(g)
		+125·5	(N)	(g)
	2 M in MeOH	+218·7	(NMe)	(g)(k)
		+134·0	(N)	(g)(k)
	2 M in H_2O	+217·7	(NMe)	(g)(h)
		+134·7	(N)	(g)(h)
	2 M in $CHCl_3$ + 1 eq. of CF_3CH_2OH	+220·2	(NMe)	(g)
		+134·0	(N)	(g)
	2 M in $CHCl_3$ + 1 eq. of MeCOOH	+219·2	(NMe)	(g)
		+140·4	(N)	(g)
	in H_2O, pH 11–13	+216·2	(NMe)	(j)
		+135·2	(N)	(j)
	CF_3COO^-, 2 M in $CHCl_3$	+217·0	(NMe)	(g)
		+196·0	(NH)	(g)
	$MeCOO^-$, 2 M in MeCOOH	+209·3	(NMe)	(g)
		+204·2	(NH)	(g)
	Cl^-, 2 M in MeOH	+208·7	(NMe)	(g)
		+206·9	(NH)	(g)
	Cl^-, 2 M in H_2O	+210·3	(NMe)	(g)(h)
		+209·8	(NH)	(g)(h)
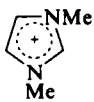	I^-, 1·4 M in MeOH	+210·7		(g)
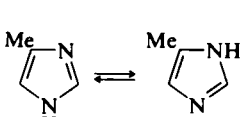	1·5 M in $CHCl_3$	+167·7	(NCMe)	(g)
		+173·2	(NCCMe)	(g)
	in H_2O	+170·6	(NCMe)	(g)
		+179·0	(NCCMe)	(g)
	2 M in $CHCl_3$ + 1 eq. of CF_3CH_2OH	+173·2	(NCMe)	(g)
		+179·5	(NCCMe)	(g)
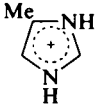	CF_3COO^-, 2 M in $CHCl_3$	+201·2	(NCMe)	(g)
		+205·3	(NCCMe)	(g)
	$MeCOO^-$, 2 M in MeOH	+203·5	(NCMe)	(g)
		+207·5	(NCCMe)	(g)
	Cl^-, 2 M in H_2O	+204·8	(NCMe)	(g)
		+208·8	(NCCMe)	(g)

TABLE 112—*cont.*

Compound	Solution	Nitrogen shielding referred to neat nitromethane	Notes
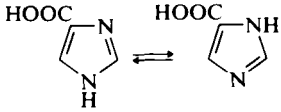	in H_2O	+186·2 (NCCCOOH) +161·8 (NCCOOH)	(h) (h)
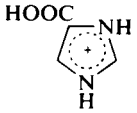	Cl^-, in H_2O	+209·2 (NCCCOOH) +205·9 (NCCOOH)	(h) (h)
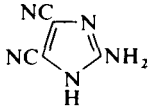	in DMSO/MeOH	+326·6 (NH_2) +201·8 (N⇄NH) +111·8 (CN)	(l) (l) (l)
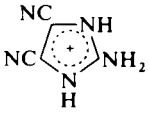	in DMSO/H_2O/HCl	+319·3 (NH_2) +205·3 (NH) +109·4 (CN)	(l) (l) (l)
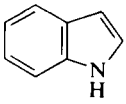 (indole)	1·0 M in $CDCl_3$ 1·0 M in DMSO	+255·4 +249·0	(m) (m)
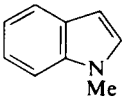	neat liquid	+250 ± 3	(f)(n)
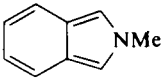 (*N*-Me-isoindole)	satd. in Et_2O	+218 ± 3	(f)(n)
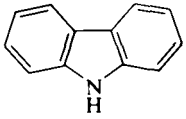 (carbazole)	0·01 M in acetone	+268 ± 1	(o)
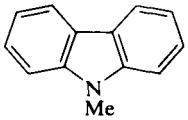	satd. in acetone	+278 ± 8 +275·4	(f) (p)

TABLE 112—*cont.*

Compound	Solution	Nitrogen shielding referred to neat nitromethane	Notes
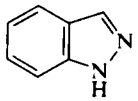 (indazole, prevailing tautomer)	1·5 M in acetone	+200·6 (NH)	(e)
		+65·1 (N)	(e)
	1·5 M in CF_3CH_2OH	+207·2 (NH)	(e)
		+90·8 (N)	(e)
	1·5 M in MeCOOH	+204·4 (NH)	(e)
		+93·1 (N)	(e)
	1·4 M in MeCOOH + 1 eq. of CF_3COOH	+207·9 (NH)	(e)
		+124·3 (N)	(e)
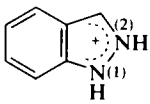	Cl^-, 1·5 M in MeCOOH	+210·4 (1-NH)	(e)
		+176·3 (2-NH)	(e)
	Cl^-, 1·2 M in H_2O, pH < −0·5	+212·2 (1-NH)	(e)
		+180·8 (2-NH)	(e)
	Cl^-, 1·3 M in MeOH	+207·3 (1-NH?)	(e)
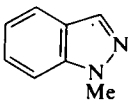	satd. in acetone	+201 ± 2 (NMe)	(f)(n)
		+62 ± 3 (N)	(f)(n)
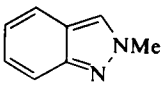	satd. in acetone	+161 ± 1 (NMe)	(f)(n)
		+86 ± 4 (N)	(f)(n)
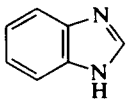 (benzimidazole)	0·15 M in acetone	+185 ± 2 (N ⇄ NH?)	(a)
	0·15 M in DMSO	+237 ± 4 (NH?)	(a)
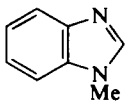	0·15 M in acetone	+231 ± 1 (NMe)	(a)
		+134 ± 1 (N)	(a)
	0·10 M in CCl_4	+237 ± 6 (NMe)	(a)
		+127 ± 6 (N)	(a)
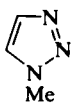 (*N*-Me-1,2,3-triazole)	neat liquid	+144 ± 1 (NMe)	(f)
		+12 ± 3 (N-2)	(f)
		+30 ± 3 (N-3)	(f)
	in acetone	+144·5 (NMe)	(q)
		+14·7 (N-2)	(q)
		+27·9 (N-3)	(q)

TABLE 112—*cont.*

Compound	Solution	Nitrogen shielding referred to neat nitromethane	Notes
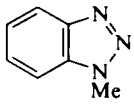		+162 ± 2 (NMe)	(f)
		+4 ± 4 (N-2)	(f)
		+40 ± 4 (N-3)	(f)
	in acetone	+164·7 (NMe)	(q)
		+1·5 (N-2)	(q)
		+41·1 (N-3)	(q)
	neat liquid	+132 ± 1 (NMe)	(f)
		+53 ± 1 (N-2, N-5)	(f)
	in MeOH(1 : 1 v/v)	+134 ± 2 (NMe)	(f)
(*N*-Me-1,2,5-triazole)		+55 ± 2 (N-2, N-5)	(f)
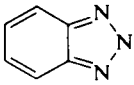	neat liquid	+119 ± 1 (NMe)	(f)(n)
		+62 ± 5 (N-2, N-5)	(f)(n)
	neat liquid	+174 ± 1 (NMe)	(f)
		+85 ± 2 (N-2)	(f)
		+131 ± 2 (N-4)	(f)
	in acetone	+173·4 (NMe)	(q)
(*N*-Me-1,2,4-triazole)		+83·7 (N-2)	(q)
		+130·1 (N-4)	(q)
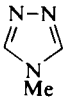	in MeOH	+222 ± 2 (NMe)	(f)
		+82 ± 4 (N-3, N-4)	(f)
(*N*-Me-1,3,4-triazole)			
	in $CDCl_3$	+158·7 (NMe)	(p)
		+14·5 (N-2)	(p)
		−8·8 (N-3)	(p)
(*N*-Me-1,2,3,4-tetrazole)		+54·4 (N-4)	(p)
	in $CDCl_3$	+98·8 (NMe)	(p)
		−4·4 (N-2)	(p)
		+42·9 (N-3)	(p)
(*N*-Me-1,2,3,5-tetrazole)		+68·7 (N-5)	(p)
	0·9 M in $CDCl_3$	+160·6 (NPh)	(r)
		+78·6 (N)	(r)

TABLE 112—*cont.*

Compound	Solution	Nitrogen shielding referred to neat nitromethane	Notes
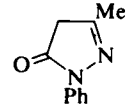 (A)	0·7 M in $CDCl_3$	+186·8 (NPh)	(r)
	(prevailing A)	+54·8 (N)	(r)
⇅			
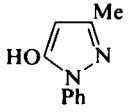 (B)			
⇅			
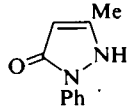 (C)	0·7 M in DMSO	+187·4 (NPh in A)	(r)
	(prevailing B ⇄ C, trace of A)	+59·1 (N= in A)	(r)
		+191·2 (NPh in B ⇄ C)	(r)
		+125 (broad, N ⇄ NH in B ⇄ C)	(r)
 (isoxazole, 1,2-oxazole)	neat liquid	−2·9	(a)
		0 ± 1	(f)
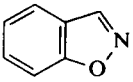 (benzisoxazole)	neat liquid	+8 ± 1	(f)
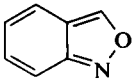 (anthranil)	neat liquid	+27 ± 1	(f)
 (oxazole, 1,3-oxazole)	in CCl_4	+124 ± 1	(o)
	in MeOH	+127 ± 1	(f)
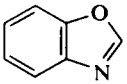 (benzoxazole)	neat liquid	+142 ± 3	(f)
 (1,2,4-oxadiazole)	1 : 1 v/v in Et_2O	+140 ± 2 (N-4)	(f)
		+20 ± 2 (N-2)	(f)

TABLE 112—*cont.*

Compound	Solution	Nitrogen shielding referred to neat nitromethane	Notes
	neat liquid	−33 ± 1	(f)
	1 : 1 v/v in acetone	−34 ± 1	(f)
	1 : 1 v/v in Et_2O	−32 ± 1	(f)(t)
(furazan, 1,2,5-oxadiazole)			
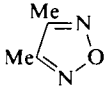	20% v/v in acetone	−24·8	(s)
	20% v/v in CF_3CH_2OH	−18·3	(s)
	20% v/v in CF_3COOH	−6·8	(s)
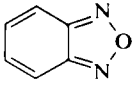	satd. in Et_2O	−36 ± 2	(f)(n)(t)
	2 M in acetone	−36·3	(s)
	2 M in CF_3CH_2OH	−29·7	(s)
(benzofurazan)	2 M in CF_3COOH	−22·3	(s)
	neat liquid	+82 ± 1	(f)
	1 : 1 v/v in acetone	+80 ± 1	(f)
	1 : 1 v/v in Et_2O	+80 ± 1	(f)
(1,3,4-oxadiazole)			
	satd. in Et_2O	+82 ± 1	(f)
(isothiazole, 1,2-thiazole)			
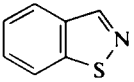	satd. in Et_2O	+76 ± 2	(f)
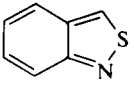	neat liquid	+121 ± 2	(f)
	neat liquid	+58 ± 1	(f)
		+57·2	(a)
	0·15 M in acetone	+55 ± 1	(a)
(thiazole, 1,3-thiazole)	0·15 M in DMSO	+53 ± 2	(a)
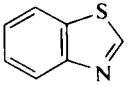	neat liquid	+62 ± 2	(f)
	0·15 M in acetone	+61 ± 1	(a)
(benzothiazole)			
	1 : 3 v/v in Et_2O	−33 ± 1 (N-2)	(f)
		−59 ± 1 (N-3)	(f)
	in acetone	−30·7 (N-2)	(q)
(1,2,3-thiadiazole)		−55·8 (N-3)	(q)

TABLE 112—*cont.*

Compound	Solution	Nitrogen shielding referred to neat nitromethane	Notes
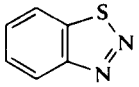	1 : 3 v/v	−42 ± 2 (N-2) −62 ± 1 (N-3)	(f) (f)
	in acetone	−44·9 (N-2) −60·9 (N-3)	(q) (q)
 (1,2,4-thiadiazole)	1 : 3 v/v in Et_2O	+106 ± 1 (N-2) +70 ± 1 (N-4)	(f) (f)
 (1,2,5-thiadiazole)	neat liquid 1 : 1 v/v in Et_2O	+35 ± 1 +34 ± 1	(f) (f)
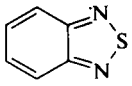	2 M in acetone 2 M in DMSO 2 M in CF_3CH_2OH 2 M in CF_3COOH satd. in Et_2O	+49·6 +50·5 +60·6 +72·3 +50 ± 1 +52 ± 2	(s) (s) (s) (s) (f)(n)(t) (u)
	1 : 1 v/v in Et_2O	+10 ± 2	(f)(t)
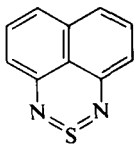	2 M in DMSO	+89·3	(s)
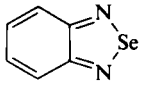	2 M in acetone 2 M in CF_3CH_2OH 2 M in CF_3COOH	+7·0 +25·5 +68·7	(s) (s) (s)
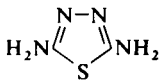	1 M in DMSO	+87·9 (N–N) +324·0 (NH_2)	(v) (v)
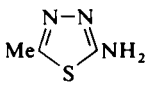	1 M in DMSO	+79·0 (N–N) +318·8 (NH_2)	(v) (v)

TABLE 112—*cont.*

Compound	Solution	Nitrogen shielding referred to neat nitromethane	Notes
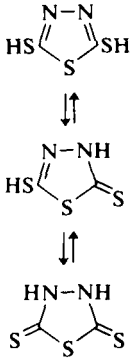	1 M in absolute EtOH	+114·2 (broad)	(v)
	2 M in DMSO	+116·8 (N=) +166·7 (NH) +314·9 (NH_2)	(v) (v) (v)

(a) Data from ref. 1, pp. 179–182, and references therein.

(b) Data from ref. 271; ^{14}N continuous-wave spectra; 4·33 MHz; high-precision differential saturation technique with full lineshape fitting; concentric spherical sample/standard containers in order to eliminate bulk susceptibility effects; referred to neat nitromethane.

(c) Data from ref. 272; ^{14}N continuous-wave spectra; 7·22 MHz; field perpendicular to sample tube; referred originally to saturated aqueous $NaNO_3$, +3·7 ppm from neat nitromethane (Table 6); conversion scheme II (Table 4).

(d) Data from ref. 137; details as in note (c).

(e) Data from ref. 273; ^{15}N natural abundance spectra; 18·25 MHz; field parallel to sample tube; referred originally to 1 M DNO_3, +6·2 ppm from neat nitromethane (Table 6); conversion scheme IV (Table 4).

(f) Data from ref. 33 and references therein; ^{14}N continuous-wave spectra; 4·33 MHz; field perpendicular to sample tube; referred originally to neat nitromethane (uncorrected for bulk susceptibility effects).

(g) Data from ref. 274; see note (e).

(h) Data from ref. 213; see note (e).

(i) Data from ref. 275; ^{15}N-labelled compounds; ^{15}N spectra; 10·158 MHz; field perpendicular to sample tube; referred originally to Me_4N^+, +337·7 ppm from neat nitromethane (Table 6); conversion scheme II (Table 4).

(j) Data from ref. 276; see note (i).

(k) Data from ref. 26; see note (e).

(l) Data from ref. 162; see note (e).

(m) Data from ref. 128; ^{15}N natural abundance spectra; 10·09 MHz; field perpendicular to sample tube; referred originally to 2·9 M NH_4Cl in 1 M HCl, but reported relative to "anhydrous ammonia", +380·2 ppm from neat nitromethane (Table 6); conversion scheme IV (Table 4).

(n) Data from ref. 201; see note (f).

(o) Data from ref. 2, pp. 210–214, and references therein; +4 ppm was added to shieldings referred to NO_3^- there in order to convert them to neat nitromethane scale.

(p) Data from ref. 179; ^{15}N natural abundance spectra; 18·25 MHz; field parallel to sample tube; referred originally to neat nitromethane (uncorrected for bulk susceptibility effects).

(q) Data from ref. 33; ^{15}N spectra as in note (p).

(r) Data from ref. 277; ^{15}N-labelled compounds; ^{15}N spectra; 9·12 MHz; field perpendicular to sample tube; referred originally to NH_4^+ in 5 M NH_4NO_3 in 2 M HNO_3, +359·0 ppm from neat nitromethane (Table 6); conversion scheme II (Table 4).

(s) Data from ref. 278; see note (e).

(t) Data from ref. 279; see note (f).

(u) Data from ref. 206; ^{14}N continuous-wave measurements; 3 MHz; wide-line spectrometer; referred originally to NH_4^+ in saturated aqueous NH_4NO_3, +359·6 ppm from neat nitromethane (Table 6); low-precision measurements.

(v) Data from ref. 163; see note (e); proton-coupled spectra.

TABLE 113

Substituent effects on nitrogen shielding in pyrrole ring system

Substituents at pyrrole ring 	Nitrogen shielding difference related to pyrrole for 10% v/v solutions in chloroform-*d*
2-NO_2	−0·6
3-CHO	−0·9
2-C(=O)Me	−4·2
3-NO_2	−4·8
5-NO_2, 2-C(=O)OMe	+0·2
2-C(=O)OMe	−5·5
4-C(=O)OMe	−7·6

Data from ref. 280; $^1H\{^{15}N\}$ double-resonance spectra; 100/10·1 MHz; referred to pyrrole in $CDCl_3$.

TABLE 114

Nitrogen shieldings obtained from factor analysis of experimental data on some imidazole complexes

Sample	Nitrogen shielding referred to neat nitromethane	Notes
 in H_2O, pH 10·4	+176·0 (N⇄NH)	(a)
(imidazole)		
Imidazole + $Zn(NO_3)_2$ + HNO_3 + H_2O pH < 9		
$Zn(imidazole)_n^{2+}$		
$n = 1$	+177·5	(a)
2	+181·5	(a)
3	+182·0	(a)
4	+182·0	(a)
5	+181·5	(a)
6	+181·2	(a)
Imidazole + $Cd(NO_3)_2$ + HNO_3 + H_2O pH < 9		
$Cd(imidazole)_n^{2+}$		
$n = 1$	+188·4	(b)
2	+186·1	(b)
3	+184·7	(b)
4	+183·5	(b)

(a) Data from ref. 275; ^{15}N-labelled imidazole; ^{15}N spectra; 10·158 MHz; field perpendicular to sample tube; referred originally to imidazole (in H_2O, pH 10·4), and the latter referred to Me_4N^+, +337·7 ppm from neat nitromethane (Table 6); conversion scheme II (Table 4).

(b) Data from ref. 281; details as above.

TABLE 115

Nitrogen shieldings in tertiary-amine and pyrrole-type moieties in Rauwolfia alkaloids and related structures

	Solution	Nitrogen shielding referred to neat nitromethane N-5	N-12
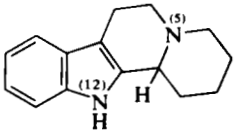	0·7 M in $CDCl_3$	+323·2	+261·8
	0·7 M in DMSO	+322·8	+255·6
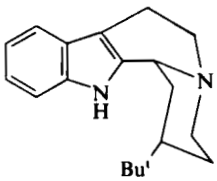	0·3 M in $CDCl_3$	+336·4	+260·6
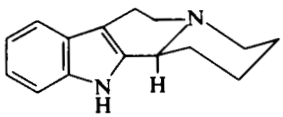	1·5 M in $CDCl_3$	+322·3	+262·0
	1·5 M in DMSO	+324·0	+255·6
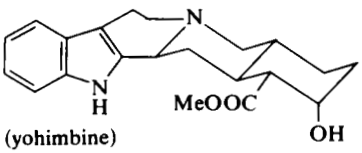 (yohimbine)	1·0 M in DMSO	+324·3	+254·8
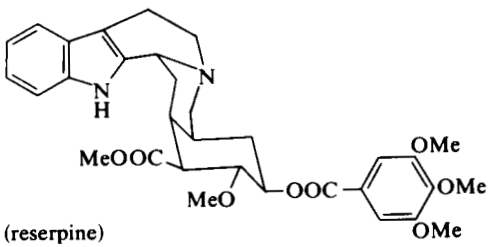 (reserpine)	0·3 M in $CDCl_3$	+348·3	+262·3
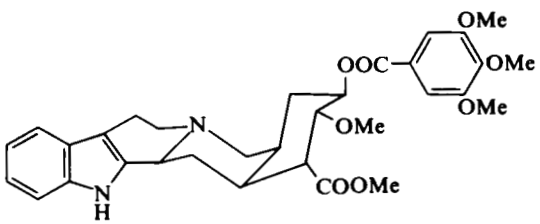 (isoreserpine)	0·4 M in $CDCl_3$	+333·2	+264·5

TABLE 115—*cont.*

	Solution	Nitrogen shielding referred to neat nitromethane N-5	N-12
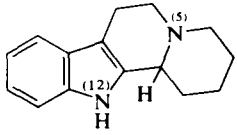			
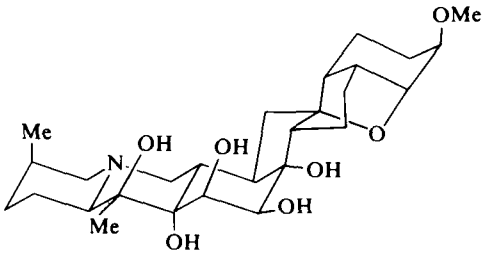 (cevadine)	1·0 M in $CDCl_3$	+338·9	
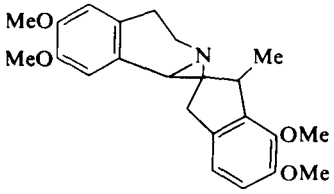 (corydaline)	1·0 M in $CDCl_3$	+341·5	
 (sparteine)	neat liquid	+331·5, +331·1	
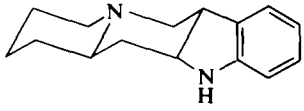	1·5 M in $CDCl_3$	+326·6	+308·8 (NH)
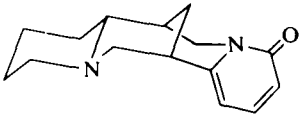 (thermopsine)	1·5 M in $CDCl_3$	+327·4	+202·2 (NC=O)

Data from ref. 128; ^{15}N natural abundance spectra; 10·09 MHz; field perpendicular to sample tube; referred originally to NH_4Cl (2·9 M in 1 M HCl), but reported relative to "anhydrous ammonia" standard, +380·2 ppm from neat nitromethane (Table 6); conversion scheme IV (Table 4).

TABLE 116

Nitrogen shieldings in porphyrin ring systems and related structures

Structure	Solution	Nitrogen shielding referred to neat nitromethane	Notes
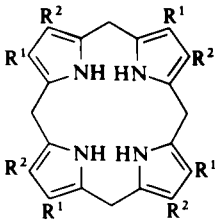 (uroporphyrinogen, "uro'gen") R^1=CH_2COOH; R^2=CH_2CH_2COOH	in D_2O	+226·7	(a)
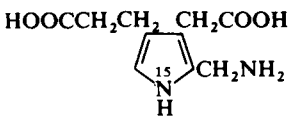 (porphobilinogen, PBG)	in D_2O	+227·4 (^{15}NH)	(a)
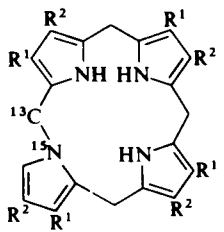 (intermediate in uro'gen formation)	in D_2O	+225·7 (NH) +208·0 (NH hydrogen bonded +189·5 to COOH) +224·5 (doublet, ^{13}C–^{15}N)	(a) (a) (a) (a)

TABLE 116—*cont.*

Structure		Solution	Nitrogen shielding referred to neat nitromethane	Notes
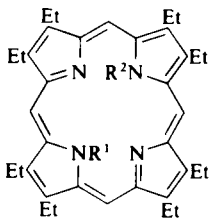				
(octaethylporphyrin, OEP structure)				
$(OEP)H_2$	$R^1 = R^2 = H$	in $CDCl_3$(+28 °C)	+194·7 (=N⇄NH)	(b)
		in $CDCl_3$(−53 °C)	+143·4 (=N)	(b)
			+247·0 (NH)	(b)
$(OEP)H_4^{2+}$		in CF_3COOH	+257·4 (NH)	(b)
(OEP)MeH	R^1 = Me, $R^2 = H$	in $CDCl_3$	+129·5 (=N–)	(b)
			+247·0 (NH)	(b)
			+259·7 (NMe)	(b)
$(OEP)MeH_3^{2+}$		in CF_3COOH	+255·0 (NH adj. to NMe)	(b)
			+256·6 (NH opposite to NMe)	(b)
			+262·7 (NMe)	(b)
$(OEP)Me_2H^+$	$R^1 = R^2$ = Me (on adjacent nitrogens)	monocation in $CDCl_3$	+187·2 (=N⇄=NH^+)	(b)
			+260·0 (NMe)	(b)
$(OEP)Me_2H_2^{2+}$		in CF_3COOH (dication)	+258·2 (NH)	(b)
			+264·5 (NMe)	(b)
OEP complexes	$R^1, R^2 = -M(N)_2-$			
Mg(OEP)		0·04 M in $CDCl_3$ + trace of pyridine	+183·6	(b)
Fe(II)(OEP)Py_2		0·04 M in pyridine	+191·6 (porphyrin)	(b),(c)
Fe(II)(OEP)(4-Me-$Py)_2$		0·04 M in 4-Me-pyridine	+189·2 (porphyrin)	(c)

Ni(OEP)	0·04 M in $CDCl_3$	+260·7	(b)
Zn(OEP)	0·04 M in $CDCl_3$/pyridine	+182·9 (porphyrin)	(b)
Cd(OEP)	0·04 M in pyridine	+176·8 (porphyrin)	(b)
Fe(II)(OEP)(Py)(octyl isocyanide)	in pyridine	+214·3 (porphyrin)	(c)
Fe(II)(OEP)(Py)(CO)	in pyridine	+235·0 (porphyrin)	(c)
Co(III)(OEP)(Br)(Py)	in CD_2Cl_2	+263·1 (porphyrin)	(c)
	in pyridine	+263·7 (porphyrin)	(c)
Co(III)(OEP)(Br)(4-acetyl-Py)	in 4-acetylpyridine	+266·2 (porphyrin)	(c)
Co(III)(OEP)(Br)(4-Me-Py)	in 4-Me-pyridine	+261·0 (porphyrin)	(c)

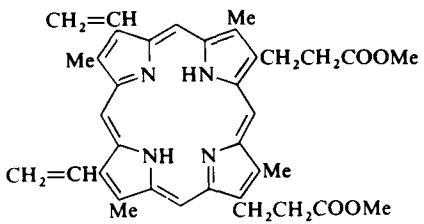

(protoporphyrin IX dimethyl ester)	0·02 M in $CDCl_3$(−60 °C)	+140·5 (singlet)	(h)
		+245·5 (doublet)	(h)
	dication in CF_3COOH	+251·5 (doublet)	(h)
coproporphyrin III tetramethyl ester	0·02 M in $CDCl_3$	+140·5 (singlet)	(h)
		+247·0 (doublet)	(h)
(probably $-CH=CH_2 \rightarrow -CH_2CH_2COOMe$)	dication in CF_3COOH	+251·5 (doublet)	(h)

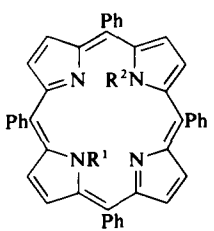

(*meso*-tetraphenylporphyrin, TPP structure)

TABLE 116—*cont.*

Structure	Solution	Nitrogen shielding referred to neat nitromethane	Notes
$(TPP)H_2$ $R^1 = R^2 = H$	in $CDCl_3/CS_2$(−80 °C)	+135·7 (=N–, singlet)	(d)
		+242·8 (NH, doublet)	(d)
	0·011 M in $CDCl_3$/acetone	+138 (=N–)	(e)
	(−12 °C)	+247 (NH)	(e)
$(TPP)H_4^{2+}$	in $CDCl_3$/acetone/ CF_3COOH	+246 (NH)	(e)
TPP complexes $R^1 = R^2 =$ 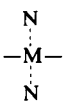			
Cd(TPP)	in $CDCl_3$ + pyridine	+169·6 (porphyrin)	(f)
Zn(TPP)	0·02 M in $CDCl_3$	+179·5	(g)
Zn(TPP) 1 : 1 complex with			
3-CN-pyridine	in $CDCl_3$	+179·4 (porphyrin)	(g)
4-CN-pyridine	in $CDCl_3$	+179·1 (porphyrin)	(g)
3-CHO-pyridine	in $CDCl_3$	+178·8 (porphyrin)	(g)
4-CHO-pyridine	in $CDCl_3$	+178·7 (porphyrin)	(g)
2-Me-pyridine	in $CDCl_3$	+178·6 (porphyrin)	(g)
4-COMe-pyridine	in $CDCl_3$	+178·5 (porphyrin)	(g)
pyridine	in $CDCl_3$	+178·0 (porphyrin)	(g)

3-Me-pyridine	in $CDCl_3$	+177·9 (porphyrin)(g)	(g)
4-Me-pyridine	in $CDCl_3$	+177·8 (porphyrin)(g)	(g)
3-NH_2-pyridine	in $CDCl_3$	+177·8 (porphyrin)(g)	(g)
4-NH_2-pyridine	in $CDCl_3$	+177·5 (porphyrin)(g)	(g)

(a) Data from ref. 282; ^{15}N-labelled pyrrole ring; ^{15}N spectra; 8·1 MHz; field perpendicular to sample tube; reference not reported, but most probably NH_3, +380·2 ppm from neat nitromethane (Table 6); conversion scheme IV (Table 4).

(b) Data from ref. 283 and ref. 284; ^{15}N-labelled compounds; ^{15}N spectra; 10·09 MHz; field perpendicular to sample tube; referred originally to NO_3^- in NH_4NO_3 in DMSO, +3·7 ppm from neat nitromethane (Table 6); conversion scheme II (Table 4).

(c) Data from ref. 285; details as in note (b).

(d) Data from ref. 286; $^1H\{^{15}N\}$ INDOR spectra; 100/10·1 MHz; field perpendicular to sample tube; referred originally to nitromethane in $CDCl_3$, +3·8 ppm from neat nitromethane (Table 6); conversion scheme II (Table 4).

(e) Data from ref. 287; ^{15}N-labelled and non-labelled compounds; ^{15}N spectra; 18·25 MHz; field parallel to sample tube; referred originally to what was reported as 0·1 M DNO_3, probably 1·0 M DNO_3, +6·2 ppm from neat nitromethane (Table 6); conversion scheme IV (Table 4).

(f) Data from ref. 288; INDOR spectra as in note (d), but referred to TMS lock at 100 MHz; recalculated using a frequency of 10 135 023 Hz for nitromethane under these conditions.

(g) Data from ref. 289; ^{15}N-labelled porphyrin ring; ^{15}N spectra; 9·12 MHz; field perpendicular to sample tube; referred originally to 1 M $NaNO_3$, +3·5 ppm from neat nitromethane (Table 6); conversion scheme II (Table 4).

(h) Data from ref. 290; ^{15}N-labelled compounds; ^{15}N spectra; 9·12 MHz; field perpendicular to sample tube; referred originally to 4 M NH_4Cl in 2 M HCl, +352·5 ppm from neat nitromethane (Table 6); conversion scheme II (Table 4).

TABLE 117

Nitrogen shieldings in some furoxans (1,2,5-oxadiazole-2-*N*-oxides) and related structures

Structure	Solution	Nitrogen shielding referred to neat nitromethane	Notes (^{14}N signals half-height width in parentheses)
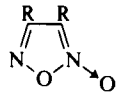			
R = Me	neat liquid	+25 ± 1 (N → O)	(a), (c) (200 Hz)
		+11 ± 3 (N)	(c) (610 Hz)
	1 : 1 v/v in Et_2O	+25 ± 1 (N → O)	(a)
	1 : 1 v/v in acetone	+25 ± 1 (N → O)	(a)
	20% v/v in acetone	+25·3 (N → O)	(b)
		+13·2 (N)	(b)
	20% v/v in CF_3CH_2OH	+27·9 (N → O)	(b)
		+14·1 (N)	(b)
	20% v/v in CF_3COOH	+31·5 (N → O)	(b)
		+12·5 (N)	(b)
Et	neat liquid	+19 ± 2 (N → O)	(a)
	1 : 1 v/v in Et_2O	+22 ± 2 (N → O)	(a)
	1 : 1 v/v in acetone	+22 ± 2 (N → O)	(a)
C(=O)Me	1 : 1 v/v in Et_2O	+22 ± 2 (N → O)	(a)
Ph	satd. in acetone	+25 ± 3 (N → O)	(a)
$C_6H_4{\cdot}NO_2p$	satd. in acetone	+24 ± 2 (N → O)	(a)
Br	in Et_2O	+26 ± 2 (N → O)	(a)
I	in Et_2O	+24 ± 3 (N → O)	(a)
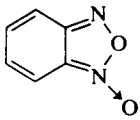	2 M in acetone (−10 °C)	+18·0 (N → O)	(b)
		+4·5 (N)	(b)
	2 M in acetone (+55 °C)	+11·2 (averaged)	(b)
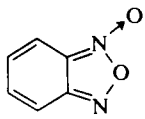	satd. in acetone	+5 ± 3 (N)	(c) (700 Hz)
		+19·0 ± 0·4 (N → O)	(c) (140 Hz)
		+18·4 ± 0·2 (NO_2)	(c) (33 Hz)
		+4·7 (N)	(d)
		+19·4 (N → O, NO_2)	(d)

TABLE 117—*cont.*

Structure	Solution	Nitrogen shielding referred to neat nitromethane	Notes (^{14}N signals half-height width in parentheses)
	satd. in acetone	−2 ± 3 (N) +16 ± 5 (N → O, N) +24 ± 1 (N → O) +23·0 ± 0·2 (NO_2) −2·4 (N) +6·5 (N) +18·8 (N → O) +22·4 (N → O, NO_2)	(c) (270 Hz) (c) (500 Hz) (c) (130 Hz) (c) (40 Hz) (d) (d) (d) (d)
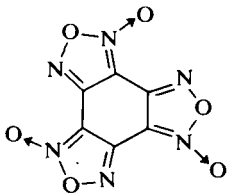	satd. in acetone	+20·9 (N → O) +1·5 (N)	(d) (d)
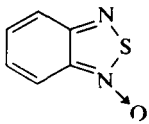	in acetone	+122 ± 1 (N → O) +26 ± 1 (N)	(a) (a)

(a) Data from ref. 279; ^{14}N continuous-wave spectra; 4·33 MHz; field perpendicular to sample tube; referred to neat nitromethane (uncorrected for bulk susceptibility effects).

(b) Data from ref. 278; ^{15}N natural abundance spectra; 18·25 MHz; field parallel to sample tube; referred originally to 1 M DNO_3, +6·2 ppm from neat nitromethane (Table 6); conversion scheme IV (Table 4).

(c) Data from ref. 291; ^{14}N spectra as in footnote (a); lineshape fitting; ^{14}N resonance half-height widths (in Hz) are given in parentheses.

(d) Data from ref. 291; ^{15}N natural abundance spectra; 18·25 MHz; field parallel to sample tube; referred to neat nitromethane (uncorrected for bulk susceptibility effects).

TABLE 118

Nitrogen shieldings in some phosphadiazoles

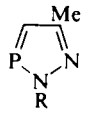
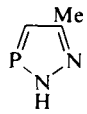
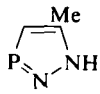
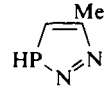

(A) (B) (C)

Substituent R	Solution and temperature	Nitrogen shielding referred to neat nitromethane for isotope and nitrogen atom specified		
			–N=	N–R
H (prevailing tautomer A)	40% in CCl_4 (70–95 °C)	^{14}N	+24 ± 5	+143 ± 3
C(=O)Me	80% in CCl_4 (70–90 °C)	^{14}N	+24 ± 5	+100 ± 3
	(ambient)	^{15}N	+26·5	+98·3
Ph	80% in CCl_4 (80–90 °C)	^{14}N	+41 ± 5	+133 ± 3
CH_2CH_2CN	40% in CCl_4 (80 °C)	^{14}N	+26 ± 5	+142 ± 3

Data from ref. 292; ^{14}N and ^{15}N natural abundance spectra; 6·5 and 9·1 MHz, respectively; field perpendicular to sample tube; referred originally to neat nitromethane (uncorrected for bulk susceptibility effects).

TABLE 119

Nitrogen shieldings in some sydnones, sydnonimines, and related structures

Structure	Solution	Nitrogen shielding referred to neat nitromethane	Notes
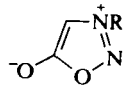			
(sydnone structure)			
R = Me	in acetone	+34·6 (N–O)	(a)
		+108 ± 1 (NMe)	(b)
	in acetone	+36·2 (N–O)	(c)
		+112·5 (NMe)	(c)
Et	in acetone	+36·9 (N–O)	(c)
		+99·1 (NEt)	(c)
Pr^i	in acetone	+35·3 (N–O)	(c)
		+85·7 ($N–Pr^i$)	(c)
Bu^t	in acetone	? (N–O)	(c)
		+80·0 ($N–Bu^t$)	(c)
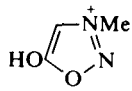	Cl^-, in acetone	+32·2 (N–O)	(a)
		+94 ± 5 (NMe)	(b)
(protonated sydnone)			
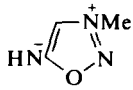			
(hypothetical sydnonimine)			
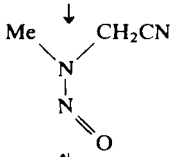	in MeOH	+156·2 (MeN)	(a)
		+131·1 (CN)	(a)
		−161·5 (NO)	(a)
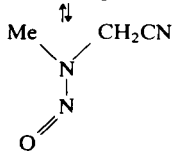	in MeOH	+151·1 (MeN)	(a)
		+126·1 (CN)	(a)
		−166·0 (NO)	(a)
	Cl^-, in MeOH	+15·0 (N–O)	(a)
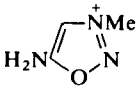		+104·0 (NMe)	(a)
		+307·3 (NH_2)	(a)
		+16·0 (N–O)	(c)
(protonated sydnonimine)		+105·8 (NMe)	(c)
		+309·5 (NH_2)	(c)

TABLE 119—*cont.*

Structure	Solution	Nitrogen shielding referred to neat nitromethane		Notes
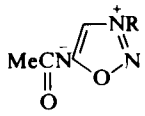				
(*N*-acetylsydnonimine)				
R = Me	in acetone	+33·6	(N–O)	(c)
		+111·2	(NMe)	(c)
		+197·5	(NCOMe)	(c)
	in MeOH	+22·7	(N–O)	(a)
		+105·5	(NMe)	(a)
		+203·6	(NCOMe)	(a)
Et	in acetone	+33·0	(N–O)	(c)
		+105·5	(NEt)	(c)
		+197·3	(NCOMe)	(c)
Pr^i	in acetone	+31·7	(N–O)	(c)
		+85·0	(N–Pr^i)	(c)
		+196·2	(NCOMe)	(c)
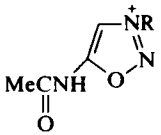				
(protonated *N*-acetylsydnonimine)				
R = Me	in MeOH	+5·5	(N–O)	(a)
		+98·9	(NMe)	(a)
		+250·0	(NHCOMe)	(a)
		+6·5	(N–O)	(c)
		+100·4	(NMe)	(c)
		+252·2	(NHCOMe)	(c)
Et	in MeOH	+6·9	(N–O)	(c)
		+88·1	(NEt)	(c)
		+252·2	(NHCOMe)	(c)
Pr^i	in MeOH	+9·6	(N–O)	(c)
		+79·7	(N–Pr^i)	(c)
		+251·5	(NHCOMe)	(c)

(a) Data from ref. 264; ^{15}N singly labelled compounds; ^{15}N spectra; 9·12 MHz; field perpendicular to sample tube; referred originally to NH_4^+ in 5 M NH_4NO_3 in 2 M HNO_3, +359·0 ppm from neat nitromethane (Table 6), but reported relative to neat nitromethane; conversion scheme II (Table 4).

(b) Data from ref. 293; ^{14}N continuous-wave spectra; 4·33 MHz; field perpendicular to sample tube; referred originally to neat nitromethane (uncorrected for bulk susceptibility effects).

(c) Data from ref. 294; ^{15}N natural abundance spectra; 18·25 MHz; field parallel to sample tube; referred originally to neat nitromethane (uncorrected for bulk susceptibility effects).

TABLE 120

Nitrogen shieldings in pyridine and its derivatives

Compound	Solution	Nitrogen shielding referred to neat nitromethane: observed	corrected for bulk susceptibility	corrected, extrapolated to inf. dilution	Notes
 (pyridine)	neat, gaseous	+54·6	+56·2 ± 1·8		(a)
	neat liquid	+62·03 ± 0·11	same		(b)
		+63·5	+62·5		(a)
		+62·2			(c)
	0·003 mol % in C_2Cl_4	+60·9	+59·1		(a)
	14·3 mol % in cyclohexane	+59·4	+58·4	+57·7	(a)
	14·3 mol % in CCl_4	+62·1	+60·8	+60·5	(a)
	14·3 mol % in benzene	+62·3	+61·3	+61·1	(a)
	0·5 M in DMSO	+63·0			(d)
	2 M in DMSO	+63·8			(e)
	14·3 mol % in DMSO	+64·0	+63·0	+63·1	(a)
	14·3 mol % in CH_2Cl_2	+66·2	+64·9	+65·3	(a)
	14·3 mol % in $CHCl_3$	+69·2	+67·8	+68·7	(a),(f)
	2 M in $CHCl_3$	+70·0			(g)
	14·3 mol % in MeOH	+79·1	+78·4	+81·1	(a)
	14·3 mol % in H_2O	+82·1	+80·9	+84·3	(a)
	0·5 M in H_2O (1 mol %)	+84·4	same		(b)
	2 M in CF_3CH_2OH	+90·2			(e)
	14·3 mol % in CF_3CH_2OH	+92·3	+91·3	+96·1	(a)
Substituted pyridines					
2-Me	neat liquid	+62·3			(c)
3-Me	neat liquid	+61·7			(c)
4-Me	neat liquid	+70·2			(c)
		+69·8			(h)
2,3-Me_2	neat liquid	+62·3			(c)
2,4-Me_2	neat liquid	+71·0			(c)
2,5-Me_2	neat liquid	+62·7			(c)
	14·5 mol % in $CHCl_3$	+70·9			(f)
	14·5 mol % in CF_3CH_2OH	+94·5			(f)
2,6-Me_2	neat liquid	+62·4			(c)
3,4-Me_2	neat liquid	+68·8			(c)
3,5-Me_2	neat liquid	+61·7			(c)
2,4,6-Me_3	neat liquid	+71·1			(h)
2-Et	neat liquid	+64·0			(c)
3-Et	0·5 M in DMSO	+61·4			(d)

TABLE 120—*cont.*

Compound	Solution	Nitrogen shielding referred to neat nitromethane			Note
		observed	corrected for bulk susceptibility	corrected, extrapolated to inf. dilution	
4-Et	neat liquid	+68·6			(h)
2-Pr^{i}	neat liquid	+67·3			(c)
4-Pr^{i}	neat liquid	+67·9			(h)
2-Bu^{t}	neat liquid	+64·7			(c)
4-Bu^{t}	neat liquid	+67·8			(h)
2,6-Bu$^{t}_2$	neat liquid	+70·4			(c)
2,4,6-Bu$^{t}_3$	in benzene	+80·8			(c)
2-CH_2Ph	0·5 M in DMSO	+64·3			(d)
4-CH_2Ph	0·5 M in DMSO	+69·7			(d)
2-Ph	0·5 M in DMSO	+71·2			(d)
4-Ph	0·5 M in DMSO	+67·7			(d)
2-$CH{=}CH_2$	0·5 M in DMSO	+71·0			(d)
4-$CH{=}CH_2$	0·5 M in DMSO	+65·1			(d)
2-CN	0·5 M in DMSO	+62·2 (N)			(d)
		+126·2 (CN)			(d)
2-C(=O)Me	0·5 M in DMSO	+65·7			(d)
4-C(=O)Me	neat liquid	+51·8			(a)
	14·3 mol % in benzene	+50·6			(a)
	14·3 mol % in MeOH	+64·3			(a)
2-CHO	0·5 M in DMSO	+60·4			(d)
3-CHO	0·5 M in DMSO	+63·3			(d)
4-CHO	0·5 M in DMSO	+47·8			(d)
2-$CONH_2$	0·5 M in DMSO	+65·7 (N)			(d)
		+282·0 (NH_2)			(d)
3-$CONH_2$	0·5 M in DMSO	+64·5 (N)			(d)
		+277·1 (NH_2)			(d)
	0·1 M in D_2O	+74·7 (N)			(i)
4-$CONH_2$	0·5 M in DMSO	+56·4 (N)			(d)
		+275·9 (NH_2)			(d)
2-COOH	0·5 M in DMSO	+65·4			(d)
3-COOH	0·5 M in DMSO	+64·4			(d)
4-COOH	0·5 M in DMSO	+52·0			(d)
3-COOMe	0·5 M in DMSO	+63·3			(d)
3-COOEt	0·5 M in DMSO	+61·9			(d)
2-Cl	0·5 M in DMSO	+72·6			(d)
3-Cl	0·5 M in DMSO	+57·8			(d)
4-Cl	0·5 M in DMSO	+67·9			(d)
2-Br	0·5 M in DMSO	+64·3			(d)
3-Br	0·5 M in DMSO	+56·7			(d)
4-Br	0·5 M in DMSO	+67·4			(d)
2,6-Cl_2	0·5 M in DMSO	+80·6			(d)
2-Cl-5-NO_2	0·5 M in DMSO	+70·6			(d)

TABLE 120—*cont.*

Compound	Solution	Nitrogen shielding referred to neat nitromethane: observed	corrected for bulk susceptibility	corrected, extrapolated to inf. dilution	Notes
2-F	neat liquid	+104·5			(p)
		+105 ± 1			(j)
	1 : 5 v/v in Et_2O	+105 ± 1			(j)
	1 : 1 v/v in acetone	+107 ± 1			(j)
	1 : 1 v/v in MeOH	+109 ± 1			(j)
3-F	neat liquid	+80·8 (??)			(p)
		+54 ± 2			(j)
	1 : 5 v/v in Et_2O	+52 ± 2			(j)
	1 : 1 v/v in acetone	+56 ± 2			(j)
	1 : 1 v/v in MeOH	+58 ± 2			(j)
4-F	1 : 5 v/v in Et_2O	+73 ± 2			(j)
2,3,4,5,6-F_5	neat liquid	+147 ± 2			(j)
	1 : 5 v/v in Et_2O	+146 ± 2			(j)
	1 : 1 v/v in acetone	+148 ± 2			(j)
	1 : 1 v/v in MeOH	+149 ± 2			(j)
2,6-F_2		+135·0			(p)
2,3,5,6-F_4-4-OH	1 : 1 v/v in acetone	+156 ± 3			(j)
	1 : 1 v/v in MeOH	+160 ± 3			(j)
2,3,5,6-F_4-4-OMe	neat liquid	+150 ± 3			(j)
	1 : 1 v/v in acetone	+152 ± 3			(j)
	1 : 1 v/v in MeOH	+157 ± 3			(j)
2,3,5,6-F_4-4-SH	1 : 1 v/v in acetone	+144 ± 3			(j)
	1 : 3 v/v in acetone	+145 ± 3			(j)
2,3,5,6-F_4-4-SMe	1 : 1 v/v in acetone	+142 ± 2			(j)
	1 : 3 v/v in acetone	+144 ± 2			(j)
2,3,5,6-F_4-4-NH_2	1 : 5 v/v in acetone	+168 ± 2 (N)			(j)
		+331 ± 3 (NH_2)			(j)
2,3,5,6-F_4-4-NMe_2	1 : 3 v/v in acetone	+165 ± 2 (N)			(j)
		+336 ± 3 (NMe_2)			(j)
	1 : 1 v/v in MeOH	+170 ± 3 (N)			(j)
		+341 ± 3 (NMe_2)			(j)
2-OH		see Table 64			
3-OH	1 : 3 v/v in acetone	+67 ± 4			(k)
	1 : 3 v/v in MeOH	+71 ± 4			(k)
4-OH		see Table 64			
2-OMe	neat liquid	+109 ± 3			(k)
	1 : 3 v/v in acetone	+111 ± 2			(k)
	1 : 3 v/v in MeOH	+119 ± 2			(k)
3-OMe	neat liquid	+60 ± 3			(k)
	1 : 3 v/v in acetone	+64 ± 3			(k)
	1 : 3 v/v in MeOH	+67 ± 4			(k)

TABLE 120—*cont.*

Compound	Solution	Nitrogen shielding referred to neat nitromethane: observed	corrected for bulk susceptibility	corrected, extrapolated to inf. dilution	Notes
4-OMe	neat liquid	+86·2			(a)
	1 : 3 v/v in acetone	+91 ± 3			(k)
	14·3 mol % in benzene	+85·1			(a)
	14·3 mol % in MeOH	+103·3			(a)
2-SH		see Table 64			
3-SH	in acetone	+74 ± 1			(l)
	in MeOH	+88 ± 5			(l)
	in acetone/MeOH	+72 ± 5			(l)
4-SH		see Table 64			
2-SMe	1 : 3 v/v in acetone	+79 ± 3			(l)
	1 : 3 v/v in MeOH	+88 ± 4			(l)
3-SMe	1 : 3 v/v in acetone	+64 ± 1			(l)
	1 : 3 v/v in MeOH	+82 ± 5			(l)
	in acetone/DMSO (4 : 1)	+64 ± 3			(l)
4-SMe	1 : 3 v/v in acetone	+77 ± 2			(l)
	1 : 3 v/v in MeOH	+86 ± 4			(l)
	in acetone/DMSO (4 : 1)	+82 ± 4			(l)
2- 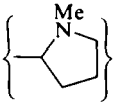	0·2 M in $CDCl_3$	+63·6 (pyridine)			(o)
3- 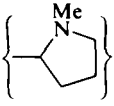	0·2 M in $CDCl_3$	+60·9 (pyridine)			(o)
4- 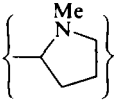	0·2 M in $CDCl_3$	+64·5 (pyridine)			(o)
2,3-$(NH_2)_2$	0·5 M in DMSO	+114·5 (N)			(d)
		+313·5 (2-NH_2)			(d)
		+330·4 (3-NH_2)			(d)
2,6-$(NH_2)_2$	0·5 M in DMSO	+149·0 (N)			(d)
		+309·1 (NH_2)			(d)
3,4-$(NH_2)_2$	0·5 M in DMSO	+99·3 (N)			(d)
		+336·9 (3-NH_2)			(d)
		+322·0 (4-NH_2)			(d)
2-NH_2-5-NO_2	0·5 M in DMSO	+11·4 (NO_2)			(d)
		+117·8 (N)			(d)
		+287·6 (NH_2)			(d)

TABLE 120—*cont.*

Compound	Solution	Nitrogen shielding referred to neat nitromethane: observed	corrected for bulk susceptibility	corrected, extrapolated to inf. dilution	Notes
2-NH_2	1 : 3 v/v in acetone	+116 ± 3 (N)			(l)
		+310 ± 3 (NH_2)			(l)
	in acetone	+115·7 (N)			(m)
		+311·8 (NH_2)			(m)
	0·5 M in DMSO	+113·8 (N)			(d)
		+307·3 (NH_2)			(d)
	0·5 M in DMSO	+116·0 (N)			(n), (m)
		+307·8 (NH_2)			(n), (m)
3-NH_2	1 : 3 v/v in acetone	+66 ± 3 (N)			(l)
		+334 ± 3 (NH_2)			(l)
	in acetone	+64·5 (N)			(m)
		+328·3 (NH_2)			(m)
	0·5 M in DMSO	+63·9 (N)			(d)
		+325·3 (NH_2)			(d)
4-NH_2	1 : 3 v/v in acetone	+106 ± 3 (N)			(l)
		+323 ± 3 (NH_2)			(l)
	in acetone	+101·5 (N)			(m)
		+317·2 (NH_2)			(m)
	0·5 M in DMSO	+103·7 (N)			(d)
		+312·0 (NH_2)			(d)
	0·5 M in DMSO	+107·2 (N)			(n), (m)
		+312·8 (NH_2)			(n), (m)
2-NHMe	1 : 3 v/v in acetone	+110 ± 3 (N)			(l)
		+308 ± 3 (NHMe)			(l)
3-NHMe	1 : 3 v/v in acetone	+65 ± 3 (N)			(l)
		+336 ± 3 (NHMe)			(l)
4-NHMe	1 : 3 v/v in acetone	+105 ± 3 (N)			(l)
		+318 ± 3 (NHMe)			(l)
2-NMe_2	1 : 3 v/v in acetone	+109 ± 3 (N)			(l)
		+319 ± 3 (NMe_2)			(l)
	in acetone	+112·6 (N)			(m)
		+323·0 (NMe_2)			(m)
3-NMe_2	1 : 3 v/v in acetone	+64 ± 3 (N)			(l)
		+342 ± 3 (NMe_2)			(l)
	in acetone	+63·6 (N)			(m)
		+340·0 (NMe_2)			(m)
4-NMe_2	1 : 3 v/v in acetone	+102 ± 3 (N)			(l)
		+329 ± 3 (NMe_2)			(l)
	in acetone	+105·6 (N)			(m)
		+328·6 (NMe_2)			(m)
2-NH_2-4-Me	0·5 M in DMSO	+119·3 (N)			(d)
		+308·1 (NH_2)			(d)

TABLE 120—*cont.*

Compound	Solution	Nitrogen shielding referred to neat nitromethane: observed	corrected for bulk susceptibility	corrected, extrapolated to inf. dilution	Note
2-NH_2-6-Me	0·5 M in DMSO	+112·4 (N)			(d)
		+307·4 (NH_2)			(d)
2-NH_2-4,6-Me_2	0·5 M in DMSO	+118·7 (N)			(d)
		+308·7 (NH_2)			(d)
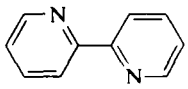 (2,2′-dipyridyl)	2 M in $CDCl_3$	+78·9			(g)

(a) Data from ref. 26; ^{15}N natural abundance spectra; 18·25 MHz; field parallel to sample tube; referred originally to 1 M DNO_3, +6·2 ppm from neat nitromethane (Table 6); conversion scheme IV (Table 4).

(b) Data from ref. 80 and ref. 85; ^{14}N continuous-wave measurements; 4·33 MHz; high-precision differential saturation technique with full lineshape fitting; concentric spherical sample/standard containers in order to eliminate bulk susceptibility effects; referred to neat nitromethane.

(c) Data from ref. 37; ^{15}N natural abundance spectra; 10·1 MHz; field perpendicular to sample tube; referred originally to *internal* nitromethane standard, +3·1 ppm from external neat nitromethane, as can be deduced from the reported shielding for pyridine.

(d) Data from ref. 115 and ref. 298; ^{15}N natural abundance spectra; 10·1 MHz; field perpendicular to sample tube; referred originally to aqueous NH_4NO_3; originally converted to neat nitromethane scale (uncorrected for bulk susceptibility effects).

(e) Data from ref. 299; see note (a).

(f) Data from ref. 300; see note (a).

(g) Data from ref. 125; ^{15}N natural abundance spectra; 10·09 MHz; field perpendicular to sample tube; referred originally to what was reported as aqueous NH_4Cl, +352·9 ppm from neat nitromethane (Table 6), but the shift reported for pyridine suggests that aqueous NH_4NO_3 was used actually, +359·6 ppm from neat nitromethane (Table 6); conversion scheme II (Table 4).

(h) Details as in note (c), but results referred to external $MeNO_2$ in deuterobenzene; conversion constant as in note (c).

(i) Data from ref. 136; ^{15}N-labelled pyridine ring; ^{15}N spectrum; 10·14 MHz; field perpendicular to sample tube; referred originally to 1 M ND_4Cl, +352·9 ppm from neat nitromethane (Table 6); conversion scheme II (Table 4).

(j) Data from ref. 301; ^{14}N continuous-wave spectra; 4·33 MHz; field perpendicular to sample tube; referred to neat nitromethane (uncorrected for bulk susceptibility effects).

(k) Data from ref. 1, p. 190, and references therein.

(l) Data from ref. 159; details as in note (j).

(m) Data from ref. 160; ^{15}N natural abundance spectra; 18·25 MHz; field parallel to sample tube; referred originally to neat nitromethane (uncorrected for bulk susceptibility effects).

(n) Data from ref. 158; see note (a).

(o) Data from ref. 26; note (a); quoted from earlier work by R. L. Lichter and J. D. Roberts, *J. Amer. Chem. Soc.*, 1972, **94**, 2495.

(p) Data from ref. 379; ^{15}N natural abundance spectra; 10·1 MHz; field perpendicular to sample tube; referred originally to neat nitromethane, but reported relative to NH_3, +380·2 ppm from neat nitromethane (Table 6); uncorrected for bulk susceptibility effects.

TABLE 121

Nitrogen shieldings in some derivatives of pyrimidine and pyrazine

Compound	Solution	Nitrogen shielding referred to neat nitromethane	Notes
	0·5 M in DMSO	+84·8	(a)
	neat liquid	+85·4	(b)
(pyrimidine)			
Substituted pyrimidines			
4-Me	0·5 M in DMSO	+93·1 (N-1)	(a)
		+84·7 (N-3)	(a)
5-Me	0·5 M in DMSO	+85·9	(a)
4-Ph	0·5 M in DMSO	+89·2 (N-1)	(a)
		+94·5 (N-3)	(a)
2-Cl	0·5 M in DMSO	+88·2	(a)
2-NH_2	0·5 M in DMSO	+129·9 (N)	(a)
		+297·9 (NH_2)	(a)
2-NMe_2	0·5 M in DMSO	+132·0 (N)	(a)
		+311·9 (NMe_2)	(a)
2-NH_2-4-Me	0·5 M in DMSO	+138·2 (N-1)	(a)
		+130·3 (N-3)	(a)
		+299·5 (NH_2)	(a)
2-NH_2-4,6-Me_2	0·5 M in DMSO	+138·0 (N)	(a)
		+300·4 (NH_2)	(a)
2-NH_2-4,6-Cl_2	0·5 M in DMSO	+141·5 (N)	(a)
		+292·0 (NH_2)	(a)
2-NH_2-4,6-$(OMe)_2$	0·5 M in DMSO	+180·2 (N)	(a)
		+296·4 (NH_2)	(a)
2,4-$(OMe)_2$	0·5 M in DMSO	+150·0 (N-1)	(a)
		+160·9 (N-3)	(a)
2-Me-4-Ph	0·5 M in DMSO	+87·5	(a)
2,4-Me_2-5-COOEt	0·5 M in DMSO	+94·5 (N-1)	(a)
		+85·4 (N-3)	(a)
2-Cl-5-NO_2	0·5 M in DMSO	+91·3 (N)	(a)
		+17·6 (NO_2)	(a)
2,4-Cl_2	0·5 M in DMSO	+92·6 (N-1)	(a)
		+94·5 (N-3)	(a)
2-SMe-4-Cl	0·5 M in DMSO	+100·5 (N-1)	(a)
		+102·4 (N-3)	(a)
4,6-Cl_2	0·5 M in DMSO	+93·7	(a)
2,6-Me_2-4-NH_2	0·5 M in DMSO	+121·0 (N-1)	(a)
		+139·2 (N-3)	(a)
		+299·0 (NH_2)	(a)
2,5-Me_2-4-NH_2	0·5 M in DMSO	+121·3 (N-1)	(a)
		+134·0 (N-3)	(a)
		+299·6 (NH_2)	(a)

TABLE 121—*cont.*

Compound	Solution	Nitrogen shielding referred to neat nitromethane	Notes
2-Me-4-NH_2-5-CN	0·5 M in DMSO	+108·9 (N-1)	(a)
		+120·2 (N-3)	(a)
		+134·2 (CN)	(a)
		+288·3 (NH_2)	(a)
2-Et-4-NH_2-5-CN	0·5 M in DMSO	+108·8 (N-1)	(a)
		+121·7 (N-3)	(a)
		+134·7 (CN)	(a)
		+288·3 (NH_2)	(a)
2-SMe-4-NH_2-5-COOEt	0·5 M in DMSO	+128·8 (N-1)	(a)
		+142·0 (N-3)	(a)
		+289·4 (NH_2)	(a)
4-NH_2-5-[CH_2·C_6H_2-3,4,5($OMe)_3$]	0·5 M in DMSO	+120·9 (N-1)	(a)
		+132·7 (N-3)	(a)
		+298·4 (NH_2)	(a)
2-Ph-4-NH_2-5-[CH_2·C_6H_2-3,4,5($OMe)_3$]	0·5 M in DMSO	+127·8 (N-1)	(a)
		+141·3 (N-3)	(a)
		+297·8 (NH_2)	(a)
2,4-$(NH_2)_2$	0·5 M in DMSO	+164·5 (N-1)	(a)
		+173·4 (N-3)	(a)
		+301·6 (2-NH_2)	(a)
		+299·6 (4-NH_2)	(a)
2,4-$(NH_2)_2$-5-[CH_2·C_6H_2-3,4,5($OMe)_3$]	0·5 M in DMSO	+163·0 (N-1)	(a)
		+174·4 (N-3)	(a)
		+304·6 (2-NH_2)	(a)
		+302·3 (4-NH_2)	(a)
2,4-$(NH_2)_2$-5-(C_6H_4·Cl*p*)-6-Et	0·5 M in DMSO	+176·3 (N-1, N-3)	(a)
		+300·9 (NH_2)	(a)
		+299·4 (NH_2)	(a)
2,4-$(NH_2)_2$-5,6-(–$CH_2CH_2CH_2CH_2$–)	0·5 M in DMSO	+174·1 (N-1, N-3)	(a)
		+305·1 (NH_2)	(a)
		+302·6 (NH_2)	(a)
2,4-$(NH_2)_2$-6-Cl	0·5 M in DMSO	+166·1 (N-1)	(a)
		+178·7 (N-3)	(a)
		+297·7 (2-NH_2)	(a)
		+296·5 (4-NH_2)	(a)
4,6-$(NH_2)_2$	0·5 M in DMSO	+149·4 (N)	(a)
		+309·1 (NH_2)	(a)
4,6-$(NH_2)_2$-5-[C_6H_3-3,4($OMe)_2$]	0·5 M in DMSO	+151·8 (N)	(a)
		+304·5 (NH_2)	(a)
4,5-$(NH_2)_2$	0·5 M in DMSO	+132·6 (N-1)	(a)
		+133·5 (N-3)	(a)
		+305·9 (4-NH_2)	(a)
		+338·0 (5-NH_2)	(a)
2,4,6-$(NH_2)_3$	0·5 M in DMSO	+189·5 (N)	(a)
		+304·0 (2-NH_2)	(a)
		+306·0 (4,6-NH_2)	(a)

TABLE 121—*cont.*

Compound	Solution	Nitrogen shielding referred to neat nitromethane	Notes
2,4,6-$(NH_2)_3$-5-[C_6H_2-3,4,5$(OMe)_3$]	0·5 M in DMSO	+191·6 (N)	(a)
		+305·5 (2-NH_2)	(a)
		+306·1 (4,6-NH_2)	(a)
2-(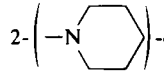)-4,6-$(NH_2)_2$	0·5 M in DMSO	+190·2 (N)	(a)
		+308·2 (piperidyl)	(a)
		+306·2 (4,6-NH_2)	(a)
2,4,5-$(NH_2)_3$	1 M in DMSO	? (N-1, N-3)	(a)
	as hydrochloride	+311·2 (2-NH_2)	(a)
	+1 eq. of 4 M NaOH	+316·3 (4-NH_2)	(a)
		+357·3 (5-NH_2)	(a)
2,4,5-$(NH_2)_3$-6-(CH=CHPh)	1 M in DMSO as	+173·0 (N-1)	(a)
	hydrochloride	+180·2 (N-3)	(a)
	+1 eq. of 4 M NaOH	+303·4 (2-NH_2)	(a)
		+311·5 (4-NH_2)	(a)
		+345·9 (5-NH_2)	(a)
4,5,6-$(NH_2)_3$	1 M in DMSO as	+152·7 (N)	(a)
	hydrochloride	+309·8 (4,6-NH_2)	(a)
	+1 eq. of 4 M NaOH	+346·9 (5-NH_2)	(a)
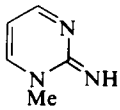	0·5 M in DMSO	+98·6 (N)	(a)
		+246·9 (NMe)	(a)
		+194·4 (=NH)	(a)
	0·5 M in DMSO	+46·3	(a)
(pyrazine)			
Substituted pyrazines			
2-[C(=O)N=C$(NH_2)_2$]-3,5-$(NH_2)_2$-6-Cl	in DMSO	+53·5 (N-1)	(c)
		+139·1 (N-4)	(c)
2-[C(=O)NH^+=C$(NH_2)_2$]-3,5-$(NH_2)_2$-6-Cl	in DMSO, Cl^-	+68·5 (N-1)	(c)
		+147·1 (N-4)	(c)
2-[C(=O)N=C$(NMe_2)_2$]-3,5-$(NH_2)_2$	in DMSO	+55·1 (N-1)	(c)
		+141·2 (N-4)	(c)
2-C(=O)N=C$(NH_2)_2$-3-NH_2-5-NMe_2	in DMSO	+46·7 (N-1)	(c)
		+126·5 (N-4)	(c)

(a) Data from ref. 115 and ref. 298; ^{15}N natural abundance spectra; 10·1 MHz; field perpendicular to sample tube; referred originally to aqueous NH_4NO_3; originally converted to neat nitromethane scale; uncorrected for bulk susceptibility effects.

(b) Data from ref. 1, p. 190, and references therein.

(c) Data from ref. 161; ^{15}N natural abundance spectra; 18·25 MHz; field parallel to sample tube; referred originally to 1 M DNO_3, +6·2 ppm from neat nitromethane (Table 6); conversion scheme IV (Table 4).

TABLE 122

Nitrogen shieldings in unsubstituted azine ring systems

Structure	Solution or state	Nitrogen shielding referred to neat nitromethane	Notes
 (pyridine)	neat liquid	+62·03 ± 0·11	(a)
	0·5 M in DMSO	+63·0	(b)
	0·3 M in acetone	+64·0	(a)
	see also Table 120		
 (pyridazine, 1,2-diazine)	0·5 M in DMSO	−20·3	(b)
 pyrimidine, 1,3-diazine)	neat liquid	+85·4	(c)
	0·5 M in DMSO	+84·8	(b)
 (pyrazine, 1,4-diazine)	0·5 M in DMSO	+46·3	(b)
 (1,2,4-triazine)	in acetone	−42 ± 1 (N-1)	(e)
		+2 ± 1 (N-2)	(e)
		+82 ± 1 (N-4)	(e)
 (1,3,5-triazine)	0·15 M in acetone	+97 ± 1	(c)
	in dioxan	+98 ± 1	(d)
 (1,2,4,5-tetrazine)	in acetone	−5 ± 1	(d)
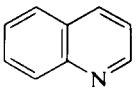 (quinoline)	1·0 M in acetone	+66·89 ± 0·15	(i)

TABLE 122—*cont.*

Structure	Solution or state	Nitrogen shielding referred to neat nitromethane	Notes
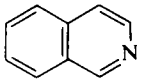 (isoquinoline)	1·0 M in acetone	+69·11 ± 0·21	(i)
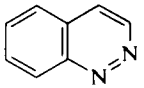 (cinnoline)	0·5 M in DMSO	−44·6 (N-1?) −41·3 (N-2?)	(b) (b)
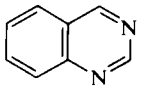 (quinazoline)	in acetone	+86·2 (N-1?) +97·4 (N-3?)	(f) (f)
	0·5 M in DMSO	+85·5 (N-1?) +96·9 (N-3?)	(b) (b)
		+87·0 (N-1?) +98·4 (N-3?)	(g) (g)
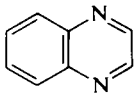 (quinoxaline)	in acetone 0·5 M in DMSO	+51·4 +49·8	(f) (b)
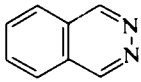 (phthalazine)	in acetone 0·5 M in DMSO	+8·8 +10·3	(f) (b)
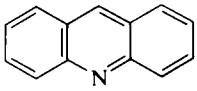 (acridine)	in CH_2Br_2	+94 ± 8	(d)
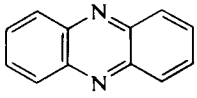 (phenazine)	in acetone	+54·0	(f)
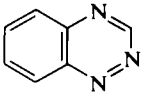 (benzo-1,2,4-triazine)	in acetone	−78 ± 2 (N-1) −26 ± 2 (N-2) +99 ± 1 (N-4)	(e) (e) (e)

TABLE 122—*cont.*

Structure	Solution or state	Nitrogen shielding referred to neat nitromethane	Notes
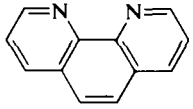	2 M in MeOH	+86·5	(h)

(a) Data from ref. 80 and ref. 85; ^{14}N continuous-wave spectra; 4·33 MHz; high-precision differential saturation technique with full lineshape fitting; spherical sample/standard containers in order to eliminate bulk susceptibility effects; referred to neat nitromethane.

(b) Data from ref. 115; ^{15}N natural abundance spectra; 10·1 MHz; field perpendicular to sample tube; referred originally to aqueous NH_4NO_3; converted originally to neat nitromethane scale (uncorrected for bulk susceptibility effects); $Cr(acac)_3$ added to samples.

(c) Data from ref. 1, p. 190, and references therein.

(d) Data from ref. 2, p. 221, and references therein.

(e) Data from ref. 36; details as in note (a), but smaller precision.

(f) Data from ref. 302; ^{15}N natural abundance spectra; 18·25 MHz; field parallel to sample tube; referred originally to neat nitromethane (uncorrected for bulk susceptibility effects).

(g) Data from ref. 158; ^{15}N natural abundance spectra; 18·25 MHz; field parallel to sample tube; referred originally to 1 M DNO_3, +6·2 ppm from neat nitromethane (Table 6); conversion scheme IV (Table 4).

(h) Data from ref. 125; ^{15}N natural abundance spectra; 10·09 MHz; field perpendicular to sample tube; referred originally to what was reported as aqueous NH_4Cl, +352·9 ppm from neat nitromethane (Table 6), but the reported shift for pyridine suggests that aqueous NH_4NO_3 was actually used, +359·6 ppm from neat nitromethane (Table 6); conversion scheme II (Table 4).

(i) Data from ref. 179; details as in note (a).

TABLE 123

Nitrogen shieldings in some azinium ions and related structures

Cation	Solution (TFA = CF_3COOH)	Nitrogen shielding referred to neat nitromethane	Notes
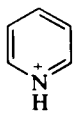 (pyridinium ion)	Cl^-, 0·5 M in 10·0 M HCl (*ca.* 1 mol %)	+178·96 ± 0·09 (doublet)	(a)
	Cl^-, 16·0 mol % in $CHCl_3$	+167·8	(b)
	Cl^-, 15·6 mol % in DMSO	+165·6	(b)
	Cl^-, 4·0 mol % in MeOH	+176·6	(b)
	Cl^-, 4·3 mol % in H_2O	+179·6	(b)
	Cl^-, 2 M in H_2O/HCl	+182·7 (?)	(c)
	CF_3COO^-, 33 mol % in TFA	+172·1	(d)
	CF_3COO^-, 20 mol % in TFA/$CHCl_3$ (1 : 1)	+175·4	(d)
	CF_3COO^-, 14·5 mol % in TFA	+184·8 (doublet)	(e)
	CF_3COO^-, 2 M in TFA	+179·0	(f)
	CF_3COO^-, 0·5 M in TFA	+182·5	(g)
	SO_3F^-, 0·5 M in FSO_3H	+186·9	(g)
Substituted pyridinium ions			
2-Me	CF_3COO^-, 33 mol % in TFA	+171·1	(d)
	CF_3COO^-, 20 mol % in TFA/$CHCl_3$ (1 : 1)	+175·8	(d)
3-Me	CF_3COO^-, 33 mol % in TFA/$CHCl_3$ (1 : 1)	+160·3	(d)
	CF_3COO^-, 20 mol % in TFA/$CHCl_3$ (1 : 1)	+175·7	(d)
	CF_3COO^-, 33 mol % in TFA	+181·9	(d)
4-Me	CF_3COO^-, 12·5 mol % in TFA/$CHCl_3$ (2 : 5)	+174·4	(d)
	CF_3COO^-, 20 mol % in TFA/$CHCl_3$ (1 : 1)	+182·2	(d)
	CF_3COO^-, 14 mol % in TFA/$CHCl_3$ (1 : 1)	+183·7	(d)
	CF_3COO^-, 33 mol % in TFA	+185·0	(d)
	CF_3COO^-, 11 mol % in TFA/$CHCl_3$ (1 : 1)	+186·2	(d)
	CF_3COO^-, 9 mol % in TFA/$CHCl_3$ (1 : 1)	+187·1	(d)
	CF_3COO^-, 7·7 mol % in TFA/$CHCl_3$ (1 : 1)	+187·5	(d)

TABLE 123—*cont.*

Cation	Solution (TFA = CF_3COOH)	Nitrogen shielding referred to neat nitromethane	Notes
2,3-Me_2	CF_3COO^-, 33 mol % in TFA/$CHCl_3$ (1:1)	+163·3	(d)
	CF_3COO^-, 20 mol % in TFA/$CHCl_3$ (1:1)	+176·4	(d)
	CF_3COO^-, 33 mol % in TFA	+176·6	(d)
2,4-Me_2	CF_3COO^-, 33 mol % in TFA/$CHCl_3$ (1:1)	+161·0	(d)
	CF_3COO^-, 20 mol % in TFA/$CHCl_3$ (1:1)	+182·3	(d)
	CF_3COO^-, 33 mol % in TFA	+182·5	(d)
2,5-Me_2	CF_3COO^-, 33 mol % in TFA/$CHCl_3$ (1:1)	+150·4	(d)
	CF_3COO^-, 20 mol % in TFA/$CHCl_3$ (1:1)	+175·5	(d)
	CF_3COO^-, 33 mol % in TFA	+172·1	(d)
2,6-Me_2	CF_3COO^-, 20 mol % in TFA/$CHCl_3$ (1:1)	+176·0	(d)
	CF_3COO^-, 33 mol % in TFA	+175·2	(d)
	CF_3COO^-, 14·5 mol % in TFA	+183·2 (doublet)	(e)
3,4-Me_2	CF_3COO^-, 12·5 mol % in TFA/$CHCl_3$ (2:5)	+178·4	(d)
	CF_3COO^-, 33 mol % in TFA	+179·1	(d)
	CF_3COO^-, 20 mol % in TFA/$CHCl_3$ (1:1)	+182·2	(d)
	CF_3COO^-, 14·3 mol % in TFA/$CHCl_3$ (1:1)	+183·5	(d)
	CF_3COO^-, 11·1 mol % in TFA/$CHCl_3$ (1:1)	+185·6	(d)
	CF_3COO^-, 9·1 mol % in TFA/$CHCl_3$ (1:1)	+186·8	(d)
	CF_3COO^-, 7·7 mol % in TFA/$CHCl_3$ (1:1)	+187·6	(d)
	CF_3COO^-, 4·8 mol % in TFA/$CHCl_3$ (1:1)	+188·8	(d)
3,5-Me_2	CF_3COO^-, 20 mol % in TFA/$CHCl_3$ (1:1)	+176·6	(d)
	CF_3COO^-, 33 mol % in TFA	+177·6	(d)
4-C(=O)Me	Cl^-, 4·0 mol % in MeOH	+169·6	(b)
	Cl^-, 3·2 mol % in H_2O	+171·3	(b)
	Cl^-, 10·5 mol % in DMSO	+145·7	(b)
4-C(OMe)$_2$Me	Cl^-, 4·0 mol % in MeOH	+178·2	(b)

3-$CONH_2$	Cl^-, 0·1 M in D_2O, pD 2	+170·9 (NH^+)	(h)
4-OMe	Cl^-, 4·0 mol % in MeOH	+197·5	(b)
	Cl^-, 4·1 mol % in H_2O	+199·9	(b)
2-NH_2	CF_3COO^-, 0·5 M in TFA	+226·0 (NH^+)	(g)
		+305·6 (NH_2)	(g)
	SO_3F^-, 0·5 M in FSO_3H	+229·5 (NH^+)	(g)
		+292·6 (NH_2)	(g)
2-NH_3^+	SO_3F^-, 0·5 M in FSO_3H	+192·4 (NH^+)	(g)
		+330·6 (NH_3^+)	(g)
3-NH_2	CF_3COO^-, 0·5 M in TFA	+184·7 (NH^+)	(g)
		+325·2 (NH_2)	(g)
	SO_3F^-, 0·5 M in FSO_3H	+181·1 (NH^+)	(g)
		+334·8 (NH_2)	(g)
3-NH_3^+	SO_3F^-, 0·5 M in FSO_3H	+181·1 (NH^+)	(g)
		+345·4 (NH_3^+)	(g)
4-NH_2	CF_3COO^-, 0·5 M in TFA	+220·7 (NH^+)	(g)
		+293·0 (NH_2)	(g)
	SO_3F^-, 0·5 M in FSO_3H	+210·8 (NH^+)	(g)
		+295·1 (NH_2)	(g)
4-NH_3^+	SO_3F^-, 0·5 M in FSO_3H	+181·6 (NH^+)	(g)
		+330·2 (NH_3^+)	(g)
2,3-$(NH_2)_2$	CF_3COO^-, 0·5 M in TFA	+219·4 (NH^+)	(g)
		+305·0 (2-NH_2)	(g)
		+337·0 (3-NH_2)	(g)
	SO_3F^-, 0·5 M in FSO_3H	+219·5 (NH^+)	(g)
		+305·0 (2-NH_2)	(g)
		+339·5 (3-NH_2)	(g)
2,6-$(NH_2)_2$	CF_3COO^-, 0·5 M in TFA	+239·3 (NH^+)	(g)
		+312·3 (NH_2)	(g)

TABLE 123—*cont.*

Cation	Solution (TFA = CF_3COOH)	Nitrogen shielding referred to neat nitromethane	Notes
3,4-$(NH_2)_2$	CF_3COO^-, 0·5 M in TFA	+216·9 (NH^+)	(g)
		+339·0 (3-NH_2)	(g)
		+290·4 (4-NH_2)	(g)
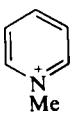	Cl^-, 3·7 mol % in H_2O	+180·2	(b)
	I^-, 4·4 mol % in H_2O	+180·7	(b)
	I^-, 1 M in DMSO	+179·9	(f)
	I^-, 1 M in CF_3CH_2OH	+181·3	(f)
	I^-, 1 M in TFA	+182·0	(f)
(*N*-Me-pyridinium ion)			
Substituted *N*-Me-pyridinium ions			
4-C(=O)Me	Cl^-, 2·6 mol % in H_2O	+174·0	(b)
	I^-, 4·4 mol % in H_2O	+174·6	(b)
3-$CONH_2$	0·1 M in D_2O	+171·2 (N^+Me)	(h)
	0·1 M in 70% MeOH	+171·2 (N^+Me)	(h)
4-OMe	Cl^-, 4·1 mol % in H_2O	+201·5	(b)
	I^-, 4·4 mol % in H_2O	+201·8	(b)
	I^-, 10·0 mol % in $CHCl_3$	+202·5	(b)
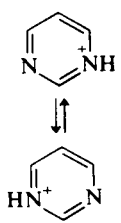	CF_3COO^-, 0·5 M in TFA	+134·8 ($N \rightleftarrows NH^+$)	(g)
(pyrimidinium monocation)			

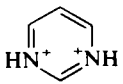	SO_3F^-, 0·5 M in FSO_3H	+182·6	(g)
(pyrimidinium dication)			
Substituted pyrimidinium mono- and di-cations			
4-NH_2-5-[$CH_2{\cdot}C_6H_2$-3,4,5$(OMe)_3$]			
dication	CF_3COO^-, 0·5 M in TFA	+217·9 (NH^+)	(g)
		+218·0 (NH^+)	(g)
		+278·3 (NH_2)	(g)
2-Ph-4-NH_2-5-[$CH_2{\cdot}C_6H_2$-3,4,5$(OMe)_3$]			
dication	CF_3COO^-, 0·5 M in TFA	+227·6 (NH^+)	(g)
		+281·2 (NH_2)	(g)
	SO_3F^-, 0·5 M in FSO_3H	+224·2 (NH^+)	(g)
		+230·9 (NH^+)	(g)
		+270·8 (NH_2)	(g)
2-NH_2			
monocation	CF_3COO^-, 0·5 M in TFA	+134·8 ($N\rightleftarrows NH^+$)	(g)
		+294·3 (NH_2)	(g)
dication	SO_3F^-, 0·5 M in FSO_3H	+220·0 (NH^+)	(g)
		+286·7 (NH_2)	(g)
2,4-$(NH_2)_2$			
dication+some N-1 monocation	CF_3COO^-, 0·5 M in TFA	+253·6 (1-NH^+)	(g)
		+231·6 (3-NH^+)	(g)
		+296·4 (2-NH_2)	(g)
		+276·4 (4-NH_2)	(g)
dication	SO_3F^-, 0·5 M in FSO_3H	+253·6 (NH^+)	(g)
		+254·6 (NH^+)	(g)
		+293·1 (2-NH_2)	(g)
		+279·0 (4-NH_2)	(g)

TABLE 123—*cont.*

Cation	Solution (TFA = CF_3COOH)	Nitrogen shielding referred to neat nitromethane	Notes
2,4-$(NH_2)_2$-5-[$CH_2 \cdot C_6H_2$-3,4,5$(OMe)_3$]			
dication+some N-1 monocation	CF_3COO^-, 0·5 M in TFA	+253·3 (1-NH^+)	(g)
		+226·3 (3-NH^+)	(g)
		+299·0 (2-NH_2)	(g)
		+279·0 (4-NH_2)	(g)
dication	SO_3F^-, 0·5 M in FSO_3H	+252·1 (NH^+)	(g)
		+254·3 (NH^+)	(g)
		+293·1 (2-NH_2)	(g)
		+271·4 (4-NH_2)	(g)
2,4-$(NH_2)_2$-5-($C_6H_4 \cdot Cl$*p*)-6-Et			
dication	CF_3COO^-, 0·5 M in TFA	+247·5 (NH^+)	(g)
		+294·5 (2-NH_2)	(g)
		+274·9 (4-NH_2)	(g)
dication	SO_3F^-, 0·5 M in FSO_3H	+249·9 (NH^+)	(g)
		+250·7 (NH^+)	(g)
		+295·8 (2-NH_2)	(g)
		+274·5 (4-NH_2)	(g)
2,4-$(NH_2)_2$-5,6-(–$CH_2CH_2CH_2CH_2$–)			
dication	CF_3COO^-, 0·5 M in TFA	+247·1 (NH^+)	(g)
		+245·1 (NH^+)	(g)
		+296·4 (2-NH_2)	(g)
		+278·7 (4-NH_2)	(g)
dication	SO_3F^-, 0·5 M in FSO_3H	+248·4 (NH^+)	(g)
		+255·2 (NH^+)	(g)
		+297·8 (2-NH_2)	(g)
		+278·0 (4-NH_2)	(g)

2,4-$(NH_2)_2$-6-Cl			
dication+some N-1 and N-3 monocations	CF_3COO^-, 0·5 M in TFA	+227·4 (1-NH^+)	(g)
		+229·1 (3-NH^+)	(g)
		+297·9 (2-NH_2)	(g)
		+283·5 (4-NH_2)	(g)
dication	SO_3F^-, 0·5 M in FSO_3H	+248·0 (1-NH^+)	(g)
		+257·0 (3-NH^+)	(g)
		+292·1 (2-NH_2)	(g)
		+271·8 (4-NH_2)	(g)
4,6-$(NH_2)_2$			
dication+some monocation	CF_3COO^-, 0·5 M in TFA	+210·3 (NH^+)	(g)
		+289·0 (NH_2)	(g)
dication	SO_3F^-, 0·5 M in FSO_3H	+233·9 (NH^+)	(g)
		+289·1 (NH_2)	(g)
4,6-$(NH_2)_2$-5-[CH_2·C_6H_3-3,4$(OMe)_2$]			
dication+some monocation	CF_3COO^-, 0·5 M in TFA	+209·9 (NH^+)	(g)
		+297·2 (NH_2)	(g)
dication	SO_3F^-, 0·5 M in FSO_3H	+230·7 (NH^+)	(g)
		+289·6 (NH_2)	(g)
4,5-$(NH_2)_2$			
dication	CF_3COO^-, 0·5 M in TFA	+215·1 (NH^+)	(g)
		+282·3 (4-NH_2)	(g)
		+335·8 (5-NH_2)	(g)
dication	SO_3F^-, 0·5 M in FSO_3H	+216·7 (NH^+)	(g)
		+220·2 (NH^+)	(g)
		+261·6 (4-NH_2)	(g)
		+340·9 (5-NH_2)	(g)
2,4,6-$(NH_2)_3$			
dication	CF_3COO^-, 0·5 M in TFA	+261·7 (NH^+)	(g)
		+291·3 (NH_2)	(g)
dication	SO_3F^-, 0·5 M in FSO_3H	+260·0 (NH^+)	(g)
		+281·4 (2-NH_2)	(g)
		+264·5 (4,6-NH_2)	(g)

TABLE 123—*cont.*

Cation	Solution (TFA = CF_3COOH)	Nitrogen shielding referred to neat nitromethane	Notes
2,4,6-$(NH_2)_3$-5-[$CH_2{\cdot}C_6H_3$-3,4$(OMe)_2$] dication	CF_3COO^-, 0·5 M in TFA	+261·5 (NH^+)	(g)
		+297·5 (2-NH_2)	(g)
		+295·6 (4,6-NH_2)	(g)
dication	SO_3F^-, 0·5 M in FSO_3H	+261·8 (NH^+)	(g)
2- 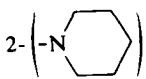 -4,6-$(NH_2)_2$ dication	CF_3COO^-, 0·5 M in TFA	+266·1 (NH^+)	(g)
		+295·8 (piperidyl)	(g)
		+293·3 (NH_2)	(g)
dication	SO_3F^-, 0·5 M in FSO_3H	+261·1 (NH^+)	(g)
		+293·9 (piperidyl)	(g)
2,4,5-$(NH_2)_3$ monocation (N-1 hydrochloride)	Cl^-, 0·5 M in DMSO+0·2 eq. HCl	+218·8 ($N{\rightleftarrows}NH^+$)	(g)
		+310·1 (2 or 4-NH_2)	(g)
		+309·0 (2 or 4-NH_2)	(g)
		+336·1 (5-NH_2)	(g)
2,4,5-$(NH_2)_3$-6-(CH=CHPh) dication	Cl^-, 0·5 M in DMSO dissolved as N-1 monohydrochloride +1·0 eq. HCl	+260·8 (NH^+)	(g)
		+303·1 (2-NH_2)	(g)
		+279·4 (4-NH_2)	(g)
		+336·1 (5-NH_2)	(g)

4,5,6-$(NH_2)_3$ monocation	Cl^-, 0·5 M in DMSO dissolved as N-1 monohydrochloride +0·2 eq. HCl	+181·7 ($N \rightleftarrows NH^+$) +301·5 (4,6-NH_2) +343·2 (5-NH_2)	(g) (g) (g)
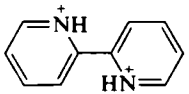	2 M in H_2O/HCl	+164·2	(c)
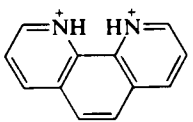	2 M in H_2O/HCl	+148·2	(c)
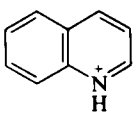 (quinolinium ion)	1:3 v/v in H_2SO_4	+193·1	(i)
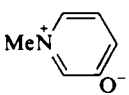 (*N*-Me-3-oxypyridyl-betaine)	1:3 v/v in MeOH	+181 ± 1	(i)

TABLE 123—*cont.*

Cation	Solution (TFA = CF_3COOH)	Nitrogen shielding referred to neat nitromethane	Notes
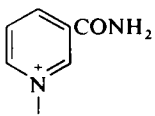 (ADP-ribose)	0·1 M in D_2O		
	pD 7	+155·0 (N^+) (dinucleotide, NAD^+)	(h)
	pD 7	+153·9 (N^+) (mononucleotide, NMN^+)	(h)
	pD 2	+154·8 (N^+) (NAD^+)	(h)
	pD 2	+154·1 (N^+) (NMN^+)	(h)

(a) Data from ref. 80; ^{14}N continuous-wave measurements; 4·33 MHz; high-precision differential saturation technique with full lineshape fitting; concentric spherical sample/standard containers in order to eliminate bulk susceptibility effects; referred to neat nitromethane.

(b) Data from ref. 26; ^{15}N natural abundance spectra; 18·25 MHz; field parallel to sample tube; referred originally to 1 M DNO_3, +6·2 ppm from neat nitromethane (Table 6); conversion scheme IV (Table 4).

(c) Data from ref. 125; ^{15}N natural abundance spectra; 10·09 MHz; field perpendicular to sample tube; referred to what was reported as aqueous NH_4Cl, +352·5 ppm from neat nitromethane (Table 6), but the reported shift for pyridine suggests that aqueous NH_4NO_3 was actually employed, +359·6 ppm from neat nitromethane (Table 6); conversion scheme II (Table 4).

(d) Data from ref. 37; ^{15}N natural abundance spectra; 10·1 MHz; field perpendicular to sample tube; referred originally to 2·9 M NH_4Cl in 1 M HCl, +355·3 ppm from neat nitromethane (Table 6); conversion scheme IV (Table 4).

(e) Data from ref. 300; details as in note (b).

(f) Data from ref. 299; details as in note (b).

(g) Data from ref. 115; ^{15}N natural abundance spectra; 10·1 MHz; field perpendicular to sample tube; referred originally to aqueous NH_4NO_3; converted originally to neat nitromethane scale (uncorrected for bulk susceptibility effects).

(h) Data from ref. 136; ^{15}N-labelled pyridine ring; ^{15}N spectra; 10·14 MHz; field perpendicular to sample tube; referred originally to 1 M ND_4Cl, +352·9 ppm from neat nitromethane (Table 6); conversion scheme II (Table 4).

(i) Data from ref. 1, p. 190, and references therein.

TABLE 124

Nitrogen shieldings in some azine *N*-oxides, their cations, and isomeric structures

Compound	Solution	Nitrogen shielding referred to neat nitromethane	Notes
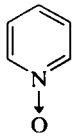	0·2 M in CS_2	+82	(a)
	1·0 M in $CDCl_3$	+84	(a)
	in acetone	+86	(b)
	in DMSO	+85·5	(c)
	2 M in DMSO	+86·8	(d)
	2 M in CF_3CH_2OH	+99·5	(d)
(pyridine *N*-oxide)	in H_2O	+99	(b)
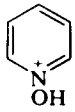	2 M in CF_3COOH	+135·7	(d)
(*N*-hydroxypyridinium cation, conjugate acid of pyridine *N*-oxide)			
Substituted pyridine *N*-oxides and corresponding cations			
2-Me	in DMSO	+85·5	(c)
	2 M in DMSO	+90·9	(d)
	in H_2O	+100·7	(c)
	2 M in CF_3CH_2OH	+103·8	(d)
	2 M in CF_3COOH (cation)	+141·8	(d)
3-Me	in DMSO	+85·5	(c)
	2 M in DMSO	+86·9	(d)
	in H_2O	+99·0	(c)
	2 M in CF_3CH_2OH	+105·2	(d)
	2 M in CF_3COOH (cation)	+141·8	(d)
4-Me	in DMSO	+94·3	(c)
	1 M in DMSO	+93·6	(d)
	1 M in CF_3CH_2OH	+106·8	(d)
	in H_2O	+108·2	(c)
	1 M in CF_3COOH (cation)	+146·0	(d)
2,6-Me_2	1 : 3 v/v in acetone	+91	(e)
	2 M in DMSO	+92·9	(d)
	2 M in CF_3CH_2OH	+107·8	(d)
	2 M in CF_3COOH (cation)	+143·1	(d)
2, 4-Me_2	1 : 3 v/v in acetone	+93	(e)
4-Ph	1 M in CF_3CH_2OH	+110·4	(d)
	1 M in CF_3COOH (cation)	+145·9	(d)

TABLE 124—*cont.*

Compound	Solution	Nitrogen shielding referred to neat nitromethane		Notes
4-Cl	1 M in CF_3CH_2OH	+106·2		(d)
	1 M in CF_3COOH (cation)	+141·7		(d)
4-NO_2	1 M in DMSO	+73·4	(N→O)	(d)
	1 M in CF_3CH_2OH	+85·8	(N→O)	(d)
	1 M in CF_3COOH (cation)	+112·9	(N^+OH)	(d)
2-Me-4-NO_2	satd. in acetone	+74	(N→O)	(e)
		+15	(NO_2)	(e)
3-Me-4-NO_2	satd. in acetone	+73	(N→O)	(e)
		+13	(NO_2)	(e)
	1 M in DMSO	+77·1	(N→O)	(d)
	1 M in CF_3CH_2OH	+90·4	(N→O)	(d)
	1 M in CF_3COOH (cation)	+122	(N^+OH)	(d)
3-Cl-4-NO_2	satd. in acetone	+72	(N→O)	(e)
		+19	(NO_2)	(e)
2-OMe	in acetone	+140±3		(f)
3-OMe	in acetone	+94		(f)
4-OMe	in acetone	+102		(f)
	2 M in DMSO	+106·4		(d)
	2 M in CF_3CH_2OH	+126·2		(d)
	2 M in CF_3COOH (cation)	+161·5		(d)
3-OH	in MeOH	+96		(f)
2-NMe_2	in MeOH	+123	(N→O)	(f)
3-NMe_2	in acetone	+85	(N→O)	(f)
4-NMe_2	in MeOH	+134	(N→O)	(f)
2-NHMe	in MeOH	+138±3	(N→O)	(f)
3-NHMe	in acetone	+86	(N→O)	(f)
4-NHMe	in MeOH	+146±3	(N→O)	(f)
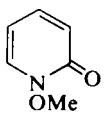 (isomeric to 2-OMe-pyridine *N*-oxide)	in acetone	+143±3		(f)

TABLE 124—*cont.*

Compound	Solution	Nitrogen shielding referred to neat nitromethane		Notes
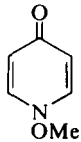 (isomeric to 4-OMe-pyridine *N*-oxide)	in acetone	+104 ± 2		(f)
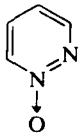 (pyridazine *N*-oxide)	in acetone	+55	(N→O)	(b)
	in acetone	+55·8	(N→O)	(g)
		+34·4	(N-2)	(g)
	0·5 M in DMSO	+55·1	(N→O)	(h)
		+33·6	(N-2)	(h)
	0·5 M in $CHCl_3$	+54·7	(N→O)	(h)
		+32·8	(N-2)	(h)
	in MeOH	+59	(N→O)	(b)
		+36	(N-2)	(b)
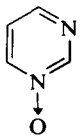 (pyrimidine *N*-oxide)	in acetone	+91	(N→O)	(b)
	0·5 M in DMSO	+90·0	(N→O)	(h)
		+80·3	(N-3)	(h)
	0·5 M in $CHCl_3$	+89·9	(N→O)	(h)
		+79·5	(N-3)	(h)
Substituted pyrimidine *N*-oxides				
2-NH_2	0·5 M in DMSO	+134·0	(N→O)	(h)
		+130·1	(N-3)	(h)
		+304·8	(NH_2)	(h)
	0·5 M in H_2O	+231·5	(N→O)	(h)
		+146·3	(N-3)	(h)
		+305·5	(NH_2)	(h)
2,6-$(NH_2)_2$	0·5 M in DMSO	+167·8	(N→O)	(h)
		+166·8	(N-3)	(h)
		+306·2	(NH_2)	(h)
		+307·4	(NH_2)	(h)
2,6-$(NH_2)_2$-5-[$CH_2{\cdot}C_6H_2$-3,4,5$(OMe)_3$]	0·5 M in DMSO	+168·8	(N→O)	(h)
		+164·9	(N-3)	(h)
		+308·6	(NH_2)	(h)
		+309·5	(NH_2)	(h)

TABLE 124—*cont.*

Compound	Solution	Nitrogen shielding referred to neat nitromethane		Notes
2,6-$(NH_2)_2$-5-(CH_2COMe)	0·5 M in DMSO	+169·2	(N→O)	(h)
		+164·8	(N-3)	(h)
		+308·1	(NH_2)	(h)
		+311·1	(NH_2)	(h)
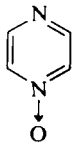	in acetone	+68	(N→O)	(b)
		+78	(N-4)	(b)(g)
	in acetone	+70·2	(N→O)	(g)
		+78·7	(N-4)	(g)
	0·5 M in DMSO	+75·7	(N→O?)	(h)
		+70·4	(N-4?)	(h)
(pyrazine *N*-oxide)	0·5 M in $CHCl_3$	+75·2	(N→O?)	(h)
		+69·1	(N-4?)	(h)
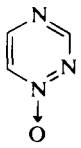	in acetone	+43	(N→O)	(i)
(1,2,4-triazine *N*-1-oxide)				
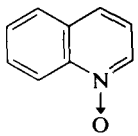	satd. in acetone	+95		(e)
	in $CHCl_3$	+99		(e)
	1 M in DMSO	+101·5		(d)
	in MeOH	+107		(e)
	1 M in CF_3CH_2OH	+112·8		(d)
(quinoline *N*-oxide)	1 M in CF_3COOH (cation)	+150·3	(N^+OH)	(d)
Substituted quinoline *N*-oxides				
2-OMe	satd. in acetone	+125 ± 2		(e)
4-OMe	satd. in acetone	+118 ± 4		(e)
	1 M in acetone	+115 ± 2		(e)
	in MeOH	+124 ± 5		(e)
2-Me	satd. in acetone	+103 ± 4		(e)
3-Me	1 M in acetone	+97		(e)
4-Me	satd. in acetone	+101 ± 4		(e)
2-Cl	satd. in acetone	+102		(e)
3-Cl	satd. in acetone	+91		(e)
4-Cl	satd. in acetone	+97		(e)
	satd. in MeOH	+108		(e)
2-Br	satd. in acetone	+102		(e)

TABLE 124—*cont.*

Compound	Solution	Nitrogen shielding referred to neat nitromethane	Notes
3-Br	satd. in acetone	+94	(e)
	satd. in MeOH	+104	(e)
4-Br	satd. in acetone	+92 ± 4	(e)
	satd. in MeOH	+104 ± 2	(e)
2-CN	satd. in acetone	+87 (N→O)	(e)
4-CN	1:3 v/v in DMSO/acetone	+77 ± 4 (N→O)	(e)
2-CHO	satd. in acetone	+90	(e)
4-CHO	satd. in acetone	+86 ± 2	(e)
2-COOH	in CH_2Br_2	+120 ± 5	(e)
3-NO_2	satd. in acetone	+91 (N→O)	(e)
		+11 (NO_2)	(e)
4-NO_2	satd. in acetone	+83 (N→O)	(e)
		+12 (NO_2)	(e)
8-OH	1 M in DMSO	+111·0	(d)
	1 M in CF_3CH_2OH	+116·1	(d)
	1 M in CF_3COOH (cation)	+144·3 (N^+OH)	(d)
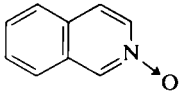	satd. in acetone	+90	(e)
	satd. in $CHCl_3$	+97	(e)
	satd. in dioxan	+100 ± 3	(e)
	satd. in MeOH	+112 ± 2	(e)
(isoquinoline *N*-oxide)			
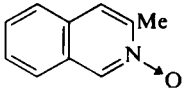	satd. in acetone	+90	(e)
	satd. in MeOH	+105 ± 2	(e)
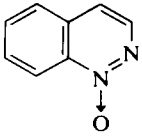	satd. in acetone	+59 (N→O)	(b)
(cinnoline *N*-1-oxide)			
Substituted cinnoline *N*-1-oxides			
4-Me	satd. in acetone	+62 (N→O)	(e)
	satd. in MeOH	+68 (N→O)	(e)
3-NO_2	satd. in acetone	+61 (N→O)	(e)
		+17 (NO_2)	(e)

TABLE 124—*cont.*

Compound	Solution	Nitrogen shielding referred to neat nitromethane		Notes
4-NO_2	satd. in acetone	+52	(N→O)	(e)
		+16	(NO_2)	(e)
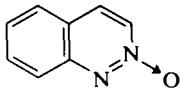	satd. in acetone	+53	(N→O)	(b)
(cinnoline *N*-2-oxide)				
Substituted cinnoline *N*-2-oxides				
4-Me	satd. in MeOH	+60	(N→O)	(e)
3-NO_2	satd. in acetone/DMSO	+51	(N→O)	(e)
4-COOH	satd. in DMSO	+57	(N→O)	(e)
	satd. in acetone/DMSO	+55	(N→O)	(e)
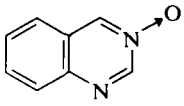	satd. in acetone	+92	(N→O)	(b)
	satd. in acetone	+92·2	(N→O)	(g)
		+74·3	(N-1)	(g)
	0·5 M in DMSO	+89·5	(N→O?)	(h)
(quinazoline *N*-3-oxide)				
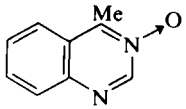	satd. in MeOH	+107	(N→O)	(e)
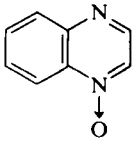	satd. in acetone	+77	(N→O)	(b)
		+83	(N-4)	(b)
	0·5 M in DMSO	+80·7	(N→O?)	(h)
		+76·8	(N-4?)	(h)
(quinoxaline *N*-oxide)				
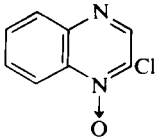	satd. in MeOH	+94 ± 2	(N→O)	(e)
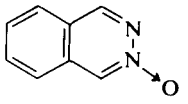	satd. in acetone	+67	(N→O)	(b)
	0·5 M in DMSO	+68·9	(N→O)	(h)
		+53·2	(N-3)	(h)
(phthalazine *N*-oxide)				

TABLE 124—*cont.*

Compound	Solution	Nitrogen shielding referred to neat nitromethane		Notes
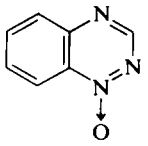 (benzo-1,2,4-triazine *N*-1-oxide)	in acetone	+46	(N→O)	(i)
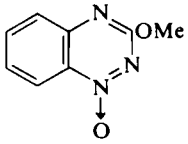	1:3 v/v in acetone	+41	(N→O)	(e)
	satd. in MeOH	+43	(N→O)	(e)
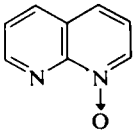 (1,8-naphthyridine *N*-oxide)	satd. in acetone	+90	(N→O)	(e)
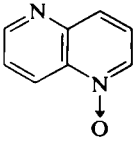 (1,5-naphthyridine *N*-oxide)	satd. in acetone	+93	(N→O)	(e)
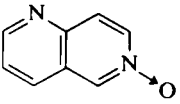 (1,6-naphthyridine *N*-6-oxide)	satd. in acetone	+89	(N→O)	(e)
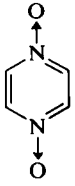 (pyrazine *N*,*N*′-dioxide)	satd. in DMSO	+98·6		(g)

TABLE 124—*cont.*

Compound	Solution	Nitrogen shielding referred to neat nitromethane	Notes
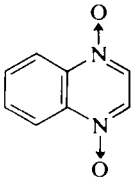 (quinoxaline *N,N'*-dioxide)	satd. in DMSO	+108·7	(g)

(a) Data from ref. 303; ^{15}N-labelled compounds; $^{1}H/^{15}N$ spectra at 100/10·1 MHz; field perpendicular to sample tube; referred originally to 0·1 M nitromethane in $CDCl_3$, +3·8 ppm from neat nitromethane (Table 6); conversion scheme II (Table 4).

(b) Data from ref. 1, pp. 196–197, and references therein.

(c) Data from ref. 37; ^{15}N natural abundance spectra; 10·1 MHz; field perpendicular to sample tube; referred to *internal* nitromethane, in DMSO, −2·0 ppm from neat nitromethane (Table 133), and in H_2O, −2·0 ppm from neat nitromethane (Table 133).

(d) Data from ref. 299; ^{15}N natural abundance spectra; 18·25 MHz; field parallel to sample tube; referred originally to 1 M DNO_3, +6·2 ppm from neat nitromethane (Table 6); conversion scheme IV (Table 4).

(e) Data from ref. 304; ^{14}N continuous-wave spectra; 4·33 MHz; field perpendicular to sample tube; referred to neat nitromethane; uncorrected for bulk susceptibility effects.

(f) Data from ref. 305; details as in note (e).

(g) Data from ref. 306; ^{15}N natural abundance spectra; 18·25 MHz; field parallel to sample tube; referred originally to neat nitromethane; uncorrected for bulk susceptibility effects.

(h) Data from ref. 115; ^{15}N natural abundance spectra; 10·1 MHz; field perpendicular to sample tube; referred originally to aqueous NH_4NO_3; converted originally to neat nitromethane scale; uncorrected for bulk susceptibility effects; $Cr(acac)_3$ added to samples.

(i) Data from ref. 307; details as in note (e).

TABLE 125

Nitrogen shieldings in thiamine and vitamin B_1

	Sample	Nitrogen shielding referred to neat nitromethane thiazole	N-3	N-1	NH_2
Thiamine 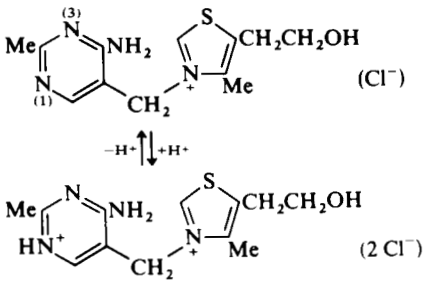 Vitamin B_1 (thiamine hydrochloride)	vitamin B_1 satd. in H_2O	+142 (singlet)	+172 (singlet)	+214 (singlet)	+274 (triplet)
	0·9 M in ethylene glycol+NaOH NaOH added (equiv.)				
	0	+136·7	+170·9	+215·0	+273·0
	0·25	+137·4	+170·1	+195·5	+278·4
	0·75	+139·0	+169·0	ca. 165	+287·0
	1·0	+140·2	+168·0	ca. 141	+294·2

Data from ref. 308; ^{15}N natural abundance spectra; proton-undecoupled and selectively decoupled; 18·25 MHz; field parallel to sample tube; referred originally to 1 M DNO_3, +6·2 ppm from neat $MeNO_2$; conversion scheme IV (Table 4).

TABLE 126

Nitrogen shieldings in some nucleosides, nucleotides, and related structures

Compound and solution	Nitrogen shielding referred to neat nitromethane for nitrogen atoms specified N-1	N-3	N-7	N-9	NH_2	Notes
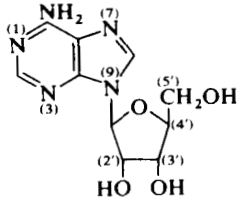						
(adenosine)						
0·4 M in DMSO (45 °C)	+142·8	+155·7	+138·1	+209·7	+298·2	(b)
0·5 M in DMSO	+145·8	+158·9	+140·9	+211·8	+300·0	(a)
$+CF_3COOH$						
0·16 eq.	+153·2	+159·2	+141·6	+211·2	+299·6	(a)
0·31 eq.	+161·8	+159·1	+141·5	+210·6	+298·4	(a)
1·6 eq.	+217·5	+157·0	+137·9	+203·6	+291·1	(a)
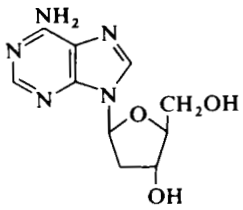						
(2′-deoxyadenosine)						
0·5 M in DMSO	+145·3	+158·3	+140·5	+208·3	+299·9	(a)
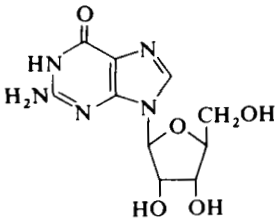						
(guanosine)						
0·8 M in DMSO (45 °C)	+231·9	+212·9	+132·2	+209·2	+306·2	(b)
0·5 M in DMSO	+234·2	+215·7	+134·8	+211·5	+308·2	(a)
$+CF_3COOH$						

TABLE 126—*cont.*

Compound and solution	Nitrogen shielding referred to neat nitromethane for nitrogen atoms specified N-1	N-3	N-7	N-9	NH_2	Notes
0·17 eq.	+233·7	+215·5	+149·8	+209·8	+306·7	(a)
0·36 eq.	+233·4	+216·1	+156·7	+209·2	+306·2	(a)
1·86 eq.	+232·2	+217·2	+210·1	+205·6	+303·0	(a)
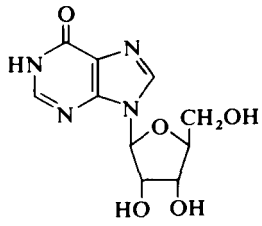 (inosine)						
0·8 M in DMSO (45 °C)	+204·1	+165·2	?	+204·7		(b)
0·5 M in DMSO	+206·9	+167·4	+132·9	+206·9		(a)
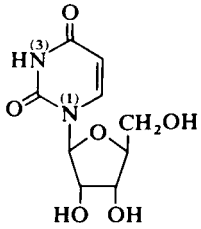 (uridine)						
0·8 M in DMSO (45 °C)	+235·6	+221·7				(b)
0·5 M in DMSO	+237·8	+223·7				(a)
1 M in H_2O (35 °C)	+234·0	+221·7				(b)
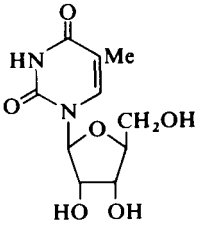 (thymidine)						
0·8 M in DMSO (45 °C)	+235·3	+223·7				(b)
0·5 M in DMSO	+237·5	+225·2				(a)

TABLE 126—*cont.*

Compound and solution	Nitrogen shielding referred to neat nitromethane for nitrogen atoms specified N-1	N-3	N-7	N-9	NH_2	Notes
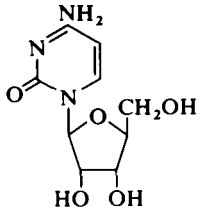						
(cytidine)						
0·8 M in DMSO (45 °C)	+226·2	+169·9			+285·5	(b)
0·5 M in DMSO + CF_3COOH 1·5 eq.	+228·4	+172·3			+287·2	(a)
	+227·3	+237·1			+275·2	(a)
1 M in H_2O	+227·3	?			+287·0	(b)
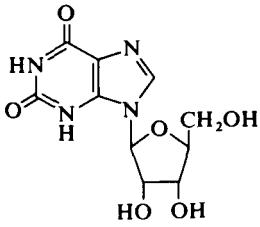						
(xanthosine)						
0·8 M in DMSO (45 °C)	+225·5	+265·5	+131·2	+213·3		(b)
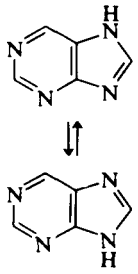						
(purine)						
(numbering system of adenosine retained)						
0·5 M in DMSO	+119·8	+100·7	+193 (broad)	+193 (broad)		(a)
1·25 M in H_2O	+128·6	+113·4		+189·6 +185·8		(b)

TABLE 126—*cont.*

Compound and solution	Nitrogen shielding referred to neat nitromethane for nitrogen atoms specified N-1	N-3	N-7	N-9	NH_2	Notes
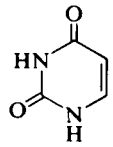						
(uracil)						
0·8 M in DMSO (45 °C)	+220·2	+247·8				(b)
2′,3′,5′-tri-*O*-benzyluridine-3-^{15}N						
0·5 M in $CDCl_3$		+226·5				(d)
+ excess of 5′-acetyl-2′,3′-isopropylideneadenosine		+221·7				(d)
adenosine 5′-monophosphate (AMP)						
0·5 M in H_2O, neutral	+158·3	+166·6	+151·0	+213·2	+303·2	(a)
adenosine 5′-triphosphate (ATP)						
0·5 M in H_2O, neutral	+157·9	+166·5	+151·2	+213·4	+303·2	(a)
pH 2·5	+220·5	+160·6	+145·7	+206·3	+295·0	(a)
guanosine 5′-monophosphate (GMP)						
0·5 M in H_2O, neutral	+235·3	+217·5	+147·4	+213·4	+309·7	(a)
uridine 5′-monophosphate						
0·5 M in H_2O, neutral	+236·2	+222·7				(a)
thymidine 5′-monophosphate						
0·5 M in H_2O, neutral	+235·4	+225·7				(a)
cytidine 5′-monophosphate						
0·5 M in H_2O, neutral	+229·7	+181·4			+289·4	(a)
adenosine 3′-monophosphate						
0·08 M in H_2O, pH 6–10	+155·8	+162·4	+148·7	+211·6	+301·1	(c)
guanosine 3′-monophosphate						
0·08 M in H_2O, pH 6–10	+233·1	+214·0	+145·3	+212·0	+307·5	(c)
uridine 3′-monophosphate						
0·08 M in H_2O, pH 3–6	+234·3	+221·6				(c)
pH 10	+234·0	+179·0				(c)
cytidine 3′-monophosphate						
0·08 M in H_2O, pH 6–10	+227·1	+178·7			+285·9	(c)
pH 2	+227·0	+238·0			+278·0	(c)
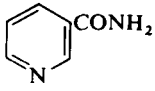						
(nicotinamide)						
0·1 M in D_2O, pH 7, potassium phosphate buffer	+74·7 (ring N)					(e)

TABLE 126—*cont.*

Compound and solution	Nitrogen shielding referred to neat nitromethane for nitrogen atoms specified	Notes
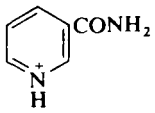		
0·1 M in D_2O + CCl_3COOH, pD 2	+170·9 (NH^+)	(e)
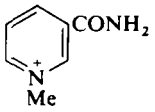		
0·1 M in H_2O, +0·05 M potassium phosphate	+171·2 (N^+Me)	(e)
0·1 M in 70% MeOH	+171·1 (N^+Me)	(e)
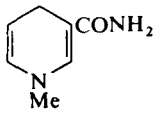		
0·1 M in D_2O + 0·05 M potassium phosphate	+279·8 (NMe)	(e)
0·1 M in 70% MeOH	+279·8 (NMe)	(e)
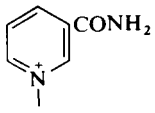	(NAD$^+$)	
(ADP-ribose)		
in D_2O, pD 7	+155·0 (N^+)	(e)
pD 2	+154·8 (N^+)	(e)
in 70% MeOH, pD 7	+154·1 (N^+)	(e)
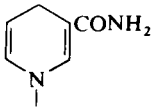	(NADH)	
(ADP-ribose)		
in D_2O, pD 7	+264·2 (ring N)	(e)
in 70% MeOH, pD 7	+264·1 (ring N)	(e)
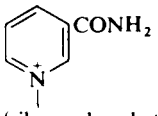	(NMN)	
(ribose-phosphate)		

TABLE 126—*cont.*

Compound and solution	Nitrogen shielding referred to neat nitromethane for nitrogen atoms specified	Notes
in D_2O, pD 7	+153·9 (N^+)	(e)
pD 2	+154·1 (N^+)	(e)
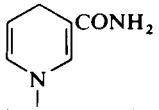 (ribose-phosphate)	(NMNH)	
in D_2O, pD 7	+264·1 (ring N)	(e)
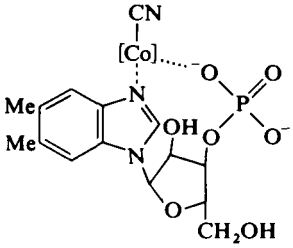 (vitamin B_{12})		
in D_2O	+221 (–N=) −130 (N···Co)	(f)

(a) Data from ref. 158; ^{15}N natural abundance spectra; 18·25 MHz; field parallel to sample tube; referred originally to what was reported as 0·1 M DNO_3, probably 1 M DNO_3, +6·2 ppm from neat nitromethane (Table 6); conversion scheme IV (Table 4); assignments from spin–spin splittings and protonation shifts.

(b) Data from ref. 181; ^{15}N natural abundance spectra; 18·25 MHz; field parallel to sample tube; referred originally to HN_4^+ in 5 M NH_4NO_3 in 2 M HNO_3, +359·0 ppm from neat nitromethane (Table 6); conversion scheme II (Table 4); original assignments for N-1 and N-3 in adenosine were reversed.

(c) Data from ref. 314 and ref. 315; ^{15}N-labelled compounds; ^{15}N spectra; 9·12 MHz; field perpendicular to sample tube; referred originally to NH_4^+ in 4 M NH_4NO_3 in 2 M HNO_3, +359·1 ppm from neat nitromethane (Table 6); conversion scheme II (Table 4).

(d) Data from ref. 316; ^{15}N-labelled N-3; ^{15}N spectrum; 10·09 MHz; field perpendicular to sample tube; referred originally to NO_3^- in aqueous NH_4NO_3, +4·0 ppm from neat nitromethane (Table 6); conversion scheme II (Table 4).

(e) Data from ref. 136; ^{15}N-labelled pyridine ring; ^{15}N spectra; 10·14 MHz; field perpendicular to sample tube; referred originally to 1·0 M ND_4Cl, +352·9 ppm from neat nitromethane (Table 6); conversion scheme II (Table 4).

(f) Data from ref. 317; ^{15}N-labelled compound; ^{15}N spectrum; 9·12 MHz; field perpendicular to sample tube; referred originally to neat nitromethane; uncorrected for bulk susceptibility effects.

TABLE 127

Nitrogen shieldings in some cyclophosphazenes

Structure	Solvent	Nitrogen shielding referred to neat nitromethane	^{14}N resonance half-height width (Hz)	Notes
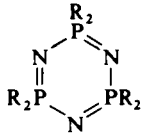				
R = NMe_2	none	+333 ± 5 (unresolved)	410	(a)
OMe	Et_2O	+325 ± 5	440	(a)
F	none	+301 ± 5	165	(a)
NCS	Et_2O	+260 ± 5 (NCS?)	750	(a)
Cl	none	+254 ± 5	224	(a)
		+258·8		(b)
Br	$CHCl_3$	+245 ± 5	400	(a)
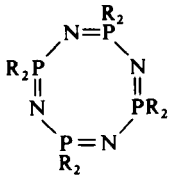				
R = OMe	Et_2O	+304 ± 5	570	(a)
F	none (50 °C)	+305 ± 5	285	(a)
Cl	none	+248·0		(b)
	Et_2O	+263 ± 5	495	(a)
	$CDCl_3$	+258·8		(c)
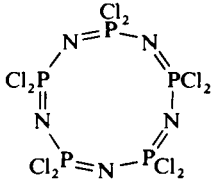	none	+253·3		(b)

TABLE 127—*cont.*

Structure	Solvent	Nitrogen shielding referred to neat nitromethane	^{14}N resonance half-height width (Hz)	Notes
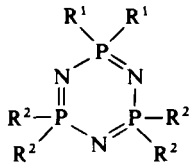				
$R^1 = SEt$; $R^2 = Cl$	$CDCl_3$	+255·9 (N between Cl) +270·9 (other two N)		(c) (c)
$R^1 = R^2 = SEt$	$CDCl_3$	+284·2 +270·0 (other two N)		(c) (c)
$R^1 = Cl$; $R^2 = SPh$	$CDCl_3$	+283·8 (N between SPh) +268·3 (other two N)		(c) (c)
$R^1 = R^2 = SPh$	$CDCl_3$	+285·0		(c)
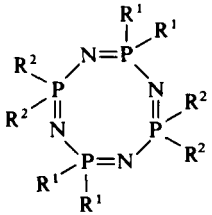				
$R^1 = SEt$; $R^2 = Cl$	$CDCl_3$	+259·8		(c)

(a) Data from ref. 143; low-precision ^{14}N continuous-wave measurements; wide-line spectrometer; 3 MHz; referred originally to NH_4^+ in saturated aqueous NH_4NO_3, +359·6 ppm from neat nitromethane (Table 6).

(b) Data from ref. 324; ^{15}N-labelled compounds; ^{15}N spectra; 9·12 MHz; field perpendicular to sample tube; referred originally to neat nitromethane; uncorrected for bulk susceptibility effects.

(c) Data from ref. 326; details as in note (b).

TABLE 128

Nitrogen shieldings in some imines and immonium cations

Parent imine (geometric isomer designation in parentheses, if data available)	Solution	Nitrogen shielding referred to neat nitromethane: imine =NR	immonium =NH^+R	Notes
(*E*)-EtC(Me)=NMe	neat liquid	+76·0		(a)
(*E*)-Pr^iC(Me)=NMe	neat liquid	+67·4		(a)
(*E*)-PhCH=CHCH=NMe	50% in $CHCl_3$	+51·8		(a)
(*E*)-PhCH=NMe	neat liquid	+59·1		(a)
	36 mol % in $CHCl_3$	+62·1		(b)
PhCH=NEt	36 mol % in $CHCl_3$	+46·8		(b)
PhCH=NPr^n	36 mol % in $CHCl_3$	+49·1		(b)
Pr^iCH=NPr^n	neat liquid	+54·3		(a)
PhCH=NBu^i	36 mol % in $CHCl_3$	+49·2		(b) (c)
	10 mol % in CF_3CH_2OH	+77·2		(c)
	9 mol % in CF_3COOH		+198·3 (doublet)	(c)
PhCH=NCH_2CMe_3	36 mol % in $CHCl_3$	+49·3		(b)
(*E*)-MeCH=NPr^i	neat liquid	+34·5		(a)
(*E*)-Pr^nCH=NPr^i	neat liquid	+34·2		(a)
(*E*)-Pr^iCH=NPr^i	neat liquid	+36·8		(a)
(*E*)-MeCH=CHCH=NPr^i	neat liquid	+31·7		(a)
PhCH=NPr^i	36 mol % in $CHCl_3$	+34·7		(b) (c)
	10 mol % in CF_3CH_2OH	+61·8		(c)
	9 mol % in CF_3COOH		+183·0	(c)
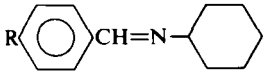				
R = OMe	20 mol % in $CHCl_3$	+44·7		(b) (c) (d)
	20 mol % in MeOH	+57·0		(b)
	10 mol % in CF_3CH_2OH	+72·5		(c)
	9 mol % in CF_3COOH		+195·5	(c)
			+193·9	(d)
Me	20 mol % in $CHCl_3$	+40·1		(b) (d)
	20 mol % in MeOH	+51·2		(b)
	9 mol % in CF_3COOH		+187·6 (doublet)	(d)
H	20 mol % in $CHCl_3$	+36·4		(b) (d)
	20 mol % in MeOH	+47·2		(b)
	9 mol % in CF_3COOH		+183·6 (doublet)	(d)
Cl	20 mol % in $CHCl_3$	+34·3		(b) (d)
	20 mol % in MeOH	+42·8		(b)
	9 mol % in CF_3COOH		+181·9 (doublet)	(d)
NO_2	20 mol % in $CHCl_3$	+20·9		(b) (c) (d)
	20 mol % in MeOH	+27·9		(b)
	10 mol % in CF_3CH_2OH	+44·7		(c)
	9 mol % in CF_3COOH		+160·2 (doublet)	(d)
			+170·3	(c)

TABLE 128—*cont.*

Parent imine (geometric isomer designation in parentheses, if data available)	Solution	Nitrogen shielding referred to neat nitromethane imine =NR	immonium =NH⁺R	Notes
PhCH=NBu^t	36 mol % in $CHCl_3$	+26·8		(b)
PhCH=NC(Et)Me$_2$	36 mol % in $CHCl_3$	+28·0		(b)
(*E*)-EtC(Me)=NCH$_2$Ph	neat liquid	+69·2		(a)
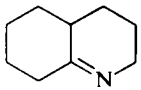	14·6 mol % in cyclohexane	+70·2		(d)
	13·5 mol % in $CHCl_3$	+83·9		(d)
	10·0 mol % in EtOH	+92·2		(d)
(*E*)-EtC(Me)=NPh	neat liquid	+55·1		(a)
(*E*)-Pr^{i}CH=NPh	neat liquid	+57·3		(a)
(*E*)-PhCH=CHCH=NPh	50 % in $CHCl_3$	+49·6		(a)
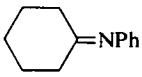	20 mol % in $CHCl_3$	+65·1		(c)
	10 mol % in CF_3CH_2OH	+87·5		(c)
	9 mol % in CF_3COOH		+184·1 (doublet)	(c)
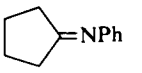	20 mol % in $CHCl_3$	+66·7		(c)
	10 mol % in CF_3CH_2OH	+88·5		(c)
	9 mol % in CF_3COOH		+187·0 (doublet)	(c)
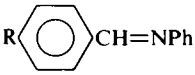				
R = NMe$_2$	20 mol % in $CHCl_3$	+72·9		(b)
OMe	20 mol % in $CHCl_3$	+62·6		(b) (c)
	20 mol % in DMSO	+61·8		(b)
	20 mol % in MeOH	+71·8		(b)
	10 mol % in CF_3COOH	+83·1		(c)
	9 mol % in CF_3COOH		+205·9 (doublet)	(c)
Me	20 mol % in $CHCl_3$	+58·1		(b) (c)
	20 mol % in DMSO	+56·8		(b)
	10 mol % in CF_3CH_2OH	+79·0		(c)
	9 mol % in CF_3COOH		+198·2 (doublet)	(c)
H	50 % in $CHCl_3$	+54·4		(a)
	23·7 mol % in $CHCl_3$	+54·1		(b) (c) (d)
	24·4 mol % in cyclohexane	+50·3		(d)
	10·7 mol % in benzene	+51·3		(d)
	20 mol % in DMSO	+53·7		(b)
	10·8 mol % in MeOH	+59·7		(b) (d)
	10 mol % in CF_3CH_2OH	+74·0		(c)
	9 mol % in CF_3COOH		+193·6 (doublet)	(c)

TABLE 128—*cont.*

Parent imine (geometric isomer designation in parentheses, if data available)	Solution	Nitrogen shielding referred to neat nitromethane imine =NR	immonium =NH⁺R	Notes
F	20 mol % in $CHCl_3$	+55·5		(b)
	20 mol % in DMSO	+55·0		(b)
Cl	20 mol % in $CHCl_3$	+52·8		(b)
	20 mol % in DMSO	+52·2		(b)
	20 mol % in MeOH	+58·1		(b)
NO_2	20 mol % in $CHCl_3$	+41·3		(b) (c)
	20 mol % in DMSO	+42·8		(b)
	10 mol % in CF_3CH_2OH	+51·0 (+55 °C)		(c)
	9 mol % in CF_3COOH		+181·7 (doublet)	(c)
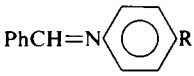				
R = OMe	20 mol % in $CHCl_3$	+57·6		(b) (c)
	20 mol % in DMSO	+56·1		(b)
	10 mol % in CF_3CH_2OH	+77·2		(c)
	9 mol % in CF_3COOH		+198·2 (doublet)	(c)
Me	20 mol % in $CHCl_3$	+56·2		(b)
	20 mol % in DMSO	+54·2		(b)
H	see data above			
Cl	20 mol % in $CHCl_3$	+58·2		(b)
	20 mol % in DMSO	+57·7		(b)
NO_2	20 mol % in $CHCl_3$	+57·9		(b) (c)
	9 mol % in CF_3COOH		+199·8	(c)
$Ph_2C{=}NPh$	20 mol % in $CHCl_3$	+52·3		(c)
	9 mol % in CF_3COOH		+198·2	(c)
PhC(Me)=NPh	20 mol % in $CHCl_3$	+50·7		(c)
	10 mol % in CF_3CH_2OH	+70·5		(c)
	9 mol % in CF_3COOH		+189·9 (doublet)	(c)
$(CH_2{=}N^+Me_2)\,CF_3COO^-$	in $CHCl_2CHCl_2$		+158·7	(e)
MeCH=NN=CHMe	neat liquid	+22 ± 3		(f)
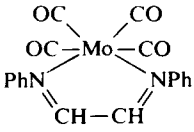	in $CDCl_3$	+76·5		(g)
	in benzene	+78·5		(g)
$Me_2NCH{=}NPh$	neat liquid	+149·5		(a)
$Me_2C{=}CHC(NMe_2){=}NPh$	neat liquid	+139·3		(a)

TABLE 128—*cont.*

Parent imine (geometric isomer designations in parentheses, if data available)	Solution	Nitrogen shielding referred to neat nitromethane imine =NR	immonium =NH⁺R	Notes
$(Me_2N)_2C{=}NPh$	neat liquid	+175·4		(a)
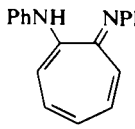				
⇃↾	0·3 M in $CDBr_3$ (26 °C)	+188·1 (=NPh ⇄ NHPh)		(h)
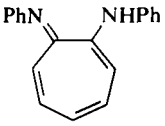				
$FSO_2N{=}SMe_2$	in acetone	+293 ± 3		(i)
$FSO_2N{=}SOF{-}NEt_2$	in Et_2O	+272 ± 3		(i)
$FSO_2N{=}SOF_2$	neat liquid	+252 ± 3		(i)
$F_2S{=}NC_6F_5$	neat liquid	+252 ± 3		(i)
$F_2S{=}NCl$	neat liquid	+233 ± 3		(i)
$F_2S{=}NC(=O)F$	neat liquid	+229 ± 3		(i)

(a) Data from ref. 171; ^{15}N natural abundance spectra; 9·117 MHz; field perpendicular to sample tube; referred originally to aqueous $NaNO_3$, +3·7 ppm from neat nitromethane (Table 6); conversion scheme II (Table 4); samples contained 0·1 M $Cr(acac)_3$.

(b) Data from ref. 172; ^{15}N natural abundance spectra; 18·25 MHz; field parallel to sample tube; referred originally to 1 M DNO_3, +6·2 ppm from neat nitromethane (Table 6); conversion scheme IV (Table 4).

(c) Data from refs 300 and 325; see note (b).

(d) Data from ref. 26; see note (b).

(e) Data from ref 40; ^{15}N natural abundance spectra; 6·08 MHz; field perpendicular to sample tube; referred originally to 0·5 M HNO_3, +3·7 ppm from neat nitromethane (Table 6); conversion scheme II (Table 4).

(f) Data from ref. 39; ^{14}N continuous-wave measurements; wide-line spectrometer; 3 MHz; referred originally to NH_4^+ in aqueous NH_4NO_3, +359·6 ppm from neat nitromethane (Table 6); low-precision data.

(g) Data from ref. 319; ^{15}N-enriched compounds; ^{15}N spectra; 30·4 MHz; field parallel to sample tube; referred originally to dimethylformamide, +277·0 ppm from neat nitromethane (Table 6); conversion scheme II (Table 4).

(h) Data from ref. 320; ^{15}N-labelled compound; ^{15}N spectrum; 10·09 MHz; field perpendicular to sample tube; referred originally to aqueous NH_4Cl, +352·9 ppm from neat nitromethane (Table 6); conversion scheme II (Table 4).

(i) Data from ref. 206; see note (f).

TABLE 129

Nitrogen shieldings in some oximes, their ethers, and protonated forms

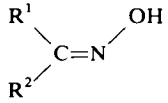

Compound		Isomer designation	Solution	Nitrogen shielding referred to neat nitromethane	Notes
R^1	R^2				
H	H		20 mol % in H_2O	+2·2	(a)
H	Me	*E*	36 mol % in $CHCl_3$	+34·6	(a) (b)
			1 : 1 v/v in $CHCl_3$	+33·9	(c)
			10 mol % in CF_3CH_2OH	+42·3	(b)
			9 mol % in CF_3COOH	+141·2	(b)
Me	H	*Z*	36 mol % in $CHCl_3$	+30·3	(a) (b)
			10 mol % in CF_3CH_2OH	+39·5	(b)
			9 mol % in CF_3COOH	+141·2	(b)
H	Et	*E*	36 mol % in $CHCl_3$	+34·4	(a)
Et	H	*Z*	36 mol % in $CHCl_3$	+32·8	(a)
H	Pr^n	*E*	36 mol % in $CHCl_3$	+33·5	(a)
Pr^n	H	*Z*	36 mol % in $CHCl_3$	+31·6	(a)
H	Pr^i	*E*	1 : 1 v/v in $CHCl_3$	+35·2	(c)
			36 mol % in $CHCl_3$	+36·3	(a)
			25 mol % in benzene	+35·4	(a)
			25 mol % in MeOH	+31·8	(a)
			25 mol % in tetrahydrofuran	+24·1	(a)
			25 mol % in DMSO	+22·9	(a)
Pr^i	H	*Z*	36 mol % in $CHCl_3$	+36·2	(a)
			25 mol % in benzene	+35·2	(a)
			25 mol % in MeOH	+33·6	(a)
			25 mol % in tetrahydrofuran	+24·1	(a)
			25 mol % in DMSO	+22·1	(a)
H	Bu^i	*E*	36 mol % in $CHCl_3$	+32·7	(a)
Bu^i	H	*Z*	36 mol % in $CHCl_3$	+32·2	(a)
H	Bu^s	*E*	36 mol % in $CHCl_3$	+35·0	(a)
Bu^s	H	*Z*	36 mol % in $CHCl_3$	+35·1	(a)
H	$EtC(\dot{M}e)HCH_2$	*E*	36 mol % in $CHCl_3$	+32·2	(a)
$EtC(Me)HCH_2$	H	*Z*	36 mol % in $CHCl_3$	+32·2	(a)
H	Et_2CH	*E*	36 mol % in $CHCl_3$	+34·2	(a)
Et_2CH	H	*Z*	36 mol % in $CHCl_3$	+32·0	(a)
H	cyclohexyl	*E*	36 mol % in $CHCl_3$	+34·2	(a)
cyclohexyl	H	*Z*	36 mol % in $CHCl_3$	+34·5	(a)
Me	Me		36 mol % in $CHCl_3$	+45·9	(a)
			1 : 1 v/v in $CHCl_3$	+44·2	(c)
			in Et_2O	+36 ± 3	(d)

TABLE 129—*cont.*

Compound		Isomer designation	Solution	Nitrogen shielding referred to neat nitromethane	Notes
Me	Et	*E*	36 mol % in $CHCl_3$	+44·5	(a)
			1 : 1 v/v in $CHCl_3$	+47·7	(c)
Et	Me	*Z*	36 mol % in $CHCl_3$	+45·1	(a)
Me	Pr^i	*E*	36 mol % in $CHCl_3$	+44·5	(a)
Pr^i	Me	*Z*	36 mol % in $CHCl_3$	+49·6	(a)
Me	Pr^n	*E*	36 mol % in $CHCl_3$	+42·2	(a)
Pr^n	Me	*Z*	36 mol % in $CHCl_3$	+45·1	(a)
Me	Bu^t	*E*	36 mol % in $CHCl_3$	+43·2	(a)
Et	Et		36 mol % in $CHCl_3$	+46·3	(a)
Et	Pr^i	*E*	36 mol % in $CHCl_3$	+44·3	(a)
Pr^i	Et	*Z*	36 mol % in $CHCl_3$	+46·5	(a)
Pr^i	Pr^i		36 mol % in $CHCl_3$	+43·5	(a)
Me	Bu^i	*E*	36 mol % in $CHCl_3$	+42·3	(a)
Bu^i	Me	*Z*	36 mol % in $CHCl_3$	+45·3	(a)
Me	Me_3CCH_2	*E*	36 mol % in $CHCl_3$	+37·6	(a)
H	p-$Me_2N{\cdot}C_6H_4$	*E*	20 mol % in $CHCl_3$	+38·4	(e)
			20 mol % in DMSO	+23·1	(e)
H	p-$MeO{\cdot}C_6H_4$	*E*	20 mol % in $CHCl_3$	+30·9	(e)
			20 mol % in DMSO	+17·2	(e)
H	p-$Me{\cdot}C_6H_4$	*E*	36 mol % in $CHCl_3$	+29·3	(a) (e)
			20 mol % in $CHCl_3$	+26·3	(b)
			10 mol % in CF_3CH_2OH	+35·5	(b)
			20 mol % in DMSO	+13·2	(e)
			9 mol % in CF_3COOH	+159·8	(b)
H	Ph	*E*	1 : 1 v/v in $CHCl_3$	+24·7	(c)
			20 mol % in $CHCl_3$	+26·3	(a) (e)
			20 mol % in DMSO	+10·7	(e)
			in acetone	+13 ± 20	(f)
H	p-$F{\cdot}C_6H_4$	*E*	20 mol % in $CHCl_3$	+26·7	(e)
			20 mol % in DMSO	+11·9	(e)
H	p-$Cl{\cdot}C_6H_4$	*E*	20 mol % in $CHCl_3$	+23·5	(a) (e)
			20 mol % in DMSO	+9·1	(e)
H	p-$O_2N{\cdot}C_6H_4$	*E*	20 mol % in DMSO	−1·4 (NOH)	(e)
				+12·7 (NO_2)	(e)
Ph	Ph		36 mol % in $CHCl_3$	+34·2	(a)
			in Et_2O	+33 ± 17	(f)
Me or cyclopropyl	cyclopropyl or Me	*E* or *Z*	36 mol % in $CHCl_3$	+47·8	(a)
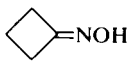			36 mol % in $CHCl_3$	+52·4	(a)
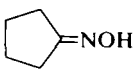			36 mol % in $CHCl_3$	+53·0	(a)

TABLE 129—*cont.*

Compound	Solution	Nitrogen shielding referred to neat nitromethane	Notes
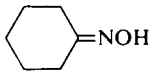	25 mol % in CF_3CH_2OH	+60·7	(a)
	neat liquid (?)	+54·8	(g)
	36 mol % in $CHCl_3$	+52·6	(a)
	25 mol % in $CHCl_3$	+52·3	(b)
	25 mol % in MeOH	+50·8	(a)
	25 mol % in benzene	+50·5	(a)
	2·5 mol % in benzene	+48·3	(a)
	25 mol % in DMSO	+38·3	(a)
	9 mol % in CF_3COOH	+141·2	(b)
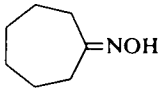	36 mol % in $CHCl_3$	+46·8	(a)
	neat liquid (?)	+32·2	(g)
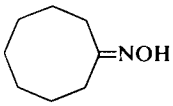	36 mol % in $CHCl_3$	+45·7	(a)
	neat liquid (?)	+29·0	(g)
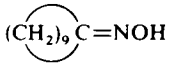	neat liquid (?)	+23·6	(g)
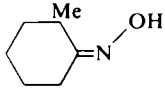	36 mol % in $CHCl_3$	+55·2	(a)
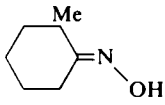	36 mol % in $CHCl_3$	+50·6	(a)
	neat liquid (?)	+54·6	(g)
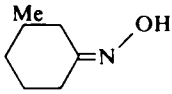	36 mol % in $CHCl_3$	+52·3	(a)
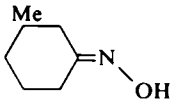	36 mol % in $CHCl_3$	+52·3	(a)
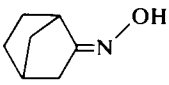	36 mol % in $CHCl_3$	+59·6	(a)

TABLE 129—*cont.*

Compound	Solution	Nitrogen shielding referred to neat nitromethane	Notes
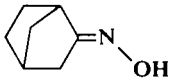	36 mol % in $CHCl_3$	+57·6	(a)
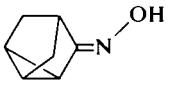	36 mol % in $CHCl_3$	+65·2	(a)
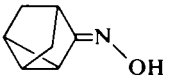	36 mol % in $CHCl_3$	+70·1	(a)
$Me_2C{=}NOMe$	in Et_2O	+8·1	(d)
$MeC(=O)C(Me){=}NOH$	in acetone	−17·6	(h)
$MeC(=O)C(Me){=}NOMe$	in acetone	−30·8	(h)

(a) Data from ref. 321; ^{15}N natural abundance spectra; 18·25 MHz; field parallel to sample tube; referred originally to 1 M DNO_3, +6·2 ppm from neat nitromethane (Table 6); conversion scheme IV (Table 4).

(b) Data from ref. 300; see note (a).

(c) Data from ref. 171; ^{15}N natural abundance spectra; 9·12 MHz; field perpendicular to sample tube; referred originally to aqueous $NaNO_3$, +3·7 ppm from neat nitromethane (Table 6); conversion scheme II (Table 4); samples contained 0·1 M $Cr(acac)_3$.

(d) Data from ref. 179; ^{14}N continuous-wave spectra; 4·33 MHz; field perpendicular to sample tube; referred originally to neat nitromethane; uncorrected for bulk susceptibility effects.

(e) Data from ref. 172; see note (a).

(f) Data from ref. 39; low-precision ^{14}N continuous-wave spectra (wide-line spectrometer); 3 MHz; referred originally to NH_4^+ in aqueous NH_4NO_3, +359·6 ppm from neat nitromethane (Table 6).

(g) Data from ref. 322; ^{15}N natural abundance spectra; 27·36 MHz; field parallel to sample tube; referred originally to saturated aqueous NH_4Cl, +352·9 ppm from neat nitromethane (Table 6); conversion scheme II (Table 4).

(h) As in note (d), but ^{15}N natural abundance spectra; 18·25 MHz; field parallel to sample tube.

TABLE 130

Nitrogen shieldings in some nitrones

Compound (satd. solution in acetone)	Nitrogen shielding referred to neat nitromethane	Notes
PhCH=N(O)Me	+104 ± 1	(a)
PhCH=N(O)Bu^t	+72 ± 1	(a)
PhCH=N(O)Ph	+95 ± 1	(a)
PhC(Me)=N(O)Me	+109 ± 1	(a)
Ph_2C=N(O)Ph	+111 ± 1	(b)
PhCH=N(O)CH_2Ph	+95 ± 1	(b)

(a) Data from ref. 1, p. 201, and references therein.
(b) Data from ref. 179; ^{14}N continuous-wave spectra; 4·33 MHz; field perpendicular to sample tube; referred originally to neat nitromethane; uncorrected for bulk susceptibility effects.

TABLE 131

Nitrogen shieldings in sulphinylamines, thionitrites, sulphodiimides, and related structures

Compound	Solution	Nitrogen shielding referred to neat nitromethane	Notes
MeN=S=O (sulphinylamine structure)	0·25 M in Et_2O	+54·8	(a)
EtN=S=O	1·9 M in Et_2O	+37·4	(a)
Pr^{n}N=S=O	neat liquid	+39·6	(a)
	1·9 M in Et_2O	+41·3	(a)
Bu^{n}N=S=O	neat liquid	+39·0	(a)
	1·9 M in Et_2O	+41·3	(a)
Bu^{i}N=S=O	neat liquid	+41·7	(a)
	1·5 M in acetone	+42·0	(a)
Pr^{i}N=S=O	neat liquid	+25·2	(a)
	1·9 M in Et_2O	+26·6	(a)
Bu^{s}N=S=O	neat liquid	+28·6	(a)
	1·8 M in Et_2O	+29·2	(a)

TABLE 131—*cont.*

Compound	Solution	Nitrogen shielding referred to neat nitromethane	Notes
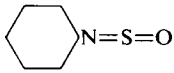	neat liquid	+28·8	(b)
$Bu^tN{=}S{=}O$	neat liquid	+26·0	(a)
	2·0 M in Et_2O	+28 ± 2	(c)
		+27·4	(a)
$PhN{=}S{=}O$	neat liquid	+62·1	(a)
		+63·8	(b)
		+66 ± 3	(c)
	1·7 M in Et_2O	+63·3	(a)
	2·0 M in acetone	+63·2	(a)
pMeO·C_6H_4·N=S=O	neat liquid	+64·6	(b)
	3 M in DMSO	+65·0	(b)
$pO_2N{\cdot}C_6H_4{\cdot}N{=}S{=}O$	3 M in DMSO	+70·9 (NSO)	(b)
		+10·9 (NO_2)	(b)
pMe·C_6H_4·N=S=O	2·0 M in Et_2O	+62·5	(a)
mMe·C_6H_4·N=S=O	2·0 M in Et_2O	+63·0	(a)
oMe·C_6H_4·N=S=O	2·0 M in Et_2O	+66·7	(a)
2,5-Bu^t_2-C_6H_3·N=S=O	2·0 M in Et_2O	+79·0	(a)
$Me_3SiN{=}S{=}O$	neat liquid	+51 ± 3	(c)
$Me_2NSN{=}S{=}O$	neat liquid	+38 ± 5 (NSO)	(c)
		+342 ± 5 (Me_2N)	(c)
$Pr^n_2NSN{=}S{=}O$	neat liquid	+57 ± 10 (NSO)	(c)
		+330 ± 10 (Pr^n_2N)	(c)
$PhSN{=}S{=}O$	neat liquid	+64 ± 4	(c)
$S(N{=}S{=}O)_2$	neat liquid (100 °C)	+78 ± 3	(c)
$FSO_2N{=}S{=}O$	neat liquid	+86 ± 3	(c)
$EtSN{=}O$ (thionitrite structure)	neat liquid	−405 ± 1	(c)
$CF_3SN{=}O$	neat liquid (−80 °C)	−335 ± 1	(c)
$PhN{=}S{=}NPh$ (sulphodiimide structure)	in Et_2O	+83 ± 3	(d)
	2 M in DMSO	+119·9	(e)

(a) Data from ref. 118; ^{14}N continuous-wave spectra; high-precision differential saturation technique with full lineshape fitting; 4·33 MHz; concentric spherical sample containers in order to eliminate bulk susceptibility effects; referred to neat nitromethane.

(b) Data from ref. 259; ^{15}N natural abundance spectra; 18·25 MHz; field parallel to sample tube; referred originally to 1 M DNO_3, +6·2 ppm from neat nitromethane (Table 6); conversion scheme IV (Table 4); the apparent discrepancy for PhNSO with the precise ^{14}N data [note (a)] comes most probably from bulk susceptibility effects in the ^{15}N spectrum.

(c) Data from ref. 323; low-precision ^{14}N continuous-wave measurements; wide-line spectrometer; 3 MHz; referred originally to NH_4^+ in saturated aqueous NH_4NO_3, +359·6 ppm from neat nitromethane (Table 6).

(d) Data from ref. 204; see note (c).

(e) Data from ref. 278; see note (b).

TABLE 132

Nitrogen shieldings in some nitramines, nitrourethanes, and their isomeric structures

Compound	Solvent	Nitrogen shielding referred to neat nitromethane	
		R_2N, RN= groups	NO_2, =N(O)OR groups
$MeNH-NO_2$	none	+222·6	+24·6
Me_2N-NO_2	none	+218·0	+25·7
$MeOC(=O)NH-NO_2$	none	+189·5	+45·3
$MeOC(=O)NMe-NO_2$	none	+184·0	+41·0
$EtOC(=O)NMe-NO_2$	none	+184·7	+41·3
$Me_3SiN(Me)-NO_2$	none, −30 °C	+202·1	+20·1
$EtOC(=O)N(NO_2)SiMe_3$*	none	+171·1	+38·9
$MeN(NO_2)_2$	none	+102·1	+41·2
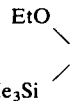	none	+118·3	+20·7
$(MeNNO_2)^-NH_4^+$	H_2O	+120·0	+27·3
$(MeOOCNNO_2)^-NH_4^+$	H_2O	+136·9	+9·6
$MeN=N(O)OMe$†	none	+110·5	+66·8
		+103·1	+52·8
$MeN=N(O)OSiMe_3$*	none	+93·8	+55·5
$MeOC(=O)N=N(O)OMe$	none	+107·3	+46·6
$EtOC(=O)N=N(O)OPr^i$	none	+101·4	+50·4

Data from ref. 263; ^{15}N-labelled compounds; ^{15}N spectra; 9·12 MHz; field perpendicular to sample tube; referred originally to aqueous $NaNO_3$, +3·7 ppm from neat nitromethane; conversion scheme II (Table 4).

* Mixture of isomeric species.

† Separate spectra of *E* and *Z* isomers were observed.

TABLE 133

Nitrogen shieldings in nitro compounds, nitrates, and related structures

Compound	Solution	Nitrogen shielding referred to neat nitromethane	Notes
$MeNO_2$ (nitromethane)	0·30 M in DMSO	−2·01 ± 0·12	(a)
	0·30 M in H_2O	−1·98 ± 0·12	(a)
	0·30 M in D_2O	−1·94 ± 0·13	(a)
	0·30 M in 11·7 M HCl	−1·95 ± 0·14	(a)
	0·30 M in Me_2NCHO	−0·69 ± 0·13	(a)
	neat liquid (18·42 M)	0·0000	(a)
	0·30 M in MeCN	+0·20 ± 0·13	(a)
	0·30 M in acetone	+0·77 ± 0·10	(a)
	0·30 M in dioxan	+1·82 ± 0·13	(a)
	0·30 M in MeOH	+2·01 ± 0·13	(a)
	0·30 M in EtOH	+2·70 ± 0·12	(a)
	0·30 M in CH_2Cl_2	+3·21 ± 0·13	(a)
	0·30 M in CH_2Br_2	+3·41 ± 0·12	(a)
	0·30 M in $CHCl_3$	+3·79 ± 0·13	(a)
	0·30 M in Et_2O	+3·91 ± 0·13	(a)
	0·30 M in benzene	+4·38 ± 0·11	(a)
	0·30 M in CCl_4	+7·10 ± 0·11	(a)
$EtNO_2$	0·30 M in DMSO	−11·37 ± 0·16	(b)
	neat liquid	−10·25 ± 0·10	(b)
	0·30 M in acetone	−9·37 ± 0·11	(b)
	0·30 M in CCl_4	−4·09 ± 0·12	(b)
Pr^nNO_2	0·30 M in DMSO	−10·09 ± 0·21	(b)
	0·30 M in acetone	−8·31 ± 0·14	(b)
	neat liquid	−7·73 ± 0·10	(b)
	0·30 M in CCl_4	−3·77 ± 0·16	(b)
Bu^nNO_2	0·30 M in acetone	−7·91 ± 0·16	(b)
	neat liquid	−7·90 ± 0·11	(b)
	0·30 M in CCl_4	−3·87 ± 0·16	(b)
$Me(CH_2)_4NO_2$	neat liquid	−7·56 ± 0·11	(b)
	0·30 M in acetone	−7·36 ± 0·18	(b)
	0·30 M in CCl_4	−3·89 ± 0·17	(b)
$Me(CH_2)_5NO_2$	neat liquid	−6·44 ± 0·12	(b)
	0·30 M in CCl_4	−3·97 ± 0·19	(b)
Pr^iNO_2	neat liquid	−19·45 ± 0·10	(b)
	0·30 M in acetone	−19·40 ± 0·15	(b)
	0·30 M in CCl_4	−14·73 ± 0·14	(b)
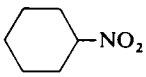	0·30 M in acetone	−18·36 ± 0·22	(b)
	neat liquid	−16·27 ± 0·11	(b)
	0·30 M in CCl_4	−13·63 ± 0·25	(b)

TABLE 133—*cont.*

Compound	Solution	Nitrogen shielding referred to neat nitromethane	Notes
Bu^tNO_2	0·30 M in DMSO	−28·20 ± 0·17	(b)
	0·30 M in acetone	−25·95 ± 0·11	(b)
	neat liquid	−25·51 ± 0·11	(b)
	0·30 M in CCl_4	−21·57 ± 0·12	(b)
$C(NO_2)_4$ (tetranitromethane)	neat liquid (8·31 M)	+46·59 ± 0·09	(a)
$PhNO_2$ (nitrobenzene)	0·7 M in $CHCl_3$ (9 mol %)	+9·55 ± 0·07	(c)
	neat liquid	+9·56 ± 0·12	(a)
	0·30 M in CCl_4	+12·18 ± 0·18	(a)
Substituted nitrobenzenes			
3-NO_2	6 mol % in $CHCl_3$	+15·6	(d)
3-CN	6 mol % in $CHCl_3$	+15·1 (NO_2)	(d)
3-Br	6 mol % in $CHCl_3$	+13·0	(d)
3-I	6 mol % in $CHCl_3$	+12·9	(d)
3-Cl	6 mol % in $CHCl_3$	+12·9	(d)
3-NH_2	6 mol % in $CHCl_3$	+8·4 (NO_2)	(d)
4-N=S=O	3 M in DMSO	+10·9 (NO_2)	(e)
4-CH=NOH	20 mol % in DMSO	+12·7 (NO_2)	(f)
4-CH=NNHPh	20 mol % in DMSO	+11·3 (NO_2)	(f)
4-CH=NPh	20 mol % in DMSO	+13·2 (NO_2)	(f)
4-N=CHPh	20 mol % in DMSO	+10·6 (NO_2)	(f)
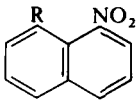			
R = NO_2	in $CHCl_3$	+8·6	(d)
CN	in $CHCl_3$	+8·9 (NO_2)	(d)
I	in $CHCl_3$	+5·4	(d)
Cl	in $CHCl_3$	+1·9	(d)
H	in $CHCl_3$	+5·6	(d)
NH_2	in $CHCl_3$	−3·1 (NO_2)	(d)
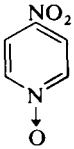	1 M in DMSO	+17·1 (NO_2)	(g)
	1 M in CF_3CH_2OH	+20·2 (NO_2)	(g)
	1 M in CF_3COOH	+24·2 (NO_2)	(g)
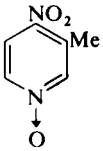	1 M in DMSO	+13·8 (NO_2)	(g)
	1 M in CF_3CH_2OH	+16·6 (NO_2)	(g)
	1 M in CF_3COOH	+20·1 (NO_2)	(g)

TABLE 133—*cont.*

Compound	Solution	Nitrogen shielding referred to neat nitromethane	Notes
$MeOOCCH(NH_3^+)CH_2CH_2CH_2C(NH_2)=NNO_2$			
	in H_2O	+12·1 (NO_2)	(h)
HNO_3	100 %, liquid	+42·5 ± 0·5	(j)
	15·71 M in H_2O (70·0 % w/w)	+31·31 ± 0·08	(a)
	10·00 M in H_2O	+18·23 ± 0·13	(a)
	7·00 M in H_2O	+12·59 ± 0·12	(a)
	1·00 M in H_2O	+4·43 ± 0·11	(a)
$MeONO_2$	neat liquid	+40 ± 2	(i)
$EtONO_2$	neat liquid	+40 ± 2	(i)
$MeC(=O)ONO_2$	neat liquid	+68 ± 1	(j)
$O_2N–O–NO_2$	neat liquid	+66 ± 2	(i)
nitramines, $R_2N–NO_2$	see Table 132		
NO_3^-	K^+, 0·30 M in H_2O	+3·55 ± 0·12	(a)
	Na^+, 0·30 M in H_2O	+3·53 ± 0·12	(a)
	Na^+, 7·93 M in H_2O (satd.)	+3·70 ± 0·12	(a)
	NH_4^+, 12·30 M in H_2O (satd.)	+3·98 ± 0·12	(a)
	NH_4^+, 5 M in 2 M HNO_3	+4·64 ± 0·12	(a)
	NH_4^+, 8 M in 2 M HCl	+4·93 ± 0·11	(a)
	NH_4^+, 5 M in 2 M HCl	+5·23 ± 0·11	(a)
	NH_4^+, 4 M in 2 M HNO_3	+5·55 ± 0·11	(a)
	NH_4^+, 4·5 M in 3 M HCl	+6·30 ± 0·10	(a)

(a) Data from ref. 80; ^{14}N continuous-wave measurements; 4·33 MHz; 30 °C; high-precision differential saturation technique with full lineshape fitting; concentric spherical sample/standard containers in order to eliminate bulk susceptibility effects; referred to neat nitromethane.

(b) Data from ref. 121; details as in note (a).

(c) Data from ref. 179; details as in note (a).

(d) Data from ref. 83; ^{15}N natural abundance spectra; 18·25 MHz; $Cr(acac)_3$ added to samples; referred to *internal* nitrobenzene (9 mol %); solutions in $CHCl_3$; recalculated using a value of +9·55 ppm from neat nitromethane for 9 mol % nitrobenzene in $CHCl_3$ (this table).

(e) Data from ref. 259; ^{15}N natural abundance spectra; 18·25 MHz; field parallel to sample tube; referred originally to 1 M DNO_3, +6·2 ppm from neat nitromethane (Table 6); conversion scheme IV (Table 4).

(f) Data from ref. 172; details as in note (e).

(g) Data from ref. 299; details as in note (e).

(h) Data from ref. 188; ^{15}N natural abundance spectra; 9·12 MHz; field perpendicular to sample tube; referred originally to 1 M $NaNO_3$, +3·7 ppm from neat nitromethane (Table 6); conversion scheme II (Table 4).

(i) Data quoted from ref. 1, p. 207, and references therein.

(j) Data from ref. 327; ^{14}N PFT measurements; 4·33 MHz; field perpendicular to sample tube; referred to neat nitromethane; uncorrected for bulk susceptibility effects.

TABLE 134

Nitrogen shieldings in some diazo compounds

Compound	Solvent	Nitrogen shielding referred to neat nitromethane $=N^+=$	$=N^-$	Notes
$PhCH=N^+=N^-$	Et_2O	+83·0	−56·3	(a)
$Ph_2C=N^+=N^-$	$CDCl_3$	+77·6	−58·5	(b)
	cyclohexane	+76·9	−59·3	(a)
	Pr^iOH	+76·2	−60·0	(a)
	DMSO	+75·4	−59·9	(a)
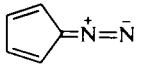	n-pentane	+112·4	−2·6	(a)
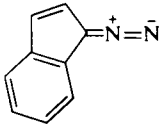	n-pentane	+102·0	−36·1	(a)
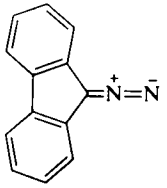	benzene	+95·2	−60·2	(a)
	$CDCl_3$	+87·0	−67·0	(c)
$PhC(=O)CH=N^+=N^-$	$CDCl_3$	+112·1	+6·5	(b)
$PhC(=O)C(Ph)=N^+=N^-$	Et_2O/tetrahydrofuran	+98·9	−25·8	(a)
	$CDCl_3$	+101·9	−19·6	(a)
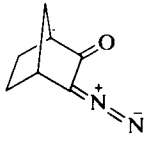	$CDCl_3$	+104·0	−30·0	(c)
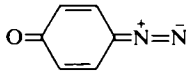	$EtOH/H_2O$	+123·3	+15·8	(a)
$EtOC(=O)CH=N^+=N^-$	$CDCl_3$ (20 °C)	+112·6	−3·6	(b) (d)
	$CDCl_3$ (−50 °C)	+113·7	−0·6	(d)
	(*E*,*Z*-isomers)	+113·3	−8·0	
$(EtOOC)_2C=N^+=N^-$	$CDCl_3$	+124·4	5·1	(b)

TABLE 134—*cont.*

Compound	Solvent	Nitrogen shielding referred to neat nitromethane =N⁺=	=N⁻		Notes
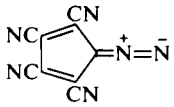	DMSO	+153·3	+47·8	+103·9 (CN) +110·0 (CN)	(a)
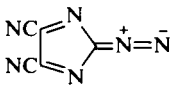	DMSO	+152·2	+65·6	+114·2 (CN) 88·9 (ring)	(a)

(a) Data from ref. 162; ^{15}N natural abundance spectra and those of selectively labelled compounds; 18·25 MHz; field parallel to sample tube; referred originally to 1 M DNO_3, +6·2 ppm from neat nitromethane (Table 6); conversion scheme IV (Table 4).

(b) Data from ref. 29; ^{15}N singly labelled compounds; ^{15}N spectra; 9·12 MHz; field perpendicular to sample tube; referred originally to urea but reported relative to Me_4N^+; however, comparison with data from ref. 67 [note (d)] shows a gross error in the calibration since the shielding for the original reference point becomes +283·6 ppm from neat nitromethane (this value is used here for conversion), far from that for the standard reported (Table 6); 1–2 M solutions.

(c) Data from ref. 328; ^{15}N natural abundance spectra; 9·12 MHz; field perpendicular to sample tube; referred to unspecified "NH_4^+", assumed here to be that in saturated aqueous NH_4Cl, +352·9 ppm from neat nitromethane (Table 6); conversion scheme II (Table 4).

(d) Data from ref. 67; singly and doubly ^{15}N-labelled compounds; ^{15}N spectra; 10·1 MHz; field parallel to sample tube; referred originally to "NH_4Cl" signal at 355·3 ppm from neat nitromethane (Table 6; this corresponds to 2·9 M NH_4Cl in 1 M HCl, uncorrected); conversion scheme IV (Table 4).

TABLE 135

Nitrogen shieldings in some diazonium salts

Diazonium cation (solution in $CHCl_3$/18-crown-6)	Counterion	Nitrogen shielding referred to neat nitromethane -N⁺≡	≡N
$pR{\cdot}C_6H_4{\cdot}N^+{\equiv}N$			
$R = O^-$	none	+123·3	+15·8
OH	Cl^-	+153·0	+57·0
OMe	BF_4^-	+154·7	+59·4
Me	BF_4^-	+155·6	+63·1
H	BF_4^-	+156·4	+63·4
NO_2	BF_4^-	+158·6	+63·2

Data from ref. 162; ^{15}N selectively labelled and unlabelled salts; ^{15}N spectra; 18·25 MHz; field parallel to sample tube; referred originally to 1 M DNO_3, +6·2 ppm from neat nitromethane (Table 6); conversion scheme IV (Table 4).

TABLE 136

Nitrogen shieldings in some azo compounds, azoxy compounds, azimines, and related structures

Compound	Solution	Nitrogen shielding referred to neat nitromethane		Notes
trans-Ph–N=N–Ph	9·4 mol % in cyclohexane	−128·5		(a)
	7·4 mol % in $CHCl_3$	−127·8		(a)
	6·3 mol % in Pr^iOH	−127·8		(a)
	3·3 mol % in $H_2SO_4/H_2O/EtOH$ (3 : 2 : 3mol ratio)	+22·6		(a)
trans-Ph–N=N–CPh_3	in benzene	−141	(NPh)	(b)
		−165	($NCPh_3$)	(b)
trans-Ph–N=N–$C(CN)Me_2$	in benzene	−131	(NPh)	(b)
		−133	($NCMe_2$)	(b)
		+122	(CN)	(b)
cis-Ph–N=N–$C(CN)Me_2$	in benzene	−150	(NPh)	(b)
		−140	($NCMe_2$)	(b)
		+112	(CN)	(b)
trans-Ph–N=N–$C(Ph)Me_2$	in benzene	−128	(NPh)	(b)
		−164	($NCMe_2$)	(b)
cis-Ph–N=N–$C(Ph)Me_2$	in benzene	−157	(NPh)	(b)
		−190	($NCMe_2$)	(b)
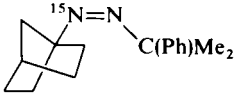	in cyclopropane			
	(−90 °C)	−164	(^{15}N)	(c) (i)
	(−40 °C)	−172	(^{15}N)	(c) (i)
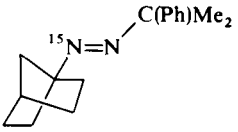	in cyclopropane			
	(−90 °C)	−150	(^{15}N)	(c) (i)
	(−40 °C)	−154	(^{15}N)	(c) (i)
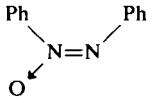	in $CDCl_3$ (−20 °C)	+36·0	(NO)	(d)
		+19·8	(N)	(d)
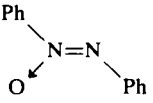	in $CDCl_3$ (−20 °C)	+54·1	(NO)	(d)
		+46·7	(N)	(d)

TABLE 136—*cont.*

Compound	Solution	Nitrogen shielding referred to neat nitromethane	Notes
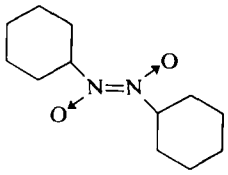	in $MeOCH_2CH_2OMe$	+73 ± 3	(e)
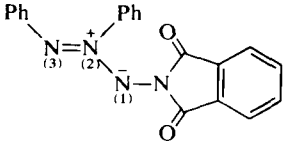 (azimine structure)	in $CDCl_3$ (−20 °C)	+63·7 (N-2) +59·6 (N-3)	(d) (d)
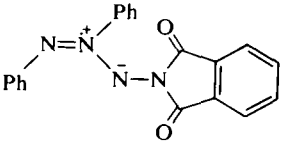 (azimine structure)	in $CDCl_3$ (−20 °C)	+64·7 (N-2) +60·5 (N-3)	(d) (d)
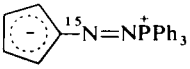	in $CH_2Cl_2/CHCl_3$	−44·1 (^{15}N)	(f)
$Me_2NN{=}NNMe_2$	neat liquid	−25 ± 3 (N=N)	(g) (h)
$(Me_3Si)_2NN{=}NN(SiMe_3)_2$	neat liquid	−41 ± 3 (N=N)	(g) (h)
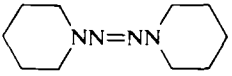	neat liquid	−37 ± 5 (N=N)	(h)
$Me_3SiON{=}NOSiMe_3$	neat liquid	−68 ± 5	(h)
$MeN{=}NSiMe_3$	neat liquid	−271 ± 5 (NMe) −302 ± 5 (NSi)	(h) (h)
$Me_3CN{=}NSiMe_3$	neat liquid	−282 ± 3 ($NCMe_3$) −290 ± 3 (NSi)	(h) (h)
$Me_3SiN{=}NSiMe_3$	neat liquid	−618 ± 3	(h)
$Me_3CN{=}NGeMe_3$	neat liquid	−233 ± 3 −252 ± 3	(h) (h)
$Me_3CN{=}NPMe_2$	neat liquid	−192 ± 3	(h)

TABLE 136—*cont.*

Compound	Solution	Nitrogen shielding referred to neat nitromethane	Notes
pMe·C_6H_4·N=$NNMe_2$ (triazene structure)	neat liquid	−65·6 (central N) +20·7 (NPh) +233·6 (NMe_2)	(j) (j) (j)
other triazenes		see ref. 1, p. 209	
Me_3N^+–N=NO_2^-	in H_2O	+118 ± 2 (central N) +17 ± 2 (NO_2)	(e) (e)
	in Et_2O	+47·5	(k)

(a) Data from ref. 26; ^{15}N natural abundance spectra; 18·25 MHz; field parallel to sample tube; referred originally to 1 M DNO_3, +6·2 ppm from neat nitromethane (Table 6); conversion scheme IV (Table 4).

(b) Data from ref. 114; ^{15}N-labelled compounds; ^{15}N spectra; 10·1 MHz; CIDNP experiments (Table 9); referred to NO_3^-, ~4 ppm from neat nitromethane (Table 6).

(c) Data from ref. 86; ^{15}N singly labelled compounds; see note (b).

(d) Data from ref. 329; ^{15}N doubly labelled compounds; ^{15}N spectra; 10·1 MHz; field perpendicular to sample tube; referred originally to neat nitromethane; uncorrected for bulk susceptibility effects.

(e) Data from ref. 39; ^{14}N continuous-wave measurements; wide-line spectrometer; 3 MHz; referred to NH_4^+ in saturated aqueous NH_4NO_3, +359·6 ppm from neat nitromethane (Table 6); low-precision data.

(f) Data from ref. 162; see note (a).

(g) Data from ref. 137; ^{14}N continuous-wave spectra; 7·22 MHz; field perpendicular to sample tube; referred originally to saturated aqueous $NaNO_3$, +3·7 ppm from neat nitromethane (Table 6); conversion scheme II (Table 4).

(h) Data from ref. 38; see note (g).

(i) Data from ref. 114; see note (g).

(j) Data from ref. 45; ^{15}N natural abundance spectra; 9·12 MHz; field perpendicular to sample tube; referred originally to aqueous $NaNO_3$, +3·7 ppm from neat nitromethane (Table 6); conversion scheme II (Table 4); $Cr(acac)_3$ added to the samples.

(k) Data from ref. 330; ^{15}N natural abundance spectrum; 18·25 MHz; field parallel to sample tube; referred originally to neat nitromethane containing some $Cr(acac)_3$; uncorrected for bulk susceptibility effects.

TABLE 137

Nitrogen shielding as a means of investigation of azo-hydrazone tautomerism

Compound	Solution	Temp. (K)	Nitrogen shielding referred to neat nitromethane N_α	N_β
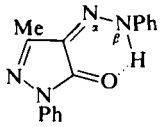	10 % v/v in $CDCl_3$	330	+205·7	+17·0
		300	+205·2	+17·3
		270	+205·4	+17·6
		240	+204·6	+17·9
(model hydrazone structure with internal hydrogen bond)				
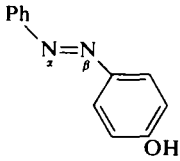	10 % v/v in DMSO	360	−112·7	−126·4
		330	−111·5	−125·2
		300	−110·2	−124·2
(model azo structure without internal hydrogen bond)				
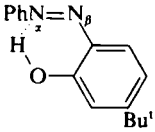	10 % v/v in $CDCl_3$	330	−70·9	−128·1
		300	−69·4	−126·9
		270	−68·1	−125·3
		240	−67·0	−123·7
(model azo structure with internal hydrogen bond)				
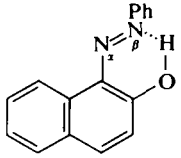	10 % v/v in $CDCl_3$	330	+108·0	−32·7
		310	+116·9	−28·0
		290	+126·2	−22·8
		270	+137·4	−17·0
		250	+148·5	−10·6
		230	+158·2	−4·7
(azo tautomer)				
⇵			calcd. hydrazone content	calcd. hydrazone content
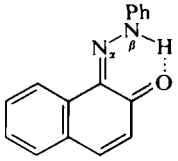		330	64·7%	65·7%
		310	67·8%	68·7%
		290	71·2%	72·0%
		270	75·3%	75·8%
		250	79·3%	80·0%
(hydrazone tautomer)		230	82·9%	83·9%

Data from ref. 331; ^{15}N selectively labelled N-α and N-β atoms; ^{15}N spectra; 10·095 MHz; field perpendicular to sample tube; referred originally to neat nitromethane; the content of hydrazone form at a given temperature is calculated from the shieldings for N-α and N-β, respectively, in model compounds with internal hydrogen bonds and in the tautomeric system investigated.

TABLE 138

Nitrogen shieldings in some nitroso-amines and related structures

Compound	Isomer	Solution or state	Nitrogen shielding referred to neat nitromethane R_2N	$N{=}O$	other	Notes
$Me_2N{-}N{=}O$		neat liquid (13·5 M, 30 °C)	+148·84 ±0·08	−155·43 ±0·12		(a)
		neat liquid (40 °C)	+150·4	−152·6		(b)
		in CF_3COOH (extrapolated to inf. dil.)	+133·7	−115·5		(b)
$Et_2N{-}N{=}O$		neat liquid (9·2 M, 30 °C)	+122·78 ±0·12	−160·67 ±0·38		(a)
		neat liquid	+126·0	−156·9		(b)
$Pr^n{}_2N{-}N{=}O$		neat liquid	+129·9	−158·8		(b)
$Bu^n{}_2N{-}N{=}O$		neat liquid	+129·9	−156·5		(b)
$Pr^i{}_2N{-}N{=}O$		neat liquid	+110·9	−162·3		(b)
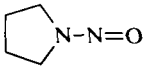		neat liquid	+125·0	−152·0		(b)
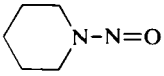		neat liquid	+135·3	−150·9		(b)
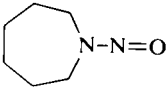		neat liquid	+142·7	−151·0		(b)
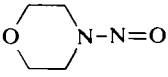		neat liquid	+125·4	−155·5		(b)
$Ph_2N{-}N{=}O$		neat liquid	+113·5	−172·2		(b)
$MeN(Et){-}N{=}O$	*Z*, 29% *E*, 71%	neat liquid	+138·9	−152·6		(b)
$MeN(Pr^n){-}N{=}O$	*Z*, 21% *E*, 79%	neat liquid	+140·8	−156·8		(b)
$MeN(Bu^t){-}N{=}O$	*E*, 100%	neat liquid	+122·4	−158·1		(b)
$MeN(Ph){-}N{=}O$	*E*, 100%	neat liquid	+145·9	−161·6		(b)
$PhCH_2N(Me){-}N{=}O$	*Z*, 29%	neat liquid	+141·6	−152·8		(b)
	E, 71%		+139·5	−155·7		(b)
$NCCH_2N(Me){-}N{=}O$	*Z*, 56%	neat liquid	+157·3	−157·0	+133·2	(b)
	E, 44%		+152·3	−161·3	+128·4	(b)
	Z	2 M in CD_3OH	+156·2	−161·5	+131·1	(c)
	E		+151·1	−166·0	+126·1	(c)
$EtN(Ph){-}N{=}O$	*Z*, 5%	neat liquid	?	?		(b)
	E, 95%		+118·3	−163·2		(b)

TABLE 138—*cont.*

Compound	Isomer	Solution or state	Nitrogen shielding referred to neat nitromethane R_2N	N=O	other	Notes
$PhCH_2N(Et)$-N=O	*Z*, 50%	neat liquid	+129·2	−153·9		(b)
	E, 50%		+126·6	−156·2		(b)
$HOCH_2CH_2N(Et)$-N=O	*Z*, 50%	neat liquid	+128·3	−154·2		(b)
	E, 50%					
$Pr^iN(Bu^t)$-N=O	*E*, 100%	neat liquid	+107·4	−173·2		(b)
$PhCH_2N(Pr^i)$-N=O	*Z*, 18%	neat liquid	+118·1	−163·1		(b)
	E, 82%		+120·2	−156·2		(b)
$NCCH_2N(Pr^i)$-N=O	*Z*, 93%	neat liquid	+134·8	−159·2	+133·2	(b)
	E, 7%		?	?		(b)
NCCH(Me)$N(Pr^i)$-N=O	*Z*, 80%	neat liquid	+126·5	−161·5	+132·7	(b)
	E, 20%		+119·7	−168·4	+126·5	(b)
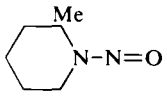	*Z*, 33% *E*, 67%	neat liquid	+126·6	−153·3		(b)
Me_2N^+=N-OMe(SO_3F^-) (cation derived from Me_2NNO under action of $MeOSO_2F$)		in $MeOSO_2F$	+114·3	−92·9	(NOMe)	(b)

(a) Data from ref. 80; ^{14}N continuous-wave spectra; 4·33 MHz; high-precision differential saturation technique with full lineshape fitting; concentric spherical sample/standard containers in order to eliminate bulk susceptibility effects; referred to neat nitromethane.

(b) Data from ref. 45; ^{15}N natural abundance spectra; 9·117 MHz; field perpendicular to sample tube; referred originally to aqueous $NaNO_3$, +3·7 ppm from neat nitromethane (Table 6); conversion scheme II (Table 4); measurements carried out at elevated (40–80 °C) temperatures; $Cr(acac)_3$ added to samples.

(c) Data from ref. 264; ^{15}N natural abundance spectra; 18·25 MHz; field parallel to sample tube; referred originally to neat nitromethane; uncorrected for bulk susceptibility effects.

TABLE 139

Protonation equilibria in dimethyl-*N*-nitrosoamine estimated by ^{15}N shielding data

$$Me_2N\text{–}N{=}O + H^+ \rightleftarrows Me_2N^+{=}N\text{–}OH$$

$$\sigma_{obs.} - \sigma_{amine} = \frac{\sigma_{cation} - \sigma_{amine}}{2f}\left(1 - \sqrt{1 + \frac{4Kf(f-1)}{K+1}}\right)$$

$$\frac{\sigma_{inf.dil.} - \sigma_{amine}}{\sigma_{cation} - \sigma_{amine}} = \frac{K}{K+1}$$

Nitrogen shielding referred to neat nitromethane			value calculated for cation (σ_{cation})	Equilibrium constant K for protonation
neat Me_2NNO (σ_{amine})	infinite dilution value ($\sigma_{inf.dil.}$)			
+150·4 (Me_2N)	+133·7	CF_3COOH	+124·4	~2
−152·6 (NO)	−115·5		−97·0	
	?	FSO_3H	+123·4	~10
			−99·0	

Data from ref. 45; originally referred to aqueous $NaNO_3$ [see Table 138, note (b)]; shieldings for the cation and values of K are obtained from concentration dependence of nitrogen shieldings of Me_2NNO, in CF_3COOH and FSO_3H respectively. *Abbreviations used*: f = mole fraction of Me_2NNO (total); K = equilibrium constant.

TABLE 140

Nitrogen shieldings in some nitroso compounds and nitrites

Compound	Solution	Nitrogen shielding referred to neat nitromethane	Notes
Bu^t-N=O	neat liquid	−578 ± 3	(a)
PhC(=O)$OCMe_2CMe_2$-N=O	in Et_2O	−568 ± 3	(a)
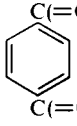	in Et_2O	−563 ± 3	(a)
Ph-N=O	satd. in acetone	−529 ± 4	(b)
	satd. in Et_2O	−536 ± 3	(b)
*p*MeO·C_6H_4·N=O	3 M in Et_2O	−428 ± 10	(b)
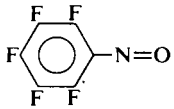	in Et_2O	−507 ± 3	(a)
$CF_2ClCFCl$-N=O	neat liquid	−428 ± 3	(a)
EtO-N=O (ethyl nitrite)	neat liquid	−190 ± 3	(a)
NO_2^-	Na^+, 0·30 M in H_2O	−227·60 ± 0·33	(c)
(nitrite ion)	Na^+, 7·56 M in H_2O (satd.)	−228·89 ± 0·25	(c)
R_2N-N=O	see Table 138		

(a) Data from ref. 39; ^{14}N continuous-wave measurements; 3 MHz; wide-line technique; referred originally to NH_4^+ in saturated aqueous NH_4NO_3, +359·6 ppm from neat nitromethane (Table 6).

(b) Data from ref. 1, p. 208, and references therein.

(c) Data from ref. 80; ^{14}N continuous-wave spectra; 4·33 MHz; high-precision differential saturation technique with full lineshape fitting; concentric spherical sample/standard containers in order to eliminate bulk susceptibility effects; referred to neat nitromethane.

TABLE 141

Nitrogen shieldings in some nitro and nitrito onium ions

Compound (solution in SO_2, −60 °C)	Nitrogen shielding referred to neat nitromethane
$NO^+ BF_4^-$ (PF_6^-)	+3·3
$NO_2^+ BF_4^-$ (FSO_3^-)	+131·5
$Me_2S^+NO_2 BF_4^-$	−257·8
$Me_2S^+ONO BF_4^-$	−616·8

Data from ref. 333; ^{15}N-labelled compounds; ^{15}N spectra; 8·059 MHz; field perpendicular to sample tube; referred to 2 M $NaNO_3$, +3·7 ppm from neat nitromethane (Table 6); conversion scheme II (Table 4).

TABLE 142

Nitrogen shieldings in dinitrogen and its complexes

Compound	Solution or state (THF = tetrahydrofuran)	Nitrogen shielding referred to neat nitromethane	Notes
N_2	in cyclopropane (−40 °C)	+70·5	(a)
	in benzene (−30 °C)	+70·5	(b)
	gaseous	+75·3	(c)
	in toluene	+71·7	(d)
trans-$[Mo(N_2)_2(Ph_2PCH_2CH_2PPh_2)_2]$	in THF	+46·5 (α-N)	(c)
		+46·2 (β-N)	(c)
trans-$[W(N_2)_2(Ph_2PCH_2CH_2PPh_2)_2]$	in THF	+63·5 (α-N)	(c)
		+52·0 (β-N)	(c)
cis-$[Mo(N_2)_2(PhPMe_2)_4]$	in THF	+42·6 (α-N)	(c)
		+34·9 (β-N)	(c)
cis-$[W(N_2)_2(PhPMe_2)_4]$	in THF	+61·2 (α-N)	(c)
		+35·9 (β-N)	(c)
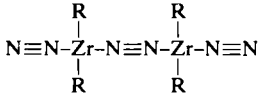	in toluene-d_8	−179 (central N_2)	(d)
		−80, −11 (terminal N_2)	(d)

(R = pentamethylcyclopentadienyl)

(a) Data from ref. 86; $^{15}N{\equiv}^{14}N$ molecules; ^{15}N spectra; 10·1 MHz; field perpendicular to sample tube; referred originally to NO_3^-, *ca.* +4 ppm from neat nitromethane (Table 6); CIDNP emission signal in experiments with diazenyl radicals.

(b) Data from ref. 86; $^{15}N_2$ molecules; details as in note (a).

(c) Data from ref. 380; ^{15}N-enriched N_2; ^{15}N spectra; 18·24 MHz; field parallel to sample tube; referred originally to neat nitromethane; uncorrected for bulk susceptibility effects.

(d) Data from ref. 332; ^{15}N-labelled N_2; ^{15}N spectra; 18·25 MHz; field parallel to sample tube; referred originally to 1 M DNO_3, +6·2 ppm from neat nitromethane (Table 6); conversion scheme IV (Table 4).

TABLE 143

Nitrogen shieldings in some diazenido ligands

Structure (M = metal)	Solution	Nitrogen shielding referred to neat nitromethane M–N=	=N–R
M–N=N \ R (singly bent structure)			
$MoBr(N{=}NEt)(Ph_2PCH_2CH_2PPh_2)_2$	in tetrahydrofuran	+29·0	+146·8
$WBr(N{=}NEt)(Ph_2PCH_2CH_2PPh_2)_2$	in tetrahydrofuran	+28·2	+164·7
$MoCl(N{=}NCOMe)(Ph_2PCH_2CH_2PPh_2)_2$	in tetrahydrofuran	+35·4	+123·7
$WCl(N{=}NCOMe)(Ph_2PCH_2CH_2PPh_2)_2$	in tetrahydrofuran	+32·2	+134·5
$ReCl_2(N{=}NCOPh)(pyridine)(PPh_3)_2$	in toluene	+55·9	+148·6
$RuCl_3(N{=}NPh)(PPh_3)_2$	in CH_2Cl_2	+46·8	non-labelled
M \ N=N \ R (doubly bent structure)			
$RhCl_2(N{=}N$–C$_6$H$_3$(NO$_2$)–$)(PPh_3)_2$	in CH_2Cl_2	−327·1	non-labelled
$RhCl_2(N{=}NPh)(PPh_3)_2$	in CH_2Cl_2	−298·4	non-labelled
$RhCl_3(NHN$–C$_6$H$_3$(NO$_2$)–$)(PPh_3)_2$	in CH_2Cl_2	−200·1	non-labelled

Data from ref. 334; ^{15}N-labelled N=N moiety; ^{15}N spectra; 18·25 MHz; field parallel to sample tube; referred originally to neat nitromethane; uncorrected for bulk susceptibility effects.

TABLE 144

Nitrogen shieldings in some complexes

Complex	Solution	Nitrogen shielding referred to neat nitromethane	Notes
$[Co(NH_3)_5(^{15}NH_3)]Cl_3$	0·3 M in H_2O	+423·4	(a)
$[Co(H_2{}^{15}NCH_2CH_2{}^{15}NH_2)_3]Cl_3$	0·3 M in H_2O	+397·2	(a)
$[Co(NH_3)_5NO]Cl_2$	in H_2O	+389 ± 5 (NH_3)	(b)
$[Co(NH_3)_5Cl]Cl_2$	in H_2O	+351 ± 10	(b)
$[Co(NH_3)_5NO_3](NO_3)_2$	in H_2O	+382 ± 10 (NH_3)	(b)
		+4 ± 5 (NO_3)	(b)
$[Co(NH_3)_5OH]Cl_2$	in H_2O	+337 ± 10	(b)
$[Ru(NH_3)_5N_2]Cl_2$	in H_2O	+396 ± 10 (NH_3)	(b)
		−24 ± 20 (N_2)	(b)
$[Ru(NH_3)_5NO]Cl_3$	in H_2O	+387 ± 10 (NH_3)	(b)
		+27 ± 10 (NO)	(b)
$[Ru(NH_3)_5CO]Cl_2$	in H_2O	+410 ± 10	(b)
$K_2(RuNOCl_5)$	in H_2O	+46 ± 10	(b)
$K_2(RuNOBr_5)$	in H_2O	+41 ± 10	(b)
$K_2(RuNOI_5)$	in H_2O	+65 ± 10	(b)
$[OsNO(NH_3)_5]Cl_3$	in H_2O	+412 ± 10 (NH_3)	(b)
		+75 ± 10 (NO)	(b)
$K_2(OsNOCl_5)$	in H_2O	+52 ± 5	(b)
$[OsNO(NH_3)_4OH]Cl$	in H_2O	+385 ± 5 (NH_3)	(b)
		+62 ± 5 (NO)	(b)
$K_3[CoNO(CN)_5]$	in H_2O	+99 ± 25	(b)
$K_2[FeNO(CN)_5]$	in H_2O	+56 ± 10	(b)
$(R)PtCl_2[H_2{}^{15}N(CH_2)_5Me]$	in $CDCl_3$		
R = $PBu^n{}_3$, *trans*		+352·2	(c)
PPh_2Me, *trans*		+353·3	(c)
$P(C_6H_4{\cdot}Me\text{-}p)_3$, *trans*		+353·1	(c)
$AsBu^n{}_3$, *trans*		+357·7	(c)
$AsPh_2Me$, *trans*		+359·7	(c)
$As(C_6H_4{\cdot}Me\text{-}p)_3$, *trans*		+359·2	(c)
$^{15}NH_2(CH_2)_5Me$, *trans*		+397·5	(c)
$CH_2{=}CH_2$, *trans*		+356·6	(c)
$CH_2{=}CH_2$, *cis*		+385·8	(c)
$(R)PdCl_2[H_2{}^{15}N(CH_2)_5Me]$	in $CDCl_3$		
R = $PBu^n{}_3$, *trans*		+357·6	(c)
PPh_2Me, *trans*		+358·8	(c)
$P(C_6H_4{\cdot}Me\text{-}p)_3$, *trans*		+358·8	(c)
$AsBu^n{}_3$, *trans*		+360·7	(c)
$AsPh_2Me$, *trans*		+363·6	(c)
$As(C_6H_4{\cdot}Me\text{-}p)_3$, *trans*		+362·1	(c)
$^{15}NH_2(CH_2)_5Me$, *trans*		+386·1	(c)
$Rh(NH_2CH_2CH_2NH_2)_3Cl_3$	in H_2O	+391·4	(d)
$Rh(MeNHCH_2CH_2NH_2)_3Cl_3$	in H_2O	+344·1 +394·1	(d)
$Rh(NH_2CH_2CH_2CH_2NH_2)_3Cl_3$	in H_2O	+403·6	(d)

TABLE 144—*cont.*

Complex	Solution	Nitrogen shielding referred to neat nitromethane	Notes
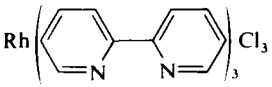	in H_2O	+173·5	(d)
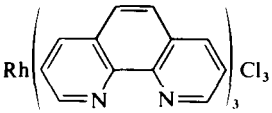	in H_2O	+178·8	(d)
trans-$Rh[(NH_2CH_2CH_2NH_2)_2Cl_2]Cl$	in H_2O	+388·2	(d)
trans- 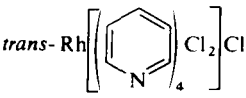	in benzyl alcohol (50 °C)	+168·6	(d)
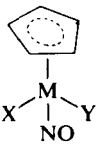	in $CDCl_3$		
$(\eta^5\text{-}C_5H_5)Cr(CO)_2(NO)$		−48·8	(e)
$(\eta^5\text{-}C_5H_5)Mo(CO)_2(NO)$		−37·4	(e)
$(\eta^5\text{-}C_5H_5)Mo(CO)(PPh_3)(NO)$		−35·2	(e)
$(\eta^5\text{-}C_5H_5)W(CO)_2(NO)$		−16·3	(e)
$(\eta^5\text{-}C_5H_5)Cr(NO)_2(Cl)$		−184·4	(e)
$(\eta^5\text{-}C_5H_5)Mo(NO)_2(Cl)$		−185·2	(e)
$(\eta^5\text{-}C_5H_5)W(NO)_2(Cl)$		−172·7	(e)
$[(\eta^5\text{-}C_5H_5)Cr(NO)_2]_2$		−121·5	(e)
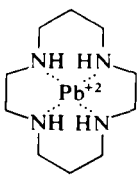 $(NO_3^-)_2$	0·9 M in DMSO	+318·8 (equatorial) +325·5 (axial) +11·8 (NO_3^-)	(f) (f) (f)

(a) Data from ref. 335; ^{15}N-labelled compounds; ^{15}N spectra; 6·058 MHz; field perpendicular to sample tube; referred originally to aqueous $NaNO_2$, −228·9 ppm from neat nitromethane (Table 6); conversion scheme II (Table 4).

(b) Data from ref. 336; ^{14}N continuous-wave spectra; 4·33 MHz; low precision (broad resonances); referred originally to NO_3^- in saturated aqueous NH_4NO_3, +4·0 ppm from neat nitromethane (Table 6).

Footnotes to Table 144—*cont.*

(c) Data from ref. 337; ^{15}N-labelled compounds; ^{15}N spectra; 9·12 MHz; field perpendicular to sample tube; referred originally to aqueous NH_4Cl, +352·9 ppm from neat nitromethane (Table 6); conversion scheme II (Table 4).

(d) Data from ref. 125; ^{15}N natural abundance spectra; 10·99 MHz; field perpendicular to sample tube; referred to what is reported as aqueous NH_4Cl, +352·5 ppm from neat nitromethane (Table 6), but the reported shift for pyridine in $CHCl_3$ suggests that aqueous NH_4NO_3 was used instead, +359·6 ppm from neat nitromethane (Table 6); conversion scheme II (Table 4).

(e) Data from ref. 338; ^{15}N natural abundance spectra; 18·25 MHz; field parallel to sample tube; referred to what was reported as 0·1 M HNO_3, probably 1 M DNO_3, +6·2 ppm from neat nitromethane (Table 6); conversion scheme IV (Table 4).

(f) Data from ref. 339; ^{15}N natural abundance spectra; 18·25 MHz; field parallel to sample tube; referred originally to neat nitromethane; uncorrected for bulk susceptibility effects.

TABLE 145

Some ^{15}N–^{1}H couplings across one bond

Compound	Solvent	$^{1}J(^{15}N-^{1}H)$ (Hz)	Ref.
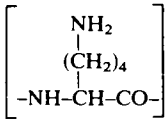	H_2O		
	pH 0·5	(−)91·2 (NH)	240
		(−)74·6 (NH_3^+)	240
	pH 4·0	(−)92·8 (NH)	240
	pH 7·0	(−)87·9 (NH)	240
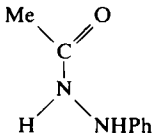	DMSO	(−)90·1 (NHPh)	77
		(−)101·6 (NHCO)	77
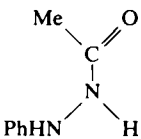	DMSO	(−)92·3 (NHPh)	77
		(−)97·6 (NHCO)	77
$HN^+(CH_2CH_2OH)_3\ Cl^-$	H_2O	(−)72·3	124
Bis(methyl-2-*O*-acetyl-4,6-*O*-benzylidene-3-deoxy-α-D-altropyranosid-3-yl)amine	DMSO	(−)86·7	341
	CCl_4	(−)78·0	342
(aniline)	$CDCl_3$	(−)78·0	342
	acetone-d_6	(−)82·1	342
	DMSO-d_6	(−)82·3	342
	D_2O	(−)82·6	83

TABLE 145—*cont.*

Compound	Solvent	$^1J(^{15}N-^1H)$ (Hz)	Ref.
Substituted anilines			
4-Me	$CDCl_3$	(−)76·5	342
4-NO_2	acetone-d_6	(−)89·9	342
	DMSO	(−)89·4	342
3-Cl	D_2O	(−)85·1	83
3-Br	D_2O	(−)85·3	83
3-I	D_2O	(−)84·4	83
3-NO_2	D_2O	(−)86·2	83
	acetone-d_6	(−)78 (+34 °C)	343
		(−)89 (−80 °C)	343
$PhNH(PMe_2)$	benzene	(−)81·0	142
$PhNH(PMe_2O)$	DMSO-d_6	(−)83·0	142
$PhNH(PMe_2S)$	dioxan	(−)82·0	142
$PhNH(PMe_2Se)$	CH_2Cl_2	(−)83·0	142
$PhNH(PMe_2Te)$	benzene/CH_2Cl_2	(−)79·5	142
$PhNH(P^+Me_3)\ I^-$	CH_2Cl_2	(−)83·3	142
$PhNH(P^+Me_2SMe)\ I^-$	$CHCl_3$	(−)84·5	142
$PhNH(P^+Me_2SeMe)\ I^-$	CH_2Cl_2	(−)82·5	142
$PhNH(PBu^n_2)$	mesitylene	(−)80·5	142
$PhNH(PBu^n_2O)$	mesitylene/CH_2Cl_2	(−)80·5	142
$PhNH(PBu^n_2S)$	mesitylene/$CHCl_3$	(−)78·5	142
$PhNH(PBu^n_2Se)$	mesitylene/$CHCl_3$	(−)78·5	142
$PhNH(P^+MeBu^n_2)\ I^-$	DMSO-d_6	(−)77·0	142
$PhNH(P^+Bu^n_2SeMe)\ I^-$	DMSO-d_6	(−)81·0	142
$PhNHP(NMe_2)_2$	benzene	(−)79·0	142
$(PhNH)_2PNMe_2$	benzene	(−)79·5	142
$PhNHP(MeNCH_2CH_2NMe)$	benzene	(−)78·5	142
$PhNHP(S)(MeNCH_2CH_2NMe)$	benzene/$CHCl_3$	(−)83·0	142
$PhNHP(Se)(MeNCH_2CH_2NMe)$	benzene	(−)85·8	142
$PhNHP^+(Me)(MeNCH_2CH_2NMe)\ I^-$	CH_2Cl_2	(−)79·8	142
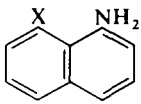			
X=NH_2	D_2O	(−)79·5	83
H	D_2O	(−)83·4	83
I	D_2O	(−)82·5	83
Br	D_2O	(−)86·0	83
CN	D_2O	(−)82·5	83
NO_2	D_2O	(−)79·9	83
Chetomin (see Table 66)	$CDCl_3$	(−)87·8 (6-NH)	201
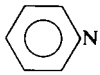	DCl_{aq}	(−)76·0	342

TABLE 145—*cont.*

Compound	Solvent	$^1J(^{15}N-^1H)$ (Hz)	Ref.
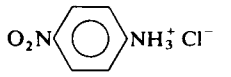	DCl_{aq}	(−)76·0	342
Nucleosides and nucleotides (see Table 126)			
adenosine	DMSO-d_6, 0·2 M	(−)92·3* (NH_2)	344
guanosine	DMSO-d_6, 0·2 M	(−)100·6* (NH)	344
		(−)91·0* (NH_2)	344
adenine	DMSO-d_6, 0·05 M	(−)88·7* (NH_2)	344
	0·10 M	(−)91·9* (NH_2)	344
9-ethylguanine	DMSO-d_6, 0·05 M	(−)87·5* (NH_2)	344
		(−)92·6* (NH)	344
	0·10 M	(−)94·3* (NH_2)	344
		(−)94·7* (NH)	344
	0·20 M	(−)97·9* (NH_2)	344
		(−)107·3* (NH)	344
1-methylthymine	DMSO-d_6, 0·10 M	(−)91·2* (NH)	344
	0·20 M	(−)92·0* (NH)	344
uracil	DMSO-d_6, 0·05 M	(−)86·4* (1-NH)	344
		(−)92·2* (3-NH)	344
guanosine-3′-phosphate	H_2O, pH 7	(−)90·7 (NH_2)	315
adenosine-3′-phosphate	H_2O, pH 7	(−)88·2 (NH_2)	315
cytidine-3′-phosphate	H_2O, pH 7	(−)86·0 (NH_2)	315
2′,3′,5′-tri-*O*-benzyluridine	$CDCl_3$, 0·5 M	(−)91·3 (3-NH)	316
same + 5′-*O*-acetyl-2′,3′-*O*-isopropylideneadenosine	$CDCl_3$	(−)87·5 (3-NH, uridine moiety)	316
$(H_2N)_2C{=}O$	D_2O	(−)90·3	66
	DMSO	(−)88·5	178
	acetone + DMSO + tetramethylurea	(−)86·8	345
$H_2NC(=O)NHC(=O)NH_2$	DMSO	(−)88·5 (NH_2)	178
		(−)89·1 (NH)	178
$(PhNH)_2C{=}O$	DMSO	(−)89·1	178
$(PhNH)_2{}^{13}C{=}O$	DMSO	(−)87·9	178
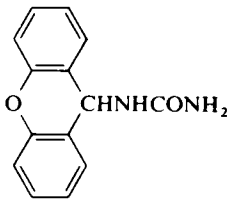	DMSO	(−)87·3 (NH)	178
		(−)87·9 (NH_2)	178

TABLE 145—*cont.*

Compound	Solvent	$^1J(^{15}N-^1H)$ (Hz)	Ref.
	DMSO	(−)88·5 (NH) (−)87·3 (NH_2)	178 178
$(MeNH)_2C{=}O$	DMSO-d_6	(−)88·7	345
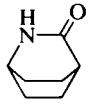	D_2O	(−)92·8	347
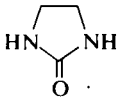	DMSO	(−)92·2	185
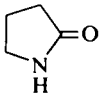	DMSO	(−)90·0	185
		(−)93	191
	H_2O	(−)93	191
	CF_3COOH	(−)93·0	185
		(−)92·5	198
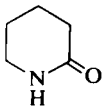	H_2O	(−)91	191
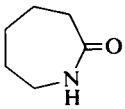	$CDCl_3$,		
	0·05 M	(−)89·9*	344
	0·10 M	(−)82·8*	344
	0·25 M	(−)85·1*	344
	H_2O	(−)90	191
	DMSO	(−)90	191
	CF_3COOH	(−)92·5	198
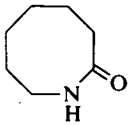	H_2O	(−)89	191
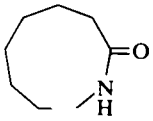	DMSO	(−)89	191

TABLE 145—*cont.*

Compound	Solvent	$^1J(^{15}N-^1H)$ (Hz)	Ref.
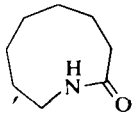	DMSO	(−)91	191
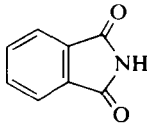	DMSO	(−)93·7	185, 362
	$HCOOH/CH_2Cl_2$	(−)96·8	185
	CF_3COOH	(−)97·7	185, 362
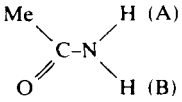	H_2O	(−)86·9; (−)91·3	346
	DMSO-d_6	(−)88·5 ($N-H_A$)	361
		(−)87·2 ($N-H_B$)	361
$MeC(=O)NH_2$	DMSO	(−)88·0	362
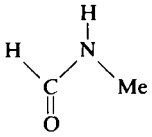	none	(−)93·8	373
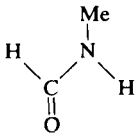	none	(−)90·2	373
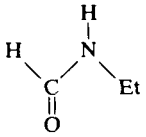	none	(−)92·2	373
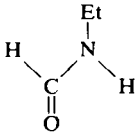	none	?	373
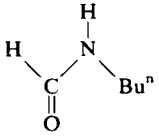	none	(−)92·2	373

TABLE 145—*cont.*

Compound	Solvent	$^1J(^{15}N-^1H)$ (Hz)	Ref.
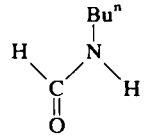	none	(−)89·8	373
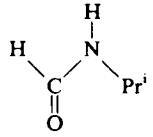	none	(−)92·4	373
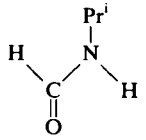	none	?	373
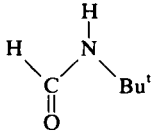	none	(−)92·3	373
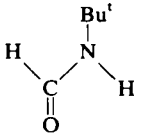	none	(−)86·6	373
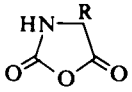			
R=Me	DMSO	(−)97·0	185
	acetone/$CDCl_3$	(−)97·8	185
	CF_3COOH	(−)100·8	185
Pr^i	acetone/$CDCl_3$	(−)98·0	185
	CF_3COOH	(−)100·0	185
Bu^i	acetone/$CDCl_3$	(−)98·0	185
	CF_3COOH	(−)100·0	185
Ph	CF_3COOH	(−)100·0	185
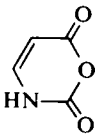	CF_3COOH	(−)94·5	185

TABLE 145—*cont.*

Compound	Solvent	$^1J(^{15}N-^1H)$ (Hz)	Ref.
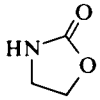	DMSO	(−)96·8	185
$PhCH_2OCONHCH_2COOH$	pyridine	(−)93·0	185
	DMSO	(−)93·7	185
	HCOOH	(−)93·0	185
$MeCO^{15}NHCH(Me)CONHMe$	D_2O	(−)93·4 (^{15}NH)	347
$[-NHCH_2CH_2C(=O)-]_n$	CF_3COOH	(−)93·5	198
$[-NHCH_2CH_2CH_2C(=O)-]_n$	CF_3COOH	(−)94·0	198
$(H_2{}^{15}N)_2C^+NHCH_2CH_2CH_2CH(NH_2)COO^-$	D_2O, pH 9·9	(−)91·7 ($^{15}NH_2$)	66
$PhNHNH_2$	none	(−)68 (NH_2)	346
trans-$[MoF(NNH_2)(Ph_2PCH_2CH_2PPh_2)]BF_4$	CH_2Cl_2	(−)86	346
$[MoCl(NNH_2)(pyridine)(PMe_2Ph)]Cl$	CH_2Cl_2	(−)83	346
$[WCl(NNH_2)(pyridine)(PMe_2Ph)]Cl$	CH_2Cl_2	(−)83	346
$MeNHNO_2$	CH_2Cl_2	(−)100 ± 5	263
	benzene	(−)96·4	348
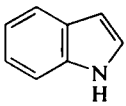	DMSO, 0·1 M	(−)96·8*	344
2-Methylindole	DMSO, 0·1 M	(−)97·1*	344
3-Methylindole	DMSO, 0·1 M	(−)96·9*	344
Tryptophan	DMSO	(−)103·0* (ring NH)	344
Octaethylporphyrin (OEP) derivatives (see Table 116)			
$(OEP)H_2$	$CDCl_3$(28 °C)	(−)24 (N⇄NH)	283
	$CDCl_3$(−53 °C)	(−)97 (NH)	283
$(OEP)H_4{}^{2+}$	CF_3COOH	(−)93 (NH^+)	283
(OEP)MeH	$CDCl_3$	(−)100 (NH)	283
$(OEP)MeH_3{}^{2+}$	CF_3COOH	(−)92 (NH^+)	283
$(OEP)Me_2H^+$	$CDCl_3$	(−)48 (N⇄NH^+)	283
Protoporphyrin-IX dimethyl ester (see Table 116)	$CDCl_3$	(−)103 ± 4	290
its dication	$CDCl_3$	(−)90 ± 3	290
Coproporphyrin-III tetramethyl ester (see Table 116)	$CDCl_3$	(−)100 ± 3	290
its dication	$CDCl_3$	(−)85 ± 3	290
$HN=N^+=N^-$ (hydrazoic acid)	Et_2O	(−)70·18	247
$pO_2N{\cdot}C_6H_4{\cdot}C(=O)^{15}NHOH$	DMSO	(−)102 (^{15}NH)	349

TABLE 145—*cont.*

Compound	Solvent	$^1J(^{15}N-^1H)$ (Hz)	Ref.
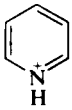	CF_3COOH	(−)96·3	300
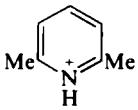	CF_3COOH	(−)96·3	300
*p*MeO·C_6H_4·CH=NH^+Ph	CF_3COOH	(−)93·7	300
*p*Me·C_6H_4·CH=NH^+Ph	CF_3COOH	(−)93·7	300
PhCH=NH^+Ph	CF_3COOH	(−)94·6	300
PhCH=NH^+·C_6H_4·OMe*p*	CF_3COOH	(−)90·2	300
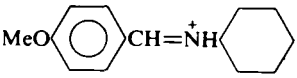	CF_3COOH	(−)91·0	300
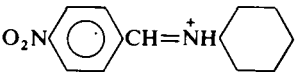	CF_3COOH	(−)92·0	300
PhCH=NH^+Pr^i	CF_3COOH	(−)92·4	300
PhCH=NH^+Bu^i	CF_3COOH	(−)89·1	300
Ph_2C=NH^+Ph	CF_3COOH	(−)92·0	300
PhC(Me)=NH^+Ph	CF_3COOH	(−)92·0	300
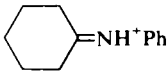	CF_3COOH	(−)92·0	300
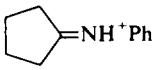	CF_3COOH	(−)95·4	300

* Recalculated from $^{14}N-^1H$ couplings obtained from analysis of relaxation times.

TABLE 146

Some ^{15}N–^{1}H couplings across two bonds (absolute values if sign not given)

Compound	Solvent	$^{2}J(^{15}N–^{1}H)$ (Hz)	Ref.
$MeNHNO_2$	CH_2Cl_2	1·0 (Me–N)	263
Me_2NNO_2	CH_2Cl_2	1·0 (Me–N)	263
$MeOOC–N(NO_2)Me$	CH_2Cl_2	0·6 (Me–N)	263
$EtOOC–N(NO_2)Me$	CH_2Cl_2	0·4 (Me–N)	263
$MeN(NO_2)_2$	CH_2Cl_2	1·8 (Me–N)	263
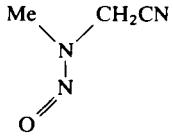	$CDCl_3$	1·5 (Me–N) 1·6 (CH_2–N)	352 352
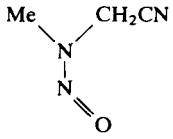	$CDCl_3$	1·7 (Me–N) 1·4 (CH_2–N)	352 352
$EtOOC–CH{=}N^{+}{=}N^{-}$	MeCN	2·8 ($HC{=}N^{+}{=}$)	67
$MeNHC(=O)NHMe$	DMSO-d_6	0·7 (Me–N)	345
$MeC(=O)NHMe$	CCl_4	+1·0 (Me–N)	360
$EtC(=O)NHMe$	CCl_4	+1·2 (Me–N)	360
$Pr^{i}C(=O)NHMe$	CCl_4	+1·2 (Me–N)	360
$PhN(Me)CH_2C{\equiv}CH$	CD_2Cl_2	>0·2 (CH_2–N) >0·2 (Me–N)	343 343
$PhN(Me)C{\equiv}CMe$	acetone-d_6	0·8 (Me–N)	343
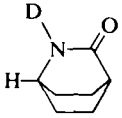	D_2O	1·5 (CH–N)	347
$MeCO^{15}NDCH(Me)CONHMe$	D_2O	1·1 (CH–^{15}N)	347
$Bu^{t}C(=O)NHMe$	CCl_4	+1·2 (Me–N)	360
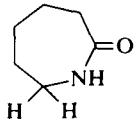	CCl_4	+0·8 (CH_2–N)	360
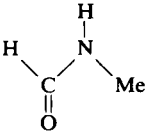	none	15·6 (N–CO–H) 1·4 (N–Me)	373 373

TABLE 146—*cont.*

Compound	Solvent	$^2J(^{15}N-^1H)$ (Hz)	Ref.
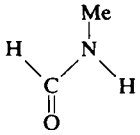	none	15·1 (N–CO–H) 1·4 (N–Me)	373 373
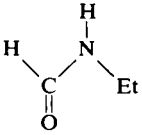	none	15·1 (N–CO–H)	373
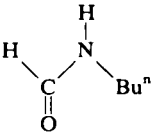	none	15·0 (N–CO–H)	373
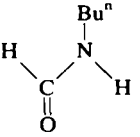	none	14·3 (N–CO–H)	373
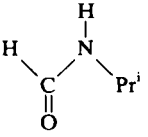	none	15·3 (N–CO–H)	373
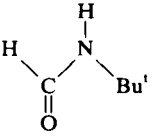	none	14·7 (N–CO–H)	373
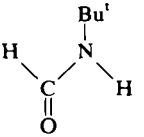	none	14·4 (N–CO–H)	373

TABLE 146—*cont.*

Compound	Solvent	$^2J(^{15}N-^1H)$ (Hz)	Ref.
PhNHC(=O)NHMe	pyridine, 1 M, 30 °C	2·0 (Me–N)	362
	DMSO, 1 M, 30 °C	1·2 (Me–N)	362
	D_2O/acetone, 1 M, 30 °C	<2·0 (Me–N)	362
	HCOOH, 1 M, 30 °C	<2·0 (Me–N)	362
	CF_3COOH, 1 M, 30 °C	2·4 (Me–N)	362
	DMSO, 0·16 M, 30 °C; 0·4 M; 1·6 M; 1·6 M, 80 °C; 1·6 M, 130 °C	1·2 (Me–N)	362
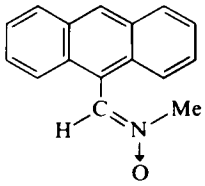	$CDCl_3$	+2·1 (HC=N)	363
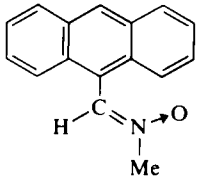	$CDCl_3$	−2·3 (HC=N)	363
$MeNO_2$	nematic phase	+2·25 (N–Me)	371
		−3·286 (direct NH coupling)	371
Silatranes (see Table 29)			
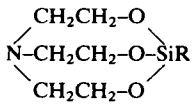			
R=Me	CD_3OD	0·2 (CH_2–N)	124
$CH=CH_2$	acetone-d_6	0·1 (CH_2–N)	124
Ph	acetone-d_6	0·1 (CH_2–N)	124
CH_2Cl	$CDCl_3$	0·1 (CH_2–N)	124

TABLE 146—*cont.*

Compound	Solvent	$^2J(^{15}N-^1H)$ (Hz)	Ref.
$F_2PN(SiH_3)_2$	$CDCl_3$	−3·8 (H_3Si–N)	138
$(F_2P)_2NSiH_3$	$CDCl_3$	−3·5 (H_3Si–N)	138
$F_2PN(SiH_3)_2 \cdot BH_3$	$CDCl_3$	4·2 (H_3Si–N)	138
Amino acid residues in alumichrome (see Table 84)	DMSO-d_6		
Gly^1		0·2, 1·1 (CH$_2$–N)	356
Gly^2		1·4, 0·9 (CH$_2$–N)	356
Gly^3		1·1, 0·4 (CH$_2$–N)	356
Orn^1		1·5, 0·1 (CH–N)	356
Orn^2		1·0 (CH–N)	
Orn^3		1·7, 0·5 (CH–N)	356
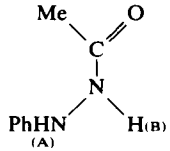	DMSO	1·1 (N–N–H_A) 1·2 (N–N–H_B)	77 77
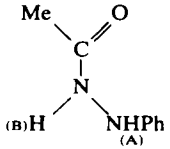	DMSO	>0·4 (N–N–H_A) 5·5 (N–N–H_B)	77 77
	none benzene-d_6	4·52 (CH–N) −5·36 (CH–N)	280 348
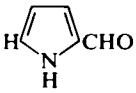	$CHCl_3$	4·05 (CH–N)	280
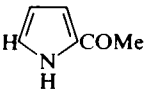	$CHCl_3$	4·00 (CH–N)	280
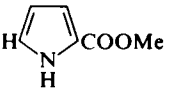	$CHCl_3$	4·10 (CH–N)	280

TABLE 146—*cont.*

Compound	Solvent	$^2J(^{15}N-^1H)$ (Hz)	Ref.
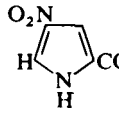	$CHCl_3$	3·45 (CH–N)	280
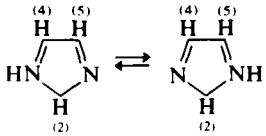	H_2O	−9·6 (2-CH–N) −7·2 (4,5-CH–N)	276 276
	H_2O	−5·5 (2-CH–N) −4·0 to −4·6 (4,5-CH–N)	276 276
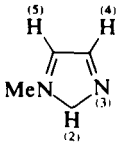	H_2O	−7·6 (2-CH–1-N) −10·8 (2-CH–3-N) −5·5 (5-CH–1-N) −9·0 (4-CH–3-N) −1·6 (Me–N)	276 276 276 276 276
	H_2O	−5·0 (2-CH–1-N) −5·4 (2-CH–3-N) −4·4 to −5·2 (4-CH–3-N) −1·9 (Me–N)	276 276 276 276
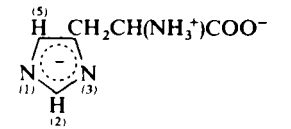	H_2O, pH 10·9	−8·8 (2-CH–1-N) −9·6 (2-CH–3-N) −6·6 (5-CH–1-N)	209, 276 209, 276 209, 276
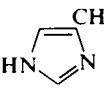 (see Table 72) (histidine)	H_2O, pH 7·6	−8·2 (2-CH–1-N) −10·2 (2-CH–3-N) −5·9 (5-CH–1-N)	208, 209 208, 209 208, 209
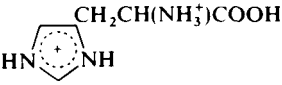	H_2O, pH 1·3	−4·6 (2-CH–1-N) −6·1 (2-CH–3-N) −4·8 (5-CH–1-N)	209, 276 209, 276 209, 276
α-*N*-Acetylhistidine, cation/amphion	H_2O	−4·8 (2-CH–1-N) −4·6 (2-CH–3-N) −4·9 (5-CH–1-N)	208 208 208
α-*N*-Acetylhistidine, anion	H_2O	−7·9 (2-CH–1-N) −9·8 (2-CH–3-N) −6·6 (5-CH–1-N)	208 208 208

TABLE 146—*cont.*

Compound	Solvent	$^2J(^{15}N-^1H)$ (Hz)	Ref.
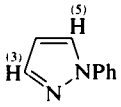	$CDCl_3$	4·4 (5-CH-1-N) 14·2 (3-CH-2-N)	277 277
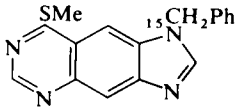	DMSO-d_6	1·2 ($^{15}N-CH_2$)	351
	acetone-d_6	−10·93 (CH-N)	358, 359
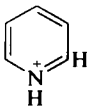	CD_3OH	−3·01 (CH-N)	359
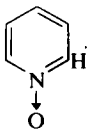	$CDCl_3$ CS_2	+0·47 (CH-N) 0·35	359, 303 303
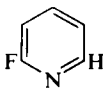	acetone-d_6	−11·35 (CH-N)	358
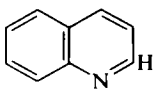	$CDCl_3$	10·2 (CH-N)	350
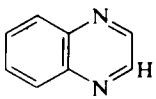	$CDCl_3$	6·5 (CH-N)	350
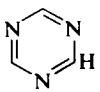	nematic phase	14·7 (CH-N)	102
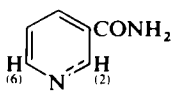 (nicotinamide)	D_2O, pH 7·0 D_2O, pH 2·0 	9·6 (2-CH-N) 10·1 (6-CH-N) 1·2 (2-CH-N) 1·3 (6-CH-N)	136 136 136 136
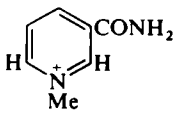	D_2O	1·2 (2-CH-N) 1·3 (6-CH-N) 1·8 (Me-N)	136 136 136

TABLE 146—*cont.*

Compound	Solvent	$^2J(^{15}N-^1H)$ (Hz)	Ref.
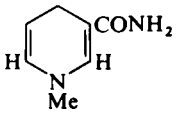	D_2O	2·4 (2-CH–N) 3·7 (6-CH–N) 5·0 (Me–N)	136 136 136
Nicotinamide nucleotides (see Table 126)			
NAD^+	D_2O	1·2 (2-CH–N) 1·4 (6-CH–N) 2·1 (1′-CH–N)	136 136 136
NADH	D_2O	1·6 (2-CH–N) 3·6 (6-CH–N)	136 136
NMN^+	D_2O	1·1 (2-CH–N) 1·1 (6-CH–N) 2·4 (1′-CH–N)	136 136 136
NMNH	D_2O	2·0 (2-CH–N) 3·4 (6-CH–N) >1·3 (1′-CH–N)	136 136 136
Antibiotic ristocetin	DMSO-d_6	5–12 (α-CH–NH)	354
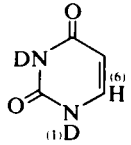	D_2O	3·30 (6-CH–1-N)	355
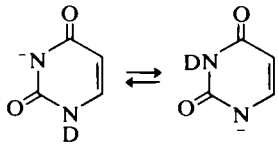	D_2O	6·34 (6-CH–1-N)	355
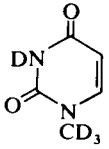	D_2O	2·48 (6-CH–1-N)	355
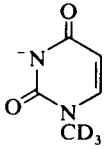	D_2O	2·32 (6-CH–1-N)	355
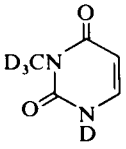	D_2O	3·36 (6-CH–1-N)	355

TABLE 146—*cont.*

Compound	Solvent	$^2J(^{15}N-^1H)$ (Hz)	Ref.
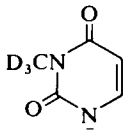	D_2O	10·46 (6-CH-1-N)	355
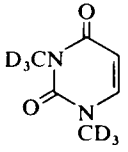	D_2O	2·54 (6-CH-1-N)	355
	D_2O, pD 12·3	2·47 (6-CH-1-N)	355
Nucleotides (see Table 126)			
adenosine-3′-phosphate	H_2O, pH 3	12·5 (2-CH-1-N)	314, 315
		14·0 (2-CH-3-N)	314, 315
		10·5 (8-CH-7-N)	314, 315
		9·5 (8-CH-9-N)	314, 315
	H_2O, pH 7	14·0 (2-CH-1-N)	314, 315
		15·5 (2-CH-3-N)	314, 315
		10·5 (8-CH-7-N)	314, 315
guanosine-3′-phosphate	H_2O, pH 7	10·0 (8-CH-7-N)	314, 315
	H_2O, pH 10	10·0 (8-CH-7-N)	314, 315
$HN{=}N^+{=}N^-$ (hydrazoic acid)	Et_2O	2·26 ($HN{=}N^+{=}$)	247
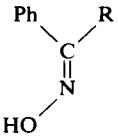			
R=CH_2Cl	Et_2O	1·93 (HO-N)	357
CH_2Br	Et_2O	1·88 (HO-N)	357
CH_2I	Et_2O	1·82 (HO-N)	357
	DMSO-d_6	1·91 (HO-N)	357
CH_2CMe_3	DMSO-d_6	1·75 (HO-N)	357
CH_2OMe	DMSO-d_6	2·01 (HO-N)	357
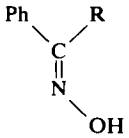			
R=Me	DMSO-d_6	1·77 (HO-N)	357
Et	DMSO-d_6	1·86 (HO-N)	357
CH_2CMe_3	DMSO-d_6	1·92 (HO-N)	357
CH_2OMe	DMSO-d_6	1·63 (HO-N)	357

TABLE 147

Comparison of experimental and calculated values of two-bond ^{15}N–^{1}H couplings in –HC=N– moieties

Structure	$^{2}J(^{15}N$–$^{1}H)$ (Hz) observed	calculated by CNDO/2-FPT or INDO-FPT methods
Pyridine	−10·8	−17·0
Pyridinium ion	−3·0	+0·5
Pyridine *N*-oxide	+0·5	
Quinoline	−11·0	
Quinolinium ion	−2·0	
Quinoline *N*-oxide	0·0	
Oxime	−15·9	−15·4 (acetaldoxime)
Imine	−9·9	−17·5 } see Table 146
Imine *N*-oxide (nitrone)	+2·1	+0·6 } see Table 146
	−2·3	−3·25 } see Table 146

Data from ref. 363, and references therein.

TABLE 148

Some ^{15}N–^{1}H couplings across three bonds (absolute values if sign not given)

Compound	Solvent	$^{3}J(^{15}N$–$^{1}H)$ (Hz)	Ref.
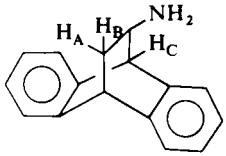	D_2O	−1·0 (N–C–CH_A) 0 (N–C–CH_C) −3·8 (N–C–CH_B)	367 367 367
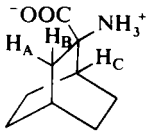	D_2O	−1·12 (N–C–CH_A) −0·42 (N–C–CH_C) −3·79 (N–C–CH_B)	367 367 367
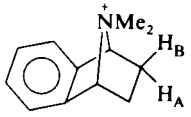	$CDCl_3$	4·2* (N–C–CH_A) 0 (N–C–CH_B)	369 369
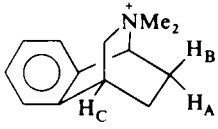	$CDCl_3$	3·5* (N–C–CH_A) 0 (N–C–CH_B) 4·9* (N–C–CH_C)	369 369 369

TABLE 148—*cont.*

Compound	Solvent	$^3J(^{15}N-^1H)$ (Hz)	Ref.
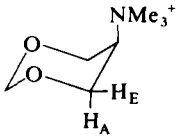	$CDCl_3$	4·8* ($N-C-CH_A$) 1·0* ($N-C-CH_E$)	369 369
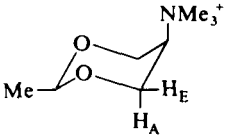	$CDCl_3$	3·6* ($N-C-CH_A$) 1·0* ($N-C-CH_E$)	369 369
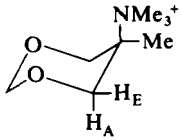	$CDCl_3$	5·0* ($N-C-CH_A$) 1·0* ($N-C-CH_E$)	369 369
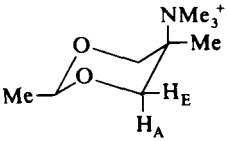	$CDCl_3$	4·8* ($N-C-CH_A$) 0·7* ($N-C-CH_E$)	369 369
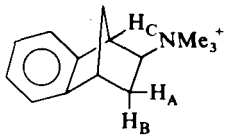	$CDCl_3$	3·9* ($N-C-CH_A$) 1·1* ($N-C-CH_B$) 0·4* ($N-C-CH_C$)	369 369 369
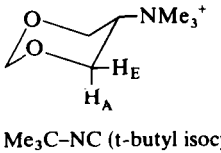	$CDCl_3$	1·3* ($N-C-CH_A$) 1·0* ($N-C-CH_E$)	369 369
Me_3C-NC (t-butyl isocyanide) in complexes with Pd (Table 110)	$CDCl_3$	2·9* ($N-C-CH_3$)	370
Leucine			
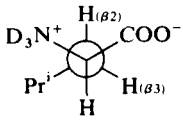 anion	D_2O	−2·15 ($N-C-CH_{\beta 2}$) −3·15 ($N-C-CH_{\beta 3}$)	368 368
cation	D_2O	−2·47 ($N-C-CH_{\beta 2}$) −3·47 ($N-C-CH_{\beta 3}$)	368 368

TABLE 148—*cont.*

Compound	Solvent	$^3J(^{15}N-^1H)$ (Hz)	Ref.
Amino acid residues in alumichrome (see Table 84)	DMSO-d_6		
Orn[1]		0·5 ($N-C-CH_{\beta 2}$)	356
		5·0 ($N-C-CH_{\beta 3}$)	356
		5·4 ($N-C-CH_{\gamma 2}$)	356
		0 ($N-C-CH_{\gamma 3}$)	356
Orn[2]		0·2 ($N-C-CH_{\beta 2}$)	356
		5·8 ($N-C-CH_{\beta 3}$)	356
		0·5 ($N-C-CH_{\gamma 2}$)	356
		0 ($N-C-CH_{\gamma 3}$)	356
Orn[3]		2·5 ($N-C-CH_{\beta 2}$)	356
		0·4 ($N-C-CH_{\beta 3}$)	356
		5·8 ($N-C-CH_{\gamma 2}$)	356
		0·3 ($N-C-CH_{\gamma 3}$)	356
$N(CH_2CH_2OH)_3$	$CDCl_3$	3·4 ($N-C-CH_2$)	124
	acetone-d_6	3·3 ($N-C-CH_2$)	124
	H_2O	2·3 ($N-C-CH_2$)	124
$NH^+(CH_2CH_2OH)_3\ Cl^-$	H_2O	2·2 ($N-C-CH_2$)	124
Silatranes (see Table 29)			
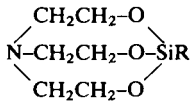			
R=Me	$CDCl_3$	2·4 ($N-C-CH_2$)	124
	CD_3OD	2·4 ($N-C-CH_2$)	124
$CH=CH_2$	acetone-d_6	2·3 ($N-C-CH_2$)	124
Ph	acetone-d_6	2·3 ($N-C-CH_2$)	124
CH_2Cl	$CDCl_3$	2·3 ($N-C-CH_2$)	124
OMe	acetone-d_6	2·2 ($N-C-CH_2$)	124
OEt	acetone-d_6	2·3 ($N-C-CH_2$)	124
$MeC(=O)NH_2$	DMSO-d_6	−1·0 ($N-CO-CH_3$)	361
$H_2NC(=O)NH_2$	acetone/DMSO/ tetramethylurea	1·7 ($N-CO-NH_2$)	345
$MeNHC(=O)NHMe$	DMSO-d_6	0·1 (N-CO-NH)	345
$PhNHC(=O)NHMe$	pyridine, 1 M, 30 °C	1·6 (N-CO-NH)	362
	DMSO, 0·16–1·6 M, 30 °C	1·8 (N-CO-NH)	362
	DMSO, 1·6 M, 130 °C	1·8 (N-CO-NH)	362
	HCOOH, 1 M, 30 °C	<2·0 (N-CO-NH)	362
	CF_3COOH, 1 M, 30 °C	2·4 (N-CO-NH)	362
	FSO_3H, 1 M, 30 °C	2·0 (N-CO-NH)	362

TABLE 148—*cont.*

Compound	Solvent	$^3J(^{15}N-^1H)$ (Hz)	Ref.
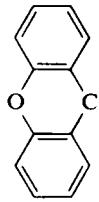	DMSO	1·8 (N–CO–NH_2)	178
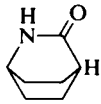	D_2O	1·3 (N–CO–CH)	347
$MeCO^{15}NHCH(Me)CONHMe$	D_2O	2·9 (^{15}N–C–CH_3)	347
		1·2 (^{15}N–CO–CH_3)	347
$MeNHNO_2$	CH_2Cl_2	3·0 (N–N–CH_3)	263
Me_2NNO_2	CH_2Cl_2	2·5 (N–N–CH_3)	263
$MeOOCN(Me)NO_2$	CH_2Cl_2	2·5 (N–N–CH_3)	263
$EtOOCN(Me)NO_2$	CH_2Cl_2	2·0 (N–N–CH_3)	263
$MeN(NO_2)SiMe_3$	CH_2Cl_2	3·0 (N–N–CH_3)	263
$MeN(NO_2)_2$	CH_2Cl_2	3·6 (N–N–CH_3)	263
$(MeNNO_2)^-\ NH_4^+$	CH_2Cl_2	5·0 (N–N–CH_3)	263
$EtOOCN(NO_2)SiMe_3$	CH_2Cl_2	0·9 (N–Si–CH_3)	263
$MeN(NO_2)SiMe_3$	CH_2Cl_2	0·6 (N–Si–CH_3)	263
$MeOOCN{=}N(O)OMe$	CH_2Cl_2	3·2 (N–O–CH_3)	263
$EtOOCN{=}N(O)OMe$	CH_2Cl_2	3·8 (N–O–CH_3)	263
$EtOOCN{=}N(O)OCHMe_2$	CH_2Cl_2	2·5 (N–O–CH)	263
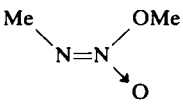	CH_2Cl_2	5·5 (N=N–CH_3)	263
		3·5 (N–O–CH_3)	263
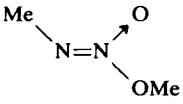	CH_2Cl_2	5·3 (N=N–CH_3)	263
		3·8 (N–O–CH_3)	263
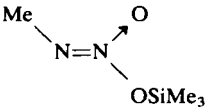	CH_2Cl_2	5·4 (N=N–CH_3)	263
$Me_2NP(NHPh)_2$	benzene	−3·5 (N–P–NH)	142
$PhNHPMe_2$	benzene	−2·7 (N–P–CH_3)	142
$PhNHPMe_2O$	DMSO-d_6	−1·2 (N–P–CH_3)	142
$PhNHPMe_2S$	dioxan	−1·2 (N–P–CH_3)	142
$PhNHPMe_2Se$	CH_2Cl_2	−1·0 (N–P–CH_3)	142
$PhNHPMe_2Te$	benzene/CH_2Cl_2	−1·7 (N–P–CH_3)	142
$(PhNHP^+Me_2SMe)\ I^-$	$CHCl_3$	−1·3 (N–P–CH_3)	142
$(PhNHP^+Me_3)\ I^-$	CH_2Cl_2	−1·4 (N–P–CH_3)	142

TABLE 148—*cont.*

Compound	Solvent	$^3J(^{15}N-^1H)$ (Hz)	Ref.
$(PhNHP^+Me_2SeMe)\ I^-$	CH_2Cl_2	−1·2 (N–P–CH_3)	142
$(PhNH–P^+Bu_2Me)\ I^-$	DMSO-d_6	−1·2 (N–P–CH_3)	142
$Me_3SnN(Ph)PMe_2$	benzene	−2·1 (N–P–CH_3)	142
$Me_3SnN(Ph)PMe_2S$	benzene	±0·2 (N–P–CH_3)	142
$PhNH\overset{+}{P}(Me)(MeNCH_2CH_2NMe)\ I^-$	CH_2Cl_2	−1·2 (N–P–CH_3)	142
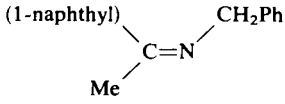	$CDCl_3$	−3·3 (N=C–CH_3)	363
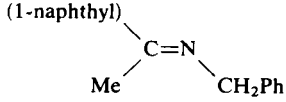	$CDCl_3$	−1·4 (N=C–CH_3)	363
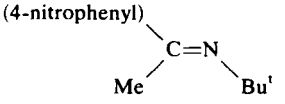	$CDCl_3$	−1·5 (N=C–CH_3)	363
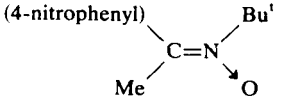	$CDCl_3$	−3·4 (N=C–CH_3)	363
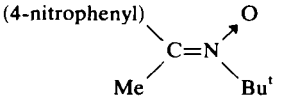	$CDCl_3$	−3·2 (N=C–CH_3)	363
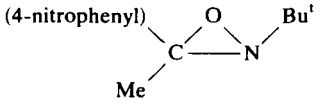	$CDCl_3$	−2·9 (N–C–CH_3)	363
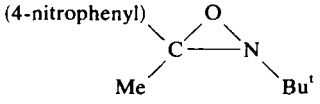	$CDCl_3$	−0·5 (N–C–CH_3)	363
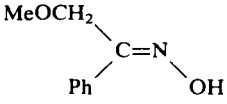	$CDCl_3$ DMSO-d_6 CCl_4 CF_3COOH	3·71 (N=C–CH_2) 3·75 (N=C–CH_2) 3·85 (N=C–CH_2) 3·00 (N=C–CH_2)	357 357 357 357
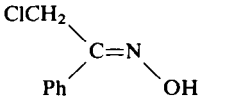	$CDCl_3$	4·10 (N=C–CH_2)	357

TABLE 148—*cont.*

Compound	Solvent	$^3J(^{15}N-^1H)$ (Hz)	Ref.
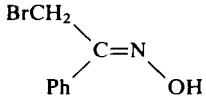	$CDCl_3$	4·33 ($N{=}C{-}CH_2$)	357
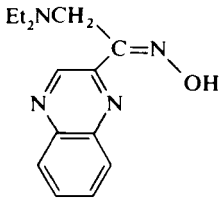	$CDCl_3$	3·68 ($N{=}C{-}CH_2$)	357
	DMSO-d_6	3·34 ($N{=}C{-}CH_2$)	357
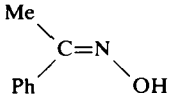	$CDCl_3$	−4·2 ($N{=}C{-}CH_3$)	366
		4·30 ($N{=}C{-}CH_3$)	357
	DMSO-d_6	4·12 ($N{=}C{-}CH_3$)	357
	CCl_4	4·23 ($N{=}C{-}CH_3$)	357
	CF_3COOH	4·85 ($N{=}C{-}CH_3$)	357
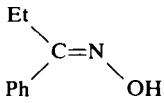	$CDCl_3$	3·72 ($N{=}C{-}CH_2$)	357
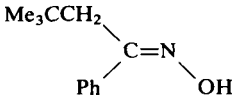	$CDCl_3$	4·60 ($N{=}C{-}CH_2$)	357
	CCl_4	4·60 ($N{=}C{-}CH_2$)	357
	CF_3COOH	5·38 ($N{=}C{-}CH_2$)	357
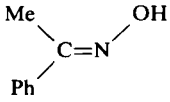	$CDCl_3$	−2·0 ($N{=}C{-}CH_3$)	366
$Me_2C{=}NOH$	?	2·2 ($N{=}C{-}CH_3$, *syn*)	365
		4·0 ($N{=}C{-}CH_3$, *anti*)	365
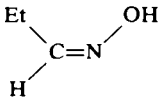	$CDCl_3$	−2·6 ($N{=}C{-}CH_2$)	366
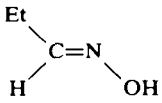	$CDCl_3$	−4·2 ($N{=}C{-}CH_2$)	366
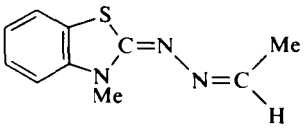	?	2·3 ($N{=}C{-}CH_3$)	365
		5·4 (N–N=CH)	365

TABLE 148—*cont.*

Compound	Solvent	$^3J(^{15}N-^1H)$ (Hz)	Ref.
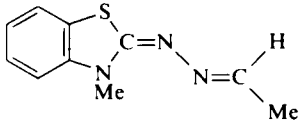	?	3·7 (N=C–CH_3) 10·0 (N–N=CH)	365 365
Me_2NCH_2, C=N, Ph, OH	$CDCl_3$ DMSO-d_6 CCl_4 CF_3COOH	3·81 (N=C–CH_2) 3·71 (N=C–CH_2) 3·81 (N=C–CH_2) 3·15 (N=C–CH_2)	357 357 357 357
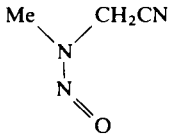	$CDCl_3$	0 (N–N–CH_2) 1·8 (N–N–CH_3) 1·5 (N≡C–CH_2)	352 352 352
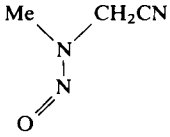	$CDCl_3$	1·7 (N–N–CH_2) 0 (N–N–CH_3) 1·5 (N≡C–CH_2)	352 352 352
$EtOOCCH=N^+=N^-$	MeCN	1·0 ($^-N=N^+=CH$)	67
$HN=N^+=N^-$ (hydrazoic acid)	Et_2O	2·25 ($^-N=N^+=N-H$)	247
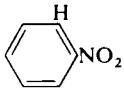	acetone-d_6	−1·9 (N–C=CH)	364
	benzene-d_6 none	−4·55 (N–C=CH) 5·39 (N–C=CH)	348 280
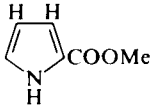	$CHCl_3$	4·31 (N–C=(3)CH) 4·95 (N–C=(4)CH)	280 280
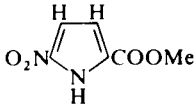	$CHCl_3$	3·05 (N–C=(3)CH) 3·63 (N–C=(4)CH)	280 280
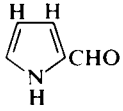	$CHCl_3$	4·15 (N–C=(3)CH) 5·00 (N–C=(4)CH)	280 280

TABLE 148—*cont.*

Compound	Solvent	$^3J(^{15}N-^1H)$ (Hz)	Ref.
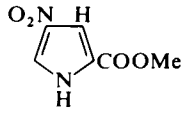	$CHCl_3$	5·05 (N–C=CH)	280
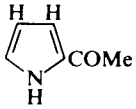	$CHCl_3$	4·60 (N–C=(3)CH) 5·10 (N–C=(4)CH)	280 280
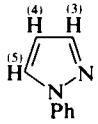	$CDCl_3$	7·4 (1-N–N=(3)CH) 6·0 (1-N–C=(4)CH) 1·0 (2-N–C=(4)CH)	277 277 277
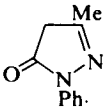	$CDCl_3$	3·5 (2-N=C–Me)	277
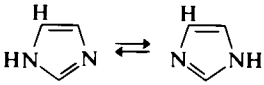	H_2O	−2·5 (N–C=CH)	276
	H_2O	−4·0 to −4·6 (N–C=CH)	276
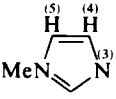	H_2O	−3·5 (1-N–C=(4)CH) −1·7 (3-N–C=(5)CH)	276 276
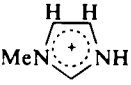	H_2O	−3·8 to −4·6 (N–C=CH)	276
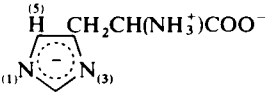	H_2O pH 10·9	−2·2 (3-N–C=(5)CH)	208, 276
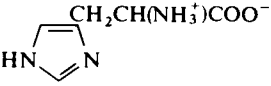	H_2O pH 7·6	−1·8 (3-N–C=(5)CH)	208, 276
histidine (see Table 72)			
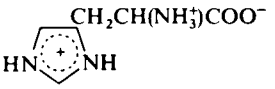	H_2O pH 1·3	−3·0 (3-N–C=(5)CH)	208, 276

TABLE 148—*cont.*

Compound	Solvent	$^3J(^{15}N-^1H)$ (Hz)	Ref.
α-*N*-Acetylhistidine, cation/amphion	H_2O	−4·2 (3-N-C=(5)CH)	208
α-*N*-Acetylhistidine, anion	H_2O	−2·0 (3-N-C=(5)CH)	208
	acetone-d_6	−1·48 (N=C-CH)	358, 359
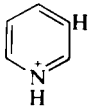	CD_3OH	−3·98 (N=C-CH)	359
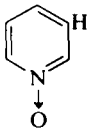	$CDCl_3$ CS_2	−5·32 (N=C-CH) −5·17 (N=C-CH)	303, 359 303
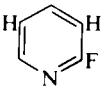	acetone-d_6	−0·69 (N-C=(3)CH) −1·94 (N-C=(5)CH)	358 358
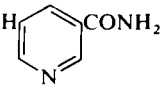 (nicotinamide)	D_2O, pD 7·0 D_2O, pD 2·0	1·8 (N-C=CH) 4·5 (N-C=CH)	136 136
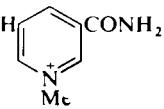	D_2O	4·7 (N-C=CH)	136
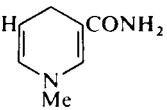	D_2O	5·0 (N-C=CH)	136
Nicotinamide nucleotides (see Table 126)			
NAD^+	D_2O	4·5 (N-C=CH)	136
NADH	D_2O	1·7 (N-C=CH)	136
NMN^+	D_2O	4·5 (N-C=CH)	136
		3·5 (N-C-2'-CH)	136
NMNH	D_2O	5·2 (N-C=CH)	136
Riboflavin tetrabutyrate			
reduced form (see Table 65)	DMSO-d_6	2·1 (5-N-C-(6)CH)	203
oxidized form (see Table 65)	DMSO-d_6	~2 (5-N-C-(6)CH)	203
		0·9 (3-N-C-(1)NH)	203

TABLE 148—*cont.*

Compound	Solvent	$^3J(^{15}N-^1H)$ (Hz)	Ref.
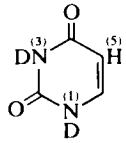	D_2O	4·46 (1-N–C–(5)CH) 2·63 (3-N–C–(5)CH)	355 355
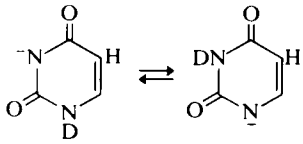	D_2O	2·81 (1-N–C–CH) 1·73 (3-N–C–CH)	355 355
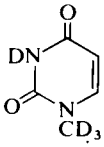	D_2O	4·73 (1-N–C–CH) 2·69 (3-N–C–CH)	355 355
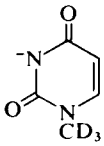	D_2O	3·97 (1-N–C–CH) 0·70 (3-N–C–CH)	355 355
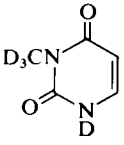	D_2O	4·49 (1-N–C–CH) 2·75 (3-N–C–CH)	355 355
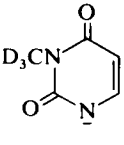	D_2O	1·68 (1-N–C–CH) 2·72 (3-N–C–CH)	355 355
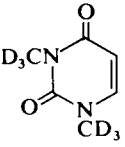	D_2O D_2O, pD 12·3	4·82 (1-N–C–CH) 2·96 (3-N–C–CH) 4·79 (1-N–C–CH) 2·93 (3-N–C–CH)	355 355 355 355

* Recalculated from $^{14}N-^1H$ couplings.

TABLE 149

Some long-range ^{15}N–^{1}H couplings (absolute values if sign not given)

Compound	Solvent	$J(^{15}N-^{1}H)$ (Hz)	Ref.
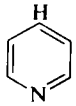	acetone-d_6	+0·27 (N=C–C=CH)	358, 359
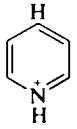	CD_3OH	+0·69 (N=C–C=CH)	359
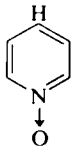	$CDCl_3$ CS_2	+1·11 (N=C–C=CH) +1·03 (N=C–C=CH)	303, 359 303
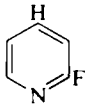	acetone-d_6	+0·69 (N=C–C=CH)	358
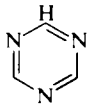	nematic phase	0·2 (N=C–N=CH)	102
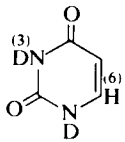	D_2O	0·25 (3-N–CCCH-6)	355
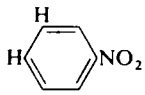	acetone-d_6	−0·8 (N-CCCH) −0·3 (N–CCCCH)	364 364

TABLE 150

Some ^{15}N–^{13}C couplings across one bond (absolute values if sign not given)

Compound	Solvent	$^1J(^{15}N-^{13}C)$ (Hz)	Ref.
$Me_3CCH_2NHCHMe_2$	$CDCl_3$	3·5 ($N-CH_2$)	374
		4·2 (N–CH)	374
its hydrochloride	$CDCl_3$	4·3 ($N-CH_2$)	374
		3·6 (N–CH)	374
	$CDCl_3$	2·5 ($N-CH_2$)	68
its hydrochloride	$CDCl_3$	4·0 ($N-CH_2$)	68
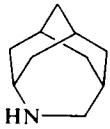	$CDCl_3$	3·4 ($N-CH_2$)	374
		3·1 (N–CH)	374
its hydrochloride	$CDCl_3$	3·7 ($N-CH_2$)	374
		3·5 (N–CH)	374
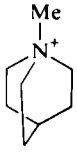	D_2O	6·3 (N–Me)	375
		4·3 ($N-CH_2$)	375
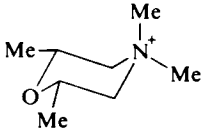	D_2O	5·3 ($N-Me_{ax}$)	375
		5·8 ($N-Me_{eq}$)	375
		4·1 ($N-CH_2$)	375
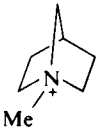	D_2O	6·0 (N–Me)	375
		4·5 ($N-CH_2$, ring)	375
		4·1 ($N-CH_2$, bridge)	375
	D_2O	2·5 (N–CH)	374
		2·6 ($N-CH_2$)	374
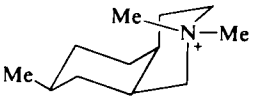	D_2O	4·9 ($N-Me_{ax}$)	375
		5·6 ($N-Me_{eq}$)	375
		3·8 ($N-2-CH_2$)	375
		4·2 ($N-6-CH_2$)	375
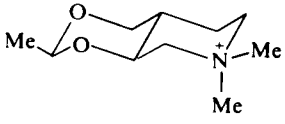	D_2O	4·8 ($N-Me_{ax}$)	375
		4·9 ($N-Me_{eq}$)	375

TABLE 150—*cont.*

Compound	Solvent	$^1J(^{15}N-^{13}C)$ (Hz)	Ref.
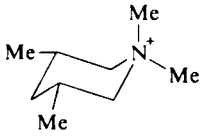	D_2O	5·5 ($N-Me_{ax}$) 5·8 ($N-Me_{eq}$) 3·6 ($N-CH_2$)	375 375 375
	D_2O	5·8 (N-Me) 1·8 (N-CH)	375 375
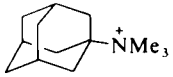	D_2O	5·6 (N-Me) ~1·0 (N-C, ring)	375 375
	D_2O	5·3 (N-Me) 1·7 (N-CH)	375 375
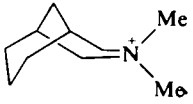	D_2O	5·8 (N-Me, "flagpole") 6·0 (N-Me, "bowsprit") 3·5 ($N-CH_2$)	375 375 375
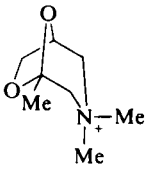	D_2O	5·0 ($N-Me_{ax}$) 5·3 ($N-Me_{eq}$) 3·9 ($N-2-CH_2$) 3·6 ($N-6-CH_2$)	375 375 375 375
Silatranes (see Table 29)			
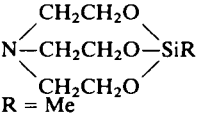			
R = Me	$CDCl_3$	7·8 ($N-CH_2$)	124
	CD_3OD	7·8 ($N-CH_2$)	124
$CH=CH_2$	acetone-d_6	7·3 ($N-CH_2$)	124
Ph	acetone-d_6	7·0 ($N-CH_2$)	124
CH_2Cl	$CDCl_3$	7·0 ($N-CH_2$)	124
OMe	acetone-d_6	6·7 ($N-CH_2$)	124
OEt	acetone-d_6	7·0 ($N-CH_2$)	124
$N(CH_2CH_2OH)_3$	$CDCl_3$	5·3 ($N-CH_2$)	124
	acetone-d_6	4·9 ($N-CH_2$)	124
	H_2O	5·0 ($N-CH_2$)	124
its hydrochloride	H_2O	4·4 ($N-CH_2$)	124
Aspartic acid	H_2O		
cation	pH 0·5–1·3	6·4 (N-CH)	376
amphion	pH 6·0–6·5	5·5 (N-CH)	376
anion	pH 12·0–12·6	3·7 (N-CH)	376

TABLE 150—*cont.*

Compound	Solvent	$^1J(^{15}N-^{13}C)$ (Hz)	Ref.
Proline	H_2O		
cation	pH 0·4	6·6 ($N-CH_\alpha$)	221
	pH 0·5–1·3	6·4 ($N-CH_\alpha$)	376
amphion	pH 6·0–6·5	5·5 ($N-CH_\alpha$)	221, 376
anion	pH 12·0–12·6	3·4 ($N-CH_\alpha$)	221
		2·7	376
cation		6·4 ($N-CH_\delta$)	221, 376
amphion		5·5 ($N-CH_\delta$)	376
		4·9	221
anion		3·5 ($N-CH_\delta$)	221
		2·7	376
Serine	H_2O		
cation		7·3 (N–CH)	376
amphion		6·4 (N–CH)	376
anion		3·7 (N–CH)	376
Glutamic acid	H_2O		
cation		6·4 (N–CH)	376
amphion		5·5 (N–CH)	376
anion.		2·7 (N–CH)	376
Glycine	H_2O		
cation		7·3 ($N-CH_2$)	376
amphion		6·4 ($N-CH_2$)	376
anion		4·6 ($N-CH_2$)	376
Alanine	H_2O		
cation		6·4 (N–CH)	376
amphion		5·5 (N–CH)	376
anion		3·7 (N–CH)	376
Valine	H_2O		
cation		6·4 (N–CH)	376
amphion		5·5 (N–CH)	376
anion		4·6 (N–CH)	376
Isoleucine	H_2O		
cation		6·4 (N–CH)	376
amphion		5·5 (N–CH)	376
Leucine	H_2O		
cation		6·4 (N–CH)	376
amphion		5·5 (N–CH)	376
anion		3·7 (N–CH)	376
$EtCH(NMe_2)-Pt(Cl)(Me_2SO)$	$CDCl_3$	5·6 (N–Me)	377
		4·3 (N–CH)	377
$MeCH(NMe_2)-Pt(Cl)(Me_2NH)$	$CDCl_3$	<2 (N–Me, ring)	377
		4·3 (N–CH, ring)	377

TABLE 150—*cont.*

Compound	Solvent	$^1J(^{15}N-^{13}C)$ (Hz)	Ref.
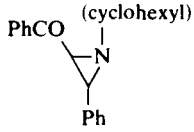	$CDCl_3$	≤2·0 (N–CH, cyclohexyl) +5·2 (N–CH, Ph) +8·2 (N–CH, PhCO)	378 378 378
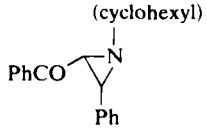	$CDCl_3$	≤3·4 (N–CH, cyclohexyl) +7·8 (N–CH, Ph) +7·3 (N–CH, PhCO)	378 378 378
$MeNHNO_2$	CH_2Cl_2	8·5 (N–Me)	263
Me_2NNO_2	CH_2Cl_2	9·1 (N–Me)	263
$EtOOCN(NO_2)Me$	CH_2Cl_2	8·1 (N–Me) 17·6 (N–CO)	263 263
$MeOOCN(NO_2)Me$	CH_2Cl_2	8·0 (N–Me) 21·0 (N–CO)	263 263
$MeN(NO_2)SiMe_3$	CH_2Cl_2	6·4 (N–Me)	263
$Me_3CC(=O)NHCHMe_2$	$CDCl_3$	9·5 (N–CH) 13·2 (N–CO)	374 374
its hydrochloride	$CDCl_3$	6·3 (N–CH) 18·8 (N–CO)	374 374
	$CDCl_3$	7·5 (N–CH) 12·1 (N–CO)	374 374
	D_2O	7·0 (N–CH) 13·2 (N–CO)	347 347
its hydrochloride	$CDCl_3$	6·3 (N–CH) 16·2 (N–CO)	374 374
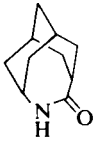	$CDCl_3$	8·3 (N–CH) 12·3 (N–CO)	374 374
its hydrochloride	$CDCl_3$	7·2 (N–CH) 15·1 (N–CO)	374 374
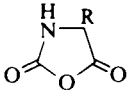			
R = Me	acetone	9·8 (N–CH) 22·5 (N–CO)	185 185
	CF_3COOH	9·8 (N–CH) 23·0 (N–CO)	185 185

TABLE 150—*cont.*

Compound	Solvent	$^1J(^{15}N-^{13}C)$ (Hz)	Ref.
Pr^i	acetone	9·8 (N–CH)	185
		23·4 (N–CO)	185
	CF_3COOH	9·8 (N–CH)	185
		24·2 (N–CO)	185
Bu^i	acetone	9·8 (N–CH)	185
		23·1 (N–CO)	185
	CF_3COOH	9·8 (N–CH)	185
		23·2 (N–CO)	185
Peptides (for abbreviations see Table 70)			
cyclo(Gly-L-Pro-Gly)$_2$	DMSO	15·9 (N–CO, Gly^1)	381
	CF_3CH_2OH	17·7 (N–CO, Gly^1)	381
	CF_3COOH	18·6 (N–CO, Gly^1)	381
cyclo(Gly-L-Pro-Gly)$_2$	DMSO	14·8 (N–CO, Gly^2)	381
	CF_3CH_2OH	15·7 (N–CO, Gly^2)	381
	CF_3COOH	16·5 (N–CO, Gly^2)	381
Bu^tOCO-Gly-L-Pro-Gly-OCH_2Ph	$CDCl_3$	14·3 (N–CO, Gly^2)	381
	DMSO	14·7 (N–CO, Gly^2)	381
	CF_3CH_2OH	16·3 (N–CO, Gly^2)	381
Bu^tOCO-Gly-Gly-OMe	$CDCl_3$	15·2 (N–CO, Gly^2)	381
	DMSO	14·6 (N–CO, Gly^2)	381
	CF_3CH_2OH	16·3 (N–CO, Gly^2)	381
$(H_2N)_2C{=}O$	DMSO (30 °C)	19·5 (N–CO)	178
	D_2O	20·2 (N–CO)	66
$(PhNH)_2C{=}O$	DMSO	20·8 (N–CO)	178
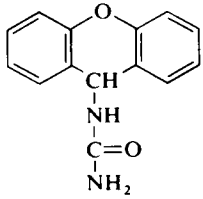	DMSO	19·5 (NH_2–CO)	178
		18·3 (NH–CO)	178
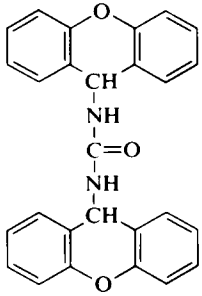	DMSO	18·6 (NH–CO)	178
$(MeNH)_2C{=}O$	DMSO-d_6	22 (N–CO)	345
		12 (N–Me)	345

TABLE 150—*cont.*

Compound	Solvent	$^1J(^{15}N-^{13}C)$ (Hz)	Ref.
MeNHC(=O)NHPh	pyridine,	15·9 (N–Ph)	362
	1 M	20·1 (N–CO)	362
	DMSO,	15·9 (N–Ph)	362
	1 M	20·1 (N–CO)	362
	DMSO,	15·9 (N–Ph)	362
	1·6 M	20·1 (N–CO)	362
	DMSO,	15·3 (N–Ph)	362
	1·6 M, 130 °C	18·9 (N–CO)	362
	D_2O/acetone,	15·9 (N–Ph)	362
	1 M	20·1 (N–CO)	362
	HCOOH,	15·3 (N–Ph)	362
	1 M	22·5 (N–CO)	362
	CF_3COOH,	14·6 (N–Ph)	362
	1 M	23·6 (N–CO)	362
	FSO_3H,	14·6 (N–Ph)	362
	1 M	26·1 (N–CO)	362
$HC(=O)NH_2$	none	14·0 (N–CO)	77
$MeC(=O)NH_2$	DMSO-d_6	−14·4 (N–CO)	361
	DMSO	14·1 (N–CO)	362
	DMSO, 130 °C	14·1 (N–CO)	362
	DMSO	14·0 (N–CO)	77
	pyridine	14·1 (N–CO)	362
	pyridine, 100 °C	13·6 (N–CO)	362
	H_2O	15·5 (N–CO)	362
	CF_3COOH	18·5 (N–CO)	362
	H_2SO_4 100%	21·0 (N–CO)	362
	FSO_3H	21·5 (N–CO)	362
$MeCONHCH_2CO^{15}NHPh$	DMSO	14·6 (^{15}N–CO)	362
		15·0 (N–Ph)	362
	DMSO, 130 °C	14·0 (^{15}N–CO)	362
		14·2 (N–Ph)	362
	CF_3COOH	14·1 (N–Ph)	362
Poly-alanine	CF_3COOH	16·5 (N–CO)	362
	FSO_3H	20·0 (N–CO)	362
Poly-leucine	CF_3COOH		
	+10% $MeSO_3H$	18·1 (N–CO)	362
	FSO_3H	19·5 (N–CO)	362
Poly-valine	CF_3COOH	17·0 (N–CO)	362
	CF_3COOH		
	+10% $MeSO_3H$	18·0 (N–CO)	362
	FSO_3H	19·5 (N–CO)	362
$MeCO^{15}NHCH(Me)CONHMe$	D_2O	11·0 (N–CH)	347
		14·5 (N–CO)	347
$PhNHCOCH_2COMe$	$CDCl_3$	14·4 (N–Ph)	382
		15·1 (N–CO)	382
oMeO·C_6H_4·$NHCOCH_2COMe$	$CDCl_3$	14·9 (N–Ph)	382
		15·4 (N–CO)	382

TABLE 150—*cont.*

Compound	Solvent	$^1J(^{15}N-^{13}C)$ (Hz)	Ref.
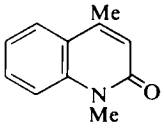	$CDCl_3$	11·5 (N–Me) 12·2 (N–CO) 14·2 (N-9-C)	382 382 382
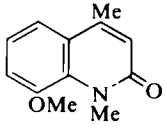	$CDCl_3$	10·2 (N–Me) 11·6 (N–CO) 13·9 (N-9-C)	382 382 382
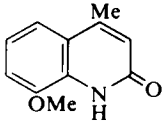	$CDCl_3$	13·3 (N–CO) 14·3 (N-9-C)	382 382
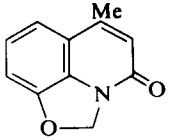	$CDCl_3$	8·8 ($N-CH_2$) 13·5 (N–CO) 13·9 (N-9-C)	382 382 382
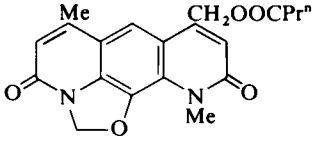	$CDCl_3$	10·1 (N–Me) 12·2 (N(Me)–CO) 15·8 (N(Me)–C) 9·3 ($N-CH_2$) 13·6 ($N(CH_2)$–CO) 12·2 ($N(CH_2)$–C)	382 382 382 382 382 382
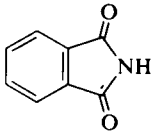	pyridine DMSO DMSO, 130 °C CF_3COOH H_2SO_4 100% FSO_3H	12·8 (N–CO) 13·4 (N–CO) 12·8 (N–CO) 14·0 (N–CO) 14·6 (N–CO) 14·6 (N–CO)	362 362 362 362 362 362
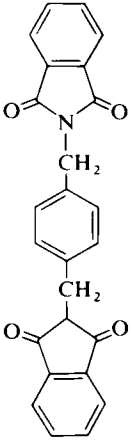	CF_3COOH FSO_3H	9·8 ($N-CH_2$) 13·4 (N–CO) 6·1 ($N-CH_2$) 14·6 (N–CO)	362 362 362 362

TABLE 150—*cont.*

Compound	Solvent	$^1J(^{15}N-^{13}C)$ (Hz)	Ref.
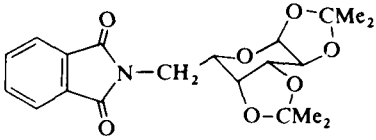	pyridine-d_5	10·0 ($N-CH_2$) 13·4 (N–CO)	383 383
MeC(=O)NHNHPh	DMSO	10 (N–Ph) 12 (N–CO)	77 77
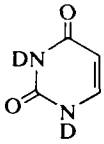	DMSO	11·2 (1-N-6-CH) 8·5 (3-N-4-CO) 16·9 (1-N-2-CO) 16·9 (3-N-2-CO)	355 355 355 355
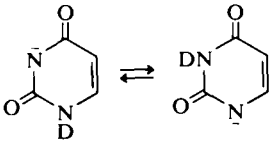	D_2O	6·7 (1-N-6-CH)	355
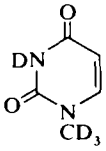	D_2O	12·8 (1-N-6-CH)	355
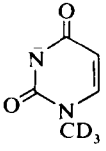	D_2O	12·8 (1-N-6-CH)	355
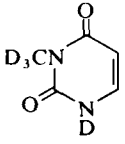	D_2O	11·6 (1-N-6-CH)	355
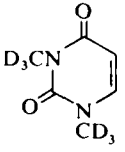	D_2O	12·2 (1-N-6-CH)	355

TABLE 150—*cont.*

Compound	Solvent	$^1J(^{15}N-^{13}C)$ (Hz)	Ref.
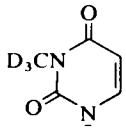	D_2O	≤1·0 (1-N–6-CH)	355
$H_2{}^{15}N-C(={}^{15}NH)-NH(CH_2)_3CH(NH_2)COOH$	D_2O		
	pD 9·9	21·3 ($^{15}N-C \rightleftarrows {}^{15}N=C$)	66
	pD 10·4	21·4 ($^{15}N-C \rightleftarrows {}^{15}N=C$)	66
	pD 13·4	18·5 ($^{15}N-C \rightleftarrows {}^{15}N=C$)	66
$PhNH_2$	$CDCl_3$	10·9 (N–Ph)	342
	none	10·9 (N–Ph)	77, 342
	DMSO-d_6	12·1 (N–Ph)	63
$PhNH_3^+$	CF_3COOH	8·9 (N–Ph)	342
	FSO_3H	8·6 (N–Ph)	63
PhNHCOMe	$CDCl_3$	14·3 (N–Ph)	342
Substituted anilines			
2-Me	$CDCl_3$	10·5 (N–Ph)	342
4-OMe	DMSO-d_6	11·0 (N–Ph)	63
4-Me	DMSO-d_6	11·8 (N–Ph)	63
3-Me	DMSO-d_6	11·8 (N–Ph)	63
4-Br	DMSO-d_6	12·5 (N–Ph)	63
4-Cl	DMSO-d_6	12·5 (N–Ph)	63
3-OMe	DMSO-d_6	12·5 (N–Ph)	63
3-CF_3	DMSO-d_6	12·5 (N–Ph)	63
3-I	DMSO-d_6	12·5 (N–Ph)	63
3-Br	DMSO-d_6	13·2 (N–Ph)	63
3-Cl	DMSO-d_6	13·2 (N–Ph)	63
4-NO_2	DMSO-d_6	14·7 (H_2N–Ph)	63
2,4-$(NO_2)_2$	DMSO-d_6	16·9 (H_2N–Ph)	63
2,4,6-Br_3	DMSO-d_6	17·6 (N–Ph)	63
2-COOH	D_2O, pD 12	10·7 (N–Ph)	342
Substituted anilinium ions			
3-Br	FSO_3H	7·9 (N–Ph)	63
4-F	FSO_3H	8·6 (N–Ph)	63
4-Cl	FSO_3H	9·1 (N–Ph)	63
4-Br	FSO_3H	9·2 (N–Ph)	63
4-NO_2	FSO_3H	9·2 (H_3N^+–Ph)	63
2-NO_2	FSO_3H	10·4 (H_3N^+–Ph)	63
2-Cl	FSO_3H	10·9 (N–Ph)	63
2-Br	FSO_3H	11·0 (N–Ph)	63
2-NO_2-4-Cl	FSO_3H	11·0 (H_3N^+–Ph)	63
2,4,6-Br_3	FSO_3H	13·5 (N–Ph)	63
PhNHMe	acetone-d_6	10·3 (N–Me)	343
		13·0 (N–Ph)	343

TABLE 150—*cont.*

Compound	Solvent	$^1J(^{15}N-^{13}C)$ (Hz)	Ref.
$PhNO_2$	acetone-d_6	−14·6 (N–Ph)	364
Azimines (R = phthalimide residue)			
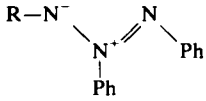	$CDCl_3$, −20 °C	12·3 (N^+–Ph) 2·0 (N–Ph)	329 329
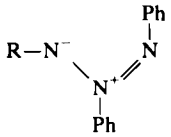	$CDCl_3$, −20 °C	13·6 (N^+–Ph) 3·0 (N–Ph)	329 329
trans-PhN(O)=NPh	$CDCl_3$, −20 °C	18·2 (NO–Ph) 3·7 (N–Ph)	329 329
cis-PhN(O)=NPh	$CDCl_3$, −20 °C	12·5 (NO–Ph) 1·3 (N–Ph)	329 329
$CH_2=N^+=N^-$	$CDCl_3$	24·0 (C=N)	29
$EtOOCCH=N^+=N^-$	$CDCl_3$	21·2 (C=N)	29
	MeCN, 20 °C	21·4 (C=N)	67
	MeCN, −35 °C	{23·2 20·8} (C=N, *s-cis*, *s-trans*)	67
	acetone-d_6	−13·0 (N–CH)	384
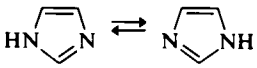	H_2O	−6·9 (N-2-C) −5·9 (N-4, 5-C)	276 276
	H_2O	−16·2 (N-2-C) −10·6 (N-4, 5-C)	276 276
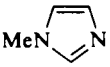	H_2O	−12·2 (1-N-2-C) −1·9 (3-N-2-C) −13·4 (1-N-5-C) +0·9 (3-N-4-C) −10·6 (1-N-Me)	276 276 276 276 276
	CH_2Cl_2	11·3 (1-N-2-C) 1 (3-N-2-C) 14·0 (1-N-5-C) 2·7 (3-N-4-C)	276 276 276 276
	H_2O	−16·7 (1-N-2-C) −16·7 (3-N-2-C) −11·4 (1-N-5-C) −10·7 (3-N-4-C) −10·1 (1-N-Me)	276 276 276 276 276

TABLE 150—*cont.*

Compound	Solvent	$^1J(^{15}N-^{13}C)$ (Hz)	Ref.
	H_2O	−6·4 (1-N-2-C) −7·3 (1-N-5-C) −6·9 (3-N-2-C) −4·7 (3-N-4-C)	276, 209 276, 209 276, 209 276, 209
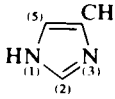 (histidine)	H_2O	−10·1 (1-N-2-C) −10·4 (1-N-5-C) −2·7 (3-N-2-C) ~0 (3-N-4-C)	276, 209 276, 209 276, 209 276, 209
	H_2O	−16·1 (1-N-2-C) −11·6 (1-N-5-C) −16·0 (3-N-2-C) −9·9 (3-N-4-C)	276, 209 276, 209 276, 209 276, 209
α-*N*-Acetylhistidine	H_2O		
amphion/cation		−16·3 (1-N-2-C) −10·6 (1-N-5-C) −16·9 (3-N-2-C) −10·7 (3-N-4-C)	208 208 208 208
anion		−7·4 (1-N-2-C) −8·2 (1-N-5-C) −6·5 (3-N-2-C) −4·2 (3-N-4-C)	208 208 208 208
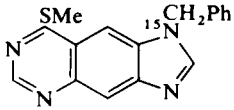	DMSO-d_6	8·6 ($^{15}N-CH_2$)	351
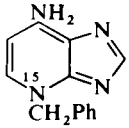	DMSO-d_6	7·2 ($^{15}N-CH_2$)	351
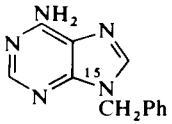	DMSO-d_6	9·3 ($^{15}N-CH_2$)	351
Intermediate in urogen formation (Table 116)	D_2O	6·0 ($^{15}N-^{13}CH_2$)	282
	$CDCl_3$	1·2 (2-N-3-C) 2·1 (1-N-5-C)	277 277

TABLE 150—*cont.*

Compound	Solvent	$^1J(^{15}N-^{13}C)$ (Hz)	Ref.
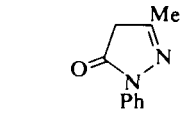	$CDCl_3$	3·1 (2-N-3-C)	277
		11·0 (1-N-5-C)	277
		12·2 (1-N-Ph)	277
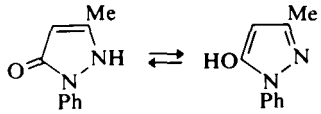	DMSO-d_6	15·9 (1-N-5-C)	277
		18·3 (1-N-Ph)	277
Chetomin 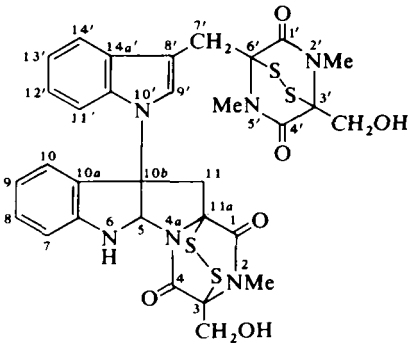	$CDCl_3$	13·7 (2-N-1-CO)	204
		7·3 (2-N-3-C)	204
		14·6 (4a-N-4-CO)	204
		5·0 (4a-N-5-C)	204
		5·0 (4a-N-11a-C)	204
		8·1 (6-N-5-C)	204
		11·8 (6-N-6a-C)	204
		13·7 (2′-N-1′-CO)	204
		7·3 (2′-N-3′-C)	204
		13·7 (5′-N-4′-CO)	204
		13·8 (10′-N-9′-C)	204
		14·5 (10′-N-10a′-C)	204
		11·5 (10′-N-10b-C)	204
Riboflavin tetrabutyrate (see Table 65)	DMSO-d_6		
reduced form		13·1 (3-N-4-C)	203
		19·5 (3-N-2-C)	203
		19·5 (1-N-2-C)	203
		17·6 (1-N-10a-C)	203
		11·0 (5-N-5a-C)	203
oxidized form		12·2 (3-N-4-C)	203
		11·4 (3-N-2-C)	203
		7·2 (1-N-2-C)	203
		7·9 (1-N-10a-C)	203
		1·2 (5-N-5a-C)	203
	acetone-d_6	+0·62 (N=C)	359
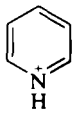	CD_3OH	−11·85 (N=C)	359

TABLE 150—*cont.*

Compound	Solvent	$^1J(^{15}N-^{13}C)$ (Hz)	Ref.
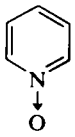	$CDCl_3$	−15·23 (N=C) −15·24 (N=C)	359 303
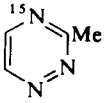	$CDCl_3$	3·6 ($4-^{15}N-3-C$) 1·0 ($4-^{15}N-5-C$)	385 385
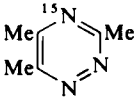	$CDCl_3$	2·6 ($4-^{15}N-3-C$) 0·7 ($4-^{15}N-5-C$)	385 385
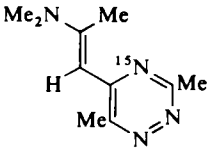	$CDCl_3$	1·2 ($4-^{15}N-3-C$) 0·3 ($4-^{15}N-5-C$)	385 385
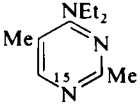	$CDCl_3$	0·8 ($1-^{15}N-2-C$) ~0 ($1-^{15}N-6-C$)	385 385
Adenosine (see Table 126)	DMSO-d_6	20·5 (NH_2-6-C) 4·4 (3-N-4-C) 19·3 (9-N-4-C) 10·4 (7-N-8-C) 8·5 (7-N-5-C) 11·1 (9-N-1′-C)	386 386 386 386 386 386
Adenine (numbering system retained from adenosine, see Table 126)	DMSO-d_6	20·5 (NH_2-6-C) 9·5 (3-N-4-C) 7·3 (7-N-5-C)	387 387 387
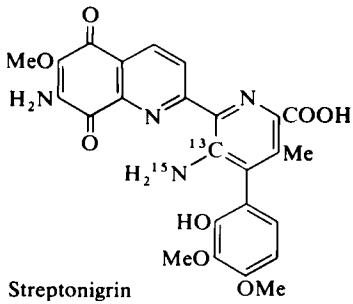 Streptonigrin	DMSO-d_6	14·6 ($H_2{}^{15}N-{}^{13}C$)	388

TABLE 150—*cont.*

Compound	Solvent	$^1J(^{15}N-^{13}C)$ (Hz)	Ref.
$PhN(Me)CH_2C{\equiv}CH$	CD_2Cl_2	9·6 (N-Me)	343
		9·6 ($N-CH_2$)	343
		12·5 (N-Ph)	343
$PhN(Me)C{\equiv}CMe$	CD_2Cl_2	12·2 (N-Me)	343
		36·2 (N-C≡)	343
		16·2 (N-Ph)	343
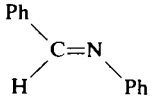	$CDCl_3$	−7·2 (C=N)	389
		<0·6 (N-Ph)	389
C-Ph-substituted derivatives	$CDCl_3$	<0·6 (N-Ph)	389
4-NO_2		7·7 (C=N)	389
4-OMe		6·6 (C=N)	389
2-Me		6·9 (C=N)	389
2,4,6-Me_3		6·8 (C=N)	389
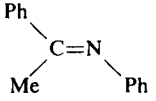	$CDCl_3$	−7·2 (C=N)	389
		0·6 (N-Ph)	389
C-Ph-substituted derivatives	$CDCl_3$		
4-Me		6·9 (C=N)	389
		0·6 (N-Ph)	389
4-NO_2		7·2 (C=N)	389
		1·0 (N-Ph)	389
4-OMe		7·1 (C=N)	389
		1·6 (N-Ph)	389
4-Cl		7·0 (C=N)	389
		1·6 (N-Ph)	389
4-Br		7·1 (C=N)	389
		1·3 (N-Ph)	389
2-Me		6·2 (C=N)	389
		0·6 (N-Ph)	389
2,4-Me_2		6·0 (C=N)	389
		1·1 (N-Ph)	389
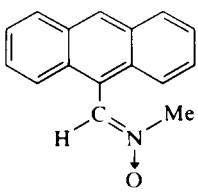	$CDCl_3$	−21·5 (C=N)	363

TABLE 150—*cont.*

Compound	Solvent	$^1J(^{15}N-^{13}C)$ (Hz)	Ref.
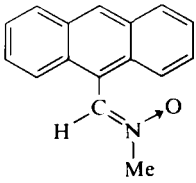	$CDCl_3$	−21·2 (C=N)	363
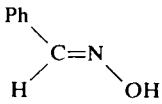	$CDCl_3$	4·8 (C=N)	390
Ph-substituted derivatives			
2,4,6-Me_3	$CDCl_3$	2·8 (C=N)	390
2-Cl	$CDCl_3$	5·0 (C=N)	390
	DMSO	4·0 (C=N)	390
3-Cl	$CDCl_3$	4·7 (C=N)	390
	DMSO	3·9 (C=N)	390
4-Cl	$CDCl_3$	4·5 (C=N)	390
	DMSO	3·9 (C=N)	390
2-OMe	$CDCl_3$	5·1 (C=N)	390
	DMSO	4·0 (C=N)	390
3-OMe	$CDCl_3$	4·9 (C=N)	390
	DMSO	4·3 (C=N)	390
4-OMe	$CDCl_3$	4·9 (C=N)	390
4-NMe_2	$CDCl_3$	4·9 (C=N)	390
	DMSO	3·7 (C=N)	390
2-NO_2	DMSO	4·2 (C=N)	390
3-NO_2	DMSO	3·8 (C=N)	390
4-NO_2	DMSO	3·7 (C=N)	390
3-CN	DMSO	4·0 (C=N)	390
4-CN	DMSO	4·9 (C=N)	390
4-CF_3	$CDCl_3$	5·1 (C=N)	390
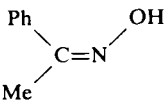	$CDCl_3$	3·1 (C=N)	69
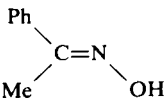	$CDCl_3$	3·9 (C=N)	69, 64
	acetone-d_6	2·4 (C=N)	64
Ph-substituted derivatives			
2-Me	$CDCl_3$	3·8 (C=N)	69
2,4,6-Me_3	$CDCl_3$	3·3 (C=N)	69

TABLE 150—*cont.*

Compound	Solvent	$^1J(^{15}N-^{13}C)$ (Hz)	Ref.
4-Me	$CDCl_3$	3·9 (C=N)	64
4-Cl	$CDCl_3$	4·0 (C=N)	64
4-Br	$CDCl_3$	3·8 (C=N)	64
4-OMe	$CDCl_3$	3·9 (C=N)	64
4-NO_2	acetone-d_6	2·7 (C=N)	64
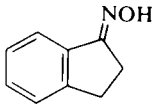	$CDCl_3$	3·8 (C=N)	69
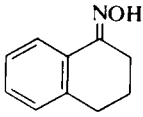	$CDCl_3$	4·2 (C=N)	69
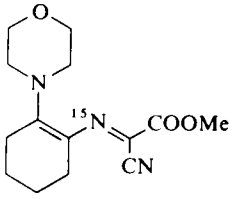	$CDCl_3$	5·8 (N–C=) 9·0 (C=N)	391 391
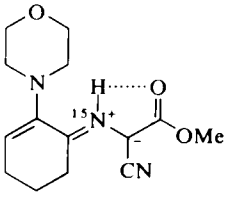	$CDCl_3$	21·6 (N^+=C) 21·3 (=N^+–C^-)	391 391
$MeN^+{\equiv}C^-$	benzene-d_6	6·33 (N^+C^-)	392
$EtN^+{\equiv}C^-$	none	9·7 (N^+C^-)	393
Myoglobin complex of EtNC	H_2O	18·5 (N^+C^-)	393
Fe(II)-tetraphenylporphyrin complex with two EtNC ligands	pyridine	22·4 (N^+C^-)	393
$Pr^nN^+{\equiv}C^-$	none	9·7 (N^+C^-)	393
Myoglobin complex of Pr^nNC	H_2O	19·6 (N^+C^-)	393
CN^-	D_2O	6·2 (C≡N)	394
$Cu(CN)_4^{3-}$ (tetrahedral)	D_2O	6·8 (C≡N)	394
$Ni(CN)_4^{2-}$ (square planar)	D_2O	9·3 (C≡N)	394
$Pt(CN)_4^{2-}$ (square planar)	D_2O	11·4 (C≡N)	394
$Cd(CN)_4^{2-}$ (tetrahedral)	D_2O	8·0 (C≡N)	394
$Hg(CN)_4^{2-}$ (tetrahedral)	D_2O	7·4 (C≡N)	394
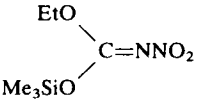	CH_2Cl_2	4·4 (C=N)	263

TABLE 151

Some ^{15}N–^{13}C couplings across more than one bond (absolute values if sign not given)

Compound (and solvent)	$^{n}J(^{15}N-^{13}C)$ (Hz)	Number of intervening bonds (n)	Ref.
$Me_3CCH_2NHCHMe_2$ (in $CDCl_3$)	1·0 (N–C–C–Me)	3	374
	1·6 ($N-CH_2-C$)	2	374
	2·6 (N–C–Me)	2	374
its hydrochloride	0·8 (N–C–C–Me)	3	374
 (in $CDCl_3$)	<0·3 (N–C–CH)	2	68
	<0·3 ($N-C-C-CH_2$)	3	68
its hydrochloride	0·3 (N–C–CH)	2	68
	0·6 ($N-C-C-CH_2$)	3	68
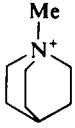 (in D_2O)	6·7 (N–C–C–CH)	3	375
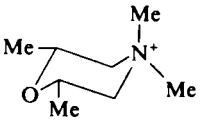 (in D_2O)	2·1 (N–C–C–Me)	3	375
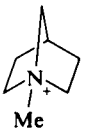 (in D_2O)	4·9 (N–C–CH)	2	375
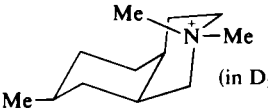 (in D_2O)	<0·6 (N–C–C–CH)	3	375
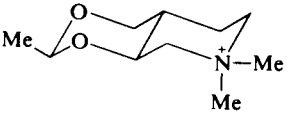 (in D_2O)	<0·4 (N–C–C–CH)	3	375
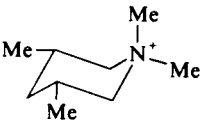 (in D_2O)	2·1 (N–C–C–Me)	3	375
 (in D_2O)	1·7 ($N-C-C-CH_2$)	3	375

TABLE 151—*cont.*

Compound (and solvent)		$^nJ(^{15}N-^{13}C)$ (Hz)	Number of intervening bonds (n)	Ref.
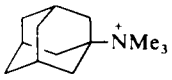	(in D_2O)	1·3 (N-C-C-CH)	3	375
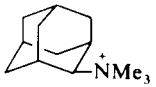	(in D_2O)	2·1 (N-C-C-CH_2)	3	375
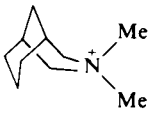	(in D_2O)	2·9 (N-C-C-CH_2, bridge)	3	375
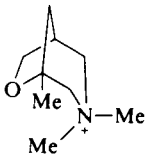	(in D_2O)	1·0 (N-C-C-CH_2)	3	375
Silatranes (see Table 29)				
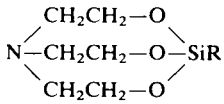				
R = Me	(in $CDCl_3$)	1·5 (N-C-C)	2	124
	(in CD_3OD)	1·5 (N-C-C)	2	124
$CH=CH_2$	(in acetone-d_6)	1·2 (N-C-C)	2	124
Ph	(in acetone-d_6)	1·2 (N-C-C)	2	124
CH_2Cl	(in $CDCl_3$)	1·2 (N-C-C)	2	124
OMe	(in acetone-d_6)	0·8 (N-C-C)	2	124
OEt	(in acetone-d_6)	0·9 (N-C-C)	2	124
$N(CH_2CH_2OH)_3$	(in $CDCl_3$)	2·5 (N-C-C)	2	124
	(in acetone-d_6)	2·8 (N-C-C)	2	124
	(in H_2O)	2·6 (N-C-C)	2	124
its hydrochloride	(in H_2O)	0·6 (N-C-C)	2	124
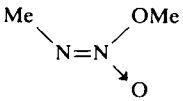	(in CH_2Cl_2)	2·8 (N=N-Me)	2	263
		1·4 (N-O-Me)	2	263
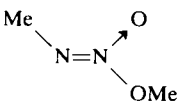	(in CH_2Cl_2)	2·3 (N=N-Me)	2	263
		1·8 (N-O-Me)	2	263

TABLE 151—*cont.*

Compound (and solvent)		$^nJ(^{15}N-^{13}C)$ (Hz)	Number of intervening bonds (n)	Ref.
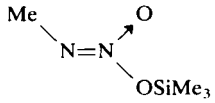	(in CH_2Cl_2)	2·0 (N=N-Me)	2	263
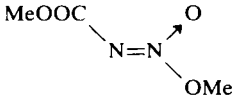	(in CH_2Cl_2)	4·5 (N=N-CO) 3·0 (N-O-Me)	2 2	263 263
Proline (see Table 70)				
(in D_2O) cation		<0·3 (N-C-CO)	2	221
		1·7 (N-C-β-C)	2	221
		4·6 (N-C-γ-C)	2	221
amphion		<0·2 (N-C-CO)	2	221
		1·7 (N-C-β-C)	2	221
		4·9 (N-C-γ-C)	2	221
anion		0·3 (N-C-CO)	2	221
		0·7 (N-C-β-C)	2	221
		3·5 (N-C-γ-C)	2	221
$Me_3CC(=O)NHCHMe_2$	(in $CDCl_3$)	6·5 (N-CO-C)	2	374
its hydrochloride		2·5 (N-CO-C)	2	374
	(in $CDCl_3$)	5·1 (N-CO-CH)	2	374
	(in D_2O)	4·2 (N-CO-CH)	2	347
		2·1 (N-CH-CH_2)	2	347
its hydrochloride (in $CDCl_3$)		2·5 (N-CO-CH)	2	374
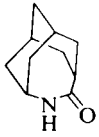	(in $CDCl_3$)	7·0 (N-CO-CH)	2	374
	its hydrochloride	3·5 (N-CO-CH)	2	374
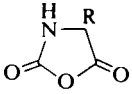				
R = Me	(in acetone)	<2 (N-CH-CO)	2	185
	(in CF_3COOH)	<2 (N-CH-CO)	2	185
Pr^i	(in acetone)	2–3 (N-CH-CO)	2	185
	(in CF_3COOH)	2–3 (N-CH-CO)	2	185
Bu^i	(in acetone)	2–3 (N-CH-CO)	2	185
	(in CF_3COOH)	<3 (N-CH-CO)	2	185

TABLE 151—*cont.*

Compound (and solvent)		$^nJ(^{15}N-^{13}C)$ (Hz)	Number of intervening bonds (n)	Ref.
$MeC(=O)NH_2$	(in pyridine)	8·8 (N–CO–Me)	2	362
	(in pyridine, 100 °C)	9·3 (N–CO–Me)	2	362
	(in DMSO)	−8·5 (N–CO–Me)	2	361
		8·8 (N–CO–Me)	2	362
	(in DMSO, 130 °C)	8·8 (N–CO–Me)	2	362
	(in H_2O)	7·3 (N–CO–Me)	2	362
	(in CF_3COOH)	3·9 (N–CO–Me)	2	362
	(in 100% H_2SO_4)	3·4 (N–CO–Me)	2	362
	(in FSO_3H)	2·9 (N–CO–Me)	2	362
$MeCONHCH_2{}^{15}NHPh$	(in DMSO)	9·5 (N–CO–CH_2)	2	362
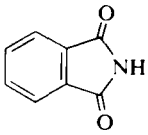	(in DMSO, 30–130 °C)	7·3 (N–CO–C)	2	362
	(in CF_3COOH)	6·1 (N–CO–C)	2	362
	(in 100% H_2SO_4)	5·3 (N–CO–C)	2	362
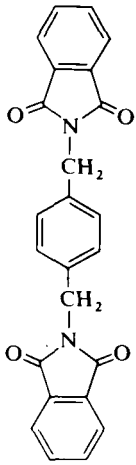	(in CF_3COOH)	7·3 (N–CO–C)	2	362
		2·0 (N–CH_2–C)	2	362
	(in FSO_3H)	2·0 (N–CH_2–C)	2	362
$PhNHCOCH_2COMe$	(in $CDCl_3$)	7·2 (N–CO–CH_2)	2	382
		0·5 (N–*ortho*-C in Ph)	2	382
		1·4 (N–*meta*-C in Ph)	3	382
o$MeO{\cdot}C_6H_4{\cdot}NHCOCH_2COMe$	(in $CDCl_3$)	7·7 (N–CO–CH_2)	2	382
		<0·5 (N–*ortho*-C in Ph)	2	382
		<0·5 (N–3-C in Ph)	3	382
		1·0 (N–5-C in Ph)	3	382
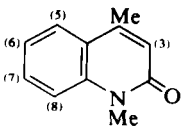	(in $CDCl_3$)	6·5 (N–CO–3-C)	2	382
		1·0 (N–C–C–5-C)	3	382
		2·0 (N–C–C–7-C)	3	382

TABLE 151—*cont.*

Compound (and solvent)		$^nJ(^{15}N-^{13}C)$ (Hz)	Number of intervening bonds (n)	Ref.
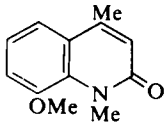	(in $CDCl_3$)	6·5 (N–CO–3-C) 0·9 (N–C–8-C) 0·9 (N–C–C–5-C)	2 2 3	382 382 382
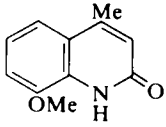	(in $CDCl_3$)	7·6 (N–CO–3-C) 1·0 (N–C–C–5-C) 0·5 (N–C–C–7-C)	2 3 3	382 382 382
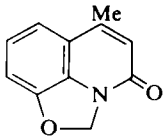	(in $CDCl_3$)	7·9 (N–CO–3-C) 3·2 (N–C–8-C) 0·5 (N–C–C–5-C) 0·5 (N–C–C–7-C)	2 2 3 3	382 382 382 382
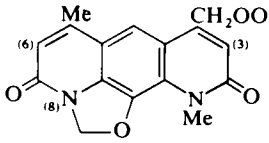	(in $CDCl_3$)	6·5 (N–CO–3-C) 7·2 (8-N–CO–6-C)	2 2	382 382
$MeC(=O)NHNHPh$	(in DMSO)	12 (N–CO–Me)	2	77
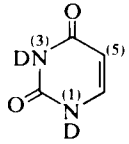	(in DMSO)	11·2 (3-N–CO–5-C)	2	355
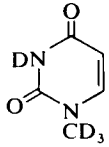	(in D_2O)	5·5 (3-N–CO–5-C)	2	355
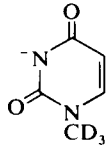	(in D_2O)	≤1·0 (3-N–CO–5-C)	2	355
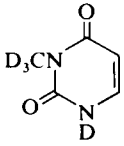	(in D_2O)	4·9 (3-N–CO–5-C)	2	355

TABLE 151—*cont.*

Compound (and solvent)		$^nJ(^{15}N-^{13}C)$ (Hz)	Number of intervening bonds (n)	Ref.
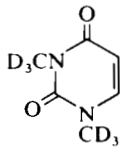	(in D_2O)	5·5 (3-N–CO–5-C)	2	355
$MeCO^{15}NHCH(Me)CONHMe$	(in D_2O)	7·2 (^{15}N–CO–Me)	2	347
$PhNO_2$	(in acetone-d_6)	−1·7 (N–C-*ortho*-C)	2	364
		−2·3 (N–C–C-meta-C)	3	364
		0·6 (N–C–C–C-*para*-C)	4	364
Azimines (R = phthalimide residue)				
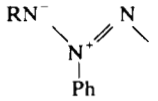	(in $CDCl_3$, −20 °C)	2·0 (N=N$^+$–Ph)	2	329
		<0·5 (N$^+$=N–Ph)	2	329
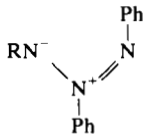	(in $CDCl_3$, −20 °C)	6·9 (N=N$^+$–Ph)	2	329
		1·5 (N$^+$=N–Ph)	2	329
trans-PhN(O)=NPh	(in $CDCl_3$, −20 °C)	9·4 (NO=N–Ph)	2	329
		<0·5 (NO=N–Ph)	2	329
cis-PhN(O)=NPh	(in $CDCl_3$, −20 °C)	2·5 (N=NO–Ph)	2	329
		<0·5 (NO=N–Ph)	2	329
PhNHMe	(in acetone)	2·5 (N-C-*ortho*-C)	2	343
		1·4 (N–C–C-*meta*-C)	3	343
		0·5 (N–C–C–C-*para*-C)	4	343
$Ph^{15}N=N^+=N^-$	(in $CDCl_3$)	4·74 (N-C-*ortho*-C)	2	248
		2·45 (N–C–C-*meta*-C)	3	248
		0·32 (N–C–C–C-*para*-C)	4	248
	(in acetone-d_6)	4·74 (^{15}N-C-*ortho*-C)	2	248
		2·02 (^{15}N–C–C-*meta*-C)	3	248
$pO_2N{\cdot}C_6H_4{\cdot}^{15}N=N^+=N^-$	(in DMSO-d_6)	3·7 (^{15}N-C-*ortho*-C)	2	248
		1·5 (^{15}N–C–C-*meta*-C)	3	248
$EtOOCCH=N^+=N^-$	(in MeCN)	3·7 (C=N$^+$=N$^-$)	2	67
		1·2 (N$^+$=CH–CO)	2	67
	(in MeCN, −50 °C)	3·2 (C=N$^+$=N$^-$)	2	67
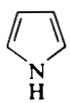	(in acetone-d_6)	−3·9 (N–C=C)	2	384
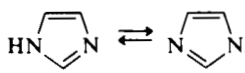	(in H_2O)	0·9 (N–C=C)	2	276

TABLE 151—*cont.*

Compound (and solvent)		$^nJ(^{15}N-^{13}C)$ (Hz)	Number of intervening bonds (n)	Ref.
	(in H_2O)	<0·5 (N–C=C)	2	276
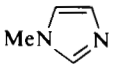	(in H_2O)	−4·8 (1-N–C–4-C)	2	276
		<0·5 (3-N–C–5-C)	2	276
	(in $CHCl_3$)	5·8 (1-N–C–4-C)	2	276
		1·5 (3-N–C–5-C)	2	276
	(in H_2O)	−0·9 (1-N–C–4-C)	2	276
		0·5 (3-N–C–5-C)	2	276
Histidine (see Table 150)				
amphion	(in H_2O)	−4·6 (3-N–C–CH_2)	2	208
anion	(in H_2O)	−3·8 (3-N–C–CH_2)	2	208
α-*N*-Acetylhistidine anion	(in H_2O)	−3·9 (3-N–C–CH_2)	2	208
	(in $CDCl_3$)	1·2 (1-N–N–3-C)	2	277
		2·1 } (1-N–C–4-C or		
		6·2 } 2-N–C–4-C)	2	277
		1·6 (1-N–C-*ortho* C in Ph)	2	277
		2·0 (1-N–C–C-*meta*-C)	3	277
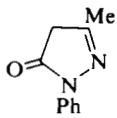	(in $CDCl_3$)	13·3 (1-N–CO–4-C)	2	277
		1·5 (2-N–C–4-C)	2	277
		3·1 (1-N–N–3-C)	2	277
		<1·2 (2-N–N–CO)	2	277
		9·8 (2-N–C–Me)	2	277
		1·2 (1-N–C-*ortho*-C in Ph)	2	277
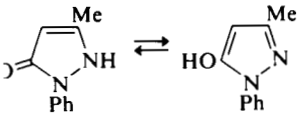		1·7 (1-N–C–C-*meta*-C)	3	277
	(in DMSO)	9·8 (1-N–C–4-C)	2	277
		7·3 (2-N–C–Me)	2	277
Chetomin (see Table 150)				
	(in $CDCl_3$)	7·3 (2-N–11a-C)	2	204
		6·2 (4a-N–3-C)	2	204
		4·2 (4a-N–10b-C)	2	204
		<1·0 (4a-N–11-C)	2	204
		3·7 (6-N–10a-C)	2	204
		1·1 (6-N–10b-C)	2	204
		7·3 (2′-N–6′-C)	2	204
		6·7 (5′-N–3′-C)	2	204
		6·3 (5′-N–6′-C)	2	204
		4·3 (10′-N–8′-C)	2	204
		4·7 (10′-N–14a′-C)	2	204
		1·5 (10′-N–5-C)	2	204
		1·3 (6-N–11a-C)	3	204

TABLE 151—*cont.*

Compound (and solvent)		$^nJ(^{15}N-^{13}C)$ (Hz)	Number of intervening bonds (n)	Ref.
	(in acetone-d_6)	+2·53 (N–C–C)	2	359
		−3·85 (N–C–C–C)	3	359
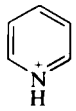	(in CD_3OH)	+2·01 (N–C–C)	2	359
		−5·30 (N–C–C–C)	3	359
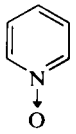	(in $CDCl_3$)	+1·43 (N–C–C)	2	359
		−5·17 (N–C–C–C)	3	359
		+1·32 (N–C–C)	2	303
		−5·13 (N–C–C–C)	3	303
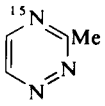	(in $CDCl_3$)	9·3 (^{15}N–C–Me)	2	385
		0·9 (^{15}N–C–6–C)	2	385
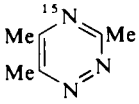	(in $CDCl_3$)	9·2 (^{15}N–3–C–Me)	2	385
		8·9 (^{15}N–5–C–Me)	2	385
		1·0 (^{15}N–C–6–C)	2	385
		0·5 (^{15}N–C–6–C–Me)	3	385
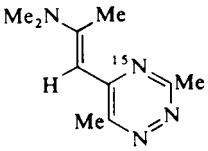	(in $CDCl_3$)	10·5 (^{15}N–3–C–Me)	2	385
		5·5 (^{15}N–5–C–CH=)	2	385
		ca. 0 (^{15}N–C–6–C)	2	385
		ca. 0 (^{15}N–C–6–C–Me)	3	385
		ca. 0 (^{15}N–5–C–C=C)	3	385
		3·9 (^{15}N–5–C–C=C–Me)	4	385
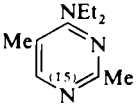	(in $CDCl_3$)	10·3 (^{15}N–2–C–Me)	2	385
		2·7 (^{15}N–C–5–C)	2	385
		2·8 (^{15}N–C–N–4–C)	3	385
		0·4 (^{15}N–C–5–C–Me)	3	385
Riboflavin tetrabutyrate (see Table 64)				
oxidized form	(in DMSO-d_6)	8·5 (4–C–5–N)	2	203
		8·9 (6–C–5–N)	2	203
		4·0 (7–C–5–N)	3	203
$PhN(Me)CH_2C{\equiv}CH$	(in CD_2Cl_2)	0·9 (N–CH_2–C)	2	343
		−2·1 (N–C–*ortho*-C in Ph)	2	343
		0·9 (N–CH_2–C–C)	3	343
		−1·1 (N–C–C–*meta*-C)	3	343
		<0·5 (N–C–C–C–*para*-C)	4	343

TABLE 151—*cont.*

Compound (and solvent)		$^nJ(^{15}N-^{13}C)$ (Hz)	Number of intervening bonds (n)	Ref.
PhN(Me)C≡CMe	(in acetone-d_6)	5·5 (N-C-C)	2	343
		−2·3 (N-C-*ortho*-C)	2	343
		0·5 (N-C≡C-Me)	3	343
		−1·8 (N-C-C-*meta*-C)	3	343
		0·5 (N-C-C-C-*para*-C)	4	343
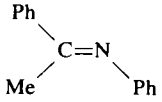	(in $CDCl_3$)	+2·7 (N=C-Me)	2	389
		8·0 (N=C-Ph)	2	389
		1·9 (N-C-*ortho*-C in Ph)	2	389
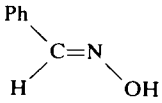	(in $CDCl_3$)	7·3 (N=C-Ph)	2	390
		2·8 (N=C-C-*ortho*-C)	3	390
		0·8 (N=C-C-C-C-*para*-C)	5	390
Ph-substituted derivatives				
2,4,6-Me_3	(in $CDCl_3$)	6·2 (N=C-Ph)	2	390
		1·2 (N=C-C-*ortho*-C)	3	390
2-Cl	(in $CDCl_3$)	7·9 (N=C-Ph)	2	390
		2·9 (N=C-C-2-C)	3	390
		0·7 (N=C-C-C-C-4-C)	5	390
	(in DMSO)	8·4 (N=C-Ph)	2	390
		2·9 (N=C-C-2-C)	3	390
3-Cl	(in $CDCl_3$)	7·6 (N=C-Ph)	2	390
		3·0 (N=C-C-2-C)	3	390
		0·9 (N=C-C-C-C-4-C)	5	390
	(in DMSO)	8·2 (N=C-Ph)	2	390
		3·4 (N=C-C-2-C)	3	390
		1·0 (N=C-C-C-C-4-C)	5	390
4-Cl	(in $CDCl_3$)	7·6 (N=C-Ph)	2	390
		3·0 (N=C-C-2-C)	3	390
	(in DMSO)	8·0 (N=C-Ph)	2	390
		3·2 (N=C-C-2-C)	3	390
2-OMe	(in $CDCl_3$)	7·3 (N=C-Ph)	2	390
		2·1 (N=C-C-2-C)	3	390
		0·7 (N=C-C-C-C-4-C)	5	390
	(in DMSO)	7·8 (N=C-Ph)	2	390
		2·5 (N=C-C-2-C)	3	390
		1·0 (N=C-C-C-C-4-C)	5	390
3-OMe	(in $CDCl_3$)	7·3 (N=C-Ph)	2	390
		3·1 (N=C-C-2-C)	3	390
		0·8 (N=C-C-C-C-4-C)	5	390
	(in DMSO)	7·8 (N=C-Ph)	2	390
		3·9 (N=C-C-2-C)	3	390

TABLE 151—*cont.*

Compound (and solvent)	$^nJ(^{15}N-^{13}C)$ (Hz)	Number of intervening bonds (n)	Ref.
4-OMe (in $CDCl_3$)	7·3 (N=C-Ph)	2	390
	3·7 (N=C-C-2-C)	3	390
4-NMe_2 (in $CDCl_3$)	7·3 (N=C-Ph)	2	390
	2·9 (N=C-C-2-C)	3	390
(in DMSO)	7·8 (N=C-Ph)	2	390
	2·9 (N=C-C-2-C)	3	390
2-NO_2 (in DMSO)	8·7 (N=C-Ph)	2	390
	2·4 (N=C-C-2-C)	3	390
	0·4 (N=C-C-C-C-4-C)	5	390
3-NO_2 (in DMSO)	8·4 (N=C-Ph)	2	390
	3·5 (N=C-C-2-C)	3	390
4-NO_2 (in DMSO)	8·5 (N=C-Ph)	2	390
	3·7 (N=C-C-2-C)	3	390
3-CN (in DMSO)	8·2 (N=C-Ph)	2	390
	3·0 (N=C-C-2-C)	3	390
4-CN (in DMSO)	7·3 (N=C-Ph)	2	390
	3·7 (N=C-C-2-C)	3	390
	1·0 (N=C-C-C-C-4-C)	5	390
4-CF_3 (in $CDCl_3$)	9·2 (N=C-Ph)	2	390
	3·2 (N=C-C-2-C)	3	390
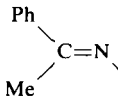 (in $CDCl_3$)	9·3 (N=C-Ph)	2	64, 69
	1·0 (N=C-Me)	2	64, 69
	2·9 (N=C-C-2-C)	3	64, 69
(in acetone)	9·7 (N=C-Ph)	2	64
	1·5 (N=C-Me)	2	64
	2·7 (N=C-C-2-C)	3	64
Ph-substituted derivatives			
2-Me (in $CDCl_3$)	8·8 (N=C-Ph)	2	69
	<0·6 (N=C-Me)	2	69
	1·1 (N=C-C-2-C)	3	69
2,4,6-Me_3 (in $CDCl_3$)	8·0 (N=C-Ph)	2	69
	<0·6 (N=C-Me)	2	69
	1·2 (N=C-C-2-C)	3	69
4-Me (in $CDCl_3$)	9·2 (N=CPh)	2	64
	0·7 (N=C-Me)	2	64
	2·8 (N=C-C-2-C)	3	64
4-Cl (in $CDCl_3$)	9·5 (N=C-Ph)	2	64
	0·8 (N=C-Me)	2	64
	2·9 (N=C-C-2-C)	3	64
4-Br (in $CDCl_3$)	9·5 (N=C-Ph)	2	64
	0·6 (N=C-Me)	2	64
	2·7 (N=C-C-2-C)	3	64
4-OMe (in $CDCl_3$)	9·3 (N=C-Ph)	2	64
	4·4 (N=C-Me)	2	64
	2·4 (N=C-C-2-C)	3	64

TABLE 151—*cont.*

Compound (and solvent)	$^nJ(^{15}N-^{13}C)$ (Hz)	Number of intervening bonds (n)	Ref.
4-NO_2 (in acetone-d_6)	10·1 (N=C-Ph)	2	64
	<0·6 (N=C-Me)	2	64
	3·4 (N=C-C-2-C)	3	64
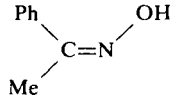 (in $CDCl_3$)	1·8 (N=C-Ph)	2	69
	−11·6 (N=C-Me)	2	69
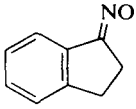 (in $CDCl_3$)	9·2 (N=C-Ph)	2	69
	+0·9 (N=C-CH_2)	2	69
	0·7 (N=C-C-CH in Ph)	3	69
	2·4 (N=C-C=C in Ph)	3	69
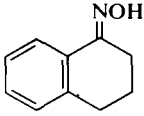 (in $CDCl_3$)	8·6 (N=C-Ph)	2	69
	+1·4 (N=C-CH_2)	2	69
	3·8 (N=C-C-CH in Ph)	3	69
	2·9 (N=C-C=C in Ph)	3	69
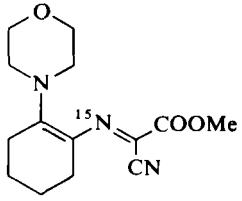 (in $CDCl_3$)	7·2 (N-C=C)	2	391
	1·9 (N-C-CH_2)	2	391
	2·2 (N=C-CN)	2	391
	10·6 (N=C-CO)	2	391
	1·7 (N-C=C-CH_2)	3	391
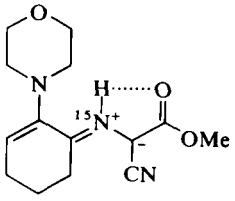 (in $CDCl_3$)	2·0 (N-C-CN)	2	391
	3·3 (N-C-CO)	2	391
	3·0 (N=C-C=C)	3	391
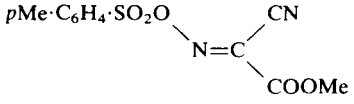 (in $CDCl_3$)	1·0 (N=C-CN)	2	391
	10·5 (N=C-CO)	2	391

TABLE 152

Some ^{15}N–^{15}N couplings (absolute values; for additional data see Table 3)

Compound (and solvent)	$^{n}J(^{15}N–^{15}N)$ (Hz)	Number of intervening bonds (n)	Ref.
$EtOOCCH{=}N^{+}{=}N^{-}$ (in MeCN)	5·6	1	67
(in MeCN, −50 °C)	5·6 (isomer *E*)	1	67
	5·1 (isomer *Z*)	1	67
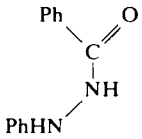 (in DMSO)	3·0	1	77
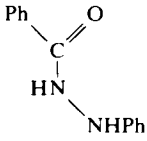 (in DMSO)	3·6	1	77
Dinitrogen complexes (DPPE = $Ph_2PCH_2CH_2PPh_2$)			
trans-$[Mo(N_2)_2(DPPE)_2]$ (in tetrahydrofuran)	4·4	1	330
trans-$[W(N_2)_2(DPPE)_2]$ (in tetrahydrofuran)	5·4	1	330
cis-$[Mo(N_2)_2(PMe_2Ph)_4]$ (in tetrahydrofuran)	6·3	1	330
cis-$[W(N_2)_2(PMe_2Ph)_4]$ (in tetrahydrofuran)	6·2	1	330
$\{[Zr(pentamethylcyclopentadienyl)_2N_2]_2(N_2)\}$ (in toluene, −28 °C)	6·2 (terminal N_2)	1	332
$MeNHNO_2$ (in CH_2Cl_2)	4·9	1	263
Me_2NNO_2 (in CH_2Cl_2)	6·7	1	263
$MeOOCNHNO_2$ (in CH_2Cl_2)	4·4	1	263
$MeOOCN(Me)NO_2$ (in CH_2Cl_2)	6·2	1	263
$EtOOCN(Me)NO_2$ (in CH_2Cl_2)	5·9	1	263
$MeN(NO_2)SiMe_3$ (in CH_2Cl_2)	7·3	1	263
$EtOOCN(NO_2)SiMe_3$ (in CH_2Cl_2)	6·7	1	263
$MeN(NO_2)_2$ (in CH_2Cl_2)	12·2	1	263
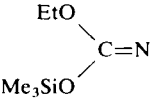 (in CH_2Cl_2)	14·0	1	263
$(MeNNO_2)^{-}\,NH_4^{+}$ (in CH_2Cl_2)	12·2	1	263
$(MeOOCNNO_2)^{-}\,NH_4^{+}$ (in CH_2Cl_2)	16·4	1	263
$MeN{=}N(O)OMe$ (in CH_2Cl_2)	14·0 (*trans*)	1	263
	12·8 (*cis*)	1	263
$MeN{=}N(O)OSiMe_3$ (in CH_2Cl_2)	11·0 (*trans*)	1	263
$MeOOCN{=}N(O)OMe$ (in CH_2Cl_2)	13·9	1	263
$EtOOCN{=}N(O)OPr^{i}$ (in CH_2Cl_2)	14·4	1	263
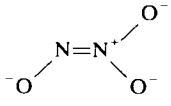 $2Na^{+}$ (in D_2O)	16·9	1	74

TABLE 152—*cont.*

Compound (and solvent)		$^nJ(^{15}N-^{15}N)$ (Hz)	Number of intervening bonds (n)	Ref.
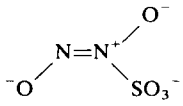	$2K^+$ (in D_2O)	21·6	1	74
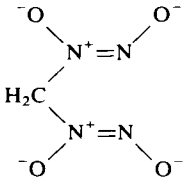	$2Na^+$ (in D_2O)	17·5	1	74
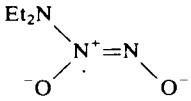	$EtNH_2^+$ (in $CDCl_3$)	16·9 (N=N)	1	74
$O{=}NNO_2$ (in CH_2Cl_2, −100 °C)		11·7	1	74
trans-PhN(O)=NPh (in $CDCl_3$)		12·5	1	329
cis-PhN(O)=NPh (in $CDCl_3$)		12·5	1	329
Azimines (R = phthalimide residue)				
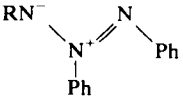 (in $CDCl_3$, −20 °C)		15·0 (N=N)	1	329
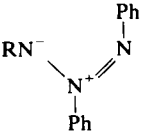 (in $CDCl_3$, −20 °C)		13·4 (N=N)	1	329
Hydrazido ligands				
$[Mo(NNH_2)$(quinolin-8-olate)$(PMe_2Ph)_3]Cl$ (in CH_2Cl_2)		~10	1	346
$[W(NNH_2)$(quinolin-8-olate)$(PMe_2Ph)_3]Cl$ (in CH_2Cl_2)		8·8	1	346
$[MoCl(NNH_2)$(pyridine)$(PMe_2Ph)_3]Cl$ (in CH_2Cl_2)		9·8	1	346
$[WCl(NNH_2)$(pyridine)$(PMe_2Ph)_3]Cl$ (in CH_2Cl_2)		10·5	1	346

TABLE 152—*cont.*

Compound (and solvent)	$^nJ(^{15}N-^{15}N)$ (Hz)	Number of intervening bonds (n)	Ref.
Diazenido ligands, DPPE = $Ph_2PCH_2CH_2PPh_2$			
$[MoBr(N{=}NEt)(DPPE)_2]$ (in tetrahydrofuran)	12·0	1	334
$[WBr(N{=}NEt)(DPPE)_2]$ (in tetrahydrofuran)	11·9	1	334
$[MoCl(N{=}NCOMe)(DPPE)_2]$ (in tetrahydrofuran)	~12	1	334
$[WCl(N{=}NCOMe)(DPPE)_2]$ (in tetrahydrofuran)	12·0	1	334
$[ReCl_2(N{=}NCOPh)(pyridine)(PPh_3)_2]$ (in toluene)	15·0	1	334
$MeN{=}N^+{=}N^-$ (in benzene-d_6)	14·4 ($N{=}N^+$)	1	248
	8·2 ($N^+{=}N^-$)	1	248
$PhN{=}N^+{=}N^-$ (in acetone-d_6)	13·4 ($N{=}N^+$)	1	248
	7·8 ($N^+{=}N^-$)	1	248
$pO_2N{\cdot}C_6H_4{\cdot}N{=}N^+{=}N^-$ (in DMSO-d_6)	13·8 ($N{=}N^+$)	1	248
	7·4 ($N^+{=}N^-$)	1	248
$2,4,6\text{-}(NO_2)_3{\cdot}C_6H_2{\cdot}N{=}N^+{=}N^-$ (in DMSO-d_6)	14·0 ($N{=}N^+$)	1	248
	6·3 ($N^+{=}N^-$)	1	248
$NCN{=}N^+{=}N^-$ (in CD_3CN, −20 °C)	16·0 ($N{=}N^+$)	1	248
	6·0 ($N^+{=}N^-$)	1	248
$(NCN{=}N^+{=}N^-)_3$ (in CD_2Cl_2)	16·1 ($N{=}N^+$)	1	248
	6·1 ($N^+{=}N^-$)	1	248
$(Me_2AlN_3)_3$ (in toluene-d_8, −100 °C)	11·5 ($N{=}N^+$)	1	256
	5·9 ($N^+{=}N^-$)	1	256
$(Me_2GaN_3)_3$ (in toluene-d_8, −90 °C)	12·6 ($N{=}N^+$)	1	256
	7·3 ($N^+{=}N^-$)	1	256
Me_2AsN_3 (in benzene-d_6)	12·2 ($N{=}N^+$, $N^+{=}N^-$)	1	256
Me_3SnN_3 (in pyridine)	~12 ($N{=}N^+$, $N^+{=}N^-$)	1	255
$Me_2P(S)N_3$ (in acetone-d_6)	13·6 ($N{=}N^+$)	1	254
	6·8 ($N^+{=}N^-$)	1	254
$Me_2P(Se)N_3$ (in benzene-d_6)	14·3 ($N{=}N^+$)	1	254
	6·8 ($N^+{=}N^-$)	1	254
$(MeO)_2P(O)N_3$ (in MeCN)	14·4 ($N{=}N^+$)	1	254
	5·8 ($N^+{=}N^-$)	1	254
$[-N{=}P(N_3)_2-]_3$ (in toluene-d_8)	12·2 ($N{=}N^+$)	1	254
	5·5 ($N^+{=}N^-$)	1	254
$HN{=}N^+{=}N^-$ (in Et_2O)	13·95 ($N{=}N^+$)	1	247
	7·20 ($N^+{=}N^-$)	1	247
$ClN{=}N^+{=}N^-$ (in CD_2Cl_2)	24·0 ($N{=}N^+$)	1	247
	7·8 ($N^+{=}N^-$)	1	247
$Li^+(N_3)^-$ (in D_2O)	11·35	1	254
$Na^+(N_3)^-$ (in D_2O)	11·32	1	254

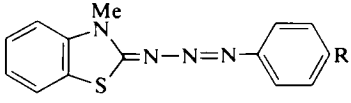

TABLE 152—*cont.*

Compound (and solvent)	$^nJ(^{15}N\text{-}^{15}N)$ (Hz)	Number of intervening bonds (n)	Ref.
cis, R = H (in pyridine)	18·9 (N=N)	1	30
	15·0 (N–N)	1	30
	0 (N=N–N)	2	30
trans, R = H (in pyridine)	13·2 (N=N)	1	30
	17·7 (N–N)	1	30
	10·7 (N=N–N)	2	30
trans, R = NO_2 (in CF_3COOH)	11·8 (N=N)	1	30
	11·8 (N–N)	1	30
	5·9 (N=N–N)	2	30
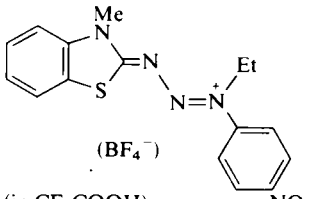 (BF_4^-) (in CF_3COOH)	13·5 (N^+=N)	1	30
	11·8 (N–N)	1	30
	5·1 (N^+=N–N)	2	30
 (in $CDCl_3$)	12·8	1	227
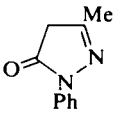 (in $CDCl_3$)	12·0	1	277
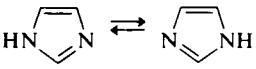 (in H_2O)	1·1 (N=C–N)	2	276
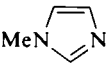 (in H_2O)	1·1 (N=C–N)	2	276
 (in H_2O)	1·7 (N=C–N)	2	276
Imidazole moiety in histidine (in H_2O)			
cation	+0·9 (N=C–N)	2	208, 276
amphion	−0·6 (N=C–N)	2	208, 209
anion	−0·9 (N=C–N)	2	208, 209
Imidazole moiety in *α*-*N*-acetylhistidine (in H_2O)			
cation	+3·4 (N=C–N)	2	208
amphion	+1·0 (N=C–N)	2	208
anion	? (N=C–N)	2	208

TABLE 152—*cont.*

Compound (and solvent)	$^nJ(^{15}N-^{15}N)$ (Hz)	Number of intervening bonds (n)	Ref.
Nucleotides (see Table 126)			
guanosine-3′-phosphate			
(in H_2O, pH 3–7)	2·2 (1-N-C-NH_2)	2	314, 315
	6·0 (3-N=C-NH_2)	2	314, 315
	3·7 (3-N-C-9-N)	2	314, 315
(in H_2O, pH 10)	6·0 (1-N-C-NH_2)	2	314, 315
	6·0 (3-N=C-NH_2)	2	314, 315
	3·7 (3-N-C-9-N)	2	314, 315
adenosine-3′-phosphate			
(in H_2O, pH 3)	1·0 (1-N-C-NH_2)	2	314, 315
	1·5 (3-N-C-9-N)	2	314, 315
(in H_2O, pH 7)	5·2 (1-N-C-NH_2)	2	314, 315
	2·2 (3-N-C-9-N)	2	314, 315
cytidine-3′-phosphate			
(in H_2O, pH 3)	1·5 (3-N=C-NH_2)	2	314, 315
(in H_2O, pH 7)	5·8 (3-N=C-NH_2)	2	314, 315
uridine-3′-phosphate			
(in H_2O, pH 3–7)	2·2 (N-CO-N)	2	314, 315
$(H_2N)_2C=O$ (in acetone + DMSO + tetramethylurea)	5·1 (N-CO-N)	2	345
$(MeNH)_2C=O$ (in DMSO-d_6)	5·3 (N-CO-N)	2	345
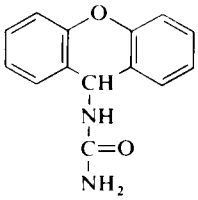 (in DMSO)	4·6 (N-CO-N)	2	178
$P(NMe_2)(NHPh)_2$ (in benzene)	2·2 (N-P-N)	2	142
cis-$Pt(NCS)_2[P(OPh)_3]_2$ (in CH_2Cl_2)	~2 (N-Pt-N)	2	396
cis-$(NH_3)_2Pt(N\text{-Me-imidazole})_2^{2+}$ (in H_2O)	5·4 (H_3N-Pt-3-N, imidazole)	2	395
$(H_2NCH_2CH_2NH_2)Pt(H_2O)(N\text{-Me-imidazole})^{2+}$ (in H_2O)	5·1 (H_2N-Pt-N, imidazole)	2	395
$(H_2NCH_2CH_2NH_2)(Pt(N\text{-Me-imidazole})_2^{2+}$ (in H_2O)	5·4 (H_2N-Pt-N, imidazole)	2	395

TABLE 153

Some ^{31}P–^{15}N couplings (absolute values if sign not given)

Compound	Solvent	$^{n}J(^{31}P–^{15}N)$ (Hz)	Number of intervening bonds (n)	Ref.
$(Me_2N)_3P$	none	+59·1	1	73, 402
$(Me_2N)_3P{=}S$	none	6·0	1	73
$(Me_2N)_3P{=}O$	none	−26·9	1	73
$PhNHPMe_2$	none	+53·0	1	73
	benzene-d_6	53·0	1	142
$PhNHP(=S)Me_2$	none	+11·3	1	73
	dioxan	11·3	1	142
$PhNHP(=O)Me_2$	none	−0·5	1	73
	DMSO-d_6	−0·5	1	142
$PhNHP(=Se)Me_2$	CH_2Cl_2	+16·5	1	142, 254
$PhNHP(=Te)Me_2$	benzene/CH_2Cl_2	36·0	1	142
$(PhNH–P^{+}Me_3)\,I^{-}$	CH_2Cl_2	4·1	1	142
$(PhNHP^{+}Me_2SMe)\,I^{-}$	$CHCl_3$	10·5	1	142
$(PhNHP^{+}Me_2SeMe)\,I^{-}$	CH_2Cl_2	14·0	1	142
$(Me_2PBH_2NPh)_n$	CH_2Cl_2	17·0	1	142
$PhNHPBu^{n}_2$	mesitylene	59·6	1	142
$PhNHP(=S)Bu^{n}_2$	mesitylene/$CHCl_3$	22·2	1	142
$PhNHP(=O)Bu^{n}_2$	mesitylene/CH_2Cl_2	11·5	1	142
$PhNHP(=Se)Bu^{n}_2$	mesitylene/$CHCl_3$	27·2	1	142
$(PhNHP^{+}MeBu^{n}_2)\,I^{-}$	DMSO-d_6	13·4	1	142
$(PhNHP^{+}Bu^{n}_2SeMe)\,I^{-}$	DMSO-d_6	23·8	1	142
$PhN(PBu^{n}_2)SnMe_3$	benzene/CH_2Cl_2	80·0	1	142
$PhN(PMe_2)SnMe_3$	benzene	71·9	1	142
$PhNP(=S)Me_2$ | $SnMe_3$	benzene	24·8	1	142

TABLE 153—*cont.*

Compound	Solvent	$^nJ(^{31}P-^{15}N)$ (Hz)	Number of intervening bonds (n)	Ref.
$PhNHP(NMe_2)_2$	benzene	53·8	1	142
$(PhNH)_2PNMe_2$	benzene	52·8	1	142
$PhNHP(MeNCH_2CH_2NMe)$	benzene	84·2	1	142
$PhNHP(=S)(MeNCH_2CH_2NMe)$	benzene/$CHCl_3$	2·6	1	142
$PhNHP(=Se)(MeNCH_2CH_2NMe)$	benzene	7·8	1	142
$PhNHP^+(Me)(MeNCH_2CH_2NMe)$	CH_2Cl_2	−3·3	1	142
$PhP(MeNCH_2CH_2NMe)$	none	49·8	1	402
$PhP[N(CH_2Ph)_2]_2$	none	76·7	1	402
$PhP(NEt_2)_2$	none	75·5	1	402
$Me_2NP(MeNCH_2CH_2NMe)$	none	51·8 (P–NMe)	1	402
		24·0 (P–NMe_2)	1	402
Cl_2PNMe_2	none	89·4	1	402
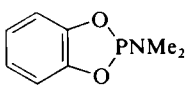	none	89·0	1	402
$(Bu^s)OP(MeNCH_2CH_2NMe)$	none	57·6	1	402
$F_3P(NH_2)_2$	none	−81·5	1	73
$F_3P{=}NPF_2$	none	−53·2	1	73
$F_2PN(SiH_3)_2$	$CDCl_3$	+77·5	1	138
$F_2PN(SiH_3)_2{\cdot}BH_3$	$CDCl_3$	40·9	1	138
$(F_2P)_2NSiH_3$	$CDCl_3$	74·6	1	138
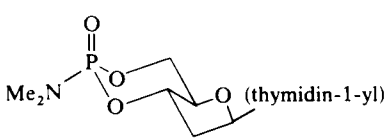	DMSO-d_6	53	1	399

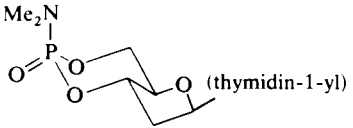	DMSO-d_6	42	1	399
$Et_2NP(=O)(OMe)_2$	benzene-d_6	42·2	1	146
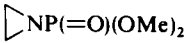	benzene-d_6	9·3	1	146
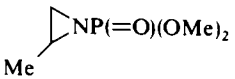	benzene-d_6	10·0	1	146
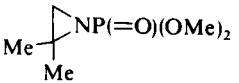	benzene-d_6	4·4	1	146
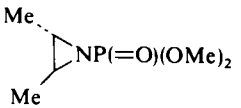	benzene-d_6	10·6	1	146
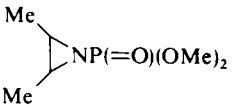	benzene-d_6	4·3	1	146
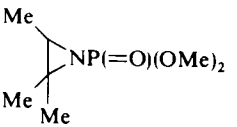	benzene-d_6	5·0	1	146
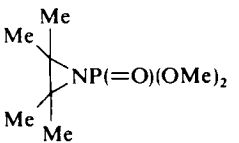	benzene-d_6	≤1	1	146

TABLE 153—*cont.*

Compound	Solvent	$^{n}J(^{31}P-^{15}N)$ (Hz)	Number of intervening bonds (n)	Ref.
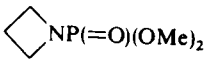	benzene-d_6	20·9	1	146
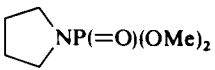	benzene-d_6	41·2	1	146
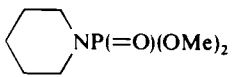	benzene-d_6	39·1	1	146
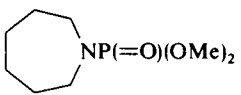	benzene-d_6	42·7	1	146
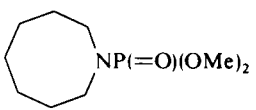	benzene-d_6	41·8	1	146
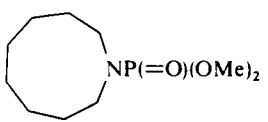	benzene-d_6	37·6	1	146
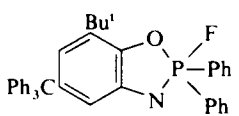	benzene-d_6	35·3	1	145
$Me_2P(=O)N=N^+=N^-$	$CDCl_3$	47·9 4·9	1 2	254 254

$Me_2P(=S)N=N^+=N^-$	acetone-d_6	54·75	1	254
		5·05	2	254
		2·70	3	254
$Me_2P(=Se)N=N^+=N^-$	benzene-d_6	57·4	1	254
$Et_2P(=O)N=N^+=N^-$	benzene-d_6	51·1	1	254
		4·5	2	254
$Et_2P(=S)N=N^+=N^-$	benzene-d_6	58·0	1	254
		5·3	2	254
$(MeO)_2P(=O)N=N^+=N^-$	MeCN	14·9	1	254
Cyclophosphazenes (see Table 127)				
$[-N=P(N_3)_2-]_3$	toluene-d_6	17 ($P-N_3$)	1	254
$[-N=PCl_2-]_3$	$CDCl_3$	31·7	1	326, 400
		31·8	1	401
$[-N=PBr_2-]_3$	$CDCl_3$	55·8	1	400
$[-N=PF_2-]_3$	$CDCl_3$	24·9	1	400
$[-N=P(SEt)_2-]_3$	$CDCl_3$	51·1	1	400
		51·0	1	326
$[-N=P(SPh)_2-]_3$	$CDCl_3$	53·3	1	326
$[-N=PCl_2-]_4$	$CDCl_3$	6·9	1	326
		6·9	1	401
$[-N=PCl_2-]_5$	$CDCl_3$	2·3	1	401
$[-N=P(SEt)_2-]_4$	$CDCl_3$	34·0	1	326
$N_3P_3Cl_4(SEt)_2$	$CDCl_3$	34·1 ($Cl_2P-N-PCl_2$)	1	326
		38·8 (Cl_2P-N)	1	326
		48·1 ($P(SEt)_2-N$)	1	326
$N_3P_3Cl_2(SEt)_4$	$CDCl_3$	40·3 (PCl_2-N)	1	326
		47·6 ($P(SEt)_2-N$)	1	326
		49·4 ($P(SEt)_2NP(SEt)_2$)	1	326
$N_4P_4Cl_4(SEt)_4$	$CDCl_3$	15·5 (PCl_2-N)	1	326
		30·6 ($P(SEt)_2-N$)	1	326
$N_3P_3Cl_4(SPh)_2$	$CDCl_3$	33·7 ($PCl_2-N-PCl_2$)	1	326
		39·4 (PCl_2-N)	1	326
		50·6 ($P(SPh)-N$)	1	326
$N_3P_3Cl_2(SPh)_4$	$CDCl_3$	39·7 (PCl_2-N)	1	326
		50·9 ($P(SPh)_2-N$)	1	326
		53·5 ($P(SPh)_2NP(SPh)_2$)	1	326

TABLE 153—*cont.*

Compound	Solvent	$^{n}J(^{31}P-^{15}N)$ (Hz)	Number of intervening bonds (n)	Ref.
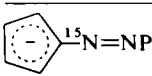	$CH_2Cl_2/CHCl_3$	18·5 ($^{15}N{=}N{-}P^{+}$)	2	162
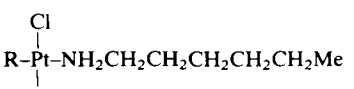				
$R = PBu^{n}_3$	$CDCl_3$	47 (N–Pt–P)	2	337
$P(Me)Ph_2$	$CDCl_3$	52 (N–Pt–P)	2	337
$P(C_6H_4Mep)_3$	$CDCl_3$	50 (N–Pt–P)	2	337
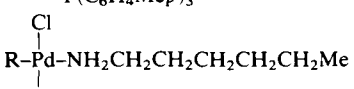				
$R = PBu^{n}_3$	$CDCl_3$	50 (N–Pd–P)	2	337
$P(Me)Ph_2$	$CDCl_3$	54 (N–Pd–P)	2	337
$P(C_6H_4Mep)_3$	$CDCl_3$	54 (N–Pd–P)	2	337
$Pt(NO_2)_2(PBu^{n}_2)_2$	$CDCl_3$			
cis-isomer		61 (*trans*-N–Pt–P)	2	337
trans-isomer		3 (*cis*-N–Pt–P)	2	337
cis-$Pt(NCS)_2[P(OPh)_3]_2$	$CDCl_3$	95 (*trans*-N–Pt–P)	2	337
		7 (*cis*-N–Pt–P)	2	337

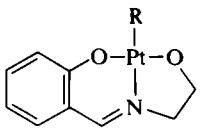

$CDCl_3$

R = PBu^n_3		50 (N–Pt–P)	2	337
$P(C_6H_4Mep)_3$		53 (N–Pt–P)	2	337
$P(OEt)_3$		76 (N–Pt–P)	2	337
cis-$Pt(NCS)(SCN)[P(OPh)_3]_2$	CH_2Cl_2	91 (*trans*-N–Pt–P)	2	396
		6 (*cis*-N–Pt–P)	2	396
trans-$[W(N_2)_2(Ph_2PCH_2CH_2PPh_2)_2]$	tetrahydrofuran	1·9 (N–W–P)	2	330
		0·9 (NN–W–P)	3	330
cis-$[Mo(N_2)_2(PMe_2Ph)_4]$	tetrahydrofuran	5·2 (*trans*-N–Mo–P)	2	330
cis-$[W(N_2)_2(PMe_2Ph)_4]$	tetrahydrofuran	16·7 (*trans*-N–W–P)	2	330
		1·2 (*cis*-N–W–P)	2	330
		0·9 (NN–W–P)	3	330
cis-$[MoF(NNH_2)(Ph_2PCH_2CH_2PPh_2)_2]BF_4$	CH_2Cl_2	6 (N–Mo–P)	2	346
trans-$[WF(NNH_2)(Ph_2PCH_2CH_2PPh_2)_2]BF_4$	CH_2Cl_2	11 (N–W–P)	2	346
$[WCl(NNH_2)(pyridine)(PMe_2Ph)_3]Cl$	CH_2Cl_2	5 (N–W–P)	2	346

TABLE 154

Some ^{19}F–^{15}N couplings (absolute values if sign not given)

Compound	Solvent	$^{n}J(^{19}F-^{15}N)$ (Hz)	Number of intervening bonds (n)	Ref.
	none	−52·5	2	379, 403
	none	3·6	3	379
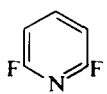	none	(−)52·3	2	379
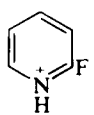	$CDCl_3/CF_3COOH$	(−)23·1	2	379
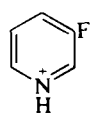	$CDCl_3/CF_3COOH$	3·1	3	379
Fluoro-anilines	none or DMSO			
2-F		0	3	379
3-F		0	4	379
4-F		1·5	5	379
2,4-F_2		1·5	5	379
2-Me-4-F		1·5	5	379

Fluoro-anilinium ions	$CDCl_3/CF_3COOH$			
2-F		1·3	3	379
3-F		0·2	4	379
4-F		0	5	379
Fluoro-substituted *N,N*-dimethylanilines	none or DMSO			
2-F		0	3	379
3-F		0	4	379
4-F		0·5	5	379
2,4-F_2		0·6	5	379
Fluoro-substituted acetanilides	DMSO			
2-F		1·0	3	379
3-F		0·9	4	379
4-F		0·5	5	379
2-Me-4-F		0·2	5	379
Fluoro-substituted benzenesulphonanilides (substituted in Ph-NH moiety of $PhNHSO_2Ph$)	DMSO			
2-F		1·9	3	379
3-F		0·5	4	379
4-F		0·8	5	379
2,4-F_2		1·3	3	379
		1·8	5	379
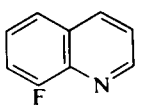	DMSO	2·9	3	379
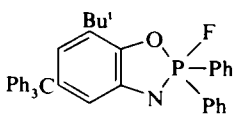	benzene-d_6	24·6 (N–P–F)	2	145
trans-$[MoF(NNH_2)(Ph_2PCH_2CH_2PPh_2)_2]BF_4$	CH_2Cl_2	77 (N–Mo–F)	2	346
trans-$[WF(NNH_2)(Ph_2PCH_2CH_2PPh_2)]BF_4$	CH_2Cl_2	58 (N–W–F)	2	346
$[WF_5(NMe)]^-$	none	56 (N–W–F)	2	404
$F_2PN(SiH_3)_2$	$CDCl_3$	−2·6 (N–P–F)	2	138
$(F_2P)_2NSiH_3$	$CDCl_3$	3·2 (N–P–F)	2	138

TABLE 155

Some ^{195}Pt–^{15}N couplings (absolute values)

Compound	Solvent	$^{n}J(^{195}Pt–^{15}N)$(Hz)	Number of intervening bonds (n)	Ref.
cis-$Pt(NH_3)_2Cl_2$	DMSO	312·2	1	405
$ClPt^{+}(NH_3)_3$	DMSO	317 (N *trans* to Cl)		
		278 (N *trans* to NH_3)	1	405
cis-$PtCl_2(NH_3)$(DMSO)	DMSO	336	1	405
trans-$PtCl_2(NH_3)$(DMSO)	DMSO	232	1	405
trans-$ClPt^{+}(NH_3)_2$(DMSO)	DMSO	287	1	405
cis-$ClPt^{+}(NH_3)_2$(DMSO)	DMSO	340·0	1	405
cis-$Pt^{2+}(NH_3)_3$(DMSO)	DMSO	288 (N *trans* to Cl)	1	405
		232 (N *trans* to DMSO)		
$Pt^{+}Cl_2(NH_2CH_2COO^{-})$	H_2O	317	1	405
trans-$PtCl_2(NH_2CH_2COOH)$(DMSO)	H_2O	244	1	405
$Pt^{+}Cl$(DMSO)$(NH_2CH_2COO^{-})$, N *trans* to DMSO	H_2O	226	1	405
$Pt^{+}Cl$(DMSO)$(NH_2CH_2COO^{-})$, N *trans* to Cl	H_2O	330	1	405
cis-$Pt(NO_2)_2(PBu^{n}_3)_2$	$CDCl_3$	390	1	406, 337
trans-$Pt(NO_2)_2(PBu^{n}_3)_2$	$CDCl_3$	453	1	406, 337
trans-$PtCl_2(R)(NH_2CH_2CH_2CH_2CH_2CH_2Me)$				
$R = PBu^{n}_3$	$CDCl_3$	138·3	1	337
$PMePh_2$	$CDCl_3$	155·9	1	337
$P(C_6H_4Mep)_3$	$CDCl_3$	158·8	1	337
$AsBu^{n}_3$	$CDCl_3$	183·8	1	337
$AsMePh_2$	$CDCl_3$	208·8	1	337
$As(C_6H_4Mep)_3$	$CDCl_3$	207·4	1	337
n-hexylamine	$CDCl_3$	286·8	1	337
$CH_2{=}CH_2$	$CDCl_3$	283·9	1	337
cis-$PtCl_2(NH_2CH_2CH_2CH_2CH_2CH_2Me)_2$	DMSO	336	1	337

cis-$PtCl_2(CH_2{=}CH_2)(NH_2CH_2CH_2CH_2CH_2CH_2Me)$	$CDCl_3$	295·6		1	337
	$CDCl_3$	296		1	407
$Pt^{2+}(H_2O)(NH_2CH_2CH_2NH_2)$	H_2O	421·4		1	395
cis-$Pt^{2+}(NH_3)_2$(*N*-Me-imidazole)$_2$	H_2O	286·5	(NH_3–Pt)	1	395
		436·5	(3-N–Pt)	1	395
		26·1	(MeN–Pt)	3	395
$Pt^{2+}(H_2O)_2(NH_3)_2$	H_2O	388·6		1	395
$Pt^{2+}(H_2O)(NH_2CH_2CH_2NH_2)$(*N*-Me-imidazole)	H_2O	{411·1 327	(NH_2–Pt)	1	395
		?	(3-N–Pt)	1	395
		24·7	(MeN–Pt)	3	395
$Pt^{2+}(NH_2CH_2CH_2NH_2)$(*N*-Me-imidazole)$_2$	H_2O	318	(NH_2–Pt)	1	395
		428·6	(3-N–Pt)	1	395
		25·5	(MeN–Pt)	3	395
$Pt^{2+}(H_2O)_2$(*N*-Me-imidazole)$_2$	H_2O	579·4	(3-N–Pt)	1	395
		32·6	(MeN–Pt)	3	395
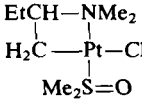	$CDCl_3$	190		1	377
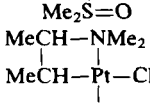	$CDCl_3$	239	(Me_2N–Pt)	1	377
		299	(HN–Pt)	1	377
trans-$PtCl_2(PPh_3)(NHMe_2)$	$CDCl_3$	171		1	408
trans-$PtCl_2(CH_2{=}CH_2)(NHMe_2)$	$CDCl_3$	299		1	408
trans-$PtCl_2(CH_2^{-}{-}CH_2N^{+}HMe_2)(NHMe_2)$	$CDCl_3$	107		1	408
		51		3	408

TABLE 156

Some miscellaneous ^{15}N–X couplings (absolute values if sign not given)

Compound		Solvent	$^nJ(^{15}N\text{–}X)$ (Hz)	Number of intervening bonds (n)	Ref.
X = ^{183}W					
$[W(NNH_2)(quinolin\text{-}8\text{-}olate)(PMe_2Ph)_3]Cl$		CH_2Cl_2	114	1	346
$[WCl(NNH_2)(pyridine)(PMe_2Ph)_3]Cl$		CH_2Cl_2	124·5	1	346
$[WF_5(NMe)]^-$		CH_2Cl_2	98	1	404, 346
trans-$\{WF_4(NMe)[(MeO)_3SO]\}$		CH_2Cl_2	140	1	404, 346
X = $^{119}Sn/^{117}Sn$					
$PhN(PMe_2S)(SnMe_2)$		benzene-d_6	−47·5 ($^{119}Sn\text{–}^{15}N$)	1	142
Stannatranes (see Table 29)	R = Me	$CDCl_3$, −30 to +33 °C	75·6; 110·0 ($^{119}Sn\text{–}^{15}N$) (non-equivalent moieties in a trimeric species)	1	140
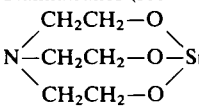			72·4; 104·6 ($^{117}Sn\text{–}^{15}N$)	1	140
	Bu^t	$CDCl_3$, −20 °C	69·9 ($^{119}Sn\text{–}^{15}N$)	1	140
			66·6 ($^{117}Sn\text{–}^{15}N$)	1	140
X = ^{111}Cd					
1:1 Adducts of ^{111}Cd-*meso*-tetraphenylporphyrin with substituted pyridines (Table 116), couplings with porphyrin nitrogens					
substituent on pyridine ring:					
4-CN			147·6	1	288
3-Cl			146·4	1	288
4-COOMe			146·3	1	288
4-COMe			146·0	1	288
none			142·5	1	288
4-Me			141·0	1	288
$4\text{-}NH_2$			137·4	1	288
X = ^{103}Rh					
$RhCl(PPr^i_3)_2(p\text{Me}\cdot C_6H_4\cdot N{=}S{=}O)$		DMSO	15·5	1 (?)	409

X = ^{71}Ga				
$(Cl_3{}^{71}GaNCS)^-$	MeCN	133*	1	410
$[Cl_2{}^{71}Ga(NCS)_2]^-$	MeCN	161*	1	410
X = ^{59}Co				
$Co^{3+}(NH_2CH_2CH_2NH_2)_3$	D_2O	63·8	1	335
$Co^{3+}(NH_3)_6$	D_2O	62·5	1	335
X = ^{57}Fe				
Fe(II) low-spin complexes with *meso*-tetraphenylporphyrin (TPP), couplings with porphyrin nitrogens				
^{57}Fe(II)(TPP)(pyridine)$_2$	pyridine/D_2O	7·8	1	411
^{57}Fe(II)(TPP)(morpholine)$_2$	$CDCl_3$	8·0	1	411
^{57}Fe(II)(TPP)(pyrrolidine)$_2$	$CDCl_3$	7·5	1	411
X = ^{27}Al				
$(Cl_3{}^{27}AlNCS)^-$	MeCN	56*	1	410
$(Cl_3{}^{27}AlNCO)^-$	MeCN	56*	1	410
$Cl_2{}^{27}Al(NCS)_2^-$	MeCN	63*	1	410
X = ^{199}Hg				
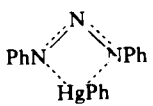 or PhN(HgPh)N=NPh ⇅ PhN=NN(HgPh)Ph	pyridine, 0·6 M	167	1	412
		<10	2	412
	pyridine, 0·1 M	165	1	412
		<10	2	412
	tetrahydrofuran, 0·2 M	154	1	412
		<10	2	412
X = ^{207}Pb				
Pb(II)(1,4,8,11-tetraazacyclotetradecane)$(NO_3)_2$ (see Table 144)	DMSO	207·5 (axial-N–Pb)	1	339
		19·8 (equatorial-N–Pb)	1	339

* Recalculated from ^{14}N couplings.

REFERENCES

1. M. Witanowski, L. Stefaniak and G. A. Webb, in "Annual Reports on NMR Spectroscopy", G. A. Webb (ed.), 1977, **7**, 117, Academic Press, London.
2. M. Witanowski and G. A. Webb (eds), "Nitrogen NMR", Plenum Press, London, 1973.
3. M. Witanowski and G. A. Webb, in "Annual Reports on NMR Spectroscopy", E. F. Mooney (ed.), 1972, **5A**, 395, Academic Press, London.
4. G. C. Levy and R. L. Lichter, "^{15}N NMR Spectroscopy", Wiley, New York, 1979.
5. J. D. Roberts, "Festschrift für F. Bloch", 1979.
6. G. J. Martin, M. L. Martin and J. P. Gouesnard, in "NMR Basic Principles and Progress", P. Diehl, E. Fluck and R. Kosfeld (eds), 1981, **18**, 1, Springer Verlag, Berlin.
7. G. A. Webb, in "NMR and the Periodic Table", R. K. Harris and B. E. Mann (eds), Academic Press, London, 1978, p. 49.
8. N. F. Ramsey, *Phys. Rev.*, 1950, **78**, 699.
9. K. A. K. Ebraheem and G. A. Webb, in "Progress in NMR Spectroscopy", J. Emsley, J. Feeney and L. H. Sutcliffe (eds), 1977, **11**, 149, Pergamon Press, Oxford.
10. P. Lazzeretti and R. Zanasi, *Int. J. Quant. Chem.*, 1977, **12**, 93.
11. S. G. Kukolich and S. C. Wofsky, *J. Chem. Phys.*, 1970, **32**, 5477.
12. U. T. Lamanna, G. Guidotti and G. P. Arrighini, *J. Chem. Phys.*, 1977, **67**, 604.
13. S. I. Chan, M. R. Baker and N. F. Ramsey, *Phys. Rev.*, 1964, **136A**, 1224.
14. J. A. Pople, *Discuss. Faraday Soc.*, 1962, **34**, 7.
15. S. T. Epstein, *J. Chem. Phys.*, 1973, **58**, 1592.
16. W. T. Raynes, in "Specialist Periodical Report on NMR", R. J. Abraham (ed.), 1978, **7**, 1, Chemical Society, London.
17. K. A. K. Ebraheem and G. A. Webb, *J. Magn. Resonance*, 1978, **30**, 211.
18. M. Jallali-Heravi and G. A. Webb, *J. Magn. Resonance*, 1978, **32**, 429.
19. M. Jallali-Heravi, G. A. Webb and M. Witanowski, *Org. Magn. Resonance*, 1979, **12**, 274.
20. J. Mason, *J. Chem. Soc. Faraday II*, 1977, 1464.
21. M. Barfield and D. M. Grant, *J. Chem. Phys.*, 1977, **67**, 3322.
22. M. Jallali-Heravi and G. A. Webb, *Org. Magn. Resonance*, 1979, **12**, 174.
23. M. J. S. Dewar, D. Landman, S. H. Suck and P. K. Weiner, *J. Amer. Chem. Soc.*, 1977, **99**, 3951.
24. J. M. Schulman, *J. Magn. Resonance*, 1977, **28**, 137.
25. I. Ando, M. Jallali-Heravi, M. Kondo, S. Watanabe and G. A. Webb, *Bull. Chem. Soc. Japan*, 1979, **52**, 2240.
26. R. O. Duthaler and J. D. Roberts, *J. Amer. Chem. Soc.*, 1978, **100**, 4969.
27. B. Wrackmeyer, *J. Magn. Resonance*, 1977, **27**, 345.
28. Y. Vysotskii, *Zh. Strukt. Khim.*, 1978, **19**, 736.
29. T. A. Albright and W. J. Freeman, *Org. Magn. Resonance*, 1977, **9**, 75.
30. E. Fanghänel, R. Radeglia, D. Hauptmann, B. Tyszkiewicz and M. Tyszkiewicz, *J. Prakt. Chem.*, 1978, **320**, 618.
31. W. McFarlane and C. J. Turner, *Bull. Soc. Chim. Belg.*, 1978, **87**, 271.
32. K. Yagi, N. Ohishi, A. Takai, K. Kawono and Y. Kyogoku, *Biochemistry*, 1976, **15**, 2877.
33. L. Stefaniak, *Bull. Acad. Pol. Sci., Ser. Sci. Chim.*, 1978, **26**, 291.
34. B. Wrackmeyer and H. Nöth, *Chem. Ber.*, 1976, **109**, 3480.
35. L. Psota, M. Franzen-Sieveking, J. Turnier and R. L. Lichter, *Org. Magn. Resonance*, 1978, **11**, 401.
36. M. Witanowski, L. Stefaniak, S. Szymanski and G. A. Webb, *Bull. Acad. Pol. Sci., Ser. Sci. Chim.*, 1978, **26**, 285.
37. A. J. Digioia, G. T. Furst, L. Psota and R. L. Lichter, *J. Phys. Chem.*, 1978, **82**, 1644.
38. J. Kroner, W. Schneid, N. Wiberg, B. Wrackmeyer and G. Ziegleder, *J. Chem. Soc. Faraday II*, 1978, 1909.

39. J. Mason, W. Van Bronswyk and J. G. Vinter, *J. Chem. Soc. Perkin II*, 1977, 469.
40. G. J. Martin, J. P. Gouesnard, J. Dorie, C. Robillier and M. L. Martin, *J. Amer. Chem. Soc.*, 1977, **99**, 1381.
41. W. Schwotzer and W. von Philipsborn, *Helv. Chim. Acta*, 1977, **60**, 1501.
42. M. P. Sibi and R. L. Lichter, *J. Org. Chem.*, 1979, **44**, 3017.
43. R. G. Jones and J. M. Wilkins, *Org. Magn. Resonance*, 1978, **11**, 20.
44. M. L. Filleux-Blanchard and N. D. An, *Org. Magn. Resonance*, 1979, **12**, 12.
45. J. P. Gouesnard and G. J. Martin, *Org. Magn. Resonance*, 1979, **12**, 263.
46. F. A. L. Anet and M. Ghiaci, *J. Amer. Chem. Soc.*, 1979, **101**, 6857.
47. G. J. Martin, J. Dorie and B. Mechin, *Org. Magn. Resonance*, 1979, **12**, 229.
48. W. T. Raynes, in "Specialist Periodical Reports on NMR", Vol. 8, R. J. Abraham (ed.), Chemical Society, London, 1979, p. 1.
49. C. J. Jameson, A. K. Jameson, H. Parker, S. M. Cohen and C. L. Lee, *J. Chem. Phys.*, 1978, **68**, 2861.
50. C. J. Jameson, A. K. Jameson and S. Wille, *J. Phys. Chem.*, 1979, **83**, 3372.
51. M. Witanowski, *Tetrahedron*, 1967, **23**, 4299.
52. J. Mason and J. G. Vinter, *J. Chem. Soc. Dalton*, 1975, 2522.
53. N. F. Ramsey, *Phys. Rev.*, 1953, **91**, 303.
54. A. D. C. Towl and K. Schaumburg, *Mol. Phys.*, 1971, **22**, 49.
55. J. A. Pople, J. W. McIver and N. S. Ostlund, *J. Chem. Phys.*, 1969, **49**, 2960, 2965.
56. A. C. Blizzard and D. P. Santry, *J. Chem. Phys.*, 1971, **55**, 950.
57. J. Kowalewski, in "Progress in NMR Spectroscopy", J. Emsley, J. Feeney and L. H. Sutcliffe (eds), 1977, **11**, 1, Pergamon Press, Oxford.
58. J. M. Schulman and T. J. Venanzi, *J. Amer. Chem. Soc.*, 1976, **98**, 4701.
59. Tun Khin and G. A. Webb, *Org. Magn. Resonance*, 1977, **10**, 175.
60. J. M. Schulman and T. J. Venanzi, *J. Amer. Chem. Soc.*, 1976, **98**, 6739.
61. J. M. Schulman, J. Ruggio and T. J. Venanzi, *J. Amer. Chem. Soc.*, 1977, **99**, 2045.
62. Tun Khin and G. A. Webb, *J. Magn. Resonance*, 1979, **33**, 159.
63. T. Axenrod, M. J. Wieder, Tun Khin, G. A. Webb, H. J. C. Yeh and S. Bulusu, *Org. Magn. Resonance*, 1979, **12**, 1.
64. L. Ernst, E. Lustig and V. Wray, *J. Magn. Resonance*, 1976, **22**, 459.
65. W. Runge and J. Firl, *Z. Naturforsch.*, 1976, **31B**, 1515.
66. R. E. London, T. E. Walker, T. W. Whaley and N. A. Matwiyoff, *Org. Magn. Resonance*, 1977, **9**, 598.
67. R. L. Lichter, P. R. Srinivasan, A. B. Smith, R. K. Dieter, C. T. Denny and J. M. Schulman, *J. Chem. Soc. Chem. Comm.*, 1977, 366.
68. S. Berger and H. Kaletsch, *Org. Magn. Resonance*, 1976, **8**, 438.
69. G. W. Buchanan and B. A. Dawson, *Canad. J. Chem.*, 1978, **56**, 2200.
70. R. E. Wasylishen, in "Annual Reports on NMR Spectroscopy", G. A. Webb (ed.), 1977, **7**, 245, Academic Press, London.
71. Tun Khin and G. A. Webb, *Org. Magn. Resonance*, 1978, **11**, 487.
72. Tun Khin, S. Duangthai and G. A. Webb, *Org. Magn. Resonance*, 1980, **13**, 240.
73. G. A. Gray and T. A. Albright, *J. Amer. Chem. Soc.*, 1976, **98**, 3857.
74. H. Schultheiss and E. Fluck, *Z. Naturforsch.*, 1977, **32B**, 257.
75. S. Bulusu, J. R. Autera and T. Axenrod, *J. Chem. Soc. Chem. Comm.*, 1973, 602.
76. T. Axenrod, P. Mangiaracina and P. S. Pregosin, *Helv. Chim. Acta*, 1976, **59**, 1655.
77. J. Elguero, B. L. Johnson, J. M. Pereillo, G. Pouzard, M. Rajzmann and E. W. Randall, *Org. Magn. Resonance*, 1977, **9**, 145.
78. M. L. Martin, M. L. Filleux-Blanchard, G. J. Martin and G. A. Webb, *Org. Magn. Resonance*, 1980, **13**, 396.
79. C. Robillier, M. L. Martin and G. J. Martin, *Nouv. J. Chimie*, 1980, **4**, 35.

80. M. Witanowski, L. Stefaniak, S. Szymański and H. Januszewski, *J. Magn. Resonance*, 1977, **28**, 217.
81. P. R. Srinivasan and R. L. Lichter, *J. Magn. Resonance*, 1977, **28**, 227.
82. R. O. Duthaler and J. D. Roberts, *J. Magn. Resonance*, 1979, **34**, 129.
83. I. I. Schuster and J. D. Roberts, *J. Org. Chem.*, 1980, **45**, 284.
84. A. J. Digioia and R. L. Lichter, *J. Magn. Resonance*, 1977, **27**, 431.
85. M. Witanowski, L. Stefaniak, B. Kamieński, S. Biernat and G. A. Webb, *J. Magn. Resonance*, 1981, **43**, 456.
86. J. G. Green, G. R. Dubay and N. A. Porter, *J. Amer. Chem. Soc.*, 1977, **99**, 1264.
87. F. W. Wehrli, in "Annual Reports on NMR Spectroscopy", G. A. Webb (ed.), 1979, **9**, 125, Academic Press, London.
88. D. Shaw, "Fourier Transform NMR Spectroscopy", Elsevier, Amsterdam, 1976.
89. G. C. Levy, J. J. Dechter and J. Kowalewski, *J. Amer. Chem. Soc.*, 1978, **100**, 2308.
90. O. A. Gansow, K. M. Triplett, T. T. Peterson, R. E. Botto and J. D. Roberts, *Org. Magn. Resonance*, 1980, **13**, 77.
91. R. D. Bertrand, W. B. Moniz, A. N. Garroway and G. C. Chingas, *J. Magn. Resonance*, 1978, **32**, 465.
92. G. C. Chingas, R. D. Bertrand, A. N. Garroway and W. B. Moniz, *J. Amer. Chem. Soc.*, 1979, **101**, 4058.
93. G. A. Morris and R. Freeman, *J. Amer. Chem. Soc.*, 1979, **101**, 760.
94. G. A. Morris, *J. Amer. Chem. Soc.*, 1980, **102**, 428.
95. G. Bodenhausen and D. J. Ruben, *Chem. Phys. Letters*, 1980, **69**, 185.
96. J. P. Marchal and D. Canet, *Biochemistry*, 1980, **19**, 1301.
97. H. J. Jakobsen, T. Lund, R. S. Hansen and P. Daugaard, *J. Magn. Resonance*, 1978, **32**, 459.
98. H. J. Jakobsen and H. Bildsoe, *J. Magn. Resonance*, 1977, **26**, 183.
99. M. Witanowski, L. Stefaniak and G. A. Webb, *J. Magn. Resonance*, 1979, **36**, 227.
100. G. C. Levy, T. Pehk and P. R. Srinivasan, *Org. Magn. Resonance*, 1980, **14**, 129.
101. H. A. L. Cordozo, J. Bulthuis and C. MacLean, *J. Magn. Resonance*, 1979, **33**, 27.
102. J. P. Marchal and D. Canet, *J. Chem. Phys.*, 1977, **66**, 2566.
103. A. Cogne, J. B. Robert and L. Wiesenfeld, *Chem. Phys. Letters*, 1978, **57**, 627.
104. E. K. Wolff, R. G. Griffin and C. Watson, *J. Chem. Phys.*, 1977, **66**, 5433.
105. G. Bodenhausen, R. E. Stark, D. J. Ruben and R. G. Griffin, *Chem. Phys. Letters*, 1979, **67**, 424.
106. R. Blinc, M. Burgar and V. Rutar, *Solid State Commun.*, 1978, **27**, 1021.
107. R. E. Stark, R. A. Haberkorn and R. G. Griffin, *J. Chem. Phys.*, 1978, **68**, 1996.
108. R. B. Creel, E. D. von Meerwall and R. G. Barnes, *Chem. Phys. Letters*, 1977, **49**, 501.
109. L. M. Ishol and T. A. Scott, *J. Magn. Resonance*, 1977, **27**, 23.
110. P. Brunner, M. Reinhold and R. R. Ernst, *J. Chem. Phys.*, 1980, **73**, 1086.
111. J. Schaefer, R. A. McKay and E. O. Stejskal, *J. Magn. Resonance*, 1979, **34**, 443.
112. H. Bösiger and P. Diehl, *J. Magn. Resonance*, 1980, **38**, 361.
113. R. Y. Dong, E. Tomchuk, J. J. Visintainer and E. Bock, *Mol. Cryst. Liq. Cryst.*, 1976, **33**, 101.
114. N. A. Porter, G. R. Dubay and J. G. Green, *J. Amer. Chem. Soc.*, 1978, **100**, 920.
115. W. Städeli, W. von Philipsborn, A. Wick and I. Kompiš, *Helv. Chim. Acta*, 1980, **63**, 504.
116. J. Mason, *Advan. Inorg. Radiochem.*, 1976, **18**, 197.
117. E. Breitmaier and W. Voelter, "^{13}C NMR Spectroscopy", Verlag Chemie, Weinheim, 1974.
118. W. Sicińska, L. Stefaniak, M. Witanowski and G. A. Webb, *Org. Magn. Resonance*, 1981, **15**, 241.
119. R. O. Duthaler and J. D. Roberts, *J. Amer. Chem. Soc.*, 1978, **100**, 3889.

120. O. W. Kolling, *Analyt. Chem.*, 1979, **51**, 1324.
121. M. Witanowski, L. Stefaniak, B. Na Lamphun and G. A. Webb, *Org. Magn. Resonance*, 1981, **16**, 57.
122. H. A. Germer, *Theoret. Chim. Acta*, 1974, **34**, 145.
123. G. C. Levy, C. E. Holloway, R. C. Rosanske, J. M. Hewitt and C. H. Bradley, *Org. Magn. Resonance*, 1976, **8**, 643.
124. E. Liepins, I. Birgele, G. Selchan and E. Lukevics, *Zh. Obshch. Khim.*, 1979, **49**, 1537.
125. K. S. Bose and E. H. Abbott, *Inorg. Chem.*, 1977, **16**, 3190.
126. P. W. Westerman and J. D. Roberts, *J. Org. Chem.*, 1977, **42**, 2249.
127. R. O. Duthaler, K. L. Williamson, D. D. Giannini, W. H. Bearden and J. D. Roberts, *J. Amer. Chem. Soc.*, 1977, **99**, 8406.
128. S. N. Y. Fanso-Free, G. T. Furst, P. R. Srinivasan, R. L. Lichter, R. B. Nelson, J. A. Panetta and G. W. Gribble, *J. Amer. Chem. Soc.*, 1979, **101**, 1549.
129. J. F. Whidby, W. B. Edwards and T. P. Pitner, *J. Org. Chem.*, 1979, **44**, 794.
130. G. T. Furst, R. L. Lichter and F. W. Vierhapper, *J. Org. Chem.*, 1980, **45**, 1521.
131. K. Crimaldi and R. L. Lichter, *J. Org. Chem.*, 1980, **45**, 1277.
132. H. R. Kricheldorf, *Makromol. Chem.*, 1978, **179**, 2687.
133. R. O. Duthaler and J. D. Roberts, *J. Amer. Chem. Soc.*, 1978, **100**, 3882.
134. G. C. Levy, T. Pehk and E. Lippmaa, *Org. Magn. Resonance*, 1980, **14**, 214.
135. F. Cavagna and H. Pietsch, *Org. Magn. Resonance*, 1978, **11**, 204.
136. N. J. Oppenheimer and R. D. Davidson, *Org. Magn. Resonance*, 1980, **13**, 14.
137. K. Barlos, G. Hübler, H. Nöth, P. Wanninger, N. Wiberg and B. Wrackmeyer, *J. Magn. Resonance*, 1978, **31**, 363.
138. E. A. V. Ebsworth, D. W. H. Rankin and J. G. Wright, *J. Chem. Soc. Dalton*, 1979, 1065.
139. V. A. Pestunovich, S. N. Tandura, B. Z. Shterenberg, B. P. Baryshok and M. G. Voronkov, *Izv. Akad. Nauk S.S.S.R., Ser. Khim.*, 1979, 2159.
140. K. Jurkschat, G. Mügge, A. Tzschach, A. Zschunke, G. Engelhardt, E. Lippmaa, M. Mägi, M. F. Larin, V. A. Pestunovich and M. G. Voronkov, *J. Organometal. Chem.*, 1979, **171**, 301.
141. K. Barlos, H. Nöth and B. Wrackmeyer, *Z. Naturforsch.*, 1978, **33b**, 515.
142. W. McFarlane and B. Wrackmeyer, *J. Chem. Soc. Dalton*, 1976, **22**, 2351.
143. J. Mason, W. von Bronswijk and J. G. Vinter, *J. Chem. Soc. Dalton*, 1977, 2337.
144. R. Appel, M. Halstenberg and F. Knoll, *Z. Naturforsch.*, 1977, **32b**, 1030.
145. H. B. Stegmann, H. V. Dumm and K. Scheffler, *Phosphorus and Sulphur*, 1978, **5**, 159.
146. G. A. Gray, G. W. Buchanan and F. G. Morin, *J. Org. Chem.*, 1979, **44**, 1768.
147. J. H. Hargis, W. B. Jennings, S. D. Worley and M. S. Tolley, *J. Amer. Chem. Soc.*, 1980, **102**, 13.
148. B. Wrackmeyer and H. Nöth, *Chem. Ber.*, 1977, **110**, 1086.
149. R. E. Botto and J. D. Roberts, *J. Org. Chem.*, 1977, **42**, 2247.
150. D. Ya. Osokin, I. A. Safin, B. I. Buzukin and P. Yu. Kitajev, *Teor. Experim. Khim.*, 1977, **13**, 79.
151. D. E. Dorman, J. W. Paschal and K. E. Merkel, *J. Amer. Chem. Soc.*, 1976, **98**, 6885.
152. J. W. Paschal and D. E. Dorman, *Org. Magn. Resonance*, 1978, **11**, 632.
153. J. D. Roberts, *Jap. J. Antibiotics*, 1979, **32** (suppl), S-112.
154. I. Yavari and J. D. Roberts, *J. Org. Chem.*, 1978, **43**, 4689.
155. T. Axenrod and M. J. Wieder, *Org. Magn. Resonance*, 1976, **8**, 350.
156. G. R. Sullivan and J. D. Roberts, *J. Org. Chem.*, 1977, **42**, 1095.
157. G. C. Levy, A. D. Godwin, J. M. Hewitt and C. Sutcliffe, *J. Magn. Resonance*, 1978, **29**, 553.
158. V. Markowski, G. R. Sullivan and J. D. Roberts, *J. Amer. Chem. Soc.*, 1977, **99**, 714.
159. L. Stefaniak, *Org. Magn. Resonance*, 1979, **12**, 379.

160. L. Stefaniak, M. Witanowski and G. A. Webb, *Polish J. Chem.*, 1981, in press.
161. R. L. Smith, D. W. Cochran, P. Gund and E. J. Cragoe, *J. Amer. Chem. Soc.*, 1979, **101**, 191.
162. R. O. Duthaler, H. G. Förster and J. D. Roberts, *J. Amer. Chem. Soc.*, 1978, **100**, 4974.
163. K. L. Williamson and J. D. Roberts, *Heterocycles*, 1978, **11**, 121.
164. M. P. Sibi and R. L. Lichter, *J. Org. Chem.*, 1977, **42**, 2999.
165. J. Chatt, M. E. Fakley, R. L. Richards, J. Mason and I. A. Stenhouse, *J. Chem. Research* (S), 1979, 322.
166. I. Yavari and J. D. Roberts, *J. Amer. Chem. Soc.*, 1978, **100**, 4662.
167. Y. Nomura and Y. Takeuchi, *J. Chem. Soc. Chem. Comm.*, 1979, 295.
168. A. W. Douglas, *J. Amer. Chem. Soc.*, 1979, **101**, 5676.
169. I. Yavari and J. D. Roberts, *Org. Magn. Resonance*, 1980, **14**, 61.
170. S. F. Nelsen and W. C. Hollinsed, *J. Org. Chem.*, 1980, **45**, 3609.
171. N. Naulet and G. J. Martin, *Tetrahedron Letters*, 1979, 1493.
172. P. W. Westerman, R. E. Botto and J. D. Roberts, *J. Org. Chem.*, 1978, **43**, 2590.
173. H. Nöth, W. Winterstein, W. Kaim and H. Bock, *Chem. Ber.*, 1979, **112**, 2494.
174. K. Kanamori, A. H. Cain and J. D. Roberts, *J. Amer. Chem. Soc.*, 1978, **100**, 4979.
175. H. R. Kricheldorf, *Org. Magn. Resonance*, 1980, **13**, 52.
176. R. E. Botto, J. H. Schwartz and J. D. Roberts, *Proc. Nat. Acad. Sci. USA*, 1980, **77**, 23.
177. W. E. Hull and H. R. Kricheldorf, *Liebigs Ann. Chem.*, 1980, 158.
178. B. Coxon, A. J. Fatiadi, A. Cohen, H. S. Hertz and R. Schaffer, *Org. Magn. Resonance*, 1980, **13**, 187.
179. L. Stefaniak and M. Witanowski, unpublished results.
180. I. Yavari and J. D. Roberts, *Org. Magn. Resonance*, 1980, **13**, 68.
181. G. E. Hawkes, E. W. Randall and W. E. Hull, *J. Chem. Soc. Perkin II*, 1977, 1268.
182. J. M. Burns, M. E. Ashley, G. C. Crockett and T. H. Koch, *J. Amer. Chem. Soc.*, 1977, **99**, 6924.
183. R. C. Haltiwanger, J. M. Burns, G. C. Crockett and T. H. Koch, *J. Amer. Chem. Soc.*, 1978, **100**, 5110.
184. H. R. Kricheldorf, *J. Macromol. Sci. Chem.*, 1980, **A14**, 959.
185. H. Kricheldorf, *Org. Magn. Resonance*, 1980, **14**, 198.
186. V. I. Stenberg, N. K. Narain, S. P. Singh, R. H. Obenauf and M. J. Albright, *J. Heterocyclic Chem.*, 1977, **14**, 407.
187. I. Yavari and J. D. Roberts, *Biochem. Biophys. Res. Comm.*, 1978, **83**, 635.
188. D. Gust, G. Dirks and G. R. Pettit, *J. Org. Chem.*, 1979, **44**, 314.
189. I. Yavari and J. D. Roberts, *J. Org. Chem.*, 1978, **43**, 4689.
190. P. W. Westerman and J. D. Roberts, *J. Org. Chem.*, 1978, **43**, 1177.
191. I. Yavari and J. D. Roberts, *Nouv. J. Chimie*, 1979, **3**, 279.
192. P. Stilbs, S. Forsén and J. S. Hartman, *J. Chem. Soc. Perkin II*, 1977, **5**, 556.
193. A. R. Bassindale and T. B. Posner, *J. Organometal. Chem.*, 1979, **175**, 273.
194. H. R. Kricheldorf, *Polymer Bull.*, 1980, **2**, 177.
195. J. Dorie, J. P. Gouesnard, B. Mechin, N. Naulet and G. J. Martin, *Org. Magn. Resonance*, 1980, **13**, 126.
196. G. J. Martin, T. Bertrand, D. Le Botlan and J. M. Letourneux, *J. Chem. Research* (S), 1979, 408.
197. J. W. Paschal, D. E. Dorman, P. R. Srinivasan and R. L. Lichter, *J. Org. Chem.*, 1978, **43**, 2013.
198. H. R. Kricheldorf and G. Schilling, *Makromol. Chem.*, 1978, **179**, 2667.
199. I. Yavari and J. D. Roberts, *Tetrahedron Letters*, 1978, 2491.
200. I. Yavari and J. D. Roberts, *J. Amer. Chem. Soc.*, 1978, **100**, 5217.
201. L. Stefaniak, *Org. Magn. Resonance*, 1978, **11**, 385.

202. W. Schwotzer, J. H. Bieri, M. Viscontini and V. von Philipsborn, *Helv. Chim. Acta*, 1978, **61**, 2108.
203. K. Kawano, N. Ohishi, A. T. Suzuki, Y. Kyogoku and K. Yagi, *Biochemistry*, 1978, **17**, 3854.
204. D. Brewer, A. G. McInnes, D. G. Smith, A. Taylor, J. A. Walter, H. R. Loosli and Z. L. Kis, *J. Chem. Soc. Perkin I*, 1978, 1248.
205. H. R. Kricheldorf, *Angew. Chem. Int. Ed. Engl.*, 1978, **17**, 442.
206. J. Mason, W. van Bronswijk and O. Glemser, *J. Phys. Chem.*, 1978, **82**, 463.
207. S. K. Knudson and J. P. Idoux, *J. Org. Chem.*, 1979, **44**, 520.
208. F. Blomberg and H. Rüterjans, in "N.M.R. Spectroscopy in Molecular Biology", B. Pullman (ed.), D. Reidel Publ. Co., Dordrecht, Holland, 1978, p. 231.
209. F. Blomberg, W. Maurer and H. Rüterjans, *J. Amer. Chem. Soc.*, 1977, **99**, 8149.
210. H. R. Kricheldorf, *Org. Magn. Resonance*, 1979, **12**, 414.
211. D. H. Live, H. R. Wyssbrod, A. J. Fischman, W. C. Agosta, C. H. Bradley and D. Cowburn, *J. Amer. Chem. Soc.*, 1979, **101**, 474.
212. K. Kawano and Y. Kyogoku, *Chem. Letters*, 1975, 1305.
213. W. W. Bachovchin and J. D. Roberts, *J. Amer. Chem. Soc.*, 1978, **100**, 8041.
214. H. R. Kricheldorf and W. E. Hull, *Org. Magn. Resonance*, 1980, **13**, 335.
215. D. Gattegno, G. E. Hawkes and E. W. Randall, *J. Chem. Soc. Perkin II*, 1976, **13**, 1527.
216. V. Markowski, T. B. Posner, P. Loftus and J. D. Roberts, *Proc. Nat. Acad. Sci. USA*, 1977, **74**, 1308.
217. H. Kricheldorf and W. E. Hull, *J. Polymer Sci., Polymer Chem.*, 1978, **16**, 583.
218. K. L. Williamson, L. G. Pease and J. D. Roberts, *J. Amer. Chem. Soc.*, 1979, **101**, 714.
219. M. A. Khaled, D. W. Urry, H. Sugano, M. Miyoshi and N. Izumiya, *Biochemistry*, 1978, **17**, 2490.
220. C. Toniolo, G. M. Bonora, G. R. Sullivan, W. H. Bearden and J. D. Roberts, *J. Org. Chem.*, 1980, **45**, 288.
221. F. Blomberg, H. Rüterjans, K. Lintner, F. Toma and S. Fermandjian, *Org. Magn. Resonance*, 1978, **11**, 598.
222. H. R. Kricheldorf and W. E. Hull, *Org. Magn. Resonance*, 1979, **12**, 607.
223. H. R. Kricheldorf and W. E. Hull, *Makromol. Chem.*, 1979, **180**, 1707.
224. G. E. Hawkes, E. W. Randall, W. E. Hull, D. Gattegno and F. Conti, *Biochemistry*, 1978, **17**, 3986.
225. M. Llinás, W. J. Horsley and M. P. Klein, *J. Amer. Chem. Soc.*, 1976, **98**, 7554.
226. M. Llinás and K. Wüthrich, *Biochim. Biophys. Acta*, 1978, **532**, 29.
227. N. Higuchi, Y. Kyogoku and H. Yajima, *Chem. Letters*, 1980, 171.
228. H. Naganawa, T. Takita, H. Umezawa and W. E. Hull, *J. Antibiotics*, 1979, **32**, 539.
229. A. Olesker, L. Valente, L. Barata, G. Lukacs, W. E. Hull, K. Tori, K. Tokura, K. Okabe, M. Ebata and H. Otsuka, *J. Chem. Soc. Chem. Comm.*, 1978, 577.
230. M. A. Khaled, K. Okamoto and D. W. Urry, *Biochim. Biophys. Acta*, 1980, **623**, 229.
231. A. Lapidot and C. S. Irving, *Biochemistry*, 1979, **18**, 704.
232. C. S. Irving and A. Lapidot, "Stable Isotopes", Proc. Third Internat. Conference, 1979, 307.
233. C. S. Irving and A. Lapidot, *Antimicrobial Agents and Chemotherapy*, 1978, **14**, 695.
234. A. Lapidot and C. S. Irving, *Biochemistry*, 1979, **18**, 1788.
235. A. Lapidot and C. S. Irving, "N.M.R. Spectroscopy in Molecular Biology", B. Pullman (ed.), D. Reidel Publ. Co., Dordrecht, Holland, 1978, p. 439.
236. C. S. Irving and A. Lapidot, *Biochim. Biophys. Acta*, 1977, **470**, 251.
237. A. Lapidot and C. S. Irving, *Proc. Nat. Acad. Sci. USA*, 1977, **74**, 1988.
238. H. Depaire, J. P. Thomas, A. Brun, W. E. Hull, A. Olesker and G. Lukacs, *Tetrahedron Letters*, 1977, **16**, 1401.

239. H. R. Kricheldorf and W. E. Hull, *Makromol. Chem.* 1979, **180**, 161.
240. W. E. Hull, H. R. Kricheldorf and M. Fehrle, *Biopolymers*, 1978, **17**, 2427.
241. H. R. Kricheldorf, *Makromol. Chem.*, 1978, **179**, 2675.
242. N. Higuchi, K. Kakiuchi, Y. Kyogoku and K. Hikichi, *Macromolecules*, 1980, **13**, 79.
243. H. R. Kricheldorf, *Makromol. Chem.*, 1979, **180**, 147.
244. H. R. Kricheldorf and W. E. Hull, *Makromol. Chem.*, 1980, **181**, 507.
245. H. R. Kricheldorf, W. E. Hull and V. Formacek, *Biopolymers*, 1977, **16**, 1609.
246. H. R. Kricheldorf and W. E. Hull, *J. Macromol. Sci. Chem.*, 1978, **A12**, 51.
247. J. Müller, *Z. Naturforsch.*, 1978, **33b**, 993.
248. J. Müller, *Z. Naturforsch.*, 1978, **34b**, 437.
249. H. Booth, B. W. Bycroft, C. M. Wels, K. Corbett and A. P. Maloney, *J. Chem. Soc. Chem. Comm.*, 1976, 110.
250. H. R. Kricheldorf and W. E. Hull, *Macromolecules*, 1980, **13**, 87.
251. H. R. Kricheldorf and W. E. Hull, *Liebigs Ann. Chem.*, 1978, 1817.
252. H. R. Kricheldorf and W. E. Hull, *Makromol. Chem.*, 1977, **178**, 253.
253. H. R. Kricheldorf and W. E. Hull, *Makromol. Chem.*, 1979, **180**, 1715.
254. J. Müller and H. F. Schröder, *Z. Anorg. Allg. Chem.*, 1979, **450**, 149.
255. J. Müller, *Z. Naturforsch.*, 1979, **34b**, 536.
256. J. Müller, *Z. Naturforsch.*, 1979, **34b**, 531.
257. C. Casewit and J. D. Roberts, *J. Amer. Chem. Soc.*, 1980, **102**, 2364.
258. A. J. Jones, H. McNab and P. Hanisch, *Aust. J. Chem.*, 1978, **31**, 1005.
259. Y. Yavari, J. S. Staral and J. D. Roberts, *Org. Magn. Resonance*, 1979, **12**, 340.
260. A. Lapidot and C. S. Irving, *J. Amer. Chem. Soc.*, 1977, **99**, 5488.
261. J. Vaes, M. Chabanel and M. L. Martin, *J. Phys. Chem.*, 1978, **82**, 2420.
262. P. S. Pregosin, N. Streit and L. M. Venanzi, *Inorg. Chim. Acta*, 1980, **38**, 237.
263. S. L. Yoffe, A. L. Blumenfeld and A. S. Shashkov, *Izv. Akad. Nauk S.S.S.R.*, 1978, 246.
264. L. Stefaniak, M. Witanowski, B. Kamieński and G. A. Webb, *Org. Magn. Resonance*, 1980, **13**, 274.
265. Y. Yamamoto and J. Uzawa, *Chemistry Letters*, 1978, 1213.
266. H. Geppert, R. Radeglia, R. Geyer and G. Rudakoff, *Z. Chem.*, 1977, **17**, 23.
267. I. Morishima and T. Inubushi, *J. Chem. Soc. Chem. Comm.*, 1977, 616.
268. I. Morishima and T. Inubushi, *J. Amer. Chem. Soc.*, 1978, **100**, 3568.
269. I. Morishima, T. Inubushi, S. Neya, S. Ogawa and T. Yonezawa, *Biochem. Biophys. Res. Comm.*, 1977, **78**, 739.
270. I. Morishima and T. Inubushi, *FEBS Letters*, 1977, **81**, 57.
271. M. Witanowski, S. Biernat, L. Stefaniak, B. A. Trofimov, A. I. Mikhaleva and G. A. Webb, *Bull. Acad. Polon. Sci., Ser. Sci. Chim.*, 1981, in press.
272. B. Wrackmeyer and H. Nöth, *Chem. Ber.*, 1976, **109**, 1075.
273. I. I. Schuster, C. Dyllick-Brenzinger and J. D. Roberts, *J. Org. Chem.*, 1979, **44**, 1765.
274. I. I. Schuster and J. D. Roberts, *J. Org. Chem.*, 1979, **44**, 3864.
275. M. Alei, L. O. Morgan and W. E. Wageman, *Inorg. Chem.*, 1978, **17**, 2288.
276. M. Alei, L. O. Morgan, E. W. Wageman and T. W. Whaley, *J. Amer. Chem. Soc.*, 1980, **102**, 2881.
277. G. E. Hawkes, E. W. Randall, J. Elguero and C. J. Marzin, *J. Chem. Soc. Perkin II*, 1977, 1024.
278. I. Yavari, R. E. Botto and J. D. Roberts, *J. Org. Chem.*, 1978, **43**, 2542.
279. M. Witanowski, L. Stefaniak, A. Grabowska and G. A. Webb, *Spectrochim. Acta*, 1978, **34A**, 877.
280. M. M. King, H. J. C. Yeh and G. O. Dudek, *Org. Magn. Resonance*, 1976, **8**, 208.
281. M. Alei, W. E. Wageman and L. O. Morgan, *Inorg. Chem.*, 1978, **17**, 3314.
282. G. Burton, H. Nordlöv, S. Hosozawa, H. Matsumoto, P. M. Jordan, P. E. Fagerness, L. M. Pryde and A. I. Scott, *J. Amer. Chem. Soc.*, 1979, **101**, 3114.

283. K. Kawano, Y. Ozaki, Y. Kyogoku, H. Ogoshi, H. Sugimoto and Z. I. Yoshida, *J. Chem. Soc. Perkin II*, 1978, 1319.
284. K. Kawano, Y. Ozaki, Y. Kyogoku, H. Ogoshi, H. Sugimoto and Z. I. Yoshida, *J. Chem. Soc. Chem. Comm.*, 1977, 226.
285. Y. Ozaki, Y. Kyogoku, H. Ogoshi, H. Sugimoto and Z. I. Yoshida, *J. Chem. Soc. Chem. Comm.*, 1979, 76.
286. H. J. C. Yeh, M. Sato and I. Morishima, *J. Magn. Resonance*, 1977, **26**, 365.
287. D. Gust and J. D. Roberts, *J. Amer. Chem. Soc.*, 1977, **99**, 3637.
288. D. D. Dominguez, M. M. King and H. J. C. Yeh, *J. Magn. Resonance*, 1978, **32**, 161.
289. D. Gust and D. N. Neal, *J. Chem. Soc. Chem. Comm.*, 1978, 681.
290. C. S. Irving and A. Lapidot, *J. Chem. Soc. Chem. Comm.*, 1977, 184.
291. M. Witanowski, L. Stefaniak, S. Biernat and G. A. Webb, *Org. Magn. Resonance*, 1980, **14**, 356.
292. V. V. Negrebetskii, L. Ya. Bogelfer, A. V. Vasilev, R. G. Bobkova, N. P. Ignatova, N. I. Shretsov-Shilovskii and N. N. Melnikov, *Zhur. Strukt. Khim.*, 1978, **19**, 532.
293. L. Stefaniak, *Tetrahedron*, 1977, **33**, 2571.
294. L. Stefaniak, M. Witanowski and G. A. Webb, *Bull. Acad. Polon. Sci., Ser. Sci. Chim.*, in press.
295. M. Alei and W. E. Wageman, *Tetrahedron Letters*, 1979, 667.
296. E. v. Goldammer, *Z. Naturforsch.*, 1979, **34c**, 1106.
297. E. v. Goldammer, *J. Mol. Struct.*, 1980, **60**, 127.
298. W. Städeli and W. von Philipsborn, *Org. Magn. Resonance*, 1981, **15**, 106.
299. I. Yavari and J. D. Roberts, *Org. Magn. Resonance*, 1979, **12**, 87.
300. M. Allen and J. D. Roberts, *J. Org. Chem.*, 1980, **45**, 130.
301. L. Stefaniak and J. Wielgat, *Bull. Acad. Polon. Sci., Ser. Sci. Chim.*, 1978, **26**, 859.
302. M. Witanowski, L. Stefaniak and G. A. Webb, *Org. Magn. Resonance*, in press.
303. T. Wamsler, J. T. Nielsen, E. J. Pedersen and K. Schaumburg, *J. Magn. Resonance*, 1978, **31**, 177.
304. L. Stefaniak, M. Witanowski and G. A. Webb, *Polish J. Chem.*, in press.
305. M. Witanowski and L. Stefaniak, *Bull. Acad. Polon. Sci., Ser. Sci. Chim.*, in press.
306. L. Stefaniak, M. Witanowski and G. A. Webb, *Bull. Acad. Polon. Sci., Ser. Sci. Chim.*, in press.
307. M. Witanowski, L. Stefaniak, B. Kamieński and G. A. Webb, *Org. Magn. Resonance*, 1980, **14**, 305.
308. A. H. Cain, G. R. Sullivan and J. D. Roberts, *J. Amer. Chem. Soc.*, 1977, **99**, 6423.
309. M. Witanowski, L. Stefaniak, H. Januszewski and G. A. Webb, *J. Magn. Resonance*, 1974, **16**, 69.
310. R. Dyllick-Brenzinger and J. D. Roberts, *J. Amer. Chem. Soc.*, 1980, **102**, 1166.
311. M. Witanowski, L. Stefaniak and J. Wielgat, *Bull. Acad. Polon. Sci., Ser. Sci. Chim.*, 1978, **26**, 865.
312. P. H. von Dreele, *J. Amer. Chem. Soc.*, 1976, **98**, 1270.
313. L. Stefaniak, *Spectrochim. Acta*, 1976, **32A**, 345.
314. P. Büchner, F. Blomberg and H. Rüterjans, in "Nuclear Magnetic Resonance Spectroscopy in Molecular Biology", B. Pullman (ed.), 1978, 53, Reidel Publishing Company, Dordrecht, Holland.
315. P. Büchner, W. Maurer and H. Rüterjans, *J. Magn. Resonance*, 1978, **29**, 45.
316. C. D. Poulter and C. L. Livingston, *Tetrahedron Letters*, 1979, 755.
317. J. A. Hörig, P. Renz and G. Heckmann, *J. Biol. Chem.*, 1978, **253**, 7410.
318. M. Watanabe, H. Iwahashi, H. Sugeta, Y. Kyogoku and M. Kainosho, "Nucleic Acids Research", Symposium Series No. 6, 1979, Information Retrieval, London.
319. L. H. Staël, D. J. Stufkens and A. Oskam, *Inorg. Chim. Acta*, 1978, **26**, 255.
320. L. M. Jackman and J. C. Trewella, *J. Amer. Chem. Soc.*, 1979, **101**, 6428.

321. R. E. Botto, P. W. Westerman and J. D. Roberts, *Org. Magn. Resonance*, 1978, **11**, 510.
322. G. C. Levy, A. D. Godwin and C. E. Holloway, *J. Magn. Resonance*, 1979, **34**, 327.
323. D. A. Armitage, J. Mason and J. G. Vinter, *Inorg. Chem.*, 1978, **17**, 776.
324. B. Thomas, G. Seifert, G. Grossmann and D. Scheller, *Z. Phys. Chem.*, 1979, **260**, 225.
325. R. E. Botto and J. D. Roberts, *J. Org. Chem.*, 1979, **44**, 140.
326. B. Thomas and G. Grossmann, *Z. Anorg. Allg. Chem.*, 1979, **448**, 107.
327. M. A. Trusule, K. K. Venter and M. Y. Mägi, *Izv. Akad. Nauk Latv. SSR, Ser. Khim.*, 1977, 465.
328. D. G. Morris and A. M. Murray, *J. Chem. Soc. Perkin II*, 1976, 1579.
329. W. Schwotzer, Ch. Leuenberger, L. Hoesch, A. S. Dreiding and W. von Philipsborn, *Org. Magn. Resonance*, 1977, **9**, 382.
330. J. Chatt, M. E. Fakley, R. L. Richards, J. Mason and I. A. Stenhouse, *J. Chem. Research* (S), 1979, 44.
331. A. Lyčka, D. Šnobl, V. Machaček and M. Večera, *Org. Magn. Resonance*, 1981, **16**, 17
332. J. M. Manriguez, D. R. McAlister, E. Rosenberg, A. M. Schiller, K. L. Williamson, S. I. Chan and J. E. Bercaw, *J. Amer. Chem. Soc.*, 1978, **100**, 3078.
333. G. A. Olah, B. G. Gupta and S. C. Narang, *J. Amer. Chem. Soc.*, 1979, **101**, 5317.
334. J. R. Dilworth, C. T. Kan, R. L. Richards, J. Mason and I. A. Stenhouse, *J. Chem. Research* (S), in press.
335. A. Yamasaki, Y. Miyakoshi, M. Fujita, Y. Yoshikawa and H. Yamatera, *J. Inorg. Nucl. Chem.*, 1979, **41**, 473.
336. A. V. Suvorov, V. A. Scherbakov and A. B. Nikolskii, *Zh. Obshch. Khim.*, 1978, **48**, 2169.
337. H. Motschi, P. S. Pregosin and L. M. Venanzi, *Helv. Chim. Acta*, 1979, **62**, 667.
338. R. E. Botto, B. W. S. Kolthammer, P. Legzdins and J. D. Roberts, *Inorg. Chem.*, 1979, **18**, 2049.
339. N. W. Allock, N. Herron and P. Moore, *Inorg. Chim. Acta*, 1979, **32**, L25.
340. E. Glozbach, P. Krommes and J. Lorberth, *J. Organometal. Chem.*, 1980, **192**, 163.
341. B. Coxon and L. Hough, *Carbohydrate Res.*, 1979, **73**, 47.
342. R. E. Wasylishen, *Canad. J. Chem.*, 1976, **54**, 833.
343. T. Bottin-Strzalko, M. J. Pouet and M. P. Simonnin, *Org. Magn. Resonance*, 1976, **8**, 120.
344. M. E. Moseley and P. Stilbs, *Canad. J. Chem.*, 1978, **56**, 1302.
345. P. Stilbs and S. Forsén, *Org. Magn. Resonance*, 1976, **8**, 384.
346. J. Chatt, M. E. Fakley, R. L. Richards, J. Mason and I. A. Stenhouse, *J. Chem. Research* (S), 1979, 322.
347. K. D. Kopple, A. Ahsan and M. Barfield, *Tetrahedron Letters*, 1978, 3519.
348. H. J. Jakobsen and W. S. Brey, *J. Amer. Chem. Soc.*, 1979, **101**, 774.
349. L. Bauer and O. Exner, *Angew Chem., Int. Ed. Engl.*, 1974, **13**, 376.
350. A. J. Jones, P. Hanisch, M. L. Heffernan and G. M. Irvine, *Aust. J. Chem.*, 1980, **33**, 499.
351. D. F. Wiemer, D. I. C. Scopes and N. J. Leonard, *J. Org. Chem.*, 1976, **41**, 3051.
352. L. Stefaniak and M. Witanowski, *Bull. Acad. Polon. Sci., Ser. Sci. Chim.*, 1977, **25**, 261.
353. J. P. Kintzinger and J. M. Lehn, *J. Chem. Soc. Chem. Comm.*, 1967, 600.
354. J. R. Kalman and D. H. Williams, *J. Amer. Chem. Soc.*, 1980, **102**, 906.
355. R. L. Lipnick and J. D. Fissekis, *J. Org. Chem.*, 1979, **44**, 1627.
356. A. Demarco, M. Llinas and K. Wüthrich, *Biopolymers*, 1978, **17**, 2727.
357. J. E. Oatis and H. P. Schultz, *Org. Magn. Resonance*, 1978, **11**, 40.
358. H. J. Jakobsen and W. S. Brey, *J. Chem. Soc. Chem. Comm.*, 1979, 478.
359. T. Bundgaard and H. J. Jakobsen, *Tetrahedron Letters*, 1976, 1621.
360. J. P. Marchal and D. Canet, *J. Magn. Resonance*, 1978, **31**, 23.
361. A. De Marco and M. Llinas, *Org. Magn. Resonance*, 1979, **12**, 454.

362. H. R. Kricheldorf, *Org. Magn. Resonance*, 1980, **14**, 455.
363. D. R. Boyd, M. E. Stubbs, N. J. Thompson, H. J. C. Yeh, D. M. Jerina and R. E. Wasylishen, *Org. Magn. Resonance*, 1980, **14**, 528.
364. L. Ernst, E. Lustig and V. Wray, *J. Magn. Resonance*, 1976, **22**, 459.
365. N. Naulet, M. Beljean and G. J. Martin, *Tetrahedron Letters*, 1976, 3597.
366. G. W. Buchanan and B. A. Dawson, *Canad. J. Chem.*, 1977, **55**, 1437.
367. A. J. Fischman, D. H. Live, H. R. Wyssbrod, W. C. Agosta and D. Cowburn, *J. Amer. Chem. Soc.*, 1980, **102**, 2533.
368. A. J. Fischman, H. R. Wyssbrod, W. C. Agosta and D. Cowburn, *J. Amer. Chem. Soc.*, 1978, **100**, 54.
369. M. J. O. Anteunis, F. A. M. Borremans, J. Gelan, A. P. Marchand and R. W. Allen, *J. Amer. Chem. Soc.*, 1978, **100**, 4050.
370. Y. Yamamoto and H. Yamazaki, *J. Coord. Chem.*, 1977, **6**, 241.
371. P. Diehl, T. Bjorholm and J. Amerin, *Org. Magn. Resonance*, 1981, **15**, 104.
372. C. D. Hall, A. P. Bell and D. Z. Denney, *Org. Magn. Resonance*, 1981, **15**, 7.
373. H. Nakanishi and J. D. Roberts, *Org. Magn. Resonance*, 1981, **15**, 7.
374. S. Berger, *Tetrahedron*, 1978, **34**, 3133.
375. L. A. Valckx, F. A. M. Borremans, C. E. Beĉu, R. H. K. De Waele and M. J. O. Anteunis, *Org. Magn. Resonance*, 1979, **12**, 302.
376. G. W. Lagodinskaya, N. G. Yuida, G. N. Nechiporenko and G. B. Manelis, *Zh. Fiz. Khim.*, 1975, **49**, 2244.
377. I. M. Al-Najjar, M. Green, I. M. Ismail, P. J. Sadler and J. K. K. Sarhan, *Inorg. Chim. Acta*, 1980, **44**, L187.
378. P. Tarburton, J. P. Edasery, C. A. Kingsbury, A. E. Sopchik and N. H. Cromwell, *J. Org. Chem.*, 1979, **44**, 2041.
379. M. P. Sibi and R. L. Lichter, *Org. Magn. Resonance*, 1980, **14**, 494.
380. N. Fangmeier and E. Leistner, *J. Biol. Chem.*, 1980, **255**, 10205.
381. J. A. Walter and J. L. C. Wright, *Tetrahedron Letters*, 1979, 3909.
382. A. M. Nadzan and K. L. Rinehart, *J. Amer. Chem. Soc.*, 1977, **99**, 4647.
383. B. Coxon and R. C. Reynolds, *Carbohydrate Res.*, 1980, **78**, 1.
384. T. Bundgaard, H. J. Jakobsen and E. J. Rahkamaa, *J. Magn. Resonance*, 1975, **19**, 345.
385. S. Braun, *Org. Magn. Resonance*, 1976, **8**, 273.
386. M. Kainosho, *J. Amer. Chem. Soc.*, 1979, **101**, 1031.
387. H. Yamada, M. Hirobe, K. Higashiyama, H. Takahashi and K. T. Suzuki, *J. Amer. Chem. Soc.*, 1978, **100**, 4617.
388. S. J. Gould and C. C. Chang, *J. Amer. Chem. Soc.*, 1978, **100**, 1624.
389. G. W. Buchanan and B. A. Dawson, *Org. Magn. Resonance*, 1980, **13**, 293.
390. A. Danoff, M. Franzen-Sieveking, R. L. Lichter and S. N. Y. Fanso-Free, *Org. Magn. Resonance*, 1979, **12**, 83.
391. H. Fritz, D. Clerin and J. P. Fleury, *Org. Magn. Resonance*, 1976, **8**, 269.
392. N. J. Koole, D. Knol and M. J. A De Bie, *J. Magn. Resonance*, 1976, **21**, 499.
393. I. Morishima, T. Hayashi, T. Inubushi, T. Yonezawa and S. Uemura, *J. Chem. Soc. Chem. Comm.*, 1979, 483.
394. R. E. Wasylishen, D. H. Muldrew and K. J. Friesen, *J. Magn. Resonance*, 1980, **41**, 341.
395. M. Alei, P. J. Vergamini and W. E. Wageman, *J. Amer. Chem. Soc.*, 1979, **101**, 5415.
396. A. J. Carty and S. E. Jacobson, *J. Chem. Soc. Chem. Comm.*, 1975, 175.
397. U. Henriksson, L. Ödberg, J. C. Eriksson and L. Westman, *J. Phys. Chem.*, 1977, **81**, 76.
398. M. Watanabe, H. Iwahashi, H. Sugeta and M. Kainosho, "Nucleic Acids Research", Symp. Ser., 1979, 75.
399. W. J. Stec and W. S. Zieliński, *Tetrahedron Letters*, 1980, 1361.
400. B. Thomas and G. Grossmann, *J. Magn. Resonance*, 1979, **36**, 333.

401. B. Thomas, G. Seifert, G. Grossmann and D. Scheller, *Z. Phys. Chem.*, 1979, **260**, 225.
402. G. A. Gray and T. A. Albright, *J. Amer. Chem. Soc.*, 1977, **99**, 3243.
403. H. J. Jakobsen and W. S. Brey, *J. Chem. Soc. Chem. Comm.*, 1979, 488.
404. O. R. Chambers, M. F. Harman, D. S. Rycroft, D. W. A. Sharp and J. M. Winfield, *J. Chem. Research* (S), 1977, 150.
405. S. J. Kerrison and P. J. Sadler, *J. Chem. Soc. Chem. Comm.*, 1977, 861.
406. P. S. Pregosin and L. M. Venanzi, *Chem. Brit.*, 1978, **14**, 276.
407. H. Motschi, S. N. Sze and P. S. Pregosin, *Helv. Chim. Acta*, 1979, **62**, 2086.
408. J. M. Al-Najjar, M. Green, S. J. S. Kerrison and P. J. Sadler, *J. Chem. Research* (S), 1979, 206.
409. R. Meij, D. J. Stufkens, K. Vrieze, W. Van Gerresheim and C. H. Stam, *J. Organometal. Chem.*, 1979, **164**, 353.
410. W. I. Tarasov, S. N. Petrosyan, G. A. Kirakosyan and Yu. A. Busalev, *Dokl. Akad. Nauk SSSR*, 1978, **242**, 156.
411. I. Morishima, T. Inubushi and M. Sato, *J. Chem. Soc. Chem. Comm.*, 1978, 106.
412. A. N. Nesmeyanov, Ye. V. Borisov, A. S. Peregudov, D. N. Kravtsov, L. A. Fedorov, E. I. Fedin and S. A. Postovoy, *Dokl. Akad. Nauk SSSR*, 1979, **247**, 1154.
413. R. E. Wasylishen, in "Annual Reports on NMR Spectroscopy", G. A. Webb (ed.), 1977, **7**, 266, Academic Press, London.
414. K. J. Friesen and R. E. Wasylishen, *J. Magn. Resonance*, 1980, **41**, 189.
415. K. T. Suzuki, H. Yamada and M. Hirobe, *J. Chem. Soc. Chem. Comm.*, 1978, 485.
416. H. Yamada, M. Hirobe, K. Higashiyama and K. T. Suzuki, *Tetrahedron Letters*, 1978, 4039.
417. G. Bodenhausen and J. D. Ruben, *Chem. Phys. Letters*, 1980, **69**, 185.
418. R. B. Jordan, *J. Magn. Resonance*, 1980, **38**, 267.
419. M. Alei, W. E. Wageman and L. O. Morgan, *Inorg. Chem.*, 1978, **17**, 3314.
420. K. D. Rose and R. G. Bryant, *Inorg. Chem.*, 1979, **18**, 2130.
421. R. Bramley, B. N. Figgis and R. S. Nyholm, *J. Chem. Soc. A*, 1967, 861.
422. C. Musikas, C. Cuillerdier and C. Chachaty, *Inorg. Chem.*, 1978, **17**, 3610.
423. V. A. Pestunovich, S. N. Tandura, B. J. Shterenberg, V. P. Beryshok and M. G. Voronkov, *Izv. Akad. Nauk SSSR, Ser. Khim.*, 1978, 2653.
424. O. Lutz and A. Nolle, *Z. Physik*, 1979, **35b**, 245.
425. J. Englich and P. Cizek, *Phys. Stat. Sol.*, 1979, **94b**, K15.
426. N. S. Dalal, J. A. Ripmeester and A. H. Reddoch, *J. Magn. Resonance*, 1978, **31**, 471.
427. R. Biehl, K. Möbius, S. E. O'Connor, R. I. Walter and H. Zimmermann, *J. Phys. Chem.*, 1979, **83**, 3449.
428. T. G. Brown and B. M. Hoffman, *Mol. Phys.*, 1980, **39**, 1073.
429. V. P. Chacko, C. A. McDowell and B. C. Singh, *J. Chem. Phys.*, 1980, **72**, 4111.
430. H. van Willigen, C. F. Mulks, A. Bouhaouss, M. Ferhat and A. H. Roufosse, *J. Amer. Chem. Soc.*, 1980, **102**, 4846.
431. B. Kirste, H. Kurreck and K. Schubert, *Tetrahedron*, 1980, **36**, 1985.
432. J. Browning, P. L. Coggin and R. J. Goodfellow, *J. Chem. Research* (S), 1978, 328.
433. N. W. Alcock, N. Herron and P. Moore, *J. Chem. Soc. Dalton*, 1979, 1486.
434. S. Martinengo, G. Ciani, A. Sironi, B. T. Meaton and J. Mason, *J. Amer. Chem. Soc.*, 1979, **101**, 7095.
435. E. J. Pedersen, R. R. Vold and R. L. Vold, *Mol. Phys.*, 1978, **35**, 997.
436. R. E. Stark, R. L. Vold and R. R. Vold, *Chem. Phys.*, 1977, **20**, 337.
437. T. Raj and R. G. Bryant, *J. Magn. Resonance*, 1979, **34**, 537.
438. D. M. Chen and J. D. Glickson, *J. Magn. Resonance*, 1977, **28**, 9.
439. N. Persson and B. Lindman, *Mol. Cryst. Liq. Cryst.*, 1977, **38**, 327.
440. A. Loewenstein, M. Brenman and R. Schwarzmann, *J. Phys. Chem.*, 1978, **82**, 1744.

441. R. E. Wasylishen and B. A. Pettitt, *Mol. Phys.*, 1978, **36**, 1459.
442. A. J. Lees, B. P. Straughan and D. J. Gardiner, *J. Mol. Struct.*, 1979, **54**, 37.
443. R. Tourki, F. Fried, M. J. Vellutini, P. Sixan and F. Gaymard, *Mol. Phys.*, 1979, **37**, 271.
444. A. Loewenstein and M. Brenman, *J. Magn. Resonance*, 1979, **34**, 193.
445. C. Brot and J. Virlet, *J. Phys.*, 1979, **40**, 573.
446. M. E. Moseley and P. Stilbs, *Canad. J. Chem.*, 1979, **57**, 1075.
447. J. Mason, *J. Chem. Soc. Faraday II*, 1976, 2064.
448. H. M. Ratajczak, J. A. Ladd, W. J. Orville-Thomas and H. Ratajczak, *Mol. Phys.*, 1977, **34**, 1019.
449. W. Suchanski and P. C. Canepa, *J. Magn. Resonance*, 1979, **33**, 389.
450. D. Ghesquiere and C. Chachaty, *Org. Magn. Resonance*, 1977, **9**, 392.
451. A. I. Andreeva, B. P. Matusin, D. Y. Osokin and I. A. Safin, *Izv. Akad. Nauk SSR, Ser. Fiz.*, 1978, **42**, 2138.
452. M. J. S. Dewar, Y. Yamaguchi, S. Doraiswamy, S. D. Sharma and S. H. Suck, *Chem. Phys.*, 1979, **41**, 21.
453. E. Jörin, F. Graf, A. Schweiger and H. H. Günthard, *Chem. Phys. Letters*, 1976, **42**, 376.
454. W. B. Mims and J. Peisach, *J. Chem. Phys.*, 1978, **69**, 4921.
455. J. A. B. Lohman, C. A. de Lange and C. MacLean, *Chem. Phys. Letters*, 1978, **55**, 29.
456. C. W. Hilbers and C. MacLean, *Mol. Phys.*, 1969, **16**, 275.
457. M. Redshaw, M. H. Palmer and R. H. Findlay, *Z. Naturforsch.*, 1979, **34a**, 220.
458. E. Hadjoudis, F. Milia, J. Seliger and R. Blinc, *Solid State Comm.*, 1977, **21**, 541.
459. E. Hadjoudis, F. Milia, J. Seliger and R. Blinc, *Chem. Phys. Letters*, 1978, **56**, 382.
460. L. S. Batchelder and J. L. Ragle, *J. Magn. Resonance*, 1980, **37**, 469.
461. K. P. Dinse and C. J. Winscom, *J. Chem. Phys.*, 1978, **68**, 1337.
462. S. E. Lowe and J. Sheridan, *Chem. Phys. Letters*, 1978, **58**, 79.
463. P. Cassoux, A. Serafini, G. Fong and R. L. Kuczkowski, *Inorg. Chem.*, 1978, **17**, 1204.
464. A. Colligiani and R. Ambrosetti, *J. Magn. Resonance*, 1978, **32**, 93.
465. J. E. Roberts, C. P. Cheng and T. L. Brown, *Inorg. Chem.*, 1978, **17**, 754.
466. C. P. Cheng, T. L. Brown, W. C. Fultz and J. L. Burmeister, *J. Chem. Soc. Chem. Comm.*, 1977, 599.
467. C. I. H. Ashby, C. P. Cheng and T. L. Brown, *J. Amer. Chem. Soc.*, 1978, **100**, 6057.
468. C. I. H. Ashby, C. P. Cheng, E. N. Duesler and T. L. Brown, *J. Amer. Chem. Soc.*, 1978, **100**, 6063.
469. A. Sasane and J. A. S. Smith, *J. Magn. Resonance*, 1978, **32**, 265.
470. T. Asaji, R. Ikeda and D. Nakamura, *J. Magn. Resonance*, 1978, **31**, 437.
471. F. O. Azizov, V. S. Greshivkin, T. G. Balisheva and I. V. Poloshi, *Zh. Fiz. Khim.*, 1979, **53**, 173.
472. F. O. Azizov, V. S. Greshivkin, T. G. Balisheva and I. V. Poloshi, *Teor. Eksp. Khim.*, 1979, **15**, 94.
473. L. Z. Pau and Y. Q. Yu, *Wu Li Hsueh Pao*, 1979, **28**, 447.
474. H. Negita, M. Maekawa, T. Kubo and T. Okuda, *Bull. Chem. Soc. Japan*, 1979, **52**, 1205.
475. R. A. Marino, Proc. New Concepts Symp., 1978, 399.
476. H. Negita, T. Hubo, M. Maekawa, A. Ueda and T. Okuda, *Bull. Chem. Soc. Japan*, 1979, **52**, 1881.
477. J. Murgich, *J. Chem. Phys.*, 1979, **70**, 1198.
478. S. N. Subbarao and P. J. Bray, *J. Chem. Phys.*, 1977, **67**, 3947.
479. C. P. Cheng and T. L. Brown, *J. Magn. Resonance*, 1977, **28**, 391.
480. S. N. Subbarao and P. J. Bray, *J. Chem. Phys.*, 1977, **67**, 1085.
481. C. P. Cheng and T. L. Brown, *J. Chem. Phys.*, 1977, **67**, 1797.
482. T. Oja and L. T. Nielsen, *J. Magn. Resonance*, 1977, **28**, 247.
483. N. S. Kim and P. J. Bray, *Phys. Letters*, 1977, **60A**, 483.

484. H. Negita, T. Kubo and M. Maekawa, *Bull. Chem. Soc. Japan*, 1977, **50**, 2215.
485. A. I. Andreyeva, I. J. Korashin, D. J. Osokin, I. A. Safin and A. P. Pudovic, *Zh. Obshch. Khim.*, 1977, **48**, 1417.
486. D. J. Osokin, B. L. Matusin and I. A. Safin, *Izv. Akad. Nauk SSSR, Ser. Fiz.*, 1978, **42**, 2116.
487. T. Asaji, R. Ikeda and D. Nakamura, *J. Phys. Chem.*, 1979, **83**, 2151.
488. T. Asaji, R. Ikeda and D. Nakamura, *Z. Naturforsch.*, 1979, **34b**, 1722.
489. J. Murgich, *J. Chem. Phys.*, 1979, **70**, 5354.
490. T. Asaji, R. Ikeda, M. Inoue and D. Nakamura, *Phys. Stat. Sol. A*, 1979, **55**, K71.
491. D. J. Osokin and G. G. Bumenko, *Zh. Fiz. Khim.*, 1979, **53**, 130.
492. K. R. Buck, *Org. Magn. Resonance*, 1978, **11**, 584.
493. S. N. Subbarao and P. J. Bray, *Phys. Letters*, 1979, **71A**, 87.
494. H. Budak, M. L. S. Garcia, I. L. Ewart, I. J. E. Poplett and J. A. S. Smith, *J. Magn. Resonance*, 1979, **35**, 309.
495. S. Pissanetzky, *J. Magn. Resonance*, 1979, **34**, 515.
496. J. C. Harding, D. A. Wade, R. A. Morino, E. G. Sauer and S. M. Klainer, *J. Magn. Resonance*, 1979, **36**, 21.
497. J. B. Lambert and D. A. Netzel, *J. Magn. Resonance*, 1977, **25**, 531.
498. P. Loftus, W. H. Bearden and J. D. Roberts, *Nouv. J. Chimie*, 1977, **1**, 283.
499. D. J. Siminovitch, M. Rance and K. R. Jeffrey, *FEBS Letters*, 1980, **112**, 79.

LIST OF TABLES

SUBJECT INDEX

B

C

O

P

Q

R

T

U

V

X

Y

Z